UNIVERSITY OF
BIRMINGHAM

Synthesis and Applications of

4*N*-Substituted Oxazoles

by

Andrew Gillie

A thesis submitted to the University of Birmingham

for the degree of DOCTOR OF PHILOSOPHY

School of Chemistry

College of Engineering and Physical Sciences

University of Birmingham

July 2015

Abstract

This thesis describes the advancement of a flexible and convergent gold-catalysed synthesis of trisubstituted oxazoles, and its application to the synthesis of novel polycyclic compounds. Following on from the initial discovery of this reaction, its scope and limitations have been have been explored, leading to a significant increase in the range of functionality which can be incorporated into the products.

This reaction, and the novel structure of the 4-amido oxazole products, was then exploited to allow the construction of other complex molecules. A one-pot reaction cascade has been developed, in which the oxazole formation is followed by an intramolecular Diels-Alder reaction, allowing the rapid construction of polyheterocyclic compounds from simple starting materials. Finally, the synthesis of the first oxazole-annulated imidazolium salts is described. These salts act as precursors to prochiral nucleophilic heterocyclic carbene ligands, the organometallic chemistry of which has been investigated.

Acknowledgements

To Paul – thank you for giving me interesting projects to work on whilst letting me pursue my own ideas, and for generally being a great supervisor. I have learnt a lot from you about what makes a good scientist.

To Elli, Holly, Matt, Tom, Fernando, Josh, Miguel, Onyeka, Matt and Elsa – thank you for being there when I needed help, for listening when I wanted someone to complain to or to bounce a crazy idea off, and for encouraging all but the craziest of them. You were great colleagues, but it is your friendship which I have valued greatest of all. The happy times with you guys are what I will remember most from my time here.

To Neil, Louise, Chi, Peter, Lianne, Stewart and Ian – thank you for all your assistance with compound characterisation and for generally keeping the place running.

To Alison Fletcher – thank you for being an inspirational chemistry teacher, if it were not for you I may well have done something completely different with the last eight years of my life!

To Mum, Dad, Michael, Susan and Chris – thank you for supporting me in all of my endeavours. I know each of you will flick through this thesis at some point and this will probably be the only page you read in full, nevertheless I appreciate the effort!

Funding for this research was provided by the Engineering and Physical Sciences Research Council and the University of Birmingham.

Table of Contents

List of Abbreviations

$\%V_{bur}$	percentage buried volume
$[\alpha]_D^{20}$	specific rotation at 20 °C using 589 nm light
°	degree(s)
1,10-phen	1,10-phenanthroline
Å	angstrom(s)
Ad	adamantyl
Ar	Aryl
$Au(pic)Cl_2$	dichloro(2-pyridinecarboxylato)gold
Boc	*tert*-butyloxycarbonyl
C	Celsius
Cbz	carboxybenzyl
cod	1,5-cyclooctadiene
d	doublet
DBN	1,5-diazabicyclo[4.3.0]non-5-ene
DBU	1,8-diazabicyclo[5.4.0]undec-7-ene
DCC	*N,N'*-dicyclohexylcarbodiimide
DFT	density functional theory
DIPP	2,6-diisopropylphenyl
DMEDA	*N,N'*-dimethylethylenediamine
DMF	dimethylformamide
DMP	Dess–Martin periodinane
DMSO	dimethyl sulfoxide
dr	diastereomeric ratio
EDG	electron-donating group

ee	enantiomeric excess
EI	electron ionisation
er	enantiomeric ratio
ES	electrospray
EWG	electron-withdrawing group
g	gram(s)
h	hour(s)
Hz	hertz
HPLC	high performance liquid chromatography
HRMS	high resolution mass spectrometry
IMes	1,3-bis(2,4,6-trimethylphenyl)imidazol-2-ylidene
IPr	1,3-bis(2,6-diisopropylphenyl)imidazol-2-ylidene
IR	infrared
J	coupling constant
K	kelvin
L	litre(s)
m	metre(s)
m	multiplet
M	molar
m/z	mass/charge
Mes	mesityl
mol	mole(s)
mp	melting point
Ms	methanesulfonyl
MS	mass spectrometry

MS	molecular sieves
NBS	*N*-bromosuccinimide
NHC	nucleophilic heterocyclic carbene
NMR	nuclear magnetic resonance
Piv	pivaloyl
p-Ns	4-nitrobenzenesulfonyl
ppm	parts per million
q	quartet
r.t.	room temperature
rac	racemic
s	singlet
t	triplet
TBAF	tetrabutylammonium fluoride
TBHP	*tert*-butyl hydroperoxide
TEP	Tolman's Electronic Parameter
Tf	trifluoromethylsulfonyl
TFA	trifluoroacetic acid
THF	tetrahydrofuran
TIPS	triisopropylsilyl
TMS	trimethylsilyl
TLC	thin layer chromatography
Ts	4-toluenesulfonyl
δ	chemical shift
μW	microwave
ν	wavenumber

CHAPTER 1:

INTRODUCTION

1.1: Synthetic Routes to Trisubstituted Oxazoles

Oxazoles are commonly encountered heterocycles which are prevalent in a variety of natural products[1] and pharmaceuticals[2] (Figure 1). A common biosynthetic pathway for their formation is believed to involve an enzyme-assisted cyclodehydration of a serine or threonine residue **1** to form an oxazoline **3**, which may then either be oxidised to the oxazole **4** or reduced to an oxazolidine **5** (Scheme 1).[3] A large number of methods are available to chemists for the synthesis of oxazoles, however the development of mild and convergent strategies remains an active area of research.[4] The first half of this introduction will briefly describe some of the reactions which are commonly used to access fully substituted oxazoles, as well as recent developments in this area.

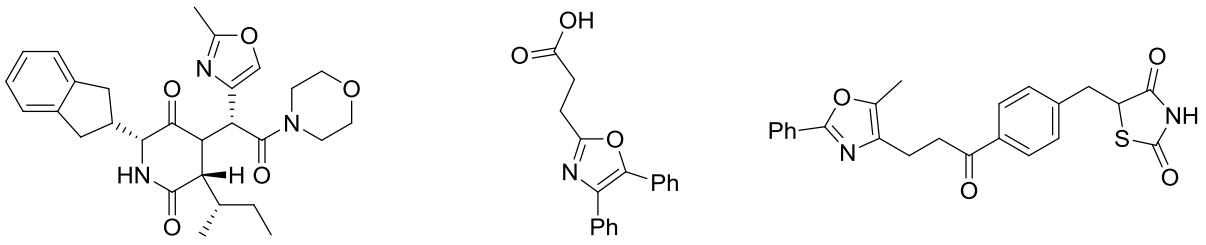

Figure 1: Examples of pharmaceuticals which contain oxazoles.[2]

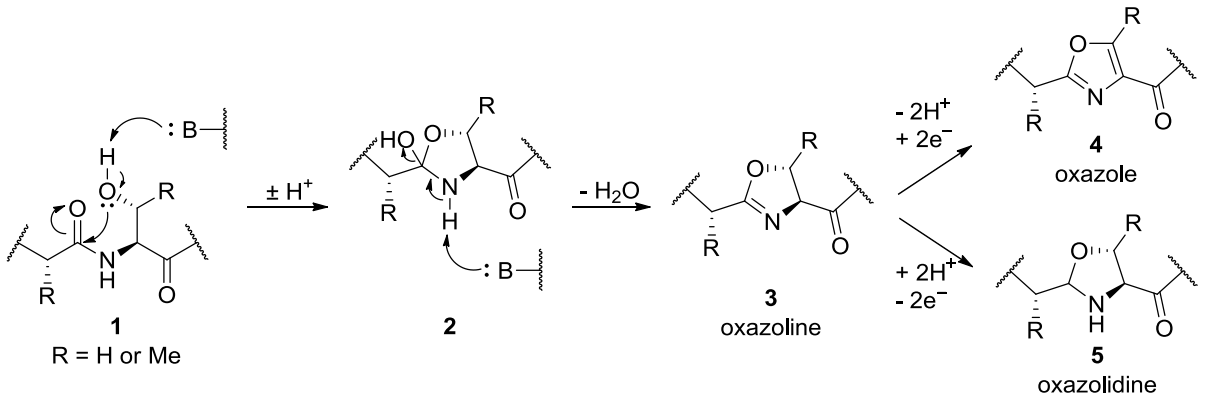

Scheme 1: Biosynthetic pathway for oxazoles and related heterocycles from serine or threonine residues.[3]

1.1.1: Intramolecular Cyclisations

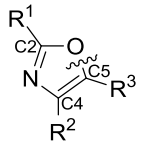

Figure 2: The O–C5 disconnection as a strategy for oxazole synthesis.

The majority of trisubstituted oxazoles are synthesised by intramolecular cyclisations which construct the O–C5 bond (Figure 2). The cyclodehydration of α-acylaminoketones **6** using either sulfuric acid or PCl_5 was reported independently by Robinson and Gabriel in 1909.[5] Since this time a number of other dehydrating reagents have been reported (including P_2O_5, $POCl_3$ and $SOCl_2$).[6] ^{18}O labelling experiments have confirmed that it is the amide oxygen which is incorporated into the oxazole (Scheme 2).[7] Despite the necessity of relatively harsh dehydrating agents, this reaction continues to be one of the most widely used methods for the construction of trisubstituted oxazoles.[8]

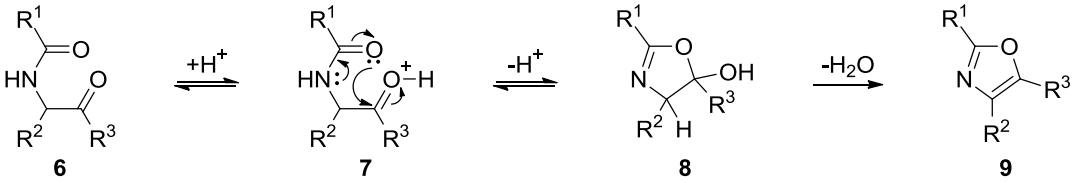

Scheme 2: The Robinson-Gabriel oxazole synthesis.[5,7]

One particularly important extension of the Robinson-Gabriel method was introduced by Wipf and Miller, where alcohols **10** are oxidised to their respective ketones **6** using Dess-Martin periodinane, and the reaction mixture filtered through alumina into a solution of PPh_3, I_2 and NEt_3 to carry out the cyclodehydration.[9] This process is generally milder, more efficient and faster than the cyclisation of **10** to oxazolines such as **3**, followed by oxidation to oxazoles, and allows the efficient construction of oxazoles within peptides.[10]

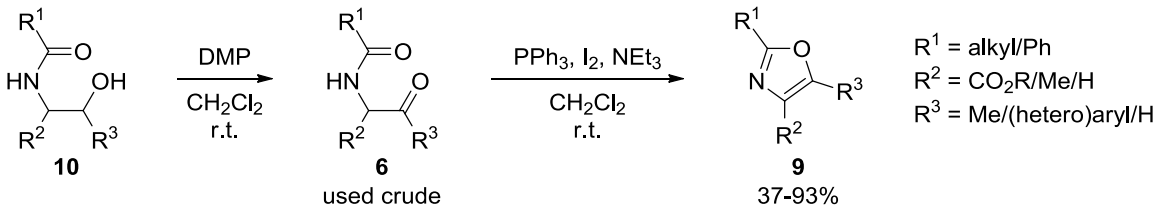

Scheme 3: Oxidation of an alcohol followed by Robinson-Gabriel oxazole synthesis.[9-10]

α-Acylaminoketones **6** may also be accessed by the rhodium(II)-catalysed reaction of amides **11** with α-diazo ketones **12** developed by the Moody group.[11] This allows a relatively convergent construction of oxazoles, which is again carried out by cyclodehydration of **6** using PPh_3, I_2 and NEt_3, and has been exploited in the total synthesis of several natural products.[12]

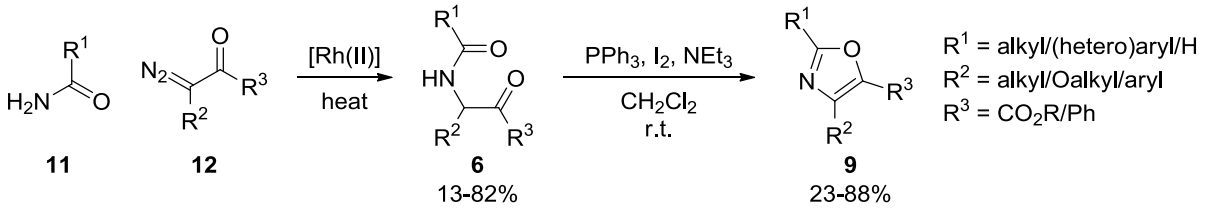

Scheme 4: Two-step oxazole synthesis by the rhodium-catalysed reaction of α-diazo ketones and amides followed by a Robinson-Gabriel cyclisation.[11]

A different intramolecular approach is the oxidative cyclisation of enamides **13** with $PhI(OAc)_2$ (Scheme 5).[13] The proposed mechanistic cycle is initiated by attack of the enamide onto the iodine species to give intermediate **14**, this may cyclise through formation of six-membered intermediate **16**, followed by reductive elimination of iodobenzene to give the oxazole. Where an electron-withdrawing substituent is α- to the amide, an alternative five-membered intermediate **17** is also reasonable. This represents a convenient method for the synthesis of tri- and disubstituted oxazoles, including the anti-inflammatory drug Oxaprozin, from a relatively simple starting material.

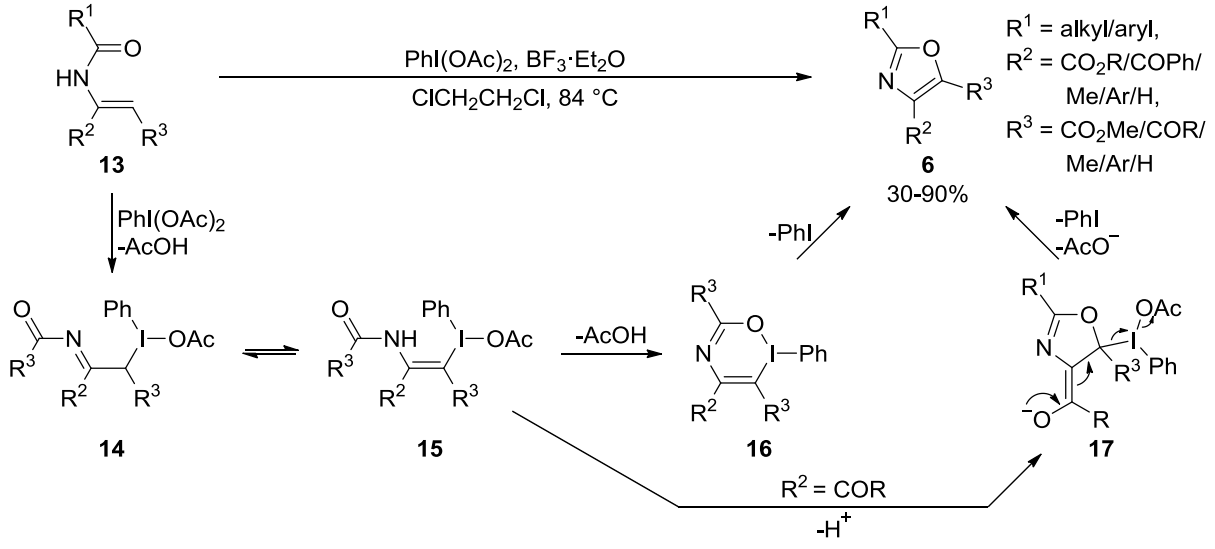

Scheme 5: Oxidative cyclisation of enamides by $PhI(OAc)_2$.[13]

1.1.2: Two-Component Reactions

1.1.2.1: By formation of the O–C2 and N–C4 bonds

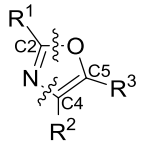

Figure 3: The O–C2 and N–C4 disconnections as a strategy for oxazole synthesis.

One of the most common intramolecular approaches to trisubstituted oxazoles is the metal-catalysed reaction of α-diazo ketones **12** with nitriles **18** (Scheme 6). This reaction was first introduced by Helquist using $Rh_2(OAc)_4$ as the catalyst.[14] The substrate scope has since been widely explored, predominantly using either rhodium(II) or copper(II) catalysts.[4a] The mechanism involves the formation of a metal carbene **19**, which is then attacked by the nitrile to generate **20**. Cyclisation to **21** may then be followed by loss of the catalyst to give the product oxazole **6**. Again, this method has been applied in a number of natural product syntheses.[12b,12c,15] One issue with this strategy is the epimerisation of stereogenic centres attached to the 2-position of the oxazole, which are prevalent in natural products;[11a,b] this can be avoided by using the methodology described in Schemes 3-4.

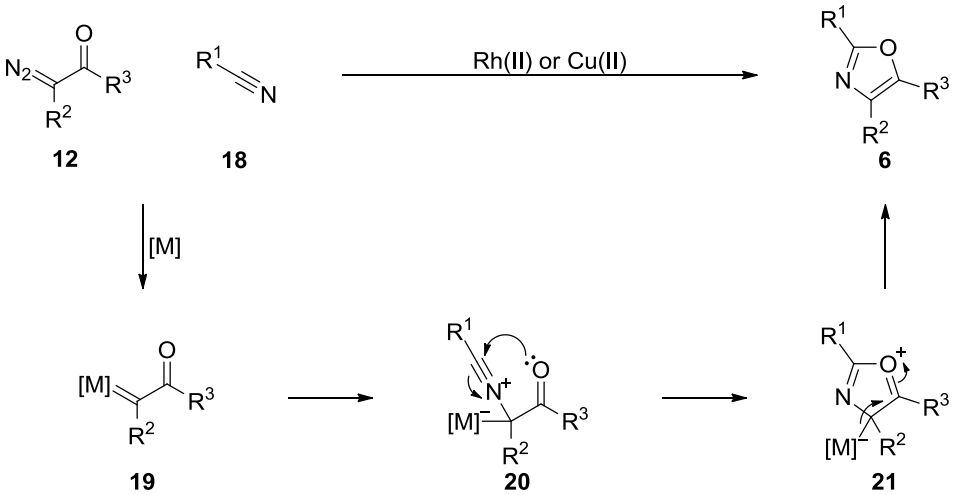

Scheme 6: Metal-catalysed oxazole formation using α-diazo ketones and nitriles.[4a,14]

Alternatively, the reaction of 1,3-dicarbonyls **22** with benzylamines **23** and I_2 produced intermediate **25**, which could undergo a copper-catalysed oxidative cyclisation to oxazoles **28**

(Scheme 7).[16] The reaction is limited to oxazoles bearing a carbonyl substituent at the 4-position and an aryl group at the 2-position. The authors suggested that only benzylamines were successful as these groups more easily underwent oxidation from **25** to **26**.

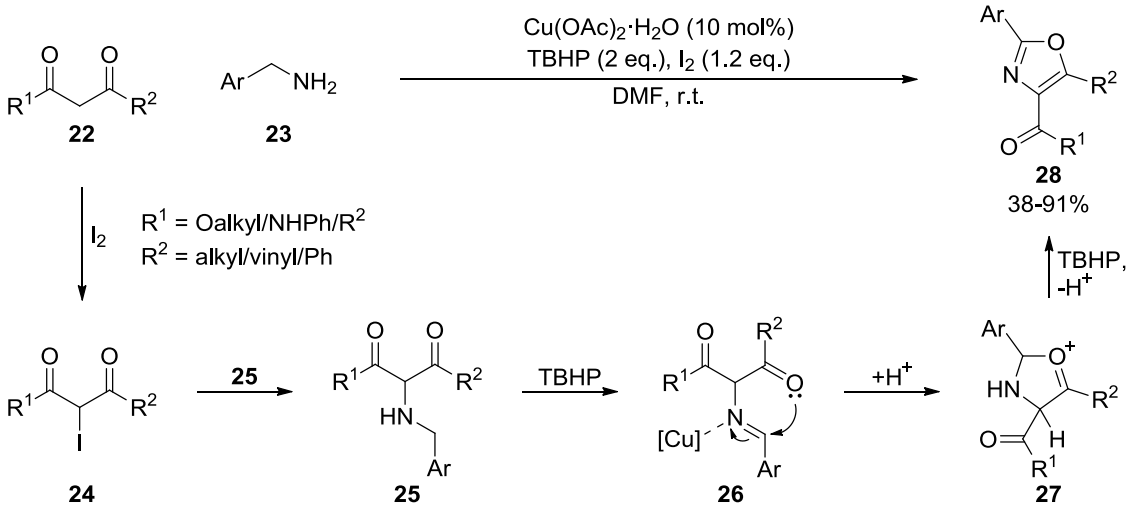

Scheme 7: Oxazole formation from 1,3-dicarbonyls and benzylamines.[16]

1.1.2.2: By formation of the O–C5 and N–C4 bonds

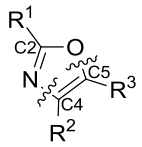

Figure 4: The O–C5 and N–C4 disconnections as a strategy for oxazole synthesis.

Buchwald and co-workers have described a one-pot synthesis of trisubstituted oxazoles from amides **11** and vinyl iodides **29** (Scheme 8).[17] The sequence begins with a copper-catalysed cross-coupling to form enamide **6**, treatment with iodine and base facilitates the formation of oxazoline **31**, which undergoes loss of HI when heated with DBU to give oxazole **9**. Where oxazoline **31** contained an alkyl substituent at the 4-position, HI elimination gave kinetic product **32**; this was isomerised to the desired oxazole **9** by refluxing in toluene with TsOH prior to its purification. The *E*/*Z* geometry of the vinyl iodide **29** proved unimportant, and the reaction could also be carried out from vinyl bromides (in which case the initial cross-coupling was carried out in toluene at 100 °C). It is also

noteworthy that iodination occurred selectively at the electron-rich enamide, allowing the synthesis of oxazoles with alkene- or thiophene-containing substituents.

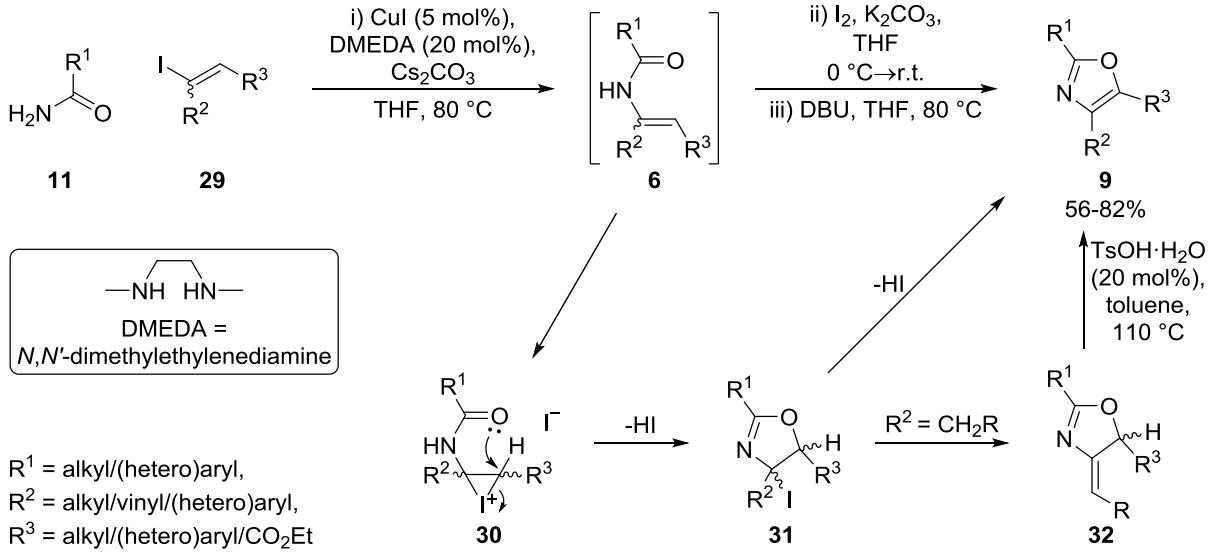

Scheme 8: One-pot copper-catalysed coupling of amides with vinyl iodides followed by oxazole formation.[17]

Moses and co-workers described a silver-mediated reaction of amide **33** and bromopyruvate ester **34**; only one trisubstituted oxazole **35** was synthesised, alongside several 2,4-disubstituted oxazoles (Scheme 9).[18] One equivalent of a silver(I) salt was required for this process, without which no reaction occurred, leading to a proposed mechanism where the silver ion assists in the cleavage of the C–Br bond of **34**, allowing the formation of imminium **36**, which can cyclise to oxazoline **37** and undergo acid-catalysed dehydration to oxazole **35**. The scope of the reaction was limited to products containing sp^2-hybridised carbon atoms at the 2-substituent; however the AgBr produced could easily be collected and recycled.

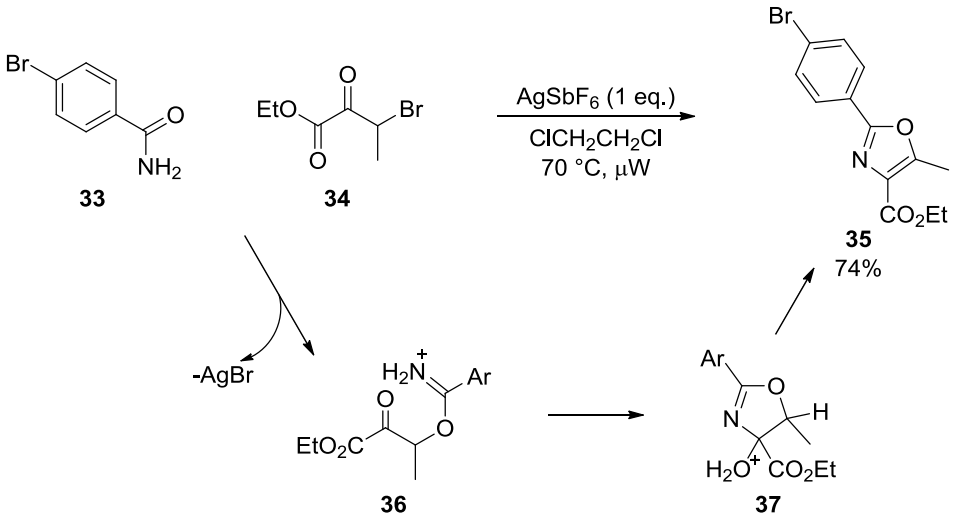

Scheme 9: Silver-mediated oxazole formation from an amide and ethyl 3-bromo-2-oxobutanoate.[18]

1.1.2.3: Alternative disconnections

The Zhu group have reported a novel, two-component approach to 5-aminooxazoles by the Lewis acid-catalysed reaction of aldehydes **38** with isocyanides **39** (Scheme 10).[19] Yields were generally good for oxazoles with a morpholine substituent at the 5-position, however other tertiary amines tested resulted in lower yields due to instability of the products.

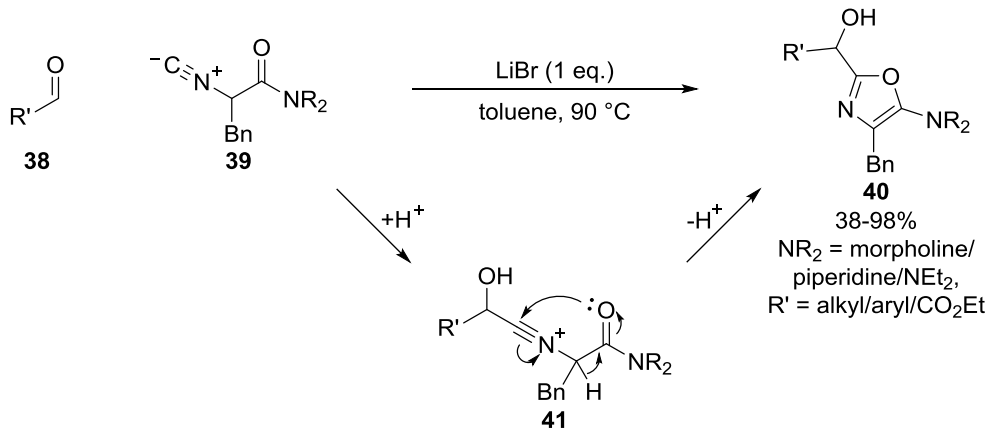

Scheme 10: Synthesis of 5-aminooxazoles from isocyanides and aldehydes.[19]

Intramolecular cyclisations of propargyl amides to oxazoles have been widely explored under gold[20] and palladium[21] catalysis, however these are generally limited to the construction of 2,5-disubstituted oxazoles. A notable exception is the synthesis of oxazoles from α-chloroglycine esters **42** and dimethylaluminium acetylides **43** (Scheme 11 – top).[22] The intermediate propargyl

amides **44** were isolable, but underwent rapid cycloisomerisation to oxazoles **45** during basic work-up. This methodology was used to construct trisubstituted oxazoles in the total syntheses of (–)-muscoride A[22] and siphonazoles A and B.[23]

Alternatively the reaction of primary amides **11** with propargyl alcohols **46** also generated propargyl amides **47** *in situ*, with TsOH catalysing both this transformation and the subsequent cyclisation of **47** into oxazoles **48** (Scheme 11 – bottom).[24] This is an efficient method for the construction of all-carbon-substituted oxazoles from relatively simple starting materials. As with all cyclisations of propargyl amides, one limitation is that the products must have a methylene substituent at the 5-position of the oxazole.

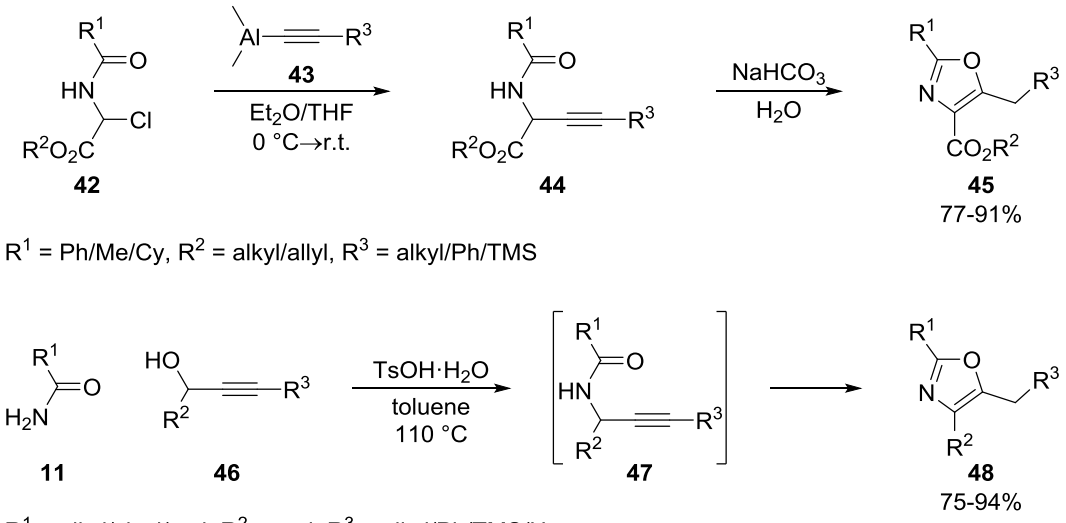

Scheme 11: Cyclisation of propargyl amides.[22,24]

1.1.3: Three-Component Reactions.

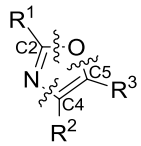

Figure 5: The N–C4, O–C2 and O–C5 disconnections as a strategy for oxazole synthesis.

Saito and co-workers recently reported a three-component synthesis of oxazoles from alkynes, nitriles and PhIO (Scheme 12).[25] The use of internal alkynes presents a regioselectivity challenge, however single isomers were formed in all cases examined using this methodology. The selectivity is

governed by the initial formation of a C–I bond at the less sterically hindered end of the alkyne to give intermediate **51**. Addition of the nitrile to form **53** is followed by the formation of the 6-membered intermediate **16** and reductive elimination of iodobenzene to give the oxazole. The evidence provided for this mechanism includes the isolation of an intermediate of type **52**, and its subsequent conversion to an oxazole when heated in H_2O/MeCN. Although the regioselectivity for this reaction is impressive, the yields were variable, and a limited substrate scope was demonstrated at both the 2- and 4-positions.

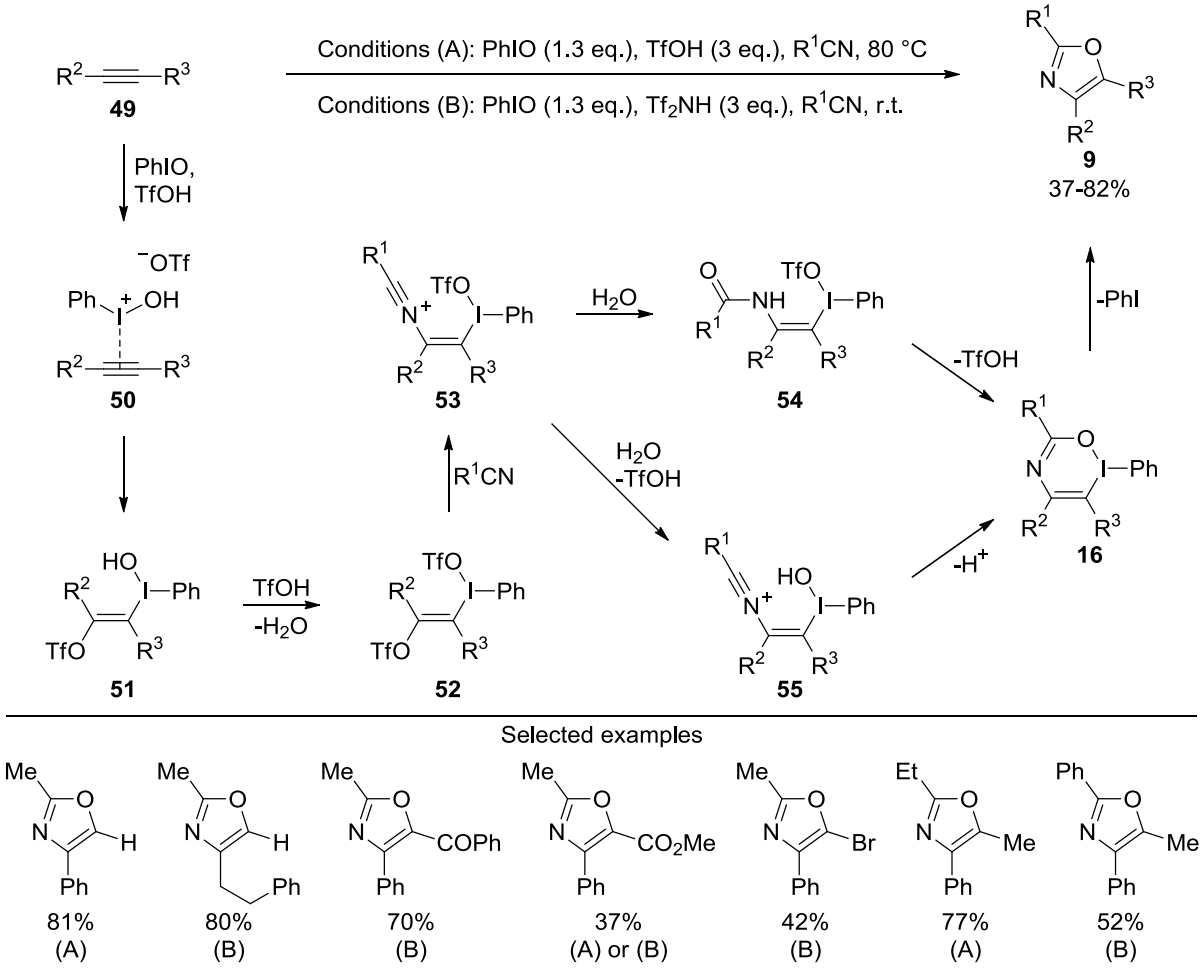

Scheme 12: Three-component oxazole synthesis from alkynes, nitriles and PhIO.[25]

An alternative oxidative cyclisation of alkynes and nitriles has been demonstrated by Jiang and co-workers (Scheme 13).[26] Isotopic labelling studies confirmed the oxygen atom in the oxazole ring came from water, allowing a similar mechanism as above to be suggested. Again the use of

unsymmetrical alkynes resulted in the formation of single regioisomers, dictated by addition of the nitrile β- to the more electron-withdrawing group on the alkyne to give intermediate **56**. Addition of water to **56** allows the formation of 6-membered intermediate **59**. Finally, reductive elimination of the catalyst from **59** gives the product **9**, whilst the copper is oxidised back to Cu(II) by molecular oxygen. Compared to Saito's methodology (Scheme 12), a slightly wider substrate scope was demonstrated at the 2-position as only three equivalents of the nitrile were required. Attempts to synthesise disubstituted oxazoles from terminal alkynes gave only trace amounts of product.

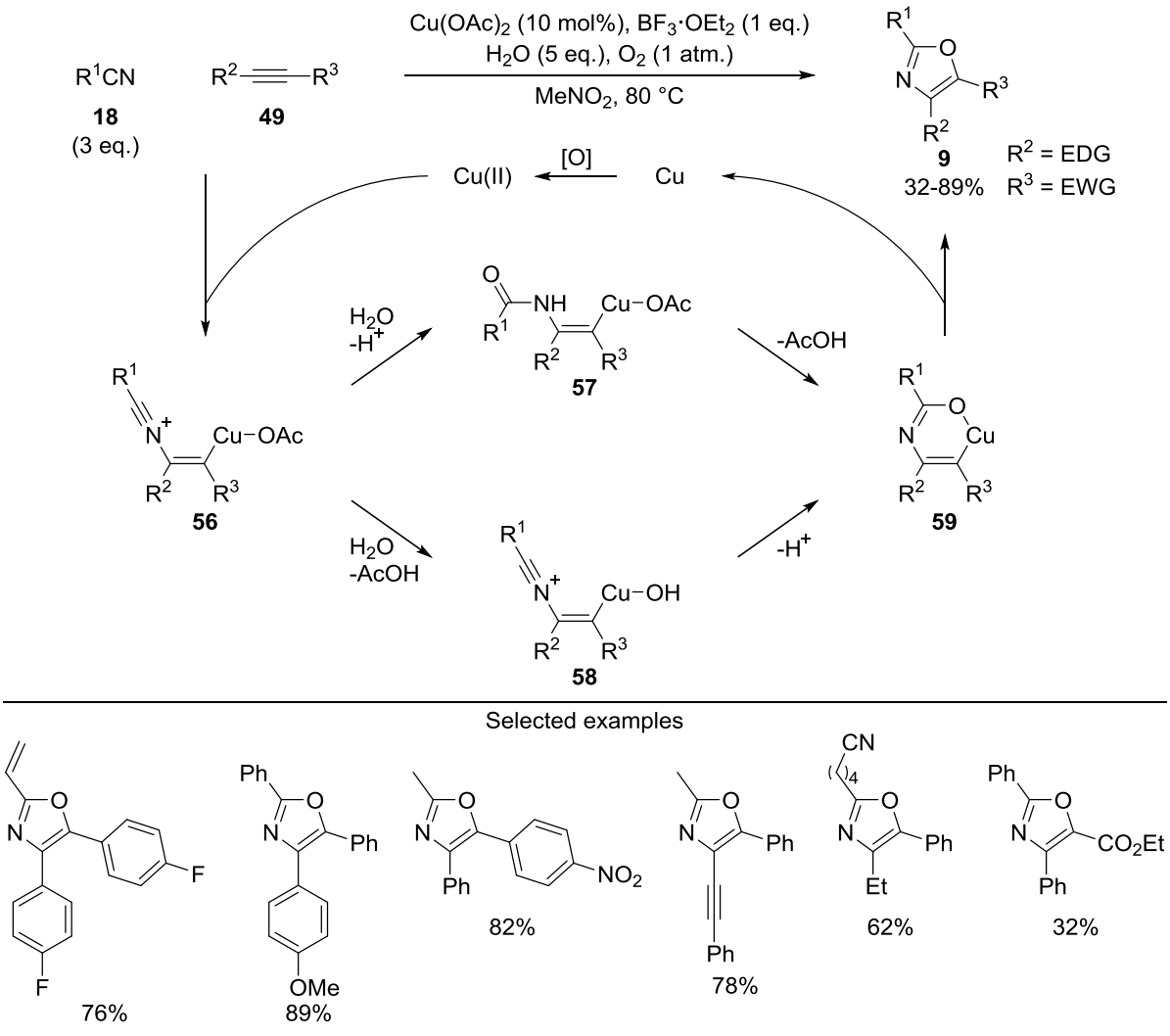

Scheme 13: Oxidative cyclisation of alkynes and nitriles.[26]

1.1.4: Conclusion

Fully substituted oxazoles are most often synthesised by Robinson-Gabriel type cyclodehydration reactions, however these generally require the treatment of a highly substituted precursor with harsh reagents. More recent developments in this field have allowed the convergent construction of these heterocycles using relatively mild conditions. There is still a need to develop new methodologies which increase the variety of substituents which can be directly incorporated onto oxazoles, ideally using robust and easily constructed starting materials.

1.2: Pyridinium Ylides in Gold-Catalysed Oxygen or Nitrene Transfer

One particularly fertile area in the burgeoning field of gold catalysis has stemmed from the ability to access electrophilic α-oxo gold carbenes **62** from alkynes.[27] Initial work in this area largely focussed on the use of tethered sulfoxides[28] or *N*-oxides (oximes/nitrones,[29] amine *N*-oxides,[30] and nitro groups[31]) as intramolecular oxidants, however pyridine-*N*-oxides and their derivatives have emerged as the most common intermolecular oxidants of choice. Activation of an alkyne by gold renders it electrophilic,[32] allowing attack of the oxidant to generate intermediate **61** (Scheme 14), loss of the pyridine delivery group then gives the gold carbene **62**, which can be trapped either inter- or intramolecularly (see below for examples). These versatile intermediates are otherwise accessible only from α-diazo ketones **63**, which are often toxic and significantly less stable and easily installed than alkynes.

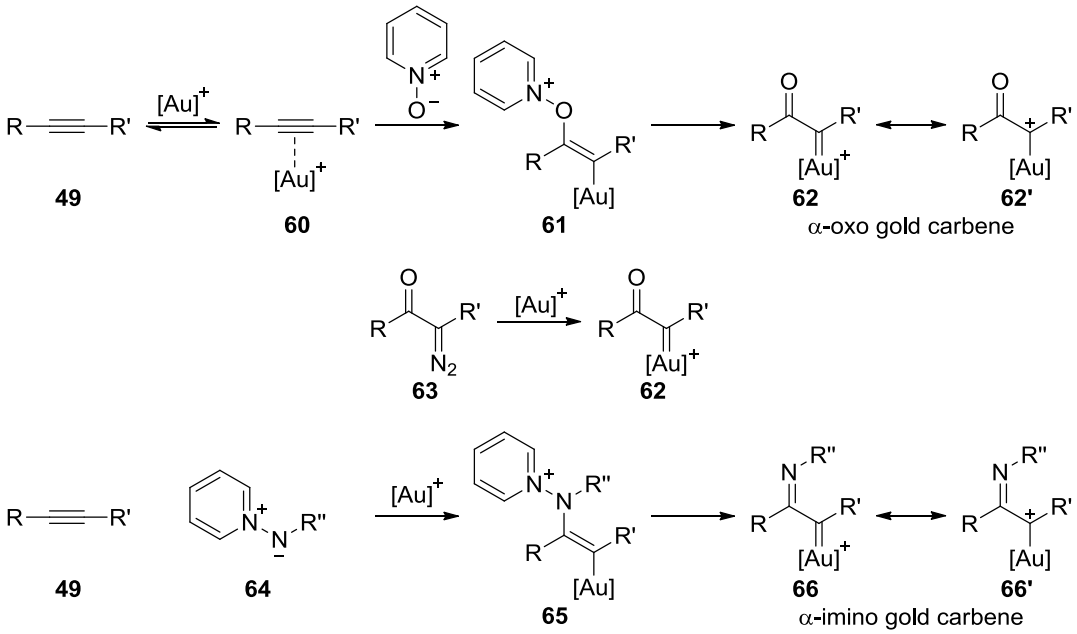

Scheme 14: Access to α-oxo gold carbenes by treatment of alkynes with pyridine-*N*-oxide under gold catalysis, or from α-diazo ketones, and adaptation of the strategy to the synthesis of α-imino gold carbenes.

This strategy has since been adapted to the synthesis of α-imino gold carbenes **66** from pyridine-*N*-aminides **64**, which are pertinent to this work (see below). It is worth noting that, whilst this route

has been significantly less widely explored, other methods for generating intermediates related to **66** under gold catalysis (primarily employing azides in place of **64**) have also been demonstrated.[33]

1.2.1: The Nature of Gold Carbenes

The precise nature of gold carbenes and where they should be invoked in reaction mechanisms is the subject of continuing debate.[34] As shown in Scheme 14, such intermediates can be drawn as one of two resonance extremes, the metal carbene form **62** and the carbocationic form **62'**. Several gold carbenes have been isolated and characterised by X-ray diffraction (Figure 6).[34b] Whilst many of the earlier examples seemed to very much resemble carbocations (due to the low rotational barrier in the C–Au bond[35] and bond lengths similar to that of C_{sp2}–Au σ bonds[36]), these examples featured an electron-donating group conjugated to the electron-deficient carbon atom (for example the OMe group in **67**/**67'**). These groups stabilise the carbocationic contribution, and reduce the possibility of Au→C backbonding, decreasing the π-character of the C–Au bond. Recently Straub and co-workers characterised a dimesityl gold carbene complex **68**/**68'**, stabilised by a very bulky N-heterocyclic carbene ligand, which features an appreciably shorter C–Au bond.[37]

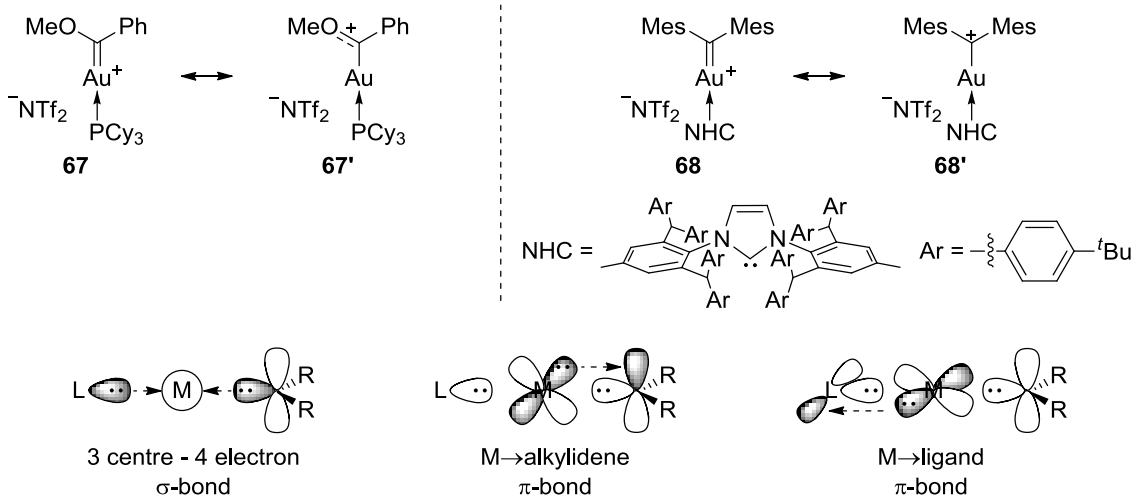

Figure 6: ***Top Left:*** **A gold carbene isolated by Fürstner and co-workers, C–Au = 2.046 Å.[35]** ***Top Right:*** **Straub and co-workers' complex, C–Au = 2.014 Å.[37]** ***Bottom:*** **Key interactions in the bonding model for $(LAu(I)CR_2)^+$ complexes proposed by Toste and co-workers (where L is a neutral, two-electron donor ligand).[38]**

Similar observations were predicted computationally, where experiments showed that the C–Au bond has both σ and π character, the contribution from each of which can be influenced by the nature of both the substrate and the ligand, however in most cases the bond order remains close to one.[38] The term "gold carbenoid" is often used to describe this structure which is intermediate between a carbene and a carbocation, however this term is used inconsistently in the literature, with some suggesting that it should be reserved for distinctly different organogold species, which have no carbene character, but may show similar reactivity (such as **61** or **65**).[34b]

The picture for α-oxo/imino gold carbenes is even more complex, no such compounds have been isolated and recent gas-phase experiments failed to observe them by mass spectrometry.[39] Alternative pathways have been proposed for several reactions that originally appeared to proceed through α-oxo carbenes,[40] for example DFT calculations predicted that the cyclisation of **69** proceeds directly from carbenoid **70** to give **71** (Scheme 15 – top).[40b] Evidence in favour of the intermediacy of α-oxo gold carbenes includes reactions that have very similar outcomes whether these supposed intermediates are generated by the oxidation of alkynes or from α-diazo ketones, for example the synthesis of **75** from either **73** or **76** (Scheme 15 – bottom).[41]

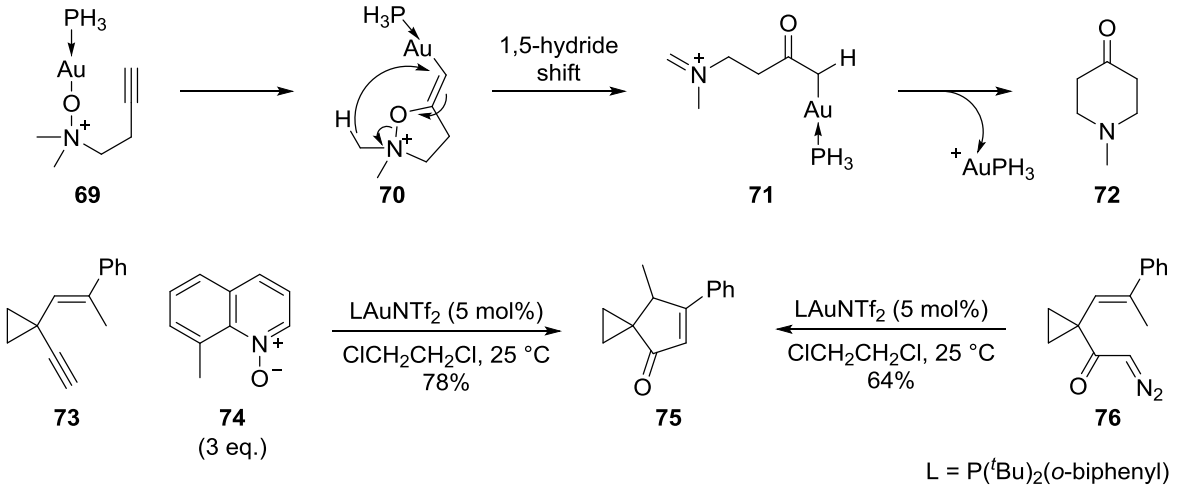

Scheme 15: ***Top:*** **Calculated lowest energy route for an example reaction.[40b]** ***Bottom:*** **Synthesis of a cyclopentenone from different starting materials.[41b]**

Although many of the reaction mechanisms described in this chapter feature α-oxo or α-imino gold carbenes, it should be kept in mind that these intermediates have considerable carbocationic character, and that in some cases alternative routes can be argued (particularly S_N2' type reactivity of **61** or **65**).

1.2.2: Applications of α-Oxo Gold Carbenes Generated from Pyridine-*N*-Oxides

The use of pyridine-*N*-oxides as intermolecular oxidants in gold catalysis was first demonstrated by Zhang and co-workers in the oxidative cyclisations of propargyl and homopropargyl alcohols to give oxetanones[42] and dihydrofuranones[43] respectively (Scheme 16). The gold carbene **78** is formed on the terminus of the alkyne, allowing predictable control of the ring size formed.

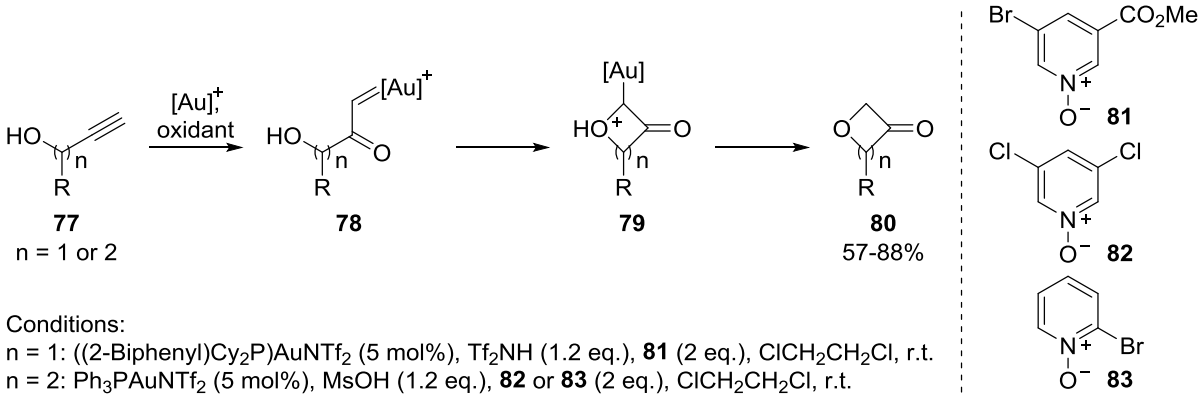

Scheme 16: Oxidative cyclisation of propargyl and homopropargyl alcohols.[42-43]

Whilst terminal alkynes generally provide excellent levels of regioselectivity under gold catalysis, this can also be achieved by using ynamides **84** (or otherwise electronically biased alkynes). In these cases the electronics of the gold-activated intermediate **85**/**85'** dictate that the nucleophile will add α- to the amide if possible (Scheme 17).[44] This allows access to more highly substituted intermediates **86** than those generated from terminal alkynes.

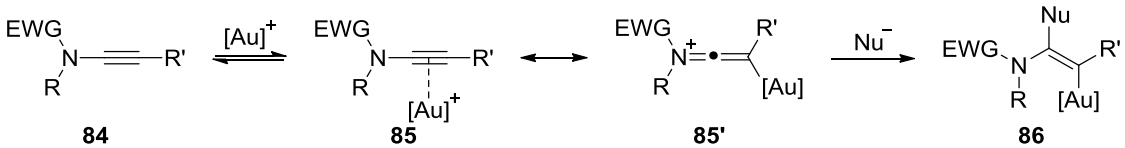

Scheme 17: Regiocontrol in nucleophilic attack onto gold-activated ynamides.

This gold-catalysed oxidation of ynamides with pyridine-*N*-oxides was first introduced by Davies and co-workers,[45] where double oxidation of a phenyl-substituted ynamide **84a** with two equivalents of pyridine-*N*-oxide to give **87** was achieved, but more interestingly a 1,2-C–H insertion with an alkyl-substituted ynamide **84b** gave α,β-unsaturated imide **88**, the initial oxidation proceeding with complete regioseletctivity (Scheme 18). Optimisation of this process allowed access to a family of compounds of type **90** using either the commercial and bench-stable catalyst dichloro(2-pyridinecarboxylato)gold (Au(pic)Cl_2) at 70 °C or $AuBr_3$ at room temperature. This reaction was later reported independently by Zhang and co-workers using sterically biased all-carbon-substituted alkynes in place of ynamides.[46]

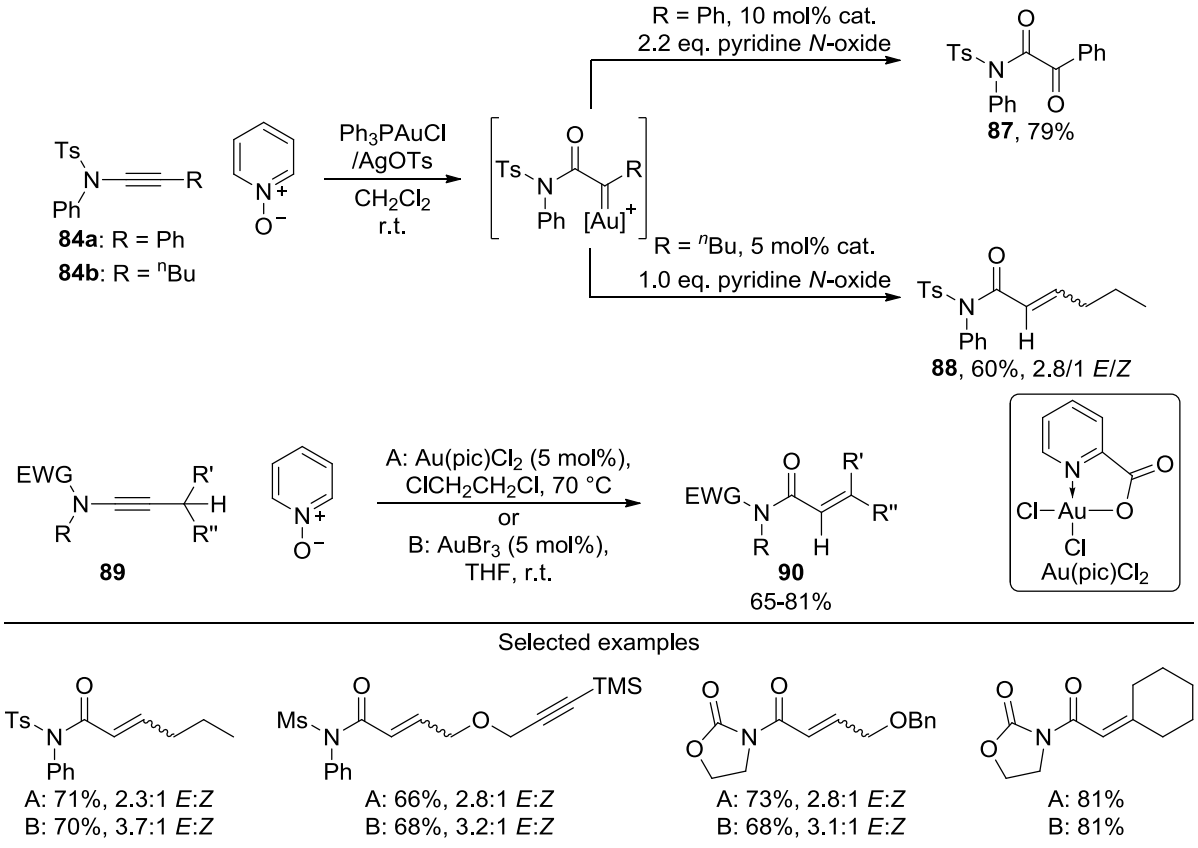

Scheme 18: Gold-catalysed oxidation of ynamides followed by 1,2-C–H insertion.[45]

Since the publication of these seminal works a plethora of other applications of α-oxo gold carbenes generated from the gold-catalysed oxidation of alkynes or ynamides with pyridine-*N*-oxides have been described, just a few of which are shown in Scheme 19.[47]

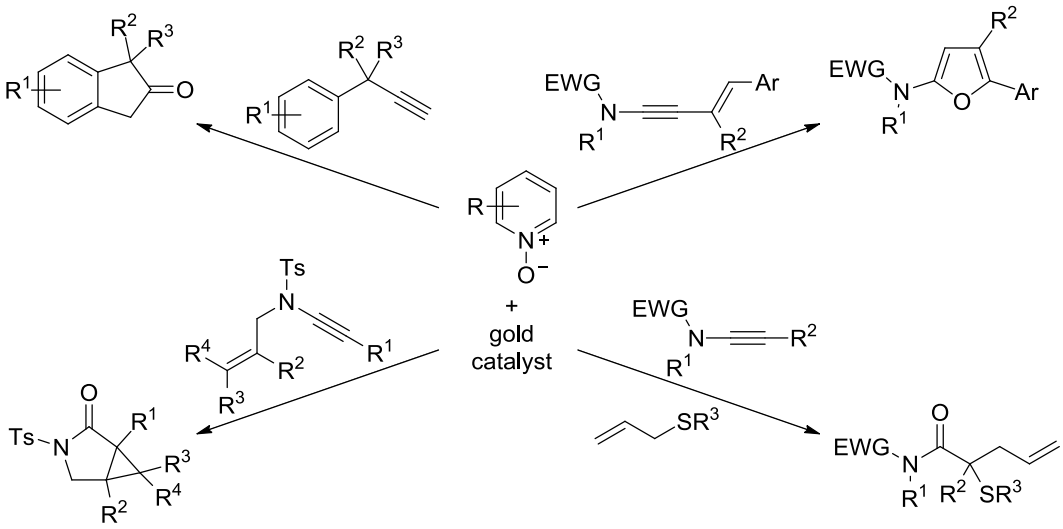

Scheme 19: Diverse reactivity initiated by gold-catalysed oxidation of alkynes or ynamides by pyridine-*N*-oxides. Clockwise from top-left: Friedel-Crafts substitution,[47a] furan synthesis,[47b] Doyle-Kirmse reaction[47c] and cyclopropanation.[47d]

1.2.3: Applications of α-Imino Gold Carbenes Generated from Pyridine-*N*-Aminides

Li and Zhang demonstrated a modification of this approach where the pyridine-*N*-oxide is replaced by an *N*-tosyl pyridine-*N*-aminide **91** (Scheme 20).[48] This effectively allows the transfer of an *N*-tosyl nitrene onto an ynamide. Again, initial attack of the ylide proceeds with complete regioselectivity, to give α-imino gold carbene **92**, which is quenched by a 1,2-C–H insertion from the alkyl group attached to the alkyne, forming amidines **93**.

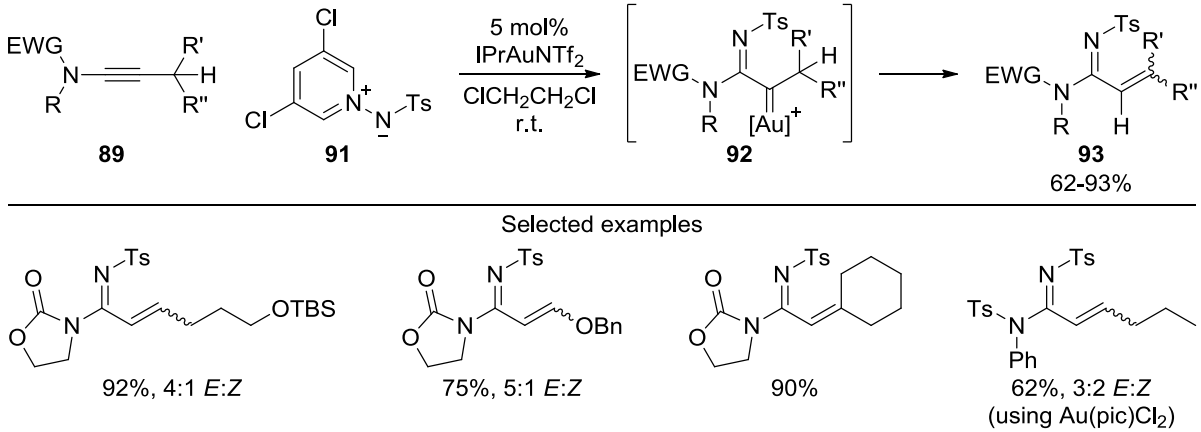

Scheme 20: Gold-catalysed nitrene transfer onto ynamides followed by 1,2-C–H insertion.[48]

The use of these nitrogen-nitrogen ylides allowed the development of a new strategy where the α-imino gold carbene could be quenched by a group appended to the nucleophilic nitrogen. This was introduced by Davies and co-workers in a formal [3+2] cycloaddition of ynamides **84** and *N*-acyl pyridine-*N*-aminides **94** for the synthesis of oxazoles **95**, which is a key reaction for this thesis (Scheme 21).[49] Several mechanistic pathways can be suggested for this process, all start with regioselective attack of the of the ylide **94** onto a gold-activated ynamide to give **96**. This may then follow path (1), and undergo cyclisation with concerted loss of pyridine to furnish intermediate **98**. Alternatively, loss of pyridine could occur prior to cyclisation to give carbene **99**, which could cyclise either through path (2): a 4π electrocyclisation; or path (3): attack of the carbonyl oxygen onto the electrophilic carbon. The oxazole would finally be formed by a deaurative aromatisation of **98**.

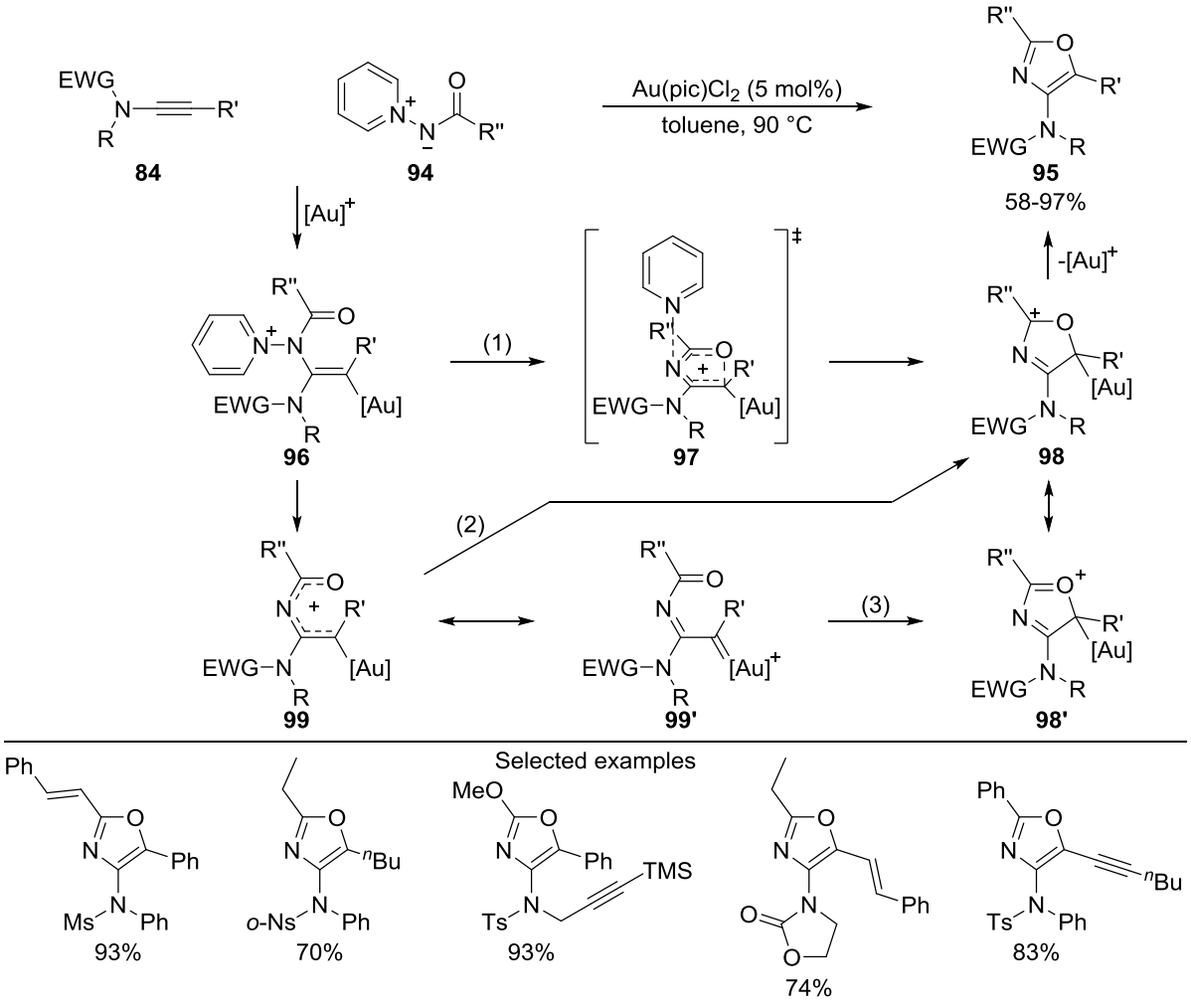

Scheme 21: Synthesis of 4-amido oxazoles.[49]

An alternative mechanism which proceeds through an electrophilic metal nitrene **100** is less likely, as this would be expected to give isomeric oxazoles **103** (Scheme 22).[50] Additionally, given that a 1.5 fold excess of aminide **94** is employed in this reaction, if nitrene **100** were formed, further reaction of **100** with alkene-containing products would be expected,[51] however this is not observed.

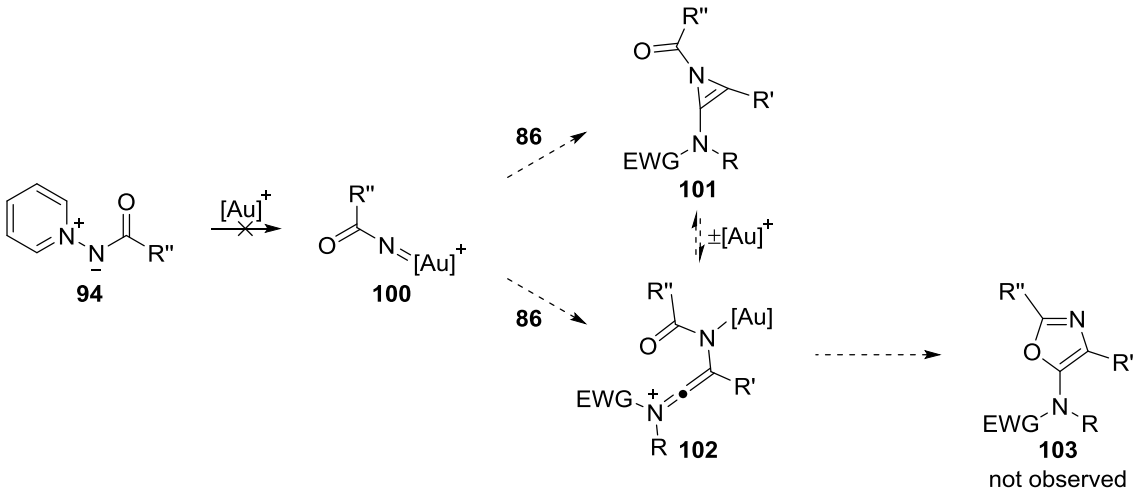

Scheme 22: Proposed alternative reactivity of a gold nitrene.

Additional mechanistic information was also provided by the divergent reactivity of ynol ether **104**, which formed oxazole **105**; and ynol ether **106** which instead gave 1,2-C–H insertion product **107** (Scheme 23). The reactivity in the latter case is related to that described in Scheme 20, and strongly supportive of the formation of an intermediate analogous to **96** (Scheme 21).

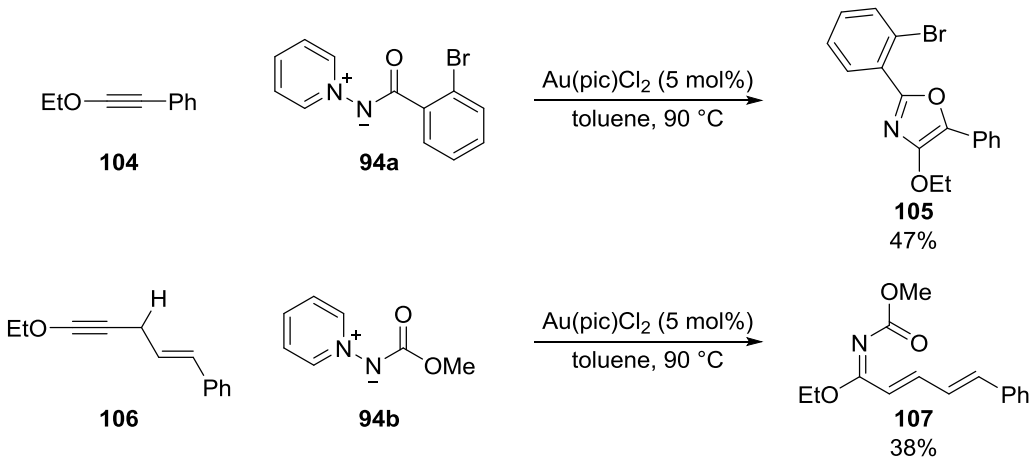

Scheme 23: Reactions of ynol ethers with *N*-acyl pyridine-*N*-aminides.[49]

Although substrate **106** was designed to favour 1,2-C–H insertion over oxazole formation, in principle these reactions can compete whenever an sp^3 hybridised C–H group is adjacent to the alkyne. In the original communication of this work, several 5-alkyl-substituted oxazoles were successfully synthesised without the isolation of competing products, it was not determined whether 1,2-C–H insertion generally competes with oxazole formation in these cases.

Overall this methodology allows the efficient synthesis of trisubstituted oxazoles *via* a [3+2] cycloaddition from simple starting materials, and has also provided access to the first oxazoles bearing a nitrogen atom at the 4-position. In addition, as it is highly convergent, employs fairly robust starting materials and has a good functional group tolerance, the substituents on the amide and on the other two positions of the oxazole can be varied widely.

In the course of the studies detailed in this thesis, co-workers in the research group investigated other ways to exploit this strategy. Chatzopoulou and Davies showed that the oxazole synthesis could also be carried out using other electron-rich alkynes, most of which were of type **108**, which are activated by conjugation to indole rings (Scheme 24).[52] These substrates provided the same level of selectivity as ynamides (only the oxazole with the electron-rich aromatic group in the 4-position is ever observed), however their reaction required higher temperatures, longer reaction times and re-optimisation of the catalyst. 4-Alkynyl anilines were also successful substrates in this reaction; however alkynes bearing anisoles and other only moderately electron-rich aromatic groups were unreactive. The use of alkyl-substituted alkynes generated a complex and inseparable mixture of oxazole and 1,2-C–H insertion products, and so these were not suitable substrates, despite the fact that oxazole formation was still the preferred pathway. This methodology complements the previous work to give all-carbon-substituted oxazoles **109**, however it is important that one substituent of the alkyne still must be strongly electron-donating.

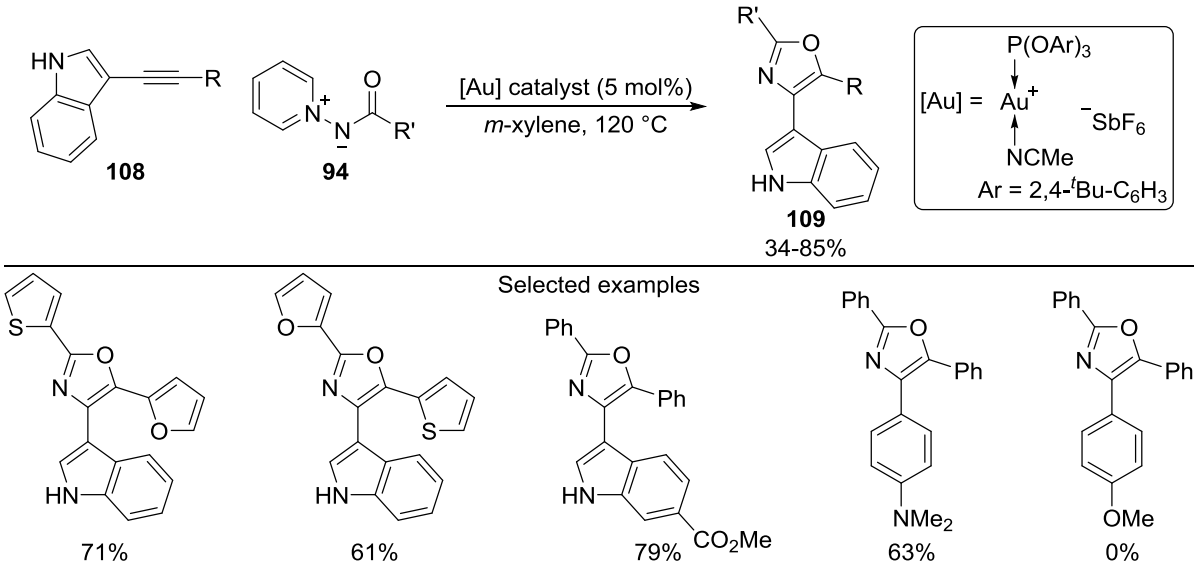

Scheme 24: Synthesis of all-carbon-substituted oxazoles.[52]

Garzón and Davies recently reported the use of a related class of nucleophiles **110**, in which the acyl group is replaced by a pyridine derivative, in the synthesis of imidazole-fused heterocycles **111** (Scheme 25).[53] Ynamides and 3-alkynyl indoles were suitable substrates. Alkyl-substituted ynamides could be used in these reactions, as the competing 1,2-C–H insertion products were separable from the imidazoles; changing from the gold(I) pre-catalyst to Au(pic)Cl_2 reduced the amount of this undesired side-reaction, allowing higher yields of the heterocycles to be achieved.

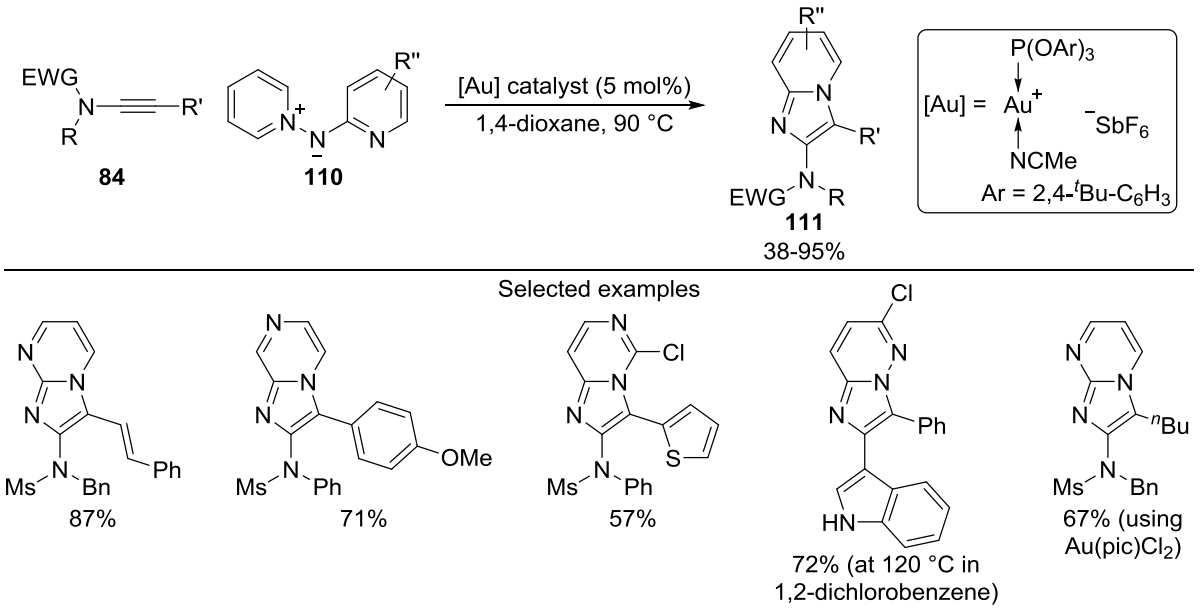

Scheme 25: Synthesis of heterocycle-fused imidazoles.[53]

1.2.4: Conclusion

A new method for the synthesis of oxazoles has been developed in the research group. The following chapter describes how the substrate scope for this reaction has been explored and enhanced. In Chapter 3 describes how the convergency of this process has been exploited to allow the synthesis of oxazoles tethered to dienophiles, followed by subsequent study of their Diels-Alder chemistry, which facilitates the rapid construction of polyheterocyclic systems. Finally, in Chapter 4 novel ligand structures incorporating these oxazoles are described.

CHAPTER 2:

EXPLORING THE SYNTHESIS OF 4-AMIDO OXAZOLES

2.1: Introduction: Starting Materials for Oxazole Synthesis

2.1.1: Applications of and Synthetic Routes to *N*-Acyl Pyridine-*N*-Aminides

Other than their use in the synthesis of oxazoles, *N*-acyl pyridine-*N*-aminides **94** have a wide variety of applications. Early work with these ylides focussed on their photochemical ring expansion to diazapines **112**.[54] A number of reactions which functionalise the pyridinium ring have since been investigated (Scheme 26)**.** Partial reduction of **94** to tetrahydropyridines **113** can be achieved by treatment with $NaBH_4$.[55] This reaction may be preceded by the regioselective *ortho*- addition of Grignard reagents to give more heavily substituted products **114** in a diastereoselective fashion.[56] Alternatively, a highly enantioselective hydrogenation of the pyridinium ring to **115** has also been demonstrated,[57] both **114** and **115** are precursors to functionalised piperidines **116**.[56] The presence of the acyl group in **94** facilitates *ortho* selective C–H activation of the pyridinium ring, to allow metal-catalysed cross-coupling with aryl[58] or alkenyl[59] halides, or *in situ*-generated copper carbenes;[60] the resulting products **117** can be deprotected to give substituted pyridines **118**.[58] Finally, *N*-alkylation of **94** to **119**, followed by intramolecular cyclisation with an enolate, generates 1,2-dihydropyrazolo[1,5-*a*]pyridines **120**.[61]

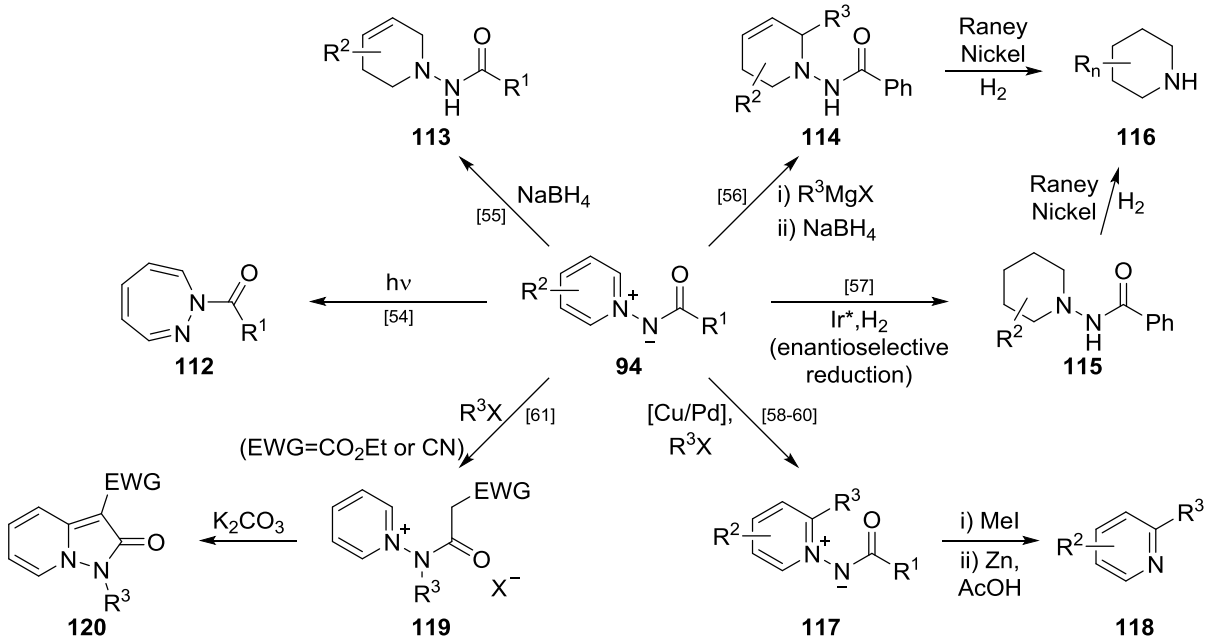

Scheme 26: Reactions of the pyridinium ring of *N*-acyl pyridine-*N*-aminides.

Ylides **94** have also been employed in a number of cycloaddition reactions, where they function primarily as 1,3-C,N-dipoles (Scheme 27). Reaction of **94** with an electron-deficient alkyne gives pyrazolo[1,5-*a*]pyridines **121**.[62] The analogous reaction can also be carried out with *in situ* generated benzynes or silver acetylides, to give products **122**[63] and **123**[64] respectively. More recently, diastereoselective nickel-catalysed addition of isoquinolinium-*N*-aminides across cyclopropanes has been demonstrated,[65] the use of a chiral nickel catalyst allowed kinetic resolution of chiral cyclopropanes to give highly enantioenriched tricyclic structures **124**.[66] The enantioselective reaction of **94** with vinylogous rhodium carbenes to form tetrahydropyridazine derivatives **125** has also recently been reported.[67] A rare example of the use of **94** as a 1,3-N,O-dipole (other than in the synthesis of oxazoles), provides oxazines **126** by the reaction of **94** with diphenylcyclopropenone.[68]

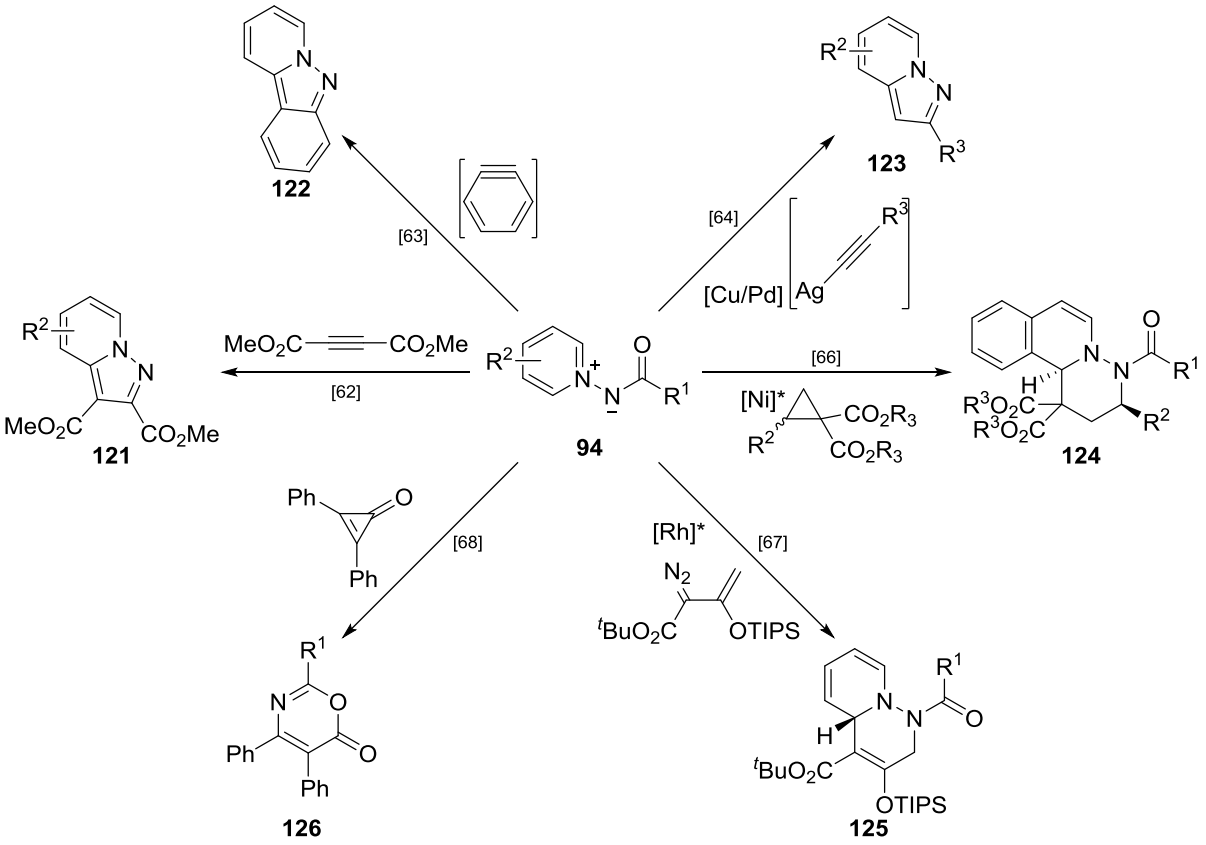

Scheme 27: Cycloaddition reactions of *N*-acyl pyridine-*N*-aminides.

The above examples show how many of the applications of these ylides focus on increasing the complexity of the pyridinium ring, whilst the acyl group is often cleaved or makes up a protecting group in the final product. As such, the synthesis of ylides with functionalised pyridinium rings has been studied, whilst relatively little structural diversity at the acyl substituent has been demonstrated. In the case of the oxazole synthesis described in Scheme 21, the nature of the acyl group dictates the substituent on the 2-position of the oxazole, whilst the pyridinium ring is not incorporated into the product. For this project it was therefore necessary to conveniently access ylides with a diverse range of functionality at the acyl substituent.

The first described synthesis of an ylide of type **94** was by the reaction of an acyl azide **127** with pyridine (Scheme 28 – route A).[69] Alternatively, they have also been accessed by attack of *N*-acyl hydrazines **128** onto 2,4-dinitrophenylpyridinium chloride **129** (route B).[55] Deprotonation of an amino pyridinium salt **130**, followed by acylation with an appropriate reagent **131** (route C) has become the most common strategy to construct **94**.[55,61,70] In most cases the latter route requires the least complex starting materials, as *N*-aminopyridinium iodide is commercially available[71] and, if required, functionalised pyridines can be readily aminated.[72]

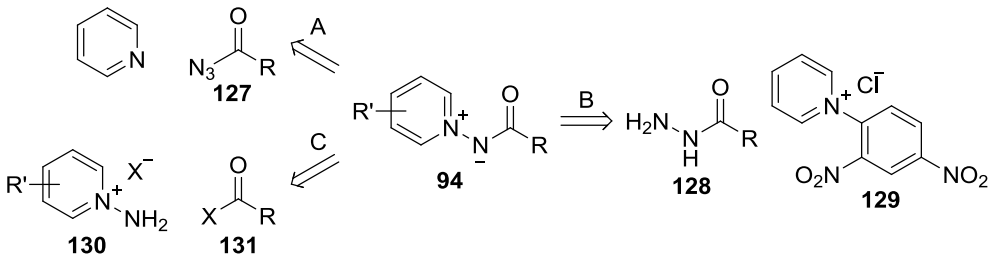

Scheme 28: General methods for the synthesis of *N*-acyl pyridine-*N*-aminides.

2.1.2: The Synthesis of Ynamides

The use of ynamides has grown in prominence in recent years due to the high and predictable reactivity of their electron-rich π-system, and the increasing ease with which they can be accessed.[73] An electron-withdrawing group is generally employed on the nitrogen atom in order to increase the stability of these molecules. The chemistry of more reactive ynamines has been studied, however

these are often subject to rapid hydration or polymerisation reactions.[74] Throughout the course of these studies it was possible to access a wide variety of ynamides for use in oxazole synthesis by using already reported methods for their synthesis (Scheme 29).

The Hsung[75] and Danheiser[76] groups independently reported the first copper-catalysed cross-couplings of amides and haloalkynes. Whilst Danheiser's protocol required fairly harsh conditions, and Hsung's procedure was initially fairly limited in scope, further optimisation by Hsung and co-workers produced one of the most attractive modern methods for the synthesis of ynamides (Scheme 29 – top).[77] This method is particularly convenient as the conditions are relatively mild, the starting materials are easily accessed, and no large excess of either reagent is required. Additionally the substrate scope is fairly wide (increasing the temperature and catalyst loading allows the use of otherwise challenging amides including acyclic carbamates and phophoramidates),[78] however protected anilines often produce poor yields using this method.

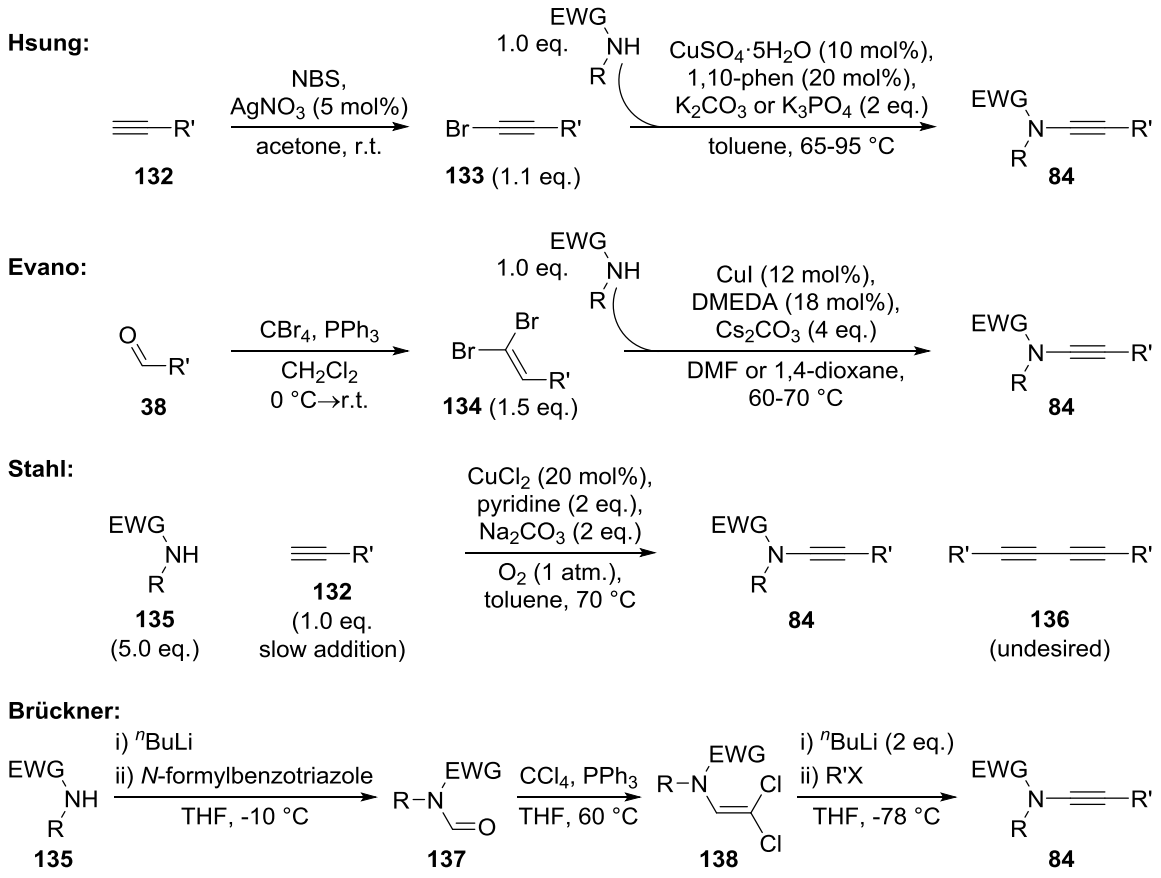

Scheme 29: Modern methods for ynamide synthesis

Although many terminal alkynes are commercially available, more complex systems are often synthesised from aldehydes using either the Corey-Fuchs[79] or Seyferth-Gilbert[80] reactions. In such scenarios the use of the Evano group's methodology is attractive, as it allows the ynamide to be accessed more quickly from an aldehyde *via* a dibromoalkene **134**.[81]

Stahl and co-workers have developed a more direct copper-catalysed oxidative cross-coupling of amides **135** and terminal alkynes **132**.[82] In order to suppress the formation of the Glazer-Hay product **136**, and increase the yield of the desired ynamide **84**, a large excess of the amide is used, and a solution of the alkyne is injected slowly into the reaction mixture over four hours. Although these requirements make the reaction inherently less convenient than the above methods, this is balanced by the direct use of terminal alkynes, and that, unlike other protocols, sulfonyl anilines generally give excellent yields when they are employed as the amide in this process. Additionally the excess amide can be recovered in the same purification process as the ynamide product.

Finally, a less convergent route has been demonstrated by Brückner,[83] where dichloroenamides **138** are converted to lithium acetylides, and trapped with various electrophiles. This allows significant structural diversity to be obtained at the *C*-terminus of the ynamide.[84] Although Scheme 29 covers all of the methods used to access the ynamides employed in this thesis, these are by no means exclusive, and the synthesis of ynamides remains an active area of research.[85]

2.2: Results and Discussion

In the initial communication of the gold-catalysed oxazole synthesis from ynamides a fairly limited substrate scope at the oxazole 2-position was demonstrated, this was in part due to the ease with which a diverse set of *N*-acyl pyridine-*N*-aminides **94** could be accessed.[49] In this chapter the modification of conditions for the synthesis of these ylides has been investigated in order to allow a wider range of functionality to be tested in the oxazole synthesis. Additionally, significant variation of the ynamide at both the *N*- and *C*-terminus has been explored above that which was originally reported, leading to an enhanced understanding of the scope and limitations of this reaction. Finally, the presence of competing 1,2-C–H insertion reactions in the synthesis of 5-alkyl oxazoles has been confirmed, and the levels of these side reactions quantified with different substrates.

2.2.1: Expanding the Scope at the Oxazole 2-Position

2.2.1.1: Modified conditions for the synthesis of polar pyridine-N-aminides

One of the most common modern methods for the synthesis of ylides **94** is the treatment of *N*-aminopyridinium iodide **139** with aqueous sodium hydroxide and an acid chloride.[49,72] These conditions were successfully applied in order to access **94c** in a good yield (Scheme 30 – equation *(1)*). However **94b**, which was originally shown to be among the most reactive ylides in the oxazole synthesis, could not be reproducibly synthesised by this method, a likely problem being **94b**'s high water solubility making extraction from water difficult. A further, more general limitation is that the synthesis of acid chlorides in acid-sensitive molecules is problematic, as can be avoiding their hydrolysis during purification and storage.

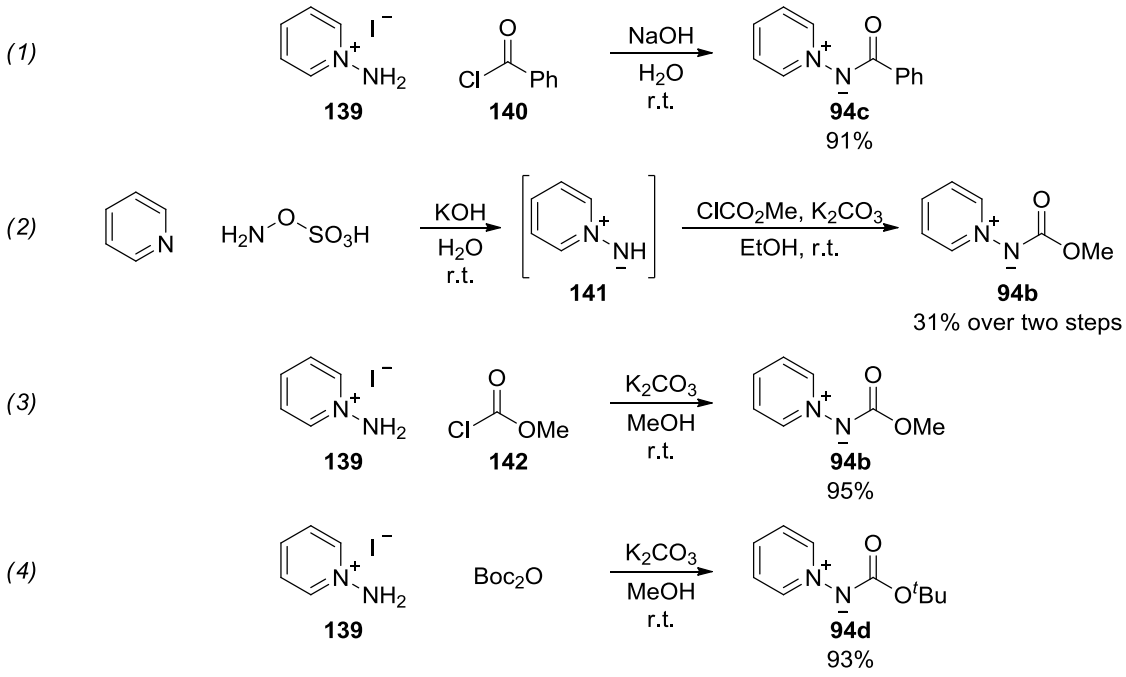

Scheme 30: ***(1):*** **Synthesis of an ylide in aqueous NaOH,** ***(2):*** **Streith's synthesis of 94b,**[86] ***(3)&(4):*** **Modified conditions for the synthesis of polar ylides.**

94b has previously been synthesised by Streith and co-workers using a freshly prepared ethanolic solution of the unstable ylide **141** (Scheme 30 – equation *(2)*).[86] Combining this procedure with the *in situ* generation of **141** resulted in an efficient route to **94b** using *N*-aminopyridinium iodide **139**, methyl chloroformate **142** and K_2CO_3 in methanol. When this reaction was originally attempted in ethanol, the isolated sample of ylide **94b** was contaminated with ~10% of the transesterification product (the CO_2Et-substituted ylide). For this synthesis of **94b**, optimisation of the purification protocol was key, as the product was too water soluble to allow aqueous work-up and too polar for chromatography on silica gel, a simple filtration of the crude residue through alumina in CH_2Cl_2/MeOH proved successful. This route was also applied to the synthesis of *tert*-butoxy-substituted ylide **94d**, where the yield was also excellent.

2.2.1.2: Oxazol-2-one formation

Oxazol-2-ones are found in several pharmaceutically active compounds[87] and are potent synthetic intermediates.[88] It was anticipated that if ylide **94d** could be used to synthesise oxazoles **143**, bearing a *tert*-butoxy group in the 2-position, the products could in turn be used to access oxazol-2-ones **144.** Similar reactivity has been used to produce pyridin-2-ones such as **146** (Scheme 31).[89]

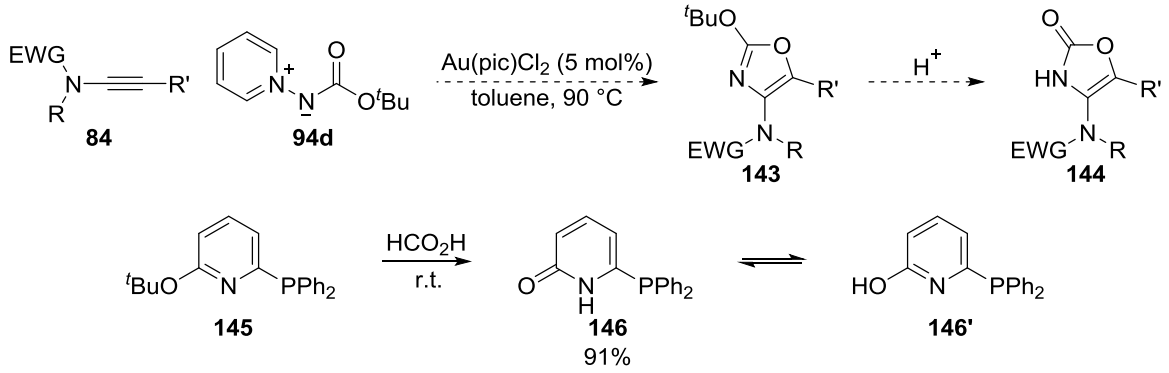

Scheme 31: *Top:* Planned route to oxazolones. *Bottom:* Literature synthesis of a pyridinone.[89d]

In an initial attempt towards this end, ylide **94d** was found to be highly reactive, allowing the rapid synthesis of oxazole **143a** (Scheme 32). Although **143a** was fairly unstable it allowed conditions to be tested for oxazolone formation. Treatment of **143a** with either TsOH in toluene or simply heating in methanol led to consumption of the oxazole, however the resulting crude residue was insoluble in most common solvents and so could not be readily purified.

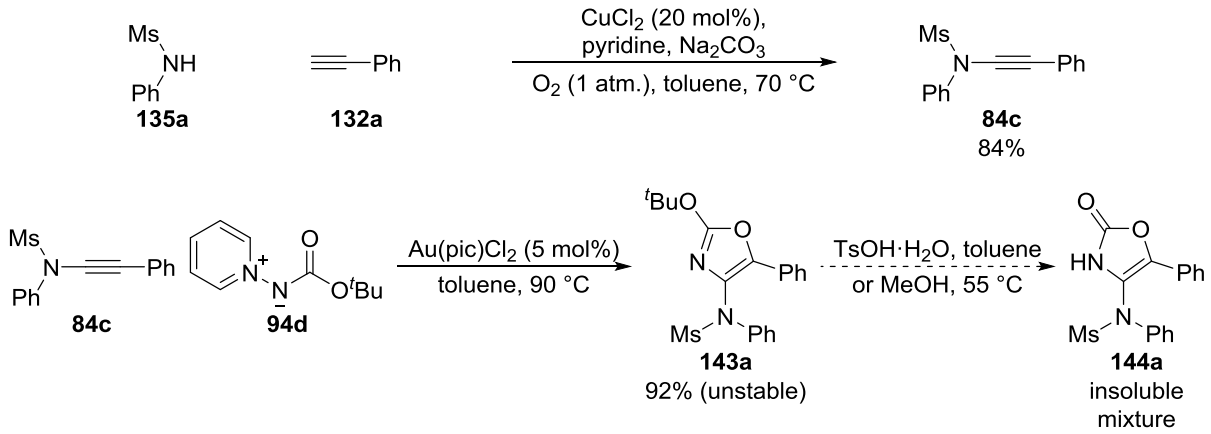

Scheme 32: Initial attempts at oxazolone formation.

As a result a second ynamide **84d** was investigated, and attempts were made to optimise a one-pot process in which unstable oxazole **143b** was formed and then converted into oxazolone **144b** (Table 1). Significant levels of oxazole **143b** remained when warming was continued in a 2:1 methanol:toluene mixture (Table 1, entry 2), or when one equivalent of trifluoroacetic acid or 20 mol% of TsOH were added to the reaction mixture (Entries 3-4). Near complete consumption of **143b** was observed when one equivalent of TsOH was employed (Entry 5). The cleanest conversion to **144b** was observed when the catalyst and excess ylide were removed by filtration through silica gel, and the crude oxazole heated in neat methanol (Entry 6).

Unfortunately when this reaction was scaled up from 0.1 to 1.0 mmol, **144b** could not be adequately purified. The synthesis of several other substrates was attempted following the same route using various ynamides **84e-g** (Figure 7), however all met similar problems, if anything producing more complex mixtures, perhaps due to instability of the products. As such, no further attempts at oxazolone synthesis were made.

Table 1: Optimisation of oxazolone formation

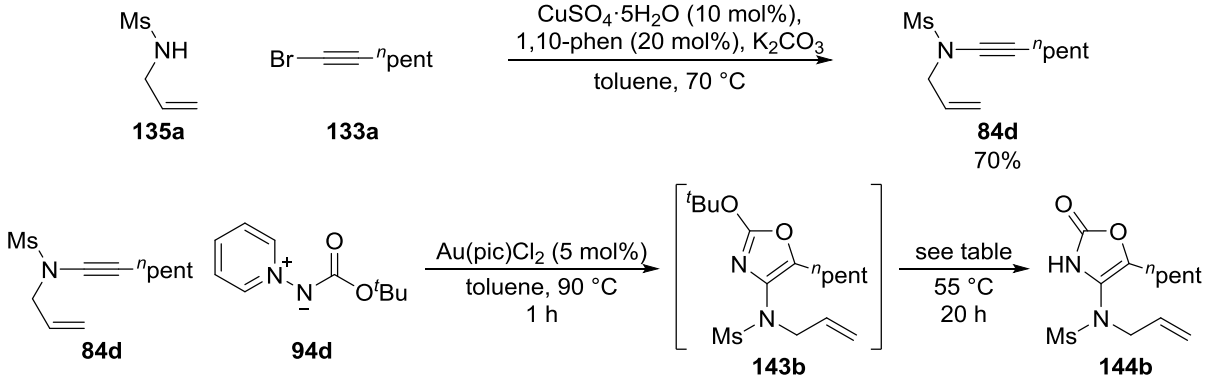

Entry	Additive after 1 hour	**143b**	**144b**
1	reaction stopped	67%	<5%
2	MeOH (2 mL)	42%	24%
3	TFA (1 eq.)	68%	<5%
4	$TsOH \cdot H_2O$ (20 mol%)	74%	<5%
5	$TsOH \cdot H_2O$ (1 eq.)	<5%	36%
6	Filter through silica, evaporate toluene and then add MeOH (2 mL)	<5%	65% (<53%)

Using **84d** (0.1 mmol), **94d** (0.15 mmol) and Au(pic)Cl_2 (5 mol%) in toluene (1 mL) at 90 °C for 1 hour before cooling to 55 °C and adding the stated additive. NMR yields calculated against 1,2,4,5-tetramethylbenzene as an internal standard (isolated yield of a product with ~90% purity from a reaction starting with 1 mmol **84d**).

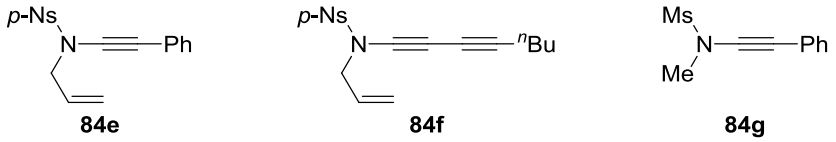

Figure 7: Other ynamides from which oxazolone synthesis was attempted.

2.2.1.3: Synthesis of functionalised pyridine-N-aminides from esters and of their respective oxazoles

Returning to the synthesis of oxazoles with structural diversity at the 2-position, the use of alternative electrophiles for the synthesis of the required ylides was investigated. Esters were identified as ideal substrates as their relative stability allows them to be easily synthesised or modified and to be stored for long periods. Ethyl esters have previously been reported to be active electrophiles in the synthesis of these ylides using very similar conditions to the ones developed here, however yields were generally moderate (possibly due to the low solubility of K_2CO_3 and *N*-aminopyridinium iodide in $CHCl_3$ which was used as the solvent) and this method has not gained widespread popularity.[61,70] Pleasingly the use of methyl esters in the K_2CO_3/methanol protocol was found to be generally applicable to a range of ylides with diverse functionality (Scheme 33).

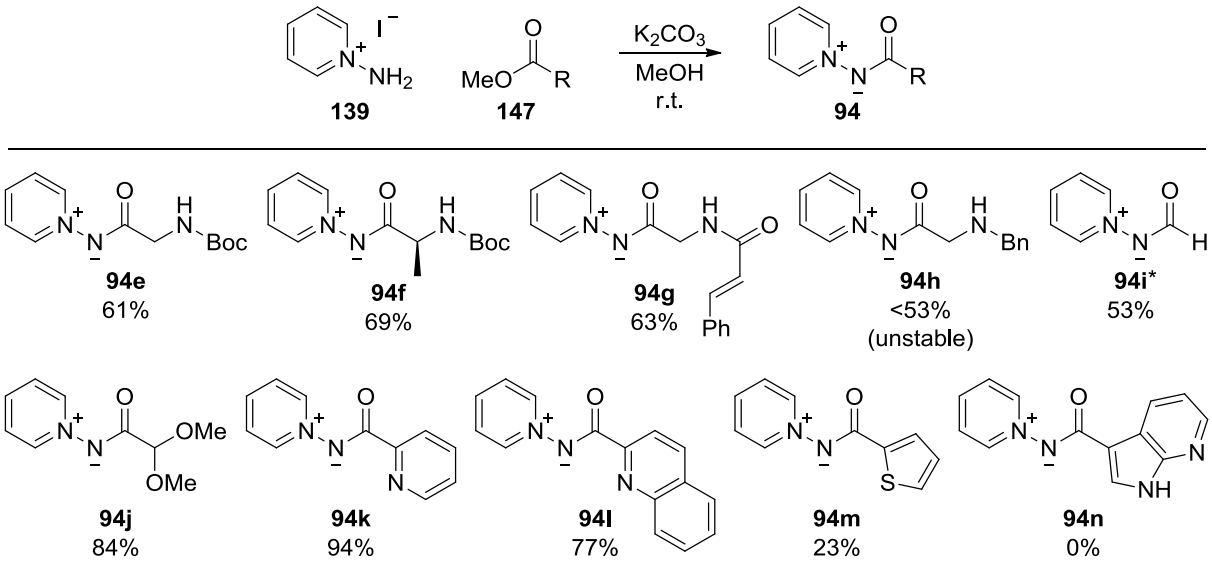

Scheme 33: Synthesis of ylides from methyl esters. *Ethyl formate was used as the electrophile.

Protected amino acid derivatives **94e-g** were accessed in satisfactory yields, which was important as variations on these substrates are used extensively in both of the subsequent chapters.

Unfortunately **94h**, bearing a secondary amine, lacked thermal stability and could not be adequately purified. Ethyl formate proved a cheap and effective formylating agent to generate **94i**, however this product had limited solubility in most common organic solvents, resulting in a reduced yield following purification. The dimethyl acetal-containing product **94j** was synthesised in a very good yield. The high reactivity of esters conjugated to electron-deficient aromatic systems gave pyridine- and quinoline-containing substrates **94k-l** in good yields. Electron-rich aromatic groups proved considerably more challenging, with 2-thiophenyl substrate **94m** formed in a low yield and an ester conjugated to an azaindole giving no product **94n**; in both cases large amounts of unreacted ester **147** was recovered, and so a more reactive electrophile was needed for these substrates.

Fortunately a variation on these conditions in which a mixed anhydride is generated from a carboxylic acid and used in the same pot had been developed by co-worker Raju Jannapureddy, to allow the direct synthesis of ylides from *N*-Boc-protected amino acids.[90] This procedure allowed thiophene-2-carboxylic acid **148** to be converted into ylide **94m** in one step, with a significantly improved yield compared to using the less reactive ester (Scheme 34 – top).

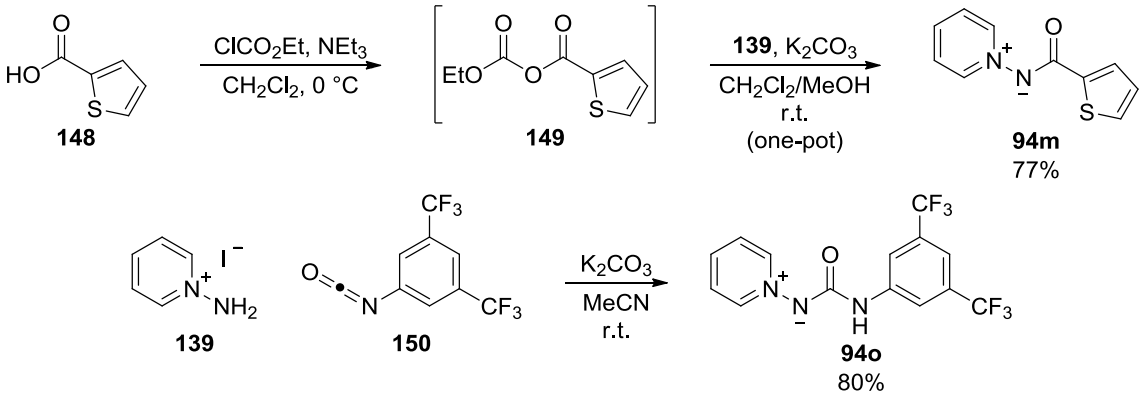

Scheme 34: Use of alternative electrophiles.

Isocyanate **150** also reacted cleanly to give the urea-type ylide **94o** (Scheme 34 – bottom). In this case the reaction was carried under an inert atmosphere in dry acetonitrile to avoid the possibility of the addition of water or methanol to **150** competing with product formation, a strategy that may be generally applicable to other sensitive electrophiles.

As these ylides have several applications (see above), the potential benefits of this improved methodology for their synthesis are significant; here they were applied in the gold-catalysed synthesis of oxazoles from ynamides described in Scheme 21. Alkyl, vinyl, aryl and alkoxy groups had previously been successfully incorporated into the 2-position of the oxazole using this methodology.[49] In order to probe the scope at the oxazole 2-position further, the ylides described above were tested alongside a standard ynamide **84g** in the synthesis of oxazoles **151** (Scheme 35).

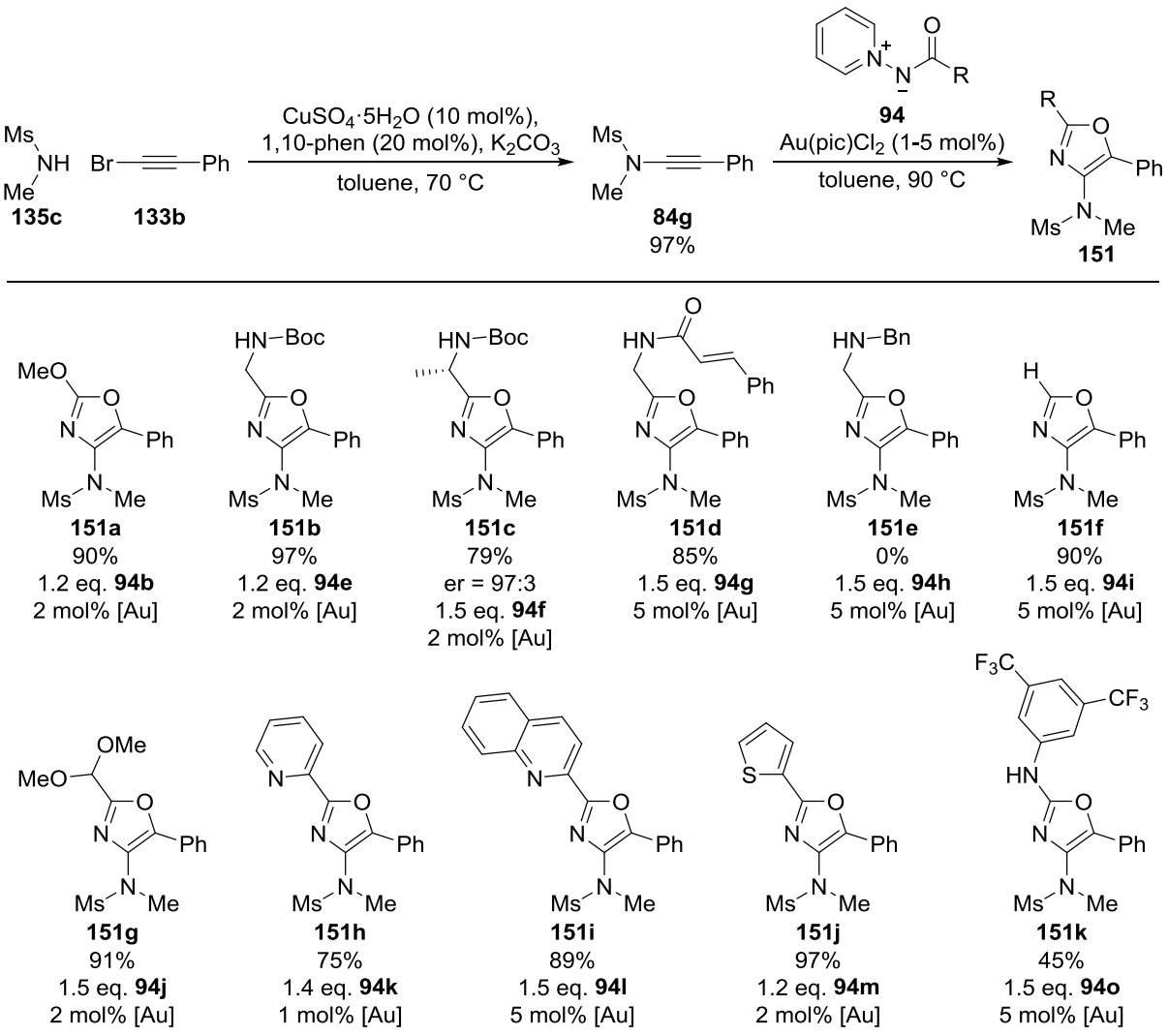

Scheme 35: Expanded scope at the oxazole 2-position.

In the original work, the oxazole synthesis was carried out using 1.5 equivalents of ylide **94** and 5 mol% of the gold catalyst with respect to the ynamide.[49] When using ylide **94b**, which had

previously been shown to be among the most reactive of the ylides trialled, the amounts of reagent were successfully cut to 1.2 equivalents of ylide and 2 mol% of catalyst whilst retaining an impressive yield of **151a** (Scheme 35). The incorporation of secondary amides was successful with **151b-d** all synthesised in good to excellent yields, however no consumption of the ynamide was observed when ylide **94h** was employed. It is unclear whether this is due to **94h**'s lack of stability, or catalyst deactivation by the amine. Despite earlier solubility concerns, ylide **94i** reacted efficiently to give the first 4,5-disubstituted oxazole **151f** synthesised by this method. The sensitive dimethyl acetal could also be incorporated into **151g** in a high yield. Remarkably the catalyst retained its activity to furnish oxazoles **151h-i**, despite the fact that both the starting materials and products resemble good bidentate ligands. Related pyridinyl-oxazolines have been used as ligands for gold(III),[91] and metal complexes of pyridine-*N*-aminides are also known.[92] 2-Thiophenyl ylide **94m** was also highly reactive, giving **151j** in an excellent yield. Finally the use of **94o** resulted in rapid consumption of ynamide **84g**, however a large amount of an insoluble by-product was also produced, resulting in a reduced yield of **151k**.

Overall these results represent a substantial increase in the scope of the reaction with regards to substituents at the 2-position, and applications of compounds related to **151b-d** as well as of **151g** are featured in later chapters of this thesis. Importantly they also show that a high level of reactivity can be obtained when a decreased excess of ylide and/or catalyst loading is employed.

In order to determine whether the process could be made even more efficient at larger scale two further reactions were performed on gram (4.8 mmol) scale (Scheme 36). The first showed that 1.21 g of oxazole **151g** could be obtained using only 1.1 equivalent of ylide **94j** and a 2 mol% catalyst loading, albeit in a slightly reduced yield. Secondly a reaction was performed in an open flask using standard grade solvent and only 1 mol% of catalyst and 1.1 equivalent of ylide **94c**. This reaction proceeded cleanly to give a 59% yield of product **151l**, however it did not reach completion within two days (most of the unreacted ynamide was recovered). For comparison, an 87% yield of

oxazole **151l** was achieved by Raju Jannapureddy using 1.1 equivalents of **94c** and 5 mol% of Au(pic)Cl_2 in dry toluene, under an argon atmosphere,[90] indicating that there is some benefit from excluding air and/or moisture in this process.

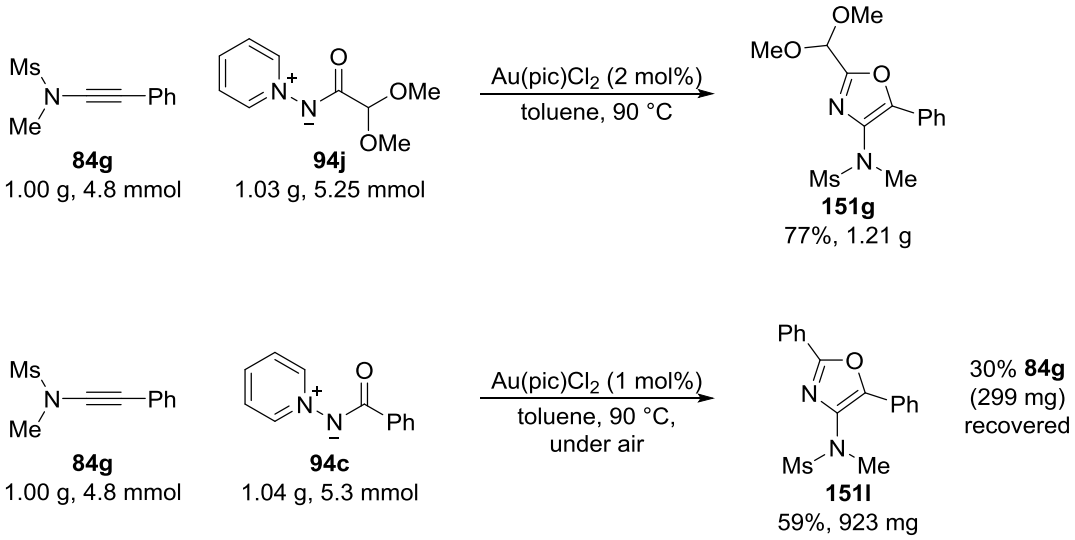

Scheme 36: Large-scale oxazole synthesis.

To assess the general suitability of amino acid-derived substrates the enantiomeric ratio of **151c** was determined to be 97:3 by chiral HPLC against a racemic sample (synthesised from racemic alanine as described in Scheme 37). In contrast the sample of ester **147f** used to synthesise **94f** was shown to be enantiopure using the same method (HPLC traces and conditions for these compounds can be found on pages 208-209). Conditions could not be found to separate the two enantiomers of ylide **94f** by HPLC.

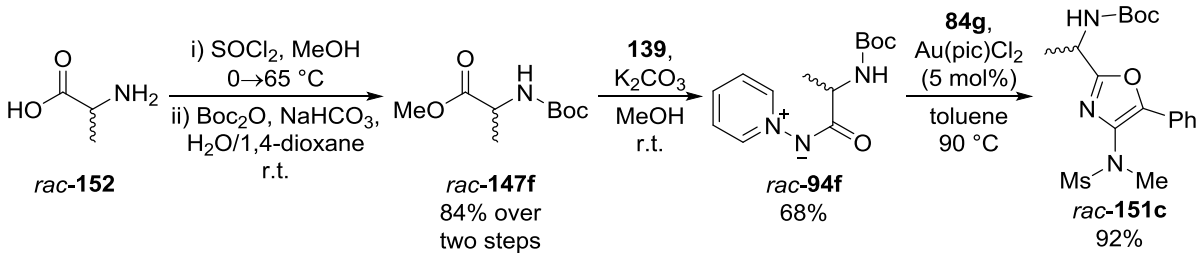

Scheme 37: Racemic synthesis of 151c

Several control experiments were carried out in order to determine the reason for the small loss enantiopurity which occurs between ester **147f** and oxazole **151c**:

Theory 1: A small amount of racemisation of ylide **94f** occurs during its purification.

Experimental result: Stirring **94f** with silica gel for 24 hours in 1:1 CH_2Cl_2:MeOH did not result in a reduction in its observed specific rotation (before $[\alpha]_D^{20}$ = −30.7 °$dm^{-1}g^{-1}cm^3$, after $[\alpha]_D^{20}$ = −32.8 °$dm^{-1}g^{-1}cm^3$).

Theory 2: A small amount of racemisation of ylide **94f** occurs by reaction with the gold catalyst and/or pyridine generated in the reaction mixture, prior to its reaction with ynamide **84g**.

Experimental result: Heating **94f** (0.23 mmol) with pyridine (0.25 mmol) and Au(pic)Cl_2 (5 mol% with respect to ynamide) in toluene (1.5 mL) for one hour at 90 °C, before the addition of ynamide **84g** (0.15 mmol) produced a sample of oxazole **151c** with an er of 98:2

Theory 3: A small amount of racemisation of oxazole **151c** occurs by reaction with the gold catalyst and/or pyridine generated in the reaction mixture.

Experimental result: Heating the original sample of **151c** (0.2 mmol) with pyridine (0.2 mmol) and Au(pic)Cl_2 (2 mol%) in toluene (2 mL) at 90 °C for 24 hours, followed by filtration through silica gel recovered **151c** with an unchanged er of 97:3.

From these results it is apparent that neither **94f** nor **151c** is particularly susceptible to racemisation under the relevant reaction conditions, and the cause of the loss of enantiopurity remains unknown. Possible explanations are that a short lived reactive intermediate in the oxazole formation is prone to racemisation, or that racemisation of **147f** or **94f** occurs very slowly during the synthesis of **94f**.

2.2.1.4: Bidentate ligands incorporating oxazoles

Attempts were made to synthesise palladium(II), copper(II) and gold(III) complexes of **151h-l**; related complexes featuring oxazolines in place of the oxazole have been described and used in catalysis.[91,93] Insoluble solids which could not be properly purified or characterised were isolated in all cases, this did at least indicate that some form of complexation had taken place (Figure 8).

(151h)$PdCl_2$ was soluble in DMSO, in which the ^{1}H-NMR spectrum showed a mixture of free and metalated **151h**, despite prior washing of the crude solid with CH_2Cl_2, indicating that exchange of DMSO and the ligand occurred using this solvent.

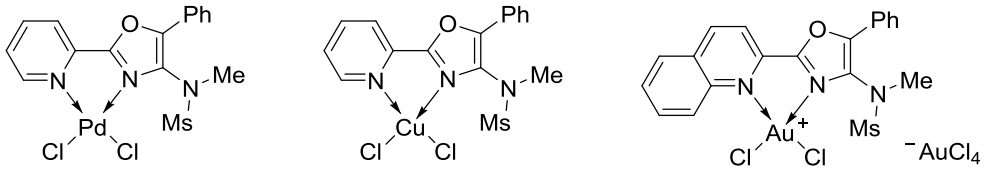

(151h)$PdCl_2$ **(151h)$CuCl_2$** **[(151i)$AuCl_2$]$AuCl_4$**

Figure 8: Targeted metal complexes of bidentate ligands.

2.2.2: Expanding the Scope at the Oxazole 4-Position

In the original publication, ynamides derived from sulfonamides or oxazolidinone were shown to be successful substrates for oxazole formation (Scheme 21).[49] The exploration of alternative amides was required in order to widen the scope at the oxazole 4-position. Several ynamides were synthesised bearing diverse substituents on the nitrogen atom and a standard phenyl group on the opposite end of the alkyne (Scheme 38). Acyclic carbamates such as **135d**, and phosphoramidates such as **135e**, have been shown to be challenging substrates in ynamide formations, however this can be overcome by following the Hsung group's protocol with increased catalyst loadings;[77b,78] pleasingly allowing the synthesis of ynamides **84h** and **84i** in good yields. Lactam **135f** was converted into ynamide **84j** using dibromoalkene **134a** following a literature procedure for this substrate.[81] Indole could also be coupled with bromophenylacetylene **133b** to produce the stable alkyne **84k**. The isolated yield of **84k** was poor as this ynamide could not be separated from **133b** by column chromatography, and so an unoptimised recrystallisation was performed instead; this problem was also encountered by Iwasawa and co-workers in the one previously reported synthesis of **84k**.[94]

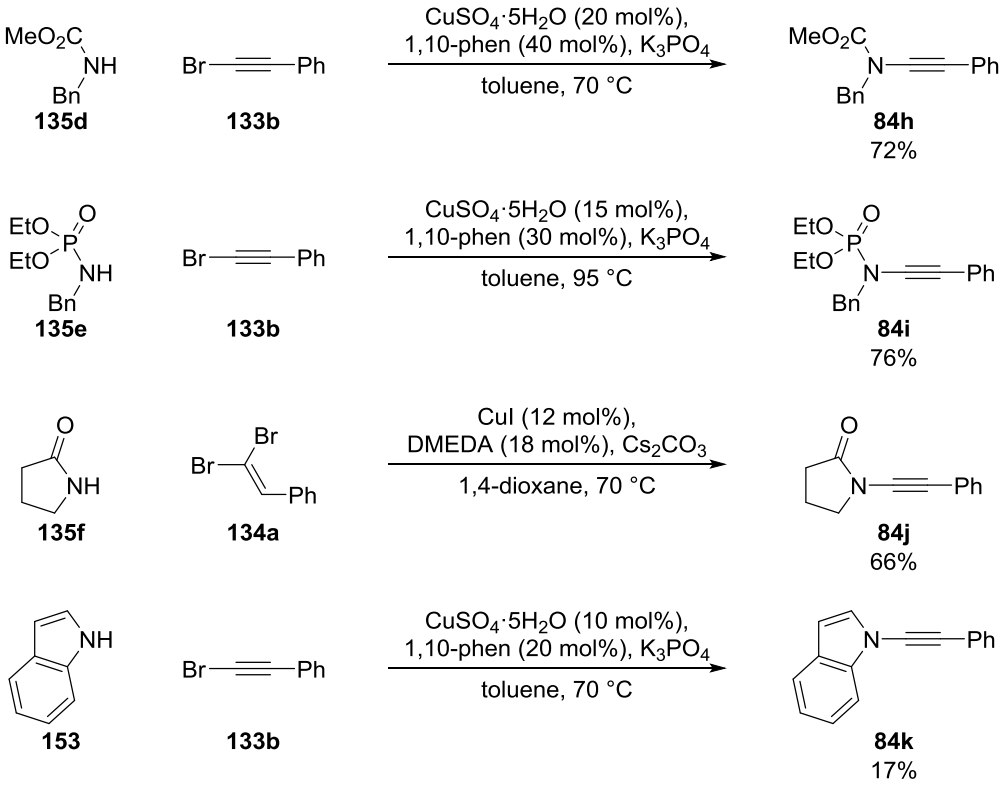

Scheme 38: Synthesis of ynamides from various amides. Ynamide 84i was synthesised by Joshua Priest.

The use of these ynamides in the gold-catalysed oxazole formation produced mixed results (Table 2). No oxazole formation was observed when **84h** was employed; however slow formation of oxazolone **155** did occur (Entry 1). The gold-catalysed formation of oxazolones by cyclisation/fragmentation of ynamides derived from *tert*-butyl carbamates has previously been reported.[95] In this analogous reaction of **84h** it seems likely that, following cyclisation to **158**, demthylation is assisted either by ylide **94c** or by water, with protodemetalation of **160** furnishing **155** (Scheme 39). Given that there should be fairly little water or acid in the mildly basic reaction mixture, it also seems likely that one or both of the demethylation (**158** to **160**) or protodemetalation (**160** to **155**) steps would be slow. This would have the effect of not only producing the low yield of **155**, but possibly also tying up the gold catalyst so that oxazole formation does not occur. In support of this theory, vinyl gold species related to **160** have been shown to be remarkably stable under basic conditions.[96]

Table 2: Use of ynamides from Scheme 38 in oxazole formation.

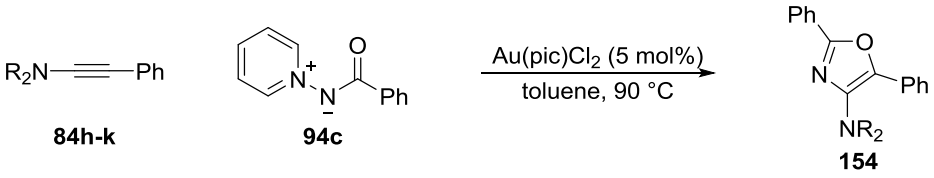

Entry	Ynamide	Time / h	Oxazole	Recovered ynamide	Side product
1	**84h**	24	0%	67%	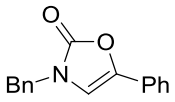 **155**, 14%
2	**84i**	5	**154a**, 81%	N/A	-
3	**84j**	24	0%	59%	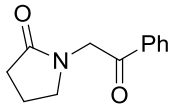 **156**, 16%
4	**84k**	96	**154b**, 64%	28%	-

Using **84** (0.4 mmol), **94c** (0.6 mmol) and Au(pic)Cl_2 (5 mol%) in toluene (4 mL) at 90 °C for the stated time. Isolated yields after flash column chromatography.

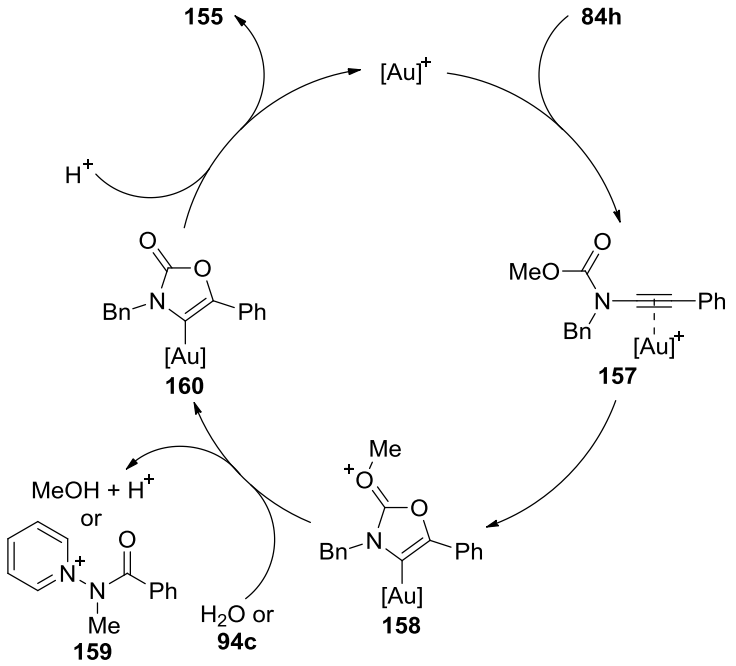

Scheme 39: Proposed mechanistic pathway for formation of oxazolone 155.

The reaction of phosphoramidate-derived ynamide **84i** was much more successful, giving oxazole **154a** in a good yield with no competing side reactions observed, providing a valuable alternative to the use of sulfonamides in this position (Table 2 – entry 2). The lactam-derived

ynamide **84j** was fairly unreactive, with only starting material and some hydration product **156** recovered (Entry 3). As **156**, with the ketone β- to the amide, is not the expected isomer for direct hydration of an ynamide,[97] an alternative mechanism for its formation is proposed (Scheme 40). Again this is initiated by attack of the carbonyl oxygen onto the alkyne to give cation **162**, hydration then reforms the lactam in **163**, with protodemetalation giving enol **164** which can tautomerise to the observed product **156**. A similar mechanism has been proposed by Hammond and co-workers in the gold-catalysed regioselective hydration of **165** to form γ-keto ester **166** (Scheme 41).[98] It should be noted that ynamide **84j** is unusually susceptible to hydration, which was also observed by TLC analysis when a solution in toluene was left for 24 hours; in this case a similar mechanism can be proposed where the gold catalyst in Scheme 40 is replaced with a proton. It is possible that the formation of **162** (not all of which can undergo hydration due to the lack of available water in the reaction mixture) prevents **161** from undergoing oxazole formation.

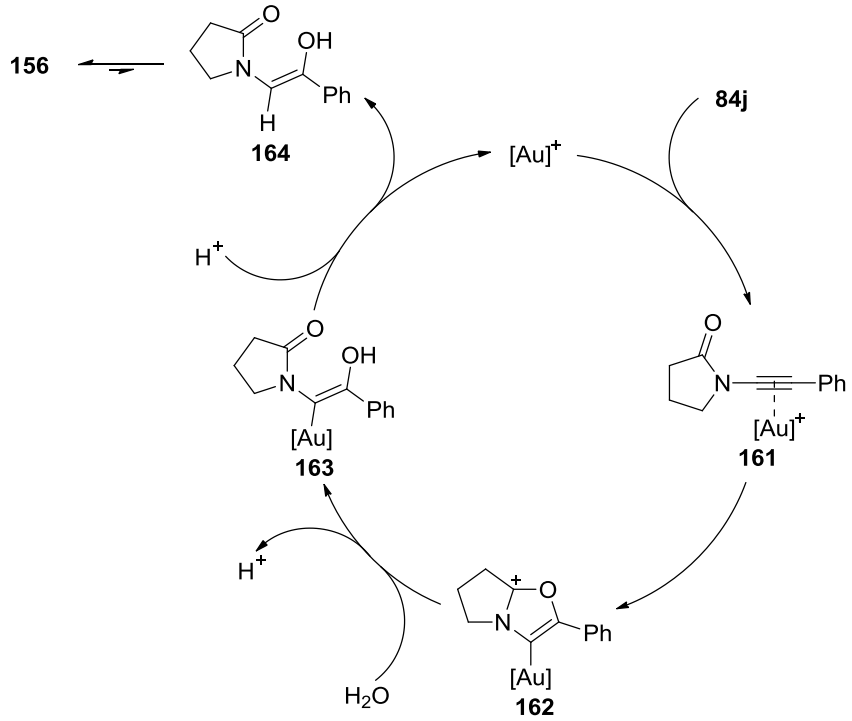

Scheme 40: Proposed mechanistic pathway for the hydration of 84j.

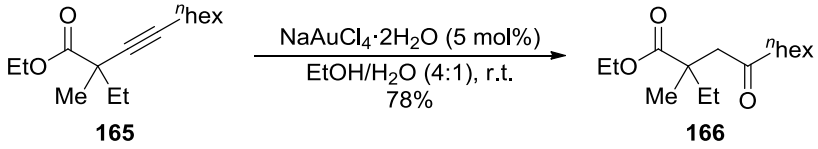

Scheme 41: Regioselective hydration of an alkyne directed by a neighbouring ester by Hammond and co-workers.[98]

The alkynyl-indole **84k** reacted much more slowly than most ynamides which participate in the oxazole formation, however leaving the reaction for four days allowed a useful amount of oxazole **154b** to be obtained (Table 2 – entry 4). This reactivity may be explained by delocalisation of the nitrogen lone pair of **154** into the indole, resulting in a less electron-rich alkyne in this substrate than in the other reactive ynamides. This appears to be the first reaction of an *N*-alkynyl indole under gold catalysis.

2.2.3: Expanding the Scope at the Oxazole 5-Position

The use of alternative functionality at the *C*-terminus of the ynamide was also investigated. Alkyl and aryl groups had previously been employed here, as were substituted vinyl groups and an alkyne.[49] Raju Jannapureddy later showed that esters and thioethers could be incorporated into the 5-position of the oxazole.[90] In order to investigate other non-carbon substituents at this position, the silylated ynamides **84l-m** were synthesised, which also allowed access to terminal ynamide **84n** (Scheme 42).

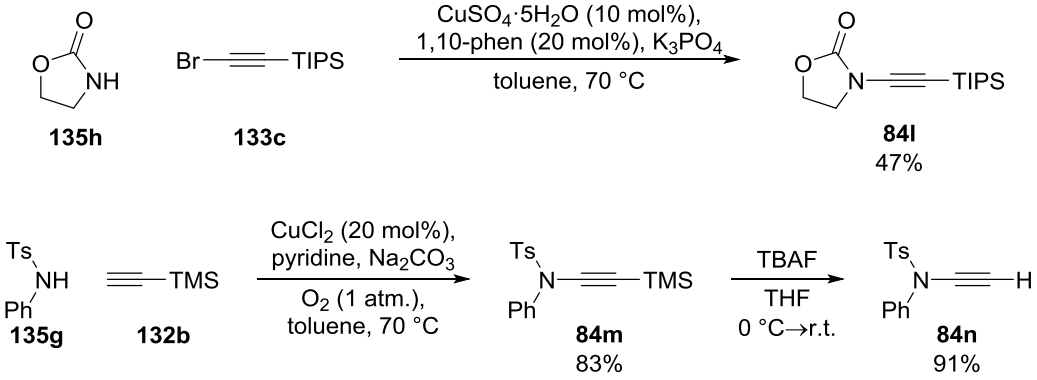

Scheme 42: Synthesis of silylated and terminal ynamides.

Ynamide **84n** successfully furnished oxazole **167**, meaning that both 2,4- and 4,5-disubstituted oxazoles can be synthesised using this methodology (Scheme 43). The use of **84m** resulted in a mixture of recovered starting material and oxazole **167**, presumably formed *via* slow desilylation of **84m** to **84n**, the other silyl ynamide **84l** was unreactive. The reason for the lack of reactivity of ynamides **84l-m** may well be steric in nature, this is supported by the fact that Raju Jannapureddy also found mesityl ynamide **84o** to be unreactive in this chemistry.

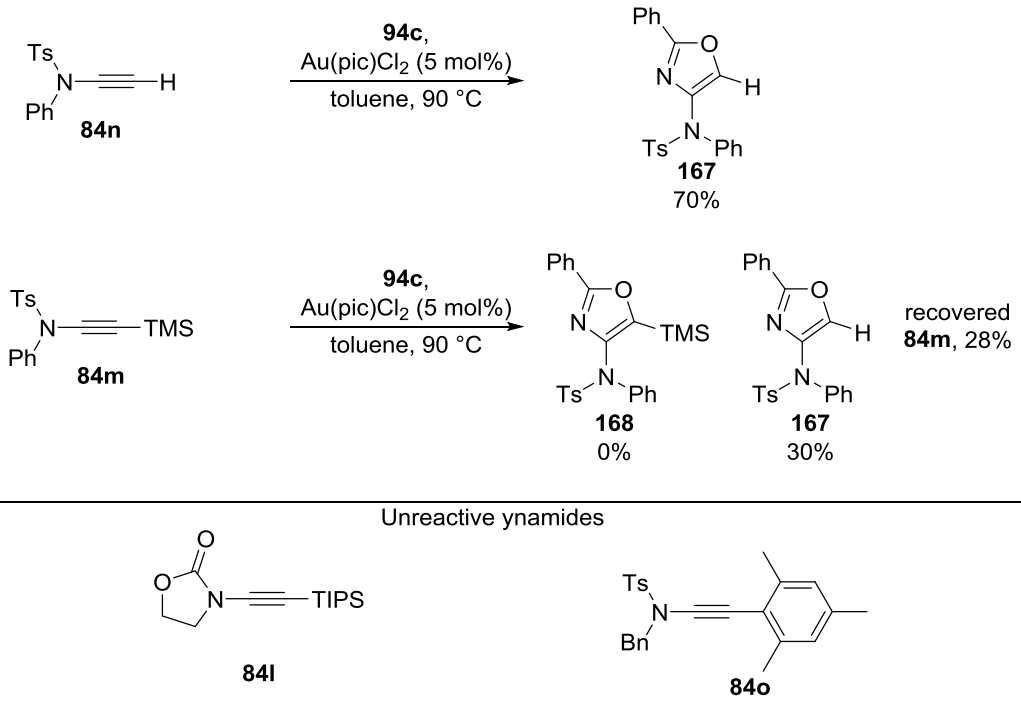

Scheme 43: Synthesis of a 2,4-disubstituted oxazole and failed synthesis of oxazoles from bulky ynamides (Ynamide 84o was synthesised and trialled in the oxazole formation by Raju Jannapureddy).

The synthesis of a 5-bromo oxazole was also attempted, which required the preparation of a previously unreported bromine-substituted ynamide. Attempts at bromination of terminal ynamide **84n** afforded a complex mixture, but elimination of HBr from dibromoenamide **169** was more successful, leading to the formation of **84q** (Scheme 44). As **84q** degraded rapidly it was used without purification, providing oxazole **170**, albeit in a modest yield.

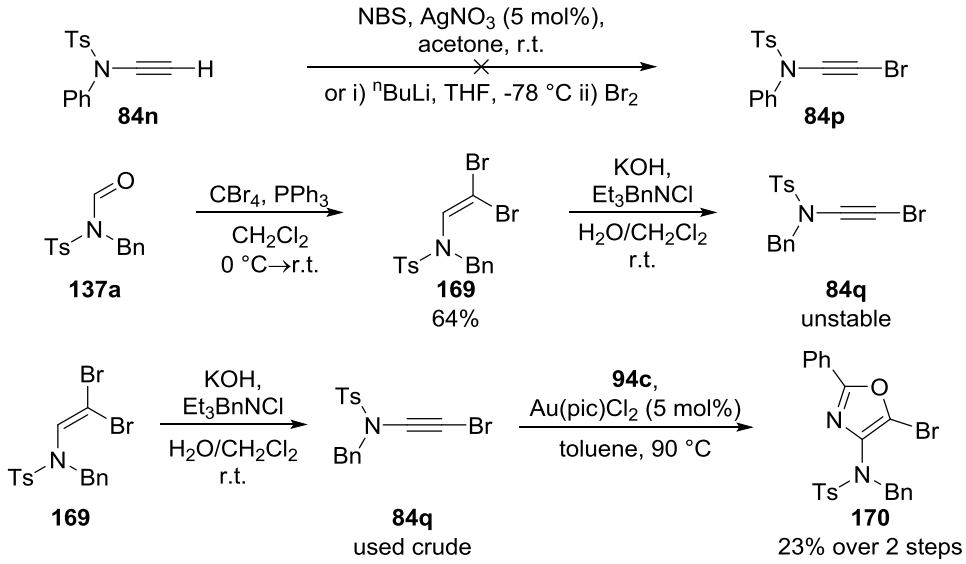

Scheme 44: Synthesis of a 5-bromooxazole.

2.2.4: Competing 1,2-C–H Insertion Pathway

5-Alkyl oxazoles had previously been synthesised using this methodology, where a competing 1,2-C–H insertion product was only isolated in one special case (Scheme 23).[49] The yields for 5-alkyl oxazoles were generally slightly depressed compared to when aryl substituents were employed in this position, and in subsequent similar reactions the competing 1,2-C–H insertion reactions were generally observed (Schemes 24-25).[52-53] In order to determine whether 1,2-insertion always competes in the synthesis of oxazoles from ynamides bearing alkyl chains, and if so what factors affect the level to which it competes, several such ynamides were synthesised (Scheme 45).

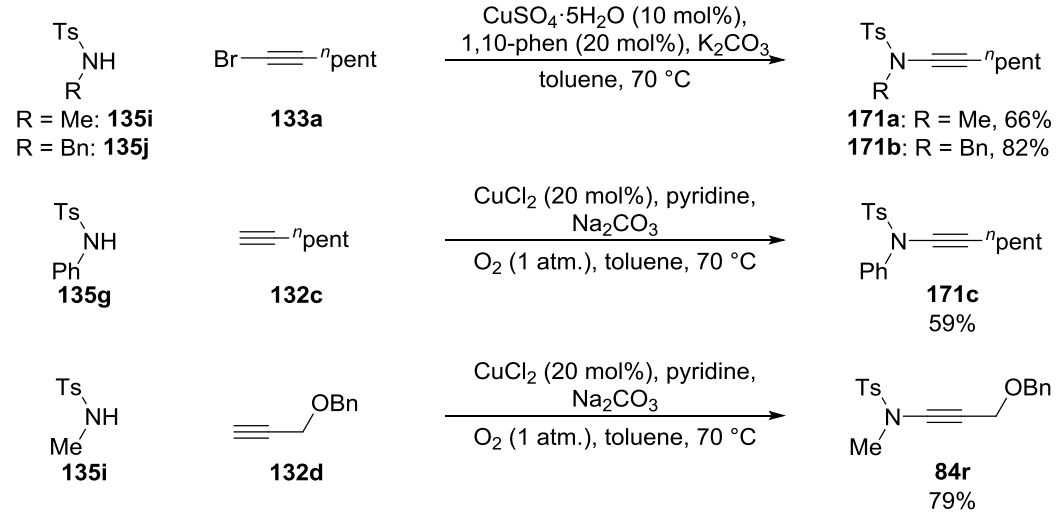

Scheme 45: Synthesis of alkyl-substituted ynamides.

The ynamides **171a-c** were investigated in reactions with ylides **94b** and **94c**, and attempts were made to isolate all of the products (Table 3). In each reaction a mixture of isomers was formed, in which the oxazole **172** was the major component. When ylide **94b** was employed, the only observed side product was the expected 1,2-insertion product **173** as a mixture of *E* and *Z* isomers. In two cases (Entries 1-2) the 1,2-insertion products were inseparable from the oxazoles by column chromatography. Where ynamide **171c** was employed alongside ylide **94b** the resulting oxazole could be separated from the side-products (Entry 3). In contrast, the major side-products with ylide **94c** were dienes **174**, tautomers of the expected 1,2-insertion products (Entries 4-6). Whilst in no cases could **174** be isolated cleanly, all 3 oxazoles were separable from the side-products.

Table 3: Competing oxazole formation and 1,2-insertion reactions.

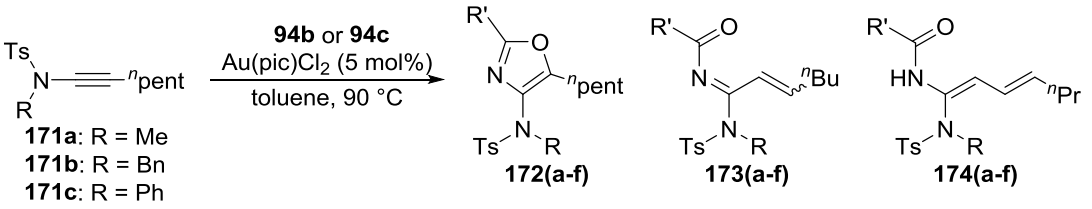

Entry	Ynamide	Ylide	R	R'	**172**	**173**	**174**
1	**171a**	**94b**	Me	OMe	inseparable – 83%[a] (64: 33(*E*):3(*Z*))		-[b]
2	**171b**	**94b**	Bn	OMe	inseparable – 77%[a] (85: 15(*E*):trace(*Z*))		-[b]
3	**171c**	**94b**	Ph	OMe	66%	21% (*E*/*Z*:15/1)	-[b]
4	**171a**	**94c**	Me	Ph	68%	-[b]	<15%[c]
5	**171b**	**94c**	Bn	Ph	62%	-[b]	<8%[c]
6	**171c**	**94c**	Ph	Ph	76%	<4%[c]	<3%[c]

Using **171** (0.4 mmol), **94** (0.6 mmol) and Au(pic)Cl_2 (5 mol%) in toluene (4 mL) at 90 °C. Isolated yields. [a] Isolated as an inseparable mixture. [b] Product not observed. [c] Isolated as the major component of a complex mixture.

Ynamide **84r** was also investigated with both ylides, giving near identical results in each case (Scheme 46). Alongside oxazoles **175**, the only side products were enols **176** which were derived from the expected 1,2-C–H insertion reaction, followed by hydrolysis of the resulting enol ether, possibly during purification by column chromatography. Only the conjugated enol tautomers of **176**

were observed by spectroscopic analysis, in which the *Z* form was predominant, possibly due to the presence of an internal hydrogen bond.

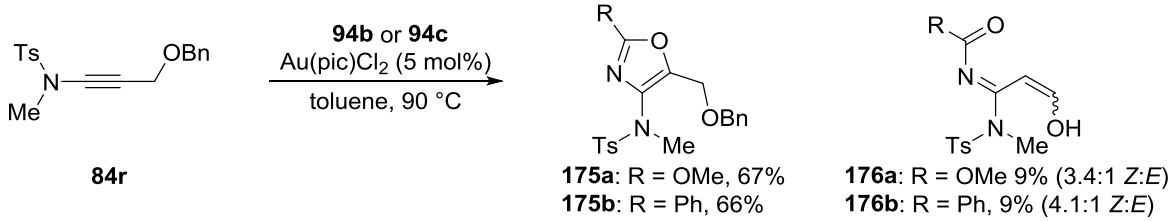

Scheme 46: Effect of a benzyl ether on oxazole formation vs. C–H-insertion.

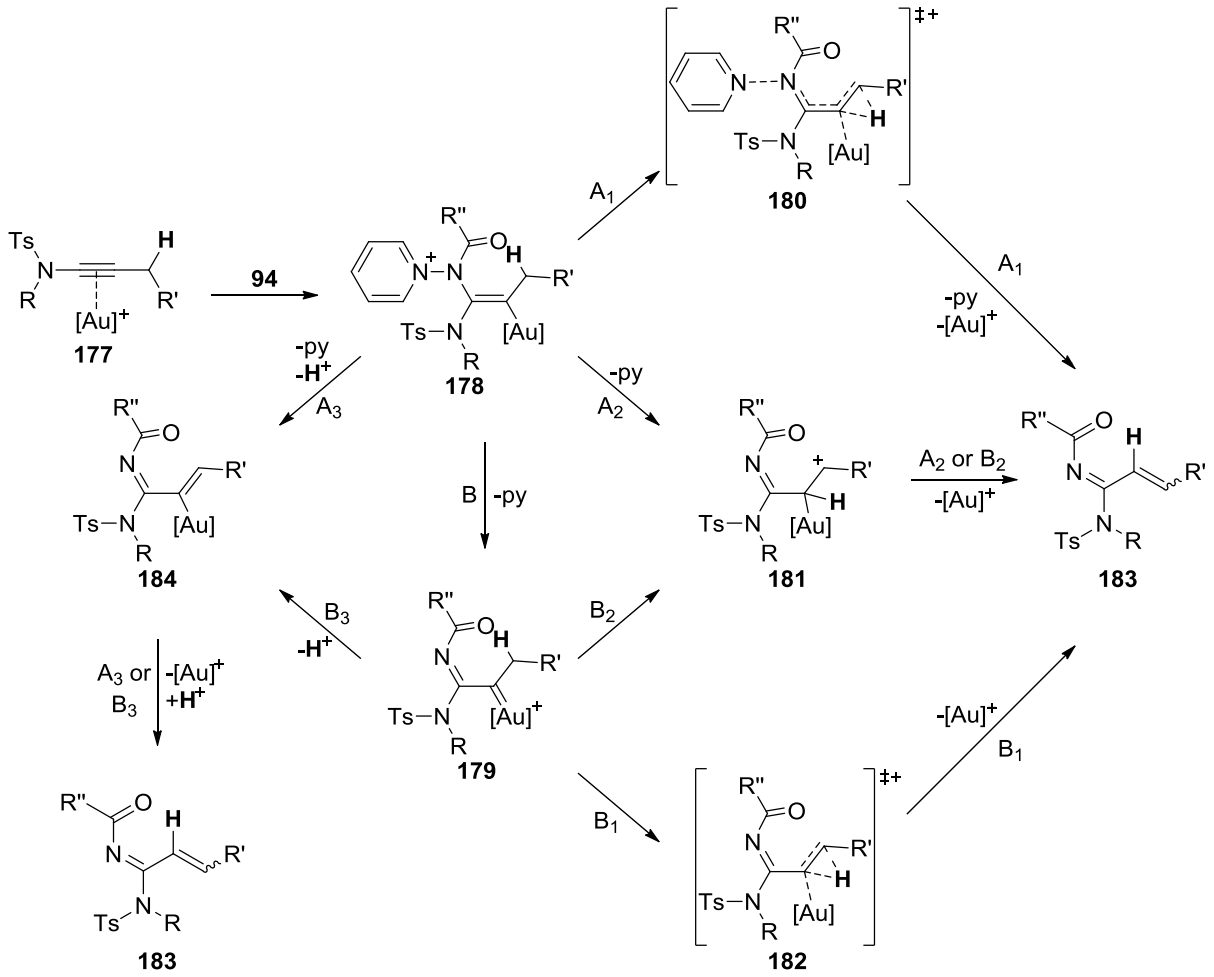

Scheme 47: Possible mechanisms for 1,2-C–H insertion.

Although it is unclear whether either oxazole formation or 1,2-insertion proceeds through carbenoid **178** or carbene **179**, pathways for the competing reaction can be suggested from either intermediate (Scheme 47). Plausible mechanisms for the formation of **183** include a concerted 1,2-hydride shift/loss of gold (A_1 or B_1) or a stepwise mechanism where the hydride shift generates

carbocation **181**, which is then quenched by loss of the metal (A_2 or B_2). Alternatively elimination of a proton may be followed by protodemetalation (A_3 or B_3). The benzyl ether in ynamide **84r** would be expected to stabilise carbocation **181**, however its reactivity was very similar to that of ynamide **171a**, suggesting that pathway 2 is less likely than pathway 1.

Regarding the substituent on the sulfonamide, the formation of 1,2-insertion products appears to be accelerated by the presence of the smaller *N*-methyl group, although an overall pattern is not clear (Table 3). It is worth noting that remarkably large remote steric effects have been observed in 1,2-hydride and -aryl shifts onto rhodium carbenes.[99] In the present case it must also be considered that the conformation of **178** as previously drawn may undergo either oxazole formation or 1,2-insertion, however the alternative conformation **178'** could only undergo 1,2-insertion, the relative concentrations of these conformations may well be affected by the size of the substituents on the amide (Scheme 48).

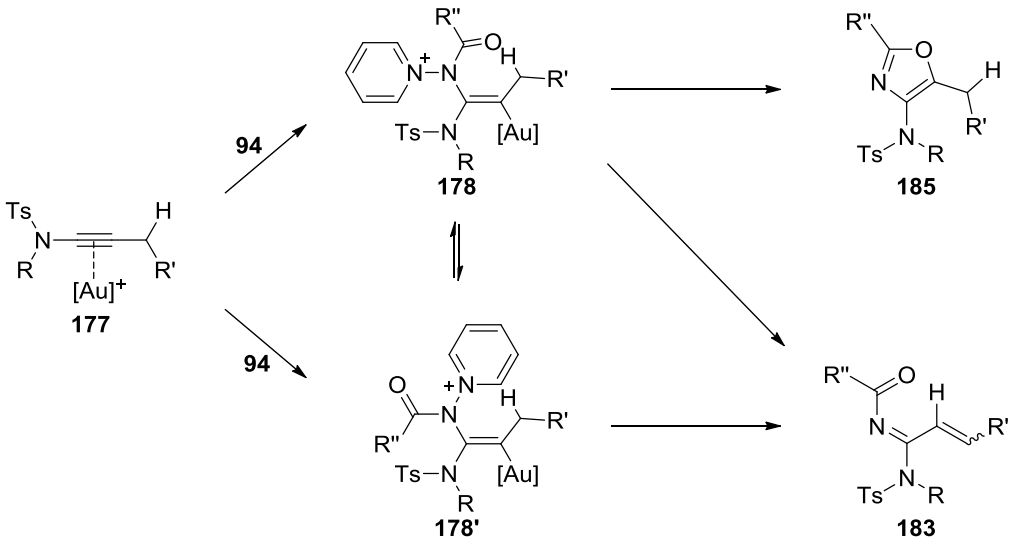

Scheme 48: Reactive pathways for different conformations of the gold carbenoid.

These results demonstrate that, where alkyl chains are incorporated into the 5-position of the oxazole, 1,2-C–H insertion competes in all cases, as it does in the similar reactions which were later reported.[52-53] The heterocycle is always the major product and can usually be isolated from the mixture by chromatography (nine additional examples in the original publication[49] as well as those

described here), and so the effect is generally to depress the yield of the desired oxazole. On two occasions the oxazole could not be separated from the side products (Table 3 – entries 1-2). The presence of products **183** is consistent with the mechanism for oxazole formation presented in Scheme 21, showing that the reaction initially proceeds through formation of the C–N bond rather than in a concerted fashion. The relatively high yields of oxazole obtained where competing reactions are possible, suggest that the formation of the C–O bond must then be relatively rapid compared to 1,2-C–H insertion.

2.2.5: Conclusion

The scope of an existing reaction for the synthesis of trisubstituted oxazoles has been significantly widened at each position. This was allowed by the improvement of routes towards the required starting materials, especially pyridine-*N*-aminides. At the 2-position the reaction was found to tolerate groups such as secondary amides/anilines, an acetal and even products which may act as bidentate ligands. At the 4-position the incorporation of a phosphoramidate and an indole was demonstrated, whilst the challenging synthesis of a 5-bromo oxazole was also achieved. Additionally both 2,4- and 4,5-disubstituted oxazoles can now be accessed using this reaction.

Some limitations to this chemistry have been found, notably including the incorporation of large substituents at the 5-position of the oxazole or of unprotected amines. Ynamides derived from lactams or acyclic carbamates were also found to be unsuitable for oxazole synthesis. In several cases products of competing reactions have been isolated, especially those of a 1,2-C–H insertion reaction, which allow some mechanistic insight into this process.

This reaction is a key step in the formation of the products described in Chapters 3 and 4 of this thesis, where this work has been applied to the synthesis of polycyclic molecules.

CHAPTER 3:

SYNTHESIS AND DIELS-ALDER REACTIONS OF OXAZOLES – DEVELOPMENT OF A ONE-POT REACTION CASCADE FOR THE CONSTRUCTION OF POLYHETEROCYCLIC MOLECULES

3.1: Introduction: Intramolecular Diels-Alder Reactions of Oxazoles

The Diels-Alder reaction of oxazoles is a powerful method for the rapid construction of (poly)heterocyclic systems.[100] Where the dienophile is an alkene these can be either oxo-bridged tetrahydropyridines, or pyridines which are derived from their fragmentation. Alternatively, the cycloaddition of oxazoles with alkynes is normally followed by a retro Diels-Alder reaction to form furans. Generally these reactions take place under normal electron demand and are significantly accelerated by the presence of electron-donating groups on the oxazole and/or with the use of electron-deficient dienophiles.

3.1.1: To Generate oxo-Bridged Tetrahydropyridines

The oxo-bridged tetrahydropyridines **187**, which can be formed by an intermolecular Diels-Alder reaction of an oxazole and an alkene are shown in Scheme 49. In comparison, intramolecular variants of this reaction are often more facile and usually allow for greater regio- and diastereocontrol, as well as allowing the formation of products fused to an additional ring system.

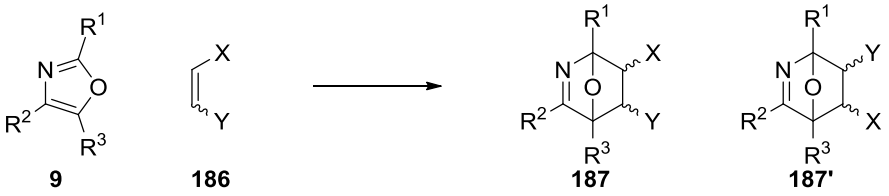

9 **186** **187** **187'**

Scheme 49: Generic intermolecular Diels-Alder reaction of an oxazole and an alkene.

Shimada and Toju first demonstrated the intramolecular Diels-Alder reaction to form stable oxo-bridged tetrahydropyridines, using oxazoles with dienophiles tethered at the 5-position.[101] These included oxazoles **188** bearing *O*-allyl carbamates, which gave products **189** when heated at 140 °C (Scheme 50). The yields were heavily dependent on the substituents on both the alkene and the oxazole, with less substituted products (especially those derived from terminal alkenes: R^3=H) generally formed more efficiently. Interestingly, each of the products was isolated as a single diastereoisomer, although the relative stereochemistry was determined only for **189a**. Here the

steric constraints of the tether between the heterocycle and the alkene lead to exclusive formation of the *exo* product.

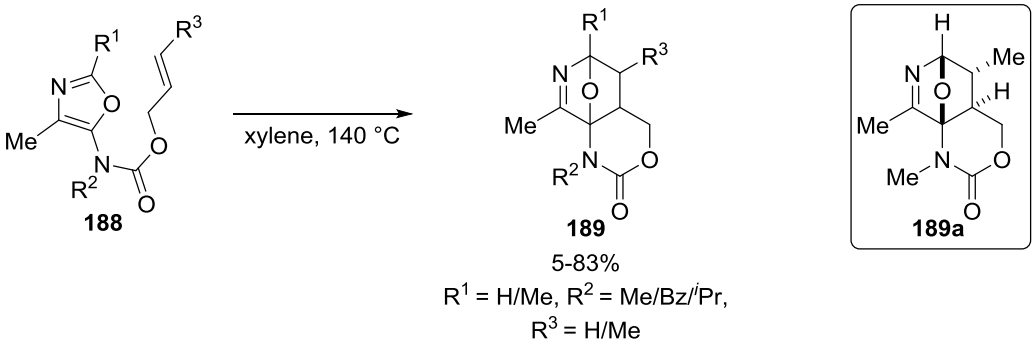

Scheme 50: Intramolecular Diels-Alder reaction of oxazoles with tethered alkenes.[101]

Zhu and co-workers have developed a multicomponent reaction for the synthesis of oxazoles, including those which subsequently undergo reactions with tethered dienophiles.[102] In a typical example the oxazole synthesis begins with a condensation of a substituted allyl amine **190** with an aldehyde (Scheme 51 – top).[102c]. The resulting iminium species **192** is attacked by isonitrile **191** to give intermediate **193**, which cyclises to oxazole **194**. Finally **194** undergoes an intramolecular Diels-Alder cyclisation to give the product **195**. Remarkably the whole process is completed within two hours, in one-pot, at room temperature and forms **195** as a single diastereoisomer, which exhibits the same relative stereochemistry at the ring junction as previously described in Scheme 50. This demonstrates how the Diels-Alder reaction of oxazoles can be accelerated where an electron-donating group is present at the 5-position of the heterocycle, and an electron-deficient alkene is employed.

In contrast, when diallylamine **196** was tested, the reaction stopped at oxazole **199** (Scheme 51 – middle). The final cycloaddition of oxazole **199** with the unactivated alkene was only triggered upon heating this substrate to 80 °C, and was followed by loss of morpholine to give pyridine **200** (this type of fragmentation is discussed below).

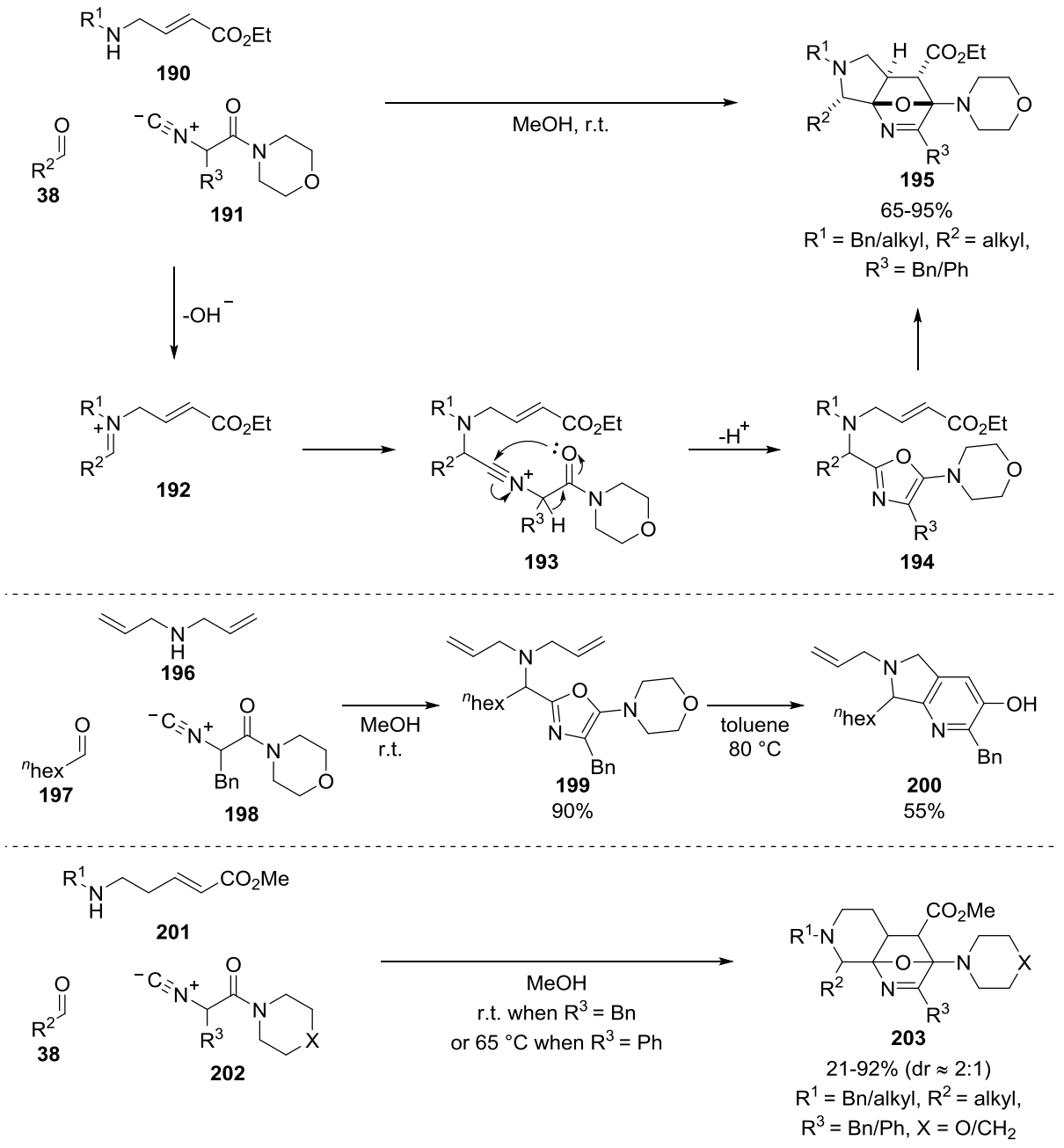

Scheme 51: Multicomponent reactions which synthesise oxo-bridged tetrahydropyridines *via* oxazoles.[100c-d]

Starting from amines **201**, the analogous reaction for the synthesis of Diels-Alder adducts fused to piperidines **203** has also been carried out (Scheme 51 – bottom).[102d] In this case most of the products were isolated in a ~2:1 diastereomeric ratio, and the yields of **203** were slightly less impressive than those for **195**, which can be explained by the increased flexibility of the longer chain alkene.

The same group has developed a similar one-pot protocol which is highly enantioselective (Scheme 52).[102f] Starting from aldehydes and primary anilines **204**, the resulting imine **205** is activated by a chiral phosphoric acid. It was proposed that the enantioselectivity for this reactions arises from addition of the isonitrile **207** to chiral iminium salt **206**. Which is followed by cyclisation of the resulting species **208** to give enantioenriched oxazole **209. 209** is then acylated and undergoes a Diels-Alder reaction to form pyrrolidinone-fused products **211**. The diastereoselectivity of the final step was governed by the nature of the substituent originally derived from the aldehyde. When R^1 = cyclohexyl the diastereomeric ratio was between 6:1 and 12:1, whilst a larger *tert*-butyl group in this position resulted in the formation of the enantioenriched products **211** as single diastereoisomers.

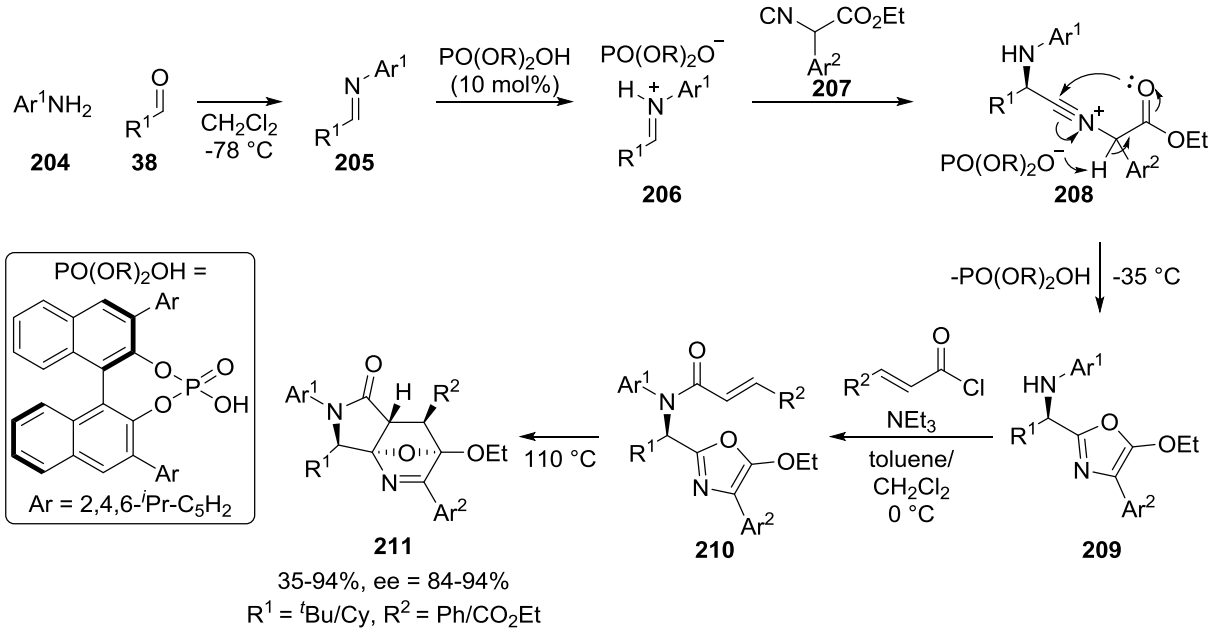

Scheme 52: Enantioselective one-pot synthesis of oxo-bridged tetrahydropyridines.[102f]

3.1.2: To Generate Pyridines (the Kondrat'eva Pyridine Synthesis)

As mentioned above, the adducts **187** can be converted into pyridines through several pathways. This process may be triggered thermally or by the addition of either acid or base, and is known as the Kondrat'eva pyridine synthesis (Scheme 53).[100a] The classic, and often targeted, fragmentation is dehydration to pyridines **212**, however other pathways may compete depending on the nature of the substituents on **187**. These include the loss of the group which originates from the oxazole 5-position (R^3) to give pyridinol **213**, or where this substituent is a proton it may facilitate elimination with its adjacent substituent (Y) to give **214**, or reduction to **215**.

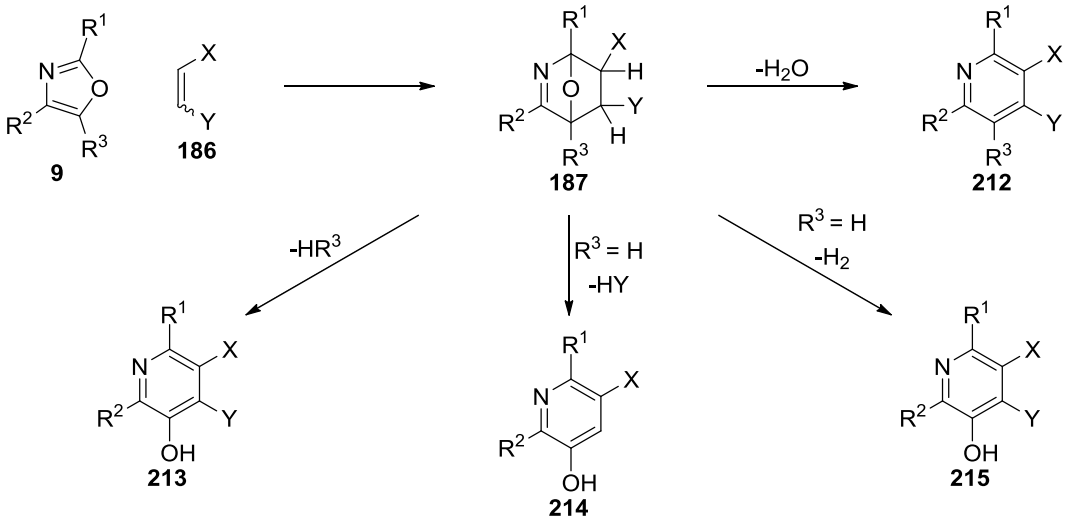

Scheme 53: Possible pathways for aromatisation of tetrahydropyridines.

An example of how these competing pathways can be controlled can be found in the total synthesis of eupolauramine by Levin and Weinreb (Scheme 54).[103] When oxazole **216** was heated in 1,2-dichlorobenzene, the reduction product **218** was produced alongside pyridinol **219**, despite the absence of any obvious oxidant. The reaction was attempted in several (degassed) solvents at various temperatures, with the only observed difference being that lower temperatures increased the ratio of **218**:**219** (suggesting that **219** is likely a product of decarboxylation of **218**). Addition of the base DBN to the reaction mixture changed the fragmentation pathway, resulting in exclusive formation of

the desired dehydration product **220**. The intramolecular Kondrat'eva pyridine synthesis has since been incorporated into several other natural product syntheses.[104]

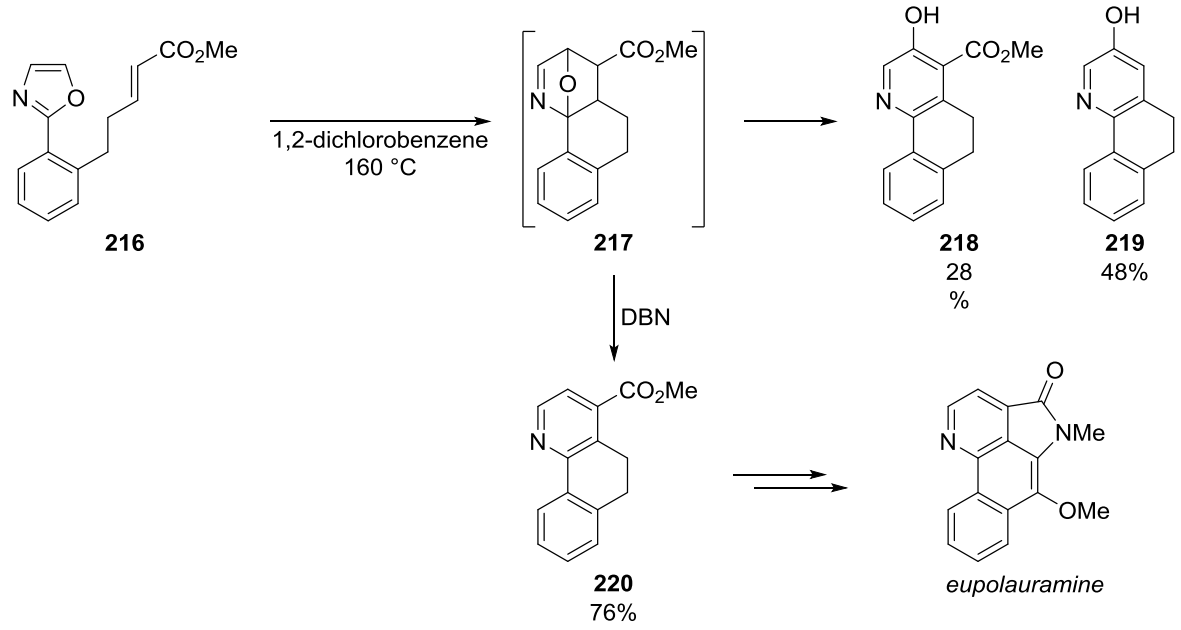

Scheme 54: Intramolecular Kondrat'eva pyridine synthesis as a key step in Levin and Weinreb's synthesis of eupolauramine.[103]

The dehydration of oxo-bridged tetrahydropyridines may also be triggered under acid catalysis. Addition of trifluoroacetic acid at low temperature to the multicomponent synthesis of **195** described in Scheme 51 led to the isolation of pyridine products **221** (Scheme 55).[102c] This is in contrast to the loss of morpholine which followed the Diels-Alder reaction of **199** in the absence of either acid or, possibly importantly, the ester substituent (Scheme 51).

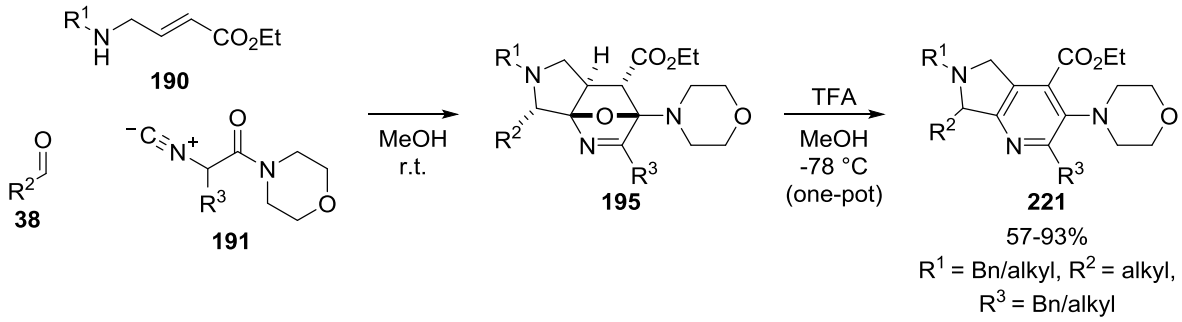

Scheme 55: Multicomponent synthesis of pyridines.[102c]

3.1.3: To Generate Furans

The first cycloadditions of oxazoles with alkynes employed 5-ethoxy-oxazoles of type **222** and dimethyl acetylenedicarboxylate **223** (Scheme 56).[105] The resulting adduct **224** was not observed before it underwent a rapid retro-Diels-Alder reaction to give furan products **225**, with loss of either a nitrile or hydrogen cyanide.

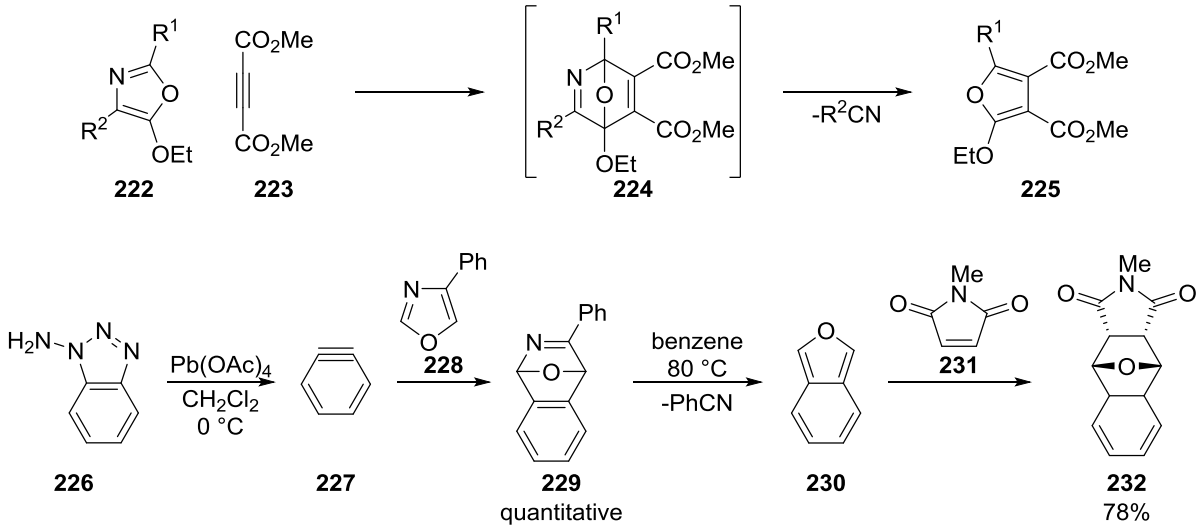

Scheme 56: Intermolecular Diels-Alder reactions of oxazoles with an alkyne[105] and a benzyne.[106]

The reaction of 4-phenyl oxazole **228** with benzyne gave the unusually stable Diels-Alder adduct **229** (Scheme 56 – bottom).[106] Compound **229** could be stored for several days at room temperature, however heating **229** produced the very reactive isobenzofuran **230**, which was trapped with *N*-methyl maleimide as **232**. A likely reason for the stability of **230** is the relatively small gain in aromatic character on going from **230** to **232** compared to going from **224** to **225**.

The Jacobi group have studied the intramolecular variant of this reaction and exploited it in the racemic synthesis of a number of furanosesquiterpene natural products, with the construction of the furan representing a robust and often efficient final step (Scheme 57).[107] Intramolecular furan syntheses of this type have also been employed at an earlier stage in a number of other natural product syntheses.[108]

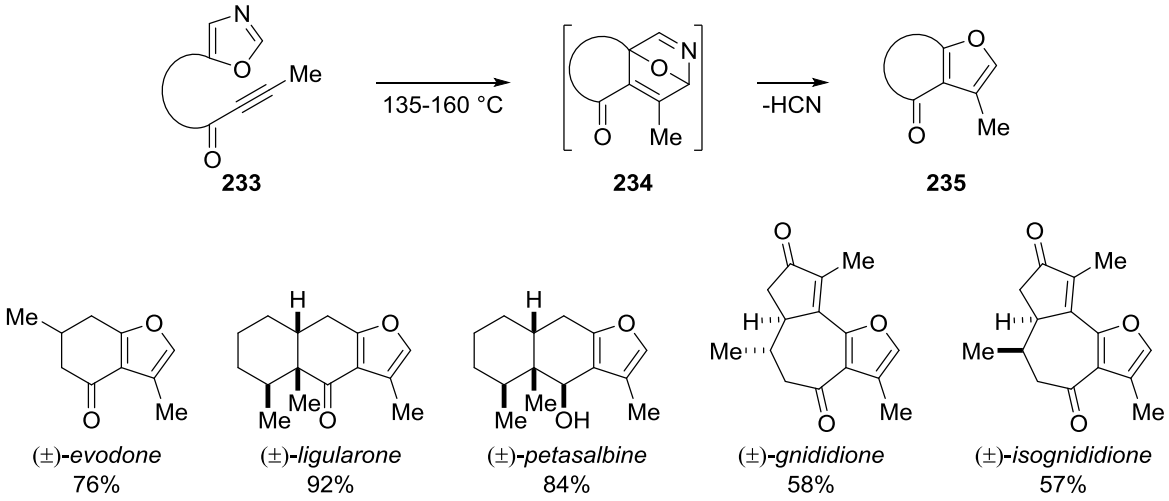

Scheme 57: Construction of the furan ring as the final step in the synthesis of furanosesquiterpene natural products.[107]

Zhu and co-workers have developed a multicomponent synthesis of fully substituted furans **239** using a route analogous to that described in Scheme 51, in which the alkene is replaced by an alkyne (Scheme 58).[109] A higher temperature was required for efficient conversion than for the reactions with alkenes, additionally the use of an electron-withdrawing group on the dienophile was essential to facilitate its reaction with the oxazole (terminal alkynes did not undergo the Diels-Alder reaction).

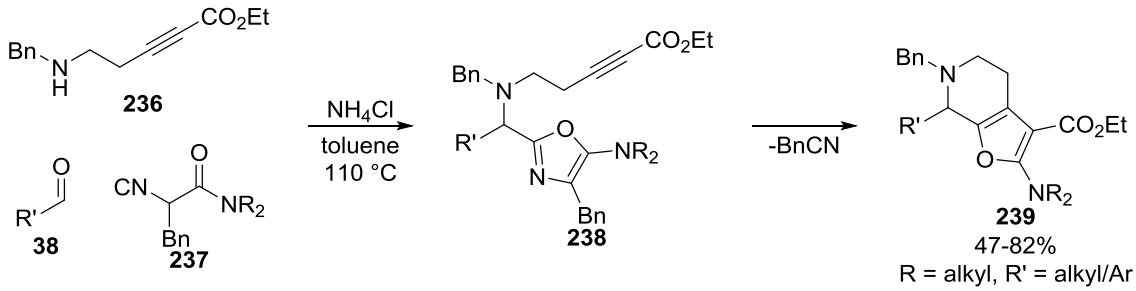

Scheme 58: Multicomponent syntheses of fully substituted furans and benzenes.[109]

3.1.4: Conclusion

The intramolecular Diels-Alder reaction of oxazoles allows the construction of oxo-bridged tetrahydropyridines, pyridines or furans fused to an additional newly formed ring system. The cycloaddition usually takes place under normal electron demand and can be accelerated by the use of electron-rich oxazoles and/or electron-deficient dienophiles. As no additional reagents or catalysts are generally required, these reactions are ideally suited to incorporation into one-pot, multi-step cascade processes for the rapid construction of polycyclic molecules.

3.2: Results and Discussion

Chapter 2 showed how oxazoles bearing diverse substituents could be convergently constructed. The substrate scope was explored particularly widely at the 2-position, for which an improved synthesis of pyridine-*N*-aminides has been developed. It was therefore anticipated that a variety of oxazoles tethered to dienophiles at the 2-position could be accessed by this gold-catalysed cycloaddition. This would allow the Diels-Alder chemistry of the new 4-amido oxazoles to be explored, and potentially facilitate the construction of heavily substituted polycyclic compounds such as tetrahydropyridine **242**, pyridine **243** or furan **247** (Scheme 59). The ultimate aim of this project would be to carry out both the synthesis of the oxazole and its subsequent Diels-Alder reaction in a one-pot process.

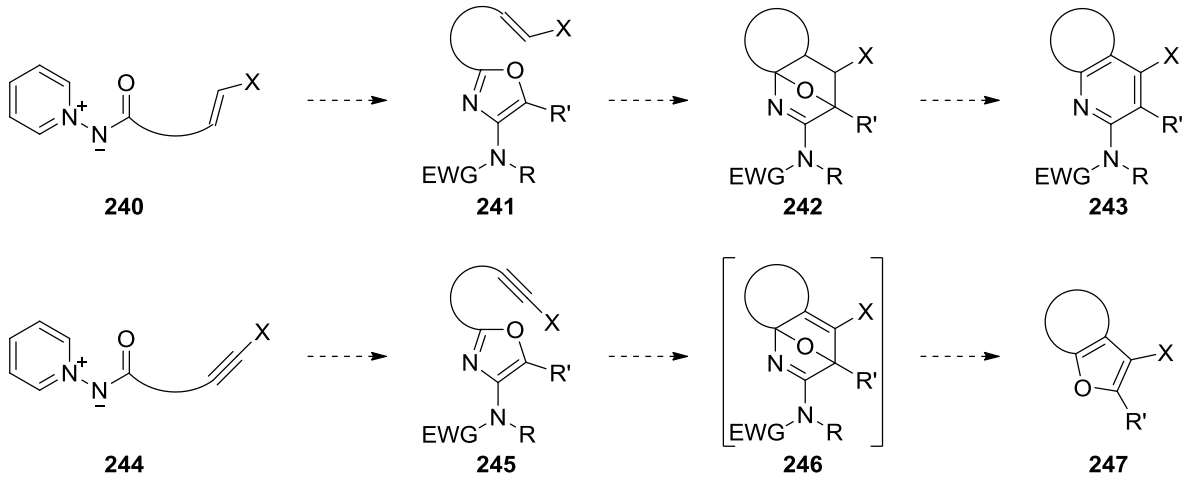

Scheme 59: Proposed route to polycyclic products from pyridine-*N*-aminides.

3.2.1: Initial Synthesis of Furans and oxo-Bridged Tetrahydropyridines

The synthesis of oxazoles **151b-d** was described in Chapter 2 (Scheme 35). It is noteworthy that no Diels-Alder reaction of **151d** was observed either during in its initial synthesis or when it was heated to higher temperatures in a sealed tube (Scheme 60). This lack of reactivity is in contrast with that of the similar substrates **210** (Scheme 52), however it can be explained by the reduced number of substituents on and α- to the nitrogen in the tether, which raises the relative energy of the required reactive rotamer. This cyclisation is further sterically disfavoured by the presence of large phenyl groups on both the alkene and at the 5-position of the oxazole.

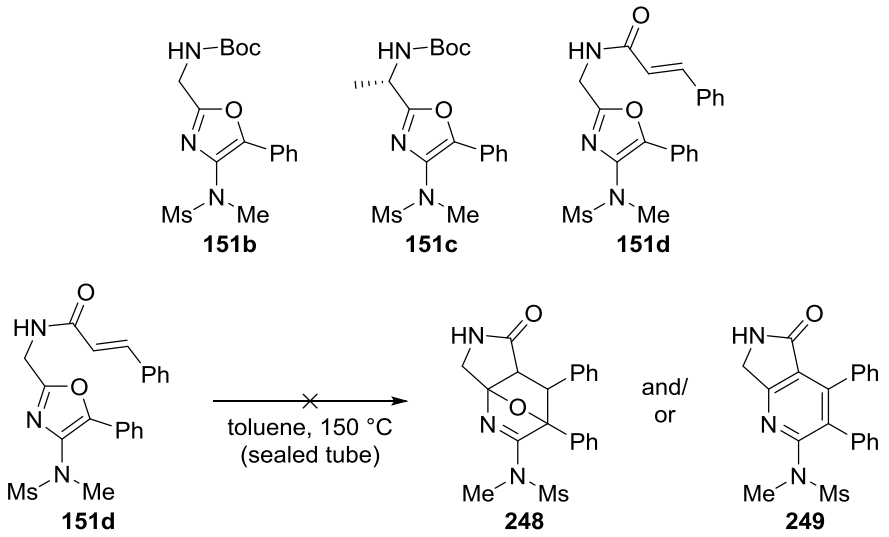

Scheme 60: Previously synthesised oxazoles including one tethered to an alkene which does not undergo a Diels-Alder reaction.

With the steric considerations above in mind, the first successful Diels-Alder reaction was carried out using the alkyne-tethered oxazole **250** (Scheme 61). In an unoptimised procedure the protecting group of oxazole **151c** was first cleaved, and the resulting primary amine was treated with excess propargyl bromide at 50 °C to give dipropargylated product **250**. Upon heating to 100 °C, some conversion of **250** was observed by TLC. The reaction was stopped after 24 hours (before the full consumption of oxazole, as some degradation was also obvious at this point), leading to the isolation of furan **253**. In keeping with the literature reviewed above, the final retro-Diels-Alder

reaction which furnished this furan appeared to be extremely rapid, as the initial intermediate **251** was not observed at any stage. Nitrile **252** was also isolated, although not with high purity.

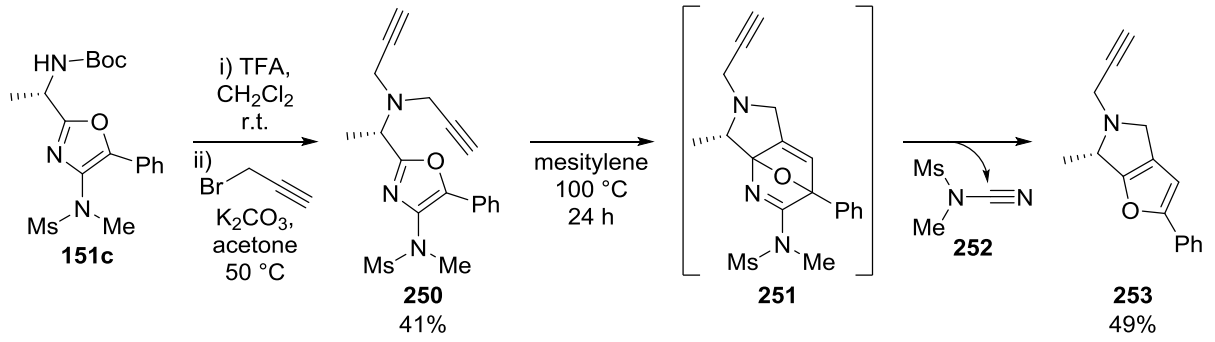

Scheme 61: First Diels-Alder reaction of a 4-amido oxazole, generating a furan.

Given the problems with the small amount of racemisation of **94f**/**151c** (Chapter 2 – Scheme 37), and the possibility of forming up to four diastereoisomers of oxo-bridged tetrahydropyridines from chiral pyridine-*N*-aminides, it was preferable to continue these early investigations from the glycine-derived oxazole **151b**, with the intention of returning to substrates based on chiral amino acids following further optimisation.

A more straightforward alkylation strategy than that described above was to treat **151b** with NaH and the appropriate alkyl bromide. The propargylation of **151b** appeared to proceed smoothly by, as evidenced by TLC analysis, so this reaction mixture was then heated to facilitate the following cycloaddition in the same pot (Scheme 62). The resulting furan **255** was isolated in a low yield, however this is likely to be due to the instability of this product. Following purification, further degradation of furan **255** occurred even at room temperature.

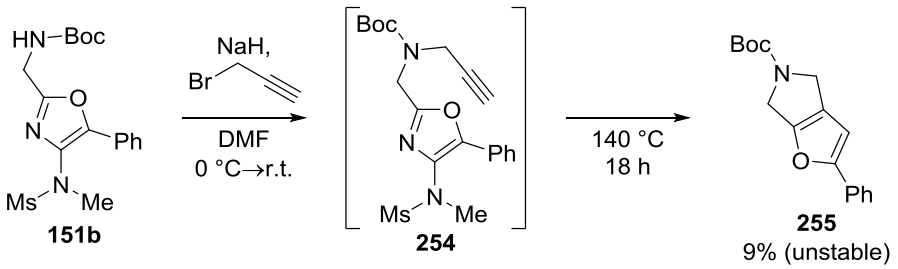

Scheme 62: One-pot propargylation and Diels-Alder reaction of an oxazole.

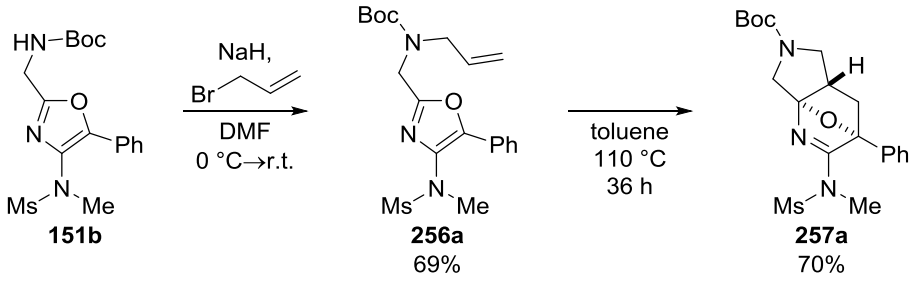

Scheme 63: Successful Diels-Alder reaction of an oxazole tethered to an alkene.

When the alkene tethered oxazole **256a** was heated to reflux in toluene, it pleasingly gave the stable tetrahydropyridine **257a** as a single diastereoisomer (Scheme 63, evidence for the relative stereochemistry drawn for products **257** is discussed from page 71). The selectivity for the *exo* product is attributed to increased strain in the tether between the oxazole and the alkene for the *endo* transition state **259** (Scheme 64). This selectivity is the same as that displayed by similar oxazoles **194**[102c] (Scheme 51) and **210**[102f] (Scheme 52), and by related furans.[110]

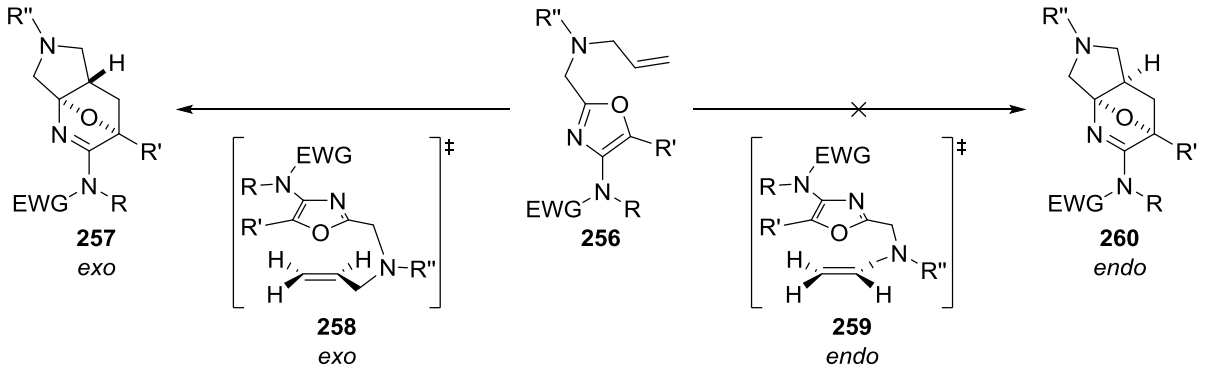

Scheme 64: Favoured and disfavoured transition states in the Diels-Alder reaction of oxazoles 256.

It is interesting to note the increased reactivity of **256a** over **151d**, despite **256a** containing the more electron-rich alkene. As inverse electron demand Diels-Alder reactions of oxazoles are known only for very deactivated heterocycles,[111] it appears that the steric effect of substituents on the oxazole-dienophile tether and/or on the alkene is very important, although further investigation into the electronics of this reaction were required.

The relative stability of the tetrahydropyridines, and the initial success in their synthesis, meant that these substrates were next targeted as part of a cascade process.

3.2.2: Cascade Reactions to Synthesise Tetrahydropyridines in One-Pot from Ynamides

3.2.2.1: Screen of protecting groups

Having found a suitably reactive substrate in **256a**, ylides based on protected *N*-allyl glycines were targeted so that such oxazoles could be prepared directly from ynamides, and the Diels-Alder reaction carried out in the same reaction vessel. Several protecting groups were investigated in order to find a highly reactive ylide which could be easily accessed.

Protected glycines **147e** and **262** were allylated in an unoptimised procedure by treatment with allyl bromide and sodium hydride. These reactions produced fairly complex mixtures from which isolation of the product was difficult, resulting in disappointing yields of **263a-b** (Scheme 65). A likely reason for this is that excess NaH was used, allowing enolate formation, which may lead to additional allylation adjacent to the carbonyl and/or Claisen condensation. In contrast, the more acidic secondary sulfonamides **264** and **265** could be allylated using K_2CO_3 when heated with allyl bromide in acetonitrile.[112] The reactions of the sulfonamides were particularly clean and **263c-d** could be purified simply by aqueous extraction following each of the two steps, making these far more easily accessed substrates.

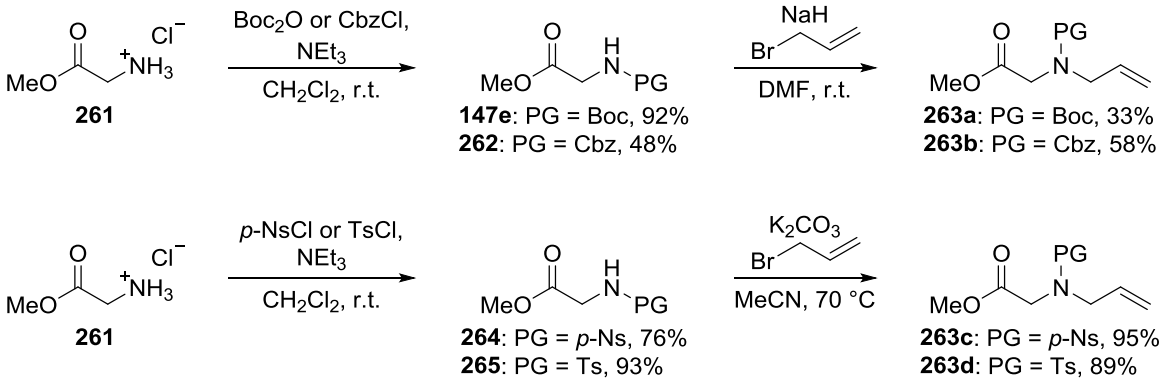

Scheme 65: Synthesis of protected *N*-allyl glycine methyl esters.

Esters **263a-d** were next used in the synthesis of ylides **263a-d**. Moderate yields were obtained for **266a-b** whilst there was a significant difference in the yield of sulfonated products **266c-d** (Table 4). Nitrobenzenesulfonamides are typically deprotected by nucleophilic substitution at

the carbon-sulfur bond with strong nucleophiles (usually thiolates), followed by loss of SO_2.[113] Side-products believed to be derived from this deprotection using the nucleophile generated by deprotonation of **139** were observed in the synthesis of **266c**, explaining the significantly lower yield for this substrate than for **266d**.

Table 4: Effect of the glycine protecting group on ylide synthesis and the cascade oxazole formation / Diels-Alder reaction.

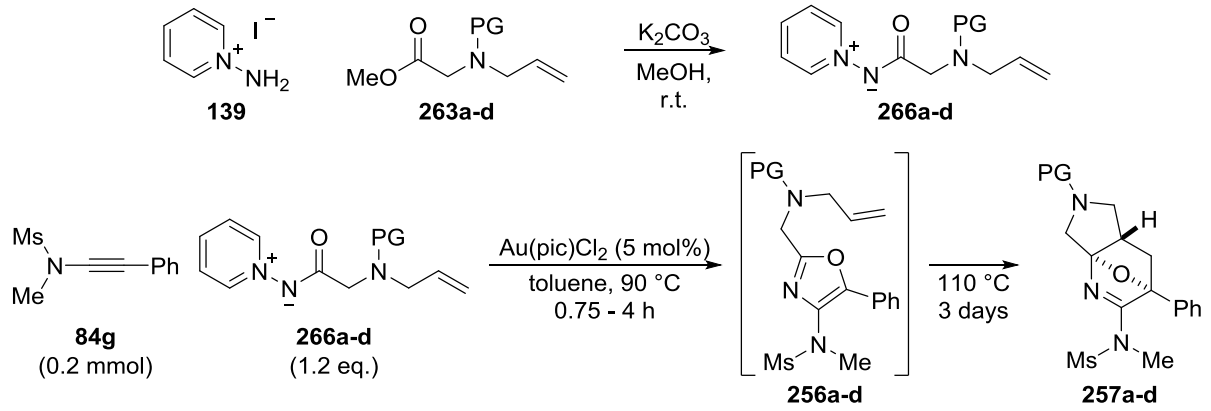

Entry	PG	**266**	Yield	**257**	Yield
1	Boc	**266a**	45%	**257a**	68%
2	CBz	**266b**	36%	**257b**	63%
3	*p*-Ns	**266c**	12%	**257c**	36%
4	Ts	**266d**	62%	**257d**	69%

Ylides **266a,b,d** all retained the very high reactivity of the similar glycine-derived ylide **94e** (Chapter 2 – Scheme 35); TLC analysis showed that ynamide **84g** was consumed within 45 minutes to cleanly form intermediate oxazoles **256**, which were heated for three days at reflux to give tetrahydropyridines **257a,b,d** in consistently good yields (Table 4 – entries 1,2 and 4). Again the yield was fairly poor using the *para*-nitrobenzenesulfonamide (Entry 3). In this case ylide **263c** did not consume ynamide **84g** as evidenced by TLC analysis within four hours at 90 °C, the reason for this is unclear as nitrobenzenesulfonamides have previously been well tolerated in the gold-catalysed oxazole synthesis.[49]

A number of important conclusions could be drawn from this study. Firstly, as envisioned, it was possible to carry out the oxazole synthesis and a subsequent Diels-Alder reaction with a tethered

N-allyl group in a one-pot protocol. This process allows a remarkably rapid increase in complexity, generating four new ring systems and three new stereogenic centres with complete diastereoselectivity for the *exo* product.

Secondly, *N*-Boc, -Cbz and -tosyl protecting groups on the amino acid can all be used in this cascade with little variation in the yield, allowing the potential development of different strategies if subsequent products containing an unprotecting pyrrolidine were desired. In these successful reactions the remaining material in the reaction mixture was mostly comprised of the intermediate oxazole **256**, for which complete consumption was never achieved (recovering the oxazoles **256** in high purity from these reactions was challenging, partially due to the small amount present). It is clear that for these substrates a balance must be struck between the required reaction time and temperature, and obtaining a good yield of the product. Identifying oxazole/dienophile combinations which more readily underwent the Diels-Alder reaction remained an objective.

It is also interesting to note that very similar yields of **257a** were obtained whether oxazole **256a** was isolated and used as the starting material (Scheme 62), or formed *in situ* from the ynamide (Table 4 – entry 1). As the formation of oxazoles **256a,b,d** directly by gold catalysis appeared by TLC analysis to proceed in a near quantitative fashion (as it had for related oxazole **151b** – Chapter 2 – Scheme 35), this implied no significant effect of the gold catalyst on the Diels-Alder reaction, and also no benefit in isolating the intermediate oxazole.

Finally, considering both the yield for the formation of ylide **266d**, and the fact that its required ester **263d** could be accessed extremely easily, **266d** was an ideal substrate to continue investigating the scope of this process. The absence of carbamate rotamers in the tosylated products, which complicated the NMR spectra of tetrahydropyridines **257a-b**, was an additional factor in this decision.

Before moving on to testing other ynamides, two further experiments were carried out with ynamide **84g**. The reactions shown in Table 4 employed 0.2 mmol of ynamide. A 1.5 mmol scale

reaction showed that the yield of **257d** remained consistent, whilst providing nearly half a gram of this substrate for subsequent investigation of its chemistry (Scheme 66).

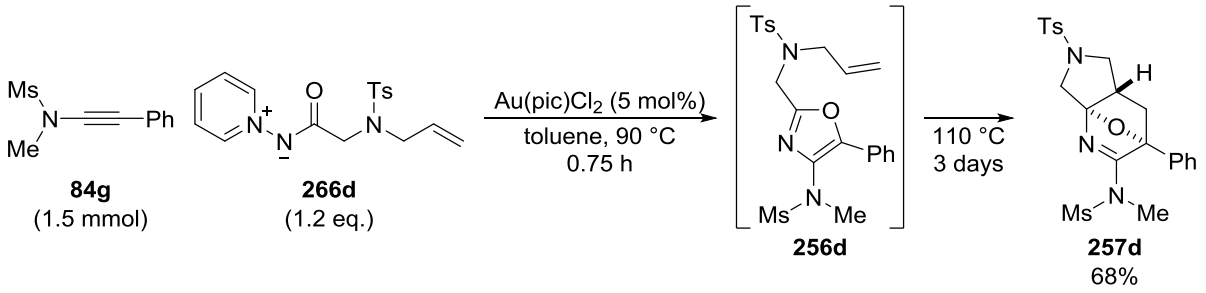

Scheme 66: Large-scale synthesis of an oxo-bridged tetrahydropyridine.

Secondly the reaction of **84g** with **266a** was repeated, however after 45 minutes (by which time all of **256a** had been consumed as evidenced by TLC) DBU was added to the reaction mixture (Scheme 67). **257a** was obtained from this reaction in a practically unchanged yield from the base-free reaction (Table 4 – entry 1) and no formation of any pyridine products was observed. Although such a dehydration has been triggered by the addition of DBU[102b] or DBN (Scheme 54)[103] to similar substrates, a key difference is that the Diels-Alder reaction of oxazole **256a** was carried out without an electron-withdrawing group attached to the alkene. Therefore, in the resulting product **257a**, none of the protons on the tetrahydropyridine ring are acidic enough to readily facilitate base-catalysed dehydration.

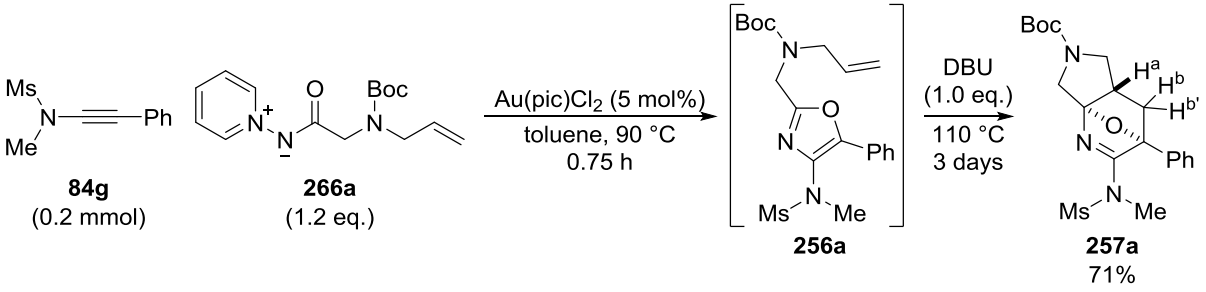

Scheme 67: Addition of DBU to the Diels-Alder reaction does not result in dehydration of the product.

3.2.2.2: Variation of the ynamide

Having already established the types of ynamides which cleanly formed oxazoles in Chapter 2, a range of these substrates were synthesised in order to investigate the effect of altering the substituents on the oxazole 4- and 5-position on their Diels-Alder reactions (Scheme 68).

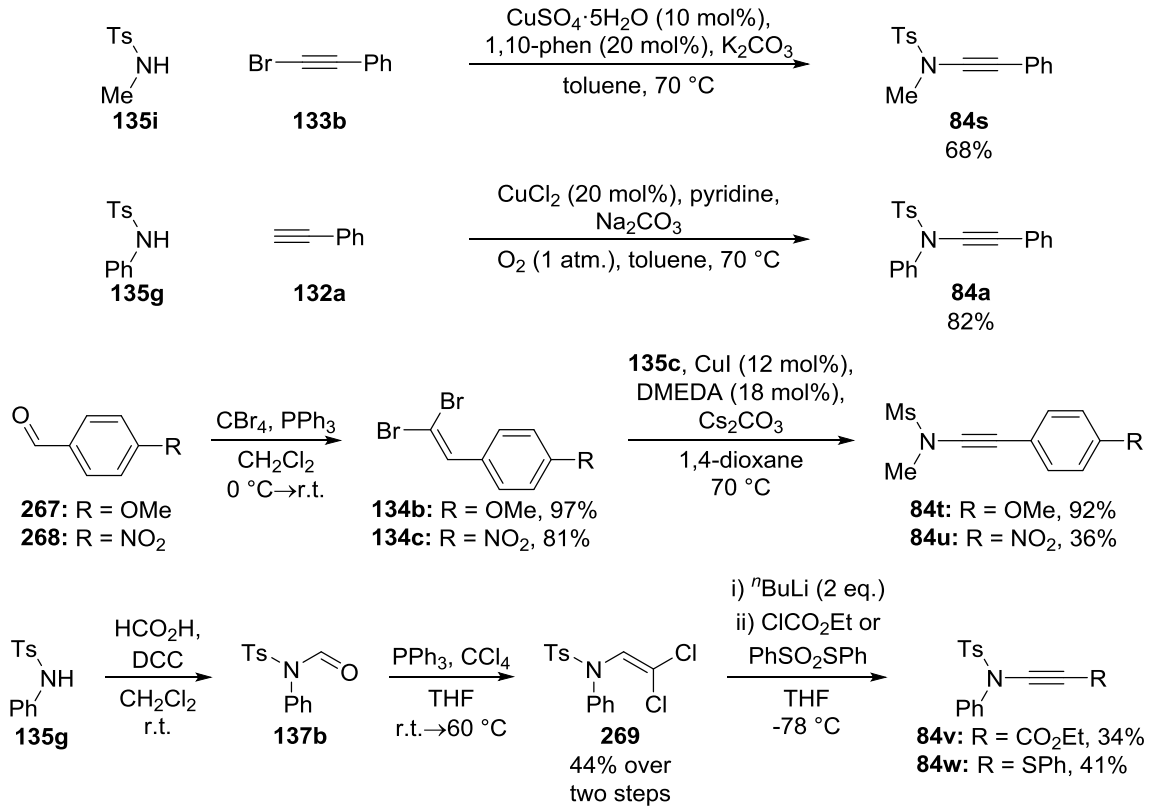

Scheme 68: Synthesis of ynamides for use in the oxazole formation/Diels-Alder reaction. Ynamide 84a was synthesised by Mickaël Dos Santos.[47c]

With several ynamides in hand, as well as **84n** and **171c** which were previously described (Chapter 2 – Schemes 42 and 45), the synthesis of oxo-bridged tetrahydropyridines **257e-l** was investigated (Scheme 69). The nature of combining two or more reactions into one process often makes it difficult to explain the relative reactivity of different substrates, as there are always several factors at play (efficiency of conversion of **84** to **256** and of **256** into **257**, as well as stability of both **256** and **257**). One particular problem in this case is that the amount of oxazole **256** remaining at the end of the reaction could usually only be roughly estimated. Levels of **256** could not be quantified by ^{1}H-NMR spectroscopic analysis of the crude reaction mixtures, due to overlap of the easily

identifiable resonances with either those of the product **267** or of unconsumed ylide **266d**. Attempts to isolate **256** were laborious and rarely gave pure oxazole.

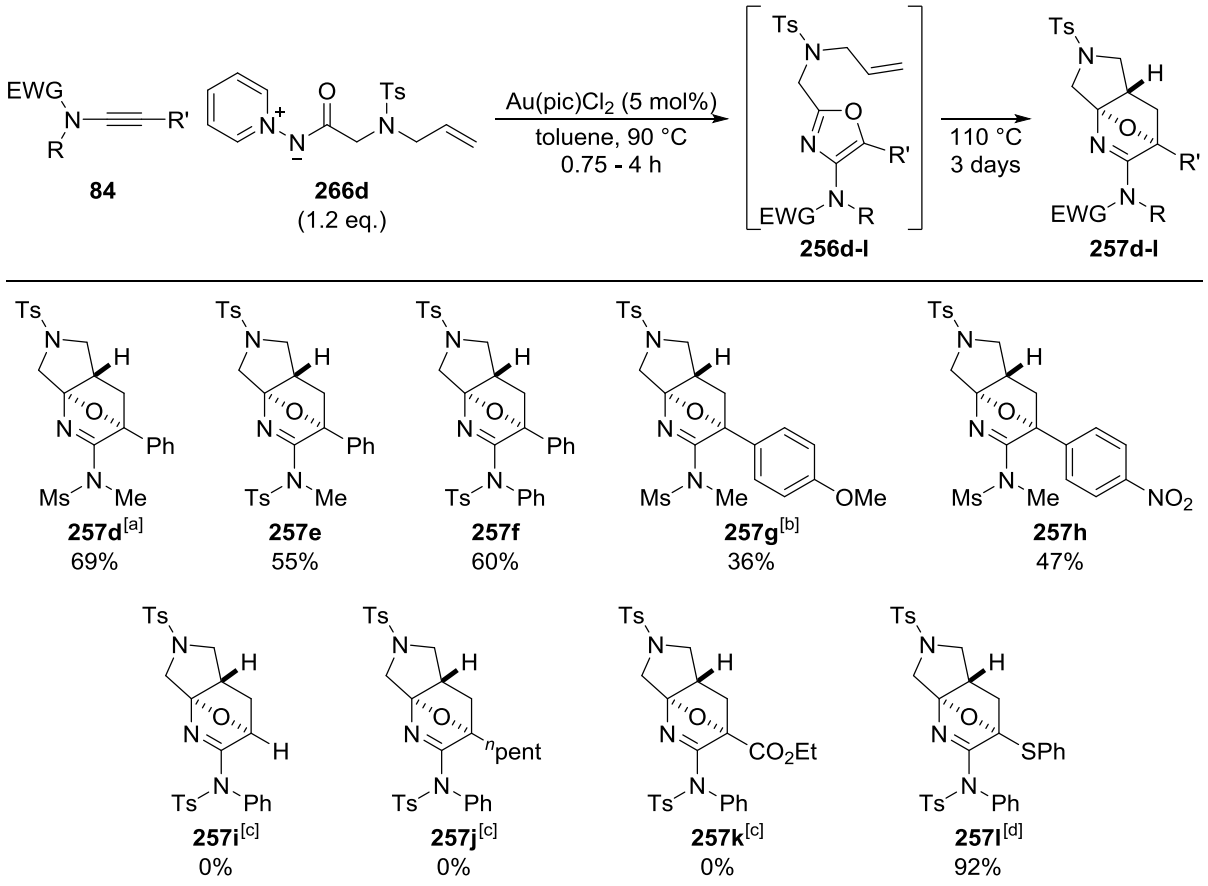

Scheme 69: Synthesis of oxo-bridged tetrahydropyridines from various ynamides. [a]: Result from Table 4 provided for comparison. [b]: Approx. 95% purity. [c]: Complex mixture from which no pure compounds could be isolated. [d]: Reaction stopped after 6 hours at 110 °C when all 256l was consumed as evidenced by TLC.

Increasing the size of the substituents on the nitrogen of the ynamide could disfavour the approach of the dienophile, however it could also affect the ability of the nitrogen lone pair to overlap with the π-system of the oxazole ring. Tetrahydropyridines **257e-f** were both formed in a reduced yield compared to **257d**, however the slightly improved yield of **257f** over **257e** means there is no obvious pattern in these results.

The low yield of **257g** is curious, as all of ynamide **84t** was consumed within 45 minutes and only <9% of impure oxazole **256g** was also isolated from this reaction. It may be that the electron-

rich aromatic substituent allows degradation of **257g** by facilitating cleavage of the adjacent C-O bond; indeed this product could not isolated with high purity, however no degradation products (pyridines or otherwise) could be isolated or identified. The reduced yield of **257h** compared to **257d** is expected, assuming the Diels-Alder reaction takes place under normal electron demand (in both cases the ynamide was consumed within 45 minutes at 90 °C, however the amount of remaining oxazole was not quantified).

Terminal ynamide **84h** was previously shown to be reactive in the oxazole synthesis (Scheme 43) and was cleanly transformed into one product (presumably oxazole **256i**) on reaction with **263d** within 45 minutes at 90 °C. The presence of a proton on the oxazole 5-position potentially opens up pathways for conversion of **257i** into a 3-hydroxypyridine (Scheme 53), however continued heating at 110 °C led to the formation of an extremely complex mixture from which no compounds could be isolated or identified. Similar behaviour was observed when ynamide **171c** was employed (further complicated by the presence of 1,2-C–H insertion products), and so none of product **257j** could be isolated.

The conversion of ynamides **84v** and **84w** into oxazoles has been demonstrated by Raju Jannupureddy, although the reactivity of ester-substituted ynamides was heavily dependent on the ylide with which they were partnered.[90] Reaction of **84v** with **263d** formed a complex mixture without full consumption of the ynamide over 90 minutes at 90 °C. Heating was continued for three days at 110 °C for consistency, but no pure compounds could be isolated after this time.

Ynamide **84w** was completely consumed within 45 minutes at 90 °C and, unlike in the other reactions, both oxazole **256l** and tetrahydropyridine **257l** were apparent by TLC analysis at this point. Continued heating at 110 °C for six hours led to complete consumption of the oxazole (this was not achieved within three days for any other reaction), and allowed **257l** to be isolated in an excellent yield.

As well as identifying some ynamides which are not well suited to this cascade process, this study indicates that the Diels-Alder reaction of these 4-amido oxazoles probably proceeds under normal electron demand given the reduced yield of **257h** compared to **257d** and the especially high reactivity of oxazole **256l**.

3.2.2.3: Diastereochemical assignment

Only one diastereoisomer of the tetrahydropyridines **257** was observed in each of the reactions described above. These have been assigned as the *exo* products based on the following observations. Tetrahydropyridine **257m** was synthesised by Matthew Ball and produced crystals suitable for single crystal X-ray diffraction, which confirmed the relative stereochemistry of this molecule (Scheme 70).

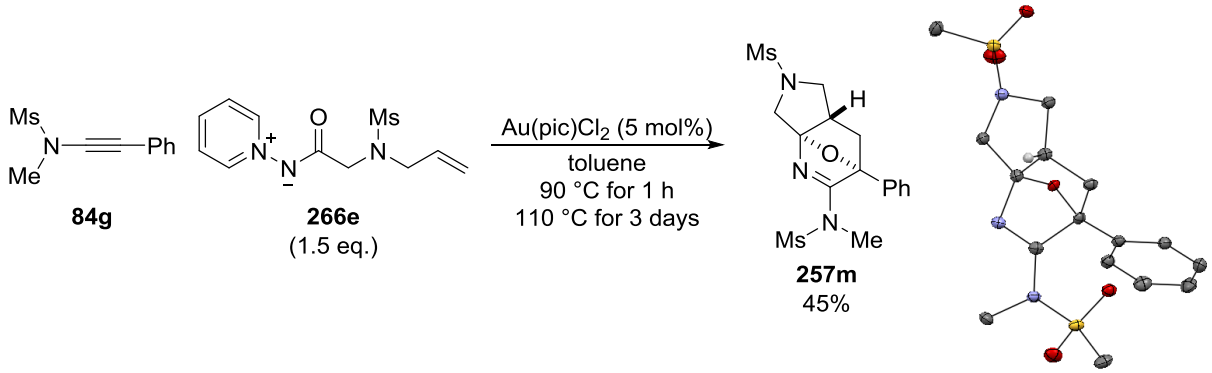

Scheme 70: Synthesis of an oxo-bridged tetrahydropyridine by Matthew Ball and its X-ray structure. Ellipsoids at 50% probability, hydrogens omitted except at the ring junction, X-ray data was obtained and solved by Dr Louise Male.

Key features of the ^{1}H- and ^{13}C-NMR spectra of the Diels-Alder adducts were then compared (Table 5). Only relatively small changes were observed in the chemical shifts of the proton and tertiary carbon at the ring junction were observed. The H-H coupling constants near to the ring junction were also very consistent across the products. Only **257l** showed notable deviation in this respect, however these changes are more likely due to the significantly different substituent (R' = SPh) in this compound, rather than a reversal of the diastereoselectivity in its formation. This data strongly suggests that the same relative stereochemistry is present in all the products **257a-m**.

Table 5: Comparison of NMR data for Diels-Alder adducts

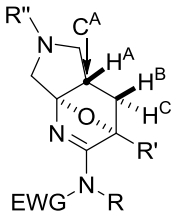

257

257	EWG	R	R'	R''	δC^A /ppm	δH^A/ ppm	$^3J(H^A\text{-}H^B)$/ Hz	$^3J(H^A\text{-}H^c)$/ Hz	$^2J(H^B\text{-}H^C)$ /Hz
257a[a]	Ms	Me	Ph	Boc	45.2, 44.5	2.62-2.48	-	-	-
257b[a]	Ms	Me	Ph	Cbz	45.2, 44.5	2.62-2.48	-	-	-
257c	Ms	Me	Ph	*p*-Ns	45.5	2.59-2.49	7.6	3.2	12.2
257d	Ms	Me	Ph	Ts	45.6	2.49-2.40	7.7	3.2	12.0
257e	Ts	Me	Ph	Ts	45.6	2.46-2.33	7.6	3.2	12.0
257f	Ts	Ph	Ph	Ts	45.6	2.53-2.44	7.6	3.2	12.0
257g	Ms	Me	4-OMe-C_6H_4	Ts	45.7	2.49-2.41	7.6	3.3	12.0
257h	Ms	Me	4-NO_2-C_6H_4	Ts	45.5	2.55-2.46	7.6	3.1	12.0
257l	Ms	Me	SPh	Ts	45.3	2.36-2.28	7.1	2.6	12.6
257m	Ms	Me	Ph	Ms	45.8	2.68-2.60	7.6	3.2	12.2

[a]: Due to the carbamate protecting groups two rotamers were observed in the NMR spectra of these compounds. As such, two values are given for δC^A and the H-H coupling constants could not be determined due to peak overlap.

3.2.2.4: Attempted synthesis of enantioenriched tetrahydropyridines from chiral starting materials

The tetrahydropyridines described so far have all been synthesised as a racemic mixture of a single diastereoisomer. The use of chiral starting materials should allow access to enantioenriched Diels-Alder adducts, however the formation of additional diastereoisomers would then be possible.

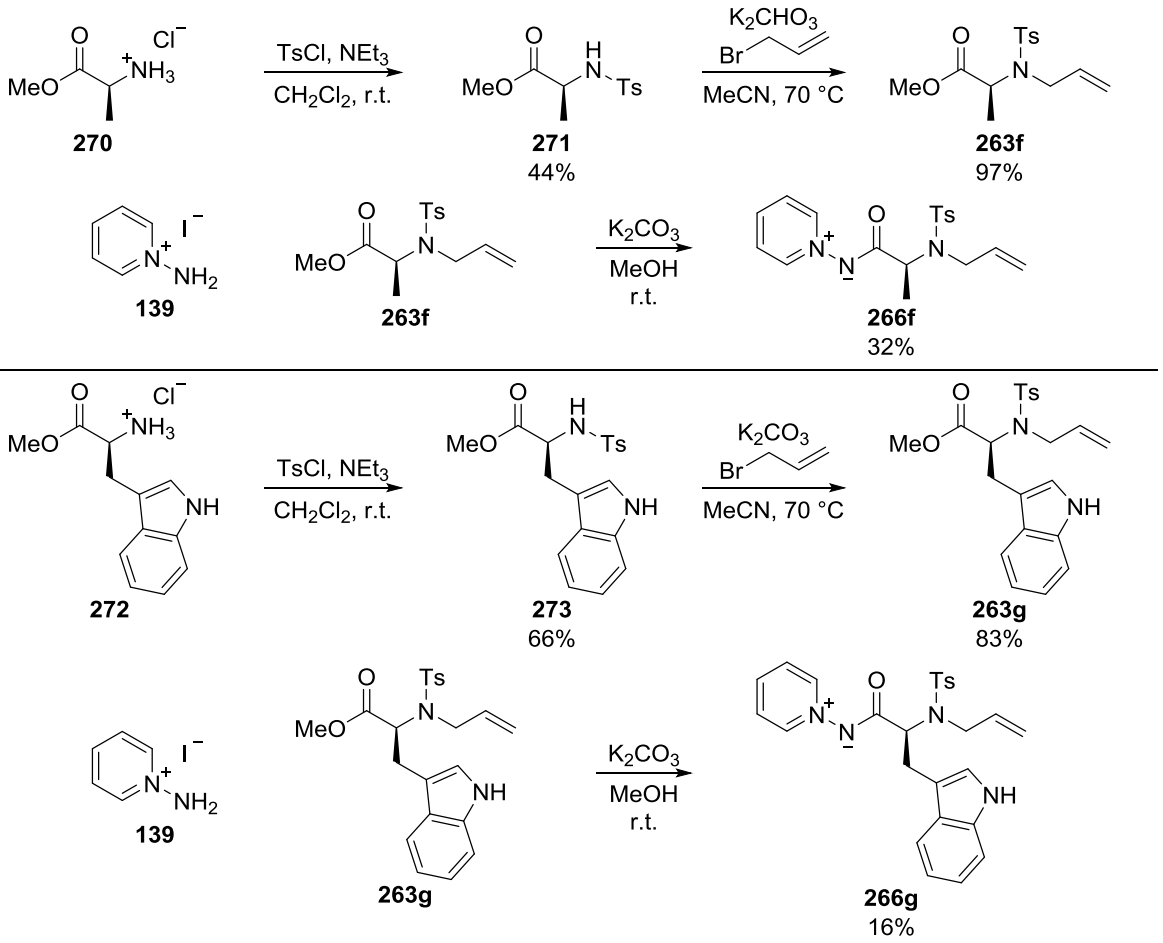

Scheme 71: Synthesis of ylides derived from proteced *N*-allyl alanine and *N*-allyl tryptophan.

The most obvious candidates for this strategy were ylides derived from amino acids other than glycine. Alanine- and tryptophan- based ylides **266f-g** were synthesised using the same methods as those described above (Scheme 71). Disappointingly the final step in each case was inefficient; the presence of large groups α- to the ester may disfavour substitution at this position. Purification of these substrates was also challenging and required a recrystallisation following flash column chromatography. Finally, given the previously encountered problem of possible racemisation of a

related compound (Scheme 37), the specific rotation of **266f** was disconcertingly low ($[\alpha]_D^{20}$ = −8.3 °dm^{-1}g^{-1}cm^3). This measurement could not be made for **266g** due to its lack of room temperature solubility in an appropriate solvent.

Ylides **266f-g** were then tested with ynamide **84g** in the cascade oxazole formation and Diels-Alder reaction (Scheme 72). Each reaction produced a mixture of two diastereoisomers (in a roughly 2:1 ratio), which presumably had the relative stereochemistry illustrated in general substrates **274** and **274'**. Whilst these compounds could be separated, all four products were contaminated with low levels of other unidentified impurities, and none showed any optical activity. The combined yield of the products **276** was also poor; this can be at least partially explained by the failure of this reaction to consume all of ynamide **84g**, which is possibly due to the steric bulk of the ylide or its low solubility. Although not properly quantified, the apparent ease with which these substrates underwent racemisation compared to **94f**/**151c** (Chapter 2 – Scheme 37) is intriguing, and likely due to the increased acidity of the proton α to an *N*-Ts group over an *N*-Boc group.

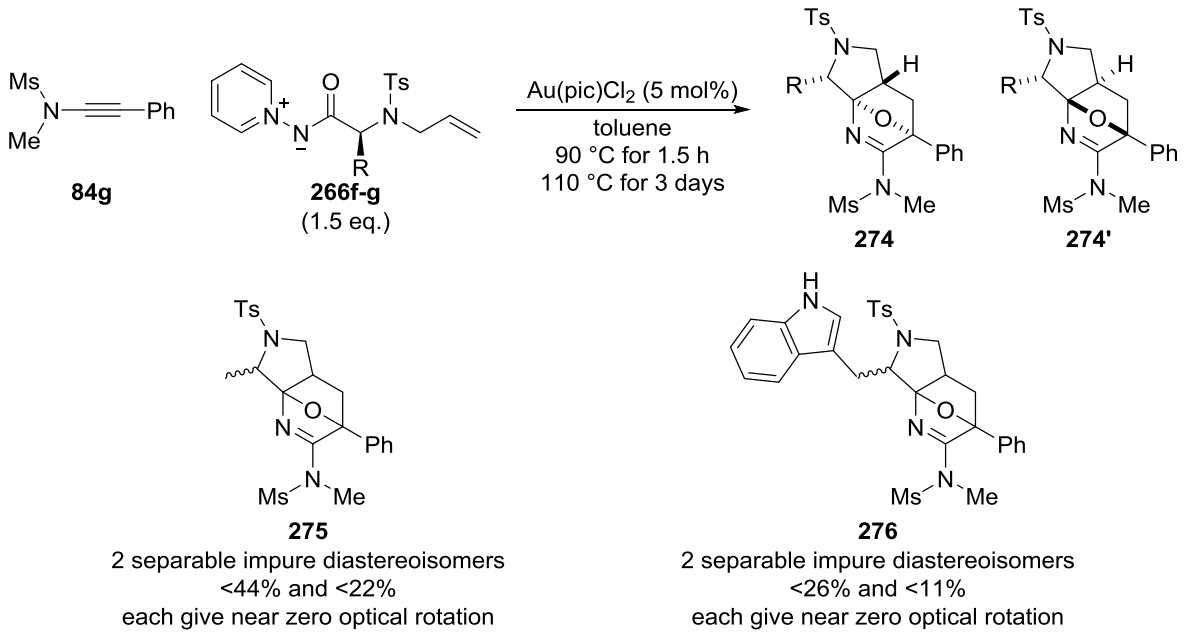

Scheme 72: Reactions of chiral ylides with an ynamide.

Given the low yield of the ylide synthesis, problems with the products' purification and probable racemisation, and the moderate diastereoselectivity of these reactions, no further investigations were undertaken with these substrates.

Chiral ynamide **84x**, derived from (-)-camphor sultam, was also tested in this reaction (Scheme 73). A much more promising diastereoselectivity of 4:1 was observed for the formation of tetrahydropyridines **277**, however the products were not easily separated in this case. Additionally, the overall recovery of this reaction was poor given that ynamide **84x** was all consumed within one hour as evidenced by TLC, but only <8% of the impure intermediate oxazole was isolated alongside products **277**. No products of competing reactions were identified.

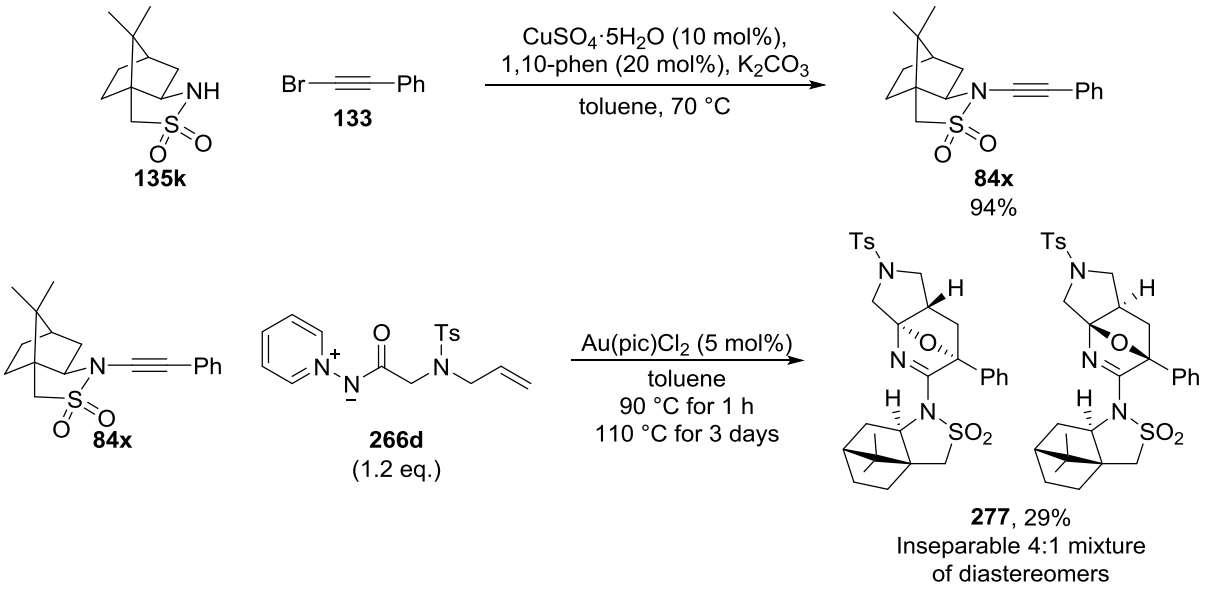

Scheme 73: Reaction of a chiral ynamide with ylide 263d.

3.2.2.5: Increased ring size

The final aspect of the Diels-Alder reaction which was investigated was the impact of increasing the length of the tether between the oxazole and the alkene; this would have the effect of increasing the size of the ring fused to the oxo-bridged tetrahydropyridine products. To this end, ylides **266h-i** were synthesised (Scheme 74).

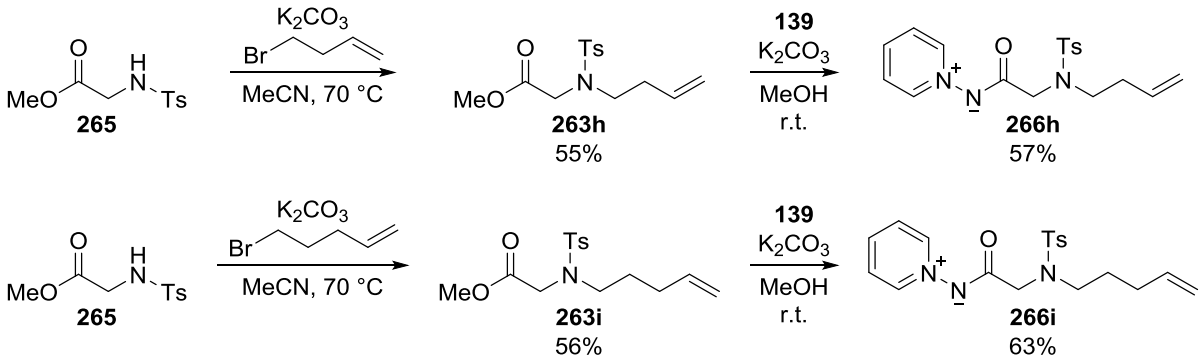

Scheme 74: Glycine-derived ylides with tethered alkenes.

The formation of a piperidine ring using **266h** was successful, furnishing **278** in a 52% yield (Scheme 75). Again only one diastereoisomer was observed and the X-ray structure of **278** revealed that it had the same relative stereochemistry as the products fused to pyrrolidine rings described above. The formation of 7-membered rings is known to be significantly more challenging than that of their 5- or 6-membered equivalents.[114] This was the case in the reaction of **266i** and ynamide **84g**, which were efficiently transformed into oxazole **279**, however no subsequent Diels-Alder reaction occurred.

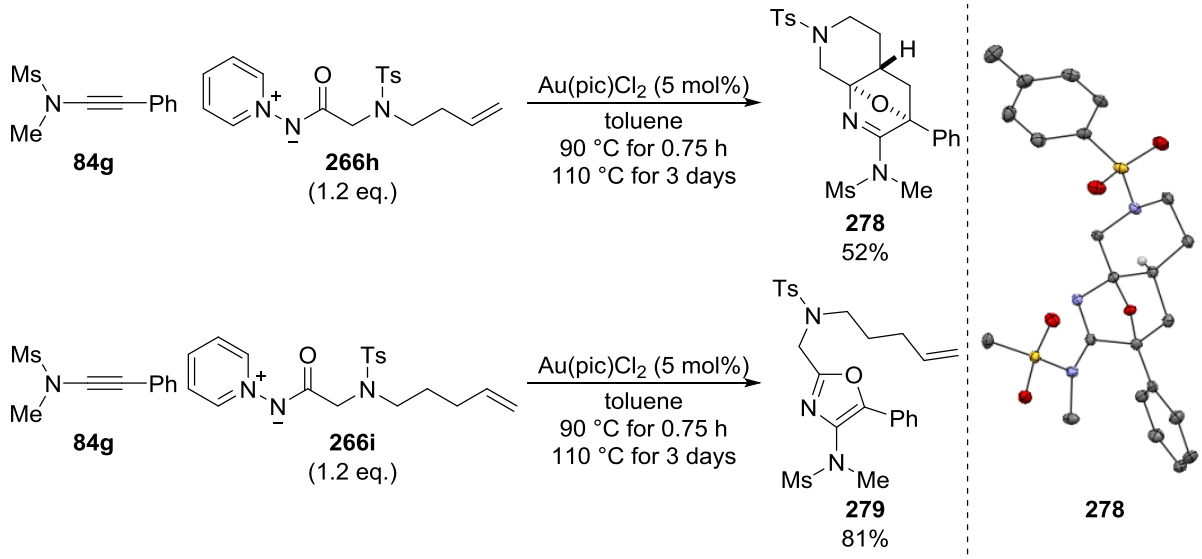

Scheme 75: *Left*: Synthesis of a Diels-Alder adduct fused to a piperidine. The reaction stops at the oxazole when a longer tether is used. *Right*: X-ray structure of 278. Ellipsoids at 50% probability, hydrogens omitted except at the ring junction, X-ray data was obtained and solved by Dr Louise Male.

3.2.3: Reactions of the Tetrahydropyridine Products

3.2.3.1: Treatment with acid

As base-catalysed dehydration of **257a** had been unsuccessful (Scheme 66), this reaction was instead attempted with **257d** using trifluoroacetic acid (Scheme 76), as described for similar substrates **195** (Scheme 55).[102c] No reaction of **257d** was observed, which can again be explained by the lack of an electron-withdrawing group on the tetrahydropyridine ring. In the case of **195** it is likely that the enol tautomer **281** assists in the in cleavage of the first C–O bond to give dihydropyridine **282**, which then readily undergoes dehydration. This pathway is not available to **257d**. This illustrates that whilst Diels-Alder reactions between oxazoles and unactivated alkenes are more challenging than with electron-deficient alkenes, they do result in products with considerably greater acid/base stability.

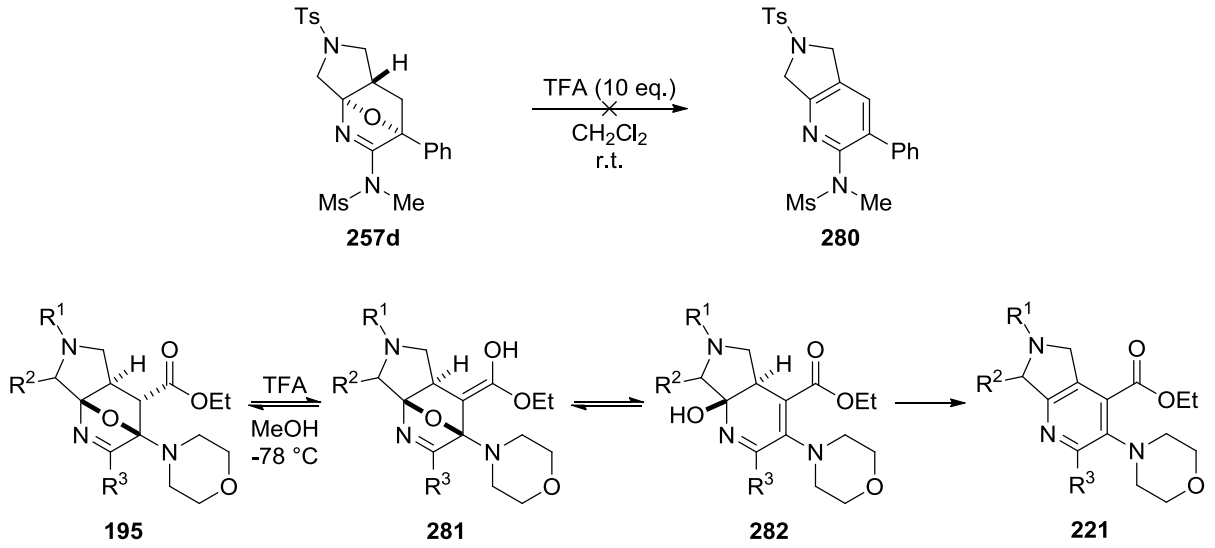

Scheme 76: *Top*: Treatment of 257d with trifluoroacetic acid does not result in dehydration. *Bottom*: Proposed mechanism for the dehydration of 195 described by Zhu and co-workers.[102c]

In contrast, **257d** was consumed within twenty minutes when treated with TsOH in methanol to generate hydration product **283**, the X-ray structure of which revealed it to be formed by hydrolysis of the amidine (Scheme 77). It is not clear whether this reaction was triggered by the use of the stronger acid or by the change in solvent.

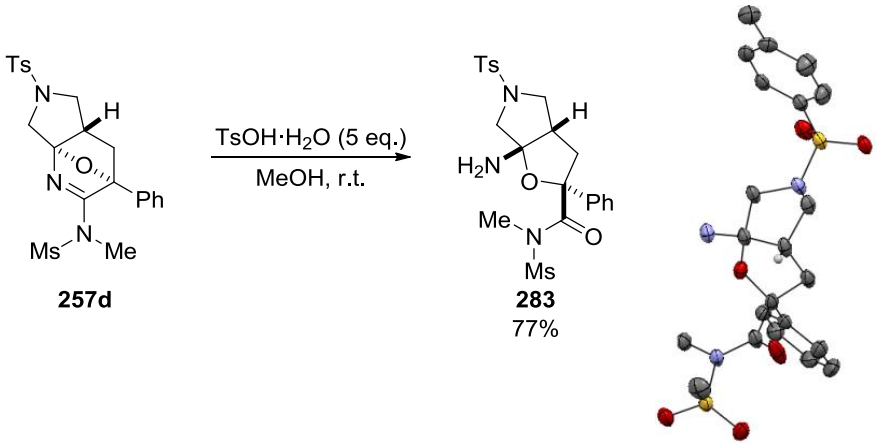

Scheme 77: *Left*: Acid-catalysed hydrolysis of the amidine. *Right*: X-ray structure of 283. Ellipsoids at 50% probability, hydrogens omitted except at the ring junction, X-ray data was obtained and solved by Dr Louise Male.

The hydrolysis of related cyclic amidines[115] and acetimidates[116] has previously been reported. The presence of the additional nitrogen or oxygen atom attached to the imine carbon prevents the reversal of these reactions from dominating, which is observed for simple six-membered cyclic imines, unless the primary amine in the product is trapped by another reagent.[117] As oxo-bridged tetrahydropyridines have not previously been synthesised with a heteroatom attached to the imine carbon, this appears to be the first example of the hydrolysis of such a C=N bond. The stability of **257d** towards acid-catalysed dehydration is also important to achieving this reactivity.

The efficiency and simplicity of this step makes for a powerful method for accessing substituted tetrahydrofurans fused to pyrrolidines in a diastereoselective fashion. Although this was achieved towards the end of the experimental work described in this thesis, a potential future line of enquiry would be to see whether the hydration reaction could be combined with deprotection of acid-sensitive protecting groups on the Diels-Alder product (eg. *N*-Boc on the pyrrolidine and/or *N*-PO(OR)$_2$ on the amidine).

3.2.3.2: Reduction with $LiAlH_4$

Amidine **257d** underwent an interesting reaction with $LiAlH_4$, where reduction of the amidine functionality was followed by hydrogenolysis of both the resulting aminal and the hemiaminal ether to give **284**, which was isolated as a single diastereoisomer (Scheme 78). In order to obtain X-ray quality crystals **284** was treated with HCl, allowing the relative stereochemistry of the resulting salt to be unambiguously determined.

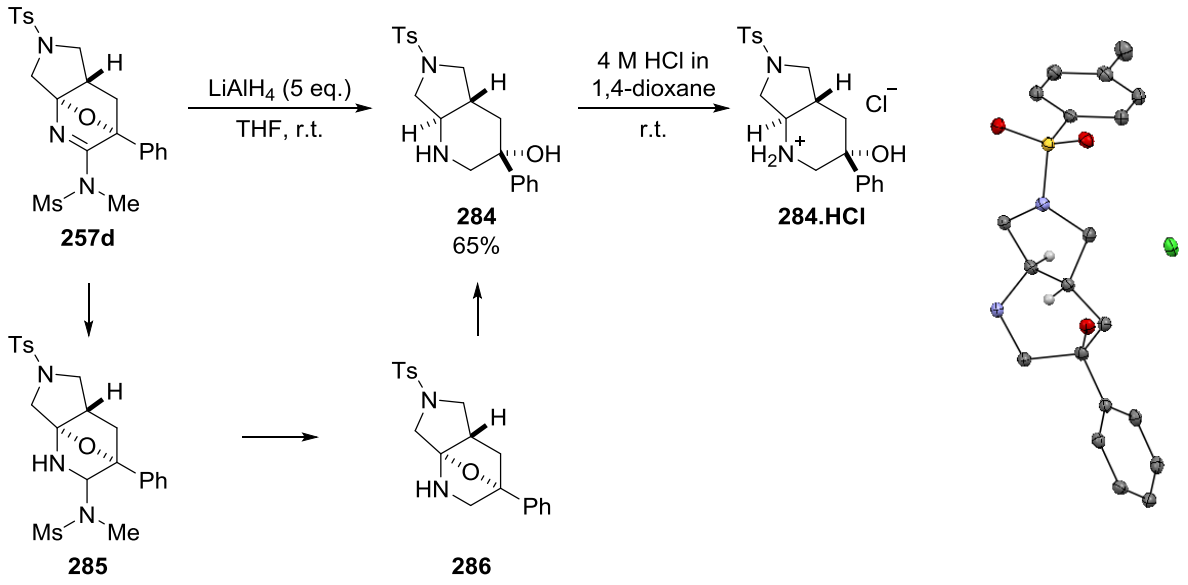

Scheme 78: Reduction of 257d with $LiAlH_4$ and X-ray structure of 284.HCl. Ellipsoids at 50% probability, hydrogens omitted except at the ring junction, X-ray data was obtained and solved by Dr Louise Male.

As with the acid-catalysed hydration, this reaction opens up a number of possibilities which there was not time to investigate. These include testing alternative reduction conditions (such as hydrogenation) in an effort to improve the yield, and attempting the reaction with *N*-Cbz protected substrates such as **257c** to give deprotected pyrrolidines fused to piperidines. It also shows a potential advantage of optimising the diastereoselective synthesis of the oxo-bridged tetrahydropyridines from chiral ynamides (Scheme 73), as this should allow a chiral auxiliary approach to enantioenriched products of the type **284**. It is noteworthy that the bicyclic system in **284** can also be found in the antibacterial agent Moxifloxacin, albeit with different relative stereochemistry at the ring junction.[118]

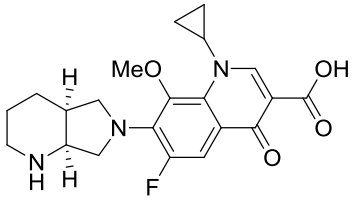

Moxifloxacin

Figure 9: Chemical structure of the antibacterial agent Moxifloxacin.

3.2.4: Conclusion

The reaction of ynamides with pyridine-*N*-aminides tethered to alkenes allows the synthesis and Diels-Alder reaction of oxazoles in one-pot to form oxo-bridged tetrahydropyridines fused to pyrrolidines or piperidines as single diastereoisomers. Overall, good yields are obtained considering the rapidly increased complexity of the products, however the Diels-Alder reaction only reached completion when the intermediate oxazole had a thioether substituent at the 5-position.

Acid-catalysed hydration of the products was demonstrated, as was their reduction by $LiAlH_4$, providing diastereoselective routes to saturated bicyclic systems. The possibility of carrying out the Diels-Alder reaction using alkynes as the dienophile, in order to give furan-containing products, was also confirmed.

Future work to develop the substrate scope of this reaction could focus on several areas. Altering the nature of the tether between the alkene and the oxazole may allow access to oxo-bridged tetrahydropyridines fused to alternative heterocycles, whilst further investigation of more substituted alkenes could also be undertaken. It is likely that the Diels-Alder reaction could be accelerated by the use of more electron deficient alkenes, although the increased steric demand of these substrates may be problematic. Finally, deprotection of the amides present in the Diels-Alder adducts, as well as the products of their hydration or reduction, could also be investigated.

CHAPTER 4:

SYNTHESIS OF NOVEL OXAZOLE-ANNULATED IMIDAZOLIUM SALTS AND INVESTIGATION OF THEIR ORGANOMETALLIC CHEMISTRY

4.1: Introduction: NHCs Fused to Aromatic Rings

Nucleophilic heterocyclic carbenes (also knowns as N-heterocyclic carbenes or NHCs) **287** are carbenes stabilised by flanking heteroatoms which are commonly employed either as organocatalysts[119] or as ligands in transition metal catalysis;[120] their most common classes, **288**-**291**, are shown in Figure 10.

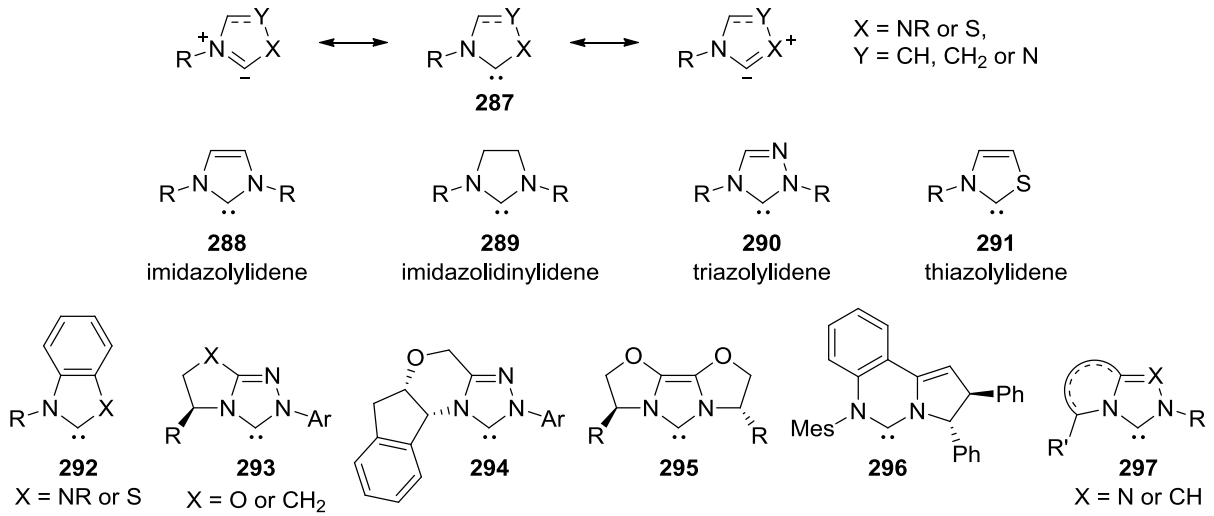

Figure 10: Common structures for monocyclic and polycyclic NHCs.

Polycyclic NHC systems have attracted considerable interest,[121] these include benzimidazolylidines and benzthiazolylidines **292** where the steric effect of the additional benzene ring is small; however variation of its substituents can exert a measurable electronic impact.[122] Among structures containing saturated ring systems 1,5-fused to the NHC, **293** and **294** have provided extremely successful architectures for asymmetric organocatalysis.[123] Promising enantioselectivities have also been achieved using ligands such as **295** and **296** in transition metal catalysis.[124] These ligands rely on the influence of stereogenic centres near to the ring junction, allowing the formation of a chiral environment which is rigid and well-defined in the area close to the carbene, the lack of which is often supposed to be a reason for poor asymmetric induction from other chiral NHCs.[125]

By contrast the 1,5-annulation of aromatic rings, as in **297**, puts the substituent *ortho* to the ring junction (R') in the same plane as, and close to, the carbene and any metals to which it is bound. This allows the design of ligands **297** where the R' substituent has a predictable steric impact, or functions as a second donor atom in bidentate ligands. Additionally the fused aromatic ring in **297** may be used to tune the electronic properties of the NHC.[126]

The synthesis of carbenes **297** and their respective azolium salts, as well as their applications as ligands is discussed in this introduction; whilst novel imidazolium salts which are fused to oxazoles are introduced in the results and discussion for this chapter.

4.1.1: Synthesis of Imidazolium Salts Fused to Aromatic Rings

The majority of imidazolylidenes fused to aromatic systems are accessed *via* imidazo[1,5-a]pyridinium salts **298**, which are generally synthesised using one of three routes (Scheme 79).

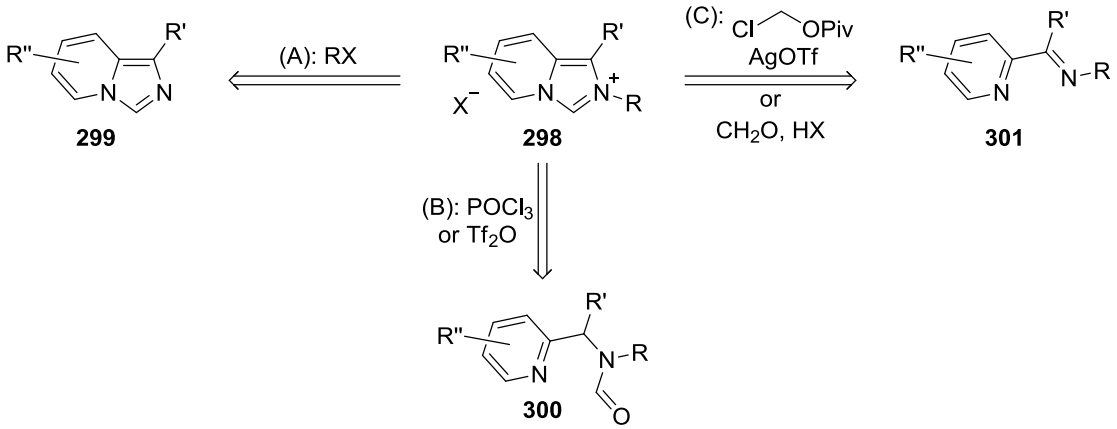

Scheme 79: General routes to imidazo[1,5-a]pyridinium salts.

N-Alkylation of imidazo[1,5-a]pyridine using methyl iodide (route A), was first described by Miyashita and co-workers in 1996,[127] although few experimental details were given. The Lassaletta group later showed that this approach was very efficient in the synthesis of salts of type **303**, although it was most suitable for simple and easily accessed imidazopyridine starting materials with

unhindered alkyl halides (Scheme 80).[128] Kunz and co-workers expanded this methodology to allow the synthesis of bidentate NHC precursors **305** and **306**.[129]

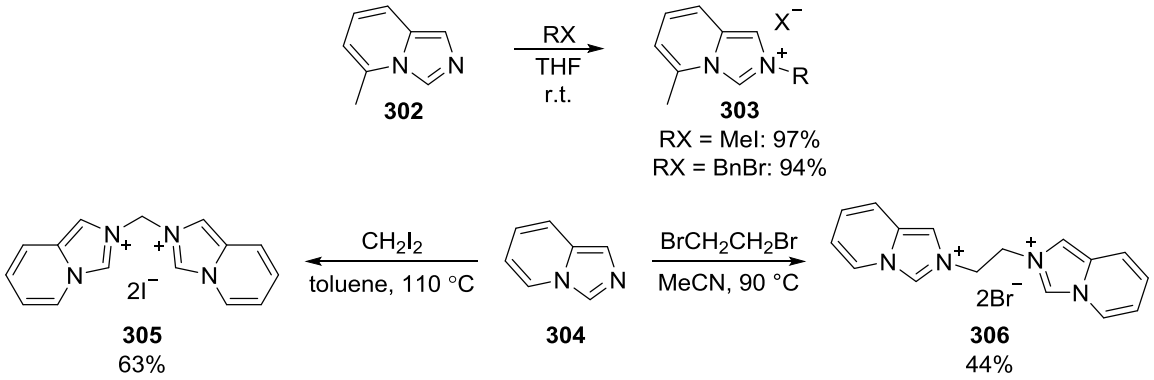

Scheme 80: Alkylations of imidazopyridines (Route A).[128-129]

Lassaletta and co-workers also described a modified Vilsmeier-Haack reaction (Scheme 79: route B), which allowed direct formation of the imidazolium ring onto pyridines or quinolines, with a range of *N*-substituents having been prebuilt into the formamide moiety (Scheme 81).[128] Where necessary, the resulting imidazolium chlorides **308** could also be converted to their respective PF_6 salts **309**. Variations on this technique have recently been described in which triflate salts such as **311** were synthesised from the same starting materials by using triflic anhydride, leading to a reduction in the required reaction temperature compared to the use of phosphoryl chloride.[130]

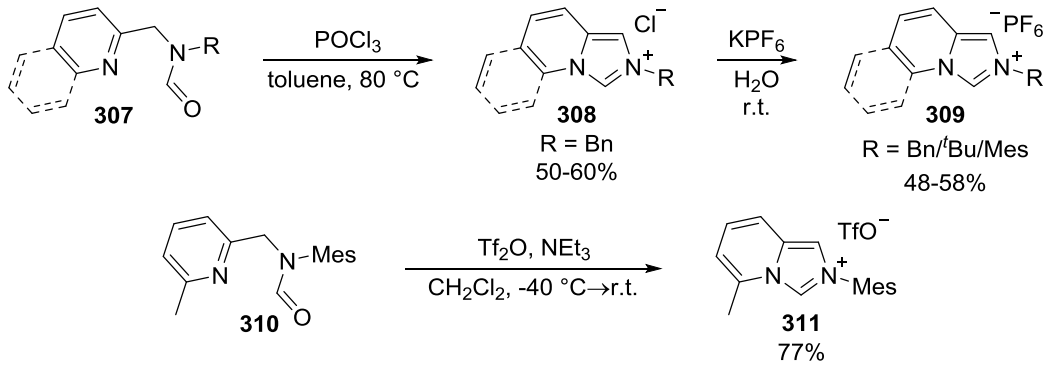

Scheme 81: Synthesis of imidazolium rings from formamides (Route B).[128,130b]

Glorius and co-workers introduced the final method, (Scheme 79: route C), where iminopyridines **313** were treated with chloromethyl pivalate (Scheme 82).[131] Suzuki couplings could be carried out using one of these products **315**, allowing significant variation at the substituent close

to the masked carbene through a divergent route. It is noteworthy that **316b** appeared to exist as a mixture of two atropisomers, however attempts to separate these were unsuccessful. The combination of chloromethyl pivalate and silver(I) triflate has since been employed to produce optically active derivates **318**,[132] and the first thiazole-annulated imidazolium salt **320**.[133]

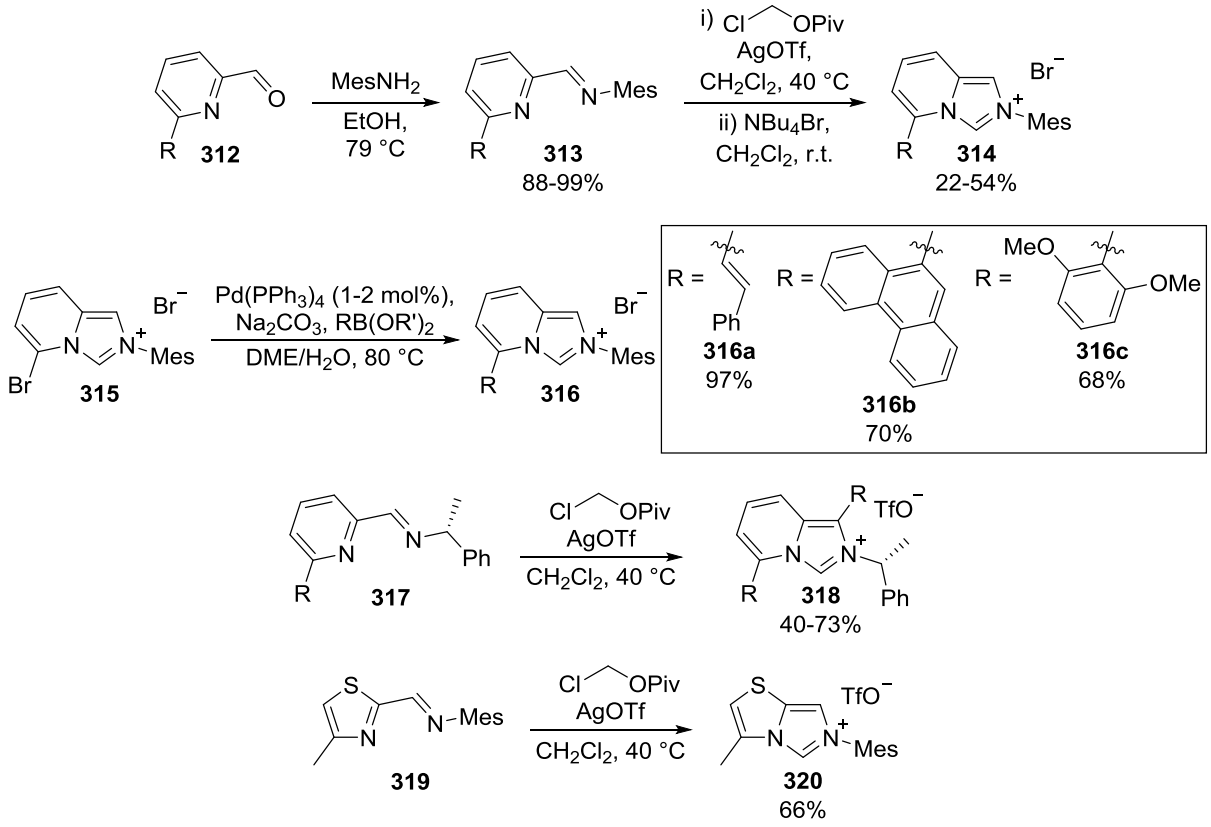

Scheme 82: Synthesis of imidazolium rings using chloromethyl pivalate (Route C).[131-133]

The formation of monocyclic imidazolium salts **321** from bisimines **322** is typically carried out using formaldehyde and acid (Scheme 83).[134] The use of iminopyridines **301** as bisimine equivalents is attractive, as these can be readily prepared from picolinaldehydes, and the application of this route to the synthesis of imidazopyridinium salts and their derivatives has become relatively common, such as in the synthesis of **325** and **328**.[135] A one-pot procedure for the rapid construction of the imidazolium ring from picolinaldehyde derivatives **329** and primary amines has also been developed,[136] this strategy was later applied to the synthesis of bidentate NHC precursor **332**.[137]

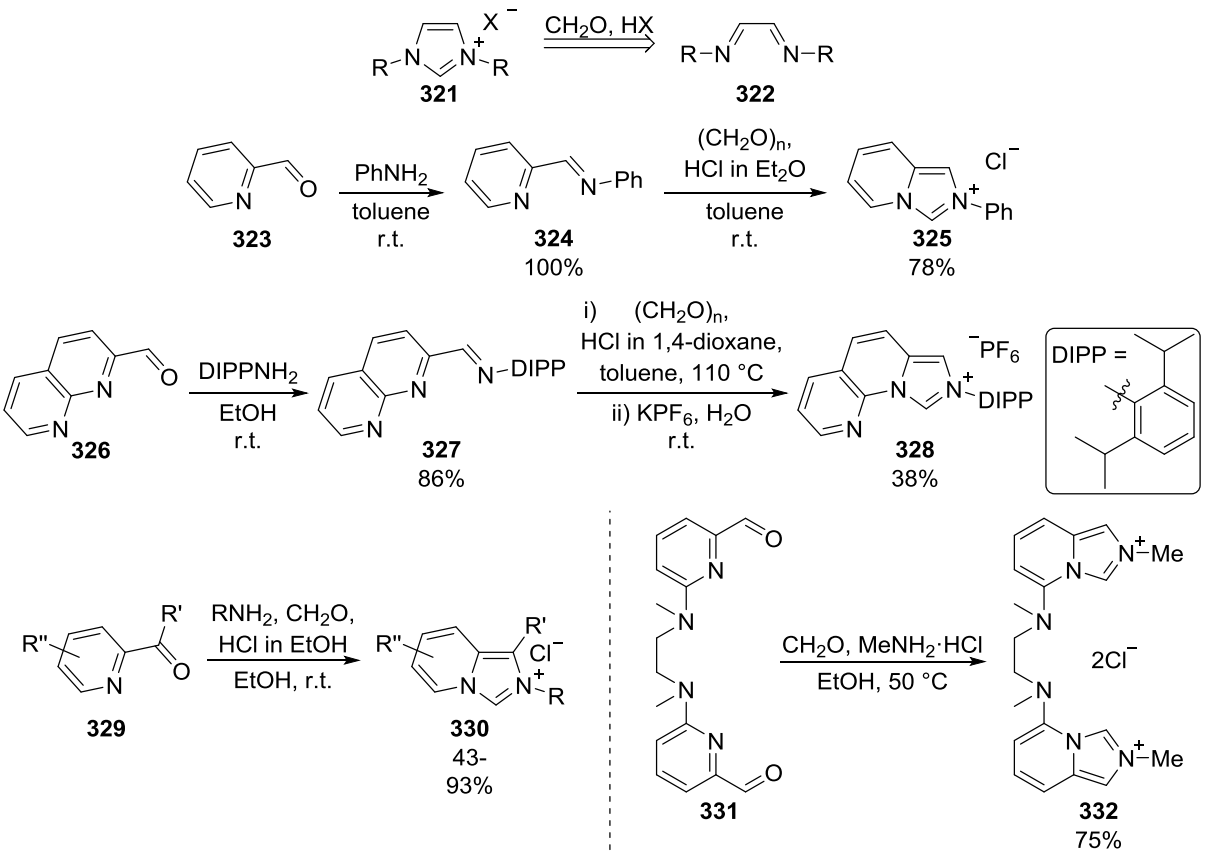

Scheme 83: Construction of imidazolium rings using formaldehyde (Route C).[135-137]

4.1.2: Isolation of Resulting Carbenes

Many NHCs are stable enough to be handled under an inert atmosphere, some even at high temperatures.[138] Lassaletta's imidazolium salts **333** provided the first precursors for isolation and characterisation of free carbenes fused to an aromatic system.[128] Interestingly, the presence of an *ortho*-substituent on the pyridine ring was essential to confer room-temperature stability on carbenes **334**, perhaps to prevent dimerization, however this problem was avoided by Kunz and co-workers by handling **336** at low temperature.[139]

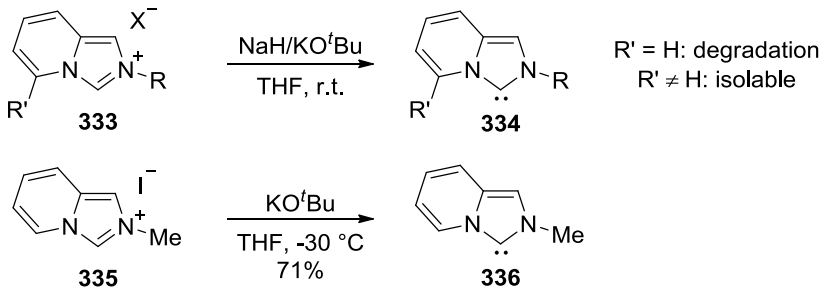

Scheme 84: Isolation of free carbenes.[128,139]

4.1.3: Applications as Ligands

Many of the azolium salts described above were subsequently transformed into their respective NHC-metal complexes. The impact of a substituent next to the ring junction was first described by Glorius and co-workers, where the X-ray structure of iridium complex **328** showed secondary interactions between the metal and the proximal benzene ring (Scheme 85).[131] Additionally, of the ligands described in this work, the palladium complex generated *in situ* from the most sterically demanding imidazolium salt **316b** was the most effective in the Suzuki coupling of a hindered aryl chloride **329**.

Recently the Lassaletta group reported the synthesis of silver(I) complex **334**, alongside several gold, silver and copper complexes featuring related ligands.[140] In **334,** large substituents, both adjacent to the ring junction and on the other nitrogen of the NHC resulted in, by one measure, the most sterically crowded monodentate NHC-metal complexes described to date (for discussion of the percentage buried volume (%V_{bur}) method see page 106).

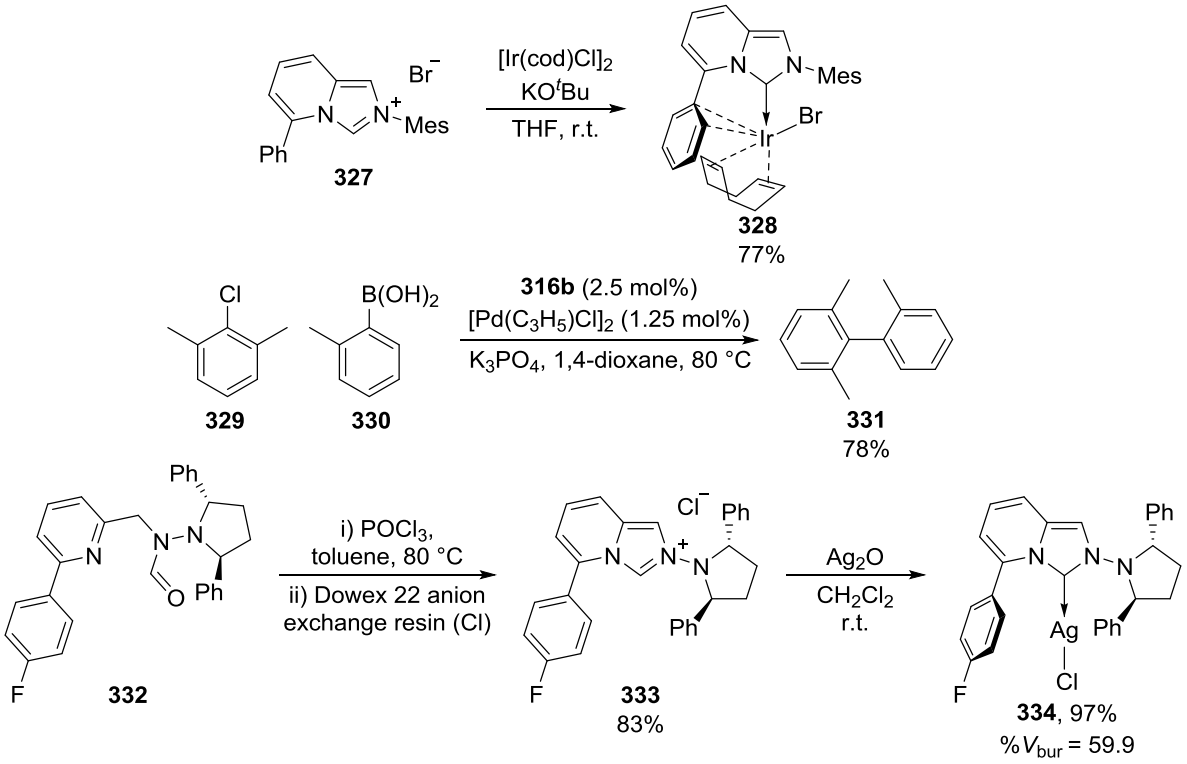

Scheme 85: Use of imidazolylidenes with bulky substituents next to the ring junction.[131,140]

The use of appropriate substitution next to the ring junction can also allow the design of multidentate ligands such as those featured in **335**,[141] **336**,[135c] and **337**[137] (Figure 11). In each case the N–M bond length suggested a relatively weak interaction (for comparison a (1,10-phenanthroline)Cu(I) complex related to **335** had average N–Cu bond lengths of 2.05 Å).[141]

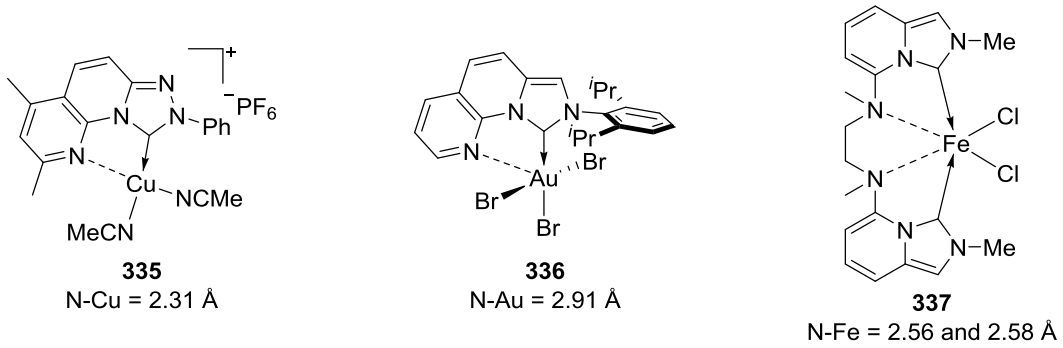

335
N-Cu = 2.31 Å

336
N-Au = 2.91 Å

337
N-Fe = 2.56 and 2.58 Å

Figure 11: Metal complexes featuring multidentate ligands.[135c,137,141]

Many of the more interesting applications of these ligands are in asymmetric transition metal catalysis. There has been considerable interest in the copper-catalysed hydroboration of enones **338**. The results of several successful attempts at this reaction are summarised in Table 6, however it must be noted that differences in the conditions used and substrates tested makes direct comparison difficult. Among the most successful chiral ligands employed in this process are **341**[142] and **296**,[124d] investigated by the Hoveyda and McQuade groups respectively. However results with the imidazopyridine-derived carbene **342a** were similarly impressive; interestingly it proved significantly more selective than the less sterically demanding ligand **342b**.[143] The authors proposed a model for this selectivity where the key intermediate **344** was disfavoured compared to **345** due to interactions between the alkene's substituents and bulky parts of the ligand (specifically the methyl group on the pyridine unit and *tert*-butyl group on the oxazoline, Figure 12). The β-pinene-derived carbene **343** was also investigated by Wang and co-workers, for which a modest enantioselectivity was observed.[135d]

Table 6: Asymmetric β-borylation of enones catalysed by (NHC)Cu(I) complexes.

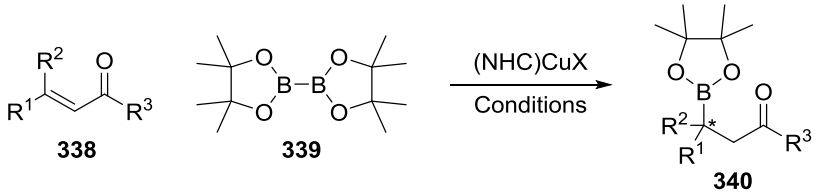

Entry	Ligand	R^1	R^2	R^3	Average Yield (best yield)	Average ee (best ee)	Ref.
1[a]	**341**	Ar or alkyl	Me or Et	Ph, Me, OEt or SEt	83% (98%)	83% (99%)	[142]
2	**296**	Ar or alkyl	H	OAlkyl	91% (95%)	91% (96%)	[124d]
3[b]	**342a**	Ar or alkyl	H	OAlkyl	85% (95%)	92% (97%)	[143]
4	**343**	Ph	H	OEt	72%	62%	[135d]

[a]: The lower average yields and enantioselectivities for Entry 1 must be set against the wider substrate scope which was investigated in this work. [b]: The products **340** were oxidised to their respective alcohols using $NaBO_3 \cdot 4H_2O$ before determination of the yield and enantioselectivity.

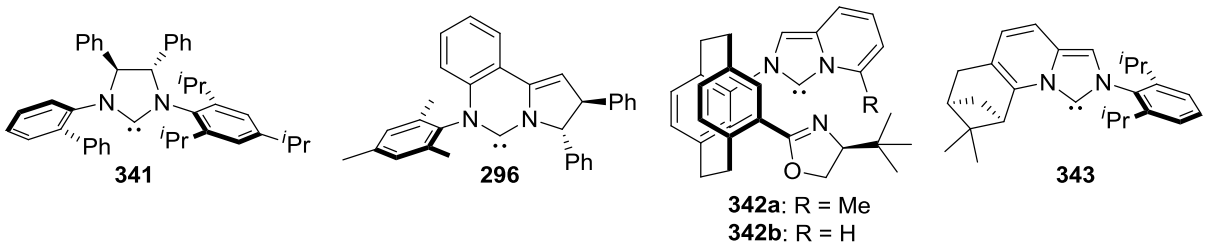

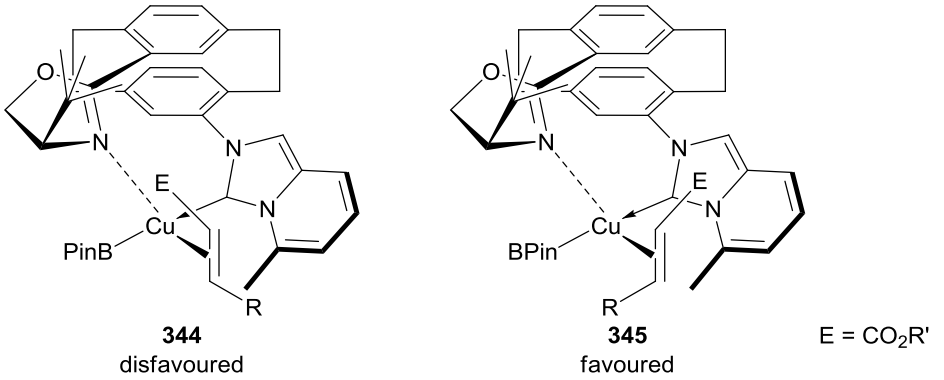

Figure 12: Selectivity model for Cu(I)-catalysed β-borylation of enones using ligand 342a.[143]

The Fernández and Lassaletta groups have investigated several chiral NHCs with *N*-linked thioethers as C-S ligands in transition metal catalysis.[144] Palladium complex **346** showed promising enantioselectivity in an allylic substitution reaction to form **347** (Scheme 86),[144b] however an enantioexcess of 98.5% for this reaction was reported in 1993 using a bidentate chiral oxazoline based N-P ligand.[145]

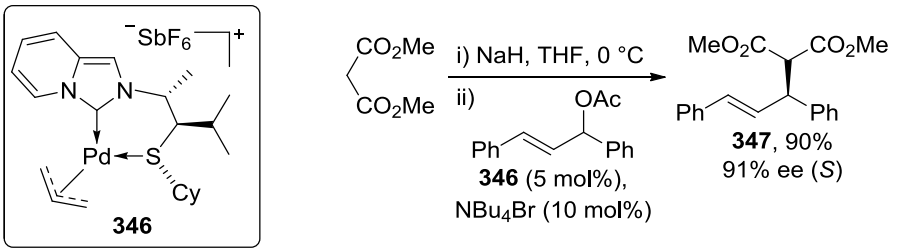

Scheme 86: Allylic substitution of 1,3-diphenylpropenyl acetate with dimethyl malonate.[144b]

A particularly exciting new ligand scaffold was recently reported by Lassaletta and co-workers. The ligand **351** employs a triazolylidene fused to an isoquinoline bearing a naphthyl substituent, placing the metal in a rigid chiral pocket (Scheme 87).[146] **(351)AuCl** was an impressive precatalyst for the enantioselective Diels-Alder reaction of allenamide **355**, outperforming several gold complexes bearing NHCs **352-354** which have been successful in other areas (Table 7).[147]

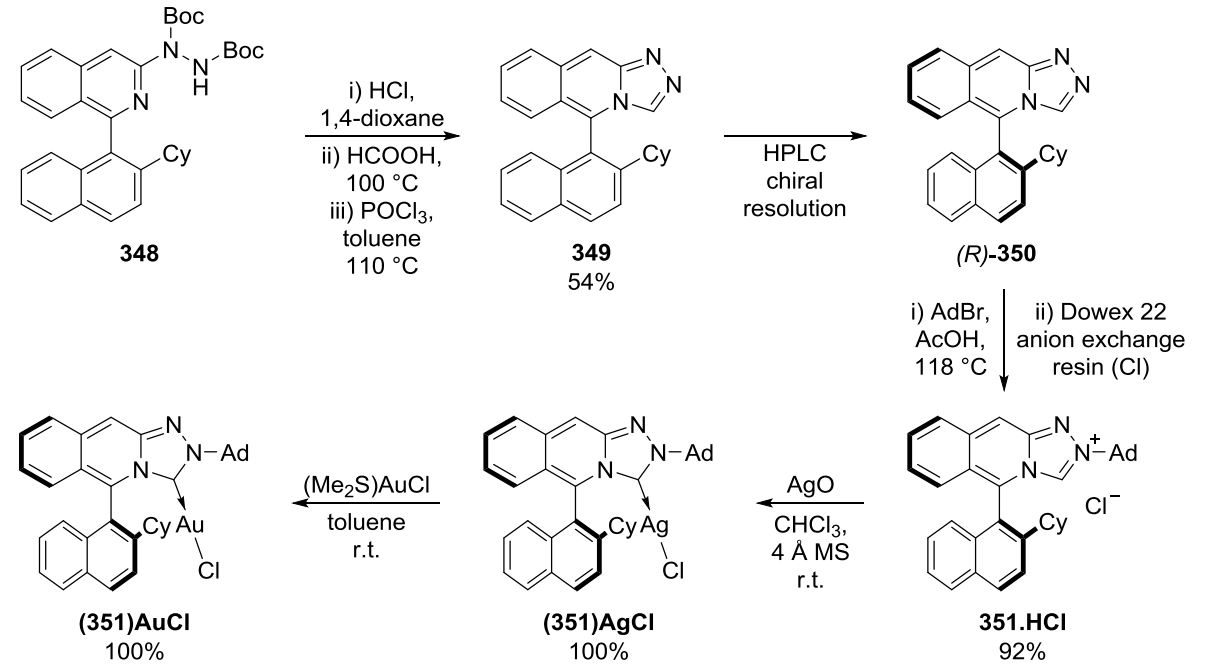

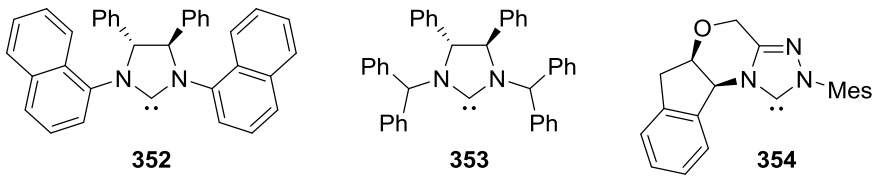

Scheme 87: ***Top:*** **Synthesis of an axially chiral gold complex.** ***Bottom:*** **Other chiral ligands used for comparison.**[146]

Table 7: Catalyst performance in the enantioselective Diels-Alder reaction of an allenamide.

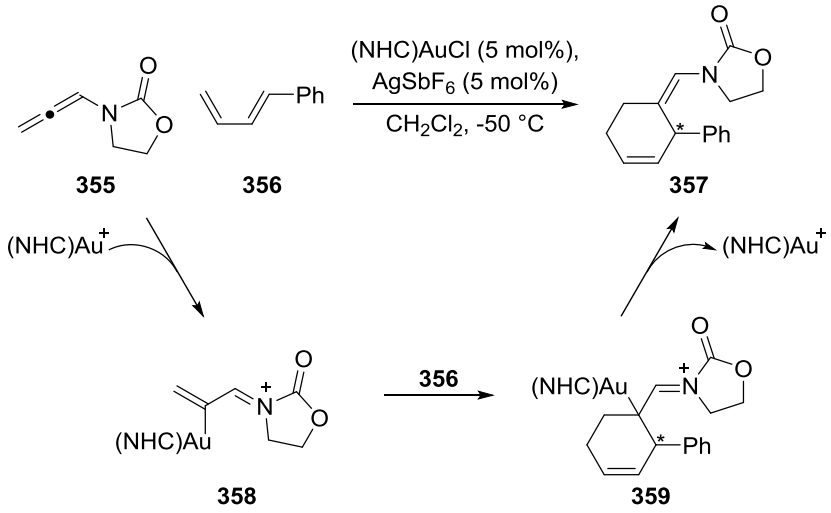

(NHC)	Yield	ee
351	81%	90%
352	76%	23%
353	51%	24%
354	91%	16%

Minor optimisation of the reaction conditions allowed a family of products **362** to be synthesised in good yields with excellent enantioselectivities (Scheme 88).

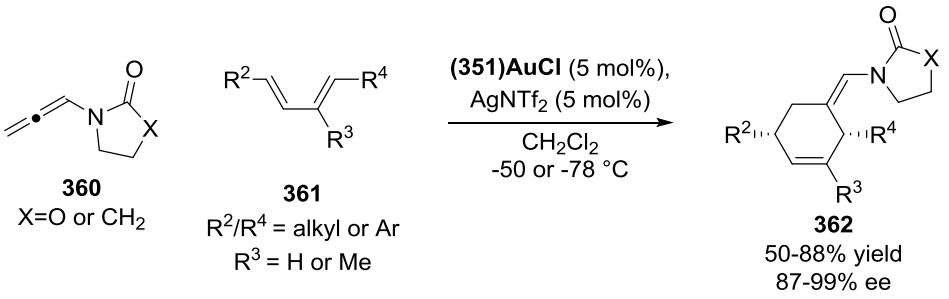

Scheme 88: Optimised conditions for the enantioselective Diels-Alder reaction of allenamides.

4.1.4: Conclusion

NHCs fused to additional aromatic rings (usually a pyridine derivative) have increased in prominence since the introduction of convenient methods for their synthesis from 2005.[128,131] Their planar geometry forces substituents *ortho* to the ring junction to sit alongside the carbene and any metals to which it is bound; this allows the design of ligands with versatile and predictable rigid steric environments.

The results and discussion section of this chapter describes efforts to synthesise novel imidazolium salts which are fused to oxazoles, and their respective metal complexes. The ligands'

steric and electronic properties have been quantified, and a preliminary study of their reactivity has been investigated in the gold-catalysed hydration of an unsymmetrical alkyne.

4.2: Results and Discussion

4.2.1: Ligand Design

Given the convergent nature of the gold-catalysed oxazole synthesis it was envisioned that oxazole-annulated imidazolium salts of the type **363.HX** could be rapidly constructed from an appropriately highly functionalised oxazole **364** (Scheme 89). These salts could be converted into their respective NHC-metal complexes, in which the amide would be placed close to the metal, allowing the design of tuneable steric environments. Additionally, this would be the first example of an NHC fused to an oxazole, and would therefore potentially have interesting electronic properties which may be affected by varying the oxazole's substituents.

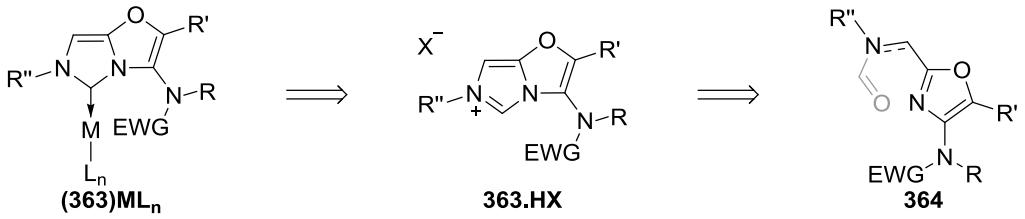

Scheme 89: Proposed route to oxazole-annulated NHCs.

4.2.2: Synthesis of Imidazolium Salts

As shown in the introduction to this chapter, there are several possible strategies for the annulation of imidazolium rings to nitrogen-containing heterocycles. In order to accomplish this from oxazoles, the first challenge was to incorporate appropriate functionality into the oxazole 2-position, which would require the synthesis of a similarly functionalised pyridine-*N*-aminide, and its use in gold catalysis. The relatively low nucleophilicity of the oxazole nitrogen, in comparison to that of pyridines (on which the annulation of imidazolium rings has most often been demonstrated) was also a potential issue.

4.2.2.1: Attempted synthesis of imidazolium salts from anilines

The first route to an imidazolium salt of type **363.HX** investigated was to attempt the annulation of the imidazolium ring onto an oxazole tethered to a secondary amine or aniline **365**, which would be derived from an ylide of type **366** (Scheme 90).

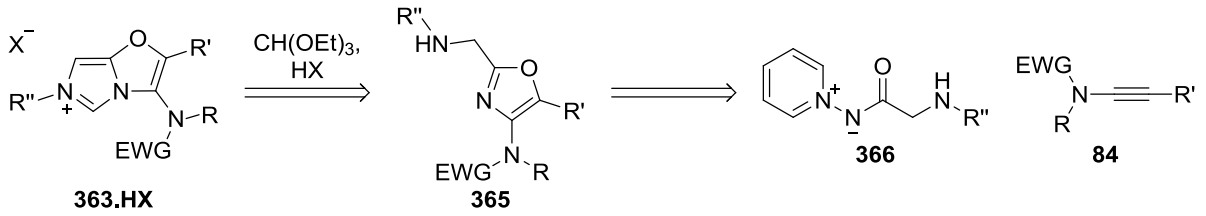

Scheme 90: Route to an imidazolium salt using an oxazole tethered to an amine or aniline.

Previous attempts to access ylide **94h**, bearing a secondary amine, gave an impure product which could not be used in gold catalysis (Chapter 1 – Scheme 33 and 35). In contrast, the use of a bulky aniline, which was ideal for incorporation into NHCs, was significantly more successful. The synthesis of ylide **94p** in two steps from commercially available reagents proved straightforward (Scheme 91). Pleasingly this unprotected aniline was tolerated by the gold-catalysed oxazole formation, providing a rapid route to oxazole **151m**.

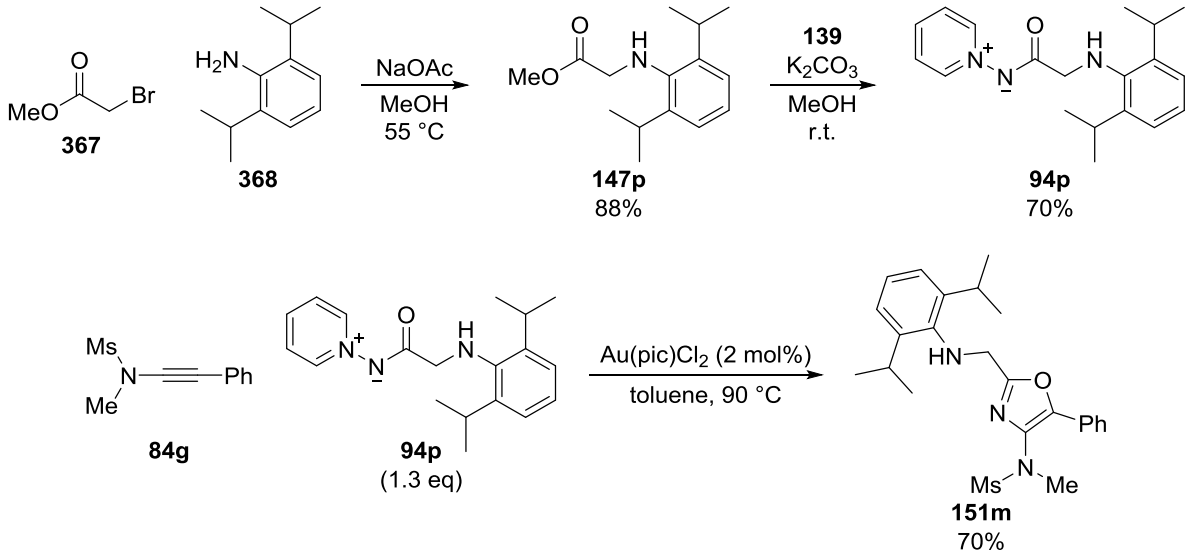

Scheme 91: Synthesis of an oxazole tethered to an aniline.

Heating oxazole **151m** with triethylorthoformate and acid led to the formation of a small amount of precipitate, however this was mostly composed of formamide **371a**, and none of the

desired imidazolium salt **363a.HX** was observed (Scheme 92). The formation of **371a** shows that the initial reaction of the aniline with $HC(OEt)_3$ occurs, however it is not followed by the desired formation of the second N–C bond.

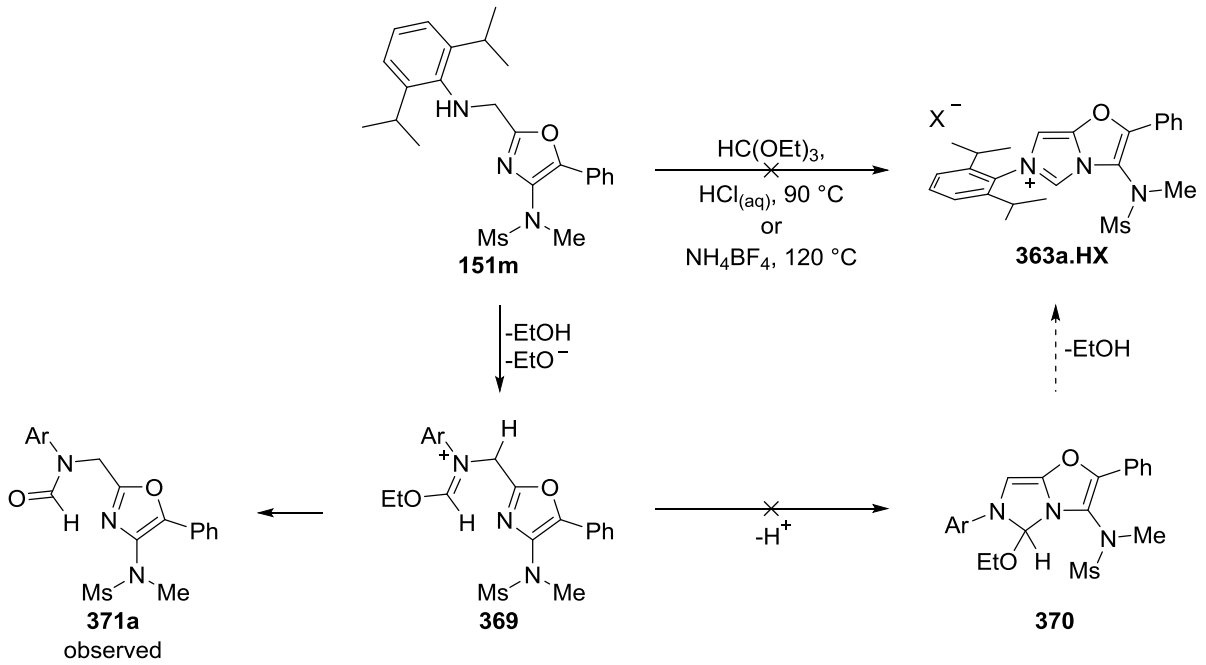

Scheme 92: Reaction of the aniline-tethered oxazole with $CH(OEt)_3$.

The use of trialkylorthoformates in the synthesis of azolium salts is common,[134b] however the mostly closely related starting materials to oxazole **151m** which have been employed in these reactions are hydrazines **374** (Scheme 93).[148] The construction of imidazolium rings from starting materials of general structure **376** has not been demonstrated, possibly due to the relatively low nucleophilicity of the nitrogen of the unactivated imine/heterocycle, a problem which would be exacerbated by using oxazoles.

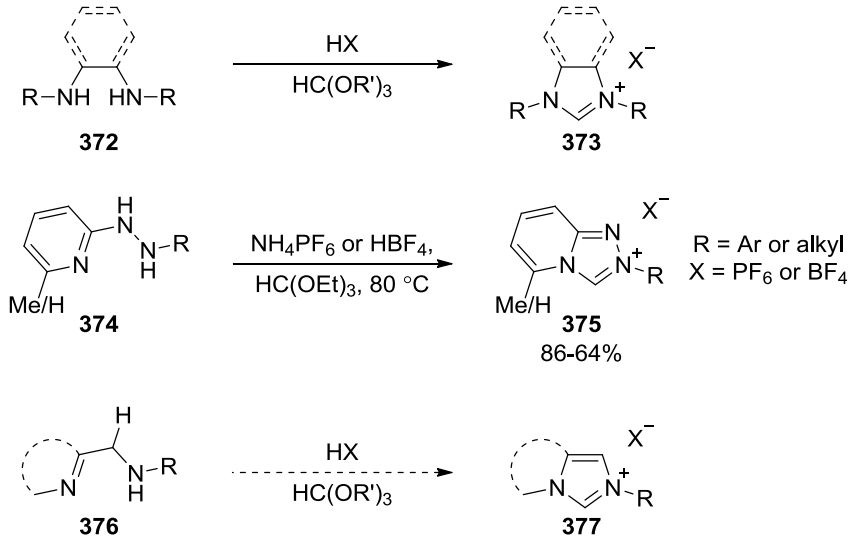

Scheme 93: Examples of the use of trialkylorthoformates in the synthesis of azolium salts.[134b,148]

Given the lack of reactivity of **151m**, and that other routes with more encouraging literature precedent were available, no further experiments were carried out using this oxazole.

4.2.2.2: Synthesis of imidazolium chloride salts from formamides

Formamide-tethered oxazole **371** was an alternative type of substrate for the construction of oxazole-annulated imidazolium salts, which could be constructed from an ylide of type **378** (Scheme 94).

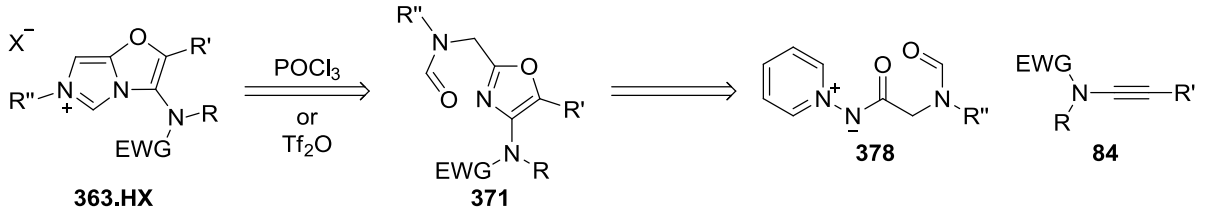

Scheme 94: Route to an imidazolium salt using an oxazole tethered to a formamide.

Ester **147q** was synthesised by formylation of **147p** and allowed access to ylide **94q** (Scheme 95). Although the yield of **94q** was moderate, this reaction was scaled up to give 2.75 g of this ylide, which would later allow access to several oxazoles.

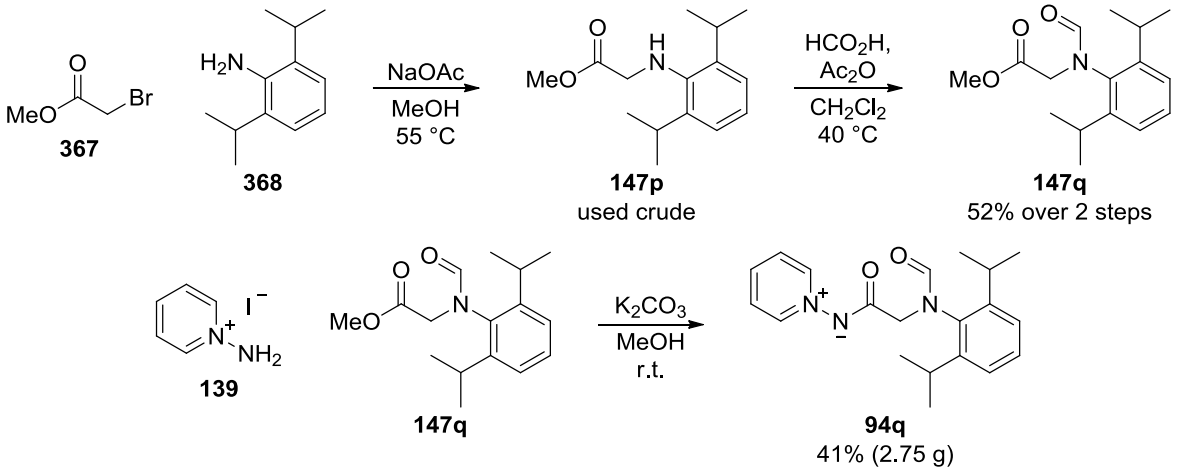

Scheme 95: Route to ylide 94q.

The formation of oxazoles **371a-b** from ylide **94q** was efficient using only 1.2 equivalents of the ylide and 2 mol% of the gold catalyst (Scheme 96). Although oxazoles of the type **371** could usually be purified, they were generally susceptible to slow degradation, and so were used within a couple of days of their purification.

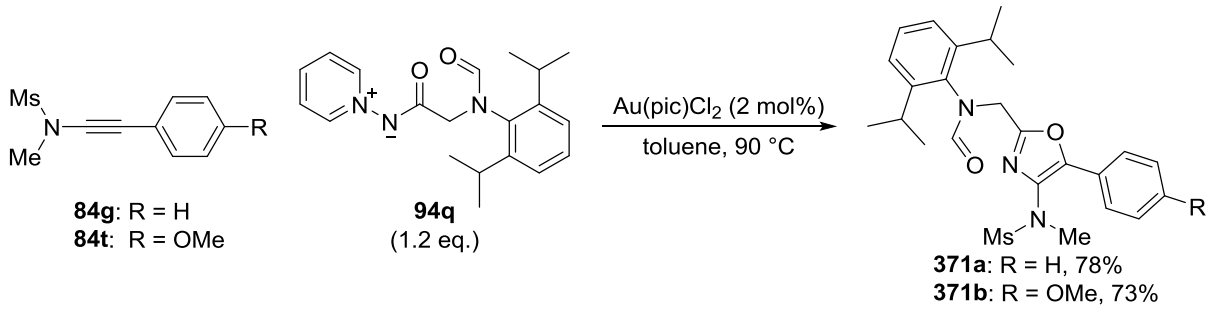

Scheme 96: Synthesis of an oxazole tethered to a formamide.

Initial attempts to cyclise **371a** with $POCl_3$ following a literature procedure were unsuccessful,[128] with no reaction at 80 °C in toluene or on heating to reflux (Table 8 – entry 1). Presumably this was again because the nitrogen atom within the oxazole ring is significantly less nucleophilic than that of a pyridine. Raising the temperature to 165 °C did facilitate formation of **363a.HCl** (Entry 2), however this could not be adequately purified despite repeated attempts at column chromatography and recrystallisations. Attempts to use impure **363a.HCl** as an NHC precursor led to the formation of a similarly impure copper complex. Oxazole **371b** was next investigated as a starting material in the hope that modifying the substrate would facilitate

purification of the products. It was found that an intermediate temperature of 140 °C gave much cleaner conversion of the oxazole to the imidazolium salt (Entry 3), a method that was generally applicable to other substrates (see below), however **363b.HCl** also could not be completely purified.

Table 8: Formation of the imidazolium ring from formamides

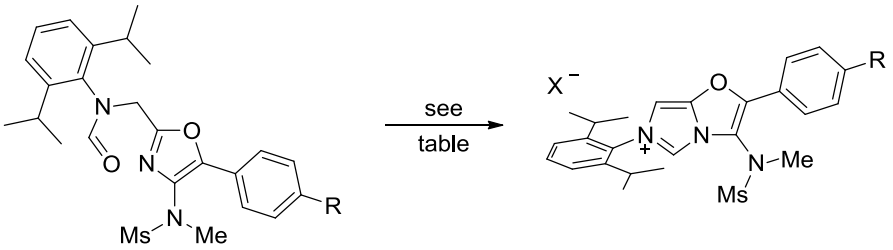

371a: R = H
371b: R = OMe

363a-b.HX

Entry	**371**	Reagent	Solvent	Temperature	Time	X	Yield
1	**371a**	$POCl_3$	toluene	80 or 110 °C	24 h	Cl	NR
2	**371a**	$POCl_3$	mesitylene	165 °C	3 days	Cl	<56% (impure)
3	**371b**	$POCl_3$	*m*-xylene	140 °C	3 days	Cl	<95% (impure)
4	**371b**	Tf_2O/NEt_3	CH_2Cl_2	0⟶40 °C	24 h	OTf	0%
5	**371b**	Tf_2O/NEt_3	1,4-dioxane	100 °C	24 h	OTf	trace
6	**371b**	Tf_2O/NEt_3	toluene	110 °C	24 h	OTf	0%

This purification issue for related ammonium/azolium.HCl salts formed by $POCl_3$-mediated reactions has also by the Alder and Organ groups, with the suggestion that contamination may be due to the presence of one or more phosphorus-containing anions.[130a,149] In an attempt to exchange these anions, the impure **363.HCl** salts were treated with Dowex® 22 chloride anion exchange resin. Despite subsequent reports of the use of this resin as part of the purification protocol in the synthesis of imidazo[1,5-a]pyridinium salts using $POCl_3$ (such as **333**, Scheme 85),[140] it had no observable effect in this case.

Triflic anhydride, which has been used in place of $POCl_3$ in a related reaction and allowed a significant reduction in the required reaction temperature (Scheme 81),[130b] was investigated for the synthesis of **363b.HOTf**, however only trace amounts of product were observed using this reagent, even at 110 °C (Table 8 – entries 4-6). As a more successful protocol had by this point been established (see below), no further attempts were made at the synthesis of imidazolium triflate salts.

4.2.2.3: Synthesis of imidazolium hexafluorophosphate salts from formamides

Although the synthesis of imidazolium hexafluorophosphate salts by the salt metathesis of chloride salts following $POCl_3$-mediated cyclisation of formamides was described in the original work of the Lassaletta group (Scheme 81),[128] these salts were not initially investigated due to the effect of changing the chloride ion to a PF_6 ion on desired subsequent organometallic reactions (described below in Schemes 101 and 106).

Applying this approach did however allow the highly crystalline salts **363a-d.HPF$_6$** to be obtained, and their purity was established by elemental analysis (Scheme 97). To carry out the salt metathesis reaction, the **363.HCl** salts were dissolved in boiling water and some insoluble material removed by filtration, following which the **363.HPF$_6$** salts were precipitated by the addition of KPF_6 to the filtrate and purified by recrystallisation from acetone/Et_2O. Whilst the $POCl_3$-mediated cyclisation was generally highly efficient, the necessity to carry out this second step led to a significant drop in yield in all cases. Addition of larger apolar groups to the sulfonamide as in **363c-d** was particularly problematic, due to the lack of water solubility of the **363.HCl** salts, leading to a further reduction in yield. It is noteworthy that a ^{31}P-NMR spectrum taken prior to the recrystallisation of **363b.HPF$_6$** showed several small resonances which were not due to the PF_6 ion, providing evidence for the presence of phosphorus-containing impurities which arise from the reaction with $POCl_3$.

This method represents a highly convergent route to previously unknown oxazole-annulated imidazolium salts which could be explored as NHC precursors, it was also the only successful method found which allowed the purification of these compounds.

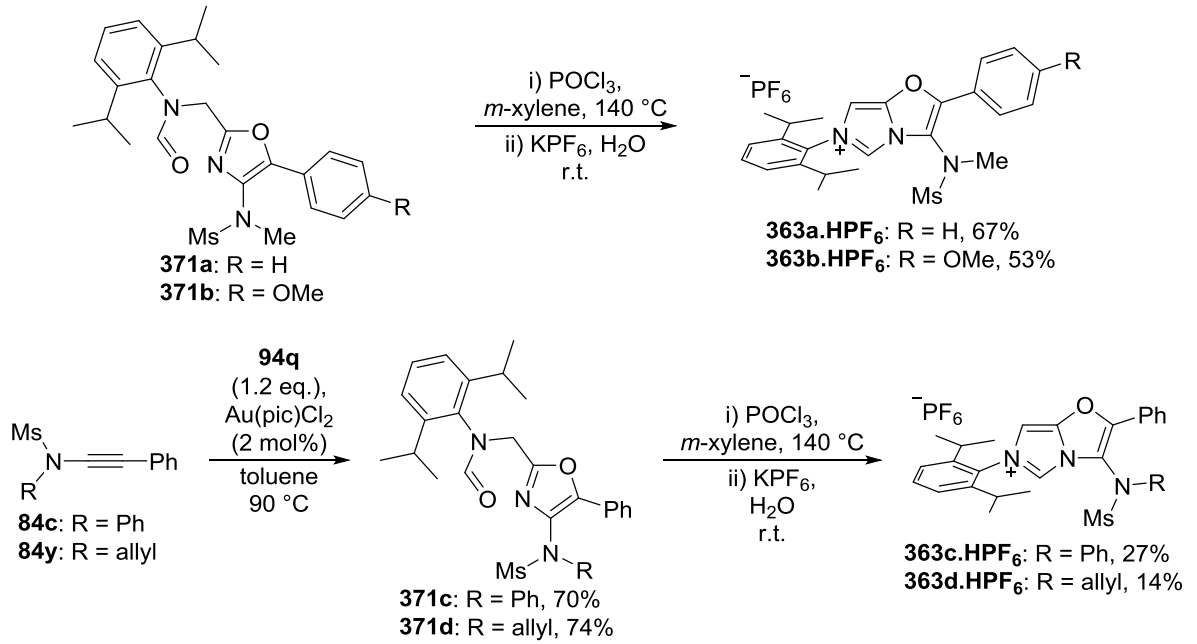

Scheme 97: Synthesis of NHC.HPF_6 salts.

4.2.2.4: Attempted synthesis of imidazolium salts from imines

Given the initial difficulties in synthesising pure imidazolium salts using formamides, it was envisioned that **363.HX** could instead be accessed from oxazoles which are tethered to an imine **380** (Scheme 98).

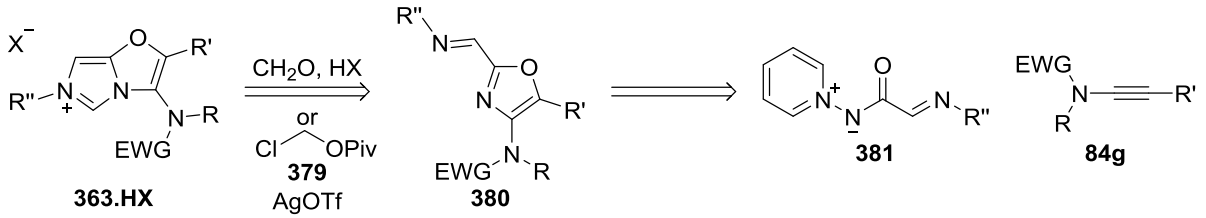

Scheme 98: Route to an imidazolium salt using an oxazole tethered to an imine.

The synthesis of such an oxazole was initially attempted using ylide **94r**, which could be formed from ester **383**; however **94r** was highly susceptible to imine hydrolysis, and material free of 2,6-diisopropylaniline **368** could not be obtained (Scheme 99). No reaction of ylide **94r** with ynamide **84g** occurred under gold catalysis, possibly due to catalyst poisoning by the aniline impurity.

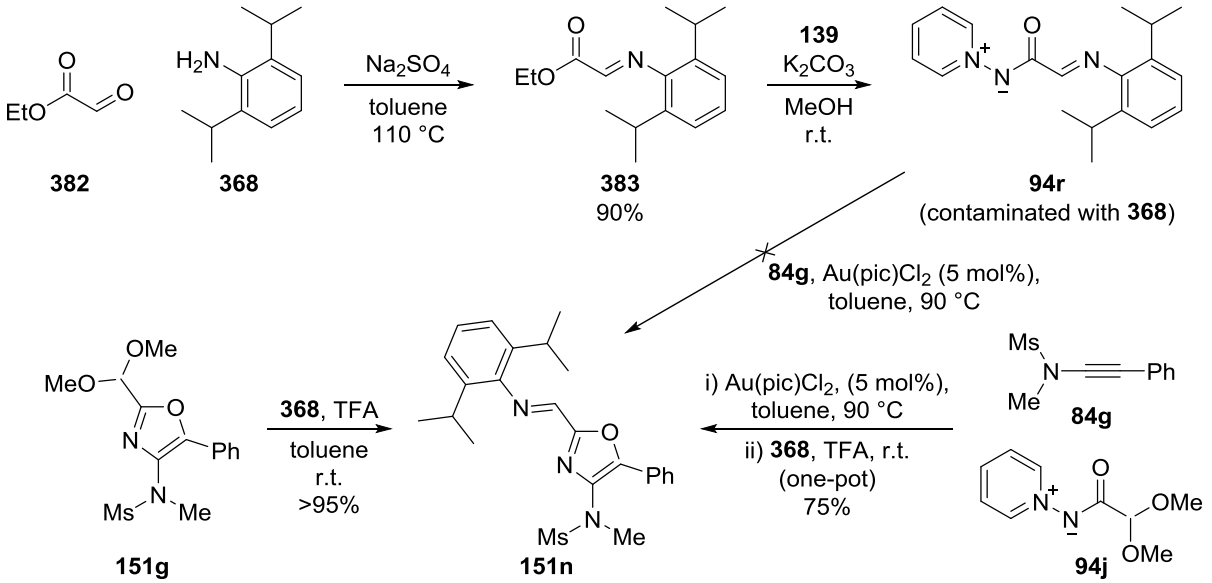

Scheme 99: Synthesis of an oxazole tethered to an imine.

Pleasingly the acetal-containing oxazole **151g** described in Chapter 1 could be converted into the desired imine **151n** in a quantitative yield (Scheme 99). Additionally, the synthesis of oxazole **151g**, using ylide **94j** and ynamide **84g**, could be followed by imine formation to give **151n** in a one-pot procedure. Given the ease with which ylide **94j** could be accessed, and the efficiency of subsequent steps, the synthesis of oxazole **151n** is considerably more straightforward than that of its formamide bearing analogue **371a**, despite the requirement of an extra late-stage synthetic operation. Additionally, **151n** was not overly sensitive to imine hydrolysis and could be stored for several months without degradation. For these reasons, a route to imidazolium salts using this imine was highly attractive. Imine **151n** also represents a potentially interesting bidentate ligand structure in its own right, although its use for this purpose was not investigated.[150]

Table 9: Attempted cyclisation of an imine tethered to an oxazole.

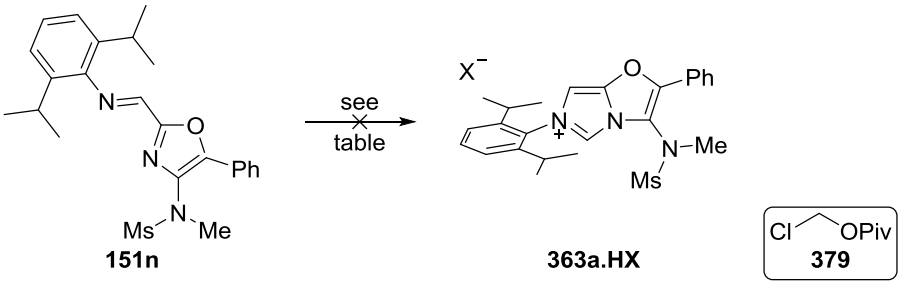

151n **363a.HX** **379**

Entry	Reagent	Solvent	Temperature[a]	X	Yield
1	**379**	MeCN	81 °C	Cl	0%
2	**379**	Ph_2O	195 °C	Cl	0%
3	**379**, AgOTf	CH_2Cl_2	40 °C	OTf	0%
4	**379**, AgOTf	1,4-dioxane	120 °C	OTf	0%
5	**379**, NaI	MeCN	70 °C	I	0%
6	**379**, NaI, $ZnCl_2$	MeCN	70 °C	I	0%
7	$(CH_2O)_n$, $ZnCl_2$, HCl	THF	60 °C	Cl	0%
8	$(CH_2O)_n$, TMSCl	EtOAc	77 °C	Cl	0%
9	CH_2I_2	MeCN	100 °C	I	0%
10	CH_2I_2, 2AgOTf	toluene	110 °C	I	0%

[a] Reactions above the normal boiling point of the solvent were carried out in a sealed tube.

Several unsuccessful attempts at the formation of the imidazolium ring from **151n** were made (Table 9). These included the use of chloromethyl pivalate **379** either on its own (Entries 1-2), or activated by AgOTf (Entries 3-4) or NaI (Entries 5-6), under literature conditions,[131,133] as well as at elevated temperatures. Paraformaldehyde[134a,135] (Entries 7-8) and CH_2I_2[151] (Entries 9-10) were also trialled as the carbon donor without success. Generally the only isolable compounds from the reaction mixtures were the starting material **151n**, and (in some cases) the products of imine hydrolysis. Following Hutt and Aron's multicomponent reaction protocol from acetal **151g** only resulted in the formation of imine **151n**, even at elevated temperature (Scheme 100).[136a]

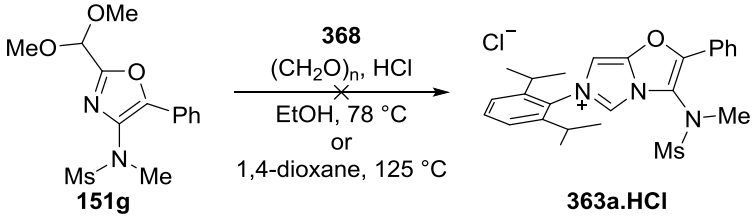

151g **363a.HCl**

Scheme 100: Unsuccessful formation of an imidazolium salt from acetal 151g.

Again the failure of these reactions to form the imidazolium ring despite success on other systems is attributed to the relatively low nucleophilicity of the oxazole nitrogen. In line with this hypothesis the chloroiminium species **384** generated by the treatment of **371a** with $POCl_3$ would be expected to be significantly more electrophilic than any of the intermediates **386** generated by the reactions described in Table 9 (Scheme 101). As such the reaction of oxazoles **371** with $POCl_3$, followed by purification by anion exchange remained the only viable route to the desired NHC precursors.

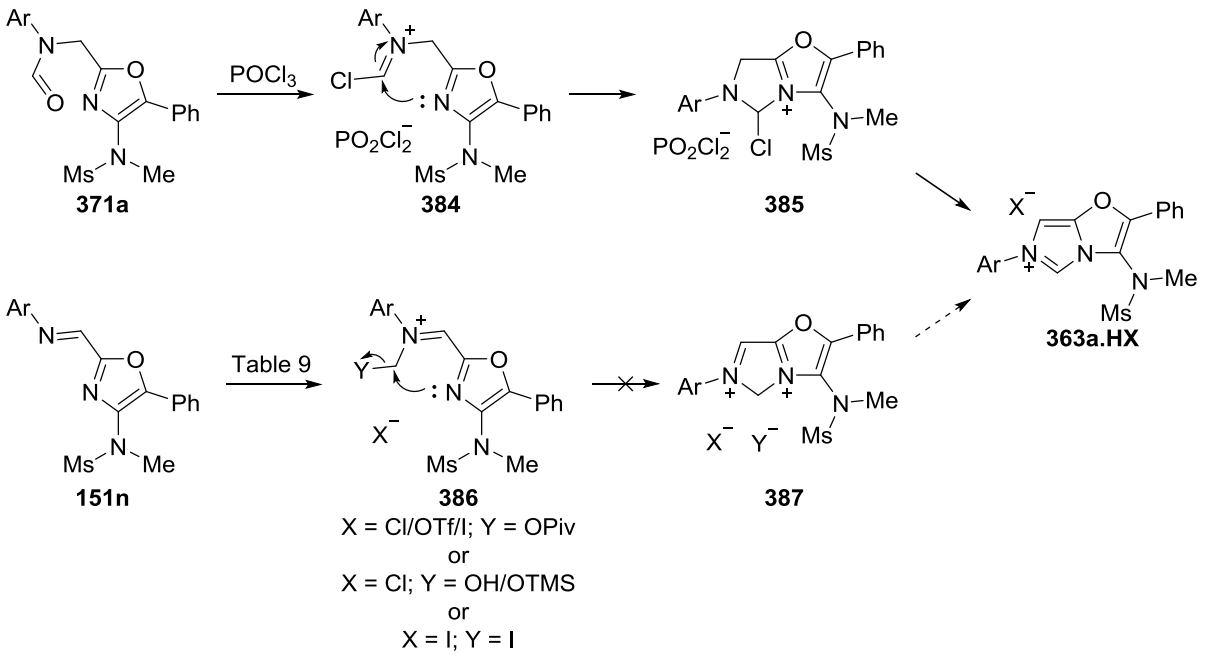

Scheme 101: Proposed mechanisms for the formation of the imidazolium ring.

4.2.3: Organometallic Complexes

With the **363.HPF$_6$** salts in hand, investigation of their conversion into NHC-metal complexes was undertaken, with the aim of examining the steric and electronic properties of the ligands, as well as their behaviour in catalysis.

4.2.3.1: Synthesis of gold and copper complexes

As the **363.HCl** salts could not be purified, a commonly employed route for synthesising the desired (NHC)MCl complexes by transmetalation from (NHC)AgCl complexes was unavailable; treatment of NHC.HPF$_6$ salts with Ag_2O results in the formation of $[(NHC)_2Ag]PF_6$ complexes, which in turn give bis-NHC metal complexes following reaction with transition metal halides (Scheme 102).[152]

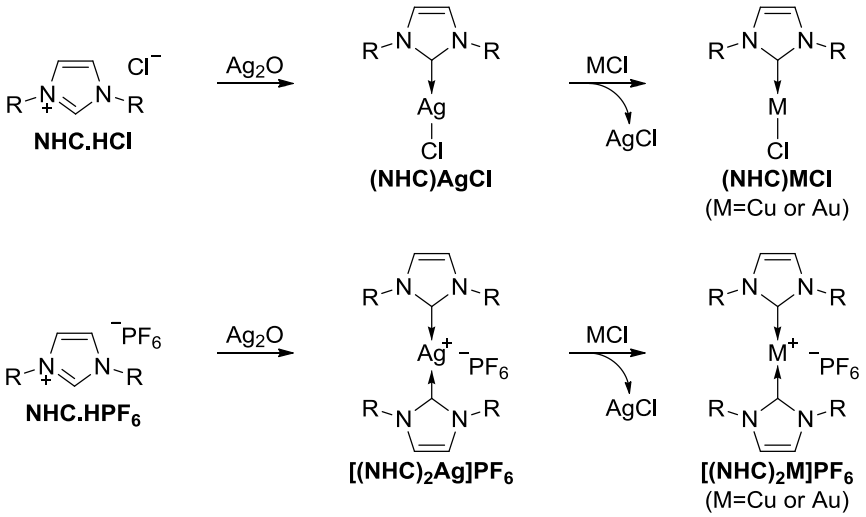

Scheme 102: Anion effect in the general synthesis of NHC complexes by a common transmetalation route.[152]

Recent reports have shown that gold(I) and copper(I) NHC halide complexes of the type (NHC)MCl can be synthesised by direct treatment of imidazolium salts and the appropriate metal halides with K_2CO_3 at room or slightly elevated temperatures.[153] Whilst following these procedures directly using the newly synthesised imidazolium salts resulted in the formation of complex mixtures, simply changing the base to NEt_3 and extending the reaction time from one to sixteen hours allowed access to **(363a)AuCl** and **(363c)AuCl** in high yields, as well as **(363a)CuCl** in a reasonable yield.

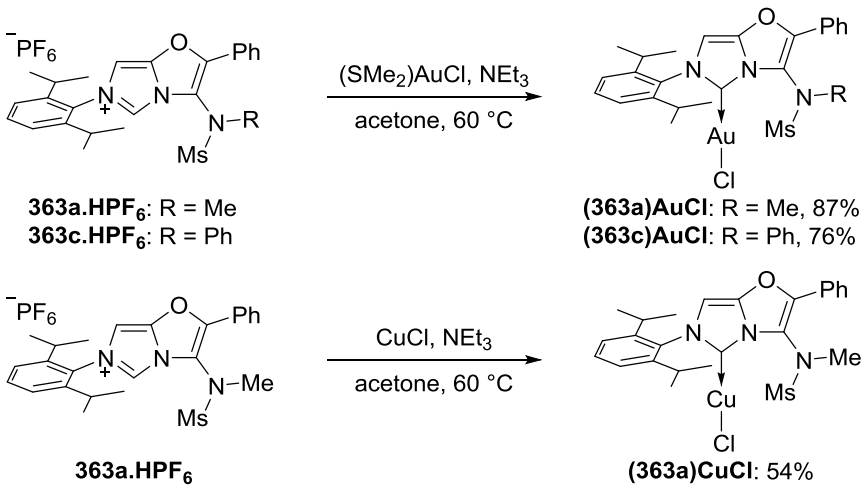

Scheme 103: Synthesis of (363)MCl complexes.

The purity of all three metal complexes was established by elemental analysis and their structures were examined by single crystal X-ray diffraction (Figures 13-15). The X-ray structures show that the two non-oxazole substituents of the sulfonamide sit in a plane approximately perpendicular to that of the metal and the biaryl unit. No co-ordination from the sulfonamide to the metal is suggested as N–M interatomic distances are between 3.53 and 3.66 Å. There is little difference in the key bond lengths or angles in the two gold complexes, whilst the slightly decreased ligand–M and M–Cl bond lengths in **(363a)CuCl** are a possible reason for the more pronounced deviation from linearity in the C–M–Cl bond angle in the copper complex.

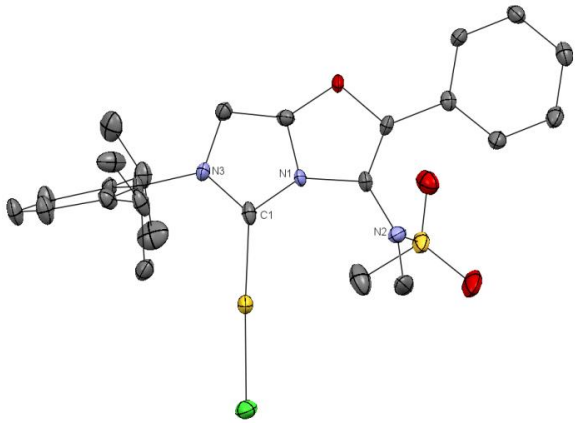

Figure 13: X-ray structure of (363a)AuCl. Ellipsoids drawn at 50% probability. C1–Au: 1.98 Å, Au–Cl: 2.28 Å, N2–Au: 3.65 Å. N1–C1–N3: 102.7°, N3–C1–Au: 129.5°, N1–C1–Au: 127.1°, C1–Au–Cl: 175.8°.

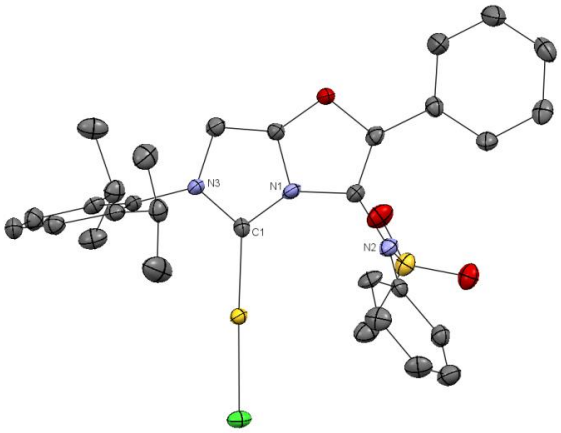

Figure 14: X-ray structure of (363c)AuCl. Ellipsoids drawn at 50% probability. C1–Au: 1.97 Å, Au–Cl: 2.28 Å, N2–Au: 3.66 Å. N1–C1–N3: 102.6°, N3–C1–Au: 129.4°, N1–C1–Au: 127.9°, C1–Au–Cl: 177.7°.

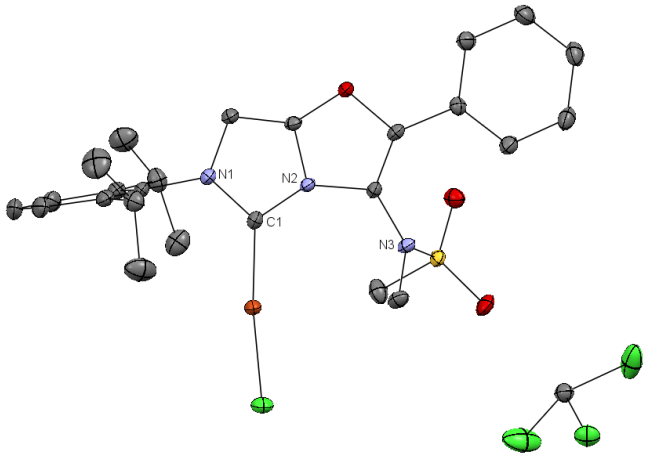

Figure 15: X-ray structure of (363a)CuCl co-crystallised with a molecule of $CDCl_3$. Ellipsoids drawn at 50% probability. C1-Cu: 1.88 Å, Cu–Cl: 2.11 Å, N3–Cu: 3.53 Å. N1–C1–N2: 102.0°, N1–C1–Cu: 131.7°, N2–C1–Cu: 126.2°, C1–Cu–Cl: 173.3°.

X-ray data for **(363a)AuCl** and **(363c)AuCl** was obtained by Dr Louise Male (University of Birmingham) whilst data for **(363a)CuCl** was obtained by the UK National Crystallography Service (University of Southampton), all structures were solved by Louise Male.

4.2.3.2: Calculation of percentage buried volume

The most common method for measuring the steric bulk of NHC ligands is the percentage buried volume ($\%V_{bur}$) method developed by the Cavallo and Nolan groups, which can also be used for other monodentate ligands (Figure 16).[154] This value can be generated using a set of Cartesian coordinates for the ligand and a calculator made freely available online by the Cavallo group.[155] The set of coordinates can be generated by DFT calculations but most commonly come from an X-ray structure of either the free ligand or one of its metal complexes. As the $\%V_{bur}$ is a property purely of the ligand, in the latter case the metal and any additional ligands must be deleted before running the calculation; however this can be advantageous as it leaves behind a ligand structure in a real conformation for metal coordination (note that the choice of metal and ancillary ligands can therefore affect the result).

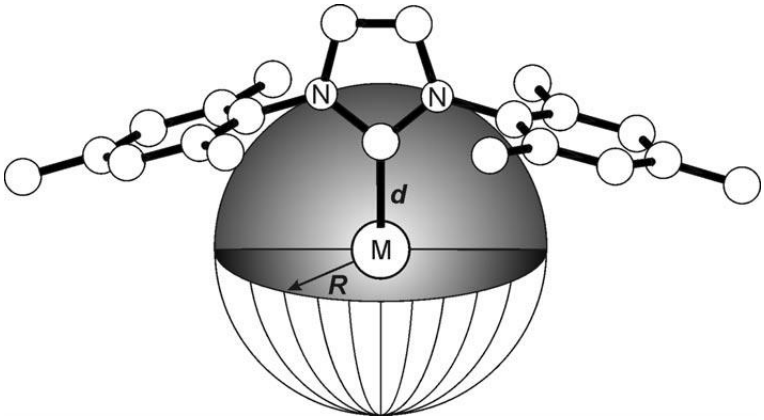

Figure 16: Representation of the $\%V_{bur}$ method reproduced from reference [154a].

For the calculation itself an imaginary metal is placed at a defined distance from the coordinating atom and a sphere of a defined radius placed around this. This sphere is divided into sections by a cubic mesh and each section is checked for whether its edges are within the Van der Waals radius of any atom of the ligand, if so the cube is assigned as buried, if not it is assigned as free, and from this the percentage buried volume is calculated.

This calculation was carried out for ligands **363a** and **363c** using the crystal structures for their gold(I) chloride complexes, and compared against literature values for several common and

particularly bulky ligands (Figure 17).[140,156] Only literature examples also derived from (NHC)AuCl complexes were selected, where in all cases a bond distance of 2.0 Å and a sphere radius of 3.5 Å was employed. The values for **363a** and **363c** were 44.9% and 43.6% respectively; similar to the ligand IPr, which is one of the most commonly used NHCs in transition metal catalysis. This perhaps unexpected result, that by this measurement **363a** is marginally more bulky than **363c**, can be explained by the fact that the sulfonamide and its substituents lie on the edge and mostly outside of the standardly used 3.5 Å sphere. When the radius of this sphere was increased this relationship was reversed, illustrating the unavoidably arbitrary nature of such measurements (Table 10).

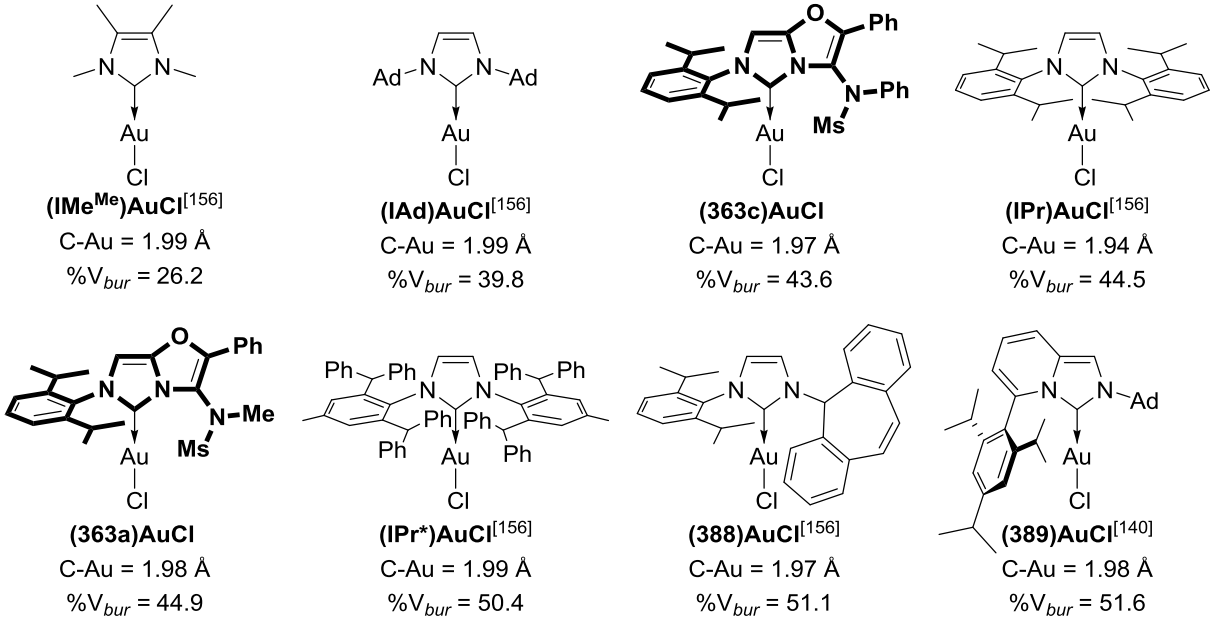

Figure 17: Gold complexes from which the %V_{bur} has been calculated for NHCs – comparison of 363a and 363c with some common and very bulky ligands from the literature. Parameters: sphere radius = 3.5 Å; distance from sphere = 2.0 Å; mesh spacing, = 0.05 Å; H atoms omitted; Bondi radii scaled by 1.17 Å.[140,156]

Table 10: %V_{bur} for NHCs at various sphere radii (r)

	%V_{bur} at r =			
Ligand	3.5 Å	4.0 Å	4.5 Å	5.0 Å
IPr	44.5	46.8	47.8	47.2
363a	44.9	45.6	45.1	43.5
363c	43.6	45.8	46.8	46.7

Parameters other than sphere radius are as in Figure 17. The values for IPr were calculated using a published X-ray structure for (IPr)AuCl: CCDC-258274.[157]

4.2.3.3: Impact of metal coordination on ligand flexibility

It is apparent from the NMR spectra of **(363a)AuCl**, **(363c)AuCl** and **(363a)CuCl** that there is a loss of symmetry in the diisopropyl phenyl group on conversion of the imidazolium salts to their metal complexes. Due to restricted rotation in the isopropyl group, the ^{1}H-NMR resonances in the imidazolium salts appear as one CH apparent heptet and two methyl doublets, but when the metal is coordinated these are separated into two CH apparent heptets and four methyl doublets (Figure 18). This effect is most pronounced in the spectra of **(363a)CuCl** and **(363c)AuCl**, however it can also be observed in **(363a)AuCl** despite there being considerably more overlap of the peaks. No coalescence of these resonances was observed when the ^{1}H-NMR spectrum of **(363a)AuCl** was recorded at 110 °C. The separation of the four methyl signals is also apparent in the ^{13}C-NMR spectra of all three metal complexes.

These observations can be explained by restriction of rotation around C–N bond at the oxazole C4 position upon coordination of the metal. This results in a racemic mixture of enantiomeric atropisomers, which no longer possess the plane of symmetry in the axis of the fused ring system, therefore rendering the two isopropyl groups diastereotopic (Scheme 104). Whilst slow interconversion of the atropisomers cannot be ruled out on the basis of these NMR experiments alone, the crystal structures of the metal complexes suggest there is little space for the required bond rotation to occur.

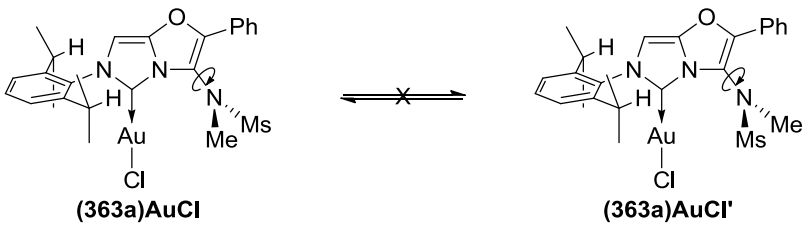

(363a)AuCl **(363a)AuCl'**

Scheme 104: Enantiomers of (363a)AuCl.

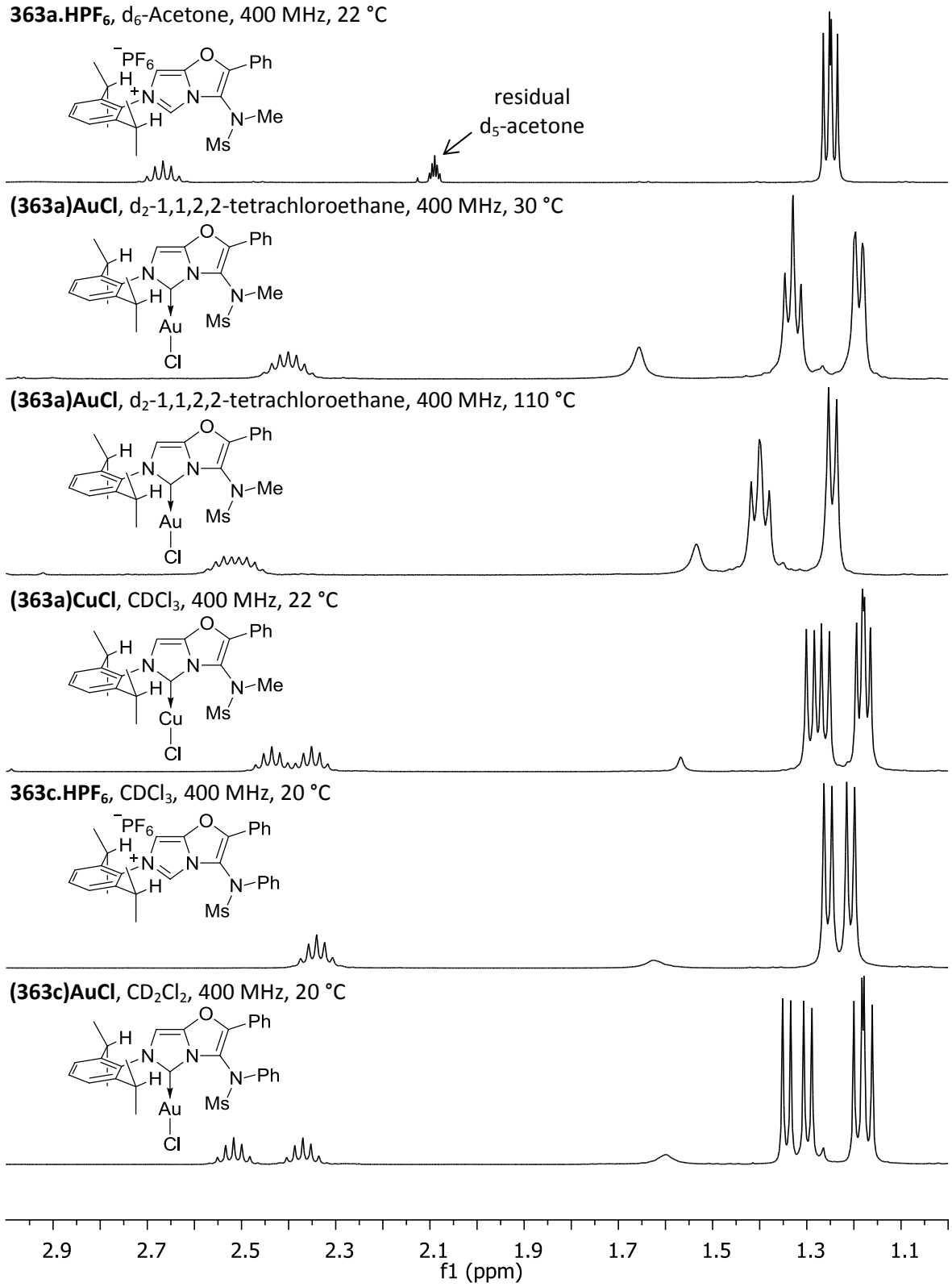

Figure 18: Section of the ^{1}H-NMR spectra of imidazolium salts 363a.HPF$_6$ and 363c.HPF$_6$ and their gold and copper complexes which show the desymmetrisation of the two isopropyl groups upon binding to a metal.

The racemic mixture of enantiomers described in Scheme 104 was also apparent in the X-ray structures of these complexes. **(363a)AuCl** (Figure 13) and **(363a)CuCl** (Figure 15) were in centrosymmetric space groups with two molecules of each enantiomer present in the unit cell. **(363c)AuCl** (Figure 14) was in a chiral space group which was refined as an inversion twin with a 1:1 mixture of enantiomers.

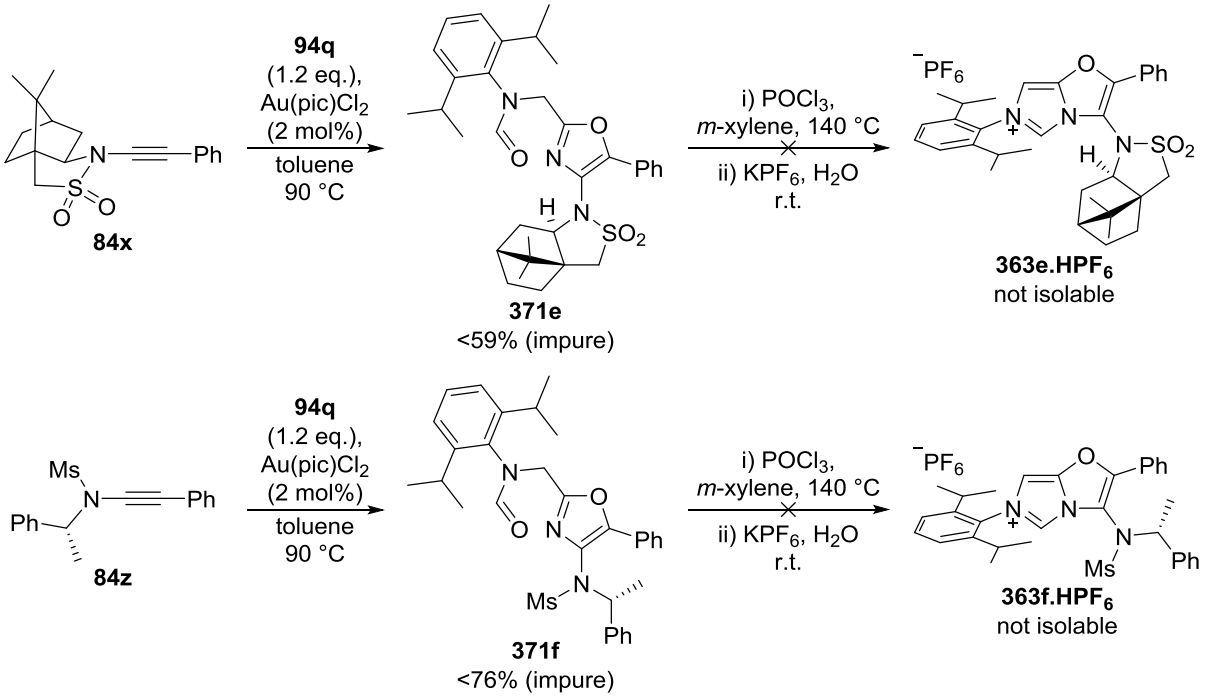

Scheme 105: Attempted synthesis of chiral imidazolium salts.

In order to assess whether this effect could be exploited in the synthesis of enantiomerically pure metal complexes, the synthesis of chiral imidazolium salts **363e-f.HPF$_6$** was attempted. The respective chiral NHCs could potentially co-ordinate diastereoselectively to a metal, particularly in the case of **363e**, where the rigid camphorsultam unit should significantly favour one conformation in the presence of a metal. Analytically pure samples of oxazoles **371e-f** were not obtained due to their limited stability; however the formation of their respective imidazolium chloride salts appeared to proceed successfully. Unfortunately the effect which led to the reduced yield of **363c-d.HPF$_6$**, namely the lack of water solubility of imidazolium chlorides bearing large apolar groups at the oxazole C4 position, was even more pronounced for these substrates, meaning that no **363e-f.HPF$_6$** salts could

be obtained. Attempts to carry out the salt metathesis of **363e.HCl** in acetonitrile were unsuccessful, as were attempts to purify the chloride salts by further chromatography or by recrystallisation.

*4.2.3.4: Attempted synthesis of a platinum complex from ligand **363d***

Given the low yield of **363d.HPF$_6$**, only enough was made for a single attempt at the synthesis of a metal complex. **(363d)PtCl$_2$** was targeted in order to assess whether any coordination between the *N*-allyl unit and the metal could be observed. Unfortunately, where an adapted literature procedure for this type of reaction was followed,[158] only a complex mixture, from which no **(363d)PtCl$_2$** could be isolated, was formed (Scheme 106).

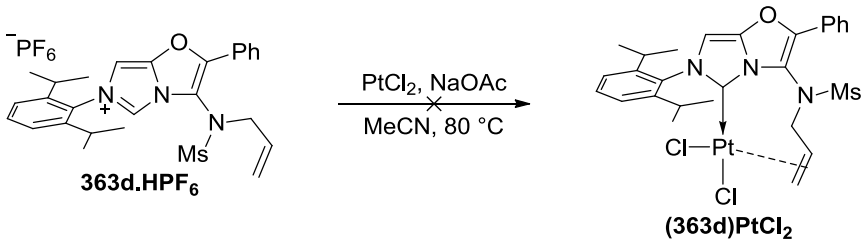

Scheme 106: Failed synthesis of (363d)PtCl$_2$

4.2.3.5: Synthesis of iridium complexes and their use in the electronic characterisation of ligands

Attempts to quantify the electronic effect that NHCs have on metals are routinely reported in the literature, in order to lead to more accurate rationalisation of structure with catalytic activity. The various methods employed for electronic characterisation have been reviewed by Dröge and Glorius[159] and most recently by Nelson and Nolan.[160]

Tolman's Electronic Parameter (TEP) is the value for the symmetrical carbonyl stretching frequency in (L)Ni(CO)$_3$ complexes.[161] The synthesis of (NHC)Ni(CO)$_3$ complexes is relatively rarely attempted due to the propensity of some ligands to instead form (NHC)Ni(CO)$_2$ complexes, as well as the high toxicity of the volatile Ni(CO)$_4$ starting material.[162] By far the most common piece of electronic characterisation data available for NHCs in the literature comes from the infra-red spectra of (NHC)Ir(CO)$_2$Cl or (NHC)Rh(CO)$_2$Cl complexes. Work by the Nolan group has allowed extrapolation of TEP values using the spectra of these complexes (Figure 19).[160,162]

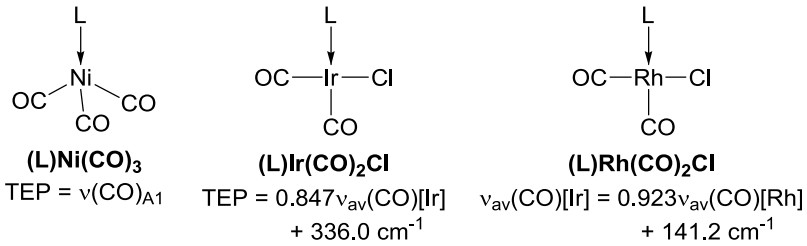

Figure 19: Nelson and Nolan's equations for the correlation of the infrared stretching frequencies of metal carbonyl compounds used in the calculation of Tolman's Electronic Parameter.[160] ν_{av} is the average wavenumber of the two CO stretches observed in the iridium or rhodium complexes.

A lower TEP value is indicative of more M→CO π* back-bonding, and so more electron-donation from the ligand to the metal. Criticisms of the TEP method are that a relatively low range of values is obtained in comparison to the sensitivity of the experiment,[163] and that secondary orbital interactions directly between the ligand under investigation and the CO being measured may affect the results,[164] however it is the most commonly employed measurement for the electronic characterisation of NHCs.

The required iridium or rhodium complexes are usually accessed from their respective (NHC)M(cod)Cl complexes (cod = 1,5-cyclooctadiene), which can be readily synthesised from an imidazolium chloride salt and the required $[M(cod)Cl]_2$ species by treatment with sodium or potassium *tert*-butoxide (Scheme 107).[162] There is again an anion effect in these reactions, for example where the above procedure was followed by Lassaletta and co-workers using **390.HPF$_6$**, the resulting product was the *bis*-NHC complex **[(390)$_2$Rh(cod)]PF$_6$**, attributed to the chloride scavenging ability of potassium ions.[128] A solution to this problem was demonstrated by the same group in the synthesis of **(391)Rh(cod)Cl** from the more acidic triazolium salt **391.BF$_4$** by using triethylamine as the base.[165]

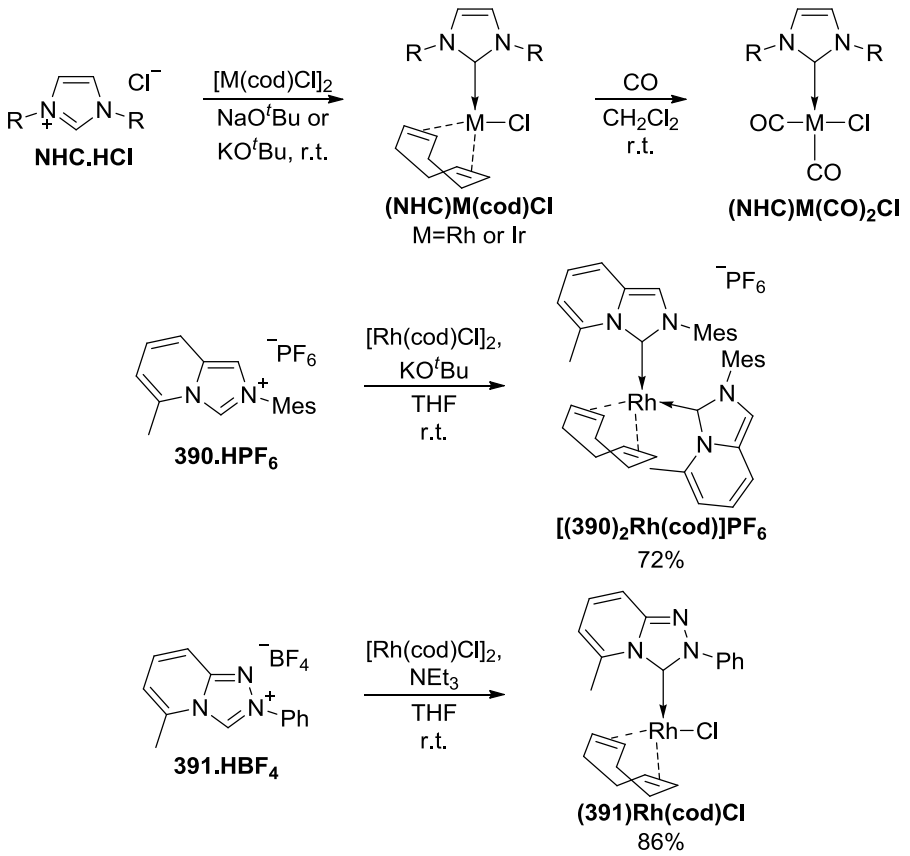

Scheme 107: Effect of the choice of base and counterion on reactions of azolium salts with $[Rh(cod)Cl]_2$.[128,165]

The measurement of a TEP value for NHCs **363a-b** would allow a comparison with those in the literature, and would show whether there was any measurable impact on the electronic donating ability of the ligands by substitution at the oxazole 5-position. As shown in Figure 19, TEP values can be estimated by extrapolation of the average value for the two C≡O stretching frequencies in **$(L)Ir(CO)_2Cl$** complexes onto the scale for nickel, whilst when rhodium complexes are used an extra extrapolation of rhodium to iridium is first carried out.

As such, **$(363a\text{-}b)Ir(CO)_2Cl$** were targeted. Surprisingly no reaction was observed between **$363a.HPF_6$** and $[Ir(cod)Cl]_2$ in the presence of NEt_3 (Scheme 108). An alternative procedure was carried out inside a nitrogen-filled glovebox: the imidazolium salts were treated with NaO^tBu and the sodium salts removed by filtration, to give solutions containing the free carbenes **363a** or **363b**, which were added to the $[Ir(cod)Cl]_2$. After stirring for one hour the reactions were removed from

the glovebox, and following column chromatography of the **(363)Ir(cod)Cl** complexes, these were treated with CO to give the desired complexes **(363a-b)Ir(CO)$_2$Cl**.

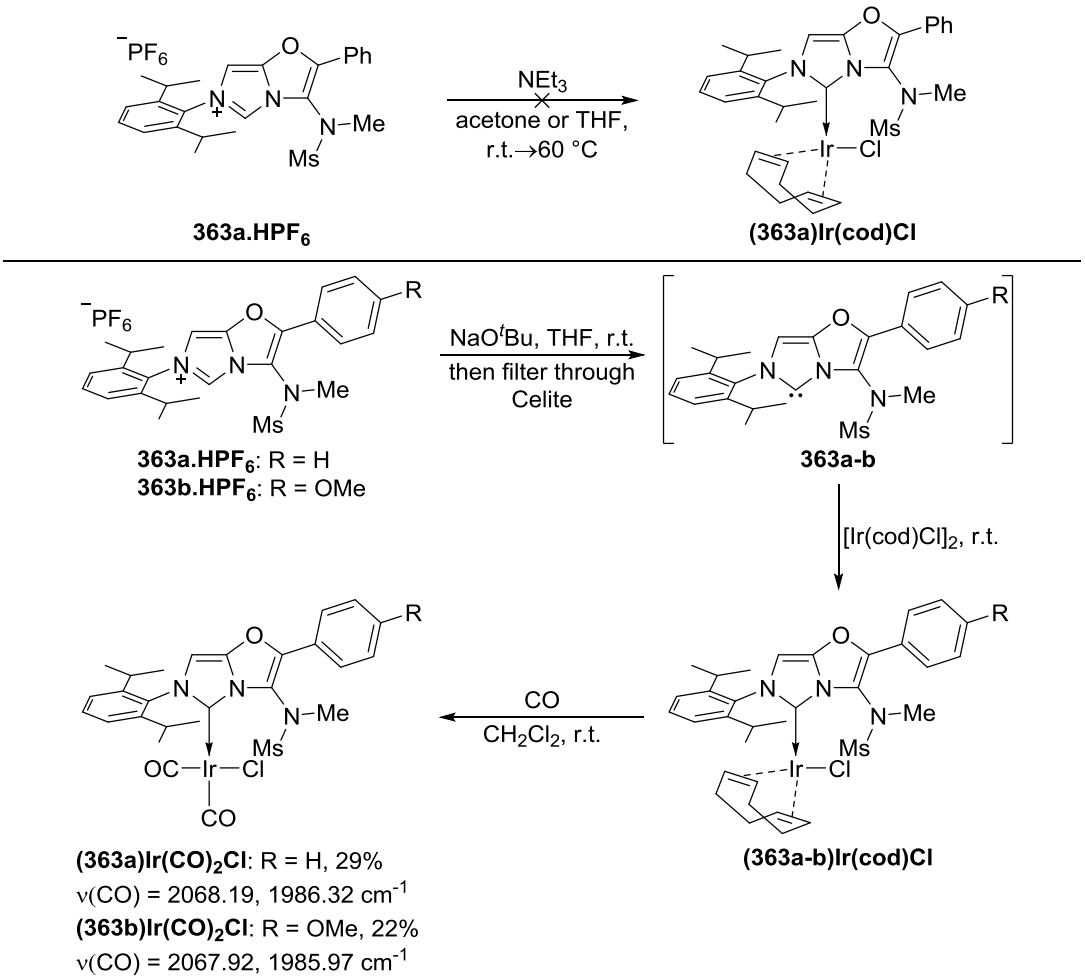

Scheme 108: Synthesis of (363a-b)Ir(CO)$_2$Cl complexes.

It is noteworthy that during the synthesis of **(363b)Ir(cod)Cl** a minor by-product with a characteristic red colour was also formed. Although this product could not be properly purified or characterised, the ^{1}H-NMR spectrum was very similar to that of **(363b)Ir(cod)Cl** – with the notable difference that the *N*-methyl signal was replaced by an AB quartet which accounted for only two protons. This is indicative of a C–H insertion by the metal at this methyl group. Related intramolecular insertions into aliphatic C–H bonds for (NHC)Ir(III) complexes have been reported, and indicate that the formation of this minor product may have occurred by the reaction of **(363b)Ir(cod)Cl** with NaO^{t}Bu.[166] The propensity of these related cyclometalated compounds to

undergo elimination of HCl (or HI) following C–H insertion, allows a tentative assignment of the side-product formed in the synthesis of **(363b)Ir(cod)Cl** as **(363b')Ir(cod)** (Figure 20).

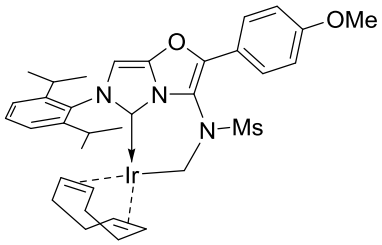

(363b')Ir(cod)

Figure 20: Potential structure of a side-product formed in the synthesis of (363b)Ir(cod)Cl.

The purity of the new **(363a-b)Ir(CO)$_2$Cl** complexes was established by elemental analysis, however their ^{1}H-NMR spectra showed three distinct sets of *N*-methyl and *N*-methylsulfonyl signals (the major one of which accounted for approximately 80% of the total in both cases). A likely explanation for this is that as well as the locked rotation around the oxazole C4–N bond, there is also some form of restricted rotation around the metal carbene bond. In the absence of crystallographic or high temperature NMR data it is difficult to say whether these different species should be properly referred to as rotamers or diastereoisomers.

Despite the above observations only two sharp C≡O stretching frequencies were observed in the infra-red spectra of each iridium complex. It is essential that the IR spectra are recorded in CH_2Cl_2 in order to compare these values with those in the literature; measurement in the solid state can lead to a difference of ~10 cm^{-1} compared to measurement in CH_2Cl_2.[133] On comparing the newly synthesised iridium complexes the difference for each peak was only a fraction of a wavenumber, indicating no real effect of the methoxy group in **363b** on the amount of electron density donated by the NHCs to the metal.

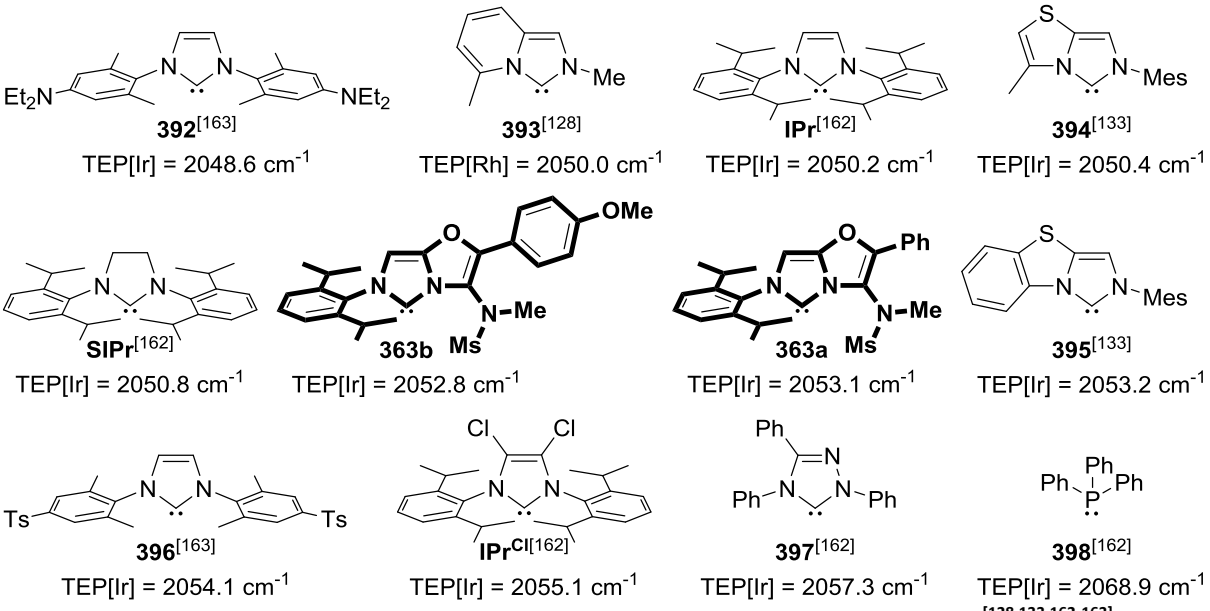

Figure 21: Comparison of estimated TEP values for 363a-b with those from the literature.[128,133,162-163] In some cases TEP values estimated using iridium complexes have been used even where the exact value from $(L)Ni(CO)_3$ complexes was available, so as to aid fair comparison of the ligands.

Comparison of the TEP values for ligands **363a-b** with those for related, common, and electronically diverse NHCs is given in Figure 21. The TEP values for the new ligands fall slightly towards the electron-deficient end, but well within the normal range for imidazolylidenes.

Given the similarity between **363a** and **363b**, and the range of ligands available on either side of the TEP scale, it is unlikely that this route to NHCs could be used to produce a ligand that is either more or less strongly electron-donating than already available imidazolylidenes, however their unique structure may still lead to interesting outcomes in catalysis.

4.2.3.5: Gold-catalysed hydration of an unsymmetrical alkyne

Nolan and co-workers have shown (IPr)AuX catalysts to be extremely efficient for the hydration of alkynes, even at very low catalyst loadings (Scheme 109).[167] Whilst terminal alkynes such as **132c** reliably give methyl ketones, there is scope for improvement in the selectivity of hydration of unsymmetrical disubstituted alkynes such as **400**.

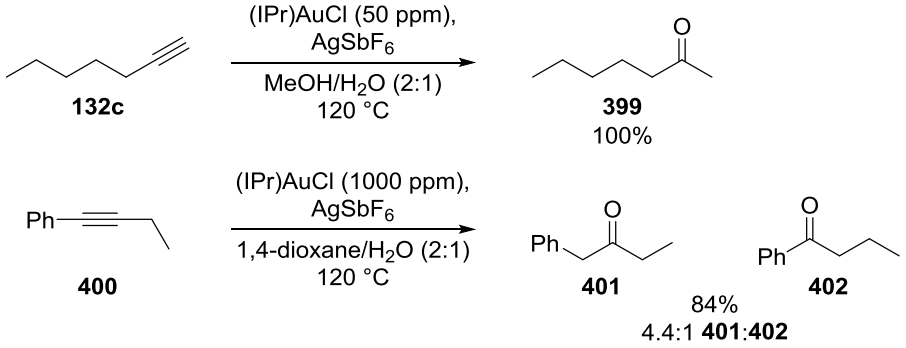

Scheme 109: Gold-catalysed hydration of unsymmetrical alkynes by Nolan and co-workers.[167a]

For the hydration reactions illustrated in Scheme 109 there is a remarkably large difference in the catalytic activity of gold complexes bearing various NHCs, for example (IMes)AuCl does not catalyse this type of reaction at all.[156,167a] With this in mind, alkyne **404** was prepared and its hydration was carried out using (IPr)AuCl, **(363a)AuCl** and **(363c)AuCl** to test both the activity and selectivity of the new catalysts (Table 11).

Table 11: Gold-catalysed hydration of an unsymmetrical alkyne.

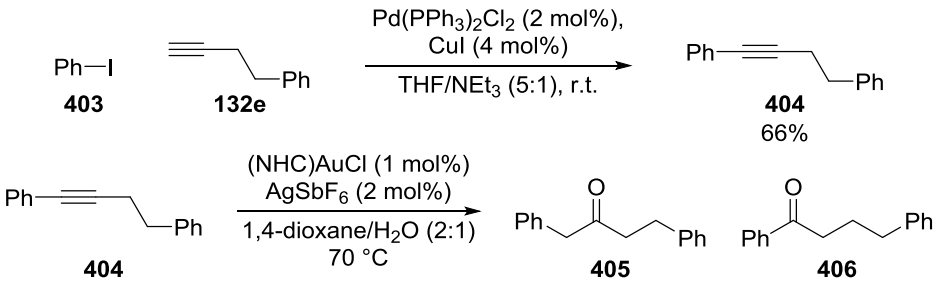

Entry	NHC	Combined yield	**405**:**406**
1	IPr	87%	1.0:1.0
2	**363a**	76%	1.1:1.0
3	**363c**	56%	1.8:1.0
4	no gold	NR	-

Isolated yield of a mixture of two isomers. Ratio determined by ^{1}H-NMR spectroscopy following purification.

(IPr)AuCl was the most active precatalyst of the three, and the only one to consume all of the starting material. The yield then decreased as the ligand was varied from IPr to **363a** to **363c**. Analysis of the crude ^{1}H-NMR spectra for these reactions showed that this reduction in yield could be entirely attributed to reduced conversion of starting material, rather than the presence of side-reactions. No reaction occurred in the absence of gold.

Interestingly (IPr)AuCl showed no selectivity in the hydration of alkyne **404**, perhaps indicating that the origin of the selectivity for the hydration of **400** is more steric than electronic, an effect that may well be diminished with **404**. **363aAuCl** and especially **363cAuCl** did show some selectivity for the benzyl ketone **405** over the phenyl ketone **406**, the same type of selectivity achieved by (IPr)AuCl in the hydration of **400**.

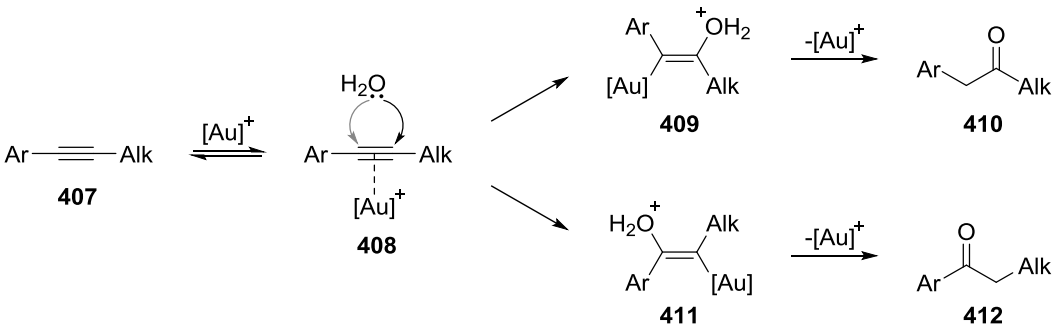

Scheme 110: Possible pathways in the gold-catalysed hydration of aryl-alkyl alkynes.

DFT studies have shown that the attack of water onto gold-activated alkynes is both the rate- and product-determining step for this reaction, so large ligands on the metal may reduce catalytic activity, but may also increase selectivity by creating greater differentiation between the energies of **409** and **411** (Scheme 110).[168] It is interesting to note that the order of selectivity (**363c**>**363a**>IPr) cannot be correlated with the percentage buried volume values for these NHCs (Table 10), showing that this measure of the steric demand of ligands is not always relevant to their behaviour in catalysis, as it does not take into account either their shape or symmetry.

In the absence of a directing group or strong electronic activation within the substrate, the regioselective gold-catalysed hydration of aryl-alkyl alkynes remains an unsolved problem.[169]

4.2.4: Conclusion

Investigation of several synthetic routes has allowed the highly convergent synthesis of the first imidazolium salts annulated to oxazoles. A current limitation of this approach is that if the imidazolium chloride salts generated by $POCl_3$-mediated cyclisation are not water soluble, then their purification is challenging.

Gold, copper and iridium NHC complexes have been prepared, allowing the steric and electronic characterisation of these ligands using the $\%V_{bur}$ and Tolman Electronic Parameter approaches respectively. The ligands have also been shown to be prochiral, due to a loss of rotational freedom upon metal binding. Finally, the gold complexes were successful in catalysing the hydration of an unsymmetrical alkyne, showing enhanced regioselectivity over the commonly used (IPr)AuCl, albeit with reduced activity.

APPENDIX

5.1: Synthetic Procedures and Characterisation Data for all Compounds

5.1.1: General Information

Commercially available chemicals/reagents were purchased from major suppliers and used without further purification except where stated. All reactions were stirred using Teflon-coated magnetic stirrer bars. Where reactions are stated as being under an argon atmosphere, glassware was pre-dried using a heat gun at high vacuum and the solvents were dried as follows: CH_2Cl_2, THF, toluene, MeCN and MeOH using a Pure Solv-MD solvent purification system; DMF, 1,4-dioxane and *m*-xylene over 4 Å Linde type molecular sieves (activated by heating with a heat gun under high vacuum). The following cooling baths were used: 0 °C (ice/water), −10 °C (ice/NaCl) and −78 °C (dry ice/acetone). For reactions above room temperature pre-heated paraffin oil baths or metal heating blocks on stirrer hotplates were employed and the temperature was controlled using an external probe. Reactions were monitored by thin layer chromatography using Merck silica gel 60 F254 (aluminium support) TLC plates which were developed using standard visualising agents: UV fluorescence (254 nm), potassium permanganate /Δ or vanillin /Δ. Flash column chromatography was carried out on silica gel except where the use of alumina is stated. Melting points were measured in open capillaries using a Stuart Scientific melting point apparatus and are uncorrected. Specific rotations were determined using a PolAAr 2001 instrument and are given in units of $°dm^{-1}g^{-1}cm^3$ with concentrations (*c*) given in g / 100 cm^3. Infra-red spectra were recorded using a Perkin-Elmer Spectrum 100 FTIR spectrometer using an ATR attachment; only selected absorbances (ν_{max}) are reported. NMR spectra were recorded using Bruker AV300 or AVIII300 (^1H = 300 MHz, ^{19}F = 282 MHz, ^{31}P = 121 MHz) and Bruker AV400 or AVIII400 (^1H = 400 MHz, ^{13}C = 101 MHz) spectrometers in commercial, TMS free, deuterated solvents. Chemical shifts (δ) are given in ppm relative to TMS and are calibrated using residual solvent peaks.[170] ^{13}C-NMR spectra were recorded using the UDEFT or PENDANT pulse sequences from the Bruker standard pulse program library. ^{13}C DEPT spectra and 2D COSY, HSQC and HMBC spectra were recorded in order to assist with NMR assignment when

necessary. NMR spectra were processed using MestReNova software. Where NMR spectra are assigned for a mixture of two rotamers these are given in the format: "4.25 and 4.13 (s, 2H)" where the two chemical shift values correspond to one singlet from each rotamer and the sum total of their relative integrations is two. Mass spectra were obtained using Waters GCT Premier (EI), Waters LCT (ES) or Waters Synapt (ES) spectrometers. High resolution spectra used a lock-mass to adjust the calibrated mass scale.

5.1.2: Precursors to Pyridine-*N*-Aminides

Ester 147e

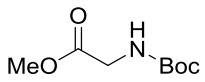

Di-*tert*-butyl dicarbonate (2.74 g, 12.6 mmol) was dissolved in CH_2Cl_2 (40 mL) and NEt_3 (4.4 mL, 31.6 mmol) and glycine methyl ester hydrochloride (1.97 g, 14.1 mmol) were added successively. The suspension was stirred for 18 hours at room temperature. The reaction mixture was cooled to 0 °C and then transferred to a separating funnel and washed with ice-cold 0.5 M $HCl_{(aq)}$ solution (2 x 50 mL). The organic phase was dried over Na_2SO_4 and concentrated under reduced pressure to give *carbamate* **147e** as a colourless oil (2.34 g, 92%); IR (neat): ν = 3371, 2979, 1753, 1697, 1513, 1367, 1207, 1156, 1056 cm^{-1}; ^{1}H-NMR (300 MHz, $CDCl_3$): δ = 5.00 (br s, NH), 3.92 (d, *J* = 5.6 Hz, 2H), 3.75 (s, 3H), 1.45 (s, 9H); ^{13}C-NMR (101 MHz, $CDCl_3$): δ = 170.9 (C), 155.8 (C), 80.0 (C), 52.2 (CH_3), 42.3 (CH_2), 28.3 ($3CH_3$). Spectroscopic data matched those reported.[171]

Ester 147f

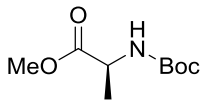

Following a literature procedure[171] solutions of $NaHCO_3$ (840 mg, 10.0 mmol) in H_2O (15 mL) and di-*tert*-butyl dicarbonate (2.19 g, 10.0 mmol) in $CHCl_3$ (5 mL), and NaCl (2.00 g), were added to a suspension of alanine methyl ester hydrochloride (1.41 g, 10.0 mmol) in $CHCl_3$ (15 mL). The biphasic solution was stirred vigorously at reflux for 2 hours. After cooling to room temperature, the reaction mixture was extracted with $CHCl_3$ (2 x 15 mL). The combined organic fractions were washed with water (20 mL), dried over Na_2SO_4, concentrated under reduced pressure and purified by flash column chromatography (4:1 hexane:EtOAc) to yield *carbamate* **147f** as a white

solid (1.38 g, 67%); mp: 25-26 °C (lit.[172] 31-33 °C); IR (neat): ν = 3361, 2980, 1743, 1696, 1514, 1366, 1160, 1068 cm^{-1}; ^{1}H-NMR (300 MHz, $CDCl_3$): δ = 5.04 (br s, NH), 4.37-4.24 (m, 1H), 3.73 (s, 3H), 1.43 (s, 9H), 1.37 (d, *J* = 7.2 Hz, 3H); ^{13}C-NMR (101 MHz, $CDCl_3$): δ = 174.0 (C), 155.2 (C), 80.0 (C), 52.5 (CH_3), 49.3 (CH), 28.5 (CH_3), 18.8 ($3CH_3$), 99% ee (HPLC trace and conditions given on page 208); Spectroscopic data matched those reported.[173]

Ester 147g

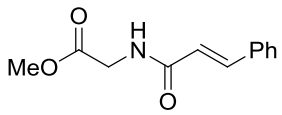

Adapted from a literature procedure[174] *trans*-cinnamic acid (742 mg, 5.0 mmol), MeCN (15 mL) and NEt_3 (700 µL, 5.0 mmol) were added to a flask under an atmosphere of argon and cooled to −10 °C. Isobutyl chloroformate (650 µL, 5.0 mmol) was added over 2 minutes and the resulting mixture was stirred for 5 minutes. MeCN (15 mL), NEt_3 (700 µL, 5.0 mmol) and glycine methyl ester hydrochloride (628 mg, 5.0 mmol) were then added before the reaction mixture was allowed to warm to room temperature and stirred for 20 hours. The solvent was removed under reduced pressure and the resulting residue was taken up in satd. $NaHCO_{3(aq)}$ solution (20 mL) and extracted with CH_2Cl_2 (3 x 20 mL). The combined organic fractions were dried over Na_2SO_4, concentrated under reduced pressure and purified by flash column chromatography (1:1 EtOAc:Hexane) to give *ester* **147g** as a white solid (785 mg, 72%); mp: 82-83 °C; IR (neat): ν = 3242, 3061, 2945, 1746, 1655, 1616, 1544, 1200, 1178, 1046, 967, 857 cm^{-1}; ^{1}H-NMR (300 MHz, $CDCl_3$): δ = 7.63 (d, *J* = 15.7 Hz, 1H), 7.49-7.42 (m, 2H), 7.37-7.28 (m, 3H), 6.66 (br t, NH), 6.51 (d, *J* = 15.7 Hz, 1H), 4.18 (d, *J* = 5.3 Hz, 2H), 3.75 (s, 3H); ^{13}C-NMR (101 MHz, $CDCl_3$): δ = 170.7 (C), 166.2 (C), 141.8 (CH), 134.7 (C), 129.9 (CH), 128.9 (2CH), 128.0 (2CH), 119.9 (CH), 52.5 (CH_2), 41.5 (CH_3); HRMS (EI): *m/z* calculated for $C_{12}H_{13}NO_3$: 219.0895, found 219.0893 $(M)^+$.

Ester 147h

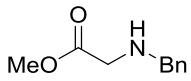

Following a literature procedure,[175] methyl bromoacetate (475 µL, 5.0 mmol), THF (5 mL), NEt_3 (1.4 mL, 10.0 mmol) and benzylamine (570 µL, 5.2 mmol) were added sequentially to a flask and the reaction mixture was stirred for 20 hours at room temperature. The precipitate was removed by filtration and the filtrate was concentrated under reduced pressure and purified by flash column chromatography (33→50% EtOAc in hexane) to give *amine* **147h** as a colourless oil (508 mg, 56%); IR (neat): ν = 3337, 1737, 1454, 1436, 1196, 1178, 1139, 735, 698 cm^{-1}; ^{1}H-NMR (300 MHz, $CDCl_3$) δ = 7.38-7.23 (m, 5H), 3.84 (s, 2H), 3.73 (s, 3H), 3.44 (s, 2H), 2.39 (br s, NH); ^{13}C-NMR (101 MHz, $CDCl_3$) δ = 172 .6 (C), 132.4 (C) 128.7 (2CH), 128. 6 (2CH), 127.5 (CH), 53.2 (CH_2), 52.0 (CH_3), 49.7 (CH_3). Spectroscopic data match those reported.[176]

Ester 147j

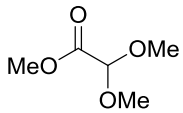

Following a literature procedure,[177] $TsOH{\cdot}H_2O$ (400 mg, 2.1 mmol) was added to a solution of glyoxylic acid monohydrate (2.00 g, 22 mmol) in trimethyl orthoformate (12 mL, 109 mmol) and the mixture was stirred for 3 hours at room temperature. K_2CO_3 (400 mg, 2.9 mmol) was added and stirring was continued for 0.5 hours before isolation of the product by distillation directly from the reaction flask (b.p. 63-64 °C at 25-28 mbar [lit.[177] 64-67 °C at 27 mbar], note that a solvent-containing fraction was collected at 25-28 mbar at room temperature prior to collection of the product fraction) to give *ester* **147j** as a clear oil (2.07 g, 71%); IR (neat) ν = 3005, 2955, 2839, 1750, 1440, 1226, 1195, 1116, 1065, 1017, 981, 913, 800 cm^{-1}; ^{1}H-NMR (300 MHz, $CDCl_3$) δ = 4.83 (s, 1H), 3.81 (s, 3H), 3.42 (s, 6H); ^{13}C-NMR (101 MHz, $CDCl_3$) δ = 167.7 (C), 99.0 (CH), 54.1 ($2CH_3$), 52.6 (CH_3). Spectroscopic data match those reported.[177]

Ester 147l

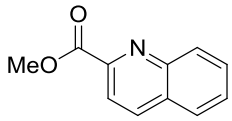

Quinaldic acid (866 mg, 5.0 mmol), MeOH (10 mL) and H_2SO_4 (500 µL, 9.3 mmol) were added to a flask and the reaction mixture was heated at reflux for 18 hours. After cooling to room temperature, the reaction mixture was concentrated under reduced pressure and partitioned between satd. $NaHCO_{3(aq)}$ solution (20 mL) and CH_2Cl_2 (20 mL). Following separation of the two layers the aqueous phase was extracted with CH_2Cl_2 (2 x 10 mL) and the combined organic fractions were dried over Na_2SO_4 and filtered through a 5 cm pad of silica gel (eluting with CH_2Cl_2). Concentration of the filtrate under reduced pressure afforded *ester* **147l** as a white solid (562 mg, 60%); mp: 80-81 °C (lit.[178] 79-80 °C); IR (neat): ν = 2953, 1710, 1449, 1317, 1299, 1196, 1140, 1106, 772 cm^{-1}; ^{1}H-NMR (300 MHz, $CDCl_3$): δ = 8.35-8.27 (m, 2H), 8.20 (d, *J* = 8.5 Hz, 1H), 7.92-7.85 (m, 1H), 7.79 (appt. td, *J* = 7.6, 1.4 Hz 1H), 7.65 (appt. td, *J* = 7.6, 1.4 Hz, 1H), 4.08 (s, 3H); ^{13}C-NMR (101 MHz, $CDCl_3$): δ = 166.1 (C), 148.1 (C), 147.7 (C), 137.5 (CH), 130.9 (CH), 130.4 (CH), 129.5 (C), 128.8 (CH), 127.7 (CH), 121.2 (CH), 53.3 (CH_3). Spectroscopic data matched those reported.[178]

Ester 147m

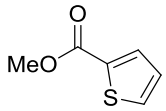

Thiophene-2-carboxylic acid (1.28 g, 10.0 mmol), MeOH (20 mL) and H_2SO_4 (1 mL, 12.0 mmol) were added to a flask and the reaction mixture was heated at reflux for 24 hours. After cooling to room temperature, satd. $NaHCO_{3(aq)}$ solution (30 mL) was added and the mixture was extracted with CH_2Cl_2 (2 x 20 mL), dried over Na_2SO_4 and concentrated under reduced pressure to yield *ester* **147m** as an orange oil (1.20 g, 84%); IR (neat): ν = 2952, 1704, 1525, 1436, 1416, 1360, 1286, 1259, 1093 cm^{-1}; ^{1}H-NMR (300 MHz, $CDCl_3$): δ = 7.81 (dd, *J* = 3.8, 1.1 Hz, 1H), 7.55 (dd, *J* = 5.0, 1.1 Hz, 1H), 7.10 (dd, *J* = 5.0, 3.8 Hz, 1H), 3.89 (s, 3H); ^{13}C-NMR (101 MHz, $CDCl_3$): δ = 162.8 (C), 133.7 (C), 133.6 (CH), 132.5 (CH), 127.9 (CH), 52.3 (CH_3). Spectroscopic data matched those reported.[179]

Ester 147n

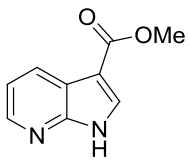

7-Azaindole-3-carboxylic acid (239 mg, 1.5 mmol), MeOH (5 mL) and H_2SO_4 (100 µL, 1.9 mmol) were added to a flask and the reaction mixture was heated at reflux for 14 hours. After cooling to room temperature, satd. $NaHCO_{3(aq)}$ solution (20 mL) was added and the mixture was extracted with CH_2Cl_2 (3 x 20 mL), dried over Na_2SO_4 and concentrated under reduced pressure to yield *ester* **147n** as a pale orange solid (97.4 mg, 38%); mp: 204-205 °C; IR (neat): ν = 3105, 1689, 1526, 1311, 1163, 1049 cm^{-1}; ^{1}H-NMR (300 MHz, $CDCl_3$): δ = 12.05 (br s, NH), 8.51 (dd, *J* = 7.9, 1.6 Hz, 1H), 8.41 (dd, *J* = 4.8, 1.5 Hz, 1H), 8.13 (s, 1H), 7.28 (dd, *J* = 7.9, 4.8 Hz, 1H), 3.94 (s, 3H); ^{13}C-NMR (101 MHz, $CDCl_3$): δ = 165.1 (C), 148.9 (C), 143.8 (CH), 131.8 (CH), 130.7 (CH), 119.2 (C), 118.1 (CH), 107.4 (C), 51.4 (CH_3); HRMS (ES): *m/z* calculated for $C_9H_9N_2O_2$: 177.0664, found 177.0667 $(M+H)^+$.

Carbamate 262

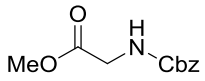

Benzyl chloroformate (700 µL, 4.6 mmol) was added to a suspension of glycine methyl ester hydrochloride (628 mg, 5.0 mmol) and NEt_3 (1.4 mL, 10.0 mmol) in CH_2Cl_2 (30 mL). The reaction mixture was stirred for 15 hours at room temperature and then washed sequentially with 0.5 M $HCl_{(aq)}$ solution (20 mL) and brine (20 mL). The organic phase was dried over Na_2SO_4, concentrated under reduced pressure and purified by flash column chromatography (15→20% EtOAc in hexane) to give *carbamate* **262** as a clear oil (537 mg, 48%); IR (neat): ν = 3351, 2954, 1706, 1524, 1276, 1207, 1054, 1005 cm^{-1}; ^{1}H-NMR (300 MHz, $CDCl_3$): δ = 7.43-7.28 (m, 5H), 5.29 (br s, NH), 5.13 (s, 2H), 3.99 (d, *J* = 5.6 Hz, 2H), 3.75 (s, 3H); ^{13}C-NMR (101 MHz, $CDCl_3$): δ = 170.6 (C), 156.4 (C), 136.3 (C), 128.7 (2CH), 128.3 (2CH), 128.2 (CH), 67.3 (CH_2), 52.5 (CH_3), 42.8 (CH_2). Spectroscopic data matched those reported.[180]

Sulfonamide 264

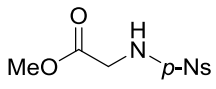

4-Nitrobenzenesulfonyl chloride (2.21 g, 10 mmol) was added to a suspension of glycine methyl ester hydrochloride (1.25 g, 10 mmol) and NEt_3 (2.8 mL, 20 mmol) in CH_2Cl_2 (75 mL). The reaction mixture was stirred for 18 hours at room temperature and then washed with 1 M $HCl_{(aq)}$ solution (100 mL). The organic phase was dried over Na_2SO_4 and concentrated under reduced pressure. The resulting residue was purified by recrystallisation from EtOAc to give *sulfonamide* **264** as a white solid (2.09 g, 76%); mp: 145-147 °C; IR (neat): ν = 3256, 1727, 1528, 1348, 1334, 1311, 1225, 1157, 1130, 826, 735 cm^{-1}; ^{1}H-NMR (300 MHz, $CDCl_3$): δ = 8.37 (d, *J* = 8.9 Hz, 2H), 8.06 (d, *J* = 8.9 Hz, 2H), 5.29 (br s, NH), 3.88 (s, 2H), 3.67 (s, 3H); ^{13}C-NMR (101 MHz, $CDCl_3$): δ = 169.1 (C), 145.5 (C), 130.4 (C), 128.6 (2CH), 124.5 (2CH), 53.0 (CH_3), 44.1 (CH_2). Spectroscopic data matched those reported.[181]

Sulfonamide 265

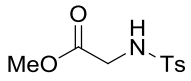

para-Toluenesulfonyl chloride (3.80 g, 20 mmol) was added to a suspension of glycine methyl ester hydrochloride (2.70 g, 21.5 mmol) and NEt_3 (6.0 mL, 43 mmol) in CH_2Cl_2 (120 mL). The reaction mixture was stirred for 20 hours at room temperature and then washed with 1 M $HCl_{(aq)}$ solution (100 mL). The organic phase was dried over Na_2SO_4, concentrated under reduced pressure to *ca.* 20 mL and filtered through a 5 cm pad of silica gel (eluting with CH_2Cl_2). Evaporation of the solvent under reduced pressure gave *sulfonamide* **265** as a white solid (4.49 g, 93%); mp: 87-88 °C (lit.[182] 89-91 °C); IR (neat): ν = 3273, 1727, 1338, 1350, 1318, 1250, 1160, 1108. 1091, 809 cm^{-1}; ^{1}H-NMR (300 MHz, $CDCl_3$): δ = 7.75 (d, *J* = 8.2 Hz, 2H), 7.31 (d, *J* = 8.2 Hz, 2H), 5.01 (br t, NH), 3.78 (d, *J* = 5.5 Hz, 2H), 3.64 (s, 3H), 2.43 (s, 3H); ^{13}C-NMR (101 MHz, $CDCl_3$): δ = 169.4 (C), 144.0 (C), 136.2 (C), 129.9 (2CH), 127.4 (2CH), 52.8 (CH_3), 44.2 (CH_2), 21.7 (CH_3). Spectroscopic data matched those reported.[183]

Sulfonamide 271

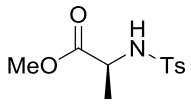

para-Toluenesulfonyl chloride (4.77 g, 25 mmol) was added to a suspension of alanine methyl ester hydrochloride (4.19 g, 30 mmol) and NEt_3 (8.4 mL, 60 mmol) in CH_2Cl_2 (100 mL). The reaction mixture was stirred for 24 hours at room temperature and then washed sequentially with 2 M $HCl_{(aq)}$ solution (2 x 100 mL) and brine (100 mL). The organic phase was dried over Na_2SO_4, concentrated under reduced pressure and partially purified by flash column chromatography (20⟶30% EtOAc in hexane). The resulting oil was further purified by precipitation from *tert*-butyl methyl ether with hexane, yielding *sulfonamide* **271** as a white solid (2.85 g, 44%); mp: 90-92 °C (lit.[184] 94-95 °C); IR (neat): ν = 3226, 1731, 1438, 1363, 1336, 1226, 1164, 1135, 1091, 991 cm^{-1}; ^{1}H-NMR (300 MHz, $CDCl_3$): δ = 7.72 (d, *J* = 8.1 Hz, 2H), 7.29 (d, *J* = 8.1 Hz, 2H), 5.16 (br d, *J* = 8.5 Hz, NH), 4.05-3.92 (m, 1H), 3.54 (s, 3H), 2.42 (s, 3H), 1.38 (d, *J* = 7.2 Hz, 3H); ^{13}C-NMR (101 MHz, $CDCl_3$): δ = 172.8 (C), 143.8 (C), 136.9 (C), 129.8 (2CH), 127.4 (2CH), 52.7 (CH), 51.6 (CH_3), 21.7 (CH_3), 20.0 (CH_3). Spectroscopic data matched those reported.[184]

Sulfonamide 273

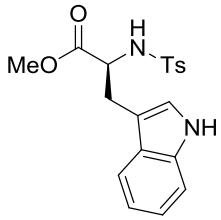

para-Toluenesulfonyl chloride (4.77 g, 25 mmol) was added to a suspension of tryptophan methyl ester hydrochloride (6.55 g, 30 mmol) and NEt_3 (8.4 mL, 60 mmol) in CH_2Cl_2 (100 mL). The reaction mixture was stirred for 24 hours at room temperature and then washed with 2 M $HCl_{(aq)}$ solution (2 x 100 mL) and brine (100 mL). The organic phase was dried over Na_2SO_4, concentrated under reduced pressure, and recrystallised from MeOH to give *sulfonamide* **273** as a white solid (6.14 g, 66%); mp: 126-128 °C; IR (neat): ν = 3395, 3283, 1735, 1456, 1446, 1426, 1343, 1335, 1250, 1221, 1165, 1091, 741 cm^{-1}; ^{1}H-NMR (300 MHz, $CDCl_3$): δ = 8.09 (s, NH), 7.60 (d, *J* = 8.3 Hz, 2H), 7.43 (d, *J* = 8.1 Hz, 1H), 7.32 (d, *J* = 8.1 Hz, 1H), 7.20-7.14 (m, 3H), 7.10-7.06 (m, 1H), 7.04-7.01 (m, 1H), 5.13 (br d, *J* = 8.9 Hz, NH), 4.30-4.20 (m, 1H), 3.43 (s, 3H), 3.23 (d, *J* = 5.5 Hz, 2H), 2.37 (s, 3H); ^{13}C-NMR (101 MHz, $CDCl_3$): δ = 171.8 (C), 143.6 (C), 136.7 (C), 136.2 (C), 129.6 (2CH), 127.3 (C), 127.2 (2CH), 123.5 (CH),

122.3 (CH), 119.8 (CH), 118.7 (CH), 111.3 (CH), 109.2 (C), 56.1 (CH), 52.5 (CH_3), 29.4 (CH_2), 21.6 (CH_3). Spectroscopic data matched those reported.[185]

Ester 263a

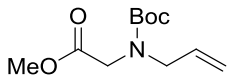

Under an argon atmosphere, allyl bromide (1.3 mL, 15 mmol) was added to a solution of ester **147e** (1.90 g, 10 mmol) in DMF (20 mL). The reaction was cooled to 0 °C and NaH (60% dispersion, 600 mg, 15 mmol) was added in portions over 5 minutes. The reaction mixture was stirred for 6 hours at room temperature and then quenched by addition of 1:1 H_2O:satd. $NH_4Cl_{(aq)}$ solution (30 mL) and extracted with EtOAc (2 x 30 mL). The combined organic phases were washed with brine (5 x 30 mL), dried over Na_2SO_4, concentrated under reduced pressure and purified by flash column chromatography (5⟶10% EtOAc in hexane) to give *ester* **263a** as a colourless oil (750 mg, 33%); IR (neat): ν = 2978, 1754, 1696, 1397, 1367, 1247, 1200, 1164, 1142 cm^{-1}; *NMR shows a mixture of two rotamers:* ^{1}H-NMR (300 MHz, $CDCl_3$): δ = 5.86-5.70 (m, 1H), 5.22-5.07 (m, 2H), 3.99-3.91 (m, 2H), 3.91-3.81 (m, 2H), 3.72 (s, 3H), 1.46 and 1.43 (s, 9H); ^{13}C-NMR (101 MHz, $CDCl_3$): δ = 170.7 (C), 155.2 (C), 133.9 and 133.8 (CH), 117.8 and 117.0 (CH_2), 80.5 (C), 52.10 and 52.07 (CH_3), 50.9 and 50.4 (CH_2), 48.0 and 47.7 (CH_2), 28.44 and 28.39 ($3CH_3$). Spectroscopic data matched those reported.[186]

Ester 263b

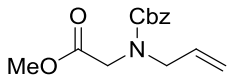

Under an argon atmosphere, allyl bromide (200 µL, 2.3 mmol) was added to a solution of ester **262** (435 mg, 1.9 mmol) in DMF (5 mL). The reaction was cooled to 0 °C and NaH (60% dispersion, 85 mg, 2.1 mmol) was added in portions over 5 minutes and the mixture was stirred for 4 hours at room temperature. The reaction was quenched H_2O (25 mL) and extracted with EtOAc (25 mL). The organic phase was washed with brine (2 x 25 mL), dried over Na_2SO_4, concentrated under reduced pressure and purified by flash column chromatography (9:1 EtOAc:hexane) to give *ester* **263b** as a colourless oil (296 mg, 58%); IR (neat): ν = 2923, 2852, 1752, 1702, 1455, 1407, 1240, 1204 cm^{-1}; *NMR shows a mixture of two rotamers in a ~ 1:1 ratio:*

^{1}H-NMR (400 MHz, $CDCl_3$): δ = 7.40-7.28 (m, 5H), 5.86-5.70 (m, 1H), 5.23-5.09 (m, 4H), 4.05-3.91 (m, 2H), 3.74 and 3.66 (s, 3H); ^{13}C-NMR (101 MHz, $CDCl_3$): δ = 170.3 (C), 136.6 (C), 133.3 and 133.2 (CH), 128.6 (2CH), 128.2 (CH and C), 127.9 (2CH), 118.3 and 117.7 (CH_2), 67.7 and 67.6 (CH_2), 52.3 and 52.2 (CH_3), 51.0 and 50.6 (CH_2), 48.0 and 47.6 (CH_2); HRMS (ES): *m/z* calculated for $C_{14}H_{17}NO_4Na$: 286.1055, found 286.1052 $(M+Na)^+$.

5.1.2.1: General procedure for alkylation of sulfonamides (GP1)

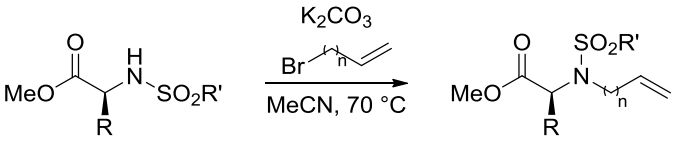

Following a literature procedure,[112] under an argon atmosphere a flask was charged sequentially with sulfonamide (1.0 eq.), K_2CO_3 (2.0 eq.), MeCN (0.1 M with respect to sulfonamide) and alkyl bromide (1.5 eq.). The reaction mixture was stirred for 18 hours at 70 °C and the volatiles were then removed under reduced pressure. The resulting solid was taken up in 1:1 EtOAc:H_2O and the organic phase was separated, washed with brine, dried over Na_2SO_4 and concentrated under reduced pressure. The crude product was purified either by filtration through a 5 cm pad of silica gel eluting with CH_2Cl_2 or by flash column chromatography to give the alkylated *sulfonamide*.

Ester 263c

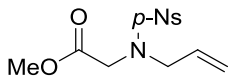

Following **GP1** using sulfonamide **264** (960 mg, 3.5 mmol), K_2CO_3 (970 mg, 7.0 mmol) and allyl bromide (450 µL, 5.2 mmol). Purification by flash column chromatography (20→25% EtOAc in hexane) gave *ester* **263c** as a white solid (1.05 g, 95%); mp: 62-63 °C; IR (neat): ν = 3114, 2957, 1753, 1610, 1545, 1348, 1313, 1203, 1160 cm^{-1}; ^{1}H-NMR (300 MHz, $CDCl_3$): δ = 8.36 (d, *J* = 9.0 Hz, 2H), 8.05 (d, *J* = 9.0 Hz, 2H), 5.71 (ddt, *J* = 16.9, 10.2, 6.5 Hz, 1H), 5.30-5.16 (m, 2H), 4.12 (s, 2H), 3.93 (d, *J* = 6.5 Hz, 2H), 3.64 (s, 3H); ^{13}C-NMR (101 MHz, $CDCl_3$): δ = 169.1 (C), 150.2 (C), 145.8 (C), 131.6 (CH), 128.8 (2CH),

124.3 (2CH), 120.8 (CH_2), 52.5 (CH_3), 50.9 (CH_2), 46.9 (CH_2); HRMS (ES): *m/z* calculated for $C_{12}H_{15}N_2O_2S$: 315.0651, found 315.0656 $(M+H)^+$.

Ester 263d

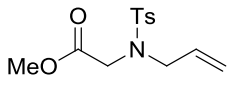

Following **GP1** using sulfonamide **265** (1.80 g, 7.4 mmol), K_2CO_3 (2.04 g, 14.8 mmol) and allyl bromide (960 µL, 11.1 mmol). Purification by filtration through a 5 cm pad of silica gel (eluting with CH_2Cl_2) gave *ester* **263d** as a colourless oil (1.88 g, 89%); IR (neat): ν = 2924, 2853, 1753, 1338, 1157, 1092, 922 cm^{-1}; ^{1}H-NMR (300 MHz, $CDCl_3$): δ = 7.73 (d, *J* = 8.2 Hz, 2H), 7.30 (d, *J* = 8.2 Hz, 2H), 5.68 (ddt, *J* = 16.8, 10.4, 6.5 Hz, 1H), 5.22-5.12 (m, 2H), 4.02 (s, 2H), 3.89 (d, *J* = 6.5 Hz, 2H), 3.63 (s, 3H), 2.43 (s, 3H); ^{13}C-NMR (101 MHz, $CDCl_3$): δ = 169.5 (C), 143.6 (C), 136.9 (C), 132.4 (CH), 129.7 (2CH), 127.5 (2CH), 120.0 (CH_2), 52.2 (CH_3), 50.9 (CH_2), 47.0 (CH_2), 21.7 (CH_3). Spectroscopic data matched those reported.[186]

Ester 263f

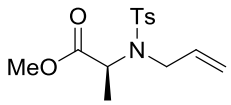

Following **GP1** using sulfonamide **271** (1.29 g, 5.0 mmol), K_2CO_3 (1.38 g, 10 mmol) and allyl bromide (650 µL, 7.5 mmol). Purification by filtration through a 5 cm pad of silica gel (eluting with CH_2Cl_2) gave *ester* **263f** as a colourless oil (1.44 g, 97%); α_D^{20} = −33.3 ($CHCl_3$, c = 1.1); IR (neat): ν = 2988, 2953, 1740, 1337, 1154, 1090, 1071 cm^{-1}; ^{1}H-NMR (300 MHz, $CDCl_3$): δ = 7.71 (d, *J* = 8.2 Hz, 2H), 7.28 (d, *J* = 8.2 Hz, 2H), 5.81 (ddt, *J* = 17.1, 10.2, 6.1 Hz, 1H), 5.23-5.14 (m, 1H), 5.13-5.07 (m, 1H), 4.66 (q, *J* = 7.3 Hz, 1H), 3.98-3.77 (m, 2H), 3.55 (s, 3H), 2.42 (s, 3H), 1.40 (d, *J* = 7.3 Hz, 3H); ^{13}C-NMR (101 MHz, $CDCl_3$): δ = 172.1 (C), 143.5 (C), 137.3 (C), 135.2 (CH), 129.6 (2CH), 127.6 (2CH), 117.7 (CH_2), 55.1 (CH), 52.2 (CH_3), 48.2 (CH_2), 21.7 (CH_3), 16.6 (CH_3); HRMS (ES): *m/z* calculated for $C_{14}H_{19}NO_4SNa$: 320.0932, found 320.0935 $(M+Na)^+$.

Ester 263g

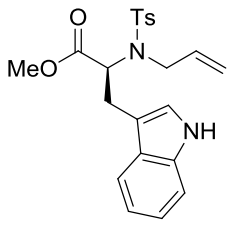

Following **GP1** using sulfonamide **273** (1.86 g, 5.0 mmol), K_2CO_3 (1.38 g, 10 mmol) and allyl bromide (650 µL, 7.5 mmol). Purification by flash column chromatography (20→50% EtOAc in hexane) gave *ester* **263g** as a white solid (1.72 g, 83%); $[\alpha]_D^{20}$ = −10.5 ($CHCl_3$, c = 1.2); mp: 82-84 °C; IR (neat): ν = 3392, 1742, 1151, 1087 cm^{-1}; ^{1}H-NMR (300 MHz, $CDCl_3$): δ = 8.00 (s, NH), 7.68-7.53 (m, 3H), 7.35 (d, *J* = 8.0 Hz, 1H), 7.23-7.06 (m, 5H), 5.76 (ddt, *J* = 17.0, 10.3, 6.3 Hz, 1H), 5.22-5.11 (m, 1H), 5.84-5.67 (m, 1H), 4.90 (appt. t, *J* = 7.5 Hz, 1H), 4.05-3.84 (m, 2H), 3.48 (s, 3H), 3.46 (dd, *J* = 14.9, 7.5 Hz, 1H), 3.15 (dd, *J* = 14.9, 7.5 Hz, 1H), 2.39 (s, 3H); ^{13}C-NMR (101 MHz, $CDCl_3$): δ = 171.4 (C), 143.3 (C), 137.3 (C), 136.2 (C), 135.0 (CH), 129.4 (2CH), 127.6 (2CH), 127.3 (C), 123.3 (CH), 122.3 (CH), 119.7 (CH), 118.7 (CH), 117.9 (CH_2), 111.3 (CH), 110.8 (C), 59.7 (CH), 52.0 (CH_3), 48.4 (CH_2), 26.8 (CH_2), 21.7 (CH_3); HRMS (ES): *m/z* calculated for $C_{22}H_{24}N_2O_4SNa$: 435.1354, found 435.1347 $(M+Na)^+$.

Ester 263h

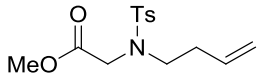

Following **GP1** using sulfonamide **265** (1.00 g, 4.1 mmol), K_2CO_3 (1.14 g, 8.2 mmol) and 4-bromo-1-butene (625 µL, 6.2 mmol). Purification by flash column chromatography (4:1 hexane:EtOAc) gave *ester* **263h** as a colourless oil (672 mg, 55%); IR (neat): ν = 2924, 2852, 1753, 1337, 1209, 1155, 1091, 926 cm^{-1}; ^{1}H-NMR (300 MHz, $CDCl_3$): δ = 7.71 (d, *J* = 8.2 Hz, 2H), 7.29 (d, *J* = 8.2 Hz, 2H), 5.69 (ddt, *J* = 17.1, 10.3, 6.8 Hz, 1H), 5.10-4.98 (m, 2H), 4.06 (s, 2H), 3.62 (s, 3H), 3.30 (t, *J* = 7.4 Hz, 2H), 2.41 (s, 3H), 2.34-2.24 (m, 2H); ^{13}C-NMR (101 MHz, $CDCl_3$): δ = 169.5 (C), 143.5 (C), 136.9 (C), 134.5 (CH), 129.6 (2CH), 127.5 (2CH), 117.4 (CH_2), 52.2 (CH_3), 48.2 (CH_2), 47.9 (CH_2), 32.7 (CH_2), 21.6 (CH_3). Spectroscopic data matched those reported.[186]

Ester 263i

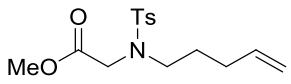

Following **GP1** using sulfonamide **265** (1.00 g, 4.1 mmol), K_2CO_3 (1.14 g, 8.2 mmol) and 5-bromo-1-pentene (730 µL, 6.2 mmol). Purification by flash column chromatography (4:1 hexane:EtOAc) gave *ester* **263i** as a colourless oil (722 mg, 56%); IR (neat): ν = 2923, 2852, 1754, 1339, 1207, 1156, 1091 cm^{-1}; ^{1}H-NMR (300 MHz, $CDCl_3$): δ = 7.71 (d, *J* = 8.2 Hz, 2H), 7.29 (d, *J* = 8.2 Hz, 2H), 5.74 (ddt, *J* = 17.0, 10.3, 6.6 Hz, 1H), 5.04-4.93 (m, 2H), 4.04 (s, 2H), 3.63 (s, 3H), 3.22 (t, *J* = 7.4 Hz, 2H), 2.42 (s, 3H), 2.10-2.01 (m, 2H), 1.71-1.59 (m, 2H); ^{13}C-NMR (101 MHz, $CDCl_3$): δ = 169.6 (C), 143.5 (C), 137.5 (CH), 136.8 (C), 129.7 (2CH), 127.5 (2CH), 115.5 (CH_2), 52.3 (CH_3), 48.11 (CH_2), 48.06 (CH_2), 30.7 (CH_2), 27.2 (CH_2), 21.7 (CH_3). Spectroscopic data matched those reported.[186]

Ester 147p

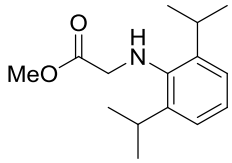

Adapted from a literature procedure,[187] methyl bromoacetate (950 µL, 10 mmol) was added to a mixture of 2,6-diisopropylaniline (1.9 mL, 10 mmol) and NaOAc (821 mg, 10 mmol) in methanol (1.5 mL) and the reaction mixture was heated at 55 °C for 6 hours. After cooling to room temperature, the reaction mixture was filtered through cotton, concentrated under reduced pressure and purified by flash column chromatography (3:17 Et_2O:hexane) to give *ester* **147p** as a red oil (2.20 g, 88%); IR (neat): ν = 2961, 2870, 1742, 1621, 1438, 1344, 1214 cm^{-1}; ^{1}H-NMR (300 MHz, $CDCl_3$): δ = 7.13-7.06 (m, 3H), 3.79 (s, 3H), 3.74 (s, 2H), 3.28 (hept, *J* = 6.8 Hz, 2H), 1.25 (d, *J* = 6.8 Hz, 12H); ^{13}C-NMR (101 MHz, $CDCl_3$): δ = 172.5 (C), 142.6 (C), 142.2 (2C), 124.1 (CH), 123.8 (2CH), 52.4 (CH_2), 52.3 (CH_3), 28.0 (2CH), 24.3 ($4CH_3$); HRMS (EI): *m/z*: calculated for $C_{15}H_{23}NO_2$: 249.1729, found 249.1727 $(M)^+$.

Ester 147q

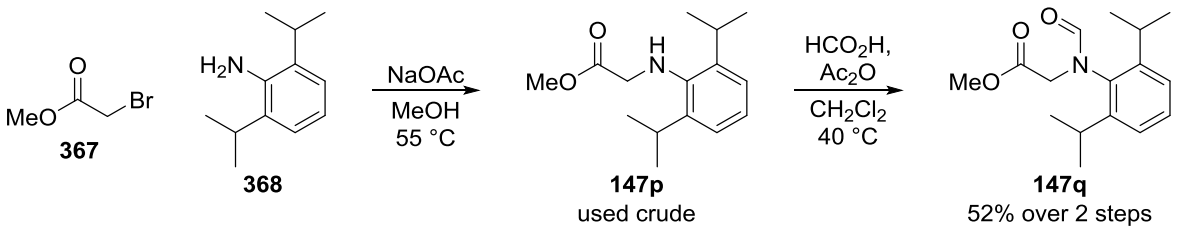

Methyl bromoacetate (6.0 mL, 63 mmol) was added to a mixture of 2,6-diisopropylaniline (11.6 mL, 62 mmol) and NaOAc (6.0 g, 118 mmol) in methanol (9.3 mL) and the reaction mixture was heated at 65 °C for 16 hours. After cooling to room temperature, satd. $NaHCO_{3(aq)}$ solution (100 mL) was added and the aqueous phase was extracted with CH_2Cl_2 (3 x 30 mL). The combined organic fractions were dried over Na_2SO_4 and concentrated under reduced pressure to give the crude ester **147p** as a red oil. Formic acid (8.9 mL, 236 mmol) and Ac_2O (7.9 mL, 84 mmol) were mixed for 1.5 hours at room temperature and this mixture was added to a solution of the crude ester **147p** in CH_2Cl_2 (30 mL). The resulting reaction mixture was stirred for 16 hours at room temperature and 3 hours at 40 °C. After cooling to room temperature, satd. $NaHCO_{3(aq)}$ solution (200 mL) was added, the phases were separated and the aqueous phase was extracted with CH_2Cl_2 (2 x 30 mL). The combined organic phases were dried over Na_2SO_4, concentrated under reduced pressure and purified by flash column chromatography (10⟶20% EtOAc:hexane) to give *ester* **147q** as a white solid (8.88 g, 52% over two steps); mp: 70-72 °C; IR (neat): ν = 2964, 2869, 1763, 1666, 1459, 1329, 1204 cm^{-1}; ^{1}H-NMR (300 MHz, $CDCl_3$): δ = 8.13 (s, 1H), 7.42-7.33 (m, 1H), 7.25-7.17 (m, 2H), 4.21 (s, 2H), 3.76 (s, 3H), 3.23 (hept, *J* = 6.8 Hz, 2H), 1.21 (d, *J* = 6.8 Hz, 6H), 1.17 (d, *J* = 6.8 Hz, 6H); ^{13}C-NMR (101 MHz, $CDCl_3$): δ = 168.2 (C), 163.7 (CH), 148.0 (2C), 135.7 (C), 129.8 (CH), 124.7 (2CH), 52.4 (CH_3), 49.9 (CH_2), 28.2 (2CH), 25.0 ($2CH_3$), 24.2 ($2CH_3$); HRMS (ES): *m/z*: calculated for $C_{16}H_{23}NO_3Na$: 300.1576, found 300.1578 $(M+Na)^+$.

Imine 383

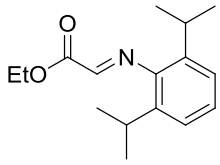

Under an argon atmosphere Na_2SO_4 (500 mg, 3.5 mmol), 2,6-diisopropylaniline (950 µL, 5.0 mmol), ethyl glyoxylate (50% solution in toluene, 1.0 mL, 4.9 mmol) and toluene (10 mL) were added squentially to a 2-neck flask fitted with a reflux condenser and the reaction mixture was heated for 1 hour at 110 °C. After cooling to room temperature, the Na_2SO_4 was removed by filtration through cotton and the filtrate was concentrated under reduced pressure and purified by flash column chromatography (95:5:1 hexane:Et_2O:NEt_3) to give *imine* **383** as a yellow oil (1.16 g, 90%); IR (neat): ν = 2962, 2932, 2870, 1751, 1723, 1283, 1195, 1032 cm^{-1}; ^{1}H-NMR (300 MHz, $CDCl_3$): δ = 7.64 (s, 1H), 7.17-7.12 (m, 3H), 4.44 (q, *J* = 7.1 Hz, 2H), 2.84 (hept, *J* = 6.9 Hz, 2H), 1.43 (t, *J* = 7.1 Hz, 3H), 1.16 (d, *J* = 6.9 Hz, 12H); ^{13}C-NMR (101 MHz, $CDCl_3$): δ = 162.7 (C), 154.7 (CH), 146.9 (C), 136.7 (2C), 125.5 (CH), 123.2 (2CH), 62.2 (CH_2), 27.9 (2CH), 23.6 ($4CH_3$), 14.2 (CH_3); HRMS (ES): m/z: calculated for $C_{16}H_{24}NO_2$: 262.1807, found 262.1812 $(M+H)^+$.

5.1.3: Pyridine-*N*-Aminides

Ylide 94c

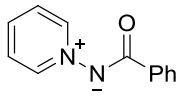

Following a literature procedure,[49] a solution of NaOH (10% in H_2O, 100 mL) was cooled to 0 °C and *N*-aminopyridinium iodide (2.22 g, 10.0 mmol) was added. Once the *N*-aminopyridinium iodide had dissolved, benzoyl chloride (2.3 mL, 19.8 mmol) was added and the reaction mixture was stirred for 16 hours at room temperature and then extracted with CH_2Cl_2 (3 x 50 mL). The combined organic phases dried over Na_2SO_4 and concentrated under reduced pressure to yield *ylide* **94c** as a pale yellow solid (1.81 g, 91%); mp: 175-177 °C (lit.[49] 187-189 °C); ^{1}H-NMR (300 MHz, $CDCl_3$): δ = 8.86-8.79 (m, 2H), 8.19-8.12 (m, 2H), 7.92 (tt, *J* = 7.7, 1.3 Hz, 1H), 7.72-7.64 (m, 2H), 7.46-7.38 (m, 3H). ^{13}C-NMR (101 MHz, $CDCl_3$): δ = 170.8 (C), 143.5 (2CH), 137.2 (C), 137.0 (CH), 130.3 (CH), 128.1 (2CH), 128.0 (2CH), 126.1 (2CH); MS (EI): *m/z* = 198.3 (M^+, 8%), 196.3 (100), 120.6 (64) 78.7 (43). Spectroscopic data matched those reported.[49]

Ylide 94b

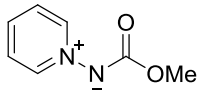

N-Aminopyridinium iodide (497 mg, 2.2 mmol) and K_2CO_3 (650 mg, 4.7 mmol) were suspended in MeOH (15 mL), methyl chloroformate (350 µL, 4.53 mmol) was added and the reaction mixture was stirred for 3 days at room temperature. The MeOH was removed under reduced pressure and the residue was suspended in 95:5 CH_2Cl_2/MeOH and filtered through a 5 cm pad of basic alumina. The filtrate was concentrated under reduced pressure to give *ylide* **94b** as pink needles (323 mg, 95%); mp: 84-85 °C (lit.[49] 92-94 °C); ^{1}H-NMR (300 MHz, $CDCl_3$): δ = 8.88-8.83 (m, 2H), 7.83 (tt, *J* = 7.7, 1.2 Hz, 1H), 7.64-7.58 (m, 2H), 3.75 (s, 3H); ^{13}C-NMR (101 MHz, $CDCl_3$): δ = 164.1 (C), 142.4 (2CH), 135.3 (CH), 126.0 (2CH), 51.9 (CH_3); MS (EI): *m/z* = 152.1 (M^+, 27%), 121.0 (59) 79.0 (100). Spectroscopic data matched those reported.[49]

Ylide 94d

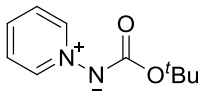

Di-*tert*-butyl dicarbonate (1.09 g, 5.0 mmol), *N*-aminopyridinium iodide (1.00 g, 4.5 mmol) and K_2CO_3 (1.37 g, 9.9 mmol) were suspended in MeOH (40 mL) and the reaction mixture was stirred for 3 days at room temperature. The MeOH was removed under reduced pressure and the residue was suspended in 95:5 CH_2Cl_2/MeOH and filtered through a 5 cm pad of basic alumina. The filtrate was concentrated under reduced pressure to give *ylide* **94d** as a pale purple powder (816 mg, 93%); mp: 129-130 °C (lit.[188] 131 °C); IR (neat): ν = 3140, 3042, 2978, 1608, 1472, 1361, 1279, 1148 cm^{-1}; ^{1}H-NMR (300 MHz, $CDCl_3$): δ = 8.90-8.85 (m, 2H), 7.75 (tt, *J* = 7.7, 1.2 Hz, 1H), 7.59-7.51 (m, 2H), 1.54 (s, 9H); ^{13}C-NMR (101 MHz, $CDCl_3$): δ = 163.5 (C), 142.4 (2CH), 134.6 (CH), 125.9 (2CH), 77.9 (C), 28.9 ($3CH_3$); HRMS (ES): *m/z* calculated for $C_{10}H_{14}N_2O_2Na$: 217.0953, found 217.0943 $(M+Na)^+$.

5.1.3.1: General procedure for synthesis of pyridine-N-aminides from esters (GP2)

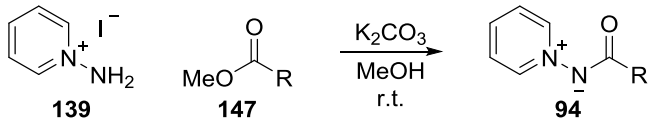

139 **147** **94**

N-Aminopyridinium iodide (1.0 eq.) and K_2CO_3 (2.4 eq.) were suspended in MeOH (0.13 M with respect to *N*-Aminopyridinium iodide) and the methyl ester (1.2 eq.) was added. The reaction mixture was stirred for 3 days at room temperature at which point the MeOH was removed under reduced pressure and the residue was suspended in 9:1 CH_2Cl_2/MeOH and filtered through a 5 cm pad of basic alumina. The filtrate was concentrated under reduced pressure and, where necessary, purified by flash column chromatography or recrystallisation.

Ylide 94e

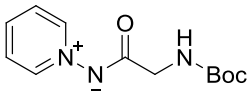

Following **GP2** using *N*-aminopyridinium iodide (1.00 g, 4.5 mmol), K_2CO_3 (1.49 g, 10.8 mmol) and ester **147e** (1.02 g, 5.4 mmol). Purification by flash column chromatography (5⟶10% MeOH in CH_2Cl_2) yielded *ylide* **94e** as a pale brown solid (694 mg, 61%); mp: 164-166 °C; IR (neat): ν = 3233, 3036, 2970, 1713, 1582, 1542, 1471, 1363, 1269, 1244, 1153, 934 cm^{-1}; ^{1}H-NMR (300 MHz, $CDCl_3$): δ = 8.71-8.63 (m, 2H), 7.92 (tt, *J* = 7.7, 1.2, Hz, 1H), 7.70-7.61 (m, 2H), 5.35 (br s, NH), 3.92 (d, *J* = 4.8 Hz, 2H), 1.44 (s, 9H); ^{13}C-NMR (101 MHz, $CDCl_3$): δ = 172.6 (C), 156.0 (C), 143.2 (2CH), 137.3 (CH), 126.2 (2CH), 79.1 (C), 44.2 (CH_2), 28.6 ($3CH_3$); HRMS (ES): *m/z* calculated for $C_{12}H_{18}N_3O_3$: 252.1348, found 252.1353 $(M+H)^+$.

Ylide 94f

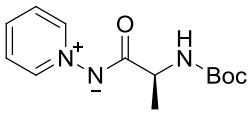

Note: To avoid degradation, room temperature water baths should be used when evaporating solvent from this compound. Following **GP2** using *N*-aminopyridinium iodide (666 mg, 3.0 mmol), K_2CO_3 (995 mg, 7.2 mmol) and ester **147f** (732 mg, 3.6 mmol). Purification by flash column chromatography (0⟶10% MeOH in CH_2Cl_2) yielded *ylide* **94f** as a pale pink solid (550 mg, 69%); mp: 120-121 °C; $[\alpha]_D^{20}$ = −30.6 (c=1.2, $CHCl_3$); IR (neat): ν = 3240, 3043, 2972, 2923, 1698, 1585, 1540, 1475, 1247, 1169, 1067, 1012, 782 cm^{-1};

^{1}H-NMR (300 MHz, $CDCl_3$): δ = 8.71-8.65 (m, 2H), 7.93 (tt, *J* = 7.7, 1.3 Hz, 1H), 7.70-7.63 (m, 2H), 5.49 (br d, NH), 4.42-4.26 (m, 1H), 1.51-1.42 (m, 12H); ^{13}C-NMR (101 MHz, $CDCl_3$): δ = 176.3 (C), 155.4 (C), 143.2 (2CH), 137.3 (CH), 126.2 (2CH), 78.9 (C), 50.4 (CH), 28.6 ($3CH_3$), 20.8 (CH_3); HRMS (ES): *m/z* calculated for $C_{13}H_{19}N_3O_3Na$: 288.1324, found 288.1316 $(M+Na)^+$.

Ylide 94g

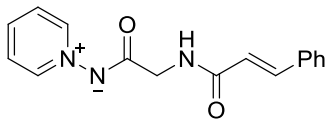

Following **GP2** using *N*-aminopyridinium iodide (222 mg, 1.0 mmol), K_2CO_3 (346 mg, 2.5 mmol) and ester **147g** (265 mg, 1.2 mmol). Purification by flash column chromatography (0⟶10% MeOH in CH_2Cl_2) yielded *ylide* **94g** as a white foam (176 mg, 63%); IR (neat): ν = 3304, 3060, 1659, 1618, 1564, 1472, 1355, 1265, 1223, 1033, 1223, 978, 730 cm^{-1}; ^{1}H-NMR (300 MHz, $CDCl_3$): δ = 8.71-8.63 (m, 2H), 7.93 (tt, *J* = 7.7, 1.3 Hz, 1H), 7.70-7.64 (m, 2H), 7.61 (d, *J* = 15.7 Hz, 1H), 7.50-7.43 (m, 2H), 7.38-7.29 (m, 3H), 6.82 (br t, NH), 6.50 (d, *J* = 15.7 Hz, 1H), 4.18 (d, *J* = 4.7 Hz, 2H); ^{13}C-NMR (101 MHz, $CDCl_3$): δ = 172.2 (C), 165.7 (C), 143.2 (2CH), 140.5 (CH), 137.6 (CH), 135.2 (C), 129.6 (CH), 128.9 (2CH), 127.9 (2CH), 126.4 (2CH), 121.2 (CH), 43.4 (CH_2); HRMS (ES): *m/z* calculated for $C_{16}H_{16}N_3O_2$: 282.1243, found 282.1248 $(M+H)^+$.

Ylide 94i

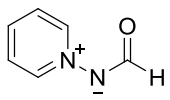

Following **GP2** using *N*-aminopyridinium iodide (444 mg, 2.0 mmol), K_2CO_3 (664 mg, 4.8 mmol) and ethyl formate (200 µL, 2.5 mmol). Filtration was carried out using 4:1 CH_2Cl_2/MeOH. Purification by flash column chromatography on neutral alumina (0⟶10% MeOH in CH_2Cl_2) gave *ylide* **94i** as a red solid (130 mg, 53%); mp: 100-102 °C; IR (neat): ν = 3107, 3073, 3028, 3012, 2949, 2817, 1620, 1581, 1567, 1473, 1355, 1265, 1241, 881, 773, 751 cm^{-1}; ^{1}H-NMR (400 MHz, d_6-DMSO): δ = 8.73 (d, *J* = 5.6 Hz, 2H), 8.19-8.12 (m, 1H), 7.90-7.84 (m, 2H), 7.83 (s, 1H); ^{13}C-NMR (101 MHz, d_6-DMSO): δ = 164.2 (CH), 143.0 (2CH), 138.7 (CH), 126.8 (2CH); HRMS (ES): *m/z* calculated for $C_6H_7N_2O$: 123.0558, found 123.0562 $(M+H)^+$.

Ylide 94j

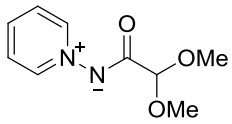

Following **GP2** using *N*-aminopyridinium iodide (666 mg, 3.0 mmol), K_2CO_3 (995 mg, 7.2 mmol) and ester **147j** (486 mg, 3.6 mmol). Purification by flash column chromatography (100:0:1→90:10:1 CH_2Cl_2:MeOH:NEt_3) yielded *ylide* **94j** as a white powder (496 mg, 84%); mp: 90-92 °C; IR (neat): ν = 3110, 3086, 2968, 2926, 2832, 1617, 1600, 1568, 1467, 1399, 1339, 1268, 1198, 1151, 1106, 1044, 983, 900, 851, 779, 749 cm^{-1}; ^{1}H-NMR (300 MHz, $CDCl_3$): δ = 8.62-8.57 (m, 2H), 7.86 (tt, *J* = 7.7, 1.1 Hz, 1H), 7.64-7.55 (m, 2H), 4.76 (s, 1H), 3.39 (s, 6H); ^{13}C-NMR (101 MHz, $CDCl_3$): δ = 170.7 (C), 142.9 (2CH), 137.6 (CH), 126.1 (2CH), 102.0 (CH), 53.7 ($2CH_3$); HRMS (ES): *m/z* calculated. for $C_9H_{13}N_2O_3$: 197.0926, found 297.0929 $(M+H)^+$.

Ylide 94k

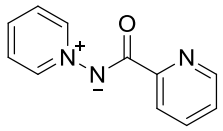

Following **GP2** using *N*-aminopyridinium iodide (444 mg, 2.0 mmol), K_2CO_3 (665 mg, 4.8 mmol) and methyl picolinate (332 mg, 2.4 mmol). The filtration through basic alumina was carried out using 95:5 CH_2Cl_2/MeOH to give *ylide* **94k** as a red solid (378 mg, 94%); mp: 178-181 °C (lit.[55a] 178-181 °C); IR (neat): ν = 3056, 3026, 1577, 1548, 1461, 1348, 1338, 1186, 1186, 989, 909, 766, 749 cm^{-1}; ^{1}H-NMR (300 MHz, $CDCl_3$): δ = 9.00-8.90 (m, 2H), 8.76 (appt. br s, 1H), 8.26 (appt. br d, *J* = 7.4 Hz, 1H), 7.99 (t, *J* = 7.5 Hz, 1H), 7.88 (appt. td, *J* = 7.7, 1.6 Hz, 1H), 7.79-7.69 (m, 2H), 7.47-7.37 (m, 1H); ^{13}C-NMR (101 MHz, $CDCl_3$): δ = 169.4 (C), 154.7 (C), 148.9 (CH), 143.6 (2CH), 137.5 (CH), 137.1 (CH), 126.2 (2CH), 125.0 (CH), 123.5 (CH); HRMS (ES): *m/z* calculated for $C_{11}H_{10}N_3O$: 200.0824, found 200.0826 $(M+H)^+$.

Ylide 94l

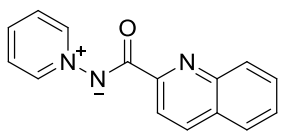

Following **GP2** using *N*-aminopyridinium iodide (222 mg, 1.0 mmol), K_2CO_3 (333 mg, 2.4 mmol) and ester **147l** (226 mg, 1.2 mmol). Following the filtration, the crude residue was dissolved in CH_2Cl_2 and the product was precipitated by addition of hexane to give *ylide* **94l** as a white solid (192 mg, 77%); mp: 142-144 °C; IR (neat): ν = 3395, 3060, 1617, 1582, 1552, 1468, 1349, 1317, 1212, 1182, 918, 845, 767 cm^{-1};

^{1}H-NMR (400 MHz, $CDCl_3$): δ = 8.88 (d, *J* = 6.2 Hz, 2H), 8.36-8.28 (m, 2H), 8.24 (d, *J* = 8.5 Hz, 1H), 7.93 (t, *J* = 7.6 Hz, 1H), 7.82 (d, *J* = 7.8 Hz, 1H), 7.74-7.65 (m, 3H), 7.53 (appt. t, *J* = 7.8 Hz, 1H); ^{13}C-NMR (101 MHz, $CDCl_3$): δ = 170.0 (C), 155.3 (C), 147.6 (C), 143.6 (2CH), 137.4 (CH), 136.7 (CH), 130.7 (CH), 129.4 (CH), 128.8 (C), 127.5 (CH), 127.1 (CH), 126.1 (2CH), 120.7 (CH); HRMS (ES): *m/z* calculated for $C_{15}H_{11}N_3ONa$: 272.0800, found 272.0791 $(M+Na)^+$.

Ylide 94m

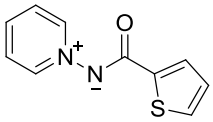

A solution of thiophene-2-carboxylic acid (255 mg, 2.0 mmol) in CH_2Cl_2 (20 mL) was cooled to 0 °C. NEt_3 (560 µL, 4.0 mmol) and ethyl chloroformate (210 µL, 2.2 mmol) were added sequentially and the reaction mixture was stirred for 1 hour before the addition of *N*-aminopyridinium iodide (488 mg, 2.2 mmol), K_2CO_3 (662 mg, 4.8 mmol) and MeOH (5 mL). The reaction mixture was allowed to warm to room temperature and stirred for 24 hours and then filtered through a 5 cm pad of silica gel. The filtrate was concentrated under reduced pressure the solid residue was dissolved in 2 M $NaOH_{(aq)}$ solution (20 mL) and CH_2Cl_2 (30 mL). The phases were separated and the aqueous phase was extracted with CH_2Cl_2 (2 x 20 mL). The combined organic phases were dried over Na_2SO_4, concentrated under reduced pressure and purified by flash column chromatography (0⟶10% MeOH in CH_2Cl_2) to give *ylide* **94m** as a white solid (315 mg, 77%); mp: 214-215 °C; IR (neat): ν = 3098, 3066, 1556, 1466, 1422, 1358, 1294, 1171, 859 cm^{-1}; ^{1}H-NMR (300 MHz, $CDCl_3$): δ = 8.89-8.82 (m, 2H), 7.92 (tt, *J* = 7.7, 1.3 Hz, 1H), 7.76 (dd, *J* = 3.6, 1.2 Hz, 1H), 7.72-7.62 (m, 2H), 7.37 (dd, *J* = 5.0, 1.2 Hz, 1H), 7.08 (dd, *J* = 5.0, 3.6 Hz, 1H); ^{13}C-NMR (101 MHz, $CDCl_3$): δ = 166.7 (C), 143.3 (2CH), 141.7 (C), 136.9 (CH), 129.2 (CH), 128.3 (CH), 127.3 (CH), 126.1 (2CH). Spectroscopic data matched those reported.[52]

Ylide 94o

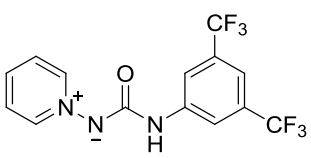

Under an argon atmosphere *N*-aminopyridinium iodide (223 mg, 1.0 mmol), K_2CO_3 (335 mg, 2.4 mmol), MeCN (7.5 mL) and 3,5-bis(trifluoromethyl)phenyl isocyanate (350 µL, 2.0 mmol) were

sequentially added to a flask and the reaction mixture was stirred for 3 days. Filtration was carried out as in **GP2**. Purification by flash column chromatography (0→8% MeOH in CH_2Cl_2) afforded *ylide* **94o** as a white solid (282 mg, 80%); mp: 180-181 °C; IR (neat): ν = 3229, 3059, 2974, 1643, 1556, 1471, 1390, 1274, 1239, 1159, 1115, 1042 cm^{-1}; ^{1}H-NMR (300 MHz, $CDCl_3$): δ = 8.82-8.73 (m, 2H), 8.15 (s, 1H), 7.94-7.85 (m, 3H), 7.69-7.61 (m, 2H), 7.32 (s, 1H); ^{13}C-NMR (101 MHz, $CDCl_3$): δ = 162.0 (C), 143.3 (2CH), 143.0 (C), 136.2 (CH), 131.9 (q, $J_{C\text{-}F}$ = 32.9 Hz, 2C), 126.3 (2CH), 123.6 (q, $J_{C\text{-}F}$ = 272.6 Hz, $2CF_3$), 117.7-117.4 (m, 2CH), 113.9-113.5 (m, CH); ^{19}F{^{1}H}-NMR (282 MHz, $CDCl_3$): δ = -63.0; HRMS (ES): *m/z* calculated for $C_{14}H_{10}F_6N_3O$: 350.0728, found 350.0725 $(M+H)^+$.

Ylide 266a

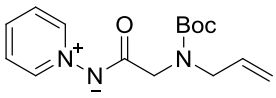

Following **GP2** using *N*-aminopyridinium iodide (490 mg, 2.2 mmol), K_2CO_3 (730 mg, 5.3 mmol) and ester **263a** (607 g, 2.65 mmol). Purification by flash column chromatography (0→5% MeOH in CH_2Cl_2) afforded *ylide* **266a** as red solid (287 mg, 45%); mp: 88-90 °C; IR (neat): ν = 3111, 2969, 1679, 1581, 1468, 1449, 1240, 1164, 1122 cm^{-1}; *NMR shows a mixture of two rotamers:* ^{1}H-NMR (300 MHz, $CDCl_3$): δ = 8.75-8.62 (m, 2H), 7.95-7.83 (m, 1H), 7.71-7.56 (m, 2H), 5.96-5.77 (m, 1H), 5.24-5.06 (m, 2H), 4.09-3.91 (m, 4H), 1.47 (s, 9H); ^{13}C-NMR (101 MHz, $CDCl_3$): δ = 173.3 (C), 156.1 (C), 143.3 and 143.1 (2CH), 136.9 (CH) 134.7 and 134.61 (CH), 126.1 and 126.0 (2CH), 116.6 and 116.0 (CH_2), 79.5 and 79.4 (C), 50.9 and 50.3 (CH_2), 50.0 and 49.6 (CH_2), 28.7 and 28.6 ($3CH_3$); HRMS (ES): *m/z* calculated for $C_{15}H_{22}N_3O_3$: 292.1661, found 292.1651 $(M+H)^+$.

Ylide 266b

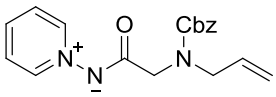

Following **GP2** using *N*-aminopyridinium iodide (185 mg, 0.83 mmol), K_2CO_3 (276 mg, 2.0 mmol) and ester **263b** (242 mg, 0.91 mmol). Purification by flash column chromatography (0→10% MeOH in CH_2Cl_2) afforded *ylide* **266b** as red oil (99 mg, 36%); IR (neat): ν = 2926, 1693, 1580, 1470, 1414, 1232 cm^{-1}; *NMR shows a mixture of two rotamers in a ~ 0.9:1.1 ratio:* ^{1}H-NMR (400 MHz, $CDCl_3$): δ = 8.59 and 8.32 (d, *J* = 6.1 Hz, 2H), 7.84-7.76 (m, 1H), 7.55

and 7.49 (appt. t, *J* = 7.1 Hz, 2H), 7.36-7.16 (m, 5H), 5.89-5.72 (m, 1H), 5.19-5.02 (m, 4H), 4.09-3.90 (m, 4H); ^{13}C-NMR (101 MHz, $CDCl_3$): δ = 172.7 (C), 156.62 and 156.57 (C), 143.1 and 143.0 (2CH), 137.4 (C), 137.1 (CH), 134.0 and 133.9 (CH), 128.35 (2CH), 127.8-127.7 (m, 3CH), 126.0 (2CH), 117.0 and 116.5 (CH_2), 67.1 and 66.8 (CH_2), 51.1 and 50.5 (CH_2), 50.0 and 49.6 (CH_2); HRMS (ES): *m/z* calculated for $C_{18}H_{19}N_3O_3Na$: 348.1324, found 348.1327 $(M+Na)^+$.

Ylide 266c

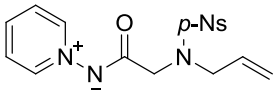

Following **GP2** using *N*-aminopyridinium iodide (480 mg, 2.2 mmol), K_2CO_3 (717 mg, 5.2 mmol) and ester **263c** (748 mg, 2.4 mmol). Purification by flash column chromatography (9:1 EtOAc:MeOH) afforded *ylide* **266c** as red oil (100 mg, 12%); IR (neat): ν = 1306, 1589, 1526, 1472, 1346, 1156, 911 cm^{-1}; ^{1}H-NMR (400 MHz, $CDCl_3$): δ = 8.51-8.47 (m, 2H), 8.28-8.23 (m, 2H), 8.16-8.10 (m, 2H), 7.91 (tt *J* = 7.7, 1.2 Hz, 1H), 7.67-7.60 (m, 2H), 5.76 (ddt, *J* = 17.0, 10.1, 6.3 Hz, 1H), 5.27-5.15 (m, 2H), 4.08 (s, 2H), 4.03 (d, *J* = 6.3 Hz, 2H); ^{13}C-NMR (101 MHz, $CDCl_3$): δ = 171.2 (C), 149.7 (C), 146.8 (C), 142.7 (2CH), 137.6 (CH), 132.5 (CH), 128.9 (2CH), 126.3 (2CH), 123.9 (2CH), 119.4 (CH_2), 50.9 (CH_2), 49.3 (CH_2); HRMS (ES): *m/z* calculated for $C_{16}H_{17}N_4O_5S$: 377.0920, found 377.0916 $(M+H)^+$.

Ylide 266d

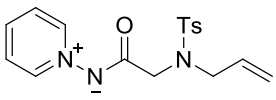

Following **GP2** using *N*-aminopyridinium iodide (1.0 g, 4.5 mmol), K_2CO_3 (1.5 g, 10.9 mmol) and ester **263d** (1.5 g, 5.4 mmol). Purification by flash column chromatography (0→10% MeOH in CH_2Cl_2) afforded *ylide* **266d** as a brown solid (962 mg, 62%); mp: 106-108 °C; IR (neat): ν = 3070, 1580, 1318, 1153, 1093 cm^{-1}; ^{1}H-NMR (400 MHz, $CDCl_3$): δ = 8.50-8.45 (m, 2H), 7.89 (tt, *J* = 7.7, 1.2 Hz 1H), 7.81 (d, *J* = 8.2 Hz, 2H), 7.64-7.57 (m, 2H), 7.24 (d, *J* = 8.2 Hz, 2H), 5.74 (ddt, *J* = 17.0, 10.2, 6.4 Hz, 1H), 5.24-5.17 (m, 1H), 5.16-5.11 (m, 1H), 4.06 (d, *J* = 6.4 Hz, 2H), 3.98 (s, 2H), 2.37 (s, 3H); ^{13}C-NMR (101 MHz, $CDCl_3$): δ = 171.9 (C), 142.9 (2CH), 142.8 (C), 138.0 (C), 137.3 (CH), 133.3 (CH), 129.4 (2C), 127.6 (2C), 126.1 (2C),

118.8 (CH_2), 51.1 (CH_2), 49.4 (CH_2), 21.6 (CH_3); HRMS (ES): *m/z* calculated for $C_{17}H_{20}N_3O_3S$: 346.1225, found 346.1214 $(M+H)^+$.

Ylide 266f

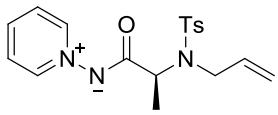

Following **GP2** using *N*-aminopyridinium iodide (666 mg, 3.0 mmol), K_2CO_3 (995 mg, 7.2 mmol) and ester **263f** (1.07 g, 3.6 mmol). Purification by flash column chromatography (0→10% MeOH in CH_2Cl_2) followed by an additional recrystallisation by precipitation from CH_2Cl_2 with Et_2O afforded *ylide* **266f** a tan solid (350 mg, 32%); $[\alpha]_D^{20}$ = −8.3 ($CHCl_3$, c = 1.0); mp: 123-125 °C; IR (neat): ν = 3078, 1584, 1468, 1327, 1240, 1153 cm^{-1}; ^{1}H-NMR (300 MHz, $CDCl_3$): δ = 8.40-8.33 (m, 2H), 7.92-7.80 (m, 3H), 7.62-7.54 (m, 2H), 7.22 (d, *J* = 8.0 Hz, 2H), 6.03-5.88 (m, 1H), 5.29-5.18 (m, 1H), 5.11-5.03 (m, 1H), 4.67 (q, *J* = 7.2 Hz, 1H), 4.31-4.20 (m, 1H), 4.16-4.05 (m, 1H), 2.38 (s, 3H), 1.43 (d, *J* = 7.2 Hz, 3H); ^{13}C-NMR (101 MHz, $CDCl_3$): δ = 174.7 (C), 143.0 (2CH), 142.5 (C), 138.6 (C), 137.3 (CH), 137.2 (CH), 129.3 (2CH), 127.9 (2CH), 125.9 (2CH), 116.1 (CH_2), 56.5 (CH), 47.8 (CH_2), 21.6 (CH_3), 17.9 (CH_3); HRMS (ES): *m/z* calculated for $C_{18}H_{21}N_3O_3SNa$: 382.1201, found 382.1199 $(M+Na)^+$.

Ylide 266g

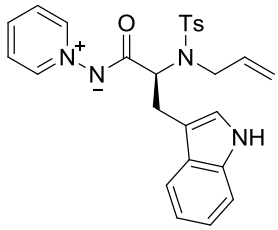

Following **GP2** using *N*-aminopyridinium iodide (666 mg, 3.0 mmol), K_2CO_3 (995 mg, 7.2 mmol) and ester **263g** (1.49 mg, 3.6 mmol). Purification by flash column chromatography (0→10% MeOH in CH_2Cl_2) followed by an additional recrystallisation by precipitation from $CHCl_3$ with Et_2O afforded *ylide* **266g** as a tan solid (234 mg, 16%); $[\alpha]_D$ = *compound was not sufficiently soluble in a solvent appropriate for measurement*; mp: 168-170 °C; IR (neat): ν = 3183, 1569, 1328, 1153, 1089 cm^{-1}; ^{1}H-NMR (300 MHz, d_6-DMSO): δ = 10.78 (s, NH), 8.16 (d, *J* = 5.6 Hz, 2H), 8.08 (t, *J* = 7.7 Hz, 1H), 7.83-7.74 (m, 2H), 7.71 (d, *J* = 8.2 Hz, 2H), 7.50 (d, *J* = 7.8 Hz, 1H), 7.34 (d, *J* = 8.0 Hz, 1H), 7.28 (d, *J* = 8.2 Hz, 2H), 7.16 (d, *J* = 2.1 Hz, 1H), 7.10-7.03 (m, 1H), 7.01-6.93 (m, 1H), 5.92-5.74 (m, 1H), 5.19 (dd, *J* = 17.3, 1.2, 1H), 4.99 (dd, *J* = 10.2, 1.2, 1H),

4.67 (dd, *J* = 8.4, 6.5 Hz, 1H), 4.43 (dd, *J* = 16.9, 6.8 Hz, 1H), 4.00 (dd, *J* = 16.9, 5.0, 1H), 3.34 (dd, *J* = 14.3, 8.4 Hz, 1H), 2.95 (dd, *J* = 14.3, 6.5 Hz, 1H), 2.33 (s, 3H); ^{13}C-NMR (101 MHz, d_6-DMSO): δ = 171.9 (C), 142.5 (C), 142.4 (2CH), 138.4 (CH), 137.7 (C), 137.4 (CH), 136.1 (C), 129.2 (2CH), 127.4 (2CH), 127.0 (C), 126.6 (2CH), 123.4 (CH), 120.8 (CH), 118.22 (CH), 118.20 (CH), 115.8 (CH_2), 111.3 (CH), 110.7 (C), 60.6 (CH), 47.0 (CH_2), 27.6 (CH_2), 21.0 (CH_3); HRMS (ES): *m/z* calculated for $C_{26}H_{26}N_4O_3SNa$: 497.1623, found 497.1614 $(M+Na)^+$.

Ylide 266h

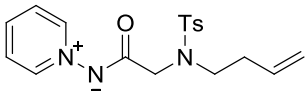

Following **GP2** using *N*-aminopyridinium iodide (355 mg, 1.6 mmol), K_2CO_3 (531 mg, 3.8 mmol) and ester **263h** (571 mg, 1.9 mmol). Purification by flash column chromatography (0→5% MeOH in CH_2Cl_2) afforded *ylide* **266h** as red solid (330 mg, 57%); mp: 86-88 °C; IR (neat): ν = 1581, 1344, 1155, 1090, 959 cm^{-1}; ^{1}H-NMR (300 MHz, $CDCl_3$): δ = 8.55-8.48 (m, 2H), 7.90 (tt, *J* = 7.7, 1.3 Hz 1H), 7.82 (d, *J* = 8.3 Hz, 2H), 7.66-7.57 (m, 2H), 7.25 (d, *J* = 8.3 Hz, 2H), 5.74 (ddt, *J* = 17.1, 10.3, 6.8 Hz, 1H), 5.10-4.95 (m, 2H), 4.04 (s, 2H), 3.53-3.40 (m, 2H), 2.47-2.34 (m, 2H), 2.39 (s, 3H); ^{13}C-NMR (101 MHz, $CDCl_3$): δ = 172.0 (C), 143.0 (2CH), 142.7 (C), 138.0 (C), 137.3 (CH), 135.3 (CH), 129.4 (2CH), 127.7 (2CH), 126.1 (2CH), 116.8 (CH_2), 50.6 (CH_2), 48.2 (CH_2), 32.8 (CH_2), 21.6 (CH_3); HRMS (ES): *m/z* calculated for $C_{18}H_{22}N_3O_3S$: 360.1746, found 360.1751 $(M+H)^+$.

Ylide 266i

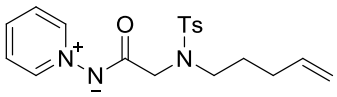

Following **GP2** using *N*-aminopyridinium iodide (403 mg, 1.8 mmol), K_2CO_3 (602 mg, 4.4 mmol) and ester **263i** (679 mg, 2.2 mmol). Purification by flash column chromatography (0→5% MeOH in CH_2Cl_2) afforded *ylide* **266i** as red solid (428 mg, 63%); mp: 48-50 °C; IR (neat): ν = 2926, 1584, 1471, 1330, 1154, 1090 cm^{-1}; ^{1}H-NMR (300 MHz, $CDCl_3$): δ = 8.49-8.41 (m, 2H), 7.88 (t, *J* = 7.7 Hz, 1H), 7.78 (d, *J* = 8.0 Hz, 2H), 7.64-7.55 (m, 2H), 7.22 (d, *J* = 8.0 Hz, 2H), 5.74 (ddt, *J* = 16.9, 10.3, 6.5 Hz, 1H), 5.01-4.86 (m, 2H), 3.99 (s, 2H), 3.41-3.29 (t, *J* = 7.5 Hz, 2H), 2.35 (s, 3H), 2.03 (appt. q, *J* = 7.0 Hz, 2H),

1.71 (appt. quin, *J* = 7.5 Hz, 2H); ^{13}C-NMR (101 MHz, $CDCl_3$): δ = 171.8 (C), 142.8 (2CH), 142.6 (C), 137.9 (CH), 137.8 (C), 137.4 (CH), 129.3 (2CH), 127.6 (2CH), 126.1 (2CH), 115.0 (CH_2), 50.4 (CH_2), 48.2 (CH_2), 30.9 (CH_2), 27.2 (CH_2), 21.50 (CH_3); HRMS (ES): *m/z* calculated for $C_{19}H_{23}N_3O_3SNa$: 396.1358, found 396.1353 $(M+Na)^+$.

Ylide 94p

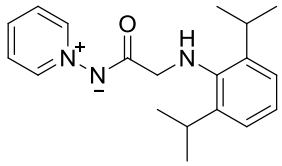

Following **GP2** using *N*-aminopyridinium iodide (1.00 g, 4.5 mmol), K_2CO_3 (1.48 g, 10.7 mmol) and ester **147p** (1.35 g, 5.4 mmol). Purification by flash column chromatography (0→10% MeOH in CH_2Cl_2) afforded *ylide* **94p** as red oil (983 mg, 70%); IR (neat): ν = 3360, 2960, 2867, 1577, 1467, 1339, 1269, 1090, 757 cm^{-1}; ^{1}H-NMR (300 MHz, $CDCl_3$): δ = 8.78-8.70 (m, 2H), 8.03-7.90 (m 1H), 7.76-7.64 (m, 2H), 7.15-7.01 (m, 3H), 3.79 (s, 2H), 3.46 (hept, *J* = 6.8 Hz, 2H), 1.28 (d, *J* = 6.8 Hz, 12H); ^{13}C-NMR (101 MHz, $CDCl_3$): δ = 174.0 (C), 144.0 (C), 143.3 (2CH), 142.1 (2C), 137.5 (CH), 126.3 (2CH), 123.7 (2CH), 123.4 (CH), 54.5 (CH_2), 27.9 (2CH), 24.4 ($4CH_3$); HRMS (ES): *m/z* calculated for $C_{19}H_{25}N_3ONa$: 334.1895, found 334.1909 $(M+Na)^+$.

Ylide 94q

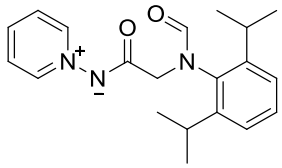

Following **GP2** using *N*-aminopyridinium iodide (4.44 g, 20 mmol), K_2CO_3 (6.64 g, 48 mmol) and ester **147q** (6.10 g, 22 mmol). Purification by flash column chromatography (0→10% MeOH in CH_2Cl_2) afforded *ylide* **94q** as red solid (*Note: in order obtain a solid after purification, hexane was added to the combined column fractions before they were concentrated, when this was not done the compound was isolated as a difficult to handle hygroscopic foam*) (2.76 g, 41%); mp: 170-172 °C; IR (neat): ν = 2963, 2927, 2869, 1670, 1590, 1469, 1349, 1259, 1192 cm^{-1}; *NMR shows a mixture of two rotamers in a ~ 0.3:0.7 ratio:* ^{1}H-NMR (300 MHz, $CDCl_3$): δ = 8.71-8.62 (m, 2H), 8.68 and 8.17 (s, 1H), 7.93 and 7.87 (tt, *J* = 7.7, 1.2 Hz, 1H), 7.70-7.57 (m, 2H), 7.37-7.26 (m, 1H), 7.23-7.15 (m, 2H), 4.25 and 4.13 (s, 2H), 3.47 and 3.17 (hept, *J* = 6.8 Hz, 2H), 1.28-1.08 (m, 12H); ^{13}C-NMR (101 MHz, $CDCl_3$): δ = 171.6 and 171.2 (C),

164.7 and 163.8 (CH), 148.2 and 146.6 (2C), 143.0 and 142.7 (2CH), 137.8 and 137.1 (CH), 136.9 and 136.1 (C), 129.3 and 128.8 (CH), 126.4 and 126.2 (2CH), 124.4 and 124.2 (2CH), 54.8 and 52.8 (CH_2), 28.6 and 28.0 (2CH), 25.1 and 24.6 ($2CH_3$), 24.4 and 24.2 ($2CH_3$); HRMS (ES): *m/z* calculated for $C_{20}H_{25}N_3O_2Na$: 362.1844, found 362.1832 $(M+Na)^+$.

5.1.4: Precursors to Ynamides

Sulfonamide 135a

MsCl (3.8 mL, 49 mmol) was added to a solution of aniline (5 mL, 55 mmol) and pyridine (8.8 mL, 109 mmol) in CH_2Cl_2 (75 mL) at 0 °C. The reaction mixture was stirred at room temperature for 2 hours. 6 M $NaOH_{(aq)}$ solution (30 mL) and H_2O (50 mL) were added. The organic phase was discarded and the aqueous phase was washed with CH_2Cl_2 (2 x 15 mL). The aqueous phase was acidified with conc. $HCl_{(aq)}$ to pH≈2 and extracted with CH_2Cl_2 (3 x 30 mL), these combined organic extracts were dried over Na_2SO_4 and the solvent was removed under reduced pressure to give *sulfonamide* **135a** as a white solid (7.72 g, 92%); mp: 98-100 °C (lit.[189] 102-103 °C); IR (neat): ν = 3253, 1495, 1471, 1393, 1320, 1145, 975, 752 cm^{-1}; ^{1}H-NMR (300 MHz, $CDCl_3$): δ = 7.42-7.31 (m, 2H), 7.26-7.16 (m, 3H), 6.66 (br s, NH), 3.02 (s, 3H); ^{13}C-NMR (101 MHz, $CDCl_3$): δ = 136.8 (C), 129.9 (2CH), 125.6 (CH), 120.9 (2CH), 39.5 (CH_3); Spectroscopic data matched those reported.[189]

Sulfonamide 135b

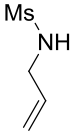

MsCl (870 µL, 11.2 mmol), was added to a solution of allylamine (750 µL, 10.0 mmol) and NEt_3 (1.55 mL, 11.1 mmol) in CH_2Cl_2 (40 mL) at 0 °C. The reaction mixture was stirred for 2 hours at room temperature and satd. NH_4Cl solution (30 mL) was added. The phases were separated and the aqueous phase was extracted with CH_2Cl_2 (2 x 30 mL). The combined organic extracts were dried over Na_2SO_4, concentrated under reduced pressure and purified by flash column chromatography (3:2 hexane:EtOAc) to give *sulfonamide* **135b** as a colourless oil (1.19 g, 88%); ^{1}H-NMR (300 MHz, $CDCl_3$): δ = 5.87 (ddt, *J* = 17.1, 10.2, 5.8 Hz, 1H), 5.30 (appt. dq, *J* = 17.1, 1.3 Hz, 1H), 5.22 (appt. dq, *J* = 10.2, 1.3 Hz, 1H), 4.62 (br s, NH), 3.81-3.73 (m, 2H), 2.97 (s, 3H);

^{13}C-NMR (101 MHz, $CDCl_3$): δ = 133.6 (CH), 117.9 (CH_2), 45.8 (CH_2), 41.2 (CH_3); MS (EI): *m/z* = 135.0 (M^+, 5%), 120.0 (100), 108.0 (33), 79.0 (78), 56.1 (92). Spectroscopic data matched those reported.[190]

Sulfonamide 135c

Following a literature procedure,[191] $MeNH_2$ (33% in EtOH, 65 mL, 527 mmol) was added to a flask fitted with a reflux condenser and MsCl (9 mL, 116 mmol) was added over 15 minutes whilst cooling with an ice/water bath. The reaction mixture was stirred for 18 hours at room temperature before CH_2Cl_2 (150 mL) was added to precipitate $MeNH_3Cl$, which was removed filtration through a 5 cm pad of silica. The filtrate was concentrated under reduced pressure and purified by flash column chromatography (3:2 EtOAc:hexane) to give *sulfonamide* **135c** as a colourless oil (8.34 g, 66%) (*note that this product is water soluble*); IR (neat): ν = 3290, 1405, 1301, 1146, 1126, 1067, 969, 834, 751 cm^{-1}; ^{1}H-NMR (300 MHz, $CDCl_3$): δ = 4.32 (br s, NH), 2.95 (s, 3H), 2.83 (d, *J* = 5.3 Hz, 3H); ^{13}C-NMR (101 MHz, $CDCl_3$): δ = 38.8 (CH_3), 29.5 (CH_3). Spectroscopic data matched those reported.[191]

Carbamate 135d

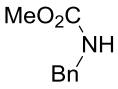

Methyl chloroformate (430 µL, 5.5 mmol), was added to a solution of $BnNH_2$ (550 µL, 5.0 mmol) and pyridine (450 µL, 5.5 mmol) in CH_2Cl_2 (15 mL) at 0 °C. The reaction mixture was stirred for 1 hour at room temperature and then washed sequentially with satd. $NH_4Cl_{(aq)}$ solution (15 mL) and satd. $Na_2CO_{3(aq)}$ solution (20 mL). The organic phase was dried over Na_2SO_4, concentrated under reduced pressure and purified by flash column chromatography (3:1 hexane:EtOAc) to give *carbamate* **135d** as a white solid (584 mg, 70%); mp: 58-59 °C (lit.[192] 62-63 °C); ^{1}H-NMR (300 MHz, d_4-MeOD): δ = 7.35-7.18 (m, 5H), 4.27 (s, 2H), 3.65 (s, 3H); ^{13}C-NMR (101 MHz, d_4-MeOD): δ = 159.7 (C), 140.6 (C), 129.4 (2CH), 128.2 (2CH), 128.1 (CH), 52.5 (CH_2), 45.5 (CH_3); MS (EI): *m/z* = 165.5 (M^+, 45%), 150.4 (61), 133.4 (31), 106.4 (31), 91.3 (65). Spectroscopic data matched those reported.[193]

Sulfonamide 135g

TsCl (7.8 g, 41 mmol), was added to a solution of aniline (5 mL, 55 mmol) and pyridine (7.2 mL, 89 mmol) in CH_2Cl_2 (100 mL) and the reaction mixture was stirred for 20 hours. The reaction mixture was washed with 4 M $HCl_{(aq)}$ solution (2 x 50 mL), dried over Na_2SO_4 and the solvent was removed under reduced pressure to give *sulfonamide* **135g** as a pink solid (9.59 g, 95%); mp: 94-96 °C (lit.[194] 96-97 °C); IR (neat): ν = 3235, 1597, 1526, 1335, 1154, 1090, 754 cm^{-1}; ^{1}H-NMR (300 MHz, $CDCl_3$): δ = 7.64 (d, *J* = 8.3 Hz, 2H), 7.26-7.18 (m, 4H), 7.11 (tt, *J* = 8.3, 1.2 Hz, 1H), 7.08-7.02 (m, 2H), 6.52 (br s, NH), 2.38 (s, 3H); ^{13}C-NMR (101 MHz, $CDCl_3$): δ = 144.0 (C), 136.7 (C), 136.1 (C), 129.8 (2CH), 129.4 (2CH), 127.4 (2CH), 125.3 (CH), 121.6 (2CH), 21.7 (CH_3). Spectroscopic data matched those reported.[195]

Sulfonamide 135i

A solution of NaOH (2.10 g, 52.5 mmol) and $MeNH_2$ (40% in H_2O, 4.5 mL, 52 mmol) in H_2O (45 mL) was cooled to 0 °C and TsCl (10.0 g, 52.5 mmol) was added over 5 minutes. The reaction mixture was stirred for 6 hours at room temperature and then extracted with EtOAc (2 x 30 mL). The combined organic extracts were washed with H_2O (30 mL) and brine (30 mL), dried over Na_2SO_4, and the solvent was removed under reduced pressure to give *sulfonamide* **135i** as a white solid (8.42 g, 87%); mp: 76-77 °C (lit.[196] 75-77 °C); IR (neat): ν = 3267, 1316, 1154, 1089, 820 cm^{-1}; ^{1}H-NMR (300 MHz, $CDCl_3$): δ = 7.75 (d, *J* = 8.2 Hz, 2H), 7.31 (d, *J* = 8.2 Hz, 2H), 4.69 (br q, NH), 2.62 (d, *J* = 5.4 Hz, 3H), 2.42 (s, 3H); ^{13}C-NMR (101 MHz, $CDCl_3$): δ = 143.6 (C), 135.9 (C), 129.9 (2CH), 127.4 (2CH), 29.4 (CH_3), 21.6 (CH_3). Spectroscopic data matched those reported.[196]

Sulfonamide 135j

Benzylamine (870 µL, 8.0 mmol) was added to a solution of TsCl (1.72 g, 9.0 mmol) and NEt_3 (1.25 mL, 9.0 mmol) in CH_2Cl_2 (20 mL) at 0 °C. The reaction mixture was stirred for 3 hours at room temperature and satd. $NH_4Cl_{(aq)}$ solution (30 mL) was added, the phases were separated, and the aqueous phase was extracted with CH_2Cl_2 (2 x 20 mL). The combined organic extracts were dried

over Na_2SO_4, concentrated under reduced pressure and purified by flash column chromatography (3:1 hexane:EtOAc) to give *sulfonamide* **135j** as a white solid (1.86 g, 89%); mp: 109-110 °C (lit.[197] 107-109 °C); ^{1}H-NMR (300 MHz, $CDCl_3$): δ = 7.76 (d, *J* = 8.3 Hz, 2H), 7.33-7.23 (m, 5H), 7.23-7.16 (m, 2H), 4.88 (br t, *J* = 6.2 Hz, NH), 4.11 (d, *J* = 6.2 Hz, 2H), 2.44 (s, 3H); ^{13}C-NMR (101 MHz, $CDCl_3$): δ = 143.6 (C), 137.0 (C), 136.4 (C), 129.9 (2CH), 128.8 (2CH), 128.0 (3CH), 127.3 (2CH), 47.4 (CH_2), 21.6 (CH_3); MS (EI): *m/z* = 261.1 (M^+, 20%), 196.1 (100), 180.1 (22), 165.1 (26). Spectroscopic data matched those reported.[198]

Sulfonamide 135l

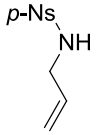

A solution of allylamine (375 µL, 5.0 mmol) and NEt_3 (780 µL, 5.6 mmol) in CH_2Cl_2 (4 mL) was added to a solution of 4-nitrobenzenesulfonyl chloride (1.27 g, 5.7 mmol) in CH_2Cl_2 (13 mL) at 0 °C. The reaction mixture was allowed to warm to room temperature and stirred for 3 hours. Satd. $NH_4Cl_{(aq)}$ solution (30 mL) was added, the phases were separated, and the aqueous phase was extracted with CH_2Cl_2 (2 x 20 mL). The combined organic phases were dried over Na_2SO_4, concentrated under reduced pressure and purified by flash column chromatography (4:1 hexane:EtOAc) to give *sulfonamide* **135l** as a yellow solid (1.12 g, 93%); mp: 110-112 °C; ^{1}H-NMR (300 MHz, $CDCl_3$): δ = 8.37 (d, *J* = 9.0 Hz, 2H), 8.06 (d, *J* = 9.0 Hz, 2H), 5.71 (ddt, *J*=17.1, 10.2, 5.8, 1H), 5.23-5.08 (m, 2H), 4.73 (t, *J* = 5.9 Hz, NH), 3.69 (apparent tt, *J* = 5.9, 1.5 Hz, 2H); ^{13}C-NMR (101 MHz, $CDCl_3$): δ = 150.3 (C), 146.3 (C), 132.5 (CH), 128.5 (2CH), 124.6 (2CH), 118.6 (CH_2), 46.0 (CH_2); MS (EI): *m/z* = 242.0 (M^+, 15%), 226.0 (10), 215.0 (8), 186.0 (49), 151.1 (28), 122.0 (100), 92.0 (24) 76.0 (49). Spectroscopic data matched those reported.[199]

Sulfonamide 135m

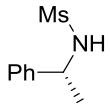

MsCl (1,3 mL, 16.8 mmol), was added to a solution of (*R*)-(+)-α-methylbenzylamine (2.5 mL, 19.6 mmol) and NEt_3 (4.7 mL, 34 mmol) in CH_2Cl_2 (30 mL) at 0 °C. The reaction mixture was stirred for 2 hours at room temperature and 2 M $HCl_{(aq)}$ solution (30 mL) was added. The phases were separated, the organic phase was dried over Na_2SO_4 and the solvent was removed

under reduced pressure to give *sulfonamide* **135m** as a white solid (2.69 g, 80%); mp: 48-50 °C (lit.[90] 46-48 °C); IR (neat): ν = 3283, 1316, 1148, 1086, 977, 755 cm^{-1}; ^{1}H-NMR (300 MHz, $CDCl_3$): δ = 7.41-7.26 (m, 5H), 5.18 (br s, NH), 4.64 (appt. quin, *J* = 6.9 Hz, 1H), 2.60 (s, 3H), 1.54 (d, *J* = 6.9 Hz, 3H); ^{13}C-NMR (101 MHz, $CDCl_3$): δ = 142.6 (C), 129.0 (2CH), 128.0 (CH), 126.4 (2CH), 53.9 (CH), 41.8 (CH_3), 24.1 (CH_3). Spectroscopic data matched those reported.[90]

Formamide 137a

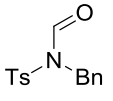

Following a literature procedure[83b] a solution of sulfonamide **135j** (724 mg, 2.8 mmol) in THF (12 mL) was cooled to 0 °C, ^{n}BuLi (2.5 M in hexane, 1.2 mL, 3.0 mmol) was added and the reaction mixture was stirred for 0.5 hours. A solution of *N*-formylbenzotriazole (338 mg, 3.0 mmol) in THF (6 mL) was added and stirring was continued for 0.5 hours at 0 °C and 1.5 hours at room temperature before the reaction was quenched with satd. $NH_4Cl_{(aq)}$ solution (15 mL) and extracted with EtOAc (3 x 30 mL). The combined organic phases were washed with 2 M $NaOH_{(aq)}$ solution (2 x 30 mL) and brine (30 mL), dried over Na_2SO_4, concentrated under reduced pressure and purified by flash column chromatography (17:3 hexane:EtOAc) to give *formamide* **137a** as a white solid (673 mg, 84%); mp: 96-97 °C (lit.[83b] 95-96 °C); IR (neat): ν = 2988, 2902, 1699, 1408, 1365, 1355, 1225, 1161, 1089, 1031, 897, 813, 755 cm^{-1}; ^{1}H-NMR (300 MHz, $CDCl_3$): δ = 9.19 (s, 1H), 7.56 (d, *J* = 8.4 Hz, 2H), 7.25-7.17 (m, 7H), 4.72 (s, 2H), 2.40 (s, 3H); ^{13}C-NMR (101 MHz, $CDCl_3$): δ = 161.7 (CH), 145.4 (C), 135.6 (C), 134.8 (C), 130.2 (2CH), 128.6 (2CH), 128.5 (2CH), 127.9 (CH), 127.5 (2CH), 45.9 (CH_2), 21.7 (CH_3). Spectroscopic data matched those reported.[83b]

Dibromoenamide 169

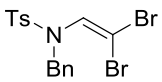

CBr_4 (998 mg, 3.0 mmol), PPh_3 (1.57 g, 6.0 mmol) and CH_2Cl_2 (20 mL) were added to a flask under an argon atmosphere whilst cooling at 0 °C. The reaction mixture was stirred for 1 hour, after which formamide **137a** (436 mg, 1.5 mmol) was added and stirring was continued for a further 18 hours at room temperature. Satd. $NaHCO_{3(aq)}$ solution (20 mL) was added, the phases were separated, and the aqueous phase was extracted with CH_2Cl_2 (2 x 15 mL). The

combined organic extracts were dried over Na_2SO_4, concentrated under reduced pressure and purified by flash column chromatography (10% EtOAc in hexane) to give *dibromoenamide* **169** as a white solid (432 mg, 64%); mp: 130-131 °C; IR (neat): ν = 3065, 3035, 2996, 1599, 1495, 1441, 1351, 1320, 1306, 1163, 1089, 954, 867, 755, cm^{-1}; ^{1}H-NMR (400 MHz, $CDCl_3$): δ = 7.75-7.70 (m, 2H), 7.37-7.26 (m, 7H), 6.61 (s, 1H), 4.54 (s, 2H), 2.46 (s, 3H); ^{13}C-NMR (101 MHz, $CDCl_3$): δ = 144.4 (C), 135.9 (C), 135.2 (C), 131.5 (CH), 130.0 (2CH), 128.8 (2CH), 128.7 (2CH), 128.2 (CH), 127.6 (2CH), 97.2 (C), 52.9 (CH_2), 21.8 (CH_3); HRMS (ES): *m/z* calculated for $C_{16}H_{15}NO_2S^{79}Br^{81}BrNa$: 467.9067, found 467.9050 $(M+Na)^+$.

Dichloroenamide 266

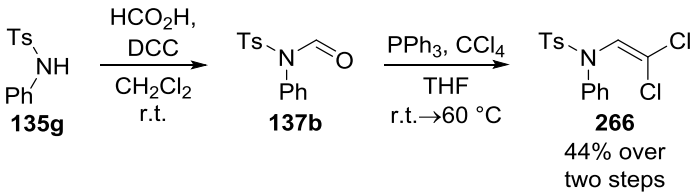

Following a literature procedure,[83b] *N,N'*-dicyclohexylcarbodiimide (5.16 g, 25 mmol) was added over 10 minutes to a solution of formic acid (750 µL, 23 mmol) and sulfonamide **135g** (2.47 g, 10 mmol) in CH_2Cl_2 (10 mL) under an argon atmosphere. After stirring for 17 hours at room temperature the reaction mixture was filtered through celite (washing with CH_2Cl_2), concentrated under reduced pressure and purified by flash column chromatography (5→10% EtOAc in hexane) to give impure formamide **137b** (contaminated with a small amount of **135g**) (2.09 g). This mixture was added to a flask containing PPh_3 (5.9 g, 22.5 mmol) and THF (75 mL) under an argon atmosphere. The reaction mixture was heated to 60 °C. and CCl_4 (7.3 mL, 75 mmol) was added by syringe pump over 7.3 hours; heating was continued for a further 10 hours. After cooling to room temperature, the solvent was removed under reduced pressure and the crude solid was taken up in satd. $NaHCO_{3(aq)}$ solution (30 mL) and extracted with CH_2Cl_2 (2 x 30 mL). The combined organic phases were dried over Na_2SO_4, concentrated under reduced pressure and purified by flash column chromatography (19:1 hexane:EtOAc) to give *dichloroenamide* **266** as a white solid (1.50 g, 44% over two steps); mp: 111-

113 °C (lit.[83b] 115-116 °C) ; IR (neat): ν = 3036, 1593, 1488, 1355, 1127, 1091, 927, 811 cm^{-1}; ^{1}H-NMR (300 MHz, $CDCl_3$): δ = 7.47 (d, *J* = 8.3 Hz, 2H), 7.33-7.23 (m, 5H), 7.10-7.03 (m, 2H), 6.97 (s, 1H), 2.43 (s, 3H); ^{13}C-NMR (101 MHz, $CDCl_3$): δ = 144.8 (C), 138.4 (C), 134.4 (C), 129.9 (2CH), 129.2 (2CH), 128.5 (2CH), 128.2 (CH), 127.9 (2CH), 126.3 (CH), 118.4 (C), 21.8 (CH_3). Spectroscopic data matched those reported.[83b]

Bromoacetylenes 133a-c

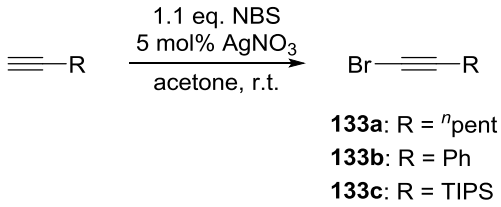

Bromoacetylenes **133a-c** were synthesised in >90% yields by mixing terminal acetylenes (1.0 eq.), NBS (1.1 eq.) and $AgNO_3$ (5 mol%) in acetone (0.2 M) for 3 hours. Silica gel was added to the reaction mixture which was then concentrated under reduced pressure. The silica-absorbed crude reaction mixture was added to a 3 cm pad of silica gel and the product was eluted with hexane. The bromoacetylenes were stored in a freezer and used within 1 week.

Alkyne 132d

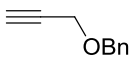

Following a literature procedure,[200] NaH (60% dispersion, 460 mg, 11.5 mmol) was suspended in DMF (10 mL) under an argon atmosphere and the suspension cooled to 0 °C. Propargyl alcohol (600 µL, 10 mmol) was added over 10 minutes and stirring was continued for a further 20 minutes before addition of benzyl bromide (1.4 mL, 12 mmol). The reaction mixture was stirred for 14 hours at room temperature and then quenched with 2 M $HCl_{(aq)}$ solution (20 mL) and extracted with EtOAc (20 mL). The organic phase was washed with brine (20 mL), dried over Na_2SO_4, concentrated under reduced pressure and purified by flash column chromatography (0⟶5% EtOAc in hexane) to give *alkyne* **132d** as a clear oil (969 mg, 64%); IR (neat): ν = 3291, 2857, 1722, 1073, 1027, 738 cm^{-1}; ^{1}H-NMR (300 MHz, $CDCl_3$): δ = 7.41-7.27 (m, 5H), 4.62 (s, 2H), 4.18 (d, *J* = 2.4 Hz, 2H), 2.47 (t, *J* = 2.4 Hz, 1H); Spectroscopic data matched those reported.[201]

5.1.4.1: General procedure for synthesis of dibromoalkenes (GP3)

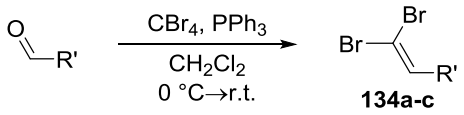

134a-c

CBr_4 (2.0 eq.) and PPh_3 (4.0 eq.) were dissolved in CH_2Cl_2 (0.13 M with respect to aldehyde) under an argon atmosphere whilst cooling with an ice/water bath. The reaction mixture was stirred for 1 hour, after which aldehyde (1.0 eq.) was added and stirring was continued for a further 18 hours at room temperature. Satd. $NaHCO_{3(aq)}$ solution and additional CH_2Cl_2 were added until all solids were dissolved and the phases were separated. The organic phase was dried over Na_2SO_4, concentrated under reduced pressure and purified by flash column chromatography to give the *dibromoalkene*.

Dibromoalkene 134a

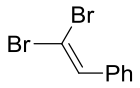

Following **GP3** using CBr_4 (1.33 g, 4.0 mmol), PPh_3 (2.10 g, 8.0 mmol) and benzaldehyde (200 µL, 2.0 mmol). Purification by flash column chromatography (9:1 hexane:EtOAc) gave *dibromoalkene* **134a** as a colourless oil (473 mg, 91%); ^{1}H-NMR (300 MHz, $CDCl_3$): δ = 7.56-7.50 (m, 2H), 7.49 (s, 1H), 7.41-7.32 (m, 3H); MS (EI): *m/z* = 263.9 (M^+, 48%), 261.9 (M^+, 100), 259.9 (M^+, 54), 181.0 (22), 102.0 (42). Spectroscopic data matched those reported.[202]

Dibromoalkene 134b

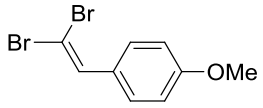

Following **GP3** using CBr_4 (2.63 g, 7.9 mmol), PPh_3 (4.23 g, 16 mmol) and 4-anisaldehyde (490 µL, 4.0 mmol). Chromatography was replaced by filtration through a 5 cm pad of silica gel (eluting with hexane) to give *dibromoalkene* **134b** as a pale yellow solid (1.14 g, 97%); mp: 33-34 °C (lit.[202] 37-38 °C); IR (neat): ν = 2964, 2840, 1603, 1567, 1507, 1254, 1177, 1026, 863 cm^{-1}; ^{1}H-NMR (300 MHz, $CDCl_3$): δ = 7.51 (d, *J* = 8.8 Hz, 2H), 7.41 (s, 1H), 6.89 (d, *J* = 8.8 Hz, 2H), 3.82 (s, 3H); ^{13}C-NMR (101 MHz, $CDCl_3$): δ = 159.8 (C), 136.5 (CH), 130.0 (2CH), 128.0 (C), 113.9 (2CH), 87.4 (C), 55.4 (CH_3). Spectroscopic data matched those reported.[203]

Dibromoalkene 134c

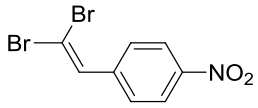

Following **GP3** using CBr_4 (2.65 g, 8.0 mmol), PPh_3 (4.23 g, 16 mmol) and 4-nitrobenzaldehyde (609 mg, 4.0 mmol). Purification by flash column chromatography (9:1 hexane:Et_2O) gave *dibromoalkene* **134c** as a white solid (999 mg, 81%); mp: 92-94 °C (lit.[202] 93-94 °C); IR (neat): ν = 3103, 3078, 2927, 2835 1586, 1505, 1488, 1332, 1108, 882, 859 cm^{-1}; ^{1}H-NMR (300 MHz, $CDCl_3$): δ = 8.23 (d, *J* = 8.8 Hz, 2H), 7.70 (d, *J* = 8.8 Hz, 2H), 7.56 (s, 1H); ^{13}C-NMR (101 MHz, $CDCl_3$): δ = 147.4 (C), 141.6 (C), 135.1 (CH), 129.3 (2CH), 123.9 (2CH), 94.3 (C). Spectroscopic data matched those reported.[204]

Dibromoalkene 134d

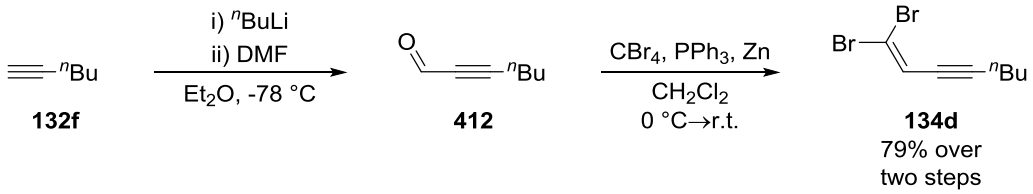

Under an Ar atmosphere ^{n}BuLi (2.5 M in hexane, 4 mL, 10 mmol) was added to a solution of 1-hexyne (1.15 mL, 10 mmol) in diethyl ether (4 mL) at −78 °C and the reaction mixture was stirred for 30 minutes. DMF (1.16 mL, 15 mmol) was then added and the solution was allowed to warm to room temperature and stirred for a further 30 minutes. The reaction mixture was cooled to 0 °C and quenched with water (10 mL) and the solution was acidified with conc. $HCl_{(aq)}$ then neutralised with satd. $NaHCO_{3(aq)}$ before extraction with diethyl ether (3 x 10 mL). The combined organic fractions were dried over Na_2SO_4, filtered and carefully concentrated (300 mbar, 40 °C) to give a crude yellow solution of aldehyde **412**. CBr_4 (6.66 g, 20.1 mmol) in CH_2Cl_2 (10 mL) was cooled to 0 °C under an argon atmosphere, PPh_3 (5.28 g, 20.1 mmol) and powdered zinc (13.3 g, 40.4 mmol) were added and the reaction mixture was stirred for 30 minutes at room temperature. The resulting red solution was cooled to 0 °C and the crude aldehyde **412** was added in CH_2Cl_2 (10 mL) and the reaction mixture was stirred for 18 hours at room temperature. The zinc residue was removed by filtration through a plug of silica before purification by flash column chromatography (hexane) gave *dibromoalkene* **134d** as a

yellow oil (2.10 g, 79%); IR (neat): ν = 3018, 2932, 2871, 2215, 1574, 1465, 1427, 850 cm^{-1}; ^{1}H-NMR (300 MHz, $CDCl_3$): δ = 6.52 (t, *J* = 2.3 Hz, 1H), 2.32 (td, *J* = 6.9, 2.3 Hz, 2H), 1.60-1.50 (m, 2H), 1.49-1.38 (m, 2H), 0.92 (t, *J* = 7.2 Hz, 3H); ^{13}C-NMR (101 MHz, $CDCl_3$): δ = 120.3 (CH), 100.2 (C), 99.6 (C), 77.9 (C), 30.4 (CH_2), 22.1 (CH_2), 19.6 (CH_2), 13.7 (CH_3); HRMS (EI): m/z: calculated. for $C_8H_{10}{}^{79}Br_2$: 263.9149, found 263.9142 $(M)^+$.

5.1.5: Synthesis of Ynamides

5.1.5.1: General procedure for synthesis of ynamides from terminal acetylenes (GP5)

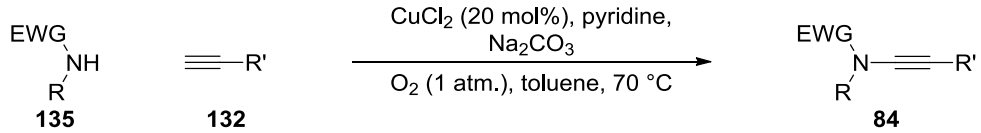

Following a literature procedure,[82] a 3 neck flask, with a volume at least 20 times greater than that of the solvent required, was charged with sulfonamide (5.0 eq.), Na_2CO_3 (2.0 eq.), and $CuCl_2$ (0.2 eq.) and purged with O_2 for 15 minutes. A balloon of O_2 gas was attached. Pyridine (2.0 eq.) and toluene (1 mL / mmol of sulfonamide) were added and the reaction mixture was heated to 70 °C before a solution of terminal acetylene (1.0 eq, 0.2 M in toluene) was added over 6 hours by syringe pump, after which stirring was continued for a further 10 hours at 70 °C. After cooling to room temperature, the reaction mixture was filtered through a 5 cm pad of silica gel (eluting with CH_2Cl_2), concentrated under reduced pressure and purified by flash column chromatography to give the *ynamide* and, where stated, some recovered amide.

Ynamide 84c

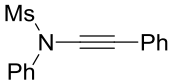

Following **GP5** using sulfonamide **135a** (2.18 g, 20 mmol), Na_2CO_3 (844 mg, 8.0 mmol), $CuCl_2$ (108 mg, 0.8 mmol), pyridine (650 µL, 8.0 mmol) and phenylacetylene (440 µL, 4.0 mmol). Purification by flash column chromatography (10→30% EtOAc in hexane) gave *ynamide* **84c** as a white solid (919 mg, 84%); mp: 74-76 °C (lit.[49] 75-77 °C); IR (neat): ν = 3078, 3010, 2923, 2243, 1589, 1485, 1365, 1165, 962 cm^{-1}; ^{1}H-NMR (300 MHz, $CDCl_3$): δ = 7.69-

7.54 (m, 2H), 7.53-7.27 (m, 8H), 3.17 (s, 3H). Spectroscopic data matched those reported.[49] Sulfonamide **135a** (634 mg, 5.8 mmol) was also recovered.

Ynamide 84m

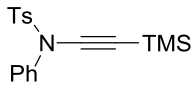

Following **GP5** using sulfonamide **135g** (3.71 g, 15 mmol), Na_2CO_3 (636 mg, 6.0 mmol), $CuCl_2$ (81 mg, 0.6 mmol), pyridine (500 µL, 6.1 mmol) and trimethylsilylacetylene (415 µL, 3.0 mmol). Purification by flash column chromatography (5→20% EtOAc in hexane) gave *ynamide* **84m** as a white solid (849 mg, 83%); mp: 92-94 °C (lit.[49] 88-91 °C); IR (neat): ν = 2962, 2166, 1490, 1365, 1160, 842 cm^{-1}; ^{1}H-NMR (400 MHz, $CDCl_3$): δ = 7.55 (d, *J* = 8.3 Hz, 2H), 7.32-7.19 (m, 7H), 2.43 (s, 3H), 0.15 (s, 9H); ^{13}C-NMR (101 MHz, $CDCl_3$): δ = 145.1 (C), 138.7 (C), 133.0 (C), 129.5 (2CH), 129.2 (2CH), 128.5 (2CH), 128.3 (CH), 126.3 (2CH), 95.4 (C), 73.4 (C), 21.9 (CH_3), 0.2 ($3CH_3$). Spectroscopic data matched those reported.[49] Sulfonamide **135g** (1.61 g, 6.5 mmol) was also recovered.

Ynamide 84r

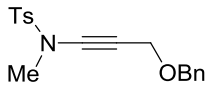

Following **GP5** using sulfonamide **135i** (930 mg, 5.0 mmol), Na_2CO_3 (213 mg, 2.0 mmol), CuCl (27 mg, 0.2 mmol), pyridine (162 µL, 2.0 mmol) and alkyne **132d** (146 µL, 1.0 mmol). Purification by flash column chromatography (17:3 hexane:EtOAc) gave *ynamide* **84r** as a white solid (260 mg, 79%); mp: 84-86 °C; IR (neat): ν = 3072, 2864, 2235, 1595, 1453, 1362, 1169, 1063, 1027, 1014, 821, 759 cm^{-1}; ^{1}H-NMR (300 MHz, $CDCl_3$): δ = 7.84-7.76 (d, *J* = 8.3 Hz, 2H), 7.39-7.28 (m, 7H), 4.53 (s, 2H), 4.28 (s, 2H), 3.09 (s, 3H), 2.43 (s, 3H); ^{13}C-NMR (101 MHz, $CDCl_3$): δ = 145.0 (C), 137.6 (C), 133.5 (C), 130.0 (2CH), 128.6 (2CH), 128.2 (2CH), 128.0 (CH), 127.9 (2CH), 81.6 (C), 71.2 (CH_2), 65.8 (C), 57.6 (CH_2), 39.3 (CH_3), 21.8 (CH_3); HRMS (ES): *m/z* calculated for $C_{18}H_{19}NO_3SNa$: 252.0983, found 252.1000 $(M+Na)^+$.

Ynamide 171c

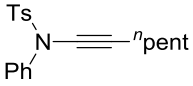

Following **GP5** using sulfonamide **135i** (2.47 g, 10 mmol), Na_2CO_3 (421 mg, 4.0 mmol), CuCl (55 mg, 0.4 mmol), pyridine (327 µL, 4.0 mmol) and hept-1-yne (263 µL, 2.0 mmol). Purification by flash column chromatography (5→15% EtOAc in hexane) gave *ynamide* **171c** as a white solid (405 mg, 59%); mp: 25-26 °C; IR (neat): ν = 2955, 2939, 2859, 2257, 1594, 1489, 1362, 1275, 1176, 1157, 1089, 935, 901, 815 cm^{-1}; ^{1}H-NMR (300 MHz, $CDCl_3$): δ = 7.58-7.51 (d, *J* = 8.2 Hz, 2H), 7.35-7.22 (m, 7H), 2.43 (s, 3H), 2.28 (t, *J* = 7.0 Hz, 2H), 1.54-1.44 (m, 2H), 1.39-1.24 (m, 4H), 0.94-0.85 (m, 3H); ^{13}C-NMR (101 MHz, $CDCl_3$): δ = 144.7 (C), 139.5 (C), 133.1 (C), 129.4 (2CH), 129.0 (2CH), 128.4 (2CH), 128.0 (CH), 126.2 (2CH), 74.0 (C), 70.6 (C), 31.1 (CH_2), 28.7 (CH_2), 22.3 (CH_2), 21.8 (CH_3), 18.6 (CH_2), 14.2 (CH_3); HRMS (ES): *m/z* calculated for $C_{20}H_{24}NO_2S$: 342.1528, found 342.1514 $(M+H)^+$. Sulfonamide **135i** (1.03 g, 4.1 mmol) was also recovered.

5.1.5.2: General procedure for synthesis of ynamides from bromoacetylenes (GP4)

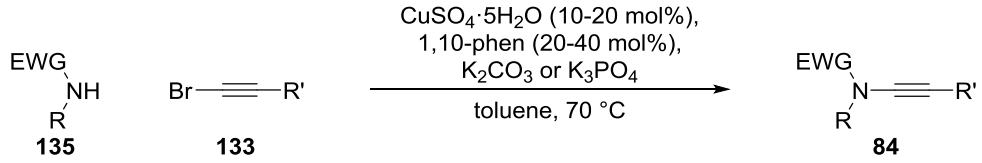

Following a literature procedure[77b] a two-neck flask under an argon atmosphere was charged with the relevant amide (1.0 eq.), K_3PO_4 or K_2CO_3 (2.0 eq.), $CuSO_4{\cdot}5H_2O$ (10-20 mol%), 1,10-phenanthroline (20-40 mol%), toluene (1 M with respect to amide) and bromoacetylene (1.1-1.5 eq.) and heated at 70 °C for the stated time. After cooling to room temperature, the reaction mixture was filtered through a 5 cm pad of silica gel, concentrated under reduced pressure, and then purified by flash column chromatography.

Ynamide 84d

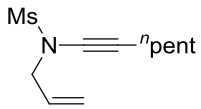

Following **GP4** using sulfonamide **135b** (1.01 g, 7.5 mmol), K_2CO_3 (2.07 g, 15 mmol), $CuSO_4 \cdot 5H_2O$ (187 mg, 0.75 mmol), 1,10-phenanthroline (270 mg, 1.5 mmol) and 1-bromohept-1-yne (1.78 g, 10 mmol) for 18 hours. Purification by flash column chromatography (9:1 hexane:EtOAc) gave *ynamide* **84d** as an orange oil (1.20 g, 70%); IR (neat): ν = 2932, 2860, 2253, 1354, 1162 cm^{-1}; ^{1}H-NMR (300 MHz, $CDCl_3$): δ = 5.93 (ddt, *J* = 17.0, 10.2, 6.4 Hz, 1H), 5.41-5.29 (m, 2H), 4.02 (appt. dt, *J* = 6.4, 1.1 Hz, 2H), 3.05 (s, 3H), 2.28 (t, *J* = 7.0 Hz, 2H), 1.55-1.46 (m, 2H), 1.41-1.25 (m, 4H), 0.89 (t, *J* = 7.1 Hz, 3H); ^{13}C-NMR (101 MHz, $CDCl_3$): δ = 131.3 (CH), 120.3 (CH_2), 72.7 (C), 71.1 (C), 54.3 (CH_2), 38.4 (CH_3), 31.1 (CH_2), 28.7 (CH_2), 22.3 (CH_2), 18.5 (CH_2), 14.1 (CH_3); HRMS (ES): *m/z* calculated for $C_{11}H_{19}NO_2SNa$: 252.1034, found 252.1030 $(M+Na)^+$.

Ynamide 84e

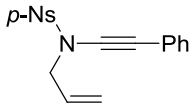

Following **GP4** using sulfonamide **135l** (143 mg, 0.59 mmol), K_2CO_3 (131 mg, 0.90 mmol), $CuSO_4 \cdot 5H_2O$ (15 mg, 0.06 mmol), 1,10-phenanthroline (22 mg, 0.12 mmol) and (bromoethynyl)benzene (163 mg, 0.90 mmol) for 18 hours. Purification by flash column chromatography (9:1 hexane:EtOAc) gave *ynamide* **84e** as a yellow solid (91.9 mg, 45%); mp: 59-61 °C (lit.[205] 65-67 °C); IR (neat): ν = 2233, 1606, 1529, 1346, 1311, 1172, 995 cm^{-1}; ^{1}H-NMR (300 MHz, $CDCl_3$): δ = 8.36 (d, *J* = 9.0 Hz, 2H), 8.10 (d, *J* = 9.0 Hz, 2H), 7.36-7.22 (m, 5H), 5.74 (ddt, *J* = 16.9, 10.2, 6.4 Hz, 1H), 5.33-5.18 (m, 2H), 4.09 (dt, *J* = 6.4, 1.1 Hz, 2H); ^{13}C-NMR (101 MHz, $CDCl_3$): δ = 150.7 (C), 143.1 (C), 131.6 (CH), 130.2 (CH), 129.1 (2CH), 128.5 (4CH), 124.5 (2CH), 122.1 (C), 120.9 (CH_2), 81.0 (C), 71.6 (C), 54.9 (CH_2). Spectroscopic data matched those reported.[205]

Ynamide 84g

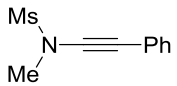

Following **GP4** using sulfonamide **135c** (811 mg, 7.4 mmol), K_2CO_3 (2.07 g, 15 mmol), $CuSO_4 \cdot 5H_2O$ (187 mg, 0.75 mmol), 1,10-phenanthroline (270 mg, 1.5 mmol) and (bromoethynyl)benzene (1.63 g, 9.0 mmol) for 18 hours. Purification by flash column chromatography (10→30% EtOAc in hexane) gave *ynamide* **84g** as a pale yellow solid (1.51 g, 97%);

mp: 54-55 °C (lit.[206] 61-63 °C); IR (neat): ν = 2241, 1347, 1320, 1155, 1107, 957, 763 cm^{-1}; ^{1}H-NMR (300 MHz, $CDCl_3$): δ = 7.46-7.37 (m, 2H), 7.36-7.27 (m, 3H), 3.30 (s, 3H), 3.13 (s, 3H); ^{13}C-NMR (101 MHz, $CDCl_3$): δ = 131.7 (2CH), 128.5 (2CH), 128.2 (CH), 122.5 (C), 83.2 (C), 69.6 (C), 39.3 (CH_3), 36.9 (CH_3). Spectroscopic data matched those reported.[207]

Ynamide 84h

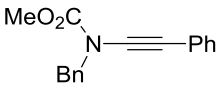

Following **GP4** using amide **135d** (498 mg, 3.0 mmol), K_3PO_4 (1.27 g, 6.0 mmol), $CuSO_4{\cdot}5H_2O$ (150 mg, 0.6 mmol), 1,10-phenanthroline (216 mg, 1.2 mmol) and (bromoethynyl)benzene (620 mg, 3.4 mmol) for 28 hours. Purification by flash column chromatography (5→10% EtOAc in hexane) gave *ynamide* **84h** as a yellow oil (572 mg, 72%); IR (neat): ν = 3033, 2955, 2260, 2238, 1724, 1441, 1392, 1291, 1232, 753 cm^{-1}; ^{1}H-NMR (300 MHz, $CDCl_3$): δ = 7.47-7.23 (m, 10H), 4.72 (s, 2H), 3.86 (s, 3H); ^{13}C-NMR (101 MHz, $CDCl_3$): δ = 155.8 (C), 136.1 (C), 131.3 (2CH), 128.8 (4CH), 128.4 (2CH), 128.3 (CH), 127.7 (CH), 123.3 (C), 83.2 (C), 71.4 (C), 54.4 (CH_3), 54.3 (CH_2). Spectroscopic data matched those reported.[77a]

Ynamide 84k

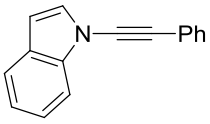

Following **GP4** using indole (702 mg, 6.0 mmol), K_3PO_4 (2.55 g, 12 mmol), $CuSO_4{\cdot}5H_2O$ (150 mg, 0.6 mmol), 1,10-phenanthroline (216 mg, 1.2 mmol) and (bromoethynyl)benzene (1.47 g, 8.1 mmol) for 28 hours. Column chromatography was replaced by filtration through a 5 cm pad of silica with hexane and, after the solvent was removed under reduced pressure, the residue was recrystallised from hexane, isolated by filtration, and washed with ice-cold hexane (20 mL) to give *ynamide* **84k** as a white solid (223 mg, 17%); mp: 54-56 °C; IR (neat): ν = 2246, 1523, 1454, 1162, 1145, 746 cm^{-1}; ^{1}H-NMR (300 MHz, $CDCl_3$): δ = 7.71-7.62 (m, 2H), 7.61-7.53 (m, 2H), 7.45-7.21 (m, 6H), 6.63 (dd, *J* = 3.4, 0.7, 1H); ^{13}C-NMR (101 MHz, $CDCl_3$): δ = 138.3 (C), 131.6 (2CH), 129.0 (CH), 128.6 (2CH), 128.2 (CH), 128.0 (C), 123.7 (CH), 122.8 (C), 122.1 (CH), 121.3 (CH), 111.5 (CH), 105.7 (CH), 80.9 (C), 70.7 (C). Spectroscopic data matched those reported.[94]

Ynamide 84l

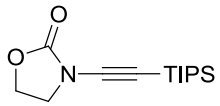

Following **GP4** using oxazolidinone (695 mg, 8.0 mmol), K_3PO_4 (3.4 g, 16 mmol), $CuSO_4 \cdot 5H_2O$ (200 mg, 0.8 mmol), 1,10-phenanthroline (288 mg, 1.6 mmol) and (bromoethynyl)triisopropylsilane (1.64 g, 6.3 mmol) for 18 hours. Purification by flash column chromatography (10⟶15% EtOAc in hexane) gave *ynamide* **84l** as a white solid (791 mg, 47%); mp: 70-72 °C; IR (neat): ν = 2943, 2865, 2177, 1758, 1479, 1463, 1399, 1103, 882 cm^{-1}; ^{1}H-NMR (300 MHz, $CDCl_3$): δ = 4.42 (dd, *J* = 8.8, 7.1 Hz, 2H), 3.94 (dd, *J* = 8.8, 7.1 Hz, 2H), 1.11-1.04 (m, 21H); ^{13}C-NMR (101 MHz, $CDCl_3$): δ = 155.9 (C), 93.2 (C), 70.2 (C), 62.9 (CH_2), 47.1 (CH_2), 18.7 ($6CH_3$), 11.4 (3CH). Spectroscopic data matched those reported.[82]

Ynamide 84s

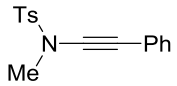

Following **GP4** using sulfonamide **135i** (1.39 g, 7.5 mmol), K_2CO_3 (2.07 g, 15.0 mmol), $CuSO_4 \cdot 5H_2O$ (187 mg, 0.75 mmol), 1,10-phenanthroline (270 mg, 1.5 mmol) and (bromoethynyl)benzene (1.49 g, 8.2 mmol) for 22 hours. Purification by flash column chromatography (5⟶10% EtOAc in hexane) gave *ynamide* **84s** as a pale yellow solid (1.46 g, 68%); mp: 60-62 °C (lit.[208] 79-81 °C); IR (neat): ν = 3241, 2234, 1594, 1579, 1359, 1167, 1115, 953, 754 cm^{-1}; ^{1}H-NMR (300 MHz, $CDCl_3$): δ = 7.84 (d, *J* = 8.3 Hz, 2H), 7.42-7.33 (m, 4H), 7.32-7.27 (m, 3H), 3.15 (s, 3H), 2.46 (s, 3H); ^{13}C-NMR (101 MHz, $CDCl_3$): δ = 144.9 (C), 133.4 (C), 131.5 (2CH), 129.9 (2CH), 128.4 (2CH), 128.0 (3CH), 122.9 (C), 84.1 (C), 69.2 (C), 39.5 (CH_3), 21.8 (CH_3). Spectroscopic data matched those reported.[208]

Ynamide 84x

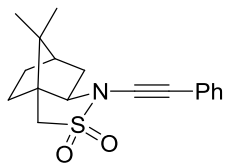

Following **GP4** using (-)-camphor sultam (2.15 g, 10 mmol), K_2CO_3 (2.76 g, 20 mmol), $CuSO_4 \cdot 5H_2O$ (250 mg, 1.0 mmol), 1,10-phenanthroline (360 mg, 2.0 mmol) and (bromoethynyl)benzene (2.0 g, 11 mmol) for 16 hours. Purification by flash column chromatography (10⟶15% EtOAc in hexane) gave *ynamide* **84x** as a colourless viscous oil (2.97 g, 94%); IR (neat): ν = 2959, 2886, 2234, 1331, 1167, 1148, 815 cm^{-1};

^{1}H-NMR (300 MHz, $CDCl_3$): δ = 7.45-7.38 (m, 2H), 7.30-7.24 (m, 3H), 3.67 (dd, *J* = 8.1, 4.2 Hz, 1H), 3.29 (s, 2H), 2.33-2.22 (m, 1H), 2.00-1.76 (m, 4H), 1.48-1.40 (m, 1H), 1.36-1.28 (m, 1H), 1.14 (s, 3H), 0.95 (s, 3H); ^{13}C-NMR (101 MHz, $CDCl_3$): δ = 131.8 (2CH), 128.3 (2CH), 128.0 (CH), 122.8 (C), 76.8 (C), 72.8 (C), 67.3 (CH), 65.9 (C), 51.3 (C), 49.9 (CH_2), 48.1 (C), 44.5 (CH), 34.5 (CH_2), 31.7 (CH_2), 27.1 (CH_2), 20.3 (CH_3), 20.1 (CH_3). Spectroscopic data matched those reported.[209]

Ynamide 84y

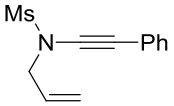

Following **GP4** using sulfonamide **135b** (405 mg, 2.9 mmol), K_2CO_3 (830 mg, 6.0 mmol), $CuSO_4 \cdot 5H_2O$ (75 mg, 0.3 mmol), 1,10-phenanthroline (108 mg, 0.6 mmol) and (bromoethynyl)benzene (600 mg, 3.3 mmol) for 18 hours. Purification by flash column chromatography (10→20% EtOAc in hexane) gave *ynamide* **84y** as a yellow solid (571 mg, 83%); mp: 49-51 °C (lit.[49] 50-52 °C); IR (neat): ν = 3030, 2934, 2242, 1441, 1344, 1158, 1023, 972, 915 cm^{-1}; ^{1}H-NMR (300 MHz, $CDCl_3$): δ = 7.45-7.37 (m, 2H), 7.34-7.27 (m, 3H), 6.00 (ddt, *J* = 16.9, 10.2, 6.4 Hz, 1H), 5.49-5.35 (m, 2H), 4.17 (d, *J* = 6.4 Hz, 2H), 3.14 (s, 3H); ^{13}C-NMR (101 MHz, $CDCl_3$): δ = 131.6 (CH), 131.0 (CH), 128.4 (2CH), 128.2 (2CH), 122.6 (C), 120.7 (CH_2), 81.7 (C), 71.3 (C), 54.5 (CH_2), 39.1 (CH_3). Spectroscopic data matched those reported.[49]

Ynamide 84z

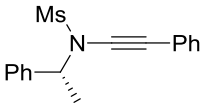

Following **GP4** using sulfonamide **135m** (1.19 g, 6.0 mmol), K_2CO_3 (1.66 g, 12.0 mmol), $CuSO_4 \cdot 5H_2O$ (150 mg, 0.6 mmol), 1,10-phenanthroline (216 mg, 1.2 mmol) and (bromoethynyl)benzene (1.19 g, 6.6 mmol) for 18 hours. Purification by flash column chromatography (10→15% EtOAc in hexane) gave *ynamide* **84z** as a yellow solid (1.13 g, 63%); mp: 77-78 °C (lit.[90] 62-64 °C); IR (neat): ν = 2236, 1688, 1354, 1163, 1129, 1099, 964, 798, 756 cm^{-1}; ^{1}H-NMR (300 MHz, $CDCl_3$): δ = 7.55-7.49 (m, 2H), 7.45-7.29 (m, 8H) 5.23 (q, *J* = 7.1 Hz, 1H), 2.75 (s, 3H), 1.78 (d, *J* = 7.1 Hz, 3H); ^{13}C-NMR (101 MHz, $CDCl_3$): δ = 139.8 (C), 131.5 (2CH), 128.9 (2CH), 128.8 (CH), 128.5 (2CH), 128.1 (CH), 127.1 (2CH), 122.9 (C), 79.7 (C), 73.8 (C), 59.3 (CH), 39.1 (CH_3), 20.2 (CH_3). Spectroscopic data matched those reported.[90]

Ynamide 171a

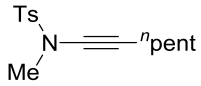

Following **GP4** using sulfonamide **135i** (429 mg, 2.3 mmol), K_2CO_3 (691 mg, 4.6 mmol), $CuSO_4 \cdot 5H_2O$ (57 mg, 0.23 mmol), 1,10-phenanthroline (83 mg, 0.46 mmol) and 1-bromohept-1-yne (608 mg, 3.48 mmol) for 16 hours. Purification by flash column chromatography (4:1 hexane:EtOAc) gave *ynamide* **171a** as a colourless oil (427 mg, 66%); IR (neat): ν = 2930, 2859, 2253, 1597, 1456, 1363, 1277, 1171, 1089, 813, 757 cm^{-1}; ^{1}H-NMR (300 MHz, $CDCl_3$): δ = 7.83-7.71 (d, *J* = 8.2 Hz, 2H), 7.40-7.29 (d, *J* = 8.2 Hz, 2H), 3.00 (s, 3H), 2.45 (s, 3H), 2.22 (t, *J* = 7.0 Hz, 2H), 1.53-1.38 (m, 2H), 1.38-1.22 (m, 4H), 0.95-0.81 (m, 3H); ^{13}C-NMR (101 MHz, $CDCl_3$): δ = 144.5 (C), 133.4 (C), 129.7 (2CH), 128.0 (2CH), 75.0 (C), 68.8 (C), 39.5 (CH_3), 31.1 (CH_2), 28.7 (CH_2), 22.3 (CH_2), 21.8 (CH_3), 18.5 (CH_2), 14.1 (CH_3); HRMS (ES): *m/z* calculated for $C_{15}H_{22}NO_2S$: 280.1371, found 280.1377 $(M+H)^+$.

Ynamide 171b

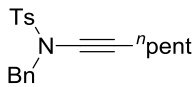

Following **GP4** using sulfonamide **135j** (524 mg, 2.0 mmol), K_2CO_3 (554 mg, 4.0 mmol), $CuSO_4 \cdot 5H_2O$ (51 mg, 0.2 mmol), 1,10-phenanthroline (72 mg, 0.4 mmol) and 1-bromohept-1-yne (384 mg, 2.2 mmol) for 18 hours. Purification by flash column chromatography (9:1 hexane:EtOAc) gave *ynamide* **171b** as a white solid (581 mg, 82%); mp: 32-33 °C (lit.[81] 45 °C); IR (neat): ν = 2255, 1427, 1354, 1168, 1088, 741 cm^{-1}; ^{1}H-NMR (300 MHz, $CDCl_3$): δ = 7.72 (d, *J* = 8.3 Hz 2H), 7.34-7.21 (m, 7H), 4.41 (s, 2H), 2.42 (s, 3H), 2.13 (t, *J* = 6.9 Hz, 2H), 1.34 (appt. quin, *J* = 6.9 Hz, 2H), 1.26-1.08 (m, 4H), 0.82 (t, *J* = 6.9 Hz, 3H); ^{13}C-NMR (101 MHz, $CDCl_3$): δ = 144.4 (C), 135.0 (C), 134.9 (C), 129.7 (2CH), 128.8 (2CH), 128.5 (2CH), 128.2 (CH), 127.8 (2CH), 73.5 (C), 71.0 (C), 55.7 (CH_2), 30.9 (CH_2), 28.6 (CH_2), 22.3 (CH_2), 21.8 (CH_3), 18.5 (CH_2), 14.1 (CH_3). Spectroscopic data matched those reported.[81]

5.1.5.3: General procedure for synthesis of ynamides from dibromoalkenes (GP6)

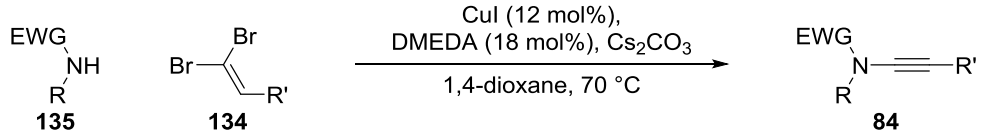

Following a literature procedure,[81] a flask under an argon atmosphere was charged with amide (1.0 eq.), Cs_2CO_3 (4.0 eq.), CuI (12 mol%), dibromoalkene (1.3-1.5 eq.), 1,4-dioxane (0.5 M with respect to amide) and *N*,*N*'-dimethylethylenediamine (DMEDA) (18 mol%) and the reaction mixture was heated at 70 °C for the indicated time. After cooling to room temperature, the reaction mixture was filtered through a 5 cm pad of silica gel (eluting with CH_2Cl_2), concentrated under reduced pressure and purified by flash column chromatography.

Ynamide 84f

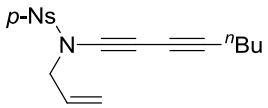

Following **GP6** using sulfonamide **135l** (818 mg, 3.4 mmol), Cs_2CO_3 (4.40 g, 13.5 mmol), CuI (76 mg, 0.40 mmol), dibromoalkene **134d** (1.16 g, 4.4 mmol) and DMEDA (65 µL, 0.60 mmol) for 18 hours. Purification by flash column chromatography (8:1 hexane:EtOAc) yielded *ynamide* **84f** as a yellow solid (732 mg, 63%); mp: 75-79 °C; IR (neat): ν = 3099, 2958, 2931, 2863, 2253, 2166, 1606, 1529, 1369, 1347 cm^{-1}; ^{1}H-NMR (300 MHz, $CDCl_3$): δ = 8.42 (d, *J* = 9.0 Hz, 2H), 8.10 (d, *J* = 9.0 Hz, 2H), 5.70 (ddt, *J* = 17.0, 10.1, 6.3 Hz, 1H), 5.33-5.22 (m, 2H), 4.04 (dt, *J* = 6.3, 1.2 Hz, 2H), 2.31 (t, *J* = 6.9 Hz, 2H), 1.59-1.33 (m, 4H), 0.92 (t, *J* = 7.2 Hz, 3H); ^{13}C-NMR (101 MHz, $CDCl_3$): δ = 150.8 (C), 143.1 (C), 129.9 (CH), 129.1 (2CH), 124.6 (2CH), 121.2 (CH_2), 85.1 (C), 65.9 (C), 63.9 (C), 59.5 (C), 54.8 (CH_2), 30.3 (CH_2), 22.1 (CH_2), 19.3 (CH_2), 13.6 (CH_3); HRMS (ES): m/z: calculated. for $C_{17}H_{18}N_2O_4NaS$: 369.0885, found 369.0842 $(M+Na)^+$.

Ynamide 84j

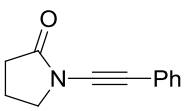

Following **GP6** using 2-pyrrolidinone (190 µL, 2.5 mmol), Cs_2CO_3 (3.25 g, 10 mmol), CuI (57 mg, 0.30 mmol), dibromoalkene **134a** (867 mg, 3.3 mmol) and DMEDA (50 µL, 0.46 mmol) for 14 hours. Purification by flash column chromatography (30→50% EtOAc in hexane) yielded *ynamide* **84j** as a yellow oil (303 mg, 66%); IR (neat): ν = 2975,

2897, 2246, 1675, 1396, 1220 cm^{-1}; ^{1}H-NMR (300 MHz, $CDCl_3$): δ = 7.48-7.41 (m, 2H), 7.34-7.27 (m, 3H), 3.83-3.75 (m, 2H), 2.53-2.45 (m, 2H), 2.24-2.12 (m, 2H); ^{13}C-NMR (101 MHz, $CDCl_3$): δ = 175.9 (C), 131.7 (2CH), 128.4 (2CH), 128.1 (CH), 122.8 (C), 80.5 (C), 72.8 (C), 50.3 (CH_2), 29.8 (CH_2), 19.0 (CH_2). Spectroscopic data matched those reported.[82]

Ynamide 84t

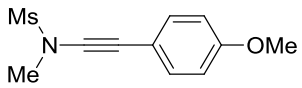

Following **GP6** using sulfonamide **135c** (218 mg, 2.0 mmol), Cs_2CO_3 (2.60 g, 8.0 mmol), CuI (48 mg, 0.25 mmol), dibromoalkene **134b** (870 mg, 3.0 mmol) and DMEDA (40 µL, 0.37 mmol) for 36 hours. Purification by flash column chromatography (20⟶30% EtOAc in hexane) yielded *ynamide* **84t** as a white solid (455 mg, 92%); mp: 91-92 °C; IR (neat): ν = 3015, 2935, 2236, 1603, 1512, 1353, 1326, 1246, 1158, 1024, 959, 839 cm^{-1}; ^{1}H-NMR (300 MHz, $CDCl_3$): δ = 7.36 (d, *J* = 8.9 Hz, 2H), 6.83 (d, *J* = 8.9 Hz, 2H), 3.81 (s, 3H), 3.28 (s, 3H), 3.11 (s, 3H); ^{13}C-NMR (101 MHz, $CDCl_3$): δ = 159.8 (C), 133.7 (2CH), 114.4 (C), 114.1 (2CH), 81.8 (C), 69.3 (C), 55.4 (CH_3), 39.4 (CH_3), 36.7 (CH_3). Spectroscopic data matched those reported.[206]

Ynamide 84u

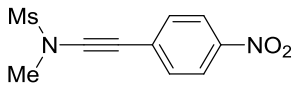

Following **GP6** using sulfonamide **135c** (218 mg, 2.0 mmol), Cs_2CO_3 (2.60 g, 8.0 mmol), CuI (48 mg, 0.25 mmol), dibromoalkene **134c** (923 mg, 3.0 mmol) and DMEDA (40 µL, 0.37 mmol) for 36 hours. Purification by flash column chromatography (20⟶30% EtOAc in hexane) yielded *ynamide* **84u** as a yellow solid (182 mg, 36%); mp: 92-94 °C; IR (neat): ν = 3013, 2930, 2227, 1592, 1510, 1360, 1337, 1161, 1103, 958, 841 cm^{-1}; ^{1}H-NMR (400 MHz, $CDCl_3$): δ = 8.16 (d, *J* = 8.8 Hz, 2H), 7.49 (d, *J* = 8.8 Hz, 2H), 3.35 (s, 3H), 3.15 (s, 3H); ^{13}C-NMR (101 MHz, $CDCl_3$): δ = 146.6 (C), 131.3 (2CH), 129.9 (C), 123.8 (2CH), 88.7 (C), 69.2 (C), 39.3 (CH_3), 37.7 (CH_3); HRMS (ES): *m/z* calculated for $C_{10}H_{10}N_2O_4SNa$: 252.0983, found 252.1000 $(M+Na)^+$.

Ynamide 84n

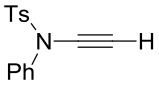

Following a literature procedure[49] a solution of ynamide **84m** (406 mg, 3.0 mmol) in THF (10 mL) was cooled to 0 °C and TBAF (1 M in THF, 3.0 mL, 3.0 mmol) was added. The reaction mixture was allowed to warm to room temperature and stirred for 10 minutes before satd. $NH_4Cl_{(aq)}$ solution (10 mL) was added and the aqueous phase was extracted with EtOAc (3 x 20 mL). The combined organic phases were washed with brine, dried over Na_2SO_4, concentrated under reduced pressure and purified by flash column chromatography (5→10% EtOAc in hexane) to give *ynamide* **84n** as a yellow solid (291 mg, 91%); mp: 77-78 °C (lit.[49] 76-78 °C); IR (neat): ν = 3276, 2166, 2125, 1594, 1489, 1363, 1164, 1097, 1086, 807 cm^{-1}; ^{1}H-NMR (300 MHz, $CDCl_3$): δ = 7.58 (d, *J* = 8.4 Hz, 2H), 7.36-7.23 (m, 7H), 2.84 (s, 1H), 2.44 (s, 3H); ^{13}C-NMR (101 MHz, $CDCl_3$): δ = 145.2 (C), 138.4 (C), 133.0 (C), 129.7 (2CH), 129.3 (2CH), 128.5 (CH), 128.4 (2CH), 126.4 (2CH), 76.7 (C), 59.0 (CH), 21.8 (CH_3). Spectroscopic data matched those reported.[49]

Ynamide 84v

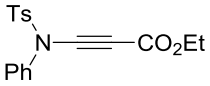

Following a literature procedure[90] a solution of dichloroenamide **266** (239 mg, 0.70 mmol) in THF (6 mL) was prepared under an argon atmosphere and cooled to −78 °C. ^{n}BuLi (2.5 M in hexane, 670 µL, 1.7 mmol) was added and the reaction mixture was stirred for 20 minutes before the addition of ethyl chloroformate (90 µL, 0.94 mmol). Stirring was continued for another 30 minutes at −78 °C and 2 hours at room temperature before the reaction was quenched by addition of satd. $NH_4Cl_{(aq)}$ solution (20 mL) and Et_2O (20 mL). The organic phase was separated, washed with brine (20 mL), dried over Na_2SO_4 and purified by flash column chromatography (9:1 hexane:EtOAc) to give *ynamide* **84v** as a white solid (82 mg, 34%); mp: 118-120 °C (lit.[90] 117-119 °C); IR (neat): ν = 2220, 1703, 1593, 1372, 1343, 1171, 1118, 1086 cm^{-1}; ^{1}H-NMR (300 MHz, $CDCl_3$): δ = 7.64 (d, *J* = 8.4 Hz, 2H), 7.40-7.29 (m, 5H), 7.24-7.16 (m, 2H), 4.23 (q, *J* = 7.1 Hz, 2H), 2.45 (s, 3H), 1.30 (t, *J* = 7.1 Hz, 3H); ^{13}C-NMR (101 MHz, $CDCl_3$): δ = 154.2 (C), 145.9 (C),

137.3 (C), 133.0 (C), 130.0 (2CH), 129.6 (2CH), 129.3 (CH), 128.5 (2CH), 126.8 (2CH), 82.3 (C), 66.6 (C), 61.8 (CH_2), 21.9 (CH_3), 14.3 (CH_3). Spectroscopic data matched those reported.[90]

Ynamide 84w

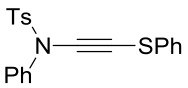

Following a literature procedure[90] a solution of dichloroenamide **266** (513 mg, 1.5 mmol) in THF (12 mL) was prepared under an argon atmosphere and cooled to −78 °C. ^{n}BuLi (2.5 M in hexane, 1.8 mL, 3.6 mmol) was added and the reaction mixture was stirred for 20 minutes before the addition of $PhSO_2SPh$ (413 mg, 1.65 mmol). Stirring was continued for another 30 minutes at −78 °C and 2 hours at room temperature before the reaction was quenched by addition of satd. $NH_4Cl_{(aq)}$ solution (20 mL) and extracted with Et_2O (2 x 10 mL). The combined organic phases were washed with brine, dried over Na_2SO_4 and purified by flash column chromatography (5→7.5% EtOAc in hexane) to give *ynamide* **84w** as a tan solid (234 mg, 41%); mp: 110-111 °C (lit.[90] 113-114 °C); IR (neat): ν = 2927, 2164, 1583, 1345, 1156, 1088 cm^{-1}; ^{1}H-NMR (300 MHz, $CDCl_3$): δ = 7.64 (d, *J* = 8.3 Hz, 2H), 7.39-7.18 (m, 12H), 2.46 (s, 3H); ^{13}C-NMR (101 MHz, $CDCl_3$): δ = 145.3 (C), 139.0 (C), 134.2 (C), 133.4 (C), 129.8 (2CH), 129.3 (2CH), 129.2 (2CH), 128.5 (CH), 128.5 (2CH), 126.6 (CH), 126.4 (2CH), 125.9 (2CH), 93.0 (C), 61.6 (C), 21.9 (CH_3). Spectroscopic data matched those reported.[90]

5.1.6: Synthesis of Oxazoles

5.1.6.1: General procedure for gold-catalysed oxazole synthesis (GP7)

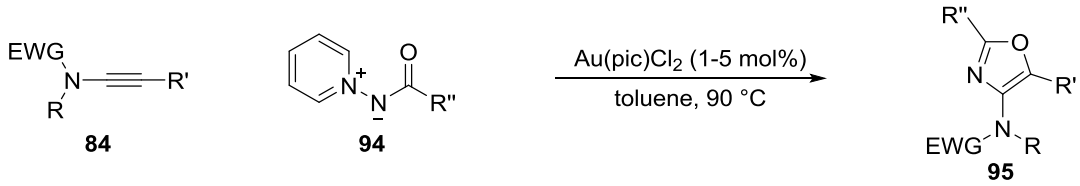

Pyridinium ylide (1.2-1.5 eq.), dichloro(2-pyridinecarboxylato)gold (1-5 mol%), and ynamide (1.0 eq.) were added to a flask under an argon atmosphere. Toluene (0.1 M with respect to ynamide) was added (where ynamides were oils these were added as a solution in toluene) and the reaction mixture was heated at 90 °C for the indicated time. After cooling to room temperature, the reaction mixture was filtered through a 5 cm plug of silica gel (washing with CH_2Cl_2 and then EtOAc) and the filtrate was concentrated under reduced pressure and purified by flash column chromatography.

Oxazole 143a

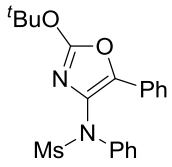

Following **GP7** with ylide **94d** (110 mg, 0.57 mmol), ynamide **84c** (101 mg, 0.37 mmol), and gold catalyst (7.6 mg, 5 mol%) for 1.5 hours. Purification by flash column chromatography (hexane:EtOAc 4:1) yielded *oxazole* **143a** as a white solid (132 mg, 92%); mp: decomp. 160 °C; IR (neat): ν = 2986, 2936, 1644, 1605, 1585, 1492, 1351, 1151 cm^{-1}; ^{1}H-NMR (300 MHz, $CDCl_3$): δ = 7.82-7.77 (m, 2H), 7.70-7.63 (m, 2H), 7.41-7.33 (m, 4H), 7.32-7.22 (m, 2H), 3.22 (s, 3H), 1.68 (s, 9H); ^{13}C-NMR (101 MHz, $CDCl_3$): δ = 156.9 (C), 140.9 (C), 140.3 (2C), 131.1 (C), 129.5 (2CH), 128.7 (2CH), 128.3 (CH), 127.9 (CH), 126.9 (2CH), 124.7 (2CH), 85.9 (C), 38.5 (CH_3), 28.0 ($3CH_3$); HRMS (ES): *m/z* calculated for $C_{20}H_{22}N_2O_4SNa$: 409.1198, found 409.1214 $(M+Na)^+$. *Degradation of this compound to a complex mixture was visible by NMR spectroscopy within 24 hours.*

Oxazole 151a

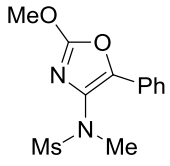

Following **GP7** with ylide **94b** (91.0 mg, 0.60 mmol), ynamide **84g** (105 mg, 0.50 mmol), and gold catalyst (4.1 mg, 2 mol%) for 1 hour. Purification by flash column chromatography (30→50% EtOAc in hexane) yielded *oxazole* **151a** as a white solid (127 mg, 90%); mp: 122-124 °C; IR (neat): ν = 3010, 2934, 1638, 1608, 1593, 1451, 1373, 1337, 1148, 1044, 967 cm^{-1}; ^{1}H-NMR (300 MHz, $CDCl_3$): δ = 7.84-7.77 (m, 2H), 7.44-7.35 (m, 2H), 7.30 (tt, *J* = 7.4, 1.3 Hz, 1H), 4.09 (s, 3H), 3.24 (s, 3H), 3.14 (s, 3H); ^{13}C-NMR (101 MHz, $CDCl_3$): δ = 159.5 (C), 141.3 (C), 132.0 (C), 128.9 (2CH), 128.4 (CH), 126.9 (C), 124.7 (2CH), 58.3 (CH_3), 37.8 (CH_3), 37.3 (CH_3); HRMS (ES): calculated for $C_{12}H_{15}N_2O_4S$: 283.0753, found 283.0760 $(M+H)^+$.

Oxazole 151b

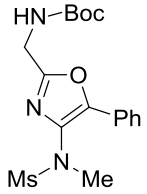

Following **GP7** with ylide **94e** (453 mg, 1.8 mmol), ynamide **84g** (314 mg, 1.5 mmol) and gold catalyst (11.6 mg, 2 mol%) for 1 hour. Purification by flash column chromatography (30→50% EtOAc in hexane) yielded *oxazole* **151b** as a white solid (553 mg, 97%); mp: 140-141 °C; IR (neat): ν = 3316, 2974, 1710, 1681, 1585, 1540, 1448, 1360, 1345, 1273, 1226, 1152, 1070, 969 cm^{-1}; ^{1}H-NMR (300 MHz, $CDCl_3$): δ = 7.89 (d, *J* = 7.3 Hz, 2H), 7.50-7.29 (m, 3H), 5.10 (br s, NH), 4.47 (d, *J* = 5.1 Hz, 2H), 3.25 (s, 3H), 3.12 (s, 3H), 1.48 (s, 9H); ^{13}C-NMR (101 MHz, $CDCl_3$): δ = 158.3 (C), 155.6 (C), 146.1 (C), 133.4 (C), 129.3 (CH), 129.0 (2CH), 126.7 (C), 125.4 (2CH), 80.5 (C), 38.5 (CH_2), 38.0 (CH_3), 37.1 (CH_3), 28.5 ($3CH_3$); HRMS (ES): *m/z* calculated for $C_{17}H_{23}N_3O_5SNa$: 404.1256, found 404.1247 $(M+Na)^+$.

Oxazole 151c

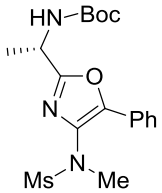

Following **GP7** with ylide **94f** (398 mg, 1.5 mmol), ynamide **84g** (209 mg, 1.0 mmol), and gold catalyst (7.8 mg, 2 mol%) for 3 hours. Purification by flash column chromatography (30→40% EtOAc in hexane) yielded *oxazole* **151c** as a white solid (314 mg, 79%); mp: 162-164 °C; $[\alpha]_D^{20}$ = −47.4 (c=1.0, $CHCl_3$); IR (neat): ν = 2978, 2933, 1700, 1518, 1345, 1247, 1153, 1069, 770 cm^{-1}; ^{1}H-NMR (300 MHz, $CDCl_3$): 7.93-7.84 (m, 2H), 7.47-7.39 (m, 2H),

7.38-7.32 (m, 1H), 5.10-4.87 (m, 2H), 3.25 (s, 3H), 3.12 (s, 3H), 1.57 (d, *J* = 6.7 Hz, 3H), 1.47 (s, 9H); ^{13}C-NMR (101 MHz, $CDCl_3$): δ = 161.9 (C), 155.0 (C), 145.8 (C), 133.2 (C), 129.2 (CH), 128.9 (2CH), 126.7 (C), 125.4 (2CH), 80.3 (C), 45.2 (CH), 38.0 (CH_3), 37.1 (CH_3), 28.5 ($3CH_3$), 20.1 (CH_3); HRMS (ES): *m/z* calculated for $C_{18}H_{25}N_3NaO_5S$: 418.1413, found 418.1399 $(M+Na)^+$; e.r. = 97:3 (HPLC trace and conditions given on page 209).

Oxazole 151d

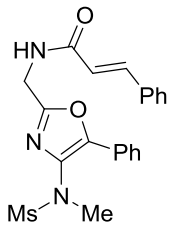

Following **GP7** with ylide **94g** (331 mg, 1.2 mmol), ynamide **84g** (163 mg, 0.77 mmol) and gold catalyst (15.2 mg, 5 mol%) for 18 hours. Purification by flash column chromatography (1:1⟶2:1 EtOAc:hexane) yielded *oxazole* **151d** as a pale pink solid (269 mg, 85%); mp: 160-163 °C; IR (neat): ν = 3374, 2990, 1669, 1624, 1517, 1494, 1450, 1359, 1335, 1211, 1148, 1065, 978 cm^{-1}; ^{1}H-NMR (400 MHz, $CDCl_3$): δ = 7.89-7.85 (m, 2H), 7.71 (d, *J* = 15.6 Hz, 1H), 7.55-7.49 (m, 2H), 7.44-7.31 (m, 6H), 6.50 (d, *J* = 15.6 Hz, 1H), 6.39 (br t, *J* = 5.4 Hz, NH), 4.70 (d, *J* = 5.4 Hz, 2H), 3.24 (s, 3H), 3.12 (s, 3H); ^{13}C-NMR (101 MHz, $CDCl_3$): δ = 166.0 (C), 157.8 (C), 146.3 (C), 142.5 (CH), 134.6 (C), 133.3 (C), 130.2 (CH), 129.4 (CH), 129.02 (2CH), 128.92 (2CH), 128.1 (2CH), 126.5 (C), 125.4 (2CH), 119.7 (CH), 37.9 (CH_3), 37.32 (CH_2), 37.28 (CH_3); HRMS (ES): *m/z* calculated for $C_{21}H_{21}N_3O_4SNa$: 434.1150, found 434.1130 $(M+Na)^+$.

Oxazole 151f

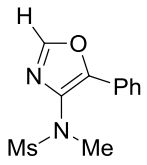

Following **GP7** with ylide **94i** (36.5 mg, 0.30 mmol), ynamide **84g** (41.8 mg, 0.20 mmol), and gold catalyst (3.9 mg, 5 mol%) for 2 hours. Purification by flash column chromatography (7:13 EtOAc/hexane) yielded *oxazole* **151f** as a white solid (45.6 mg, 90%); mp: 155-157 °C; IR (neat): ν = 3676, 3151, 2989, 2902, 1626, 1599, 1449, 1361, 1342, 1321, 1239, 1148, 1061, 978, 849 cm^{-1}; ^{1}H-NMR (300 MHz, $CDCl_3$): δ = 8.00-7.90 (m, 2H), 7.82 (s, 1H), 7.50-7.34 (m, 3H), 3.28 (s, 3H), 3.14 (s, 3H); ^{13}C-NMR (101 MHz, $CDCl_3$): δ = 148.2 (CH), 146.0 (C), 133.3 (C), 129.5 (CH), 129.0 (2CH), 126.6 (C), 125.6 (2CH), 38.0 (CH_3), 36.9 (CH_3); HRMS (ES): *m/z* calculated for $C_{11}H_{12}N_2O_3SNa$: 275.0466, found 275.0463 $(M+Na)^+$.

Oxazole 151g

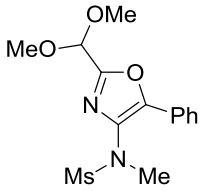

Note: To avoid degradation, room temperature water baths should be used when evaporating solvent from this compound.

1.0 mmol scale: Following **GP7** with ylide **94j** (295 mg, 1.5 mmol), ynamide **84g** (209 mg, 1.0 mmol) and gold catalyst (8.2 mg, 2 mol%) for 2.5 hours. Purification by flash column chromatography (80:20:1→50:50:1 hexane:EtOAc:NEt_3) yielded *oxazole* **151g** as a white solid (296 mg, 91%); mp: 108-110 °C; IR (neat): ν = 3016, 2956, 2909, 2833, 1451, 1358, 1337, 1324, 1152, 1116, 1059, 961, 841, 763 cm^{-1}; ^{1}H-NMR (300 MHz, $CDCl_3$): δ = 7.98-7.93 (m, 2H), 7.48-7.41 (m, 2H), 7.41-7.34 (m, 1H), 5.50 (s, 1H), 3.49 (s, 6H), 3.29 (s, 3H), 3.14 (s, 3H); ^{13}C-NMR (101 MHz, $CDCl_3$): δ = 156.4 (C), 146.5 (C), 133.2 (C), 129.5 (CH), 128.9 (2CH), 126.5 (C), 125.7 (2CH), 97.0 (CH), 53.9 ($2CH_3$), 38.0 (CH_3), 37.2 (CH_3); HRMS (ES): *m/z* calculated for $C_{14}H_{18}N_2O_5SNa$: 349.0834, found 349.0840 $(M+Na)^+$.

4.8 mmol scale: Following **GP7** with ylide **94j** (1.03 g, 5.25 mmol), ynamide **84g** (1.00 g, 4.8 mmol), gold catalyst (37 mg, 2 mol%) for 4 hours. After filtration and evaporation of the solvent under reduced pressure the crude residue was recrystallised by precipitation from CH_2Cl_2 with hexane to give *oxazole* **151g** as a tan solid (790 mg, 51%); the filtrate was concentrated under reduced pressure and purified by flash column chromatography (70:30:1 hexane:EtOAc:NEt_3) yielding additional *oxazole* **151g** as a white solid (416 mg, 26% – combined to give a 77% overall yield for the process).

Oxazole 151h

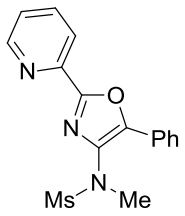

Following **GP7** with ylide **94k** (345 mg, 1.7 mmol), ynamide **84g** (242 mg, 1.2 mmol) and gold catalyst (4.6 mg, 1 mol%) for 16 hours. Purification by flash column chromatography (EtOAc:hexane 2:1→3:1) yielded *oxazole* **151h** as a white powder (284 mg, 75%); mp: 164-166 °C; IR (neat): ν = 3028, 2939, 1588, 1549, 1428, 1371, 1338, 1150, 1066, 952, 856 cm^{-1}; ^{1}H-NMR (300 MHz, $CDCl_3$): δ = 8.80 (ddd, *J* = 4.8, 1.7, 0.9 Hz, 1H), 8.16-8.03 (m, 3H), 7.87 (appt. td, *J* = 7.8, 1.7 Hz, 1H), 7.52-7.35 (m, 4H), 3.36 (s, 3H), 3.21 (s, 3H); ^{13}C-NMR (101 MHz, $CDCl_3$): δ = 157.0 (C), 150.4 (CH), 146.9 (C), 145.5 (C), 137.3 (CH), 135.1 (C), 129.6 (CH), 129.0 (2CH), 126.6 (C), 125.8 (2CH), 125.1 (CH), 122.3 (CH), 38.1 (CH_3), 37.2 (CH_3); HRMS (ES): *m/z* calculated for $C_{16}H_{15}N_3O_3SNa$: 352.0732, found 352.0733 $(M+Na)^+$.

Oxazole 151i

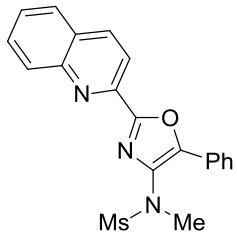

Following **GP7** with ylide **94l** (73.7 mg, 0.30 mmol), ynamide **84g** (42.3 mg, 0.20 mmol) and gold catalyst (3.9 mg, 5 mol%) for 1 hour. Purification by flash column chromatography (30→50% EtOAc in hexane) yielded *oxazole* **151i** as a white solid (67.9 mg, 89%); mp: 225-227 °C; IR (neat): ν = 3012, 2931, 1615, 1596, 1497, 1449, 1338, 1162, 1146, 969, 839, 760 cm^{-1}; ^{1}H-NMR (300 MHz, $CDCl_3$): δ = 8.33-8.26 (m, 2H), 8.20 (d, *J* = 8.6 Hz, 1H), 8.17-8.11 (m, 2H), 7.86 (d, *J* = 8.1 Hz, 1H), 7.83-7.75 (m, 1H), 7.66-7.57 (m, 1H), 7.54-7.46 (m, 2H), 7.44-7.37 (m, 1H), 3.38 (s, 3H), 3.26 (s, 3H); ^{13}C-NMR (101 MHz, $CDCl_3$): δ = 157.3 (C), 148.2 (C), 147.3 (C), 145.3 (C), 137.3 (CH), 135.3 (C), 130.5 (CH), 130.3 (CH), 129.7 (CH), 129.0 (2CH), 128.4 (C), 128.0 (CH), 127.8 (CH), 126.6 (C), 126.0 (2CH), 119.4 (CH), 38.1 (CH_3), 37.4 (CH_3); HRMS (ES): *m/z* calculated for $C_{20}H_{17}N_3O_3SNa$: 402.0888, found 402.0885 $(M+Na)^+$.

Oxazole 151j

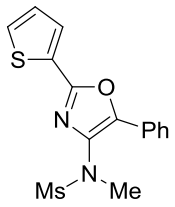

Following **GP7** with ylide **94m** (123 mg, 0.60 mmol), ynamide **84g** (105 mg, 0.50 mmol), and gold catalyst (3.9 mg, 2 mol%) for 1 hour. Purification by flash column chromatography (CH_2Cl_2) yielded *oxazole* **151j** as a white solid (162 mg, 97%); mp: 154-156 °C; IR (neat): ν = 1613, 1572, 1335, 1151, 955, 851 cm^{-1}; ^{1}H-NMR (300 MHz, $CDCl_3$): δ = 8.02-7.96 (m, 2H), 7.74 (dd, *J* = 3.7, 1.1 Hz, 1H), 7.50-7.42 (m, 3H), 7.41-7.34 (m, 1H), 7.15 (dd, *J* = 5.0, 3.7 Hz, 1H), 3.32 (s, 3H), 3.20 (s, 3H); ^{13}C-NMR (101 MHz, $CDCl_3$): δ = 154.9 (C), 145.0 (C), 134.6 (C), 129.6 (C), 129.2 (CH), 129.1 (CH), 129.0 (2CH), 128.4 (CH), 128.2 (CH), 126.8 (C), 125.4 (2CH), 38.1 (CH_3), 37.1 (CH_3); HRMS (ES): calculated for $C_{15}H_{14}N_2O_3S_2Na$: 357.0344, found 357.0341 $(M+Na)^+$.

Oxazole 151k

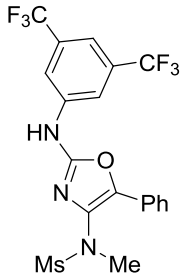

Following **GP7** with ylide **94o** (105 mg, 0.30 mmol), ynamide **84g** (43.1 mg, 0.20 mmol) and gold catalyst (4.0 mg, 5 mol%) for 1 hour. Purification by flash column chromatography (4:1 hexane/EtOAc) yielded *oxazole* **151k** as a white solid (44.7 mg, 45%); mp: 229-231 °C; IR (neat): ν = 3302, 1648, 1610, 1595, 1478, 1382, 1334, 1273, 1150, 1125, 950, 876, 865 cm^{-1}; ^{1}H-NMR (300 MHz, d_6-acetone): δ = 10.16 (s, NH), 8.39 (s, 2H), 7.87-7.79 (m, 2H), 7.66 (s, 1H), 7.50-7.41 (m, 2H), 7.38-7.29 (m, 1H), 3.31 (s, 3H), 3.27 (s, 3H); ^{13}C-NMR (101 MHz, d_6-acetone): δ = 153.9 (C), 141.7 (C), 140.0 (C), 134.4 (C), 132.9 (q, $J_{C\text{-}F}$ = 33.1 Hz, 2C), 129.6 (2CH), 129.0 (CH), 128.0 (C), 125.2 (2CH), 124.5 (q, $J_{C\text{-}F}$ = 272.1 Hz, $2CF_3$), 117.9-117.5 (m, 2CH), 115.7-115.3 (m, CH), 38.1 (CH_3), 36.9 (CH_3); ^{19}F{^{1}H}-NMR (282 MHz, d_6-acetone): δ = -63.7; HRMS (ES): *m/z* calculated for $C_{19}H_{16}N_3O_3F_6S$: 480.0817, found 480.0807 $(M+H)^+$.

Oxazole 151l

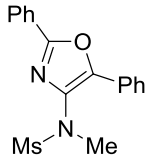

Ynamide 84g (1.00 g, 4.8 mmol), ylide **94c** (1.04 g, 5.3 mmol), gold catalyst (18.3 mg, 1 mol%) and unpurified toluene (48 mL) were added to an open flask, a reflux condenser was fitted and the reaction mixture was heated at 90 °C for 48 hours. After cooling to room temperature, the reaction mixture was filtered through a 5 cm pad of silica gel (eluting with CH_2Cl_2) and purified by flash column chromatography (CH_2Cl_2) to yield recovered *ynamide* **84g** (299 mg, 30%) and *oxazole* **151l** (923 mg, 59%); mp: 184-186 °C; IR (neat): ν = 3063, 3021, 2974, 2936, 1617, 1557, 1494, 1447, 1364, 1338, 1327, 1237, 1145, 1065, 965, 847, 765; ^{1}H-NMR (300 MHz, $CDCl_3$): δ = 8.11-7.99 (m, 4H), 7.53-7.43 (m, 5H), 7.41-7.34 (m, 1H), 3.33 (s, 3H), 3.22 (s, 3H); ^{13}C-NMR (101 MHz, $CDCl_3$): δ = 158.6 (C), 145.6 (C), 134.9 (C), 131.0 (CH), 129.2 (CH), 129.0 (4CH), 127.1 (C), 127.0 (C), 126.5 (2CH), 125.5 (2CH), 38.1 (CH_3), 37.1 (CH_3); HRMS (ES) m/z: calc. for $C_{17}H_{17}N_2O_3S$: 329.0960, found 329.0955 $(M+H)^+$.

Oxazole 154a

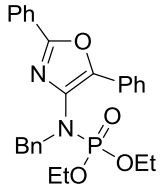

Following **GP7** using ylide **94c** (58.4 mg, 0.29 mmol), gold catalyst (3.6 mg, 5 mol%) and a solution of ynamide **84i** (70.1 mg, 0.20 mmol) in toluene (2 mL) for 5 hours. Purification by flash column chromatography (25→50% EtOAc in hexane) yielded *oxazole* **154a** as a colourless oil (75.3 mg, 81%); IR (neat): ν = 3063, 2982, 2930, 1616, 1598, 1491, 1448, 1386, 1254, 1049, 1019, 958, 774 cm^{-1}; ^{1}H-NMR (400 MHz, $CDCl_3$): δ = 8.08-8.02 (m, 2H), 7.61-7.56 (m, 2H), 7.48-7.42 (m, 3H), 7.32-7.22 (m, 5H), 7.18-7.14 (m, 3H), 4.69 (d, *J* = 7.3 Hz, 2H), 4.13 (appt. quin, *J* = 7.1 Hz, 4H), 1.24 (td, *J* = 7.1, 0.9 Hz, 6H); ^{13}C-NMR (101 MHz, $CDCl_3$): δ = 158.0 (C), 144.5 (d, $J_{C\text{-}P}$ = 6.2 Hz, C), 137.3 (d, $J_{C\text{-}P}$ = 4.2 Hz, C), 135.35 (C), 135.32 (C), 130.4 (CH), 129.3 (2CH), 128.8 (2CH), 128.3 (5CH), 127.7 (CH), 127.6 (C), 126.3 (2CH), 125.7 (2CH), 63.2 (d, $J_{C\text{-}P}$ = 5.4 Hz, $2CH_2$), 53.5 (d, $J_{C\text{-}P}$ = 5.1 Hz, CH_2), 16.1 (d, $J_{C\text{-}P}$ = 7.3 Hz, $2CH_3$); ^{31}P{^{1}H}-NMR (121 MHz, $CDCl_3$): δ = 5.76; HRMS (ES): *m/z* calculated for $C_{26}H_{28}N_2O_4P$: 463.1787, found 463.1798 $(M+H)^+$.

Oxazole 154b

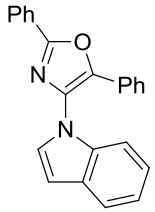

Following **GP7** using ylide **94c** (60.0 mg, 0.30 mmol), ynamide **84k** (42.8 mg, 0.20 mmol) and gold catalyst (4.1 mg, 5 mol%) for 4 days. Purification by flash column chromatography (0→10% ethyl acetate in hexane) gave recovered *ynamide* **84k** (11.9 mg, 28%) and *oxazole* **154b** as a white solid (42.8 mg, 64%); mp: 120-121 °C; IR (neat): ν = 3141, 3061, 1741, 1709, 1624, 1454, 1309, 1211, 1184, 933 cm^{-1}; ^{1}H-NMR (300 MHz, $CDCl_3$): δ = 8.13-8.04 (m, 2H), 7.67-7.57 (m, 1H), 7.48-7.38 (m, 3H), 7.32-7.26 (m, 2H), 7.25-7.17 (m, 5H), 7.14-7.06 (m, 2H), 6.68 (d, *J* = 3.3 Hz, 1H); ^{13}C-NMR (101 MHz, $CDCl_3$): δ = 159.0 (C), 142.0 (C), 136.2 (C), 133.5 (C), 131.0 (CH), 129.2 (C), 129.04 (2CH), 128.98 (2CH), 128.8 (CH), 127.6 (CH), 127.1 (C), 127.0 (C), 126.6 (2CH), 125.1 (2CH), 122.9 (CH), 121.1 (CH), 121.0 (CH), 111.6 (CH), 105.1 (CH); HRMS (ES): *m/z* calculated for $C_{23}H_{17}N_2O$: 337.1341, found 337.1340 $(M+H)^+$.

Oxazolone 155

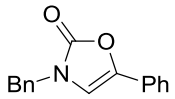

Following **GP7** using ylide **94c** (116 mg, 0.59 mmol), gold catalyst (8.1 mg, 5 mol%) and a solution of ynamide **84h** (106 mg, 0.40 mmol) in toluene (4 mL) for 24 hours. Purification by flash column chromatography (10→50% EtOAc in petroleum ether) yielded recovered *ynamide* **X** as a yellow oil (70.8 mg, 67%) and *oxazolone* **155** as a white solid (14.3 mg, 14%); mp: 150-152 °C; IR (neat): ν = 3131, 3036, 1734, 1647, 1497, 1452, 1439, 1400, 1362, 1281, 1184, 1097, 1023, 965, 731 cm^{-1}; ^{1}H-NMR (400 MHz, $CDCl_3$): δ = 7.46-7.31 (m, 9H), 7.26 (tt, *J* = 7.3, 1.3 Hz, 1H), 6.64 (s, 1H), 4.80 (s, 2H); ^{13}C-NMR (101 MHz, $CDCl_3$): δ = 155.2 (C), 139.5 (C), 135.4 (C), 129.2 (2CH), 128.9 (2CH), 128.6 (CH), 128.3 (CH), 128.2 (2CH), 127.4 (C), 123.1 (2CH), 109.0 (CH), 48.0 (CH_2); HRMS (ES): *m/z* calculated for $C_{16}H_{14}NO_2$: 252.1025, found 252.1024 $(M+H)^+$.

Ketone 156

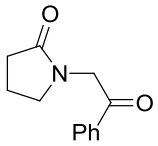

Following **GP7** using ylide **94c** (60.1 mg, 0.30 mmol), gold catalyst (4.1 mg, 5 mol%) and a solution of ynamide **84j** (36.9 mg, 0.20 mmol) in toluene (2 mL) for 24 hours. Purification by flash column chromatography (30→100% EtOAc in hexane) yielded recovered *ynamide* **84j** as an orange oil (21.7 mg, 59%) and *ketone* **156** as an orange oil (6.4 mg, 16%); IR (neat): ν = 2922, 1677, 1449, 1290, 1226, 987, 758 cm^{-1}; ^{1}H-NMR (400 MHz, $CDCl_3$): δ = 7.99-7.93 (m, 2H), 7.60 (tt, *J* = 7.4, 1.6 Hz, 1H), 7.51-7.45 (m, 2H), 4.74 (s, 2H), 3.50 (t, *J* = 7.1 Hz, 2H), 2.48 (t, *J* = 8.1 Hz, 2H), 2.17-2.06 (m, 2H); ^{13}C-NMR (101 MHz, $CDCl_3$): δ = 194.0 (C), 175.9 (C), 135.1 (C), 133.9 (CH), 129.0 (2CH), 128.2 (2CH), 49.2 (CH_2), 48.0 (CH_2), 30.5 (CH_2), 18.2 (CH_2). Spectroscopic data matched those reported.[210]

Oxazole 167

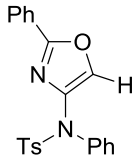

Following **GP7** using ylide **94c** (59.6 mg, 0.30 mmol), ynamide **84n** (53.9 mg, 0.20 mmol) and gold catalyst (3.9 mg, 5 mol%) for 1 hour. Purification by flash column chromatography (toluene) yielded *oxazole* **167** as a white solid (54.4 mg, 70%); mp: 122-124 °C; IR (neat): ν = 2926, 2865, 1583, 1344, 1232, 1160, 1089 cm^{-1}; ^{1}H-NMR (400 MHz, $CDCl_3$): δ = 7.91-7.82 (m, 2H), 7.73 (s, 1H), 7.59 (d, *J* = 8.2 Hz, 2H), 7.38-7.30 (m, 5H), 7.28-7.21 (m, 3H), 7.19 (d, *J* = 8.2 Hz, 2H), 2.35 (s, 3H); ^{13}C-NMR (101 MHz, $CDCl_3$): δ = 160.1 (C), 144.1 (C), 140.4 (C), 139.6 (C), 135.9 (C), 133.5 (CH), 130.7 (CH), 129.4 (2CH), 129.1 (2CH), 128.8 (4CH), 128.6 (2CH), 128.2 (CH), 127.3 (C), 126.5 (2CH), 21.7 (CH_3); HRMS (ES): *m/z* calculated for $C_{22}H_{19}N_2O_3S$: 391.1116, found 391.1111 $(M+H)^+$.

Oxazole 170

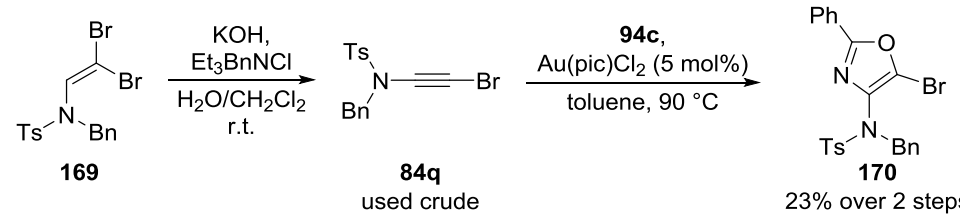

169 **84q** used crude **170** 23% over 2 steps

KOH (85%, 1.21 g, 18.3 mmol) was dissolved in H_2O (1 mL) and left to cool to room temperature before adding to a solution of dibromoenamide **169** (174 mg, 0.39 mmol) and $BnNEt_3Cl$ (75 mg, 0.33 mmol) in CH_2Cl_2 (1.5 mL). The biphasic mixture was stirred for 6 hours after which H_2O (10 mL) and CH_2Cl_2 (10 mL) were added. The phases were separated and the aqueous phase was extracted with CH_2Cl_2 (2 x 10 mL). The combined organic extracts were dried over Na_2SO_4, filtered through a 5 cm pad of silica gel (eluting with CH_2Cl_2) and the filtrate was concentrated under reduced pressure to give crude ynamide **84q** as a colourless oil. A magnetic stirrer bar, ylide **94c** (116 mg, 0.58 mmol) and gold catalyst (7.8 mg, 5 mol%) were added to the flask containing crude ynamide **84q**. This was then evacuated and back-filled with argon. Toluene (4 mL) was added and the reaction mixture was heated at 90 °C for 16 hours. After cooling to room temperature, the reaction mixture was filtered through a 5 cm plug of NEt_3 deactivated silica gel (washing with CH_2Cl_2 and then EtOAc) and the filtrate concentrated under reduced pressure and purified by flash column chromatography (95:5:1→90:10:1 hexane:EtOAc:NEt_3) yielded *oxazole* **170** as a white solid (43.7 mg, 23% over two steps); mp: 140-141 °C; IR (neat): ν = 3064, 3026, 2921, 1595, 1557, 1488, 1449, 1353, 1167, 1121, 1090, 1064, 814 cm^{-1}; ^{1}H-NMR (400 MHz, $CDCl_3$): δ = 7.87 (dd, *J* = 7.8, 1.6 Hz, 2H), 7.81 (d, *J* = 8.3 Hz, 2H), 7.49-7.41 (m, 3H), 7.36 (d, *J* = 8.3 Hz, 2H), 7.33-7.29 (m, 2H), 7.29-7.22 (m, 3H), 4.60 (s, 2H), 2.49 (s, 3H); ^{13}C-NMR (101 MHz, $CDCl_3$): δ = 161.0 (C), 144.2 (C), 136.7 (C), 135.7 (C), 135.1 (C), 131.1 (CH), 129.8 (2CH), 128.94 (2CH), 128.87 (2CH), 128.5 (4CH), 128.1 (CH), 126.6 (C), 126.2 (2CH), 122.3 (C), 53.3 (CH_2), 21.8 (CH_3); HRMS (ES): *m/z* calculated for $C_{23}H_{20}N_2O_3S^{79}Br$: 483.0378, found 483.0366 $(M+H)^+$.

Compounds 172a and 173a

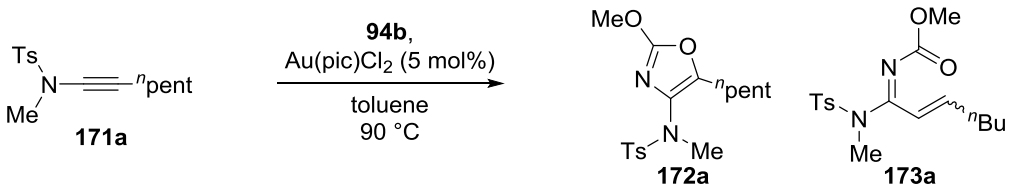

83% (64:33:3 oxazole:*E* alkene:*Z* alkene)
inseperable mixture

Following **GP7** using ylide **94b** (91 mg, 0.60 mmol), gold catalyst (7.7 mg, 5 mol%) and a solution of ynamide **171a** (111 mg, 0.40 mmol) in toluene (4 mL) for 6 hours. Purification by flash column chromatography (5⟶30% EtOAc in hexane) gave a colourless oil containing a mixture of products in the ratio 64:33:3 *oxazole:E alkene:Z alkene* (117 mg, 83%); ratio determined by ^{1}H-NMR using the characteristic alkene signals and the CH_2 signal α to C5 of the oxazole. HRMS (ES): *m/z* calculated for $C_{17}H_{25}N_2O_4S$: 353.1535, found 353.1531 $(M+H)^+$.

Compounds 172b and 173b

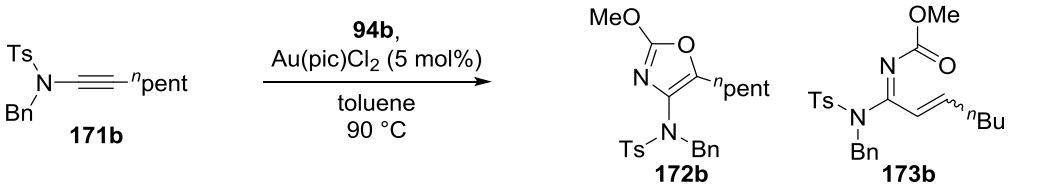

77% (85:15:trace oxazole:*E* alkene:*Z* alkene)
inseperable mixture

Following **GP7** with ylide **94b** (91 mg, 0.60 mmol), ynamide **171b** (142 mg, 0.40 mmol) and gold catalyst (7.9 mg, 5 mol%) for 2 hours. Purification by flash column chromatography (5⟶30% EtOAc in hexane) gave a colourless oil containing a mixture of products in the ratio 85:15:trace *oxazole:E alkene:Z alkene* (132 mg, 77%); ratio determined by ^{1}H-NMR using the characteristic alkene signals and the CH_2 signal α to C5 of the oxazole. HRMS (ES): *m/z* calculated for $C_{23}H_{29}N_2O_4S$: 429.1848, found 429.1845 $(M+H)^+$.

Compounds 172c and 173c

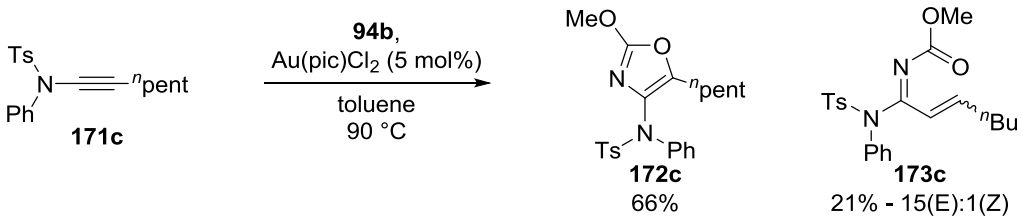

Following **GP7** with ylide **94b** (91 mg, 0.60 mmol), ynamide **171c** (128 mg, 0.38 mmol) and gold catalyst (7.8 mg, 5 mol%) for 2 hours. Purification by flash column chromatography (5⟶30% EtOAc in hexane) gave *oxazole* **172c** as a colourless oil (102 mg, 66%) and a mixture of alkenes **173c** in a 15:1 *E*:*Z* ratio as a pale yellow solid (32 mg, 21%).

Oxazole **172c**: IR (neat): ν = 2954, 2930, 2862, 1609, 1488, 1166, 1092, 813 cm^{-1}; ^{1}H-NMR (300 MHz, $CDCl_3$): δ = 7.67-7.61 (m, 2H), 7.38-7.32 (m, 2H), 7.29-7.22 (m, 4H), 7.21-7.18 (m, 1H), 3.97 (s, 3H), 2.62 (t, *J* = 7.6 Hz, 2H), 2.41 (s, 3H), 1.62-1.50 (m, 2H), 1.31-1.17 (m, 4H), 0.82 (t, *J* = 6.9 Hz, 3H); ^{13}C-NMR (101 MHz, $CDCl_3$): δ = 159.0 (C), 145.5 (C), 143.7 (C), 140.5 (C), 136.0 (C), 131.7 (C), 129.1 (2CH), 129.0 (2CH), 128.8 (2CH), 127.7 (2CH), 127.5 (CH), 57.9 (CH_3), 31.3 (CH_2), 27.1 (CH_2), 24.1 (CH_2), 22.3 (CH_2), 21.7 (CH_3), 14.0 (CH_3); HRMS (ES): *m/z* calculated for $C_{22}H_{26}N_2O_4SNa$: 437.1511, found 437.1502 $(M+Na)^+$.

Alkenes **173c**: mp: 66-68 °C; ν = 2956, 2931, 2869, 1718, 1648, 1593, 1490, 1436, 1364, 1210, 1167, 1064 cm^{-1}; ^{1}H-NMR (400 MHz, $CDCl_3$) *only peaks for the major (E) isomer are listed*: δ = 7.72-7.66 (m, 2H), 7.40-7.33 (m, 3H), 7.29-7.18 (m, 4H), 6.31 (dt, *J* = 15.8, 7.2 Hz, 1H), 5.59 (dt, *J* = 15.8, 1.2 Hz, 1H), 3.74 (s, 3H), 2.42 (s, 3H), 1.93 (appt. qd, *J* = 7.2, 1.2 Hz, 2H), 1.20-1.11 (m, 2H), 1.08-0.98 (m, 2H), 0.74 (t, *J* = 7.2 Hz, 3H); ^{13}C-NMR (101 MHz, $CDCl_3$) *only peaks for the major (E) isomer are listed*: δ = 161.1 (C), 156.6 (C), 147.0 (CH), 144.6 (C), 137.7 (C), 135.5 (C), 130.3 (2CH), 129.6 (2CH), 129.3 (2CH), 129.2 (3CH), 121.9 (CH), 53.5 (CH_3), 32.4 (CH_2), 30.1 (CH_2), 21.82 (CH_3), 21.77 (CH_2), 13.8 (CH_3); HRMS (ES): *m/z* calculated for $C_{22}H_{27}N_2O_4S$: 415.1692, found 415.1685 $(M+H)^+$.

Compounds 172d and 174d

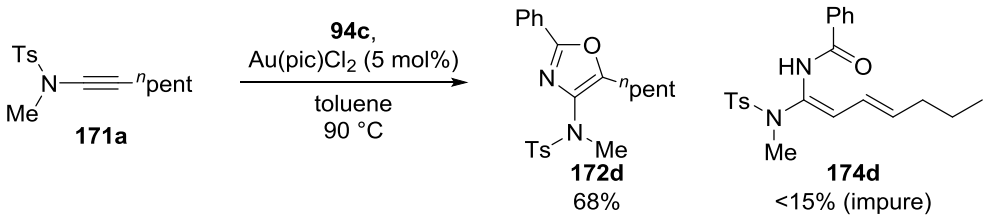

Following **GP7** using ylide **94c** (119 mg, 0.60 mmol), gold catalyst (7.7 mg, 5 mol%) and a solution of ynamide **171a** (108 mg, 0.39 mmol) in toluene (4 mL) 2 hours. Purification by flash column chromatography (5⟶20% EtOAc in hexane) gave *oxazole* **172d** as a white solid (102 mg, 66%) and a complex mixture containing **174d** as the major component as a yellow oil (22.9 mg, <15%).

Oxazole **172d**: mp: 80-82 °C, IR (neat): ν = 2950, 2930, 2868, 1639, 1597, 1559, 1449, 1341, 1152, 1087, 1042, 867, 806, 781 cm^{-1}; ^{1}H-NMR (300 MHz, $CDCl_3$): δ = 7.91-7.83 (m, 2H), 7.72-7.65 (m, 2H), 7.46-7.39 (m, 3H), 7.30 (d, *J* = 8.1 Hz, 2H), 3.11 (s, 3H), 2.84 (t, *J* = 7.7 Hz, 2H), 2.44 (s, 3H), 1.84-1.70 (m, 2H), 1.49-1.34 (m, 4H), 0.93 (t, *J* = 7.0 Hz, 3H); ^{13}C-NMR (101 MHz, $CDCl_3$): δ = 158.0 (C), 149.5 (C), 143.8 (C), 135.0 (C), 134.6 (C), 130.2 (CH), 129.5 (2CH), 128.8 (2CH), 128.5 (2CH), 127.7 (C), 126.0 (2CH), 37.4 (CH_3), 31.6 (CH_2), 27.3 (CH_2), 24.7 (CH_2), 22.4 (CH_2), 21.7 (CH_3), 14.1 (CH_3); HRMS (ES): *m/z* calculated for $C_{22}H_{27}N_2O_3S$: 399.11742, found 399.1751 $(M+H)^+$.

Alkene **174d**: ^{1}H-NMR (400 MHz, $CDCl_3$) *only peaks assigned to **174d** are reported*: δ = 7.78-7.74 (m, 2H), 7.66-7.62 (m, 2H), 7.43-7.36 (m, 3H), 7.23 (d, *J* = 8.0 Hz, 2H), 5.94 (ddt, *J* = 15.2, 10.8, 1.3 Hz, 1H), 5.62 (dt, *J* = 15.2, 7.0 Hz, 1H), 5.48 (d, *J* = 10.8 Hz, 1H), 2.99 (s, 3H), 2.36 (s, 3H), 1.98 (appt. q, *J* = 7.0 Hz, 2H), 1.36-1.26 (m, 2H), 0.80 (t, *J* = 7.4 Hz, 3H).

Compounds 172e and 174e

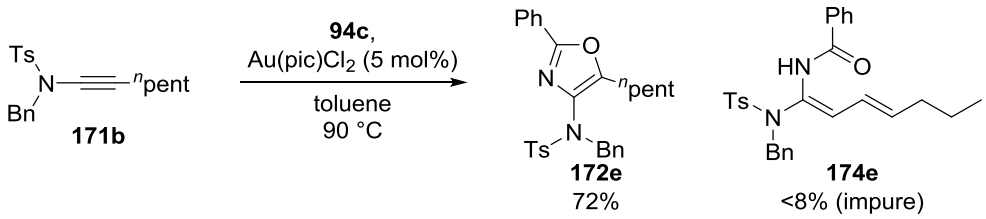

Following **GP7** with ylide **94c** (118 mg, 0.60 mmol), ynamide **171b** (143 mg, 0.40 mmol) and gold catalyst (8.0 mg, 5 mol%) for 5 hours. Purification by flash column chromatography (5→40% EtOAc in hexane) gave *oxazole* **172e** as a clear oil (118 mg, 62%) and a complex mixture containing **174e** as the major component as a yellow oil (15.7 mg, <8%).

Oxazole **172e**: IR (neat): ν = 2956, 2929, 2864, 1637, 1598, 1560, 1450, 1351, 1164, 1091, 1027, 858 cm^{-1}; ^{1}H-NMR (300 MHz, $CDCl_3$): δ = 7.90-7.83 (m, 2H), 7.81-7.75 (m, 2H), 7.45-7.38 (m, 3H), 7.37-7.20 (m, 7H), 4.57 (s, 2H), 2.50 (t, *J* = 7.5 Hz, 2H), 2.46 (s, 3H), 1.33-1.17 (m, 4H), 1.17-1.05 (m, 2H), 0.84 (t, *J* = 7.1 Hz, 3H); ^{13}C-NMR (101 MHz, $CDCl_3$): δ = 157.9 (C), 151.8 (C), 143.8 (C), 136.03 (C), 135.95 (C), 132.4 (C), 130.2 (CH), 129.6 (2CH), 129.2 (2CH), 128.8 (2CH), 128.5 (2CH), 128.4 (2CH), 127.9 (CH), 127.7 (C), 126.1 (2CH), 53.3 (CH_2), 31.5 (CH_2), 27.1 (CH_2), 24.4 (CH_2), 22.4 (CH_2), 21.7 (CH_3), 14.1 (CH_3); HRMS (ES): *m/z* calculated for $C_{28}H_{31}N_2O_3S$: 475.2055, found 475.2062 $(M+H)^+$.

Alkene **174e**: ^{1}H-NMR (400 MHz, $CDCl_3$) *only peaks assigned to **174e** are reported*: δ = 7.74-7.69 (m, 2H), 7.67-7.63 (m, 2H), 7.54-7.49 (m, 1H), 7.45-7.19 (m, 9H), 5.89 (ddt, *J* = 15.2, 10.8, 1.3 Hz, 1H), 5.57 (dt, *J* = 15.2, 7.0 Hz, 1H), 5.44 (d, *J* = 10.8 Hz, 1H), 4.61 (s, 2H), 2.42 (s, 3H), 2.06-1.97 (m, 2H), 1.40-1.29 (m, 2H), 0.84 (t, *J* = 7.4 Hz, 3H).

Compounds 172f, 173f and 174f

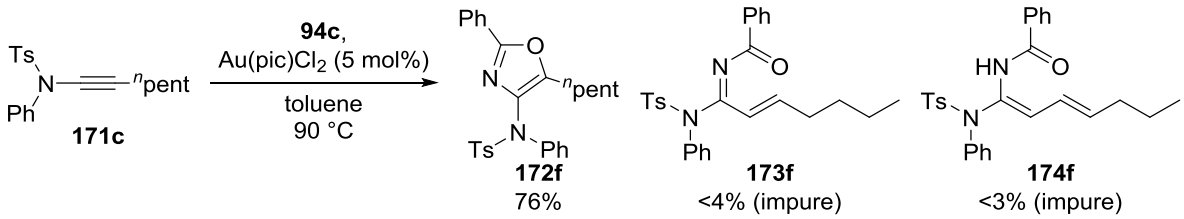

Following **GP7** with ylide **94c** (118 mg, 0.60 mmol), ynamide **171c** (138 mg, 0.40 mmol) and gold catalyst (7.8 mg, 5 mol%) for 5 hours. Purification by flash column chromatography (5→50% EtOAc in hexane) gave *oxazole* **172f** as a white solid (141 mg, 76%) and a 2 complex mixtures, the first containing **173f** as the major component of a clear oil (6.5 mg, <4%), and the second containing **174f** as a component of a clear oil (5.7 mg, <3%).

Oxazole **172f**: IR (neat): ν = 2931, 2863, 1635, 1594, 1557, 1486, 1450, 1357, 1167, 1092, 810 cm^{-1}; ^{1}H-NMR (300 MHz, $CDCl_3$): δ = 8.01-7.87 (m, 2H), 7.73-7.62 (m, 2H), 7.51-7.37 (m, 5H), 7.33-7.18 (m, 5H), 2.82 (t, *J* = 7.6 Hz, 2H), 2.43 (s, 3H), 1.76-1.62 (m, 2H), 1.39-1.22 (m, 4H), 0.85 (t, *J* = 6.8 Hz, 3H); ^{13}C-NMR (101 MHz, $CDCl_3$): δ = 157.9 (C), 150.5 (C), 143.8 (C), 140.5 (C), 135.9 (C), 134.9 (C), 130.3 (CH), 129.2 (2CH), 129.00 (2CH), 128.96 (2CH), 128.8 (2CH), 128.0 (2CH), 127.8 (C), 127.6 (CH), 126.1 (2CH), 31.5 (CH_2), 27.3 (CH_2), 24.5 (CH_2), 22.4 (CH_2), 21.8 (CH_3), 14.0 (CH_3); HRMS (ES): *m/z* calculated for $C_{27}H_{29}N_2O_3S$: 461.1899, found 461.1888 $(M+H)^+$.

Alkene **173f**: ^{1}H-NMR (400 MHz, $CDCl_3$) *only peaks assigned to **173f** are reported, aromatic peaks could not be assigned*: δ = 6.33 (dt, *J* = 15.6, 7.2 Hz, 1H), 5.48 (dt, *J* = 15.6, 1.4 Hz, 1H), 2.40 (s, 3H), 1.84-1.72 (m, 2H), 1.06-0.93 (m, 2H), 0.91-0.75 (m, 2H), 0.62 (t, *J* = 7.1 Hz, 3H).

Alkene **174f**: ^{1}H-NMR (400 MHz, $CDCl_3$) *only peaks assigned to **174f** are reported, aromatic peaks could not be assigned*: δ = 5.93 (ddt, *J* = 15.0, 10.8, 1.2 Hz, 1H), 5.78 (d, *J* = 10.8 Hz, 1H), 5.63 (dt, *J* = 15.0, 7.0 Hz, 1H), 2.32 (s, 3H), 1.97 (appt. q, *J* = 7.0 Hz, 2H), 1.38-1.21 (m, 2H), 0.79 (t, *J* = 7.3, 3H).

Compounds 175a and 176a

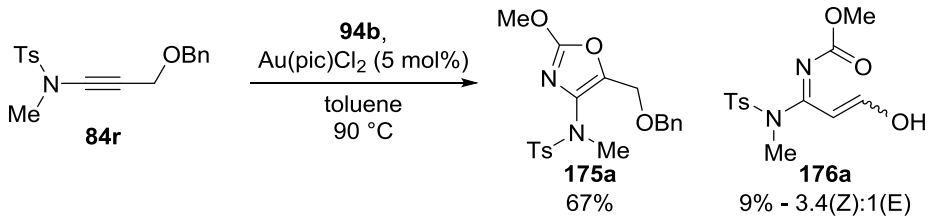

Following **GP7** with ylide **94b** (90 mg, 0.59 mmol), ynamide **84r** (131 mg, 0.40 mmol) and gold catalyst (8.0 mg, 5 mol%) for 2 hours. Purification by flash column chromatography (10⟶50% EtOAc in hexane) gave *oxazole* **175a** as a colourless oil (107 mg, 67%) and a mixture of *enols* **176a** in a 3.4:1 *Z*:*E* ratio as a white solid (11.2 mg, 9%).

Oxazole **175a**: IR (neat): ν = 3032, 2949, 1664, 1608, 1454, 1368, 1351, 1217, 1158, 1088, 1052, 969 cm^{-1}; ^{1}H-NMR (300 MHz, $CDCl_3$): δ = 7.68-7.60 (m, 2H), 7.41-7.27 (m, 7H), 4.59 (s, 2H), 4.56 (s, 2H), 3.90 (s, 3H), 3.04 (s, 3H), 2.43 (s, 3H); ^{13}C-NMR (101 MHz, $CDCl_3$): δ = 160.2 (C), 144.0 (C), 139.7 (C), 137.8 (C), 135.6 (C), 134.3 (C), 129.5 (2CH), 128.6 (2CH), 128.4 (2CH), 128.1 (2CH), 127.9 (CH), 72.7 (CH_2), 60.6 (CH_2), 58.2 (CH_3), 37.0 (CH_3), 21.7 (CH_3); HRMS (ES): *m/z* calculated for $C_{20}H_{23}N_2O_5S$: 403.1328, found 403.1331 $(M+H)^+$.

Enols **176a**: mp: 122-128 °C; IR (neat): ν = 2949, 1745, 1627, 1528, 1353, 1222, 1162, 1142, 1041, 929 cm^{-1}; ^{1}H-NMR (400 MHz, $CDCl_3$): δ = 9.52 (br s, OH_Z), 9.39 (d, *J* = 4.0 Hz, $1H_Z$), 8.98 (d *J* = 7.8 Hz, $1H_E$), 7.75-7.68 (m, $2H_E$+$2H_Z$), 7.38-7.30 (m, $2H_E$+$2H_Z$), 6.69 (br s, OH_E), 6.49 (d, *J* = 7.8 Hz, $1H_E$), 5.26 (d, *J* = 4.0 Hz, $1H_Z$), 3.78 (s, $3H_E$) 3.76 (s, $3H_Z$), 3.24 (s, $3H_E$), 3.07 (s, $3H_Z$), 2.44 (s, $3H_E$+$3H_Z$); ^{13}C-NMR (101 MHz, $CDCl_3$): δ = 190.0 (CH_Z), 189.7 (CH_E), 152.7 (C_Z), 152.4 (C_E), 149.6 (C_Z), 149.0 (C_E), 145.6 (C_E), 145.1 (C_Z), 133.6 (C_Z), 133.5 (C_E), 130.4 ($2CH_E$), 129.9 ($2CH_Z$), 128.2 ($2CH_Z$), 127.8 ($2CH_E$), 112.4 (CH_E), 103.4 (CH_Z), 53.4 (CH_{3E}+CH_{3Z}), 39.7 (CH_{3E}), 37.3 (CH_{3Z}), 21.8 (CH_{3E}+CH_{3Z}); HRMS (ES): *m/z* calculated for $C_{13}H_{17}N_2O_5S$: 313.0858, found 313.0852 $(M+H)^+$.

Compounds 175b and 176b

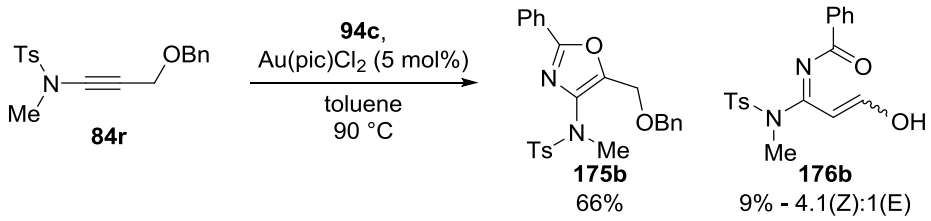

Following **GP7** with ylide **94c** (119 mg, 0.60 mmol), ynamide **84r** (131 mg, 0.40 mmol) and gold catalyst (7.9 mg, 5 mol%) for 3 hours. Purification by flash column chromatography (10⟶50% EtOAc in hexane) gave *oxazole* **175b** as a colourless oil (117 mg, 66%) and a mixture of *enols* **176b** in a 4.1:1 *Z*:*E* ratio as a colourless oil (13.1 mg, 9%).

Oxazole **175b**: IR (neat): ν = 2864, 2259, 1637, 1450, 1352, 1163, 1089, 1070, 1050, 908 cm^{-1}; ^{1}H-NMR (400 MHz, $CDCl_3$): δ = 7.95-7.90 (m, 2H), 7.66-7.61 (m, 2H), 7.47-7.39 (m, 5H), 7.39-7.34 (m, 2H), 7.33-7.27 (m, 3H), 4.78 (s, 2H), 4.67 (s, 2H), 3.14 (s, 3H), 2.44 (s, 3H); ^{13}C-NMR (101 MHz, $CDCl_3$): δ = 159.7 (C), 144.5 (C), 144.1 (C), 138.0 (C), 137.8 (C), 134.2 (C), 130.8 (CH), 129.6 (2CH), 128.8 (2CH), 128.6 (2CH), 128.5 (2CH), 128.1 (2CH), 128.0 (CH), 127.2 (C), 126.5 (2CH), 73.0 (CH_2), 61.0 (CH_2), 37.2 (CH_3), 21.7 (CH_3); HRMS (ES): *m/z* calculated for $C_{25}H_{25}N_2O_4S$: 449.1535, found 449.1538 $(M+H)^+$.

Enols **176b**: IR (neat): ν = 3301 (br), 2924, 2853, 1693, 1662, 1597, 1471, 1358, 1264, 1157, 1087, 1023 cm^{-1}; ^{1}H-NMR (400 MHz, $CDCl_3$) (*the OH signal from the E isomer was not observed)*: δ = 11.00 (br s, OH_Z), 9.44 (appt. br s, $1H_Z$), 9.02 (d, *J* = 7.3 Hz, $1H_E$), 8.00-7.94 (m, $2H_Z$), 7.84-7.80 (m, $2H_E$), 7.79-7.73 (m, $2H_E$+$2H_Z$), 7.63-7.57 (m, $1H_E$+$1H_Z$), 7.54-7.48 (m, $2H_E$+$2H_Z$), 7.36 (d, *J* = 8.1 Hz, $2H_E$), 7.32 (d, *J* = 8.1 Hz, $2H_Z$), 6.94 (d, *J* = 7.3 Hz, $1H_E$), 5.57 (d, *J* = 3.8 Hz, $1H_Z$), 3.35 (s, $3H_E$), 3.17 (s, $3H_Z$), 2.45 (s, $3H_E$), 2.43 (s, $3H_Z$); ^{13}C-NMR (101 MHz, $CDCl_3$) *only peaks for the major (Z) isomer are listed*: 190.5 (CH), 165.1 (C), 149.3 (C), 145.1 (C), 133.8 (C), 133.2 (CH), 133.0 (C), 129.9 (2CH), 129.1 (2CH), 128.4 (2CH), 128.1 (2CH), 104.1 (CH), 37.2 (CH_3), 21.8 (CH_3); HRMS (ES): *m/z* calculated for $C_{18}H_{18}N_2O_4SNa$, found 381.0878 $(M+Na)^+$.

Oxazole 250

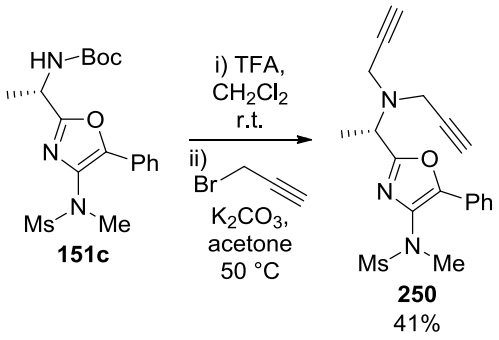

In an unoptimised procedure oxazole **151c** (99 mg, 0.25 mmol) was deprotected by stirring in a 1:1 trifluoroacetic acid:CH_2Cl_2 solution (4 mL) for 1 hour. The reaction mixture was poured into satd. $NaHCO_{3(aq)}$ solution (30 mL) and extracted with CH_2Cl_2 (3 x 10 mL). The combined organic extracts were dried over Na_2SO_4 and concentrated under reduced pressure. To the resulting crude primary amine was added K_2CO_3 (110 mg, 0.80 mmol), acetone (2.5 mL) and propargyl bromide (80% in toluene, 70 µL, 0.63 mmol). The reaction mixture was stirred at 50 °C for 22 hours, filtered through cotton and concentrated under reduced pressure. As the crude ^{1}H-NMR showed a large amount of mono-propargylated product the crude reaction mixture was re-subjected to K_2CO_3 (200 mg, 1.45 mmol) and propargyl bromide (80% in toluene, 100 µL, 0.90 mmol) in acetone (2.5 mL) for a further 5 hours. Again the reaction mixture was filtered through cotton, concentrated under reduced pressure, and then purified by flash column chromatography (1:1 EtOAc:hexane) to give *oxazole* **250** as a colourless oil (38 mg, 41% over two steps); $[\alpha]_D^{20}$ = −42.5 (c=3.1, $CHCl_3$); IR (neat): ν = 3287, 1342, 1151, 964 cm^{-1}; ^{1}H-NMR (300 MHz, $CDCl_3$): δ = 7.95-7.88 (m, 2H), 7.48-7.39 (m, 2H), 7.39-7.31 (m, 1H), 4.18 (q, *J* = 7.1 Hz, 1H), 3.73-3.59 (m, 4H), 3.26 (s, 3H), 3.10 (s, 3H), 2.19 (t, *J* = 2.4, 2H), 1.60 (d, *J* = 7.1 Hz, 3H); ^{13}C-NMR (101 MHz, $CDCl_3$): δ = 160.8 (C), 145.5 (C), 133.3 (C), 129.1 (CH), 128.9 (2CH), 127.0 (C), 125.5 (2CH), 78.7 (2C), 73.4 (2CH), 53.9 (CH), 39.6 ($2CH_2$), 38.2 (CH_3), 36.8 (CH_3), 16.9 (CH_3); HRMS (ES): *m/z* calculated for $C_{19}H_{22}N_3O_3S$: 372.1382, found 372.1393 $(M+H)^+$.

Oxazole 256a

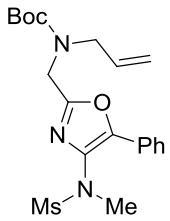

Oxazole **151b** (95 mg, 0.25 mmol) was added to a suspension of NaH (60% dispersion, 20 mg, 0.50 mmol) in DMF (2.25 mL). The reaction mixture was stirred for 10 minutes before allyl bromide (40 µL, 0.46 mmol) was added and stirring was continued for 4 hours. The reaction mixture was quenched with H_2O (30 mL) and extracted with EtOAc (2 x 20 mL). The combined organic phases were washed with brine (25 mL), dried over Na_2SO_4, concentrated under reduced pressure and purified by flash column chromatography (2:1 hexane:EtOAc) to give *oxazole* **256a** as a colourless oil (73 mg, 69%); IR (neat): ν = 2977, 2932, 1964, 1345, 1244, 1152 cm^{-1}; *NMR shows a mixture of two rotamers:* ^{1}H-NMR (400 MHz, $CDCl_3$): δ = 7.92-7.85 (m, 2H), 7.46-7.37 (m, 2H), 7.34 (t, *J* = 7.2 Hz, 1H), 5.89-5.70 (m, 1H), 5.24-5.05 (m, 2H), 4.59-4.37 (m, 2H), 4.06-3.87 (m, 2H), 3.23 (s, 3H), 3.10 (s, 3H), 1.48 and 1.43 (s, 9H); ^{13}C-NMR (101 MHz, $CDCl_3$): δ = 158.5 and 158.2 (C), 155.3 and 155.0 (C), 145.9 and 145.7 (C), 133.4 (CH), 133.3 (C) 129.1 (CH), 128.9 (2CH), 126.7 (C), 125.3 (2CH), 117.9 and 117.1 (CH_2), 80.8 (C), 50.1 (CH_2), 43.9 and 43.4 (CH_2), 38.0 (CH_3), 36.9 (CH_3), 28.5 and 28.4 ($3CH_3$); HRMS (ES): *m/z* calculated for $C_{20}H_{27}N_3O_5SNa$: 444.1569, found 444.1574 $(M+H)^+$.

Oxazole 151m

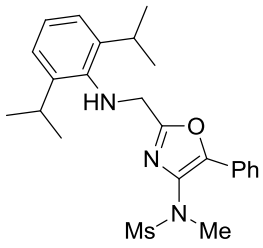

Following **GP7** using ylide **94p** (402 mg, 1.3 mmol), ynamide **84g** (180 mg, 0.86 mmol) and gold catalyst (6.7 mg, 2 mol%) for 17 hours. Purification by flash column chromatography (15→20% EtOAc in hexane) yielded *oxazole* **151m** as a white solid (266 mg, 70%); mp: 160-162 °C; IR (neat): ν = 2966, 1452, 1364, 1342, 1069, 969, cm^{-1}; ^{1}H-NMR (300 MHz, $CDCl_3$): δ = 7.93-7.83 (m, 2H), 7.50-7.33 (m, 3H), 7.17-7.07 (m, 3H), 4.24 (s, 2H), 3.36 (hept, *J* = 6.8 Hz, 2H), 3.27 (s, 3H), 3.11 (s, 3H), 1.27 (d, *J* = 6.8 Hz, 12H); ^{13}C-NMR (101 MHz, $CDCl_3$): δ = 159.7 (C), 146.0 (C), 142.8 (2C), 141.6 (C), 133.2 (C), 129.2 (CH), 128.9 (2CH), 126.7 (C), 125.4 (2CH), 124.8 (CH), 123.9 (2CH), 48.2 (CH_2), 38.0 (CH_3),

36.9 (CH_3), 27.9 (2CH), 24.3 ($4CH_3$); HRMS (ES): *m/z* calculated for $C_{24}H_{31}N_3O_3SNa$: 464.1984, found 464.1995 $(M+Na)^+$.

Oxazole 371a

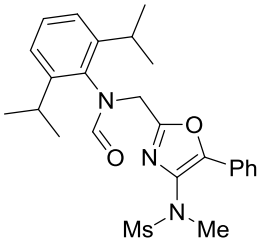

Following **GP7** using ylide **94q** (611 mg, 1.8 mmol), ynamide **84g** (314 mg, 1.5 mmol) and gold catalyst (12 mg, 2 mol%) for 4 hours. Purification by flash column chromatography (25⟶50% EtOAc in hexane) yielded *oxazole* **371a** as a white solid (549 mg, 78%); mp: 193-195 °C; IR (neat): ν = 2971, 2855, 1675, 1495, 1348, 1153 cm^{-1}; NMR *shows a mixture of two rotamers in a ~ 0.2:0.8 ratio:* ^{1}H-NMR (300 MHz, $CDCl_3$): δ = 8.75 and 8.19 (s, 1H), 7.88-7.80 (m, 2H), 7.48-7.31 (m, 4H), 7.20 (d, *J* = 7.7 Hz, 2H), 4.90 and 4.75 (s, 2H), 3.20 and 3.19 (s, 3H), 3.06 and 2.98 (s, 3H), 2.96 and 2.81 (hept, *J* = 6.9 Hz, 2H), 1.18-1.03 (m, 12H); ^{13}C-NMR (101 MHz, $CDCl_3$): *only the peaks for the major rotamer are reported* δ = 163.5 (CH), 155.9 (C), 148.1 (2C), 146.8 (C), 134.3 (C), 133.4 (C), 130.1 (CH), 129.4 (CH), 129.0 (2CH), 126.5 (C), 125.5 (2CH), 124.7 (2CH), 43.9 (CH_2), 38.0 (CH_3), 36.9 (CH_3), 28.5 (2CH), 25.3 ($2CH_3$), 23.8 ($2CH_3$); HRMS (ES): *m/z* calculated for $C_{25}H_{31}N_3O_4SNa$: 492.1933, found 492.1943 $(M+Na)^+$.

Oxazole 371b

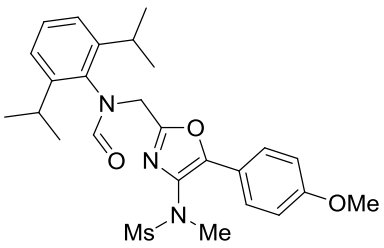

Following **GP7** using ylide **94q** (1.84 g, 5.4 mmol), ynamide **84t** (1.08 g, 4.5 mmol) and gold catalyst (35 mg, 2 mol%) for 4 hours. Purification by flash column chromatography (30⟶50% EtOAc in hexane) yielded *oxazole* **371b** as a white solid (1.64 mg, 73%); mp: 148-151 °C; IR (neat): ν = 2969, 1686, 1509, 1345, 1177, 1151, 837 cm^{-1}; *NMR shows a mixture of two rotamers in a ~ 0.3:0.7 ratio:* ^{1}H-NMR (300 MHz, $CDCl_3$): δ = 8.75 and 8.18 (s, 1H), 7.82-7.75 (m, 2H), 7.41-7.31 (m, 1H), 7.20 (d, *J* = 7.7 Hz, 2H), 6.99-6.90 (m, 2H), 4.89 and 4.73 (s, 2H), 3.85 and 3.84 (s, 3H), 3.18 and 3.16 (s, 3H), 3.04 and 2.96 (s, 3H), 2.95 and 2.81 (hept, *J* = 6.9 Hz, 2H), 1.19-1.02 (m, 12H); ^{13}C-NMR (101 MHz, $CDCl_3$): *only the peaks for the major rotamer are reported* δ = 163.3 (CH), 160.4 (C), 155.0 (C), 148.0 (2C), 146.9 (C), 134.2 (C), 131.8 (C), 130.0 (CH), 127.1 (2CH), 124.6 (2CH),

119.2 (C), 114.3 (2CH), 55.4 (CH_3), 43.7 (CH_2), 37.9 (CH_3), 36.7 (CH_3), 28.4 (2CH), 25.3 ($2CH_3$), 23.6 ($2CH_3$); HRMS (ES): *m/z* calculated for $C_{26}H_{34}N_3O_5S$: 500.2219, found 500.2215 $(M+H)^+$.

Oxazole 371c

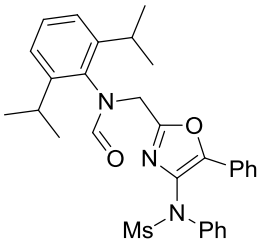

Following **GP7** using ylide **94q** (611 mg, 1.8 mmol), ynamide **84c** (410 mg, 1.5 mmol) and gold catalyst (12 mg, 2 mol%) for 4 hours. Purification by flash column chromatography (20⟶30% EtOAc in hexane) yielded *oxazole* **371c** as a white solid (562 mg, 70%); mp: 185-187 °C; IR (neat): ν = 2964, 2868, 1663, 1360, 1162, 967 cm^{-1}; *NMR shows a mixture of two rotamers in a ~ 0.1:0.9 ratio:* ^{1}H-NMR (400 MHz, $CDCl_3$): δ = 8.80 and 8.21 (s, 1H), 7.85-7.79 (m, 2H), 7.55-7.26 (m, 9H), 7.21 (d, *J* = 7.8 Hz, 2H), 4.98 and 4.81 (s, 2H), 3.18 and 3.12 (s, 3H), 2.98 and 2.82 (hept, *J* = 6.8 Hz, 2H), 1.17-1.11 (m, 6H), 1.03 and 0.96 (d, *J* = 6.8 Hz, 6H); ^{13}C-NMR (101 MHz, $CDCl_3$): *only the peaks for the major rotamer are reported* δ = 163.4 (CH), 155.6 (C), 148.2 (2C), 147.2 (C), 140.0 (C), 134.1 (C), 133.0 (C), 130.1 (CH), 129.5 (3CH), 128.9 (2CH), 127.9 (CH), 127.0 (2CH), 126.3 (C), 125.6 (2CH), 124.7 (2CH), 43.7 (CH_2), 38.6 (CH_3), 28.5 (2CH), 25.4 ($2CH_3$), 23.6 ($2CH_3$); HRMS (ES): *m/z* calculated for $C_{30}H_{33}N_3O_4SNa$: 554.2089, found 554.2092 $(M+Na)^+$.

Oxazole 371d

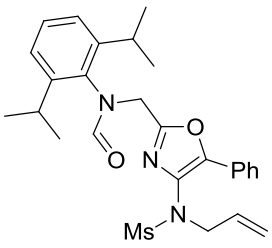

Following **GP7** using ylide **94q** (611 mg, 1.8 mmol), ynamide **84y** (353 mg, 1.5 mmol) and gold catalyst (12 mg, 2 mol%) for 4 hours. Purification by flash column chromatography (20⟶30% EtOAc in hexane) yielded *oxazole* **371d** as a white solid (552 mg, 74%); mp: 117-121 °C; IR (neat): ν = 2962 2868, 1684, 1343, 1164, 964 cm^{-1}; *NMR shows a mixture of two rotamers a ~ 0.1:0.9 ratio:* ^{1}H-NMR (400 MHz, $CDCl_3$): δ = 8.74 and 8.19 (s, 1H), 7.90-7.83 (m, 2H), 7.45-7.30 (m, 4H), 7.20 (d, *J* = 7.8 Hz, 2H), 5.93-5.82 and 5.77-5.66 (m, 1H), 5.36-5.29 and 5.12-4.99 (m, 2H), 4.91 and 4.76 (s, 2H), 4.18 and 4.14 (d, *J* = 6.7 Hz, 2H), 3.06 and 2.97 (s, 3H), 2.99 and 2.83 (hept, *J* = 6.9 Hz, 2H), 1.18-1.13 (m, 6H), 1.10 and 1.06 (d, *J* = 6.9 Hz, 6H); ^{13}C-NMR (101 MHz, $CDCl_3$): *only the peaks for the major*

rotamer are reported δ = 163.4 (CH), 155.7 (C), 148.1 (2C), 148.0 (C), 134.3 (C), 131.71 (C), 131.66 (CH), 130.1 (CH), 129.4 (CH), 128.8 (2CH), 126.5 (C), 125.6 (2CH), 124.7 (2CH), 120.2 (CH_2), 53.8 (CH_2), 43.9 (CH_2), 38.7 (CH_3), 28.5 (2CH), 25.3 ($2CH_3$), 23.8 ($2CH_3$); HRMS (ES): *m/z* calculated for $C_{27}H_{33}N_3O_4SNa$: 518.2089, found 518.2084 $(M+Na)^+$.

Oxazole 151n

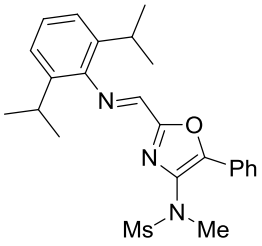

Trifluoroacetic acid (3.75 mL, 49 mmol) was added to a solution of oxazole **151g** (248 mg, 0.76 mmol) and diisopropylaniline (160 µL, 0.85 mmol) in toluene (7.5 mL). The reaction mixture was stirred for 14 hours at room temperature before cooling in an ice/water bath whilst NEt_3 (7.5 mL, 54 mmol) was added over 10 minutes resulting in a colour change from red to yellow. The solvent was removed under reduced pressure and the crude product was purified by flash column chromatography (80:20:1 hexane:EtOAc:NEt_3) to give *oxazole* **151n** as a yellow solid (331 mg, 99%); mp: 198-202 °C; IR (neat): ν = 2967, 1618, 1451, 1345, 1154, 970 cm^{-1}; ^{1}H-NMR (400 MHz, $CDCl_3$): δ = 8.14-8.08 (m, 2H), 8.02 (s, 1H), 7.53-7.40 (m, 3H), 7.22-7.14 (m, 3H), 3.37 (s, 3H), 3.21 (s, 3H), 2.97 (hept, *J* = 6.9 Hz, 2H), 1.21 (d, *J* = 6.9 Hz, 12H); ^{13}C-NMR (101 MHz, $CDCl_3$): δ = 155.0 (C), 148.6 (CH), 148.2 (C), 147.8 (C), 137.4 (2C), 135.4 (C), 130.3 (CH), 129.1 (2CH), 126.3 (2CH), 126.1 (C), 125.4 (CH), 123.4 (2CH), 38.1 (CH_3), 37.2 (CH_3), 28.1 (2CH), 23.8 ($4CH_3$); HRMS (ES): *m/z* calculated for $C_{24}H_{30}N_3O_3S$: 440.2008, found 440.1997 $(M+H)^+$.

5.1.7: Diels-Alder Reactions of Oxazoles

Furan 251

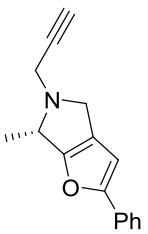

A solution of oxazole **250** (31 mg, 83 µmol) in mesitylene (0.5 mL) was heated at 100 °C for 22 hours. After cooling to room temperature, the reaction mixture was directly purified by flash column chromatography (10→30% EtOAc in hexane) to give *furan* **251** as a colourless oil (9.7 mg, 49%); $[\alpha]_D^{20}$ = +63.6 (c=0.4, $CHCl_3$); IR (neat): ν = 3295, 2922, 1602, 1375, 1077, 922, 760 cm^{-1}; ^{1}H-NMR (400 MHz, $CDCl_3$): δ = 7.65-7.59 (m, 2H),

7.39-7.33 (m, 2H), 7.23 (tt, J = 7.4, 1.1 Hz, 1H), 6.55 (s, 1H), 4.21-4.12 (m, 1H), 4.00 (dd, J = 11.4, 3.8 Hz, 1H), 3.84 (dd, J = 11.4, 3.6 Hz, 1H), 3.63 (AB part of an ABX system, $J_{A\text{-}B}$ = 17.5 Hz, $J_{A\text{-}X} \approx J_{B\text{-}X}$ = 2.3 Hz, 2H), 2.26 (appt. t, J = 2.3 Hz, 1H), 1.41 (d, J = 6.3 Hz, 3H); ^{13}C-NMR (101 MHz, $CDCl_3$): δ = 159.0 (C), 157.9 (C), 131.5 (C), 128.8 (2CH), 127.2 (CH), 123.5 (2CH), 123.0 (C), 102.2 (CH), 79.5 (C), 73.8 (CH), 56.1 (CH), 50.7 (CH_2), 41.5 (CH_2), 18.9 (CH_3); HRMS (ES): *m/z* calculated for $C_{16}H_{16}NO$: 238.1232, found 2381228 $(M+H)^+$.

Furan 255

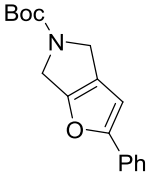

NaH (60% dispersion, 9.0 mg, 0.62 mmol) was suspended in DMF (2 mL) under an argon atmosphere and the solution cooled to 0 °C. Oxazole **151b** (90 mg, 0.20 mmol) was added and after 5 minutes this was followed by propargyl bromide (80% in toluene, 25 µL, 0.28 mmol). After stirring for 90 minutes at room temperature TLC analysis showed that all the oxazole had been consumed and the reaction mixture was heated to 140 °C for 22 hours. After cooling to room temperature, the reaction mixture was purified directly by flash column chromatography (9:1 hexane:EtOAc) to give *furan* **255** as a white solid (5.1 mg, 9%) *this compound was unstable and only characterised by proton NMR*; ^{1}H-NMR (300 MHz, $CDCl_3$): δ = 7.66-7.59 (m, 2H), 7.42-7.34 (m, 2H), 7.29-7.22 (m, 1H), 6.61 and 6.56 (s [2 conformers], 1H), 4.55-4.46 (m, 2H), 4.43-4.34 (m, 2H), 1.52 (s, 9H).

5.1.7.1: General procedure for cascade oxazole formation and Diels-Alder reactions (GP8)

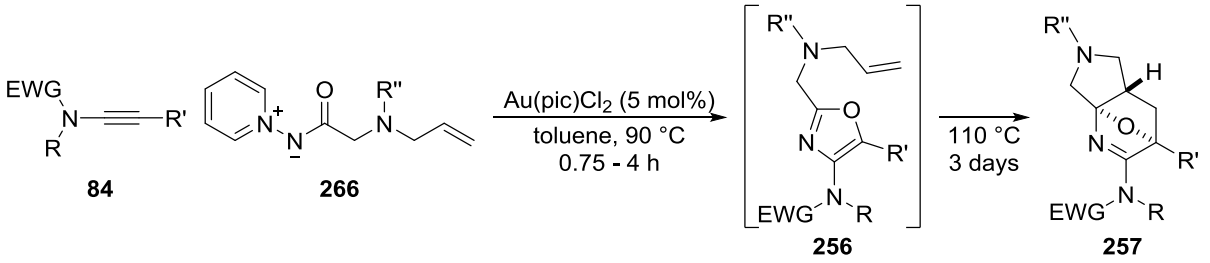

Pyridinium ylide (1.2 eq.), dichloro(2-pyridinecarboxylato)gold (5 mol%), and ynamide (1.0 eq.) were added to a heat-gun dried flask under an argon atmosphere. Toluene (0.1 M with respect to ynamide) was added (where ynamides were oils these were added as a solution in toluene) and the reaction mixture was heated to 90 °C until all of the ynamide had consumed by TLC or for 4 hours. The temperature was then increased to 110 °C for 72 hours. After cooling to room temperature, the reaction mixture was filtered through a 5 cm plug of silica gel (washing with CH_2Cl_2 and then EtOAc) and the filtrate was concentrated and purified by flash column chromatography.

Tetrahydropyridine 257a

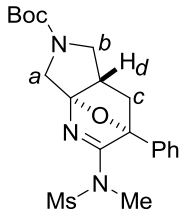

Following **GP8** using ylide **266a** (71.0 mg, 0.24 mmol), ynamide **84g** (42.8 mg, 0.20 mmol) and gold catalyst (3.9 mg, 5 mol%). Purification by flash column chromatography (10⟶30% EtOAc in hexane) yielded *tetrahydropyridine* **257a** as a white solid (58.1 mg , 68%); mp: 133-134 °C; IR (neat): ν = 2976, 2888, 1689, 1582, 1404, 1348, 1244, 1158, 1120, 960, 873 cm^{-1}; *NMR shows a mixture of two rotamers in a ~ 1.2:1 ratio:* ^{1}H-NMR (400 MHz, $CDCl_3$): δ = 7.55-7.49 (m, 2H), 7.46-7.37 (m, 3H), 4.11-4.06 (m, 1H_a), 4.03-3.97 (m, 1H_b), 3.94-3.86 (m, 1H_a), 3.05-2.96 (m, 1H_b), 2.81 and 2.80 (s, 3H), 2.76 and 2.73 (s, 3H), 2.62-2.48 (m, 1H_d), 2.43-2.35 (m, 1H_c), 2.03-1.92 (m, 1H_c), 1.46 and 1.44 (s, 9H); ^{13}C-NMR (101 MHz, $CDCl_3$): δ = 170.6 (C), 154.3 and 154.2 (C), 135.43 and 135.37 (C), 129.43 and 129.38 (CH), 128.78 (2CH), 127.83 and 127.75 (2CH), 107.8 and 107.1 (C), 93.8 and 93.6 (C), 79.77 and 79.75 (C), 51.4 and 50.8 (CH_{2b}), 48.4 and 48.0 (CH_{2a}), 45.2 and 44.5 (CH_d), 39.94 and 39.91 (CH_3), 35.6 and 35.5 (CH_3),

33.6 and 33.4 (CH_{2c}), 28.59 ($3CH_3$); HRMS (ES): *m/z* calculated for $C_{20}H_{28}N_3O_5S$: 422.1750, found 422.1759 $(M+H)^+$.

Tetrahydropyridine 257b

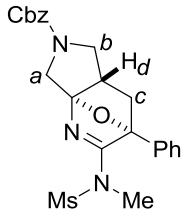

Following **GP8** using ylide **266b** (92.1 mg, 0.28 mmol), ynamide **84g** (49.0 mg, 0.23 mmol) and gold catalyst (4.6 mg, 5 mol%). Purification by flash column chromatography (30⟶50% EtOAc in hexane) yielded *tetrahydropyridine* **257b** as a white solid (65.7 mg, 63%); mp: 69-70 °C; IR (neat): ν = 2954, 1699, 1584, 1417, 1348, 1158, 1114, 957 cm^{-1}; *NMR shows a mixture of two rotamers in a ~ 1:1 ratio:* ^{1}H-NMR (400 MHz, $CDCl_3$): δ = 7.55-7.49 (m, 2H), 7.46-7.28 (m, 8H), 5.20-5.09 (m, 2H, OCH_2Ph), 4.20-4.13 (m, 1H_a), 4.11-4.05 (m, 1H_b) 4.05-3.97 (m, 1H_a), 3.14-3.05 (m, 1H_b), 2.81 (s, 3H), 2.75 and 2.73 (s, 3H), 2.64-2.52 (m, 1H_d), 2.46-2.37 (m, 1H_c), 2.05-1.94 (m, 1H_c); ^{13}C-NMR (101 MHz, $CDCl_3$): δ = 170.7 (C), 154.7 and 154.5 (C), 136.83 and 136.78 (C), 135.3 and 135.2 (C), 129.44 and 129.40 (CH), 128.8 (2CH), 128.6 (2CH), 128.1 (CH), 128.0 and 127.9 (2CH), 127.8 and 127.7 (2CH), 107.7 and 106.9 (C), 93.8 and 93.7 (C), 67.02 and 67.00 (CH_2), 51.4 and 51.2 (CH_{2b}), 48.4 and 48.2 (CH_{2a}), 45.2 and 44.4 (CH_d), 39.90 and 39.87 (CH_3), 35.6 and 35.5 (CH_3), 33.6 and 33.4 (CH_{2c}); HRMS (ES): *m/z* calculated for $C_{23}H_{25}N_3O_5SNa$: 478.1413, found 478.1406 $(M+Na)^+$.

Tetrahydropyridine 257c

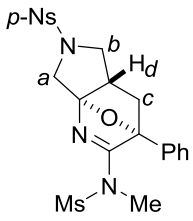

Following **GP8** using ylide **266c** (101.1 mg, 0.27 mmol), ynamide **84g** (46.8 mg, 0.22 mmol) and gold catalyst (4.4 mg, 5 mol%). Purification by flash column chromatography (10⟶40% EtOAc in hexane) yielded *tetrahydropyridine* **257c** as a white solid (39.8 mg, 36%); mp: 184-186 °C; IR (neat): ν = 1605, 1527, 1345, 1307, 1164, 977 cm^{-1}; ^{1}H-NMR (400 MHz, $CDCl_3$): δ = 8.31 (d, *J* = 8.8 Hz, 2H), 7.99 (d, *J* = 8.8 Hz, 2H), 7.40-7.33 (m, 5H), 4.16 (d, *J* = 12.0 Hz, 1H_a), 4.03-3.95 (m, 1H_b), 3.81 (d, *J* = 12.0 Hz, 1H_a), 2.87 (appt. t, *J* = 9.8 Hz, 1H_b), 2.79 (s, 3H), 2.65 (s, 3H), 2.59-2.49 (m, 1H_d), 2.37 (dd, *J* = 12.2, 7.6 Hz, 1H_c), 1.87 (dd, *J* = 12.2, 3.2 Hz, 1H_c); ^{13}C-NMR (101 MHz, $CDCl_3$): δ = 170.9 (C), 150.3 (C), 143.1 (C),

134.7 (C), 129.7 (CH), 128.7 (2CH), 128.6 (2CH), 127.8 (2CH), 124.5 (2CH), 106.9 (C), 93.8 (C), 53.2 (CH_{2b}), 49.8 (CH_{2a}), 45.5 (CH_d), 39.9 (CH_3), 35.5 (CH_3), 33.3 (CH_{2c}); HRMS (ES): *m/z* calculated for $C_{21}H_{22}N_4O_7S_2Na$: 529.0828, found 529.0835 $(M+Na)^+$.

Tetrahydropyridine 257d

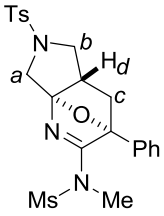

Following **GP8** using ylide **266d** (82.9 mg, 0.24 mmol), ynamide **84g** (41.9 mg, 0.20 mmol) and gold catalyst (3.9 mg, 5 mol%). Purification by flash column chromatography (20⟶50% EtOAc in hexane) yielded *tetrahydropyridine* **257d** as a white solid (65.6 mg, 69%) (*this reaction was also run on 1.5 mmol scale*, *giving a 68% yield*); mp: 103-104 °C; IR (neat): ν = 2929, 1583, 1526, 1344, 1155, 1096, 958, 762 cm^{-1}; ^{1}H-NMR (400 MHz, $CDCl_3$): δ = 7.70 (d, *J* = 8.2 Hz, 2H), 7.44-7.36 (m, 5H), 7.28 (d, *J* = 8.2 Hz, 2H), 4.11 (d, *J* = 11.8 Hz, 1H_a), 3.94-3.87 (m, 1H_b), 3.75 (d, *J* = 11.8 Hz, 1H_a), 2.83 (appt. t, *J* = 9.9 Hz, 1H_b), 2.77 (s, 3H), 2.67 (s, 3H), 2.49-2.40 (m, 1H_d), 2.39 (s, 3H), 2.32 (dd, *J* = 12.0, 7.7 Hz, 1H_c), 1.86 (dd, *J* = 12.0, 3.2 Hz, 1H_c); ^{13}C-NMR (101 MHz, $CDCl_3$): δ = 170.8 (C), 143.8 (C), 135.1 (C), 134.2 (C), 129.9 (2CH), 129.5 (CH), 128.8 (2CH), 127.9 (2CH), 127.6 (2CH), 107.5 (C), 93.8 (C), 53.0 (CH_{2b}), 49.6 (CH_{2a}), 45.6 (CH_d), 39.9 (CH_3), 35.6 (CH_3), 32.7 (CH_{2c}), 21.7 (CH_3); HRMS (ES): *m/z* calculated for $C_{22}H_{25}N_3O_5S_2Na$: 498.1133, found 498.1123 $(M+Na)^+$.

Tetrahydropyridine 257e

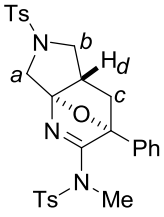

Following **GP8** using ylide **266d** (82.7 mg, 0.24 mmol), ynamide **84s** (57.2 mg, 0.20 mmol) and gold catalyst (3.9 mg, 5 mol%). Purification by flash column chromatography (20⟶40% EtOAc in hexane) yielded *tetrahydropyridine* **257e** as a white solid (60.4 mg, 55%); mp: 174-175 °C; IR (neat): ν = 1581, 1344, 1234, 1163, 1078, 1014 cm^{-1}; ^{1}H-NMR (400 MHz, $CDCl_3$): δ = 7.70 (d, *J* = 8.2 Hz, 2H), 7.46 (d, *J* = 8.2 Hz, 2H), 7.40-7.34 (m, 5H), 7.29 (d, *J* = 8.2 Hz, 2H), 7.21 (d, *J* = 8.2 Hz, 2H), 4.13 (d, *J* = 11.8 Hz, 1H_a), 3.96-3.88 (m, 1H_b), 3.68 (d, *J* = 11.8 Hz, 1H_a), 2.79 (appt. t, *J* = 9.9 Hz, 1H_b), 2.68 (s, 3H), 2.46-2.33 (m, 1H_d), 2.41 (s, 3H), 2.39 (s, 3H), 2.28 (dd, *J* = 12.0, 7.6 Hz, 1H_c), 1.88 (dd, *J* = 12.0, 3.2 Hz, 1H_c);

^{13}C-NMR (101 MHz, $CDCl_3$): δ = 170.0 (C), 144.7 (C), 143.7 (C), 135.2 (C), 134.5 (C), 134.1 (C), 129.9 (2CH), 129.5 (2CH), 129.2 (CH), 128.7 (2CH), 128.5 (2CH), 127.6 (2CH), 127.5 (2CH), 107.5 (C), 94.0 (C), 52.9 (CH_{2b}), 49.6 (CH_{2a}), 45.6 (CH_d), 35.4 (CH_3), 32.4 (CH_{2c}), 21.7 (CH_3), 21.6 (CH_3); HRMS (ES): *m/z* calculated for $C_{28}H_{30}N_3O_5S_2$: 552.1627, found 552.1619 $(M+H)^+$.

Tetrahydropyridine 257f

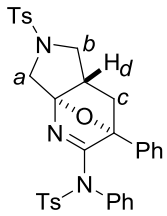

Following **GP8** using ylide **266d** (82.9 mg, 0.24 mmol), ynamide **84a** (69.5 mg, 0.20 mmol) and gold catalyst (3.9 mg, 5 mol%). Purification by flash column chromatography (20→30% EtOAc in hexane) yielded *tetrahydropyridine* **257f** as a white solid (73.1 mg, 60%); mp: 108-110 °C; IR (neat): ν = 1583, 1344, 1233, 1160, 1089, 806 cm^{-1}; ^{1}H-NMR (400 MHz, $CDCl_3$): δ = 7.71 (d, *J* = 8.2 Hz, 2H), 7.65 (d, *J* = 8.2 Hz, 2H), 7.28 (d, *J* = 8.2 Hz, 2H), 7.22 (d, *J* = 8.2 Hz, 2H), 7.08-7.00 (m, 2H), 6.99-6.89 (m, 4H), 6.85 (d, *J* = 7.3 Hz, 2H), 6.64 (d, *J* = 7.5 Hz, 2H), 4.24 (d, *J* = 11.8 Hz, 1H_a), 3.97-3.89 (m, 1H_b), 3.72 (d, *J* = 11.8 Hz, 1H_a), 2.73 (appt. t, *J* = 9.9 Hz, 1H_b), 2.53-2.44 (m, 1H_d), 2.42 (s, 3H), 2.38 (s, 3H), 2.15 (dd, *J* = 12.0, 7.6 Hz, 1H_c), 1.68 (dd, *J* = 12.0, 3.2 Hz, 1H_c); ^{13}C-NMR (101 MHz, $CDCl_3$): δ = 168.4 (C), 144.7 (C), 143.7 (C), 135.5 (C), 134.5 (C), 134.0 (2C), 129.9 (2CH), 129.7 (2CH), 129.6 (2CH), 129.1 (2CH), 128.8 (CH), 128.6 (2CH), 128.3 (CH), 127.9 (2CH), 127.5 (2CH), 126.9 (2CH), 108.1 (C), 93.8 (C), 52.7 (CH_{2b}), 49.7 (CH_{2a}), 45.6 (CH_d), 32.7 (CH_{2c}), 21.8 (CH_3), 21.6 (CH_3); HRMS (ES): *m/z* calculated for $C_{33}H_{31}N_3O_5S_2Na$: 636.1603, found 636.1595 $(M+Na)^+$.

Tetrahydropyridine 257g

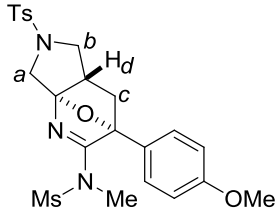

Following **GP8** using ylide **266d** (82.7 mg, 0.24 mmol), ynamide **84t** (47.6 mg, 0.20 mmol) and gold catalyst (3.8 mg, 5 mol%). Purification by flash column chromatography (70:30:1→60:40:1 hexane:EtOAc:NEt_3) yielded *tetrahydropyridine* **257g** as a white solid with approximately 95% purity (36.3 mg, 36%); mp: 90-92 °C; IR (neat): ν = 1581, 1518, 1343, 1246, 1158, 1093, 962 cm^{-1}; ^{1}H-NMR (400 MHz, $CDCl_3$): δ = 7.70 (d, *J* = 8.2 Hz, 2H), 7.33 (d, *J* = 8.8 Hz, 2H), 7.28 (d, *J* = 8.2 Hz, 2H),

6.91 (d, *J* = 8.8 Hz, 2H), 4.10 (d, *J* = 11.7 Hz, 1H_a), 3.90 (dd, *J* = 9.4, 8.3 Hz, 1H_b), 3.81 (s, 3H), 3.72 (d, *J* = 11.7 Hz, 1H_a), 2.86-2.78 (m, 4H, 1H_b+CH_3), 2.69 (s, 3H), 2.49-2.41 (m, 1H_d), 2.40 (s, 3H), 2.29 (dd, *J* = 12.0, 7.6 Hz, 1H_c), 1.85 (dd, *J* = 12.0, 3.3 Hz, 1H_c); ^{13}C-NMR (101 MHz, $CDCl_3$): δ = 171.0 (C), 160.4 (C), 143.7 (C), 134.2 (C), 129.9 (2CH), 129.2 (2CH), 127.6 (2CH), 127.0 (C), 114.1 (2CH), 107.3 (C), 93.6 (C), 55.5 (CH_3), 52.9 (CH_{2b}), 49.6 (CH_{2a}), 45.7 (CH_d), 40.0 (CH_3), 35.5 (CH_3), 32.7 (CH_{2c}), 21.7 (CH_3); HRMS (ES): *m/z* calculated for $C_{23}H_{28}N_3O_6S_2$: 506.1420, found 506.1418 $(M+H)^+$.

Tetrahydropyridine 257h

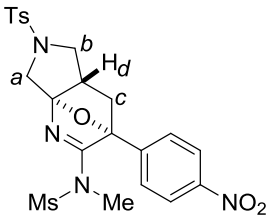

Following **GP8** using ylide **266d** (82.9 mg, 0.24 mmol), ynamide **84u** (50.9 mg, 0.20 mmol) and gold catalyst (3.9 mg, 5 mol%). Purification by flash column chromatography (30→50% EtOAc in hexane) yielded *tetrahydropyridine* **257h** as a pale yellow solid (48.6 mg, 47%); mp: 114-116 °C; IR (neat): ν = 1598, 1522, 1344, 1158, 1096, 853, cm^{-1}; ^{1}H-NMR (400 MHz, $CDCl_3$): δ = 8.28 (d, *J* = 8.8 Hz, 2H), 7.74 (d, *J* = 8.2 Hz, 2H), 7.63 (d, *J* = 8.8 Hz, 2H), 7.33 (d, *J* = 8.2 Hz, 2H), 4.13 (d, *J* = 11.9 Hz, 1H_a), 3.97-3.90 (m, 1H_b), 3.81 (d, *J* = 11.9 Hz, 1H_a), 2.87 (appt. t, *J* = 9.9 Hz, 1H_b), 2.82 (s, 3H), 2.80 (s, 3H), 2.55-2.46 (m, 1H_d), 2.43 (s, 3H), 2.38 (dd, *J* = 12.0, 7.6 Hz, 1H_c), 1.86 (dd, *J* = 12.0, 3.1 Hz, 1H_c); ^{13}C-NMR (101 MHz, $CDCl_3$): δ = 169.6 (C), 148.3 (C), 143.9 (C), 142.0 (C), 134.1 (C), 129.9 (2CH), 128.6 (2CH), 127.6 (2CH), 123.8 (2CH), 108.0 (C), 92.9 (C), 52.7 (CH_{2b}), 49.4 (CH_{2a}), 45.5 (CH_d), 39.8 (CH_3), 35.8 (CH_3), 33.4 (CH_{2c}), 21.7 (CH_3); HRMS (ES): *m/z* calculated for $C_{22}H_{25}N_4O_7S_2$: 521.1165, found 521.1163 $(M+H)^+$.

Tetrahydropyridine 257l

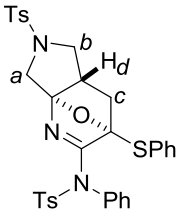

Following **GP8** using ylide **266d** (82.9 mg, 0.24 mmol), ynamide **84w** (75.9 mg, 0.20 mmol) and gold catalyst (3.9 mg, 5 mol%). Reaction times were adjusted to 45 minutes at 90 °C (at which point all ynamide was consumed by TLC) and 6 hours at 110 °C (at which point all oxazole was consumed by TLC). Purification by flash column chromatography (1:4 EtOAc:hexane) yielded *tetrahydropyridine* **257l** (119 mg, 92%);

mp: 184-186 °C; IR (neat): ν = 2951, 1582, 1518, 1343, 1242, 1158, 1093, 809 cm^{-1}; ^{1}H-NMR (400 MHz, $CDCl_3$): δ = 7.71 (d, *J* = 8.3 Hz, 2H), 7.64 (d, *J* = 8.3 Hz, 2H), 7.41-7.30 (m, 5H), 7.28-7.18 (m, 5H), 7.16-7.10 (m, 2H), 7.09-7.04 (m, 2H), 4.14 (d, *J* = 12.1 Hz, 1H_a), 3.73 (d, *J* = 12.1 Hz, 1H_a), 3.73-3.68 (m, 1H_b), 2.44 (s, 3H), 2.41 (s, 3H), 2.39-2.27 (m, 2H, 1H_b+1H_d), 1.56 (dd, *J* = 12.6, 7.1 Hz, 1H_c), 1.26 (dd, *J* = 12.6, 2.6 Hz, 1H_c); ^{13}C-NMR (101 MHz, $CDCl_3$): δ = 165.7 (C), 144.8 (C), 143.8 (C), 135.5 (C), 134.3 (C), 134.1 (2CH), 133.7 (C), 130.0 (2CH), 129.8 (3CH), 129.74 (C), 129.69 (2CH), 129.11 (2CH), 129.05 (2CH), 129.0 (CH), 128.8 (2CH), 127.6 (2CH), 106.9 (C), 97.3 (C), 52.1 (CH_{2b}), 49.6 (CH_{2a}), 45.3 (CH_d), 32.7 (CH_{2c}), 21.8 (CH_3), 21.6 (CH_3); HRMS (ES): *m/z* calculated for $C_{33}H_{32}N_3O_5S_3$: 646.1504, found 646.1513 $(M+H)^+$.

Tetrahydropyridines 277

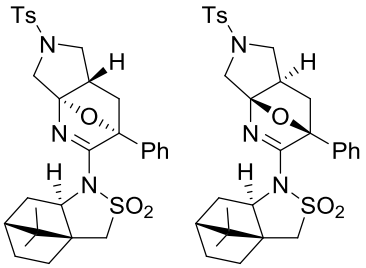

Inseparable 4:1 mixture of diastereomers

Following **GP8** using ylide **266d** (207 mg, 0.60 mmol), ynamide **84x** (158 mg, 0.50 mmol) and gold catalyst (9.7 mg, 5 mol%). Purification by flash column chromatography (25→50% EtOAc in hexane) yielded an inseparable mixture of diastereoisomers (4:1 ratio) of *tetrahydropyridines* **277** as a white solid (83.7 mg, 29%); mp: 128-133 °C; IR (neat): ν = 2958, 2879, 1568, 1333, 1234, 1160, 1140 cm^{-1}; ^{1}H-NMR (400 MHz, $CDCl_3$): δ = 7.74-7.64 (m, 2H_{major}+2H_{minor}), 7.46-7.31 (m, 5H_{major}+5H_{minor}), 7.30-7.21 (m, 2H_{major}+2H_{minor}), 4.18 (d, *J* = 11.9 Hz, 1H_{minor}), 4.14 (d, *J* = 11.7 Hz, 1H_{major}), 3.99-3.79 (m, 2H_{major}+2H_{minor}), 3.77 (d, *J* = 11.9 Hz, 1H_{minor}), 3.62 (d, *J* = 11.7 Hz, 1H_{major}), 3.25-3.10 (m, 2H_{major}+2H_{minor}), 2.82-2.70 (m, 1H_{major}+1H_{minor}), 2.54-2.31 (m, 5H_{major}+5H_{minor}), 2.11-1.72 (m, 6H_{major}+6H_{minor}), 1.43-1.23 (m, 2H_{major}+2H_{minor}), 1.07 (s, 3H_{minor}), 0.98 (s, 3H_{major}), 0.87 (s, 3H); ^{13}C-NMR (101 MHz, $CDCl_3$) *only signals assigned to the major diastereoisomer are reported*: δ = 168.7 (C), 143.7 (C), 134.1 (C), 133.8 (C), 129.9 (2CH), 129.6 (CH), 129.1 (2CH), 128.0 (2CH), 127.5 (2CH), 107.6 (C), 93.5 (C), 67.3 (CH), 53.2 (CH_2), 52.4 (CH_2), 49.7 (CH_2), 49.6 (C), 47.8 (C), 45.5 (CH), 44.9 (CH), 38.0 (CH_2), 33.0 (CH_2),

30.9 (CH_2), 26.5 (CH_2), 21.6 (CH_3), 20.8 (CH_3), 20.0 (CH_3); HRMS (ES): *m/z* calculated for $C_{30}H_{36}N_3O_5S_2$: 582.2096, found 582.2097 $(M+H)^+$.

Tetrahydropyridine 278

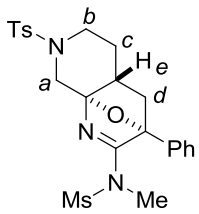

Following **GP8** using ylide **266h** (86.3 mg, 0.24 mmol), ynamide **84g** (41.9 mg, 0.20 mmol) and gold catalyst (3.9 mg, 5 mol%). Purification by flash column chromatography (30→40% EtOAc in hexane) yielded *tetrahydropyridine* **278** as a white solid (51.0 mg, 52%); mp: 200-202 °C; IR (neat): ν = 1601, 1346, 1162, 1097, 939 cm^{-1}; ^{1}H-NMR (400 MHz, $CDCl_3$): δ = 7.70 (d, *J* = 8.2 Hz, 2H), 7.53-7.48 (m, 2H), 7.45-7.38 (m, 3H), 7.32 (d, *J* = 8.2 Hz, 2H), 4.41 (d, *J* = 13.2 Hz, 1H_a), 3.86-3.78 (m, 1H_b), 3.19 (d, *J* = 13.2 Hz, 1H_a), 2.86 (s, 3H), 2.68 (s, 3H), 2.43 (s, 3H), 2.42-2.33 (m, 2H, 1H_b+1H_d), 2.06-1.98 (m, 1H_c), 1.92-1.83 (m, 1H_e), 1.65-1.53 (m, 2H, 1H_c+1H_d); ^{13}C-NMR (101 MHz, $CDCl_3$): δ = 170.2 (C), 143.8 (C), 135.3 (C), 133.3 (C), 129.8 (2CH), 129.3 (CH), 128.8 (2CH), 128.0 (2CH), 127.5 (2CH), 97.7 (C), 91.9 (C), 48.5 (CH_{2a}), 45.6 (CH_{2b}), 39.8 (CH_3), 38.2 (CH_e), 35.9 (CH_{2d}), 35.4 (CH_3), 30.7 (CH_{2c}), 21.7 (CH_3); HRMS (ES): *m/z* calculated for $C_{23}H_{27}N_3O_5S_2Na$: 512.1290, found 512.1281 $(M+Na)^+$. Crystals suitable for single crystal X-ray diffraction were grown by diffusion of hexane into a solution of **278** in CH_2Cl_2.

Oxazole 279

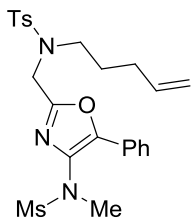

Following **GP8** using ylide **266i** (89.6 mg, 0.24 mmol), ynamide **84g** (42.2 mg, 0.20 mmol) and gold catalyst (4.0 mg, 5 mol%). Purification by flash column chromatography (7:3 hexane:EtOAc) yielded *oxazole* **279** as a white solid (81.6 mg, 81%); mp: 128-130 °C; IR (neat): ν = 1333, 1309, 1162, 1148, 972 cm^{-1}; ^{1}H-NMR (400 MHz, $CDCl_3$): δ = 7.71-7.66 (m, 2H), 7.62 (d, *J* = 8.2 Hz, 2H), 7.42-7.31 (m, 3H), 7.18 (d, *J* = 8.2 Hz, 2H), 5.76 (ddt, *J* = 17.0, 10.3, 6.6 Hz, 1H), 5.06-4.93 (m, 2H), 4.56 (s, 2H), 3.32 (t, *J* = 7.5 Hz, 2H), 3.17 (s, 3H), 3.04 (s, 3H), 2.23 (s, 3H), 2.09 (appt. q, *J* = 7.1 Hz, 2H), 1.76-1.66 (m, 2H); ^{13}C-NMR (101 MHz, $CDCl_3$): δ = 156.5 (C), 146.2 (C), 143.7 (C), 137.3 (CH), 136.5 (C), 133.2 (C), 129.8 (2CH), 129.3 (CH), 128.8 (2CH), 127.1 (2CH), 126.3 (C), 125.3 (2CH),

115.5 (CH_2), 47.9 (CH_2), 44.0 (CH_2), 37.9 (CH_3), 36.9 (CH_3), 30.6 (CH_2), 27.2 (CH_2), 21.4 (CH_3); HRMS (ES): *m/z* calculated for $C_{24}H_{29}N_3O_5S_2Na$: 526.1446, found 526.1439 $(M+Na)^+$.

Tetrahydrofuran 283

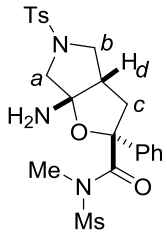

$TsOH{\cdot}H_2O$ (190 mg, 1.0 mmol) was added to a solution of tetrahydropyridine **257d** (95.1 mg, 0.20 mmol) in MeOH (2 mL) and the reaction mixture was stirred at room temperature for 20 minutes. Satd. $NaHCO_{3(aq)}$ solution (5 mL) was added and the mixture was extracted with CH_2Cl_2 (3 x 15 mL). The combined organic extracts were dried over Na_2SO_4, concentrated under reduced pressure and purified by flash column chromatography (40⟶75% EtOAc in hexane) to give *tetrahydrofuran* **283** as a white solid (76.1 mg, 77%); mp: 88-90 °C; IR (neat): ν = 3398, 2928, 2861, 1683, 1341, 1158, 761 cm^{-1}; ^{1}H-NMR (400 MHz, $CDCl_3$): δ = 7.66 (d, *J* = 8.2 Hz, 2H), 7.41-7.29 (m, 7H), 3.91 (d, *J* = 9.7 Hz, 1H_a), 3.43 (dd, *J* = 12.9, 8.1 Hz, 1H_c), 3.35 (s, 3H), 3.30 (d, *J* = 9.7 Hz, 1H_b), 3.03-2.92 (m, 4H, CH_3+1H_b), 2.85 (d, *J* = 9.7 Hz, 1H_a), 2.60-2.51 (m, 1H_d), 2.43 (s, 3H), 2.12 (br s, 2O*H*), 1.79 (dd, *J* = 12.9, 9.2 Hz, 1H_c); ^{13}C-NMR (101 MHz, $CDCl_3$): δ = 174.9 (C), 144.1 (C), 139.0 (C), 132.0 (C), 129.9 (2CH), 129.4 (2CH), 128.5 (CH), 128.0 (2CH), 123.4 (2CH), 104.0 (C), 90.9 (C), 60.7 (CH_{2a}), 53.1 (CH_{2b}), 49.5 (CH_d), 46.2 (CH_{2c}), 42.0 (CH_3), 33.5 (CH_3), 21.7 (CH_3); HRMS (ES): *m/z* calculated for $C_{22}H_{27}N_3O_6S_2Na$: 516.1239, found 516.1251 $(M+Na)^+$. Crystals suitable for single crystal X-ray diffraction were grown by diffusion of hexane into a solution of **283** in CH_2Cl_2.

Piperidine 284

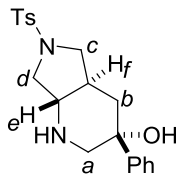

$LiAlH_4$ (32 mg, 0.84 mmol) was added to a solution of tetrahydropyridine **257d** (80.0 mg, 0.17 mmol) in THF (2 mL) and the reaction mixture was stirred at room temperature for 20 minutes. Satd. sodium potassium tartrate$_{(aq)}$ solution (10 mL) was added and the mixture was extracted with CH_2Cl_2 (3 x 10 mL). The combined organic extracts were dried over Na_2SO_4, concentrated under reduced pressure and purified by flash column chromatography (80⟶100% EtOAc in hexane) to give *piperidine* **284** as a white solid (41.0 mg, 65%); mp: 64-66 °C; IR (neat): ν = 3322, 2930, 1334, 1152, 1092, 1015, 702 cm^{-1}; ^{1}H-NMR (400 MHz, $CDCl_3$): δ = 7.69-7.63 (m, 4H), 7.37-7.31 (m, 2H), 7.31-7.26 (m, 3H), 3.64-3.55 (m, 2H, 1H_a+1H_d), 3.39 (dd, J = 9.3, 7.1 Hz, 1H_c), 2.94-2.81 (m, 3H, 1H_a+1H_c+1H_d), 2.58 (appt. td, J = 10.4, 7.0 Hz, 1H_e), 2.45-2.37 (m, 4H, CH_3+1H_b), 1.84 (br s, 2H, OH+NH), 1.58 (appt. t, J = 12.5 Hz, 1H_b), 1.48-1.35 (m, 1H_f); ^{13}C-NMR (101 MHz, $CDCl_3$): δ = 145.0 (C), 143.5 (C), 134.8 (C), 129.9 (2CH), 128.6 (2CH), 128.0 (CH), 127.4 (2CH), 126.7 (2CH), 71.4 (C), 61.8 (CH_e), 57.1 (CH_{2a}), 51.4 (CH_{2d}), 50.8 (CH_{2c}), 41.29 (CH_f), 41.25 (CH_{2b}), 21.7 (CH_3); HRMS (ES): *m/z* calculated for $C_{20}H_{25}N_2O_3S$: 373.1586, found 373.1576 $(M+H)^+$. In order to obtain crystals suitable for X-ray diffraction **284** was dissolved in 4 M HCl in 1,4-dioxane. The dioxane was removed under reduced pressure and crystals of **284.HCl** were grown by dissolving in refluxing MeCN/H_2O followed by slow evaporation of the solvent.

5.1.8: Imidazolium Salts

5.1.8.1: General procedure for synthesis of NHC.HPF$_6$ salts (GP9)

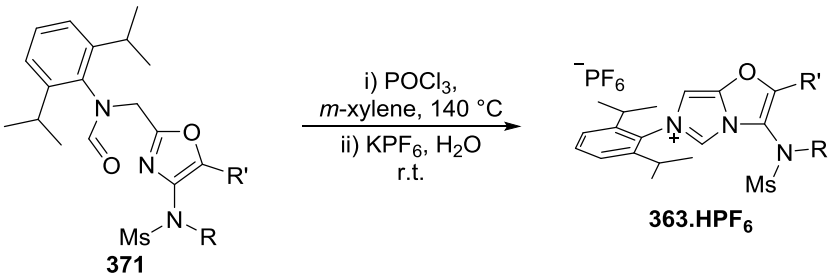

Adapted from a literature procedure,[128] under an argon atmosphere $POCl_3$ (3.0 eq.) was added to a solution of oxazole (1.0 eq.) in *m*-xylene (0.1 M with respect to oxazole) and the reaction mixture was heated at 140 °C for 64 hours. After cooling to room temperature, the impure NHC.HCl salt was isolated either by flash column chromatography (0→10% MeOH in CH_2Cl_2) or by filtration of the of the reaction mixture through a 5 cm pad of silica gel (washing first with CH_2Cl_2 to remove apolar impurities and then eluting the crude NHC.HCl salt with 10% MeOH in CH_2Cl_2). The resulting brown solid was taken up in refluxing H_2O (~10 mL) and the hot solution was filtered through glass wool, the flask was then washed out with additional boiling H_2O (~5 mL) which was also filtered though the glass wool. The aqueous filtrate was allowed to cool to room temperature and a saturated solution of $KPF_{6(aq)}$ (2.0 eq.) was added, leading to instant precipitation of the crude NHC.HPF$_6$ salt. The solid was collected by filtration, washed with ice-cold water and Et_2O, and then recrystallised from acetone by addition of Et_2O to give the *NHC.HPF$_6$ salt*.

363a.HPF$_6$

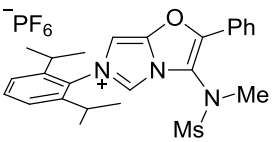

Following **GP9** using oxazole **371a** (827 mg, 1.8 mmol) and $POCl_3$ (500 µL, 5.4 mmol), purification by flash column chromatography and ion exchange with KPF_6 (644 mg, 3.5 mmol) gave **363a.HPF$_6$** as a white solid (706 mg, 67%); mp: 236-238 °C; IR (neat): ν = 3148, 2967, 1622, 1346, 1236, 1156, 1061, 830 cm^{-1}; ^{1}H-NMR (400 MHz, d_6-acetone): δ = 9.81 (d, *J* = 1.5 Hz, 1H), 8.16-8.12 (m, 2H), 8.10 (d, *J* = 1.5 Hz, 1H),

7.77-7.69 (m, 4H), 7.55 (d, *J* = 7.8 Hz, 2H), 3.62 (s, 3H), 3.41 (s, 3H), 2.67 (hept, *J* = 6.8 Hz, 2H), 1.26 (d, *J* = 6.8 Hz, 6H), 1.24 (d, *J* = 6.8 Hz, 6H); ^{13}C-NMR (101 MHz, d_6-acetone): δ = 152.4 (C), 146.9 (2C), 145.7 (C), 133.08 (CH), 133.05 (CH), 132.6 (C), 130.6 (2CH), 127.7 (2CH), 125.7 (C), 125.6 (2CH), 121.8 (CH), 119.2 (C), 101.4 (CH), 40.1 (CH_3), 37.1 (CH_3), 29.2 (2CH), 24.7 ($2CH_3$), 24.3 ($2CH_3$); ^{19}F{^{1}H}-NMR (282 MHz, Acetone): δ = -72.6 (d, J_{F-P} = 708 Hz); ^{31}P{^{1}H}-NMR (121 MHz, d_6-acetone): δ = -145.2 (hept, J_{F-P} = 708 Hz); HRMS (ES): *m/z* calculated for $C_{25}H_{30}N_3O_3S$: 452.2008, found 452.2004 $(M\text{-}PF_6)^+$; Anal. calculated for $C_{25}H_{30}F_6N_3O_3PS$: C, 50.25; H, 5.06; N, 7.03. Found: C, 50.19; H, 4.86; N, 7.10.

363b.HPF$_6$

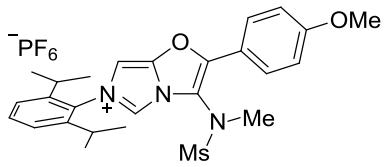

Following **GP9** using oxazole **371b** (343 mg, 0.7 mmol) and $POCl_3$ (200 µL, 2.1 mmol), purification by flash column chromatography and ion exchange with KPF_6 (254 mg, 1.4 mmol) gave **363b.HPF$_6$** as a white solid (232 mg, 53%); mp: 146-148 °C; IR (neat): ν = 3148, 2969, 1620, 1608, 1346, 1261, 1178, 1155, 830 cm^{-1}; ^{1}H-NMR (400 MHz, $CDCl_3$): δ = 8.51 (d, *J* = 1.5 Hz, 1H), 7.84 (d, *J* = 9.0 Hz, 2H), 7.56 (t, *J* = 7.9 Hz, 1H), 7.33 (d, *J* = 7.9 Hz, 2H), 7.09 (d, *J* = 9.0 Hz, 2H), 7.03 (d, *J* = 1.5 Hz, 1H), 3.89 (s, 3H), 3.42 (s, 3H), 3.18 (s, 3H), 2.39 (hept, *J* = 6.8 Hz, 2H), 1.21 (d, *J* = 6.8 Hz, 6H), 1.18 (d, *J* = 6.8 Hz, 6H); ^{13}C-NMR (101 MHz, $CDCl_3$): δ = 162.9 (C), 152.5 (C), 146.0 (2C), 143.8 (C), 132.4 (CH), 131.0 (C), 128.9 (2CH), 124.8 (2CH), 119.9 (CH), 116.4 (C), 116.1 (C), 115.4 (2CH), 99.4 (CH), 55.7 (CH_3), 40.2 (CH_3), 36.9 (CH_3), 28.7 (2CH), 24.6 ($2CH_3$), 24.2 ($2CH_3$); ^{19}F{^{1}H}-NMR (282 MHz, $CDCl_3$): δ = -72.9 (d, J_{F-P} = 713 Hz); ^{31}P{^{1}H}-NMR (121 MHz, $CDCl_3$): δ = -144.6 (hept, J_{F-P} = 713 Hz); HRMS (ES): *m/z* calculated for $C_{26}H_{32}N_3O_4S$: 482.2114, found 482.2117 $(M\text{-}PF_6)^+$; Anal. calculated for $C_{26}H_{32}F_6N_3O_4PS$: C, 49.76; H, 5.14; N, 6.70. Found: C, 49.81; H, 5.15; N, 6.77.

363c.HPF$_6$

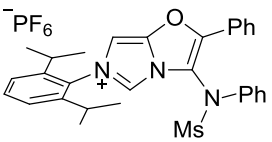

Following **GP9** using oxazole **371c** (459 mg, 0.86 mmol) and $POCl_3$ (240 µL, 2.6 mmol), purification by filtration through silica gel and ion exchange with KPF_6 (317 mg, 1.7 mmol) gave **363c.HPF$_6$** as a white solid (154 mg, 27%); mp: 146-148 °C; IR (neat): ν = 3147, 2968, 1618, 1496, 1365, 1236, 1161, 1060, 966, 834, 766 cm^{-1}; ^{1}H-NMR (400 MHz, $CDCl_3$): δ = 9.03 (d, *J* = 1.3 Hz, 1H), 8.04-7.93 (m, 2H), 7.63-7.53 (m, 4H), 7.52-7.48 (m, 2H), 7.42-7.29 (m, 5H), 7.17 (d, *J* = 1.3 Hz, 1H), 3.36 (s, 3H), 2.34 (hept, *J* = 6.8 Hz, 2H), 1.26 (d, *J* = 6.8 Hz, 6H), 1.21 (d, *J* = 6.8 Hz, 6H); ^{13}C-NMR (101 MHz, $CDCl_3$): δ = 153.6 (C), 145.5 (2C), 143.8 (C), 138.0 (C), 132.9 (CH), 132.5 (CH), 131.0 (C), 130.6 (2CH), 129.6 (2CH), 129.4 (CH), 127.7 (2CH), 125.7 (2CH), 124.8 (2CH), 123.6 (C), 120.8 (CH), 117.4 (C), 100.0 (CH), 41.0 (CH_3), 29.0 (2CH), 24.6 ($2CH_3$), 24.0 ($2CH_3$); ^{19}F{^{1}H}-NMR (282 MHz, $CDCl_3$): δ = -72.1 (d, J_{F-P} = 713 Hz); ^{31}P{^{1}H}-NMR (121 MHz, $CDCl_3$): δ = -144.4 (hept, J_{F-P} = 713 Hz); HRMS (ES): *m/z* calculated for $C_{30}H_{32}N_3O_3S$: 514.2164, found 514.2171 $(M\text{-}PF_6)^+$; Anal. calculated for $C_{30}H_{32}F_6N_3O_3PS$: C, 54.63; H, 4.89; N, 6.37. Found: C, 54.49; H, 4.76; N, 6.40.

363d.HPF$_6$

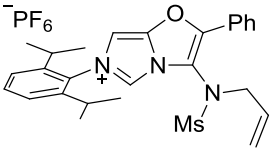

Following **GP9** using oxazole **371d** (435 mg, 0.88 mmol) and $POCl_3$ (250 µL, 2.7 mmol), purification by flash column chromatography and ion exchange with KPF_6 (324 mg, 1.8 mmol) gave **363d.HPF$_6$** as a yellow solid (80 mg, 14%); mp: 200-202 °C; IR (neat): ν = 2968, 2934, 1619, 1353, 1299, 1164, 1060, 842, 730 cm^{-1}; ^{1}H-NMR (400 MHz, $CDCl_3$): δ = 8.60 (s, 1H), 8.01-7.92 (m, 2H), 7.64-7.54 (m, 4H), 7.33 (d, *J* = 7.8 Hz, 2H), 7.16 (s, 1H), 6.08-5.96 (m, 1H), 5.30 (d, *J* = 16.9 Hz, 1H), 5.17 (d, *J* = 10.0 Hz, 1H), 4.46-4.30 (m, 2H), 3.18 (s, 3H), 2.32 (hept, *J* = 6.7 Hz, 2H), 1.19 (appt. d, *J* = 6.7 Hz, 12H); ^{13}C-NMR (101 MHz, $CDCl_3$): δ = 153.4 (C), 145.7 (2C), 144.0 (C), 132.7 (CH), 132.5 (CH), 131.2 (CH), 130.9 (C), 129.8 (2CH), 127.0 (2CH), 124.8 (2CH), 123.9 (C), 123.1 (CH_2), 119.9 (CH), 116.3 (C), 100.1 (CH), 53.9 (CH_2), 41.2 (CH_3), 28.8 (2CH), 24.31 ($2CH_3$), 24.27 ($2CH_3$); ^{19}F{^{1}H}-NMR (282 MHz, $CDCl_3$): δ = -72.6 (d, J_{F-P} = 713 Hz);

$^{31}P\{^{1}H\}$-NMR (121 MHz, $CDCl_3$): δ = -144.5 (hept, J_{F-P} = 713 Hz); HRMS (ES): *m/z* calculated for $C_{27}H_{32}N_3O_3S$: 478.2164, found 478.2161 $(M\text{-}PF_6)^+$; Anal. calculated for $C_{27}H_{32}F_6N_3O_3PS$: C, 52.00; H, 5.17; N, 6.74. Found: C, 51.82; H, 5.11; N, 6.85.

5.1.9: Organometallic complexes

5.1.9.1: General procedure for synthesis of (NHC)MCl complexes (GP10)

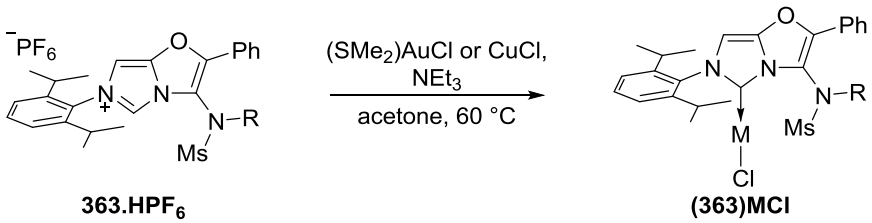

363.HPF$_6$ **(363)MCl**

Adapted from a literature procedure,[153b] a vial was charged sequentially with NHC.HX, the corresponding metal chloride, NEt_3 (70 µL, 0.50 mmol) and acetone (2 mL). and heated at 60 °C for 18 hours. The solvent was removed under reduced pressure and the crude mixture was taken up in CH_2Cl_2 (~10 mL) and washed with H_2O (2 x 10 mL). The organic phase was dried over Na_2SO_4, concentrated under reduced pressure and purified by flash column chromatography to give the (NHC)MCl complex.

(IPr)AuCl

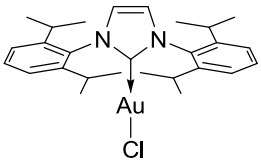

Following **GP10** using IPr.HCl (85 mg, 0.20 mmol) and (DMS)AuCl (65 mg, 0.22 mmol). Flash column chromatography was replaced by filtration through a 5 cm pad of silica gel (eluting with CH_2Cl_2) to give **(IPr)AuCl** as a white solid (68.6 mg, 55%); mp: decomp. 280 °C; IR (neat): ν = 2965, 2926, 2869, 1470, 1456, 1416, 1059, 938, 808, 763, cm^{-1}; ^{1}H-NMR (400 MHz, $CDCl_3$): δ = 7.50 (t, *J* = 7.8 Hz, 2H), 7.29 (d, *J* = 7.8 Hz, 4H), 7.17 (s, 2H), 2.55 (hept, *J* = 6.9 Hz, 4H), 1.35 (d, *J* = 6.9 Hz, 12H), 1.22 (d, *J* = 6.9 Hz, 12H). Spectroscopic data matched those reported.[211]

(363a)AuCl

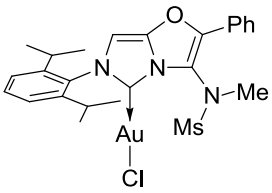

Following **GP10** using **363a.HPF$_6$** (100 mg, 0.17 mmol) and (DMS)AuCl (59.2 mg, 0.20 mmol). Purification by flash column chromatography (30→50% EtOAc in hexane) gave **(363a)AuCl** as a white solid (99.6 mg, 87%); mp: decomp. 230 °C; IR (neat): ν = 3144, 2968, 1621, 1351, 1158, 1055, 965 cm^{-1}; ^{1}H-NMR (400 MHz, $CDCl_3$): δ = 8.01-7.95 (m, 2H), 7.59-7.49 (m, 4H), 7.28 (d, *J* = 7.8 Hz, 2H), 6.79 (s, 1H), 3.73 (s, 3H), 3.53 (s, 3H), 2.48-2.31 (m, 2H), 1.34-1.28 (m, 6H), 1.20-1.14 (m, 6H); ^{13}C-NMR (101 MHz, $CDCl_3$): δ = 154.6 (C), 151.0 (C), 145.9 (C), 145.7 (C), 144.5 (C), 135.1 (C), 131.5 (CH), 131.2 (CH), 129.4 (2CH), 126.1 (2CH), 125.4 (C), 124.5 (2CH), 118.0 (C), 97.4 (CH), 43.0 (CH_3), 37.8 (CH_3), 28.6 (2CH), 24.7 ($2CH_3$), 24.6 (CH_3), 24.5 (CH_3); Anal. calculated for $C_{25}H_{29}AuClN_3O_3S$: C, 43.90; H, 4.27; N, 6.14. Found: C, 44.10; H, 4.17; N, 6.15. Crystals suitable for single crystal X-ray diffraction were grown by slow evaporation of a solution of **(363a)AuCl** in EtOAc.

(363c)AuCl

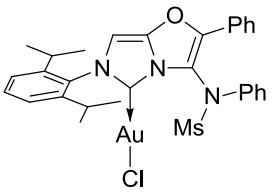

Following **GP10** using **363c.HPF$_6$** (100 mg, 0.15 mmol) and (DMS)AuCl (53.5 mg, 0.18 mmol). Purification by flash column chromatography (20→50% EtOAc in hexane) gave **(363c)AuCl** as a white solid (85.5 mg, 76%); mp: 258-260 °C; IR (neat): ν = 3127, 2967, 2930, 2873, 1671, 1616, 1364, 1230, 1162, 1063, 961 cm^{-1}; ^{1}H-NMR (400 MHz, $CDCl_3$): δ = 8.08-8.01 (m, 2H), 7.75-7.69 (m, 2H), 7.61-7.54 (m, 4H), 7.44-7.38 (m, 2H), 7.38-7.31 (m, 3H), 6.88 (s, 1H), 3.72 (s, 3H), 2.52 (hept, *J* = 6.9 Hz, 1H), 2.37 (hept, *J* = 6.9 Hz, 1H), 1.34 (d, *J* = 6.9 Hz, 3H), 1.30 (d, *J* = 6.9 Hz, 3H), 1.19 (d, *J* = 6.9 Hz, 3H), 1.17 (d, *J* = 6.9 Hz, 3H); ^{13}C-NMR (101 MHz, $CDCl_3$): δ = 155.5 (C), 152.4 (C), 146.3 (C), 146.2 (C), 145.1 (C), 139.5 (C), 135.8 (C), 132.0 (CH), 131.3 (CH), 130.4 (2CH), 129.6 (2CH), 128.2 (CH), 127.2 (2CH), 125.4 (C), 124.7 (CH), 124.6 (CH), 124.4 (2CH), 117.9 (C), 97.9 (CH), 43.2 (CH_3), 28.9 (2CH), 24.6 ($2CH_3$), 24.52 (CH_3), 24.45 (CH_3); Anal. calculated for $C_{30}H_{31}AuClN_3O_3S$: C, 48.30; H, 4.19; N, 5.63.

Found: C, 48.12; H, 3.85; N, 5.81. Crystals suitable for single crystal X-ray diffraction were grown by diffusion of pentane into a solution of **(363c)AuCl** in CH_2Cl_2.

(363a)CuCl

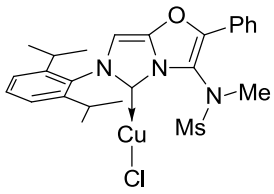

Following **GP10** using **363a.HPF$_6$** (100 mg, 0.17 mmol) and CuCl (34 mg, 0.34 mmol). Purification by flash column chromatography (30% EtOAc in hexane) gave **(363a)CuCl** as a white solid (49.9 mg, 54%); mp: 216-217 °C; IR (neat): ν = 3149, 2962, 2926, 2869, 1620, 1351, 1157, 1057, 1036, 964 cm^{-1}; ^{1}H-NMR (400 MHz, $CDCl_3$): δ = 8.01-7.95 (m, 2H), 7.58-7.48 (m, 4H), 7.29 (d, *J* = 8.0 Hz, 2H), 6.76 (s, 1H), 3.73 (s, 3H), 3.48 (s, 3H), 2.44 (hept, *J* = 6.8 Hz, 1H), 2.35 (hept, *J* = 6.8 Hz, 1H), 1.29 (d, *J* = 6.8 Hz, 3H), 1.26 (d, *J* = 6.8 Hz, 3H), 1.19 (d, *J* = 6.8 Hz, 3H), 1.17 (d, *J* = 6.8 Hz, 3H); ^{13}C-NMR (101 MHz, $CDCl_3$): δ = 159.2 (C), 150.5 (C), 145.9 (C), 145.7 (C), 145.1 (C), 135.5 (C), 131.3 (CH), 131.1 (CH), 129.4 (2CH), 126.1 (2CH), 125.6 (C), 124.4 (2CH), 118.1 (C), 97.5 (CH), 43.1 (CH_3), 37.3 (CH_3), 28.6 (2CH), 25.1 (CH_3), 25.0 (CH_3), 24.5 (CH_3), 24.2 (CH_3); Anal. calculated for $C_{25}H_{29}ClCuN_3O_3S$: C, 54.54; H, 5.31; N, 7.63. Found: C, 54,76; H, 5.32; N, 7.70. Crystals suitable for single crystal X-ray diffraction were grown by diffusion of pentane into a solution of **(363a)CuCl** in CH_2Cl_2/$CDCl_3$.

(363a)Ir(CO)$_2$Cl

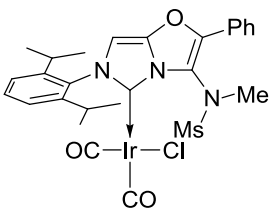

Inside a N_2 filled glovebox NaO^tBu (21.0 mg, 0.22 mmol) was added to a solution of **363a.HPF$_6$** (119 mg, 0.20 mmol) in THF (2 mL) and the suspension was stirred at room temperature for 20 minutes before filtration through a 3 cm pad of celite (washing with 1 mL of THF) into a vial containing $[Ir(cod)Cl]_2$ (71.8 mg, 0.107 mmol, 1.07 eq.) and the resulting suspension was stirred for 1 hour at room temperature. The vial was removed from the glovebox and the contents filtered through a 3 cm pad of silica gel and the filtrate purified by flash column chromatography (4:1 hexane:EtOAc). The resulting yellow solid **(363a)Ir(cod)Cl** was dissolved in CH_2Cl_2 (3 mL) and CO (balloon pressure) was bubbled through the stirred solution for 5 minutes. The solvent was removed under reduced pressure and the resulting solid purified by flash column chromatography (3:1 hexane:EtOAc) to give **(363a)Ir(CO)$_2$Cl** as a yellow solid (43.0 mg, 29% over two steps); mp: 110-112 °C; IR (CH_2Cl_2): ν = 2068.19 (CO), 1986.32 (CO) cm^{-1}; *Restricted rotation around the metal-carbene bond results in 3 sets of signals (1 major, 2 minor)*; ^{1}H-NMR (400 MHz, $CDCl_3$): δ = 8.00-7.92 (m, 2H), 7.61-7.50 (m, 4H), 7.37-7.28 (m, 2H), 6.80 (s, 1H), 3.75_{minor} and 3.68_{major} and 3.63_{minor} (s, 3H), 3.71_{minor} and 3.47_{major} and 3.43_{minor} (s, 3H), 2.87-2.76 (m, 1H), 2.53-2.41 (m, 1H), $1.44\text{-}1.40_{minor}$ and $1.36\text{-}1.27_{major}$ (m, 6H), 1.13 (d, *J* = 6.7 Hz, 3H), 1.11-1.04 (m, 3H); ^{13}C-NMR (101 MHz, $CDCl_3$) *Only the major rotamer is reported*: δ = 180.4 (CO), 167.7 (CO), 159.8 (C), 150.3 (C), 147.2 (C), 145.6 (C), 145.3 (C), 136.1 (C), 131.3 (CH), 131.0 (CH), 129.5 (2CH), 126.7 (2CH), 125.5 (C), 124.5 (CH), 123.8 (CH), 119.7 (C), 99.0 (CH), 42.4 (CH_3), 38.1 (CH_3), 28.6 (2CH), 27.3 (CH_3), 26.4 (CH_3), 23.5 (CH_3), 22.1 (CH_3); Anal. calculated for $C_{27}H_{29}ClIrN_3O_5S$: C, 44.10; H, 3.98; N, 5.71. Found: C, 44.29; H, 4.06; N, 5.43.

(363b)Ir(CO)$_2$Cl

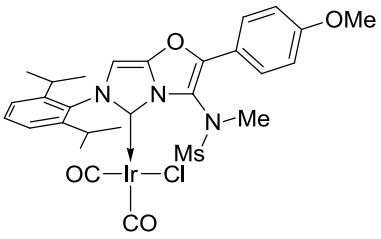

Inside a N_2 filled glovebox NaO^tBu (21.0 mg, 0.22 mmol) was added to a solution of **363b.HPF$_6$** (125 mg, 0.20 mmol) in THF (2 mL) and the suspension was stirred at room temperature for 20 minutes before filtration through a 3 cm pad of celite (washing with 1 mL of THF) into a vial containing $[Ir(cod)Cl]_2$ (70.0 mg, 0.104 mmol, 1.04 eq.) and the resulting suspension was stirred for 1 hour at room temperature. The vial was removed from the glovebox and the contents filtered through a 3 cm pad of silica gel and the filtrate purified by flash column chromatography (4:1 hexane:EtOAc). The resulting yellow solid **(363b)Ir(cod)Cl** was dissolved in CH_2Cl_2 (3 mL) and CO (balloon pressure) was bubbled through the stirred solution for 5 minutes. The solvent was removed under reduced pressure and the resulting solid purified by flash column chromatography (3:1 hexane:EtOAc) to give **(363b)Ir(CO)$_2$Cl** as a yellow solid (34.2 mg, 22% over two steps); mp: 114-116 °C; IR (CH_2Cl_2): ν = 2067.92 (CO), 1985.97 (CO) cm^{-1}; *Restricted rotation around the metal-carbene bond results in 3 sets of signals (1 major, 2 minor)*; ^{1}H-NMR (400 MHz, $CDCl_3$): δ = 7.94-7.87 (m, 2H), 7.56-7.49 (m, 1H), 7.36-7.28 (m, 2H), 7.10-7.03 (m, 2H), 6.78 (s, 1H), 3.89 (s, 3H), 3.74_{minor} and 3.68_{major}* and 3.62_{minor} (s, 3H), 3.68_{minor}* and 3.46_{major} and 3.42_{minor} (s, 3H), 2.88-2.74 (m, 1H), 2.55-2.41 (m, 1H), 1.44-1.39 and 1.35-1.27 (m, 6H), 1.16-1.10 (m, 3H), 1.10-1.03 (m, 3H); ^{13}C-NMR (101 MHz, $CDCl_3$) *Only the major rotamer is reported*: δ = 180.4 (CO), 167.7 (CO), 161.9 (C), 159.3 (C), 150.5 (C), 147.3 (C), 145.5 (C), 145.4 (C), 136.1 (C), 131.0 (CH), 128.4 (2CH), 124.5 (CH), 124.4 (C), 123.8 (CH), 117.8 (C), 114.9 (2CH), 98.9 (CH), 55.6 (CH_3), 42.4 (CH_3), 38.0 (CH_3), 28.62 (CH), 28.61 (CH), 27.3 (CH_3), 26.4 (CH_3), 23.5 (CH_3), 22.1 (CH_3); Anal. calculated for $C_{28}H_{31}ClIrN_3O_6S$: C, 43.94; H, 4.08; N, 5.49. Found: C, 44.25; H, 4.22; N, 5.32. *The overlap of these two signals was determined using an HSQC spectrum.

Alkyne 404

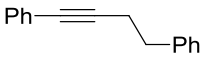

Following a literature procedure,[212] under an argon atmosphere $Pd(PPh_3)_4Cl_2$ (151 mg, 2 mol%), CuI (82 mg, 4 mol%), degassed THF (54 mL), PhI (2.19 g, 10.7 mmol), degassed NEt_3 (10.5 mL) and 4-phenyl-1-butyne (1.54 g, 11.8 mmol) were added sequentially to a two neck flask and the reaction mixture was stirred for 20 hours at room temperature. After this time the mixture was concentrated to a volume of ~5 mL and filtered through a 5 cm plug of silica gel (eluting with Et_2O) and the filtrate was concentrated under reduced pressure and purified by flash column chromatography (0⟶4% EtOAc in hexane) to give *alkyne* **404** as a colourless oil (1.46 g, 66%); IR (neat): ν = 3028, 2927, 1599, 1490, 1454, 1442, 753, 690 cm^{-1}; ^{1}H-NMR (400 MHz, $CDCl_3$): δ = 7.38-7.17 (m, 10H), 2.91 (t, *J* = 7.5 Hz, 2H), 2.67 (t, *J* = 7.5 Hz, 2H); ^{13}C-NMR (101 MHz, $CDCl_3$): δ = 140.9 (C), 131.7 (2CH), 128.7 (2CH), 128.5 (2CH), 128.3 (2CH), 127.8 (CH), 126.5 (CH), 124.0 (C), 89.6 (C), 81.5 (C), 35.3 (CH_2), 21.8 (CH_2). Spectroscopic data matched those reported.[212]

5.1.10: Hydration of alkyne 404

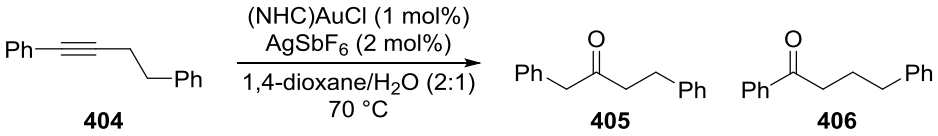

Following a literature procedure,[167a] $AgSbF_6$ (6.9 mg, 2 mol%), (NHC)AuCl (1 mol%), degassed 1,4-dioxane (670 µL), alkyne **404** (206 mg, 1.0 mmol) and degassed H_2O (330 µL) were added to a Schlenk tube under an argon atmosphere and the reaction mixture was heated at 70 °C for 17 hours. H_2O (5 mL) was added and the mixture was extracted with CH_2Cl_2 (2 x 5 mL). The combined organic extracts were dried over Na_2SO_4 and purified by flash column chromatography (19:1 hexane:EtOAc) to give a mixture of *ketones* **405** and **406** as a clear oil. Product ratios were determined by ^{1}H-NMR spectroscopy with comparison to the literature spectra for **405**[213] and **406**.[214]

5.2: HPLC Traces

5.2.1: Ester 147f

Using a Phenominex® Cellulose 1 column (250 x 4.6 mm) in 20% MeCN in H_2O at 25 °C with a flow rate of 1 mL/min, injection volume of 20 µL and a detection wavelength of 210 nm.

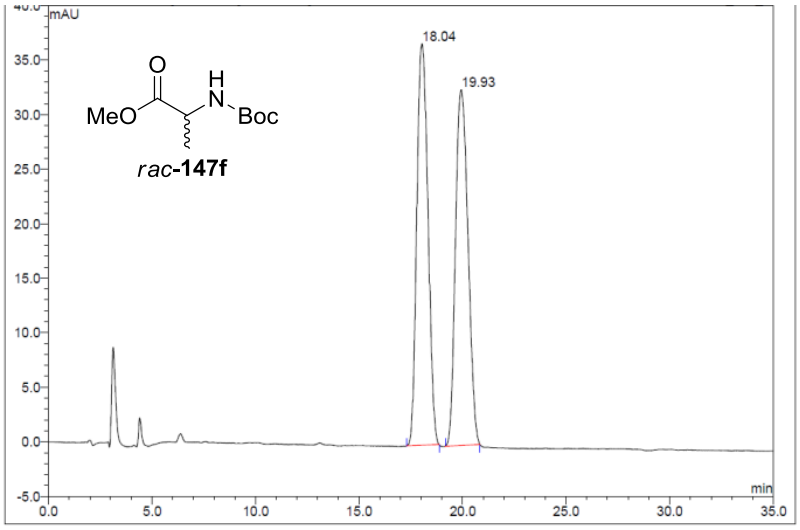

No.	Ret.Time min	Peak Name	Height mAU	Area mAU*min	Rel.Area %	Amount	Type
1	18.04	n.a.	36.833	22.964	50.12	n.a.	BMB*
2	19.93	n.a.	32.632	22.856	49.88	n.a.	BMB*
Total:			69.465	45.820	100.00	0.000	

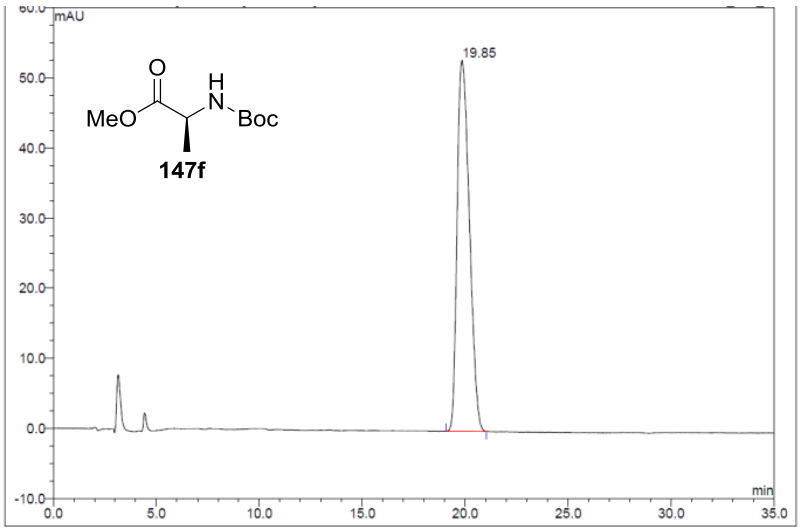

No.	Ret.Time min	Peak Name	Height mAU	Area mAU*min	Rel.Area %	Amount	Type
1	19.85	n.a.	52.929	36.543	100.00	n.a.	BMB
Total:			52.929	36.543	100.00	0.000	

5.2.2: Oxazole 151c

Using a Phenominex® Cellulose 3 column (250 x 4.6 mm) in 35% MeCN in H_2O at 25 °C with a flow rate of 0.75 mL/min, injection volume of 10 µL and a detection wavelength of 210 nm.

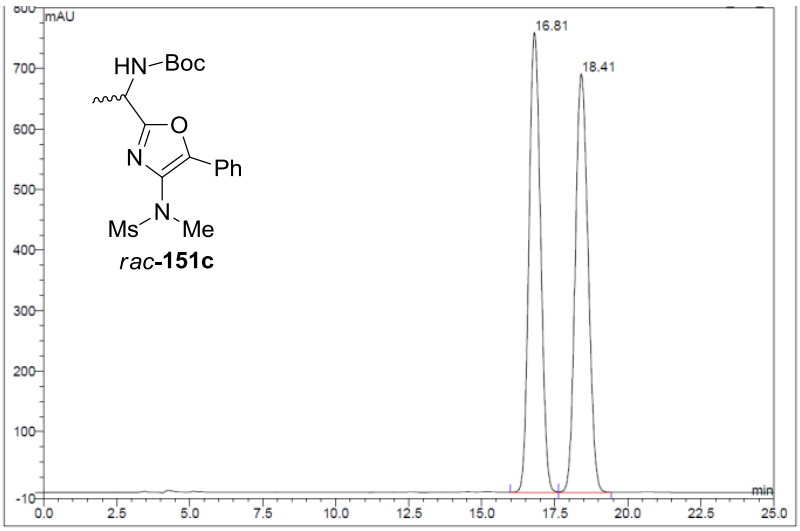

No.	Ret.Time min	Peak Name	Height mAU	Area mAU*min	Rel.Area %	Amount	Type
1	16.81	n.a.	758.896	349.779	49.89	n.a.	BM
2	18.41	n.a.	690.636	351.349	50.11	n.a.	MB
Total:			1449.532	701.127	100.00	0.000	

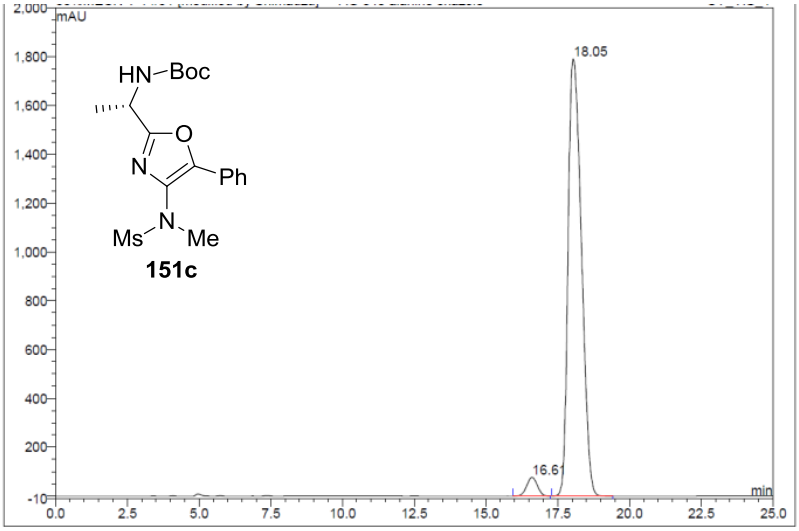

No.	Ret.Time min	Peak Name	Height mAU	Area mAU*min	Rel.Area %	Amount	Type
1	16.61	n.a.	76.060	32.645	3.29	n.a.	BMB
2	18.05	n.a.	1790.683	960.555	96.71	n.a.	BMB
Total:			1866.743	993.200	100.00	0.000	

5.3: X-Ray Data

5.3.1: Tetrahydropyridine 278

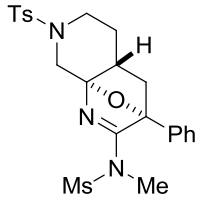

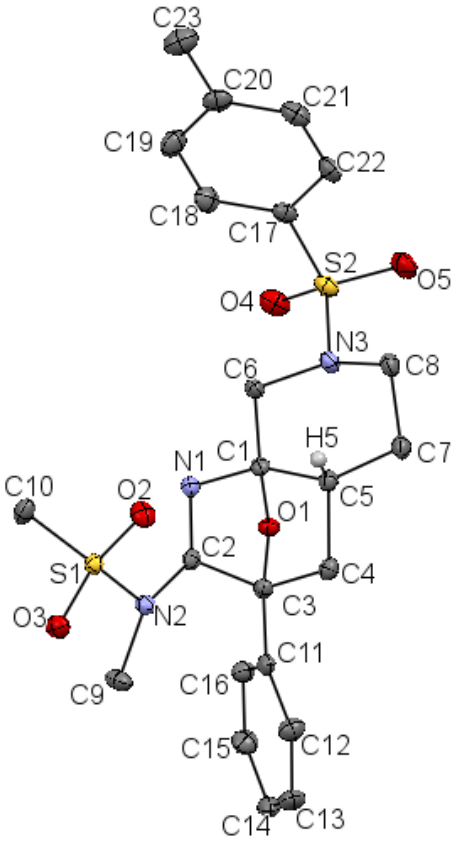

Table 1 Crystal data and structure refinement for 278.

Identification code	**278**
Empirical formula	$C_{23}H_{27}N_3O_5S_2$
Formula weight	489.59
Temperature/K	100.00(10)
Crystal system	monoclinic
Space group	$P2_1/n$
a/Å	10.94883(18)
b/Å	10.88873(18)
c/Å	19.5589(3)
α/°	90
β/°	102.1791(16)
γ/°	90
Volume/Å^3	2279.31(7)
Z	4
ρ_{calc}g/cm^3	1.427
μ/mm^{-1}	0.275
F(000)	1032.0
Crystal size/mm^3	0.3425 × 0.1255 × 0.1122
Radiation	MoKα (λ = 0.71073)
2Θ range for data collection/°	6.038 to 52.742
Index ranges	-13 ≤ h ≤ 13, -13 ≤ k ≤ 13, -24 ≤ l ≤ 24
Reflections collected	24092
Independent reflections	4667 [R_{int} = 0.0263, R_{sigma} = 0.0205]
Data/restraints/parameters	4667/0/301
Goodness-of-fit on F^2	1.045
Final R indexes [I>=2σ (I)]	R_1 = 0.0326, wR_2 = 0.0807
Final R indexes [all data]	R_1 = 0.0391, wR_2 = 0.0851
Largest diff. peak/hole / e Å^{-3}	0.38/-0.40

Table 2 Fractional Atomic Coordinates (×10^4) and Equivalent Isotropic Displacement Parameters (Å^2×10^3) for 278. U_{eq} is defined as 1/3 of of the trace of the orthogonalised U_{IJ} tensor.

Atom	*x*	*y*	*z*	U(eq)
C1	5902.7(14)	2626.9(14)	2586.2(8)	12.1(3)
C2	4947.7(14)	1770.1(14)	3316.2(8)	12.4(3)
C3	5822.6(14)	2822.2(14)	3661.4(8)	12.7(3)
C4	5087.9(14)	3983.9(14)	3329.9(8)	15.0(3)
C5	5202.1(14)	3861.6(14)	2557.6(8)	13.5(3)
C6	6521.0(14)	2352.6(14)	1984.0(8)	13.5(3)
C7	5966.7(15)	4886.2(15)	2324.0(8)	16.7(3)
C8	6393.1(15)	4544.7(15)	1658.3(8)	17.1(3)
C9	4349.7(15)	811.8(17)	4354.7(8)	19.5(3)
C10	3460.0(16)	-761.8(15)	2771.4(9)	19.5(3)
C11	6395.4(14)	2860.3(14)	4428.5(8)	14.0(3)
C12	5785.8(16)	3436.9(16)	4897.9(9)	20.2(4)
C13	6316.4(17)	3435.3(16)	5611.1(9)	22.5(4)
C14	7463.6(17)	2886.7(16)	5860.7(9)	21.1(4)
C15	8078.7(16)	2325.5(16)	5392.6(9)	21.2(4)
C16	7547.5(15)	2305.5(15)	4682.6(8)	17.0(3)
C17	7175.2(15)	2549.9(16)	488.3(8)	16.6(3)
C18	7054.7(16)	1285.3(16)	404.1(9)	21.4(4)
C19	6282.0(17)	808.2(17)	-190.8(9)	24.3(4)
C20	5619.0(16)	1585.5(17)	-707.0(9)	21.2(4)
C21	5768.2(16)	2847.6(17)	-616.3(9)	21.3(4)
C22	6539.1(15)	3339.5(16)	-23.9(9)	19.1(3)
C23	4748.9(18)	1068.6(19)	-1343.2(10)	29.3(4)
N1	5019.5(12)	1656.5(12)	2676.8(7)	13.0(3)
N2	4050.2(12)	1213.6(12)	3617.8(7)	13.7(3)
N3	7185.6(12)	3438.0(12)	1797.7(7)	14.6(3)
O1	6765.4(9)	2701.1(10)	3250.9(5)	12.5(2)
O2	2309.2(10)	1349.8(11)	2544.0(6)	20.0(3)
O3	2051.7(10)	138.3(11)	3567.4(6)	18.0(2)
O4	8951.1(10)	2197.9(12)	1574.1(6)	21.8(3)
O5	8607.4(11)	4311.3(12)	1096.8(6)	23.2(3)
S1	2824.0(3)	532.8(3)	3101.5(2)	13.08(10)
S2	8117.8(4)	3151.4(4)	1259.4(2)	16.57(11)

Table 3 Anisotropic Displacement Parameters (Å^2×10^3) for 278. The Anisotropic displacement factor exponent takes the form: $-2\pi^2[h^2a^{*2}U_{11}+2hka^*b^*U_{12}+\ldots]$.

Atom	U_{11}	U_{22}	U_{33}	U_{23}	U_{13}	U_{12}
C1	11.9(7)	12.7(7)	11.0(7)	-0.1(6)	0.6(6)	-0.8(6)
C2	12.3(7)	10.8(7)	13.6(7)	0.2(6)	1.3(6)	1.2(6)
C3	11.7(7)	12.6(7)	14.6(8)	-0.7(6)	4.7(6)	-0.4(6)
C4	14.5(7)	13.4(8)	17.1(8)	-1.1(6)	3.0(6)	1.1(6)
C5	13.9(7)	11.7(8)	14.4(8)	0.2(6)	1.9(6)	0.3(6)

C6	15.4(7)	12.4(7)	13.4(7)	1.4(6)	4.8(6)	-1.0(6)
C7	19.5(8)	12.0(8)	18.0(8)	1.1(6)	2.7(6)	-1.0(6)
C8	19.8(8)	13.2(8)	18.2(8)	3.7(6)	3.7(6)	-0.4(6)
C9	18.8(8)	27.0(9)	12.6(8)	3.7(7)	3.2(6)	-2.5(7)
C10	19.8(8)	15.1(8)	25.2(9)	-5.6(7)	8.7(7)	-2.0(6)
C11	15.9(7)	12.3(7)	14.2(8)	-0.3(6)	3.9(6)	-3.2(6)
C12	19.9(8)	22.2(9)	19.0(8)	-2.5(7)	4.9(7)	1.8(7)
C13	29.8(9)	22.8(9)	17.2(8)	-4.4(7)	10.0(7)	-0.4(7)
C14	30.7(9)	18.9(8)	12.8(8)	-0.3(6)	2.3(7)	-4.1(7)
C15	21.5(8)	22.5(9)	17.8(8)	2.5(7)	-0.1(7)	2.9(7)
C16	18.7(8)	17.8(8)	14.6(8)	-1.2(6)	3.7(6)	1.8(6)
C17	14.9(8)	21.1(8)	15.4(8)	1.6(6)	6.6(6)	0.9(6)
C18	22.5(8)	20.1(9)	22.0(9)	3.5(7)	5.5(7)	6.1(7)
C19	27.2(9)	19.4(9)	26.8(9)	-4.2(7)	7.2(7)	4.5(7)
C20	17.4(8)	28.4(10)	19.8(9)	-2.5(7)	8.8(7)	2.2(7)
C21	17.1(8)	28.7(10)	18.8(8)	7.3(7)	5.1(7)	1.7(7)
C22	18.6(8)	19.6(9)	20.8(8)	4.6(7)	7.8(7)	-1.9(7)
C23	25.7(9)	37.5(11)	24.8(10)	-8.2(8)	5.5(8)	0.7(8)
N1	14.4(6)	10.9(6)	13.8(6)	0.9(5)	3.4(5)	-0.5(5)
N2	13.5(6)	15.3(7)	12.3(6)	0.3(5)	2.9(5)	-2.8(5)
N3	14.7(6)	14.4(7)	15.7(7)	2.8(5)	5.6(5)	-0.8(5)
O1	11.2(5)	15.3(6)	11.1(5)	0.2(4)	2.6(4)	0.0(4)
O2	17.4(6)	20.5(6)	19.8(6)	3.9(5)	-1.5(5)	-0.5(5)
O3	15.2(5)	20.6(6)	19.1(6)	-1.4(5)	5.9(5)	-4.8(5)
O4	15.0(6)	29.3(7)	21.6(6)	5.7(5)	4.8(5)	3.9(5)
O5	21.5(6)	26.2(7)	23.3(6)	3.3(5)	7.8(5)	-8.6(5)
S1	12.28(19)	12.66(19)	14.34(19)	-0.65(14)	2.90(14)	-1.64(14)
S2	13.35(19)	21.1(2)	16.0(2)	3.44(15)	4.70(15)	-1.76(15)

Table 4 Bond Lengths for 278.

Atom	Atom	Length/Å	Atom	Atom	Length/Å
C1	C5	1.543(2)	C12	C13	1.393(2)
C1	C6	1.507(2)	C13	C14	1.383(3)
C1	N1	1.4681(19)	C14	C15	1.388(2)
C1	O1	1.4390(18)	C15	C16	1.388(2)
C2	C3	1.553(2)	C17	C18	1.390(2)
C2	N1	1.276(2)	C17	C22	1.390(2)
C2	N2	1.3875(19)	C17	S2	1.7641(17)
C3	C4	1.564(2)	C18	C19	1.387(3)
C3	C11	1.500(2)	C19	C20	1.398(3)
C3	O1	1.4413(17)	C20	C21	1.391(3)
C4	C5	1.547(2)	C20	C23	1.508(2)
C5	C7	1.522(2)	C21	C22	1.389(2)
C6	N3	1.4734(19)	N2	S1	1.6733(13)
C7	C8	1.519(2)	N3	S2	1.6433(13)

C8	N3	1.476(2)	O2	S1	1.4278(12)
C9	N2	1.4754(19)	O3	S1	1.4336(11)
C10	S1	1.7546(16)	O4	S2	1.4326(12)
C11	C12	1.393(2)	O5	S2	1.4338(12)
C11	C16	1.392(2)			

Table 5 Bond Angles for 278.

Atom	Atom	Atom	Angle/˚	Atom	Atom	Atom	Angle/˚
C6	C1	C5	116.50(13)	C18	C17	C22	120.44(16)
N1	C1	C5	107.24(12)	C18	C17	S2	119.53(13)
N1	C1	C6	111.56(12)	C22	C17	S2	120.02(13)
O1	C1	C5	102.15(11)	C19	C18	C17	119.76(16)
O1	C1	C6	113.56(12)	C18	C19	C20	120.73(17)
O1	C1	N1	104.77(11)	C19	C20	C23	120.77(17)
N1	C2	C3	109.74(13)	C21	C20	C19	118.49(16)
N1	C2	N2	124.76(14)	C21	C20	C23	120.73(17)
N2	C2	C3	124.36(13)	C22	C21	C20	121.45(16)
C2	C3	C4	101.55(12)	C21	C22	C17	119.11(16)
C11	C3	C2	123.00(13)	C2	N1	C1	103.11(12)
C11	C3	C4	117.53(13)	C2	N2	C9	120.89(13)
O1	C3	C2	97.98(11)	C2	N2	S1	119.13(10)
O1	C3	C4	102.07(11)	C9	N2	S1	116.29(10)
O1	C3	C11	111.25(12)	C6	N3	C8	113.50(12)
C5	C4	C3	101.22(12)	C6	N3	S2	114.33(10)
C1	C5	C4	100.45(12)	C8	N3	S2	117.19(10)
C7	C5	C1	110.42(12)	C1	O1	C3	95.60(10)
C7	C5	C4	113.13(13)	N2	S1	C10	104.35(7)
N3	C6	C1	111.16(12)	O2	S1	C10	110.06(8)
C8	C7	C5	111.46(13)	O2	S1	N2	108.79(7)
N3	C8	C7	108.45(13)	O2	S1	O3	118.77(7)
C12	C11	C3	120.96(14)	O3	S1	C10	109.04(8)
C16	C11	C3	120.08(14)	O3	S1	N2	104.76(6)
C16	C11	C12	118.96(15)	N3	S2	C17	106.73(7)
C11	C12	C13	120.18(16)	O4	S2	C17	107.64(8)
C14	C13	C12	120.63(15)	O4	S2	N3	106.72(7)
C13	C14	C15	119.22(16)	O4	S2	O5	119.97(7)
C14	C15	C16	120.52(16)	O5	S2	C17	108.42(8)
C15	C16	C11	120.48(15)	O5	S2	N3	106.66(7)

Table 6 Torsion Angles for 278.

A	B	C	D	Angle/˚	A	B	C	D	Angle/˚
C1	C5	C7	C8	50.89(17)	C11	C12	C13	C14	1.4(3)
C1	C6	N3	C8	-53.83(17)	C12	C11	C16	C15	0.1(2)
C1	C6	N3	S2	168.15(10)	C12	C13	C14	C15	-0.6(3)
C2	C3	C4	C5	-68.17(13)	C13	C14	C15	C16	-0.5(3)
C2	C3	C11	C12	-90.11(19)	C14	C15	C16	C11	0.7(3)
C2	C3	C11	C16	89.32(19)	C16	C11	C12	C13	-1.1(2)
C2	C3	O1	C1	46.80(12)	C17	C18	C19	C20	-0.2(3)
C2	N2	S1	C10	69.39(13)	C18	C17	C22	C21	0.9(2)
C2	N2	S1	O2	-48.07(13)	C18	C17	S2	N3	-94.54(14)
C2	N2	S1	O3	-176.05(11)	C18	C17	S2	O4	19.72(15)
C3	C2	N1	C1	-1.14(16)	C18	C17	S2	O5	150.90(13)
C3	C2	N2	C9	-46.8(2)	C18	C19	C20	C21	1.1(3)
C3	C2	N2	S1	155.66(12)	C18	C19	C20	C23	-178.13(16)
C3	C4	C5	C1	3.23(14)	C19	C20	C21	C22	-1.0(2)
C3	C4	C5	C7	-114.46(14)	C20	C21	C22	C17	0.1(2)
C3	C11	C12	C13	178.30(15)	C22	C17	C18	C19	-0.8(2)
C3	C11	C16	C15	-179.35(15)	C22	C17	S2	N3	84.17(14)
C4	C3	C11	C12	37.3(2)	C22	C17	S2	O4	-161.57(12)
C4	C3	C11	C16	-143.26(15)	C22	C17	S2	O5	-30.39(15)
C4	C3	O1	C1	-56.90(13)	C23	C20	C21	C22	178.18(15)
C4	C5	C7	C8	162.58(13)	N1	C1	C5	C4	71.34(14)
C5	C1	C6	N3	43.91(18)	N1	C1	C5	C7	-168.99(12)
C5	C1	N1	C2	-74.46(14)	N1	C1	C6	N3	167.50(12)
C5	C1	O1	C3	59.83(12)	N1	C1	O1	C3	-51.91(13)
C5	C7	C8	N3	-60.82(17)	N1	C2	C3	C4	73.44(15)
C6	C1	C5	C4	-162.88(13)	N1	C2	C3	C11	-152.52(14)
C6	C1	C5	C7	-43.21(18)	N1	C2	C3	O1	-30.70(15)
C6	C1	N1	C2	156.86(13)	N1	C2	N2	C9	146.71(16)
C6	C1	O1	C3	-173.89(12)	N1	C2	N2	S1	-10.9(2)
C6	N3	S2	C17	60.08(12)	N2	C2	C3	C4	-94.83(16)
C6	N3	S2	O4	-54.80(12)	N2	C2	C3	C11	39.2(2)
C6	N3	S2	O5	175.82(11)	N2	C2	C3	O1	161.04(13)
C7	C8	N3	C6	62.71(16)	N2	C2	N1	C1	167.07(14)
C7	C8	N3	S2	-160.54(11)	O1	C1	C5	C4	-38.53(13)
C8	N3	S2	C17	-76.32(13)	O1	C1	C5	C7	81.14(14)
C8	N3	S2	O4	168.80(11)	O1	C1	C6	N3	-74.38(16)
C8	N3	S2	O5	39.42(13)	O1	C1	N1	C2	33.58(15)
C9	N2	S1	C10	-89.19(13)	O1	C3	C4	C5	32.70(14)
C9	N2	S1	O2	153.36(11)	O1	C3	C11	C12	154.41(14)
C9	N2	S1	O3	25.37(13)	O1	C3	C11	C16	-26.2(2)
C11	C3	C4	C5	154.66(13)	S2	C17	C18	C19	177.86(13)
C11	C3	O1	C1	176.93(12)	S2	C17	C22	C21	-177.81(12)

Table 7 Hydrogen Atom Coordinates (Å×10^4) and Isotropic Displacement Parameters (Å^2×10^3) for 278.

Atom	*x*	*y*	*z*	U(eq)
H4A	4223	3959	3374	18
H4B	5473	4735	3539	18
H5	4375	3805	2247	16
H6A	7108	1682	2111	16
H6B	5893	2097	1582	16
H7A	5466	5628	2244	20
H7B	6692	5054	2692	20
H8A	5674	4382	1285	21
H8B	6863	5217	1514	21
H9A	3936	1338	4628	29
H9B	5237	854	4529	29
H9C	4071	-18	4386	29
H10A	3871	-1269	3153	29
H10B	4053	-504	2503	29
H10C	2804	-1221	2478	29
H12	5023	3824	4735	24
H13	5895	3806	5922	27
H14	7818	2894	6337	25
H15	8853	1960	5556	25
H16	7964	1919	4374	20
H18	7491	761	745	26
H19	6204	-38	-247	29
H21	5342	3374	-960	26
H22	6629	4186	29	23
H23A	5025	262	-1440	44
H23B	4749	1594	-1737	44
H23C	3918	1020	-1258	44

Crystal structure determination of [278]

Crystal Data for $C_{23}H_{27}N_3O_5S_2$ (*M* =489.59 g/mol): monoclinic, space group $P2_1/n$ (no. 14), *a* = 10.94883(18) Å, *b* = 10.88873(18) Å, *c* = 19.5589(3) Å, *β* = 102.1791(16)°, *V* = 2279.31(7) Å^3, *Z* = 4, *T* = 100.00(10) K, μ(MoKα) = 0.275 mm^{-1}, *Dcalc* = 1.427 g/cm^3, 24092 reflections measured (6.038° ≤ 2Θ ≤ 52.742°), 4667 unique (R_{int} = 0.0263, R_{sigma} = 0.0205) which were used in all calculations. The final R_1 was 0.0326 (I > 2σ(I)) and wR_2 was 0.0851 (all data).

Refinement model description

Number of restraints - 0, number of constraints - unknown. Details: 1. Fixed Uiso At 1.2 times of: All C(H) groups, All C(H,H) groups At 1.5 times of: All C(H,H,H) groups. 2.a Ternary CH refined with riding coordinates: C5(H5). 2.b Secondary CH2 refined with riding coordinates: C4(H4A,H4B), C6(H6A,H6B), C7(H7A,H7B), C8(H8A,H8B). 2.c Aromatic/amide H refined with riding coordinates: C12(H12), C13(H13), C14(H14), C15(H15), C16(H16), C18(H18), C19(H19), C21(H21), C22(H22). 2.d Idealised Me refined as rotating group: C9(H9A,H9B,H9C), C10(H10A,H10B,H10C), C23(H23A,H23B,H23C)

5.3.2: Tetrahydrofuran 283

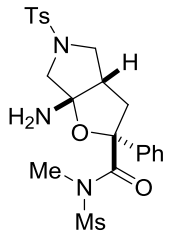

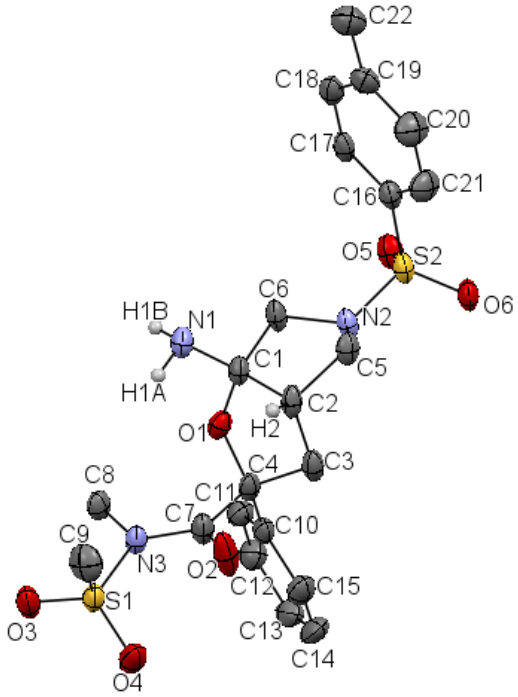

Table 1 Crystal data and structure refinement for 283.

Identification code	**283**
Empirical formula	$C_{22}H_{27}N_3O_6S_2$
Formula weight	493.58
Temperature/K	99.99(10)
Crystal system	orthorhombic
Space group	$P2_12_12_1$
a/Å	8.34939(14)
b/Å	10.43121(16)
c/Å	26.3933(3)
α/°	90
β/°	90
γ/°	90
Volume/Å^3	2298.70(6)
Z	4
ρ_{calc}g/cm^3	1.426
μ/mm^{-1}	2.485
F(000)	1040.0
Crystal size/mm^3	0.3004 × 0.1094 × 0.0566
Radiation	CuKα (λ = 1.54184)
2Θ range for data collection/°	6.698 to 136.482
Index ranges	-10 ≤ h ≤ 9, -12 ≤ k ≤ 12, -31 ≤ l ≤ 31
Reflections collected	20637
Independent reflections	4205 [R_{int} = 0.0316, R_{sigma} = 0.0211]
Data/restraints/parameters	4205/0/310
Goodness-of-fit on F^2	1.091
Final R indexes [I>=2σ (I)]	R_1 = 0.0302, wR_2 = 0.0777
Final R indexes [all data]	R_1 = 0.0311, wR_2 = 0.0784
Largest diff. peak/hole / e Å^{-3}	0.47/-0.24
Flack parameter	0.550(19)

Table 2 Fractional Atomic Coordinates (×10^4) and Equivalent Isotropic Displacement Parameters (Å^2×10^3) for 283. U_{eq} is defined as 1/3 of of the trace of the orthogonalised U_{IJ} tensor.

Atom	*x*	*y*	*z*	U(eq)
C1	11490(3)	3935(3)	1254(1)	27.4(6)
C2	10248(4)	3947(3)	1689.7(10)	30.2(6)
C3	9952(3)	5368(3)	1775.5(10)	32.8(6)
C4	11555(3)	5980(3)	1641.8(10)	29.2(6)
C5	8801(3)	3247(3)	1472.5(10)	30.4(6)
C6	10534(3)	3671(3)	765.2(10)	31.3(6)
C7	12684(4)	5940(3)	2116(1)	32.6(6)
C8	15178(4)	6188(3)	1574.3(10)	31.4(6)
C9	15346(5)	4910(4)	2912.2(13)	47.8(8)
C10	11423(3)	7376(3)	1480.4(10)	30.0(6)
C11	12019(4)	7812(3)	1021.5(11)	32.7(7)
C12	11907(4)	9088(3)	888.9(13)	38.9(7)
C13	11169(4)	9946(3)	1210.4(13)	42.2(8)
C14	10532(5)	9527(3)	1664.0(14)	48.1(9)
C15	10667(4)	8256(4)	1801.3(12)	43.0(8)
C16	7500(3)	1568(3)	503.7(10)	29.8(6)
C17	8500(3)	1008(3)	148.8(10)	31.0(6)
C18	8601(4)	-312(3)	119.6(11)	36.4(7)
C19	7706(4)	-1103(3)	446.5(11)	37.5(7)
C20	6698(5)	-508(4)	790.1(14)	48.1(9)
C21	6585(4)	814(3)	828.0(13)	41.8(8)
C22	7880(5)	-2537(4)	428.9(14)	50.7(9)
N1	12709(3)	2987(2)	1323.1(10)	31.8(5)
N2	8845(3)	3694(2)	940.0(8)	27.0(5)
N3	14302(3)	6153(2)	2058.9(8)	28.7(5)
O1	12139(2)	5230.1(19)	1231.9(7)	29.1(4)
O2	12124(3)	5773(3)	2536.7(8)	54.1(7)
O3	16967(2)	6651(3)	2432.8(8)	42.4(5)
O4	14593(3)	7337(2)	2896.9(8)	44.6(6)
O5	7804(3)	3786(2)	69.8(7)	36.2(5)
O6	5948(2)	3577(2)	800.0(8)	35.5(5)
S1	15373.3(8)	6386.8(7)	2596.3(2)	30.49(17)
S2	7429.2(8)	3250.4(7)	555.6(2)	28.76(16)

Table 3 Anisotropic Displacement Parameters (Å^2×10^3) for 283. The Anisotropic displacement factor exponent takes the form: $-2\pi^2[h^2a^{*2}U_{11}+2hka^*b^*U_{12}+\ldots]$.

Atom	U_{11}	U_{22}	U_{33}	U_{23}	U_{13}	U_{12}
C1	18.4(14)	37.7(15)	26.2(13)	3.0(11)	-0.8(10)	3.4(12)
C2	19.2(13)	49.9(17)	21.4(12)	7.2(11)	2.1(11)	3.4(13)

C3	20.1(14)	56.4(18)	21.8(12)	-1.6(12)	1.2(10)	1.6(13)
C4	20.1(14)	48.6(16)	18.8(13)	-4.3(11)	1.5(10)	4.5(12)
C5	23.5(14)	45.2(16)	22.5(12)	7.4(12)	3.1(10)	1.5(13)
C6	16.8(13)	52.6(17)	24.5(12)	2.4(12)	0.3(11)	-1.5(13)
C7	20.8(14)	53.4(17)	23.7(13)	0.5(12)	-0.2(11)	2.6(13)
C8	23.4(14)	46.3(16)	24.6(12)	-1.2(11)	6.5(11)	-1.1(13)
C9	48(2)	59(2)	36.4(15)	10.2(15)	-11.0(16)	3.9(18)
C10	19.9(14)	42.5(16)	27.7(14)	-7.6(12)	-5.5(11)	5.5(13)
C11	30.9(16)	37.2(15)	30.1(14)	-6.4(11)	-0.1(12)	5.2(12)
C12	36.0(18)	39.1(16)	41.5(17)	-2.3(13)	-4.0(14)	5.1(14)
C13	36.9(17)	37.2(17)	52.3(19)	-11.9(14)	-13.8(15)	8.9(14)
C14	40(2)	49.4(19)	55(2)	-25.0(16)	-7.4(17)	19.4(17)
C15	34.6(17)	61(2)	33.6(15)	-13.6(15)	0.1(13)	9.7(16)
C16	21.1(13)	41.8(15)	26.6(12)	0.3(11)	-1.0(11)	-2.0(13)
C17	19.0(14)	52.8(18)	21.3(13)	-1.8(12)	-2.3(10)	-1.0(13)
C18	25.4(15)	56.9(19)	26.8(14)	-10.7(13)	-1.8(12)	1.6(14)
C19	36.4(18)	46.0(17)	30.1(14)	-8.6(12)	-8.2(13)	-0.4(15)
C20	50(2)	47.9(19)	46.1(19)	1.8(15)	15.2(17)	-8.3(17)
C21	37.7(18)	46.2(18)	41.4(17)	-2.3(14)	18.5(15)	-4.8(15)
C22	53(2)	54(2)	45.3(19)	-12.1(16)	-4.6(17)	-0.5(18)
N1	21.1(12)	39.0(13)	35.4(13)	2.7(10)	1.7(11)	4.2(11)
N2	17.7(11)	41.6(13)	21.8(11)	5.4(9)	-0.5(9)	-2.9(10)
N3	19.8(12)	44.6(14)	21.7(10)	0.2(9)	0.2(9)	4.2(10)
O1	26.7(10)	35.3(10)	25.1(9)	0.5(7)	6.5(8)	4.8(9)
O2	23.9(11)	117(2)	21.4(10)	4.7(11)	1.7(9)	-7.6(12)
O3	23(1)	66.6(15)	37.6(11)	-10.0(11)	-0.8(9)	-1.7(10)
O4	34.5(12)	64.6(15)	34.7(11)	-17(1)	-2.7(10)	12.2(11)
O5	30.3(11)	50.7(12)	27.8(10)	10.9(9)	-4.4(8)	-1.6(9)
O6	18.1(10)	49.1(13)	39.2(11)	-1.1(10)	-2.3(8)	2.3(9)
S1	20.2(3)	44.9(4)	26.4(3)	-4.4(3)	-1.3(3)	5.1(3)
S2	17.6(3)	42.8(4)	25.9(3)	4.4(3)	-2.4(3)	-0.5(3)

Table 4 Bond Lengths for 283.

Atom	Atom	Length/Å	Atom	Atom	Length/Å
C1	C2	1.549(4)	C11	C12	1.380(5)
C1	C6	1.541(4)	C12	C13	1.378(5)
C1	N1	1.431(4)	C13	C14	1.381(5)
C1	O1	1.457(4)	C14	C15	1.379(5)
C2	C3	1.519(4)	C16	C17	1.384(4)
C2	C5	1.524(4)	C16	C21	1.391(4)
C3	C4	1.524(4)	C16	S2	1.761(3)
C4	C7	1.567(4)	C17	C18	1.381(5)
C4	C10	1.522(4)	C18	C19	1.408(5)
C4	O1	1.421(3)	C19	C20	1.384(5)
C5	N2	1.481(3)	C19	C22	1.504(5)

C6	N2	1.484(3)	C20	C21	1.386(5)
C7	N3	1.378(4)	N2	S2	1.625(2)
C7	O2	1.217(4)	N3	S1	1.694(2)
C8	N3	1.474(3)	O3	S1	1.426(2)
C9	S1	1.752(4)	O4	S1	1.427(2)
C10	C11	1.386(4)	O5	S2	1.433(2)
C10	C15	1.399(4)	O6	S2	1.436(2)

Table 5 Bond Angles for 283.

Atom	Atom	Atom	Angle/˚	Atom	Atom	Atom	Angle/˚
C6	C1	C2	106.0(2)	C17	C16	C21	120.6(3)
N1	C1	C2	112.8(2)	C17	C16	S2	119.6(2)
N1	C1	C6	110.6(2)	C21	C16	S2	119.8(2)
N1	C1	O1	112.4(2)	C18	C17	C16	119.7(3)
O1	C1	C2	105.7(2)	C17	C18	C19	121.1(3)
O1	C1	C6	108.9(2)	C18	C19	C22	120.9(3)
C3	C2	C1	103.2(2)	C20	C19	C18	117.5(3)
C3	C2	C5	113.2(2)	C20	C19	C22	121.6(3)
C5	C2	C1	104.3(2)	C19	C20	C21	122.3(3)
C2	C3	C4	103.4(2)	C20	C21	C16	118.7(3)
C3	C4	C7	109.4(2)	C5	N2	C6	108.3(2)
C10	C4	C3	113.7(3)	C5	N2	S2	118.98(19)
C10	C4	C7	107.0(2)	C6	N2	S2	119.52(18)
O1	C4	C3	104.3(2)	C7	N3	C8	125.9(2)
O1	C4	C7	112.8(2)	C7	N3	S1	116.71(19)
O1	C4	C10	109.8(2)	C8	N3	S1	117.43(19)
N2	C5	C2	100.7(2)	C4	O1	C1	110.6(2)
N2	C6	C1	103.2(2)	N3	S1	C9	105.35(15)
N3	C7	C4	119.9(2)	O3	S1	C9	109.05(17)
O2	C7	C4	120.1(3)	O3	S1	N3	105.51(12)
O2	C7	N3	120.0(3)	O3	S1	O4	117.37(16)
C11	C10	C4	122.2(3)	O4	S1	C9	109.90(17)
C11	C10	C15	118.4(3)	O4	S1	N3	108.93(13)
C15	C10	C4	119.4(3)	N2	S2	C16	107.95(13)
C12	C11	C10	120.9(3)	O5	S2	C16	108.13(13)
C13	C12	C11	120.0(3)	O5	S2	N2	106.77(12)
C12	C13	C14	120.0(3)	O5	S2	O6	119.85(13)
C15	C14	C13	120.1(3)	O6	S2	C16	107.47(14)
C14	C15	C10	120.5(3)	O6	S2	N2	106.17(12)

Table 6 Hydrogen Bonds for 283.

D	H	A	d(D-H)/Å	d(H-A)/Å	d(D-A)/Å	D-H-A/°
N1	H1A	O4[1]	0.97(4)	2.29(5)	3.126(3)	144(4)
N1	H1B	O6[2]	0.86(4)	2.35(4)	3.098(3)	146(3)

[1]3-X,-1/2+Y,1/2-Z; [2]1+X,+Y,+Z

Table 7 Torsion Angles for 283.

A	B	C	D	Angle/˚	A	B	C	D	Angle/˚
C1	C2	C3	C4	-31.3(3)	C8	N3	S1	O4	130.2(2)
C1	C2	C5	N2	-36.5(3)	C10	C4	C7	N3	-71.7(3)
C1	C6	N2	C5	-30.5(3)	C10	C4	C7	O2	105.3(4)
C1	C6	N2	S2	-171.1(2)	C10	C4	O1	C1	-148.8(2)
C2	C1	C6	N2	5.9(3)	C10	C11	C12	C13	-1.1(5)
C2	C1	O1	C4	6.5(3)	C11	C10	C15	C14	-0.5(5)
C2	C3	C4	C7	-84.9(3)	C11	C12	C13	C14	-0.5(5)
C2	C3	C4	C10	155.5(2)	C12	C13	C14	C15	1.5(5)
C2	C3	C4	O1	35.9(3)	C13	C14	C15	C10	-1.0(5)
C2	C5	N2	C6	42.6(3)	C15	C10	C11	C12	1.6(5)
C2	C5	N2	S2	-176.6(2)	C16	C17	C18	C19	-0.2(4)
C3	C2	C5	N2	74.9(3)	C17	C16	C21	C20	0.2(5)
C3	C4	C7	N3	164.6(3)	C17	C16	S2	N2	-86.7(2)
C3	C4	C7	O2	-18.4(4)	C17	C16	S2	O5	28.5(3)
C3	C4	C10	C11	-124.7(3)	C17	C16	S2	O6	159.2(2)
C3	C4	C10	C15	54.8(3)	C17	C18	C19	C20	1.3(5)
C3	C4	O1	C1	-26.5(3)	C17	C18	C19	C22	-177.1(3)
C4	C7	N3	C8	-12.2(5)	C18	C19	C20	C21	-1.7(6)
C4	C7	N3	S1	168.2(2)	C19	C20	C21	C16	1.0(6)
C4	C10	C11	C12	-178.9(3)	C21	C16	C17	C18	-0.6(4)
C4	C10	C15	C14	180.0(3)	C21	C16	S2	N2	91.6(3)
C5	C2	C3	C4	-143.5(2)	C21	C16	S2	O5	-153.2(3)
C5	N2	S2	C16	-62.2(2)	C21	C16	S2	O6	-22.5(3)
C5	N2	S2	O5	-178.2(2)	C22	C19	C20	C21	176.7(4)
C5	N2	S2	O6	52.8(3)	N1	C1	C2	C3	139.5(2)
C6	C1	C2	C3	-99.3(3)	N1	C1	C2	C5	-102.0(3)
C6	C1	C2	C5	19.2(3)	N1	C1	C6	N2	128.5(3)
C6	C1	O1	C4	120.0(2)	N1	C1	O1	C4	-117.0(2)
C6	N2	S2	C16	74.3(2)	O1	C1	C2	C3	16.2(3)
C6	N2	S2	O5	-41.7(3)	O1	C1	C2	C5	134.8(2)
C6	N2	S2	O6	-170.7(2)	O1	C1	C6	N2	-107.5(2)
C7	C4	C10	C11	114.4(3)	O1	C4	C7	N3	49.1(4)
C7	C4	C10	C15	-66.1(3)	O1	C4	C7	O2	-133.9(3)
C7	C4	O1	C1	92.0(3)	O1	C4	C10	C11	-8.2(4)
C7	N3	S1	C9	67.8(3)	O1	C4	C10	C15	171.3(2)
C7	N3	S1	O3	-176.9(2)	O2	C7	N3	C8	170.9(3)
C7	N3	S1	O4	-50.1(3)	O2	C7	N3	S1	-8.8(4)
C8	N3	S1	C9	-111.9(2)	S2	C16	C17	C18	177.7(2)
C8	N3	S1	O3	3.4(3)	S2	C16	C21	C20	-178.0(3)

Table 8 Hydrogen Atom Coordinates (Å×10^4) and Isotropic Displacement Parameters (Å^2×10^3) for 283.

Atom	*x*	*y*	*z*	U(eq)
H2	10659	3526	1995	36
H3A	9667	5537	2125	39
H3B	9106	5682	1557	39
H5A	8924	2324	1495	37
H5B	7817	3501	1640	37
H6A	10729	4330	513	38
H6B	10810	2843	623	38
H8A	15366	5329	1459	47
H8B	16185	6617	1622	47
H8C	14555	6643	1327	47
H9A	14258	4672	2984	72
H9B	15932	4980	3224	72
H9C	15832	4267	2702	72
H11	12502	7236	800	39
H12	12328	9370	582	47
H13	11100	10807	1122	51
H14	10012	10102	1877	58
H15	10251	7981	2110	52
H17	9101	1517	-69	37
H18	9272	-684	-120	44
H20	6075	-1014	1003	58
H21	5910	1190	1066	50
H22A	8191	-2847	757	76
H22B	8683	-2764	185	76
H22C	6875	-2915	334	76
H1A	13310(60)	3110(40)	1634(17)	63(13)
H1B	13340(50)	3070(40)	1068(15)	46(11)

Crystal structure determination of [283]

Crystal Data for $C_{22}H_{27}N_3O_6S_2$ (*M* =493.58 g/mol): orthorhombic, space group $P2_12_12_1$ (no. 19), *a* = 8.34939(14) Å, *b* = 10.43121(16) Å, *c* = 26.3933(3) Å, *V* = 2298.70(6) Å^3, *Z* = 4, *T* = 99.99(10) K, μ(CuKα) = 2.485 mm^{-1}, *Dcalc* = 1.426 g/cm^3, 20637 reflections measured (6.698° ≤ 2Θ ≤ 136.482°), 4205 unique (R_{int} = 0.0316, R_{sigma} = 0.0211) which were used in all calculations. The final R_1 was 0.0302 (I > 2σ(I)) and wR_2 was 0.0784 (all data).

Refinement model description

Number of restraints - 0, number of constraints - unknown. Details: 1. Twinned data refinement Scales: 0.450(19) 0.550(19). 2. Fixed Uiso At 1.2 times of: All C(H) groups, All C(H,H) groups At 1.5 times of: All C(H,H,H) groups. 3.a Ternary CH refined with riding coordinates: C2(H2). 3.b Secondary CH2 refined with riding coordinates: C3(H3A,H3B), C5(H5A,H5B), C6(H6A,H6B). 3.c Aromatic/amide H refined with riding coordinates: C11(H11), C12(H12), C13(H13), C14(H14), C15(H15), C17(H17), C18(H18), C20(H20), C21(H21). 3.d Idealised Me refined as rotating group: C8(H8A,H8B,H8C), C9(H9A,H9B,H9C), C22(H22A,H22B,H22C)

5.3.3: Piperidine 284.HCl

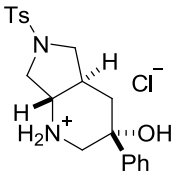

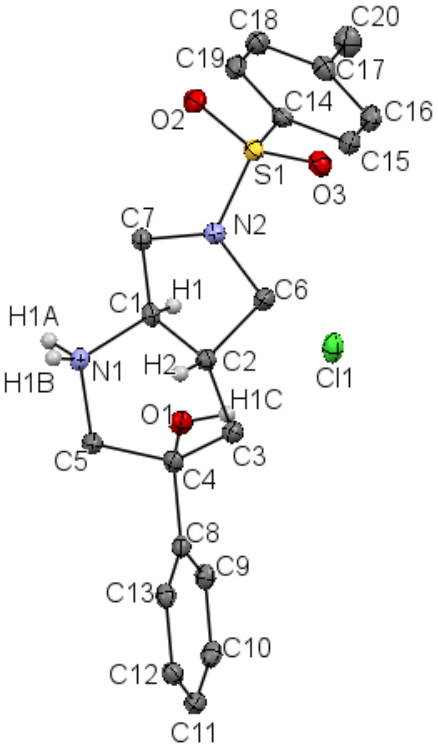

Table 1 Crystal data and structure refinement for 284.HCl.

Identification code	**284.HCl**
Empirical formula	$C_{20}H_{25}ClN_2O_3S$
Formula weight	408.93
Temperature/K	99.98(11)
Crystal system	triclinic
Space group	P-1
a/Å	8.0819(4)
b/Å	9.4116(6)
c/Å	13.7236(8)
α/°	97.294(5)
β/°	96.498(4)
γ/°	107.359(5)
Volume/Å^3	975.60(10)
Z	2
ρ_{calc}g/cm^3	1.392
μ/mm^{-1}	2.928
F(000)	432.0
Crystal size/mm^3	0.1938 × 0.1746 × 0.0597
Radiation	CuKα (λ = 1.54184)
2Θ range for data collection/°	6.578 to 138.278
Index ranges	-6 ≤ h ≤ 9, -11 ≤ k ≤ 11, -16 ≤ l ≤ 16
Reflections collected	6365
Independent reflections	3626 [R_{int} = 0.0301, R_{sigma} = 0.0378]
Data/restraints/parameters	3626/0/257
Goodness-of-fit on F^2	1.041
Final R indexes [I>=2σ (I)]	R_1 = 0.0386, wR_2 = 0.1012
Final R indexes [all data]	R_1 = 0.0458, wR_2 = 0.1081
Largest diff. peak/hole / e Å^{-3}	0.54/-0.40

Table 2 Fractional Atomic Coordinates ($\times 10^4$) and Equivalent Isotropic Displacement Parameters ($Å^2 \times 10^3$) for 284.HCl. U_{eq} is defined as 1/3 of of the trace of the orthogonalised U_{IJ} tensor.

Atom	*x*	*y*	*z*	U(eq)
C1	2876(2)	8184(2)	5553.6(14)	15.1(4)
C2	2409(2)	6481(2)	5265.7(14)	15.3(4)
C3	3031(3)	6024(2)	4300.5(14)	15.8(4)
C4	3189(2)	7239(2)	3620.4(14)	14.9(4)
C5	1792(3)	8030(2)	3729.6(14)	17.1(4)
C6	3169(3)	6086(2)	6217.7(15)	17.9(4)
C7	2439(3)	8419(2)	6604.1(14)	16.1(4)
C8	2983(2)	6525(2)	2532.5(14)	15.3(4)
C9	4388(3)	6890(2)	2007.0(15)	17.5(4)
C10	4189(3)	6239(2)	1012.2(16)	19.2(4)
C11	2596(3)	5217(2)	539.6(15)	19.4(4)
C12	1195(3)	4829(2)	1063.8(15)	18.3(4)
C13	1389(3)	5481(2)	2052.9(15)	16.7(4)
C14	5619(3)	8326(2)	8367.4(14)	15.7(4)
C15	6905(3)	7702(2)	8110.1(15)	18.2(4)
C16	8645(3)	8626(2)	8254.3(16)	20.2(4)
C17	9114(3)	10158(2)	8654.6(16)	20.5(4)
C18	7807(3)	10749(2)	8912.9(15)	19.8(4)
C19	6061(3)	9842(2)	8771.7(15)	18.7(4)
C20	11009(3)	11152(3)	8814.0(18)	26.3(5)
N1	1871(2)	8749.4(19)	4796.8(12)	15.8(3)
N2	2633(2)	7052.4(18)	6979.0(12)	15.9(3)
O1	4822.3(18)	8433.7(16)	3915.1(11)	17.9(3)
O2	2457.3(18)	7971.8(17)	8710.9(11)	19.9(3)
O3	3329.6(18)	5672.3(16)	8271.2(11)	19.8(3)
S1	3406.0(6)	7178.0(5)	8151.9(3)	15.08(14)
Cl1	7967.9(6)	7843.8(5)	5093.8(4)	22.09(15)

Table 3 Anisotropic Displacement Parameters ($Å^2 \times 10^3$) for 284.HCl. The Anisotropic displacement factor exponent takes the form: $-2\pi^2[h^2a^{*2}U_{11}+2hka^*b^*U_{12}+\ldots]$.

Atom	U_{11}	U_{22}	U_{33}	U_{23}	U_{13}	U_{12}
C1	13.2(9)	15.8(9)	17.2(9)	4.1(7)	1.3(7)	5.8(7)
C2	14.0(9)	15.4(9)	16.6(10)	2.7(7)	1.1(7)	5.2(7)
C3	17.0(9)	15.1(9)	15.5(9)	2.0(7)	1.7(7)	6.0(7)
C4	11.3(9)	14.5(9)	17.4(10)	1.1(7)	0.2(7)	3.1(7)
C5	19.8(10)	18.9(10)	14.9(9)	2.0(7)	1.8(7)	10.2(8)
C6	21.9(10)	16.7(9)	17.0(9)	1.5(7)	3.1(8)	9.4(8)
C7	17.9(9)	16.4(9)	16.7(9)	3.5(7)	2.6(7)	8.9(8)
C8	16.1(9)	15.4(9)	16.7(10)	4.1(7)	3.3(7)	7.9(7)
C9	12.5(9)	18.4(10)	22.2(10)	4.0(8)	3.2(8)	5.7(7)
C10	19.4(10)	20.2(10)	22.5(10)	6.2(8)	8.7(8)	9.9(8)
C11	25(1)	20.7(10)	16(1)	2.8(8)	3.4(8)	12.4(8)

C12	17.6(9)	19.4(10)	17.4(10)	3.4(8)	-0.6(8)	6.1(8)
C13	14.7(9)	18.6(9)	19(1)	5.2(8)	4.4(7)	7.1(8)
C14	13.6(9)	20.5(10)	13.4(9)	2.4(7)	0.9(7)	6.4(7)
C15	19.5(10)	18.8(10)	18.5(10)	2.4(8)	3.3(8)	9.4(8)
C16	17.2(10)	23.6(10)	22.7(10)	3.8(8)	4.3(8)	10.3(8)
C17	17.5(10)	24.2(11)	21(1)	7.1(8)	2.4(8)	7.6(8)
C18	20.7(10)	16.9(10)	20.8(10)	1.5(8)	0.8(8)	6.1(8)
C19	19.2(10)	21.8(10)	19(1)	4.1(8)	4.9(8)	11.2(8)
C20	19.4(11)	23.0(11)	34.8(12)	5.5(9)	3.5(9)	4.5(9)
N1	16.4(8)	16.2(9)	16.8(8)	2.5(7)	2.2(6)	8.5(7)
N2	17.5(8)	16.3(8)	14.5(8)	2.1(6)	2.1(6)	6.7(6)
O1	14.1(7)	15.1(7)	22.1(7)	1.5(6)	1.1(6)	2.3(6)
O2	17.1(7)	25.9(8)	19.5(7)	3.5(6)	6.1(6)	10.0(6)
O3	19.0(7)	22.2(7)	19.9(7)	7.2(6)	3.7(6)	7.4(6)
S1	13.5(2)	18.6(3)	14.8(2)	3.68(18)	3.54(17)	6.72(18)
Cl1	15.5(2)	17.8(2)	32.8(3)	3.6(2)	0.33(19)	6.57(18)

Table 4 Bond Lengths for 284.HCl.

Atom	Atom	Length/Å	Atom	Atom	Length/Å
C1	C2	1.520(3)	C10	C11	1.384(3)
C1	C7	1.527(3)	C11	C12	1.392(3)
C1	N1	1.493(2)	C12	C13	1.388(3)
C2	C3	1.525(3)	C14	C15	1.394(3)
C2	C6	1.517(3)	C14	C19	1.386(3)
C3	C4	1.551(3)	C14	S1	1.760(2)
C4	C5	1.537(3)	C15	C16	1.391(3)
C4	C8	1.527(3)	C16	C17	1.397(3)
C4	O1	1.431(2)	C17	C18	1.392(3)
C5	N1	1.519(2)	C17	C20	1.512(3)
C6	N2	1.484(2)	C18	C19	1.391(3)
C7	N2	1.488(2)	N2	S1	1.6356(17)
C8	C9	1.394(3)	O2	S1	1.4366(14)
C8	C13	1.396(3)	O3	S1	1.4310(15)
C9	C10	1.394(3)			

Table 5 Bond Angles for 284.HCl.

Atom	Atom	Atom	Angle/˚	Atom	Atom	Atom	Angle/˚
C2	C1	C7	104.59(15)	C13	C12	C11	120.07(19)
N1	C1	C2	108.76(16)	C12	C13	C8	120.58(18)
N1	C1	C7	114.89(15)	C15	C14	S1	119.41(16)
C1	C2	C3	112.56(16)	C19	C14	C15	120.71(19)
C6	C2	C1	100.76(15)	C19	C14	S1	119.87(15)
C6	C2	C3	118.42(16)	C16	C15	C14	119.16(19)
C2	C3	C4	111.51(15)	C15	C16	C17	120.94(18)
C5	C4	C3	111.37(16)	C16	C17	C20	120.64(19)

C8	C4	C3	110.44(16)	C18	C17	C16	118.75(19)
C8	C4	C5	108.91(16)	C18	C17	C20	120.61(19)
O1	C4	C3	110.89(15)	C19	C18	C17	120.99(19)
O1	C4	C5	104.15(15)	C14	C19	C18	119.44(18)
O1	C4	C8	110.92(15)	C1	N1	C5	114.08(15)
N1	C5	C4	112.68(16)	C6	N2	C7	111.00(15)
N2	C6	C2	101.17(15)	C6	N2	S1	118.78(13)
N2	C7	C1	101.97(14)	C7	N2	S1	119.51(13)
C9	C8	C4	120.63(17)	N2	S1	C14	107.88(9)
C9	C8	C13	118.99(18)	O2	S1	C14	107.29(9)
C13	C8	C4	120.37(17)	O2	S1	N2	106.15(9)
C8	C9	C10	120.32(18)	O3	S1	C14	108.94(9)
C11	C10	C9	120.27(18)	O3	S1	N2	105.12(9)
C10	C11	C12	119.75(19)	O3	S1	O2	120.85(9)

Table 6 Hydrogen Bonds for 284.HCl.

D	H	A	d(D-H)/Å	d(H-A)/Å	d(D-A)/Å	D-H-A/°
N1	H1A	Cl1[1]	0.89(3)	2.32(3)	3.1534(18)	157(2)
N1	H1B	Cl1[2]	0.94(3)	2.17(4)	3.1010(18)	179(3)
O1	H1C	Cl1	0.83(3)	2.30(3)	3.0866(16)	158(3)

[1]1-X,2-Y,1-Z; [2]-1+X,+Y,+Z

Table 7 Torsion Angles for 284.HCl.

A	B	C	D	Angle/˚	A	B	C	D	Angle/˚
C1	C2	C3	C4	-26.0(2)	C8	C4	C5	N1	178.79(15)
C1	C2	C6	N2	42.23(18)	C8	C9	C10	C11	-0.5(3)
C1	C7	N2	C6	0.7(2)	C9	C8	C13	C12	-0.8(3)
C1	C7	N2	S1	144.79(13)	C9	C10	C11	C12	-0.5(3)
C2	C1	C7	N2	26.53(18)	C10	C11	C12	C13	0.8(3)
C2	C1	N1	C5	-41.9(2)	C11	C12	C13	C8	-0.2(3)
C2	C3	C4	C5	-33.2(2)	C13	C8	C9	C10	1.1(3)
C2	C3	C4	C8	-154.34(16)	C14	C15	C16	C17	0.3(3)
C2	C3	C4	O1	82.29(19)	C15	C14	C19	C18	0.6(3)
C2	C6	N2	C7	-27.4(2)	C15	C14	S1	N2	-80.90(17)
C2	C6	N2	S1	-171.72(13)	C15	C14	S1	O2	165.12(15)
C3	C2	C6	N2	165.38(16)	C15	C14	S1	O3	32.70(18)
C3	C4	C5	N1	56.8(2)	C15	C16	C17	C18	0.3(3)
C3	C4	C8	C9	-113.7(2)	C15	C16	C17	C20	179.68(19)
C3	C4	C8	C13	65.5(2)	C16	C17	C18	C19	-0.4(3)
C4	C5	N1	C1	-17.1(2)	C17	C18	C19	C14	0.0(3)
C4	C8	C9	C10	-179.64(18)	C19	C14	C15	C16	-0.7(3)
C4	C8	C13	C12	179.96(18)	C19	C14	S1	N2	97.86(17)
C5	C4	C8	C9	123.68(19)	C19	C14	S1	O2	-16.12(19)
C5	C4	C8	C13	-57.1(2)	C19	C14	S1	O3	-148.53(16)
C6	C2	C3	C4	-143.08(17)	C20	C17	C18	C19	-179.80(19)

C6	N2	S1	C14	74.34(16)	N1	C1	C2	C3	66.1(2)
C6	N2	S1	O2	-170.92(14)	N1	C1	C2	C6	-166.74(15)
C6	N2	S1	O3	-41.79(16)	N1	C1	C7	N2	145.69(16)
C7	C1	C2	C3	-170.66(15)	O1	C4	C5	N1	-62.82(19)
C7	C1	C2	C6	-43.53(18)	O1	C4	C8	C9	9.6(2)
C7	C1	N1	C5	-158.68(16)	O1	C4	C8	C13	-171.17(16)
C7	N2	S1	C14	-66.98(16)	S1	C14	C15	C16	178.07(15)
C7	N2	S1	O2	47.75(16)	S1	C14	C19	C18	-178.18(15)
C7	N2	S1	O3	176.89(14)					

Table 8 Hydrogen Atom Coordinates (Å×10^4) and Isotropic Displacement Parameters (Å^2×10^3) for 284.HCl.

Atom	*x*	*y*	*z*	U(eq)
H1	4137	8657	5569	18
H2	1128	6041	5172	18
H3A	2207	5072	3949	19
H3B	4164	5879	4455	19
H5A	1957	8804	3313	21
H5B	637	7299	3496	21
H6A	2662	5023	6249	21
H6B	4436	6343	6288	21
H7A	3255	9336	7005	19
H7B	1251	8458	6592	19
H9	5464	7570	2321	21
H10	5129	6493	665	23
H11	2463	4791	-126	23
H12	128	4133	751	22
H13	447	5220	2399	20
H15	6603	6682	7846	22
H16	9508	8216	8082	24
H18	8105	11767	9184	24
H19	5199	10249	8947	22
H20A	11725	10566	8589	39
H20B	11395	11555	9509	39
H20C	11111	11967	8445	39
H1A	2250(40)	9750(40)	4860(20)	31(7)
H1B	690(50)	8470(40)	4890(20)	48(9)
H1C	5580(40)	8050(30)	4110(20)	32(7)

Crystal structure determination of [284.HCl]

Crystal Data for $C_{20}H_{25}ClN_2O_3S$ (*M* =408.93 g/mol): triclinic, space group P-1 (no. 2), *a* = 8.0819(4) Å, *b* = 9.4116(6) Å, *c* = 13.7236(8) Å, *α* = 97.294(5)°, *β* = 96.498(4)°, *γ* = 107.359(5)°, *V* = 975.60(10) Å^3, *Z* = 2, *T* = 99.98(11) K, μ(CuKα) = 2.928 mm^{-1}, *Dcalc* = 1.392 g/cm^3, 6365 reflections measured (6.578° ≤ 2Θ ≤ 138.278°), 3626 unique (R_{int} = 0.0301, R_{sigma} = 0.0378) which were used in all calculations. The final R_1 was 0.0386 (I > 2σ(I)) and wR_2 was 0.1081 (all data).

Refinement model description
Number of restraints - 0, number of constraints - unknown. Details: 1. Fixed Uiso At 1.2 times of: All C(H) groups, All C(H,H) groups At 1.5 times of: All C(H,H,H) groups. 2.a Ternary CH refined with riding coordinates: C1(H1), C2(H2). 2.b Secondary CH2 refined with riding coordinates: C3(H3A,H3B), C5(H5A,H5B), C6(H6A,H6B), C7(H7A,H7B). 2.c Aromatic/amide H refined with riding coordinates: C9(H9), C10(H10), C11(H11), C12(H12), C13(H13), C15(H15), C16(H16), C18(H18), C19(H19). 2.d Idealised Me refined as rotating group: C20(H20A,H20B,H20C)

5.3.4: (363a)AuCl

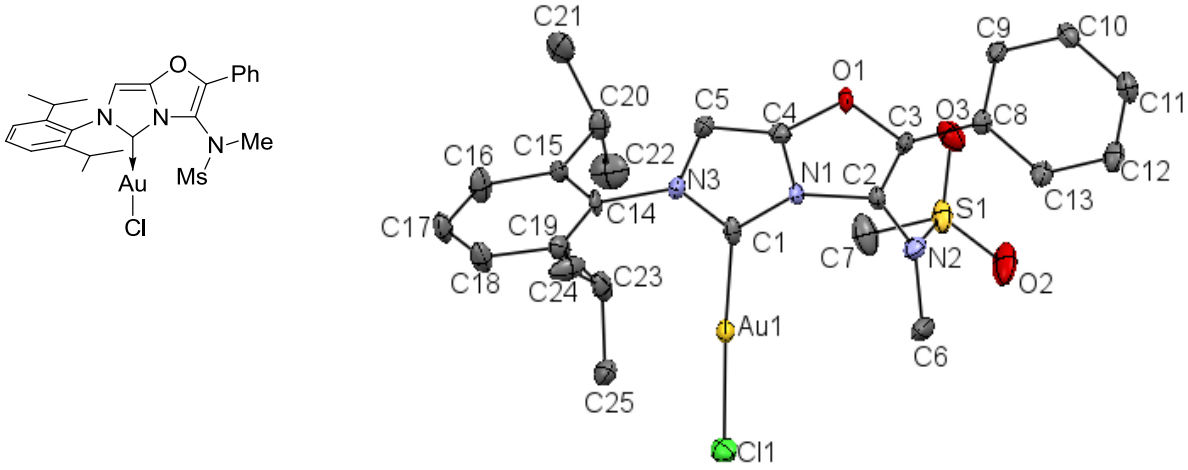

Table 1 Crystal data and structure refinement for (363a)AuCl.

Identification code	**(363a)AuCl**
Empirical formula	$C_{25}H_{29}AuClN_3O_3S$
Formula weight	683.99
Temperature/K	100.00(10)
Crystal system	monoclinic
Space group	$P2_1/n$
a/Å	9.9647(3)
b/Å	20.0858(10)
c/Å	12.9728(4)
α/°	90
β/°	100.759(3)
γ/°	90
Volume/Å^3	2550.85(16)
Z	4
ρ_{calc}g/cm^3	1.781
μ/mm^{-1}	5.986
F(000)	1344.0
Crystal size/mm^3	0.1924 × 0.1637 × 0.0228
Radiation	MoKα (λ = 0.71073)
2Θ range for data collection/°	6.052 to 52.738
Index ranges	-12 ≤ h ≤ 11, -21 ≤ k ≤ 25, -16 ≤ l ≤ 16

Reflections collected	13654
Independent reflections	5207 [R_{int} = 0.0310, R_{sigma} = 0.0429]
Data/restraints/parameters	5207/0/313
Goodness-of-fit on F^2	1.078
Final R indexes [I>=2σ (I)]	R_1 = 0.0360, wR_2 = 0.0728
Final R indexes [all data]	R_1 = 0.0461, wR_2 = 0.0779
Largest diff. peak/hole / e $Å^{-3}$	1.96/-1.59

Table 2 Fractional Atomic Coordinates (×10^4) and Equivalent Isotropic Displacement Parameters ($Å^2$×10^3) for (363a)AuCl. U_{eq} is defined as 1/3 of of the trace of the orthogonalised U_{IJ} tensor.

Atom	*x*	*y*	*z*	U(eq)
C1	3322(5)	3257(3)	5230(4)	16.7(11)
C2	5280(5)	3872(3)	6507(4)	14.8(11)
C3	5105(5)	4266(3)	7299(4)	13.8(11)
C4	3043(5)	3976(3)	6494(4)	16.0(11)
C5	1761(5)	3797(3)	6039(4)	16.8(11)
C6	7069(6)	3045(3)	6337(5)	27.7(14)
C7	6317(7)	4061(4)	4095(5)	35.3(16)
C8	6056(5)	4584(3)	8147(4)	15.2(11)
C9	5610(5)	5081(3)	8760(4)	17.0(11)
C10	6484(5)	5343(3)	9608(4)	19.8(12)
C11	7824(5)	5125(3)	9860(4)	21.9(12)
C12	8286(5)	4635(3)	9256(4)	22.0(13)
C13	7404(5)	4369(3)	8409(4)	19.2(12)
C14	859(5)	3034(3)	4562(4)	16.2(11)
C15	361(5)	3341(3)	3608(4)	17.0(11)
C16	-734(6)	3030(3)	2948(5)	25.2(13)
C17	-1294(6)	2452(3)	3265(5)	24.6(13)
C18	-780(6)	2167(3)	4214(4)	24.2(13)
C19	334(5)	2441(3)	4881(4)	19.6(12)
C20	958(5)	3979(3)	3260(4)	22.0(13)
C21	-126(6)	4513(3)	2899(5)	31.5(15)
C22	1805(7)	3828(4)	2423(6)	38.1(17)
C23	966(6)	2086(3)	5891(4)	23.7(13)
C24	-89(6)	1922(3)	6574(5)	30.0(15)
C25	1703(5)	1456(3)	5632(5)	23.6(13)
Cl1	5277.5(13)	1790.9(7)	3647.5(11)	23.6(3)
Au1	4184.2(2)	2586.0(2)	4441.5(2)	16.50(7)
N1	3958(4)	3665(2)	5998(3)	13.9(9)
N2	6465(4)	3712(2)	6146(3)	18.6(10)
N3	1982(4)	3353(2)	5261(3)	16(1)
O1	3707(3)	4355.6(19)	7308(3)	16.3(8)
O2	8515(4)	4115(3)	5527(4)	40.0(12)
O3	6627(4)	4901(2)	5634(3)	28.6(10)
S1	7088.0(13)	4256.7(8)	5396.0(11)	24.0(3)

Table 3 Anisotropic Displacement Parameters ($Å^2×10^3$) for (363a)AuCl. The Anisotropic displacement factor exponent takes the form: $-2π^2[h^2a^{*2}U_{11}+2hka*b*U_{12}+…]$.

Atom	U_{11}	U_{22}	U_{33}	U_{23}	U_{13}	U_{12}
C1	16(2)	21(3)	11(3)	2(2)	-2(2)	-6(2)
C2	12(2)	16(3)	15(3)	-1(2)	-1(2)	-4(2)
C3	8(2)	16(3)	17(3)	3(2)	0(2)	-1(2)
C4	17(2)	15(3)	16(3)	-2(2)	3(2)	2(2)
C5	13(2)	16(3)	20(3)	0(2)	0(2)	1(2)
C6	20(3)	27(3)	32(4)	-7(3)	-7(2)	10(3)
C7	38(4)	47(4)	20(3)	-4(3)	3(3)	-17(3)
C8	15(2)	17(3)	12(3)	2(2)	1(2)	-3(2)
C9	11(2)	20(3)	19(3)	-1(2)	2(2)	2(2)
C10	21(3)	19(3)	20(3)	-6(2)	5(2)	-4(2)
C11	21(3)	26(3)	18(3)	-2(2)	0(2)	-8(2)
C12	14(2)	32(3)	20(3)	-2(3)	4(2)	-3(2)
C13	16(2)	24(3)	17(3)	-3(2)	3(2)	0(2)
C14	12(2)	20(3)	14(3)	-3(2)	-5(2)	-6(2)
C15	12(2)	13(3)	25(3)	0(2)	0(2)	-2(2)
C16	27(3)	29(3)	16(3)	9(3)	-6(2)	-9(3)
C17	25(3)	23(3)	21(3)	0(3)	-9(2)	-7(2)
C18	28(3)	20(3)	21(3)	5(2)	-6(2)	-9(2)
C19	23(3)	19(3)	14(3)	-1(2)	-4(2)	2(2)
C20	21(3)	24(3)	18(3)	6(2)	-2(2)	-6(2)
C21	28(3)	21(3)	44(4)	8(3)	4(3)	-9(3)
C22	42(4)	36(4)	41(4)	11(3)	21(3)	-4(3)
C23	29(3)	21(3)	17(3)	2(2)	-10(2)	-4(2)
C24	41(4)	33(4)	15(3)	3(3)	1(3)	19(3)
C25	15(3)	23(3)	31(3)	0(3)	2(2)	1(2)
Cl1	19.7(6)	22.3(7)	31.1(8)	-4.6(6)	10.6(6)	-0.1(5)
Au1	12.43(10)	19.03(12)	17.22(12)	-3.23(9)	0.66(7)	-2.21(8)
N1	10.9(19)	16(2)	12(2)	-4.5(18)	-3.1(17)	0.0(17)
N2	15(2)	23(3)	17(2)	-3(2)	2.4(18)	4.2(19)
N3	9.6(19)	18(2)	18(2)	-2.1(19)	-1.9(17)	-0.1(18)
O1	8.7(16)	23(2)	17(2)	-6.3(16)	0.5(14)	-4.3(15)
O2	16(2)	68(4)	37(3)	-15(2)	9.6(19)	-9(2)
O3	30(2)	26(2)	32(3)	-5.9(19)	11.4(19)	-10.7(19)
S1	14.4(6)	37.3(9)	21.4(8)	-8.1(7)	6.4(5)	-6.8(6)

Table 4 Bond Lengths for (363a)AuCl.

Atom	Atom	Length/Å	Atom	Atom	Length/Å
C1	Au1	1.982(6)	C12	C13	1.379(8)
C1	N1	1.353(7)	C14	C15	1.389(8)
C1	N3	1.357(6)	C14	C19	1.394(8)
C2	C3	1.333(7)	C14	N3	1.451(6)
C2	N1	1.421(6)	C15	C16	1.402(7)

C2	N2	1.387(6)	C15	C20	1.517(8)
C3	C8	1.458(7)	C16	C17	1.383(8)
C3	O1	1.407(6)	C17	C18	1.368(8)
C4	C5	1.352(7)	C18	C19	1.388(8)
C4	N1	1.363(6)	C19	C23	1.520(8)
C4	O1	1.368(6)	C20	C21	1.532(8)
C5	N3	1.395(7)	C20	C22	1.525(8)
C6	N2	1.471(7)	C23	C24	1.532(8)
C7	S1	1.763(6)	C23	C25	1.532(8)
C8	C9	1.399(7)	Cl1	Au1	2.2841(14)
C8	C13	1.392(7)	N2	S1	1.660(5)
C9	C10	1.374(7)	O2	S1	1.429(4)
C10	C11	1.386(8)	O3	S1	1.427(5)
C11	C12	1.388(8)			

Table 5 Bond Angles for (363a)AuCl.

Atom	Atom	Atom	Angle/˚	Atom	Atom	Atom	Angle/˚
N1	C1	Au1	127.1(4)	C18	C17	C16	121.0(5)
N1	C1	N3	102.8(4)	C17	C18	C19	121.1(5)
N3	C1	Au1	129.5(4)	C14	C19	C23	122.6(5)
C3	C2	N1	106.8(4)	C18	C19	C14	117.0(5)
C3	C2	N2	129.8(5)	C18	C19	C23	120.4(5)
N2	C2	N1	123.3(5)	C15	C20	C21	112.9(5)
C2	C3	C8	132.9(5)	C15	C20	C22	110.0(5)
C2	C3	O1	110.8(4)	C22	C20	C21	111.9(5)
O1	C3	C8	116.3(4)	C19	C23	C24	112.4(5)
C5	C4	N1	109.4(5)	C19	C23	C25	109.7(5)
C5	C4	O1	140.1(5)	C25	C23	C24	111.0(5)
N1	C4	O1	110.5(4)	C1	Au1	Cl1	175.79(15)
C4	C5	N3	102.9(4)	C1	N1	C2	141.8(5)
C9	C8	C3	120.7(5)	C1	N1	C4	111.3(4)
C13	C8	C3	120.7(5)	C4	N1	C2	106.9(4)
C13	C8	C9	118.5(5)	C2	N2	C6	120.1(5)
C10	C9	C8	120.5(5)	C2	N2	S1	118.7(4)
C9	C10	C11	120.4(5)	C6	N2	S1	120.9(4)
C10	C11	C12	119.8(5)	C1	N3	C5	113.7(4)
C13	C12	C11	119.6(5)	C1	N3	C14	124.5(5)
C12	C13	C8	121.2(5)	C5	N3	C14	121.8(4)
C15	C14	C19	123.5(5)	C4	O1	C3	105.1(4)
C15	C14	N3	117.8(5)	N2	S1	C7	105.7(3)
C19	C14	N3	118.7(5)	O2	S1	C7	108.4(3)
C14	C15	C16	117.0(5)	O2	S1	N2	105.7(3)
C14	C15	C20	123.0(5)	O3	S1	C7	108.0(3)
C16	C15	C20	120.0(5)	O3	S1	N2	107.5(2)
C17	C16	C15	120.3(5)	O3	S1	O2	120.6(3)

Table 6 Torsion Angles for (363a)AuCl.

A	B	C	D	Angle/˚	A	B	C	D	Angle/˚
C2	C3	C8	C9	167.3(6)	C16	C15	C20	C22	-74.1(7)
C2	C3	C8	C13	-16.9(9)	C16	C17	C18	C19	-1.2(10)
C2	C3	O1	C4	1.8(6)	C17	C18	C19	C14	2.9(9)
C2	N2	S1	C7	-89.9(5)	C17	C18	C19	C23	-174.9(6)
C2	N2	S1	O2	155.3(4)	C18	C19	C23	C24	-53.7(7)
C2	N2	S1	O3	25.2(5)	C18	C19	C23	C25	70.2(7)
C3	C2	N1	C1	-174.3(7)	C19	C14	C15	C16	0.5(8)
C3	C2	N1	C4	2.7(6)	C19	C14	C15	C20	-178.8(5)
C3	C2	N2	C6	107.3(7)	C19	C14	N3	C1	93.3(7)
C3	C2	N2	S1	-78.9(7)	C19	C14	N3	C5	-86.9(7)
C3	C8	C9	C10	175.0(5)	C20	C15	C16	C17	-179.3(6)
C3	C8	C13	C12	-175.5(5)	Au1	C1	N1	C2	7.9(10)
C4	C5	N3	C1	0.1(6)	Au1	C1	N1	C4	-169.1(4)
C4	C5	N3	C14	-179.7(5)	Au1	C1	N3	C5	169.5(4)
C5	C4	N1	C1	-2.1(6)	Au1	C1	N3	C14	-10.7(8)
C5	C4	N1	C2	179.9(5)	N1	C1	N3	C5	-1.3(6)
C5	C4	O1	C3	177.7(7)	N1	C1	N3	C14	178.5(5)
C6	N2	S1	C7	83.8(5)	N1	C2	C3	C8	174.2(5)
C6	N2	S1	O2	-31.0(5)	N1	C2	C3	O1	-2.8(6)
C6	N2	S1	O3	-161.0(4)	N1	C2	N2	C6	-78.1(7)
C8	C3	O1	C4	-175.7(5)	N1	C2	N2	S1	95.7(6)
C8	C9	C10	C11	1.0(8)	N1	C4	C5	N3	1.2(6)
C9	C8	C13	C12	0.4(8)	N1	C4	O1	C3	0.0(6)
C9	C10	C11	C12	-0.5(9)	N2	C2	C3	C8	-10.5(10)
C10	C11	C12	C13	0.0(9)	N2	C2	C3	O1	172.5(5)
C11	C12	C13	C8	0.1(9)	N2	C2	N1	C1	10.0(10)
C13	C8	C9	C10	-0.9(8)	N2	C2	N1	C4	-173.0(5)
C14	C15	C16	C17	1.4(9)	N3	C1	N1	C2	178.9(6)
C14	C15	C20	C21	-128.9(6)	N3	C1	N1	C4	2.0(6)
C14	C15	C20	C22	105.2(6)	N3	C14	C15	C16	-179.3(5)
C14	C19	C23	C24	128.6(6)	N3	C14	C15	C20	1.4(8)
C14	C19	C23	C25	-107.4(6)	N3	C14	C19	C18	177.1(5)
C15	C14	C19	C18	-2.6(8)	N3	C14	C19	C23	-5.2(8)
C15	C14	C19	C23	175.1(5)	O1	C3	C8	C9	-15.9(7)
C15	C14	N3	C1	-87.0(7)	O1	C3	C8	C13	159.9(5)
C15	C14	N3	C5	92.8(6)	O1	C4	C5	N3	-176.6(7)
C15	C16	C17	C18	-1.1(10)	O1	C4	N1	C1	176.4(4)
C16	C15	C20	C21	51.8(7)	O1	C4	N1	C2	-1.6(6)

Table 7 Hydrogen Atom Coordinates (Å×10^4) and Isotropic Displacement Parameters (Å^2×10^3) for (363a)AuCl.

Atom	*x*	*y*	*z*	U(eq)
H5	936	3936	6203	20
H6A	7942	3079	6796	42
H6B	7185	2851	5683	42
H6C	6476	2769	6657	42
H7A	5350	4133	4003	53
H7B	6490	3603	3955	53
H7C	6691	4340	3619	53
H9	4716	5235	8591	20
H10	6173	5668	10017	24
H11	8413	5306	10432	26
H12	9185	4487	9421	26
H13	7717	4041	8007	23
H16	-1086	3213	2295	30
H17	-2030	2254	2826	30
H18	-1183	1782	4415	29
H20	1583	4159	3871	26
H21A	-734	4362	2280	47
H21B	312	4917	2745	47
H21C	-636	4594	3445	47
H22A	2493	3505	2687	57
H22B	2233	4229	2245	57
H22C	1221	3655	1808	57
H23	1649	2384	6293	28
H24A	-470	2328	6786	45
H24B	346	1681	7185	45
H24C	-805	1655	6180	45
H25A	1069	1174	5183	35
H25B	2065	1223	6269	35
H25C	2435	1576	5282	35

Crystal structure determination of [(363a)AuCl]

Crystal Data for $C_{25}H_{29}AuClN_3O_3S$ (*M* =683.99 g/mol): monoclinic, space group $P2_1/n$ (no. 14), *a* = 9.9647(3) Å, *b* = 20.0858(10) Å, *c* = 12.9728(4) Å, *β* = 100.759(3)°, *V* = 2550.85(16) Å^3, *Z* = 4, *T* = 100.00(10) K, μ(MoKα) = 5.986 mm^{-1}, *Dcalc* = 1.781 g/cm^3, 13654 reflections measured (6.052° ≤ 2Θ ≤ 52.738°), 5207 unique (R_{int} = 0.0310, R_{sigma} = 0.0429) which were used in all calculations. The final R_1 was 0.0360 (I > 2σ(I)) and wR_2 was 0.0779 (all data).

Refinement model description

Number of restraints - 0, number of constraints - unknown. Details: 1. Fixed Uiso At 1.2 times of: All C(H) groups At 1.5 times of: All C(H,H,H) groups. 2.a Ternary CH refined with riding coordinates: C20(H20), C23(H23). 2.b Aromatic/amide H refined with riding coordinates: C5(H5), C9(H9), C10(H10), C11(H11), C12(H12), C13(H13), C16(H16), C17(H17), C18(H18). 2.c Idealised Me refined as rotating group: C6(H6A,H6B,H6C), C7(H7A,H7B,H7C), C21(H21A,H21B,H21C), C22(H22A,H22B,H22C), C24(H24A,H24B,H24C), C25(H25A,H25B,H25C)

5.3.5: (363c)AuCl

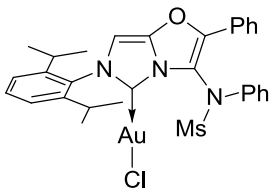

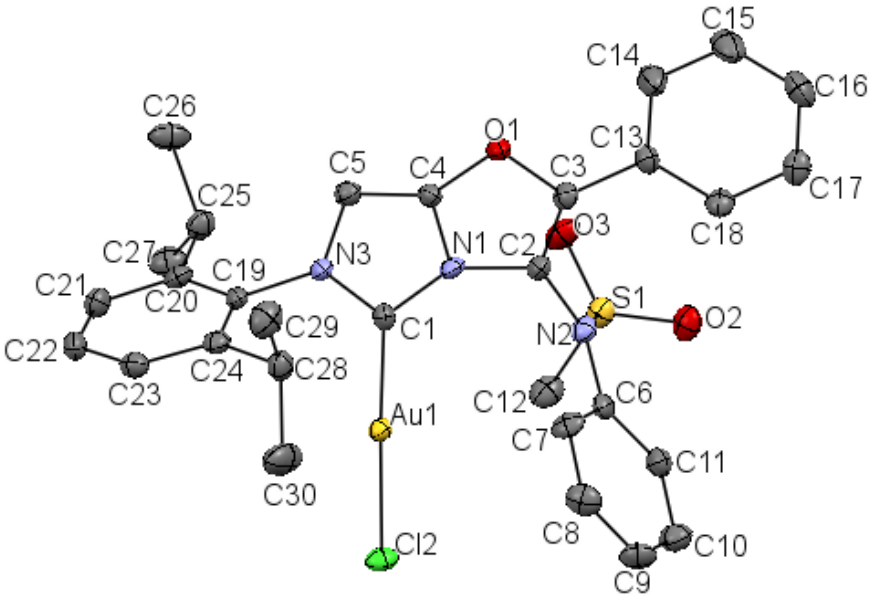

Table 1 Crystal data and structure refinement for (363c)AuCl.

Identification code	**(363c)AuCl**
Empirical formula	$C_{30}H_{31}AuClN_3O_3S$
Formula weight	746.05
Temperature/K	100.00(10)
Crystal system	orthorhombic
Space group	$P2_12_12_1$
a/Å	9.41339(16)
b/Å	13.4993(2)
c/Å	23.0896(5)
α/°	90
β/°	90
γ/°	90
Volume/Å^3	2934.10(9)
Z	4
ρ_{calc}g/cm^3	1.689
μ/mm^{-1}	5.212
F(000)	1472.0
Crystal size/mm^3	0.2982 × 0.2203 × 0.0968
Radiation	MoKα (λ = 0.71073)
2Θ range for data collection/°	6.036 to 54.964
Index ranges	-12 ≤ h ≤ 11, -17 ≤ k ≤ 17, -29 ≤ l ≤ 29
Reflections collected	31735
Independent reflections	6686 [R_{int} = 0.0350, R_{sigma} = 0.0295]
Data/restraints/parameters	6686/0/358
Goodness-of-fit on F^2	1.047

Final R indexes [I>=2σ (I)]	R_1 = 0.0209, wR_2 = 0.0389
Final R indexes [all data]	R_1 = 0.0233, wR_2 = 0.0400
Largest diff. peak/hole / e Å^{-3}	1.06/-1.02
Flack parameter	0.502(5)

Table 2 Fractional Atomic Coordinates (×10^4) and Equivalent Isotropic Displacement Parameters (Å^2×10^3) for (363c)AuCl. U_{eq} is defined as 1/3 of of the trace of the orthogonalised U_{IJ} tensor.

Atom	*x*	*y*	*z*	U(eq)
C1	898(5)	4618(3)	2166.6(18)	16.8(10)
C2	1186(5)	5100(3)	1070(2)	17.9(10)
C3	510(5)	5852(3)	806(2)	18.9(10)
C4	-290(5)	5821(3)	1699(2)	17.4(10)
C5	-760(5)	5862(3)	2247(2)	19.6(10)
C6	3617(5)	4452(3)	939(2)	18.2(10)
C7	4137(5)	5135(3)	1335(2)	22.2(11)
C8	5564(6)	5192(4)	1454(2)	26.6(11)
C9	6519(6)	4594(4)	1158(2)	27.8(12)
C10	6024(6)	3929(4)	753(2)	27.6(12)
C11	4575(5)	3854(4)	637(2)	22.7(11)
C12	1849(6)	2378(3)	951(2)	28.4(12)
C13	586(5)	6313(3)	231.5(19)	19.6(10)
C14	-325(6)	7092(4)	94(2)	34.2(13)
C15	-234(7)	7553(4)	-438(3)	39.2(15)
C16	752(6)	7246(4)	-837(2)	30.2(12)
C17	1668(5)	6480(4)	-711.7(19)	24.4(10)
C18	1592(6)	6008(3)	-174(2)	22.6(11)
C19	-67(5)	4968(3)	3146(2)	16.8(10)
C20	-1122(5)	4350(4)	3375(2)	19.5(10)
C21	-1175(5)	4261(4)	3975(2)	24.1(11)
C22	-248(5)	4782(4)	4327(2)	23.2(11)
C23	775(5)	5394(3)	4082(2)	21.9(11)
C24	902(5)	5502(3)	3486(2)	19.3(10)
C25	-2204(6)	3828(3)	2998(2)	23.5(10)
C26	-3629(5)	4366(4)	3038(3)	31.1(12)
C27	-2374(6)	2732(3)	3151(2)	29.8(12)
C28	2044(5)	6157(3)	3230(2)	23.0(11)
C29	1772(6)	7243(4)	3364(2)	32.7(13)
C30	3521(6)	5843(5)	3438(3)	44.0(17)
Au1	2246.8(2)	3550.6(2)	2347.0(2)	15.53(5)
Cl2	3820.6(12)	2304.6(8)	2515.8(5)	21.7(3)
N1	683(4)	5076(3)	1648.6(17)	17.7(9)
N2	2116(5)	4383(3)	837.9(16)	19.3(8)
N3	-8(4)	5106(3)	2522.4(15)	16.7(8)
O1	-435(3)	6309(2)	1189.5(13)	18.6(7)
O2	1949(4)	3260(2)	-37.9(14)	27.2(8)

O3	-149(3)	3554(3)	577.3(15)	29.7(8)
S1	1343.7(13)	3389.2(9)	524.3(5)	21.7(3)

Table 3 Anisotropic Displacement Parameters ($Å^2×10^3$) for (363c)AuCl. The Anisotropic displacement factor exponent takes the form: $-2π^2[h^2a^{*2}U_{11}+2hka^*b^*U_{12}+…]$.

Atom	U_{11}	U_{22}	U_{33}	U_{23}	U_{13}	U_{12}
C1	19(2)	18(2)	13(2)	0.2(16)	1.0(18)	-0.7(18)
C2	17(2)	20(2)	17(2)	-0.5(19)	2(2)	3(2)
C3	20(3)	20(2)	17(2)	-5.2(18)	0(2)	1(2)
C4	17(2)	20(2)	15(2)	-0.7(18)	-1.6(19)	3.2(19)
C5	18(2)	21(2)	20(3)	-2.4(18)	-0.6(19)	1.9(18)
C6	19(3)	19(2)	17(2)	5.3(18)	2.0(19)	1.1(19)
C7	20(3)	16(2)	30(3)	-9(2)	0(2)	3.5(19)
C8	29(3)	21(2)	30(3)	-6(2)	-8(2)	-3(2)
C9	18(3)	30(3)	36(3)	-2(2)	-7(2)	-1(2)
C10	24(3)	29(3)	31(3)	-3(2)	0(2)	6(2)
C11	24(3)	27(3)	17(3)	-2.4(19)	-1(2)	1(2)
C12	28(3)	20(2)	37(3)	-1(2)	5(2)	0(2)
C13	23(2)	20(2)	16(2)	-0.8(18)	-0.4(18)	-1(2)
C14	41(3)	37(3)	24(3)	2(2)	4(3)	16(3)
C15	53(4)	36(3)	28(3)	2(2)	-1(3)	21(3)
C16	43(3)	28(3)	20(3)	4(2)	-5(2)	-1(3)
C17	30(3)	20(2)	23(2)	-6(2)	3(2)	-6(3)
C18	26(3)	18(2)	24(3)	0.5(19)	2(2)	3(2)
C19	15(2)	21(2)	14(2)	0.0(18)	0.7(19)	5.4(19)
C20	13(2)	22(2)	24(3)	-1.3(19)	1.7(19)	2.9(19)
C21	21(3)	28(3)	23(3)	3(2)	4(2)	-2(2)
C22	24(3)	29(3)	17(3)	4(2)	4(2)	4(2)
C23	20(3)	23(3)	23(3)	-1(2)	-3(2)	2(2)
C24	18(3)	18(2)	23(3)	0.5(19)	1(2)	5(2)
C25	19(2)	27(2)	25(2)	-0.2(18)	2(2)	-3(2)
C26	21(3)	26(3)	46(3)	1(2)	-9(2)	-2(2)
C27	26(3)	24(2)	40(3)	-5(2)	-3(2)	3(2)
C28	22(3)	27(2)	21(2)	2.1(17)	3(2)	-3(2)
C29	33(3)	26(3)	40(3)	1(2)	7(3)	-4(2)
C30	23(3)	50(4)	59(4)	24(3)	8(3)	0(3)
Au1	14.46(7)	14.39(7)	17.73(8)	0.28(7)	2.04(7)	1.23(7)
Cl2	17.8(5)	15.5(5)	31.9(7)	1.6(4)	-0.5(4)	2.0(4)
N1	13(2)	20(2)	20(2)	-2.5(16)	2.0(17)	5.6(16)
N2	20(2)	17.5(18)	20.5(19)	-2.3(15)	3.0(18)	2.6(18)
N3	14.7(19)	20.4(18)	15(2)	-0.8(14)	1.5(14)	5.0(15)
O1	19.0(16)	20.1(17)	16.7(16)	0.0(13)	0.3(13)	6.5(14)
O2	30(2)	29.1(18)	23.1(18)	-8.3(13)	1.9(15)	-3.8(15)
O3	18.1(17)	31.5(18)	39(2)	-6(2)	2.6(15)	-3.0(19)
S1	20.9(6)	21.8(6)	22.4(6)	-4.9(5)	1.4(5)	-3.1(5)

Table 4 Bond Lengths for (363c)AuCl.

Atom	Atom	Length/Å	Atom	Atom	Length/Å
C1	Au1	1.965(4)	C14	C15	1.380(8)
C1	N1	1.361(6)	C15	C16	1.372(8)
C1	N3	1.355(5)	C16	C17	1.376(7)
C2	C3	1.345(7)	C17	C18	1.397(7)
C2	N1	1.417(6)	C19	C20	1.400(7)
C2	N2	1.410(6)	C19	C24	1.403(7)
C3	C13	1.468(6)	C19	N3	1.452(6)
C3	O1	1.398(5)	C20	C21	1.393(7)
C4	C5	1.343(6)	C20	C25	1.514(7)
C4	N1	1.366(6)	C21	C22	1.384(7)
C4	O1	1.354(5)	C22	C23	1.388(7)
C5	N3	1.395(6)	C23	C24	1.389(7)
C6	C7	1.388(7)	C24	C28	1.512(7)
C6	C11	1.396(7)	C25	C26	1.528(7)
C6	N2	1.435(6)	C25	C27	1.529(6)
C7	C8	1.374(7)	C28	C29	1.520(7)
C8	C9	1.388(7)	C28	C30	1.530(7)
C9	C10	1.378(7)	Au1	Cl2	2.2750(11)
C10	C11	1.394(7)	N2	S1	1.689(4)
C12	S1	1.749(5)	O2	S1	1.428(3)
C13	C14	1.393(7)	O3	S1	1.428(3)
C13	C18	1.394(7)			

Table 5 Bond Angles for (363c)AuCl.

Atom	Atom	Atom	Angle/˚	Atom	Atom	Atom	Angle/˚
N1	C1	Au1	128.0(3)	C19	C20	C25	122.5(4)
N3	C1	Au1	129.4(3)	C21	C20	C19	116.9(4)
N3	C1	N1	102.6(4)	C21	C20	C25	120.6(4)
C3	C2	N1	106.6(4)	C22	C21	C20	121.2(5)
C3	C2	N2	129.7(4)	C21	C22	C23	120.0(5)
N2	C2	N1	123.4(4)	C22	C23	C24	121.7(5)
C2	C3	C13	135.0(5)	C19	C24	C28	123.0(4)
C2	C3	O1	110.3(4)	C23	C24	C19	116.4(4)
O1	C3	C13	114.6(4)	C23	C24	C28	120.6(4)
C5	C4	N1	109.3(4)	C20	C25	C26	109.5(4)
C5	C4	O1	140.0(4)	C20	C25	C27	112.8(4)
O1	C4	N1	110.6(4)	C26	C25	C27	110.7(4)
C4	C5	N3	103.4(4)	C24	C28	C29	111.4(4)
C7	C6	C11	119.0(4)	C24	C28	C30	111.2(4)
C7	C6	N2	119.8(4)	C29	C28	C30	110.9(5)
C11	C6	N2	121.2(4)	C1	Au1	Cl2	177.62(13)
C8	C7	C6	120.9(5)	C1	N1	C2	142.0(4)
C7	C8	C9	120.1(5)	C1	N1	C4	111.1(4)

C10	C9	C8	119.6(5)	C4	N1	C2	106.7(4)
C9	C10	C11	120.5(5)	C2	N2	C6	120.4(4)
C10	C11	C6	119.7(5)	C2	N2	S1	116.2(3)
C14	C13	C3	119.7(4)	C6	N2	S1	122.9(3)
C14	C13	C18	119.2(4)	C1	N3	C5	113.5(4)
C18	C13	C3	121.0(4)	C1	N3	C19	124.2(4)
C15	C14	C13	120.4(5)	C5	N3	C19	121.7(4)
C16	C15	C14	120.2(5)	C4	O1	C3	105.8(3)
C15	C16	C17	120.7(5)	N2	S1	C12	105.2(2)
C16	C17	C18	119.8(5)	O2	S1	C12	107.9(2)
C13	C18	C17	119.8(5)	O2	S1	N2	108.4(2)
C20	C19	C24	123.7(4)	O3	S1	C12	109.9(2)
C20	C19	N3	118.5(4)	O3	S1	N2	105.2(2)
C24	C19	N3	117.7(4)	O3	S1	O2	119.3(2)

Table 6 Torsion Angles for (363c)AuCl.

A	B	C	D	Angle/˚	A	B	C	D	Angle/˚
C2	C3	C13	C14	178.4(6)	C20	C19	N3	C1	-99.2(5)
C2	C3	C13	C18	-3.9(9)	C20	C19	N3	C5	89.8(5)
C2	C3	O1	C4	1.2(5)	C20	C21	C22	C23	-1.1(8)
C2	N2	S1	C12	-115.6(4)	C21	C20	C25	C26	74.1(6)
C2	N2	S1	O2	129.2(3)	C21	C20	C25	C27	-49.6(6)
C2	N2	S1	O3	0.5(4)	C21	C22	C23	C24	0.0(7)
C3	C2	N1	C1	-173.7(6)	C22	C23	C24	C19	0.6(7)
C3	C2	N1	C4	0.5(5)	C22	C23	C24	C28	-178.8(4)
C3	C2	N2	C6	104.7(6)	C23	C24	C28	C29	-68.0(6)
C3	C2	N2	S1	-83.4(6)	C23	C24	C28	C30	56.3(6)
C3	C13	C14	C15	177.9(5)	C24	C19	C20	C21	-1.0(7)
C3	C13	C18	C17	-178.1(4)	C24	C19	C20	C25	176.5(4)
C4	C5	N3	C1	0.4(5)	C24	C19	N3	C1	83.7(5)
C4	C5	N3	C19	172.3(4)	C24	C19	N3	C5	-87.3(5)
C5	C4	N1	C1	-1.1(6)	C25	C20	C21	C22	-176.0(4)
C5	C4	N1	C2	-177.3(4)	Au1	C1	N1	C2	-2.5(9)
C5	C4	O1	C3	175.6(6)	Au1	C1	N1	C4	-176.6(3)
C6	C7	C8	C9	3.2(8)	Au1	C1	N3	C5	176.8(3)
C6	N2	S1	C12	56.2(4)	Au1	C1	N3	C19	5.2(7)
C6	N2	S1	O2	-59.1(4)	N1	C1	N3	C5	-1.1(5)
C6	N2	S1	O3	172.2(4)	N1	C1	N3	C19	-172.7(4)
C7	C6	C11	C10	2.2(7)	N1	C2	C3	C13	175.8(5)
C7	C6	N2	C2	9.6(7)	N1	C2	C3	O1	-1.1(5)
C7	C6	N2	S1	-161.8(3)	N1	C2	N2	C6	-82.0(6)
C7	C8	C9	C10	-1.5(8)	N1	C2	N2	S1	89.9(5)
C8	C9	C10	C11	0.2(8)	N1	C4	C5	N3	0.4(5)
C9	C10	C11	C6	-0.6(8)	N1	C4	O1	C3	-0.9(5)
C11	C6	C7	C8	-3.5(7)	N2	C2	C3	C13	-10.0(10)

C11	C6	N2	C2	-169.3(4)	N2	C2	C3	O1	173.1(4)
C11	C6	N2	S1	19.3(6)	N2	C2	N1	C1	11.6(9)
C13	C3	O1	C4	-176.4(4)	N2	C2	N1	C4	-174.1(4)
C13	C14	C15	C16	0.2(9)	N2	C6	C7	C8	177.6(5)
C14	C13	C18	C17	-0.4(7)	N2	C6	C11	C10	-179.0(4)
C14	C15	C16	C17	-0.4(9)	N3	C1	N1	C2	175.4(6)
C15	C16	C17	C18	0.2(8)	N3	C1	N1	C4	1.3(5)
C16	C17	C18	C13	0.2(7)	N3	C19	C20	C21	-177.9(4)
C18	C13	C14	C15	0.1(8)	N3	C19	C20	C25	-0.4(7)
C19	C20	C21	C22	1.6(7)	N3	C19	C24	C23	176.9(4)
C19	C20	C25	C26	-103.3(5)	N3	C19	C24	C28	-3.8(6)
C19	C20	C25	C27	133.0(5)	O1	C3	C13	C14	-4.8(6)
C19	C24	C28	C29	112.6(5)	O1	C3	C13	C18	172.9(4)
C19	C24	C28	C30	-123.0(5)	O1	C4	C5	N3	-176.1(6)
C20	C19	C24	C23	-0.1(7)	O1	C4	N1	C1	176.5(4)
C20	C19	C24	C28	179.3(4)	O1	C4	N1	C2	0.2(5)

Table 7 Hydrogen Atom Coordinates (Å×10^4) and Isotropic Displacement Parameters (Å^2×10^3) for (363c)AuCl.

Atom	*x*	*y*	*z*	U(eq)
H5	-1428	6291	2406	24
H7	3510	5561	1521	27
H8	5891	5631	1734	32
H9	7487	4642	1233	33
H10	6663	3527	555	33
H11	4248	3407	361	27
H12A	2866	2359	981	43
H12B	1515	1777	776	43
H12C	1443	2444	1330	43
H14	-997	7302	362	41
H15	-843	8075	-526	47
H16	802	7558	-1195	36
H17	2335	6278	-984	29
H18	2210	5491	-87	27
H21	-1846	3845	4143	29
H22	-310	4723	4727	28
H23	1391	5740	4323	26
H25	-1877	3869	2595	28
H26A	-3974	4333	3429	47
H26B	-4300	4056	2783	47
H26C	-3507	5046	2928	47
H27A	-1476	2402	3110	45
H27B	-3056	2434	2896	45
H27C	-2695	2672	3544	45
H28	2017	6076	2809	28

H29A 892	7444	3190	49
H29B 2533	7637	3210	49
H29C 1719	7334	3776	49
H30A 3599	5956	3847	66
H30B 4230	6223	3238	66
H30C 3660	5151	3358	66

Crystal structure determination of [(363c)AuCl]

Crystal Data for $C_{30}H_{31}AuClN_3O_3S$ (*M* =746.05 g/mol): orthorhombic, space group $P2_12_12_1$ (no. 19), *a* = 9.41339(16) Å, *b* = 13.4993(2) Å, *c* = 23.0896(5) Å, *V* = 2934.10(9) Å^3, *Z* = 4, *T* = 100.00(10) K, μ(MoKα) = 5.212 mm^{-1}, *Dcalc* = 1.689 g/cm^3, 31735 reflections measured (6.036° ≤ 2Θ ≤ 54.964°), 6686 unique (R_{int} = 0.0350, R_{sigma} = 0.0295) which were used in all calculations. The final R_1 was 0.0209 (I > 2σ(I)) and wR_2 was 0.0400 (all data).

Refinement model description

Number of restraints - 0, number of constraints - unknown.

Details: 1. Twinned data refinement Scales: 0.498(5) 0.502(5). 2. Fixed Uiso At 1.2 times of: All C(H) groups At 1.5 times of: All C(H,H,H) groups. 3.a Ternary CH refined with riding coordinates: C25(H25), C28(H28). 3.b Aromatic/amide H refined with riding coordinates: C5(H5), C7(H7), C8(H8), C9(H9), C10(H10), C11(H11), C14(H14), C15(H15), C16(H16), C17(H17), C18(H18), C21(H21), C22(H22), C23(H23). 3.c Idealised Me refined as rotating group: C12(H12A,H12B,H12C), C26(H26A,H26B,H26C), C27(H27A,H27B,H27C), C29(H29A,H29B, H29C), C30(H30A,H30B,H30C).

5.3.6: (363a)CuCl.CDCl$_3$

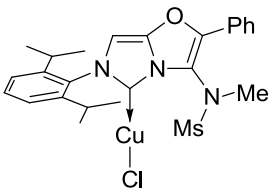

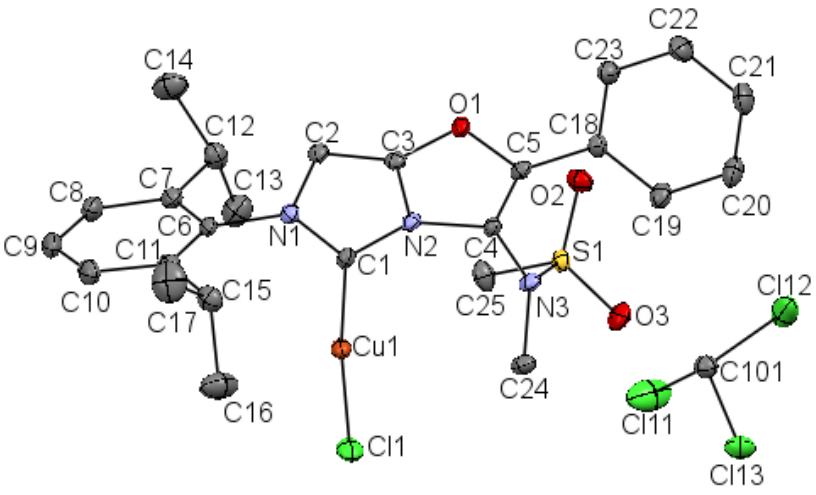

Table 1. Crystal data and structure refinement for (363a)CuCl.

Identification code	**(363a)CuCl**	
Empirical formula	$C_{25}H_{29}ClCuN_3O_3S$, $CDCl_3$	
Formula weight	670.97	
Temperature	100(2) K	
Wavelength	0.71075 Å	
Crystal system	Monoclinic	
Space group	P 2_1/n	
Unit cell dimensions	a = 16.9828(3) Å	□= 90°.
	b = 10.1478(2) Å	□= 95.615(7)°.
	c = 17.4535(12) Å	□ = 90°.

Volume	2993.5(2) $Å^3$
Z	4
Density (calculated)	1.489 Mg/m^3
Absorption coefficient	1.189 mm^{-1}
F(000)	1376
Crystal size	0.28 x 0.25 x 0.15 mm^3
Theta range for data collection	3.09 to 27.48°.
Index ranges	-22<=h<=22, -13<=k<=13, -21<=l<=22
Reflections collected	39227
Independent reflections	6850 [R(int) = 0.0259]
Completeness to theta = 27.48°	99.8 %
Absorption correction	Semi-empirical from equivalents
Max. and min. transmission	0.8418 and 0.7319
Refinement method	Full-matrix least-squares on F^2
Data / restraints / parameters	6850 / 0 / 350
Goodness-of-fit on F^2	1.006
Final R indices [I>2sigma(I)]	R1 = 0.0319, wR2 = 0.0825
R indices (all data)	R1 = 0.0337, wR2 = 0.0836
Largest diff. peak and hole	1.572 and -0.992 $e.Å^{-3}$

Notes:
Selected Parameters: C(1)-Cu(1) = 1.8801 (17) Å, N(3)…Cu(1) = 3.530 (2) Å.
The hydrogen and deuterium atoms have been fixed as riding models.

Table 2. Atomic coordinates (x 10^4) and equivalent isotropic displacement parameters ($Å^2$x 10^3) for (363a)CuCl. U(eq) is defined as one third of the trace of the orthogonalized U^{ij} tensor.

	x	y	z	U(eq)
C(1)	1976(1)	5179(2)	1260(1)	13(1)
C(2)	978(1)	5916(2)	367(1)	15(1)
C(3)	1632(1)	6648(2)	308(1)	13(1)
C(4)	2899(1)	6980(2)	741(1)	12(1)
C(5)	2676(1)	7871(2)	189(1)	13(1)
C(6)	673(1)	4037(2)	1205(1)	14(1)
C(7)	706(1)	2758(2)	906(1)	17(1)
C(8)	161(1)	1843(2)	1139(1)	21(1)
C(9)	-396(1)	2206(2)	1627(1)	23(1)
C(10)	-419(1)	3481(2)	1906(1)	22(1)
C(11)	120(1)	4430(2)	1709(1)	17(1)
C(12)	1299(1)	2359(2)	350(1)	21(1)
C(13)	2031(1)	1710(2)	773(1)	28(1)
C(14)	934(1)	1440(2)	-292(1)	32(1)
C(15)	130(1)	5801(2)	2060(1)	21(1)
C(16)	535(2)	5755(2)	2885(1)	35(1)
C(17)	-694(1)	6398(2)	2053(2)	39(1)
C(18)	3064(1)	8977(2)	-152(1)	14(1)
C(19)	3743(1)	9554(2)	224(1)	19(1)

C(20)	4079(1)	10647(2)	-98(1)	22(1)
C(21)	3754(1)	11156(2)	-796(1)	24(1)
C(22)	3082(1)	10584(2)	-1173(1)	23(1)
C(23)	2735(1)	9504(2)	-851(1)	18(1)
C(24)	3694(1)	7029(2)	2011(1)	18(1)
C(25)	4169(1)	4254(2)	1003(1)	22(1)
N(1)	1211(1)	5021(1)	957(1)	13(1)
N(2)	2223(1)	6193(1)	830(1)	12(1)
N(3)	3627(1)	6785(2)	1169(1)	13(1)
O(1)	1886(1)	7667(1)	-100(1)	14(1)
O(2)	4228(1)	6119(1)	-14(1)	20(1)
O(3)	5054(1)	6320(1)	1234(1)	21(1)
S(1)	4329(1)	5931(1)	803(1)	13(1)
Cl(1)	3353(1)	3548(1)	2984(1)	23(1)
Cu(1)	2572(1)	4346(1)	2087(1)	15(1)
C(101)	6798(1)	5186(2)	1406(1)	18(1)
Cl(11)	6913(1)	3538(1)	1686(1)	48(1)
Cl(12)	7430(1)	5585(1)	698(1)	41(1)
Cl(13)	6996(1)	6249(1)	2201(1)	24(1)

Table 3. Bond lengths [Å] and angles [°] for (363a)CuCl.

C(1)-N(1)	1.363(2)	C(10)-H(10)	0.9500	C(19)-H(19)	0.9500
C(1)-N(2)	1.364(2)	C(11)-C(15)	1.520(3)	C(20)-C(21)	1.387(3)
C(1)-Cu(1)	1.8801(17)	C(12)-C(13)	1.531(3)	C(20)-H(20)	0.9500
C(2)-C(3)	1.350(2)	C(12)-C(14)	1.541(3)	C(21)-C(22)	1.387(3)
C(2)-N(1)	1.402(2)	C(12)-H(12)	1.0000	C(21)-H(21)	0.9500
C(2)-H(2)	0.9500	C(13)-H(13A)	0.9800	C(22)-C(23)	1.388(3)
C(3)-O(1)	1.350(2)	C(13)-H(13B)	0.9800	C(22)-H(22)	0.9500
C(3)-N(2)	1.368(2)	C(13)-H(13C)	0.9800	C(23)-H(23)	0.9500
C(4)-C(5)	1.349(2)	C(14)-H(14A)	0.9800	C(24)-N(3)	1.482(2)
C(4)-N(3)	1.394(2)	C(14)-H(14B)	0.9800	C(24)-H(24A)	0.9800
C(4)-N(2)	1.420(2)	C(14)-H(14C)	0.9800	C(24)-H(24B)	0.9800
C(5)-O(1)	1.4018(19)	C(15)-C(17)	1.524(3)	C(24)-H(24C)	0.9800
C(5)-C(18)	1.457(2)	C(15)-C(16)	1.534(3)	C(25)-S(1)	1.7629(19)
C(6)-C(7)	1.402(3)	C(15)-H(15)	1.0000	C(25)-H(25A)	0.9800
C(6)-C(11)	1.405(2)	C(16)-H(16A)	0.9800	C(25)-H(25B)	0.9800
C(6)-N(1)	1.449(2)	C(16)-H(16B)	0.9800	C(25)-H(25C)	0.9800
C(7)-C(8)	1.400(2)	C(16)-H(16C)	0.9800	N(3)-S(1)	1.6520(15)
C(7)-C(12)	1.521(2)	C(17)-H(17A)	0.9800	O(2)-S(1)	1.4315(13)
C(8)-C(9)	1.383(3)	C(17)-H(17B)	0.9800	O(3)-S(1)	1.4348(13)
C(8)-H(8)	0.9500	C(17)-H(17C)	0.9800	Cl(1)-Cu(1)	2.1125(5)
C(9)-C(10)	1.384(3)	C(18)-C(23)	1.397(2)	C(101)-Cl(11)	1.7475(19)
C(9)-H(9)	0.9500	C(18)-C(19)	1.398(2)	C(101)-Cl(12)	1.7605(18)
C(10)-C(11)	1.395(3)	C(19)-C(20)	1.391(3)	C(101)-Cl(13)	1.7636(18)

N(1)-C(1)-N(2)	101.98(13)	C(12)-C(13)-H(13B)	109.5	C(20)-C(21)-H(21)	120.0
N(1)-C(1)-Cu(1)	131.72(13)	H(13A)-C(13)-H(13B)	109.5	C(21)-C(22)-C(23)	120.06(18)
N(2)-C(1)-Cu(1)	126.21(12)	C(12)-C(13)-H(13C)	109.5	C(21)-C(22)-H(22)	120.0
C(3)-C(2)-N(1)	103.69(14)	H(13A)-C(13)-H(13C)	109.5	C(23)-C(22)-H(22)	120.0
C(3)-C(2)-H(2)	128.2	H(13B)-C(13)-H(13C)	109.5	C(22)-C(23)-C(18)	120.36(17)
N(1)-C(2)-H(2)	128.2	C(12)-C(14)-H(14A)	109.5	C(22)-C(23)-H(23)	119.8

C(2)-C(3)-O(1)	140.34(15)	C(12)-C(14)-H(14B)	109.5	C(18)-C(23)-H(23)	119.8
C(2)-C(3)-N(2)	108.61(15)	H(14A)-C(14)-H(14B)	109.5	N(3)-C(24)-H(24A)	109.5
O(1)-C(3)-N(2)	111.05(14)	C(12)-C(14)-H(14C)	109.5	N(3)-C(24)-H(24B)	109.5
C(5)-C(4)-N(3)	130.58(15)	H(14A)-C(14)-H(14C)	109.5	H(24A)-C(24)-H(24B)	109.5
C(5)-C(4)-N(2)	106.33(14)	H(14B)-C(14)-H(14C)	109.5	N(3)-C(24)-H(24C)	109.5
N(3)-C(4)-N(2)	123.09(14)	C(11)-C(15)-C(17)	112.74(17)	H(24A)-C(24)-H(24C)	109.5
C(4)-C(5)-O(1)	110.50(14)	C(11)-C(15)-C(16)	109.68(16)	H(24B)-C(24)-H(24C)	109.5
C(4)-C(5)-C(18)	134.54(15)	C(17)-C(15)-C(16)	110.30(19)	S(1)-C(25)-H(25A)	109.5
O(1)-C(5)-C(18)	114.94(14)	C(11)-C(15)-H(15)	108.0	S(1)-C(25)-H(25B)	109.5
C(7)-C(6)-C(11)	123.33(16)	C(17)-C(15)-H(15)	108.0	H(25A)-C(25)-H(25B)	109.5
C(7)-C(6)-N(1)	118.51(15)	C(16)-C(15)-H(15)	108.0	S(1)-C(25)-H(25C)	109.5
C(11)-C(6)-N(1)	118.10(15)	C(15)-C(16)-H(16A)	109.5	H(25A)-C(25)-H(25C)	109.5
C(8)-C(7)-C(6)	117.03(16)	C(15)-C(16)-H(16B)	109.5	H(25B)-C(25)-H(25C)	109.5
C(8)-C(7)-C(12)	120.46(17)	H(16A)-C(16)-H(16B)	109.5	C(1)-N(1)-C(2)	113.55(14)
C(6)-C(7)-C(12)	122.52(16)	C(15)-C(16)-H(16C)	109.5	C(1)-N(1)-C(6)	124.78(14)
C(9)-C(8)-C(7)	120.88(18)	H(16A)-C(16)-H(16C)	109.5	C(2)-N(1)-C(6)	121.66(13)
C(9)-C(8)-H(8)	119.6	H(16B)-C(16)-H(16C)	109.5	C(1)-N(2)-C(3)	112.15(14)
C(7)-C(8)-H(8)	119.6	C(15)-C(17)-H(17A)	109.5	C(1)-N(2)-C(4)	141.23(14)
C(8)-C(9)-C(10)	120.69(17)	C(15)-C(17)-H(17B)	109.5	C(3)-N(2)-C(4)	106.60(13)
C(8)-C(9)-H(9)	119.7	H(17A)-C(17)-H(17B)	109.5	C(4)-N(3)-C(24)	119.00(13)
C(10)-C(9)-H(9)	119.7	C(15)-C(17)-H(17C)	109.5	C(4)-N(3)-S(1)	120.15(11)
C(9)-C(10)-C(11)	121.12(18)	H(17A)-C(17)-H(17C)	109.5	C(24)-N(3)-S(1)	118.88(11)
C(9)-C(10)-H(10)	119.4	H(17B)-C(17)-H(17C)	109.5	C(3)-O(1)-C(5)	105.48(12)
C(11)-C(10)-H(10)	119.4	C(23)-C(18)-C(19)	119.39(16)	O(2)-S(1)-O(3)	119.86(8)
C(10)-C(11)-C(6)	116.93(17)	C(23)-C(18)-C(5)	119.52(15)	O(2)-S(1)-N(3)	107.15(7)
C(10)-C(11)-C(15)	120.97(17)	C(19)-C(18)-C(5)	121.04(15)	O(3)-S(1)-N(3)	105.49(8)
C(6)-C(11)-C(15)	122.03(16)	C(20)-C(19)-C(18)	119.76(17)	O(2)-S(1)-C(25)	108.70(9)
C(7)-C(12)-C(13)	111.32(16)	C(20)-C(19)-H(19)	120.1	O(3)-S(1)-C(25)	107.65(9)
C(7)-C(12)-C(14)	112.35(16)	C(18)-C(19)-H(19)	120.1	N(3)-S(1)-C(25)	107.37(8)
C(13)-C(12)-C(14)	109.90(17)	C(21)-C(20)-C(19)	120.50(17)	C(1)-Cu(1)-Cl(1)	173.29(5)
C(7)-C(12)-H(12)	107.7	C(21)-C(20)-H(20)	119.7	Cl(11)-C(101)-Cl(12)	110.94(10)
C(13)-C(12)-H(12)	107.7	C(19)-C(20)-H(20)	119.7	Cl(11)-C(101)-Cl(13)	110.94(10)
C(14)-C(12)-H(12)	107.7	C(22)-C(21)-C(20)	119.92(17)	Cl(12)-C(101)-Cl(13)	109.19(10)
C(12)-C(13)-H(13A)	109.5	C(22)-C(21)-H(21)	120.0		

Symmetry transformations used to generate equivalent atoms:

Table 4. Anisotropic displacement parameters ($Å^2 x\ 10^3$)for (363a)CuCl. The anisotropic displacement factor exponent takes the form: $-2\pi^2[h^2 a^{*2} U^{11} + ... + 2\ h\ k\ a^*\ b^*\ U^{12}]$

	U^{11}	U^{22}	U^{33}	U^{23}	U^{13}	U^{12}
C(1)	11(1)	14(1)	15(1)	-1(1)	1(1)	-1(1)
C(2)	12(1)	16(1)	15(1)	2(1)	-2(1)	-1(1)
C(3)	12(1)	15(1)	13(1)	1(1)	-2(1)	1(1)
C(4)	9(1)	14(1)	13(1)	-1(1)	1(1)	-1(1)
C(5)	10(1)	15(1)	14(1)	-2(1)	-1(1)	0(1)
C(6)	10(1)	17(1)	14(1)	3(1)	-2(1)	-3(1)
C(7)	15(1)	20(1)	16(1)	2(1)	-1(1)	-2(1)
C(8)	23(1)	20(1)	21(1)	0(1)	-1(1)	-7(1)
C(9)	18(1)	29(1)	23(1)	6(1)	0(1)	-10(1)
C(10)	14(1)	31(1)	21(1)	4(1)	3(1)	-2(1)

C(11)	12(1)	22(1)	16(1)	3(1)	-1(1)	1(1)
C(12)	24(1)	19(1)	23(1)	-1(1)	7(1)	-1(1)
C(13)	23(1)	27(1)	33(1)	-7(1)	3(1)	2(1)
C(14)	34(1)	35(1)	25(1)	-8(1)	2(1)	2(1)
C(15)	20(1)	23(1)	21(1)	1(1)	4(1)	3(1)
C(16)	50(1)	28(1)	25(1)	-4(1)	-5(1)	2(1)
C(17)	30(1)	34(1)	54(2)	1(1)	9(1)	12(1)
C(18)	14(1)	12(1)	16(1)	0(1)	3(1)	0(1)
C(19)	15(1)	19(1)	23(1)	2(1)	-2(1)	-1(1)
C(20)	16(1)	19(1)	32(1)	1(1)	0(1)	-4(1)
C(21)	22(1)	18(1)	32(1)	5(1)	6(1)	-3(1)
C(22)	29(1)	20(1)	21(1)	6(1)	0(1)	-3(1)
C(23)	21(1)	16(1)	18(1)	1(1)	-1(1)	-2(1)
C(24)	17(1)	23(1)	14(1)	-3(1)	-2(1)	0(1)
C(25)	23(1)	15(1)	29(1)	3(1)	9(1)	1(1)
N(1)	10(1)	16(1)	14(1)	2(1)	0(1)	-1(1)
N(2)	9(1)	13(1)	12(1)	0(1)	-2(1)	0(1)
N(3)	10(1)	18(1)	12(1)	-1(1)	-1(1)	1(1)
O(1)	11(1)	16(1)	16(1)	4(1)	-2(1)	-2(1)
O(2)	18(1)	25(1)	17(1)	2(1)	5(1)	4(1)
O(3)	10(1)	25(1)	27(1)	0(1)	-2(1)	0(1)
S(1)	9(1)	15(1)	16(1)	2(1)	2(1)	0(1)
Cl(1)	20(1)	27(1)	21(1)	9(1)	-4(1)	2(1)
Cu(1)	12(1)	17(1)	15(1)	4(1)	-1(1)	-1(1)
C(101)	17(1)	20(1)	16(1)	0(1)	1(1)	1(1)
Cl(11)	79(1)	21(1)	40(1)	3(1)	-18(1)	3(1)
Cl(12)	32(1)	65(1)	27(1)	-19(1)	16(1)	-22(1)
Cl(13)	29(1)	26(1)	16(1)	-5(1)	2(1)	2(1)

Table 5. Hydrogen coordinates (x 10^4) and isotropic displacement parameters (Å^{2}x 10^3) for (363a)CuCl.

	x	y	z	U(eq)
H(2)	476	5990	77	18
H(8)	173	960	959	25
H(9)	-766	1574	1772	28
H(10)	-809	3713	2237	26
H(12)	1477	3180	100	26
H(13A)	2255	2294	1185	42
H(13B)	2425	1550	410	42
H(13C)	1880	871	995	42
H(14A)	835	572	-74	47
H(14B)	1300	1347	-689	47
H(14C)	433	1815	-522	47
H(15)	451	6385	1749	25
H(16A)	241	5160	3196	52
H(16B)	544	6641	3108	52
H(16C)	1078	5433	2877	52

H(17A)	-963	6355	1530	58
H(17B)	-650	7320	2219	58
H(17C)	-1000	5904	2404	58
H(19)	3973	9202	698	23
H(20)	4535	11048	162	27
H(21)	3991	11894	-1016	28
H(22)	2859	10931	-1651	28
H(23)	2271	9121	-1107	22
H(24A)	4050	7775	2134	27
H(24B)	3906	6242	2283	27
H(24C)	3170	7231	2170	27
H(25A)	3660	3973	739	33
H(25B)	4161	4134	1559	33
H(25C)	4595	3723	822	33
D(101)	6238	5324	1185	22

Table 6. Torsion angles [°] for (363a)CuCl.

N(1)-C(2)-C(3)-O(1)	-179.7(2)
N(1)-C(2)-C(3)-N(2)	0.78(19)
N(3)-C(4)-C(5)-O(1)	178.04(16)
N(2)-C(4)-C(5)-O(1)	-1.73(18)
N(3)-C(4)-C(5)-C(18)	-3.1(3)
N(2)-C(4)-C(5)-C(18)	177.15(18)
C(11)-C(6)-C(7)-C(8)	-0.9(3)
N(1)-C(6)-C(7)-C(8)	-177.99(15)
C(11)-C(6)-C(7)-C(12)	178.81(16)
N(1)-C(6)-C(7)-C(12)	1.7(2)
C(6)-C(7)-C(8)-C(9)	1.6(3)
C(12)-C(7)-C(8)-C(9)	-178.11(17)
C(7)-C(8)-C(9)-C(10)	-0.9(3)
C(8)-C(9)-C(10)-C(11)	-0.5(3)
C(9)-C(10)-C(11)-C(6)	1.2(3)
C(9)-C(10)-C(11)-C(15)	-175.67(17)
C(7)-C(6)-C(11)-C(10)	-0.5(3)
N(1)-C(6)-C(11)-C(10)	176.63(15)
C(7)-C(6)-C(11)-C(15)	176.36(16)
N(1)-C(6)-C(11)-C(15)	-6.5(2)
C(8)-C(7)-C(12)-C(13)	-84.2(2)
C(6)-C(7)-C(12)-C(13)	96.1(2)
C(8)-C(7)-C(12)-C(14)	39.5(2)
C(6)-C(7)-C(12)-C(14)	-140.16(18)
C(10)-C(11)-C(15)-C(17)	-46.3(2)
C(6)-C(11)-C(15)-C(17)	137.02(19)
C(10)-C(11)-C(15)-C(16)	77.1(2)
C(6)-C(11)-C(15)-C(16)	-99.7(2)
C(4)-C(5)-C(18)-C(23)	163.67(19)
O(1)-C(5)-C(18)-C(23)	-17.5(2)
C(4)-C(5)-C(18)-C(19)	-19.0(3)

O(1)-C(5)-C(18)-C(19)	159.88(16)
C(23)-C(18)-C(19)-C(20)	0.3(3)
C(5)-C(18)-C(19)-C(20)	-177.04(17)
C(18)-C(19)-C(20)-C(21)	-1.1(3)
C(19)-C(20)-C(21)-C(22)	0.9(3)
C(20)-C(21)-C(22)-C(23)	0.0(3)
C(21)-C(22)-C(23)-C(18)	-0.7(3)
C(19)-C(18)-C(23)-C(22)	0.5(3)
C(5)-C(18)-C(23)-C(22)	177.97(17)
N(2)-C(1)-N(1)-C(2)	-1.06(18)
Cu(1)-C(1)-N(1)-C(2)	175.65(13)
N(2)-C(1)-N(1)-C(6)	178.97(15)
Cu(1)-C(1)-N(1)-C(6)	-4.3(3)
C(3)-C(2)-N(1)-C(1)	0.2(2)
C(3)-C(2)-N(1)-C(6)	-179.83(15)
C(7)-C(6)-N(1)-C(1)	-82.8(2)
C(11)-C(6)-N(1)-C(1)	99.9(2)
C(7)-C(6)-N(1)-C(2)	97.21(19)
C(11)-C(6)-N(1)-C(2)	-80.0(2)
N(1)-C(1)-N(2)-C(3)	1.55(18)
Cu(1)-C(1)-N(2)-C(3)	-175.41(12)
N(1)-C(1)-N(2)-C(4)	-179.88(19)
Cu(1)-C(1)-N(2)-C(4)	3.2(3)
C(2)-C(3)-N(2)-C(1)	-1.5(2)
O(1)-C(3)-N(2)-C(1)	178.77(13)
C(2)-C(3)-N(2)-C(4)	179.40(14)
O(1)-C(3)-N(2)-C(4)	-0.30(18)
C(5)-C(4)-N(2)-C(1)	-177.4(2)
N(3)-C(4)-N(2)-C(1)	2.8(3)
C(5)-C(4)-N(2)-C(3)	1.24(18)
N(3)-C(4)-N(2)-C(3)	-178.56(15)
C(5)-C(4)-N(3)-C(24)	113.9(2)
N(2)-C(4)-N(3)-C(24)	-66.3(2)
C(5)-C(4)-N(3)-S(1)	-82.2(2)
N(2)-C(4)-N(3)-S(1)	97.51(17)
C(2)-C(3)-O(1)-C(5)	179.7(2)
N(2)-C(3)-O(1)-C(5)	-0.72(18)
C(4)-C(5)-O(1)-C(3)	1.55(18)
C(18)-C(5)-O(1)-C(3)	-177.57(14)
C(4)-N(3)-S(1)-O(2)	30.27(15)
C(24)-N(3)-S(1)-O(2)	-165.86(13)
C(4)-N(3)-S(1)-O(3)	159.05(13)
C(24)-N(3)-S(1)-O(3)	-37.08(15)
C(4)-N(3)-S(1)-C(25)	-86.35(15)
C(24)-N(3)-S(1)-C(25)	77.52(15)
N(1)-C(1)-Cu(1)-Cl(1)	178.4(3)
N(2)-C(1)-Cu(1)-Cl(1)	-5.6(6)

Symmetry transformations used to generate equivalent atoms:

5.4: References

[1] V. S. C. Yeh, *Tetrahedron* **2004**, *60*, 11995-12042.

[2] a) J. Liddle, M. J. Allen, A. D. Borthwick, D. P. Brooks, D. E. Davies, R. M. Edwards, A. M. Exall, C. Hamlett, W. R. Irving, A. M. Mason, G. P. McCafferty, F. Nerozzi, S. Peace, J. Philp, D. Pollard, M. A. Pullen, S. S. Shabbir, S. L. Sollis, T. D. Westfall, P. M. Woollard, C. Wu, D. M. B. Hickey, *Bioorg. Med. Chem. Lett.* **2008**, *18*, 90-94; b) D. J. Greenblatt, R. Matlis, J. M. Scavone, G. T. Blyden, J. S. Harmatz, R. I. Shader, *Br. J. Clin. Pharmacol.* **1985**, *19*, 373-378; c) B. Hulin, D. A. Clark, S. W. Goldstein, R. E. McDermott, P. J. Dambek, W. H. Kappeler, C. H. Lamphere, D. M. Lewis, J. P. Rizzi, *J. Med. Chem.* **1992**, *35*, 1853-1864.

[3] R. Sinha Roy, A. M. Gehring, J. C. Milne, P. J. Belshaw, C. T. Walsh, *Nat. Prod. Rep.* **1999**, *16*, 249-263.

[4] a) S. Bresciani, N. C. O. Tomkinson, *Heterocycles* **2014**, *89*, 2479-2543; b) I. J. Turchi, *Ind. Eng. Chem. Prod. Res. Dev.* **1981**, *20*, 32-76.

[5] a) R. Robinson, *J. Chem. Soc., Trans.* **1909**, *95*, 2167-2174; b) S. Gabriel, *Ber. Dtsch. Chem. Ges.* **1910**, *43*, 134-138.

[6] T. Moriya, M. Seki, S. Takabe, K. Matsumoto, K. Takashima, T. Mori, A. Odawara, S. Takeyama, *J. Med. Chem.* **1988**, *31*, 1197-1204.

[7] H. H. Wasserman, F. J. Vinick, *J. Org. Chem.* **1973**, *38*, 2407-2408.

[8] a) K. C. Nicolaou, D. Y. K. Chen, X. Huang, T. Ling, M. Bella, S. A. Snyder, *J. Am. Chem. Soc.* **2004**, *126*, 12888-12896; b) R. L. Parsons, C. H. Heathcock, *J. Org. Chem.* **1994**, *59*, 4733-4734; c) P. Wipf, S. Venkatraman, *J. Org. Chem.* **1996**, *61*, 6517-6522.

[9] P. Wipf, C. P. Miller, *J. Org. Chem.* **1993**, *58*, 3604-3606.

[10] a) A. Plant, F. Stieber, J. Scherkenbeck, P. Lösel, H. Dyker, *Org. Lett.* **2001**, *3*, 3427-3430; b) E. Biron, J. Chatterjee, H. Kessler, *Org. Lett.* **2006**, *8*, 2417-2420.

[11] a) M. C. Bagley, R. T. Buck, S. L. Hind, C. J. Moody, A. M. Z. Slawin, *Synlett* **1996**, 825-826; b) M. C. Bagley, R. T. Buck, S. Lucy Hind, C. J. Moody, *J. Chem. Soc., Perkin Trans. 1* **1998**, 591-600; c) J. R. Davies, P. D. Kane, C. J. Moody, *Tetrahedron* **2004**, *60*, 3967-3977.

[12] a) M. C. Bagley, K. E. Bashford, C. L. Hesketh, C. J. Moody, *J. Am. Chem. Soc.* **2000**, *122*, 3301-3313; b) J. Linder, A. J. Blake, C. J. Moody, *Org. Biomol. Chem.* **2008**, *6*, 3908-3916; c) J. Linder, T. P. Garner, H. E. L. Williams, M. S. Searle, C. J. Moody, *J. Am. Chem. Soc.* **2011**, *133*, 1044-1051.

[13] Y. Zheng, X. Li, C. Ren, D. Zhang-Negrerie, Y. Du, K. Zhao, *J. Org. Chem.* **2012**, *77*, 10353-10361.

[14] a) R. Connell, F. Scavo, P. Helquist, B. Åkermark, *Tetrahedron Lett.* **1986**, *27*, 5559-5562; b) R. D. Connell, M. Tebbe, A. R. Gangloff, P. Helquist, B. Åkermark, *Tetrahedron* **1993**, *49*, 5445-5459; c) R. D. Connell, M. Tebbe, P. Helquist, B. Åkermark, *Tetrahedron Lett.* **1991**, *32*, 17-20.

[15] Y. Wang, J. Janjic, S. A. Kozmin, *J. Am. Chem. Soc.* **2002**, *124*, 13670-13671.

[16] C. Wan, J. Zhang, S. Wang, J. Fan, Z. Wang, *Org. Lett.* **2010**, *12*, 2338-2341.

[17] R. Martín, A. Cuenca, S. L. Buchwald, *Org. Lett.* **2007**, *9*, 5521-5524.

[18] D. J. Ritson, C. Spiteri, J. E. Moses, *J. Org. Chem.* **2011**, *76*, 3519-3522.

[19] G. Cuny, R. Gámez-Montaño, J. Zhu, *Tetrahedron* **2004**, *60*, 4879-4885.

[20] a) A. S. K. Hashmi, J. P. Weyrauch, W. Frey, J. W. Bats, *Org. Lett.* **2004**, *6*, 4391-4394; b) J. P. Weyrauch, A. S. K. Hashmi, A. Schuster, T. Hengst, S. Schetter, A. Littmann, M. Rudolph, M. Hamzic, J. Visus, F. Rominger, W. Frey, J. W. Bats, *Chem. Eur. J.* **2010**, *16*, 956-963; c) C. L. Paradise, P. R. Sarkar, M. Razzak, J. K. De Brabander, *Org. Biomol. Chem.* **2011**, *9*, 4017-4020.

[21] a) A. Arcadi, S. Cacchi, L. Cascia, G. Fabrizi, F. Marinelli, *Org. Lett.* **2001**, *3*, 2501-2504; b) E. M. Beccalli, E. Borsini, G. Broggini, G. Palmisano, S. Sottocornola, *J. Org. Chem.* **2008**, *73*, 4746-4749; c) A. Saito, K. Iimura, Y. Hanzawa, *Tetrahedron Lett.* **2010**, *51*, 1471-1474.

[22] P.-Y. Coqueron, C. Didier, M. A. Ciufolini, *Angew. Chem. Int. Ed.* **2003**, *42*, 1411-1414.

[23] J. Zhang, M. A. Ciufolini, *Org. Lett.* **2009**, *11*, 2389-2392.

[24] Y.-m. Pan, F.-j. Zheng, H.-x. Lin, Z.-p. Zhan, *J. Org. Chem.* **2009**, *74*, 3148-3151.

[25] A. Saito, A. Taniguchi, Y. Kambara, Y. Hanzawa, *Org. Lett.* **2013**, *15*, 2672-2675.

[26] X. Li, L. Huang, H. Chen, W. Wu, H. Huang, H. Jiang, *Chem. Sci.* **2012**, *3*, 3463-3467.

[27] a) J. Xiao, X. Li, *Angew. Chem. Int. Ed.* **2011**, *50*, 7226-7236; b) L. Zhang, *Acc. Chem. Res.* **2014**, *47*, 877-888; c) H.-S. Yeom, S. Shin, *Acc. Chem. Res.* **2014**, *47*, 966-977.

[28] a) N. D. Shapiro, F. D. Toste, *J. Am. Chem. Soc.* **2007**, *129*, 4160-4161; b) G. Li, L. Zhang, *Angew. Chem. Int. Ed.* **2007**, *46*, 5156-5159; c) P. W. Davies, S. J. C. Albrecht, *Angew. Chem. Int. Ed.* **2009**, *48*, 8372-8375.

[29] H.-S. Yeom, Y. Lee, J.-E. Lee, S. Shin, *Org. Biomol. Chem.* **2009**, *7*, 4744-4752.

[30] L. Cui, Y. Peng, L. Zhang, *J. Am. Chem. Soc.* **2009**, *131*, 8394-8395.

[31] N. Asao, K. Sato, Y. Yamamoto, *Tetrahedron Lett.* **2003**, *44*, 5675-5677.

[32] A. Fürstner, P. W. Davies, *Angew. Chem. Int. Ed.* **2007**, *46*, 3410-3449.

[33] P. W. Davies, M. Garzón, *Asian J. Org. Chem.* **2015**, *4*, 694-708.

[34] a) A. S. K. Hashmi, *Angew. Chem. Int. Ed.* **2008**, *47*, 6754-6756; b) Y. Wang, M. E. Muratore, A. M. Echavarren, *Chem. Eur. J.* **2015**, *21*, 7332-7339.

[35] G. Seidel, R. Mynott, A. Fürstner, *Angew. Chem. Int. Ed.* **2009**, *48*, 2510-2513.

[36] G. Seidel, B. Gabor, R. Goddard, B. Heggen, W. Thiel, A. Fürstner, *Angew. Chem. Int. Ed.* **2014**, *53*, 879-882.

[37] M. W. Hussong, F. Rominger, P. Krämer, B. F. Straub, *Angew. Chem. Int. Ed.* **2014**, *53*, 9372-9375.

[38] D. Benitez, N. D. Shapiro, E. Tkatchouk, Y. Wang, W. A. Goddard, F. D. Toste, *Nature Chem.* **2009**, *1*, 482-486.

[39] a) J. Schulz, L. Jašíková, A. Škríba, J. Roithová, *J. Am. Chem. Soc.* **2014**, *136*, 11513-11523; b) C. A. Swift, S. Gronert, *Organometallics* **2014**, *33*, 7135-7140.

[40] a) S. Bhunia, S. Ghorpade, D. B. Huple, R.-S. Liu, *Angew. Chem. Int. Ed.* **2012**, *51*, 2939-2942; b) E. L. Noey, Y. Luo, L. Zhang, K. N. Houk, *J. Am. Chem. Soc.* **2012**, *134*, 1078-1084; c) B. Lu, Y. Li, Y. Wang, D. H. Aue, Y. Luo, L. Zhang, *J. Am. Chem. Soc.* **2013**, *135*, 8512-8524; d) M. Chen, Y. Chen, N. Sun, J. Zhao, Y. Liu, Y. Li, *Angew. Chem. Int. Ed.* **2015**, *54*, 1200-1204.

[41] a) L.-Q. Yang, K.-B. Wang, C.-Y. Li, *Eur. J. Org. Chem.* **2013**, 2775-2779; b) S. Ghorpade, M.-D. Su, R.-S. Liu, *Angew. Chem. Int. Ed.* **2013**, *52*, 4229-4234.

[42] L. Ye, W. He, L. Zhang, *J. Am. Chem. Soc.* **2010**, *132*, 8550-8551.

[43] L. Ye, L. Cui, G. Zhang, L. Zhang, *J. Am. Chem. Soc.* **2010**, *132*, 3258-3259.

[44] X.-N. Wang, H.-S. Yeom, L.-C. Fang, S. He, Z.-X. Ma, B. L. Kedrowski, R. P. Hsung, *Acc. Chem. Res.* **2014**, *47*, 560-578.

[45] P. W. Davies, A. Cremonesi, N. Martin, *Chem. Commun.* **2011**, *47*, 379-381.

[46] B. Lu, C. Li, L. Zhang, *J. Am. Chem. Soc.* **2010**, *132*, 14070-14072.

[47] a) G. Henrion, T. E. J. Chavas, X. Le Goff, F. Gagosz, *Angew. Chem. Int. Ed.* **2013**, *52*, 6277-6282; b) R. B. Dateer, K. Pati, R.-S. Liu, *Chem. Commun.* **2012**, *48*, 7200-7202; c) M. D. Santos, P. W. Davies, *Chem. Commun.* **2014**, *50*, 6001-6004; d) K.-B. Wang, R.-Q. Ran, S.-D. Xiu, C.-Y. Li, *Org. Lett.* **2013**, *15*, 2374-2377.

[48] C. Li, L. Zhang, *Org. Lett.* **2011**, *13*, 1738-1741.

[49] P. W. Davies, A. Cremonesi, L. Dumitrescu, *Angew. Chem. Int. Ed.* **2011**, *50*, 8931-8935.

[50] H. Li, R. P. Hsung, *Org. Lett.* **2009**, *11*, 4462-4465.

[51] Z. Li, X. Ding, C. He, *J. Org. Chem.* **2006**, *71*, 5876-5880.

[52] E. Chatzopoulou, P. W. Davies, *Chem. Commun.* **2013**, *49*, 8617-8619.

[53] M. Garzón, P. W. Davies, *Org. Lett.* **2014**, *16*, 4850-4853.

[54] a) J. Streith, J.-M. Cassal, *Angew. Chem. Int. Ed. Engl.* **1968**, *7*, 129-129; b) V. Snieckus, *J. Chem. Soc. D* **1969**, 831-831; c) T. Sasaki, K. Kanematsu, A. Kakehi, *J. Chem. Soc. D* **1969**, 432-433; d) A. Balasubramanian, J. M. McIntosh, V. Snieckus, *J. Org. Chem.* **1970**, *35*, 433-438; e)

T. Sasaki, K. Kanematsu, A. Kakehi, I. Ichikawa, K. Hayakawa, *J. Org. Chem.* **1970**, *35*, 426-433; f) J. Streith, J. P. Luttringer, M. Nastasi, *J. Org. Chem.* **1971**, *36*, 2962-2967.

[55] a) E. E. Knaus, K. Redda, *J. Heterocycl. Chem.* **1976**, *13*, 1237-1240; b) J. M. Yeung, L. A. Corleto, E. E. Knaus, *J. Med. Chem.* **1982**, *25*, 191-195; c) J. M. Yeung, E. E. Knaus, *J. Med. Chem.* **1987**, *30*, 104-108.

[56] C. Legault, A. B. Charette, *J. Am. Chem. Soc.* **2003**, *125*, 6360-6361.

[57] C. Y. Legault, A. B. Charette, *J. Am. Chem. Soc.* **2005**, *127*, 8966-8967.

[58] A. Larivée, J. J. Mousseau, A. B. Charette, *J. Am. Chem. Soc.* **2008**, *130*, 52-54.

[59] J. J. Mousseau, J. A. Bull, A. B. Charette, *Angew. Chem. Int. Ed.* **2010**, *49*, 1115-1118.

[60] Q. Xiao, L. Ling, F. Ye, R. Tan, L. Tian, Y. Zhang, Y. Li, J. Wang, *J. Org. Chem.* **2013**, *78*, 3879-3885.

[61] A. Kakehi, S. Ito, Y. Konno, T. Maeda, *Bull. Chem. Soc. Jpn.* **1978**, *51*, 251-256.

[62] T. Sasaki, K. Kanematsu, A. Kakehi, *J. Org. Chem.* **1971**, *36*, 2978-2986.

[63] Y. Yamashita, T. Hayashi, M. Masamura, *Chem. Lett.* **1980**, 1133-1136.

[64] a) J. J. Mousseau, J. A. Bull, C. L. Ladd, A. Fortier, D. Sustac Roman, A. B. Charette, *J. Org. Chem.* **2011**, *76*, 8243-8261; b) S. Ding, Y. Yan, N. Jiao, *Chem. Commun.* **2013**, *49*, 4250-4252.

[65] C. Perreault, S. R. Goudreau, L. E. Zimmer, A. B. Charette, *Org. Lett.* **2008**, *10*, 689-692.

[66] Y.-Y. Zhou, J. Li, L. Ling, S.-H. Liao, X.-L. Sun, Y.-X. Li, L.-J. Wang, Y. Tang, *Angew. Chem. Int. Ed.* **2013**, *52*, 1452-1456.

[67] X. Xu, P. Y. Zavalij, M. P. Doyle, *Angew. Chem. Int. Ed.* **2013**, *52*, 12664-12668.

[68] T. Sasaki, K. Kanematsu, A. Kakehi, *J. Org. Chem.* **1971**, *36*, 2451-2453.

[69] K. Hafner, D. Zinser, K.-L. Moritz, *Tetrahedron Lett.* **1964**, *5*, 1733-1737.

[70] A. Kakehi, S. Ito, Y. Hashimoto, *Bull. Chem. Soc. Jpn.* **1996**, *69*, 1769-1776.

[71] R. Gösl, A. Meuwsen, *Org. Synth.* **1963**, *43*, 1-2.

[72] C. Legault, A. B. Charette, *J. Org. Chem.* **2003**, *68*, 7119-7122.

[73] a) K. A. DeKorver, H. Li, A. G. Lohse, R. Hayashi, Z. Lu, Y. Zhang, R. P. Hsung, *Chem. Rev.* **2010**, *110*, 5064-5106; b) G. Evano, A. Coste, K. Jouvin, *Angew. Chem. Int. Ed.* **2010**, *49*, 2840-2859; c) G. Evano, K. Jouvin, A. Coste, *Synthesis* **2013**, *45*, 17-26.

[74] J. Ficini, *Tetrahedron* **1976**, *32*, 1449-1486.

[75] M. O. Frederick, J. A. Mulder, M. R. Tracey, R. P. Hsung, J. Huang, K. C. M. Kurtz, L. Shen, C. J. Douglas, *J. Am. Chem. Soc.* **2003**, *125*, 2368-2369.

[76] J. R. Dunetz, R. L. Danheiser, *Org. Lett.* **2003**, *5*, 4011-4014.

[77] a) Y. Zhang, R. P. Hsung, M. R. Tracey, K. C. M. Kurtz, E. L. Vera, *Org. Lett.* **2004**, *6*, 1151-1154; b) X. Zhang, Y. Zhang, J. Huang, R. P. Hsung, K. C. M. Kurtz, J. Oppenheimer, M. E. Petersen, I. K. Sagamanova, L. Shen, M. R. Tracey, *J. Org. Chem.* **2006**, *71*, 4170-4177.

[78] K. A. DeKorver, M. C. Walton, T. D. North, R. P. Hsung, *Org. Lett.* **2011**, *13*, 4862-4865.

[79] E. J. Corey, P. L. Fuchs, *Tetrahedron Lett.* **1972**, *13*, 3769-3772.

[80] G. J. Roth, B. Liepold, S. G. Müller, H. J. Bestmann, *Synthesis* **2004**, *2004*, 59-62.

[81] A. Coste, G. Karthikeyan, F. Couty, G. Evano, *Angew. Chem. Int. Ed.* **2009**, *48*, 4381-4385.

[82] T. Hamada, X. Ye, S. S. Stahl, *J. Am. Chem. Soc.* **2008**, *130*, 833-835.

[83] a) D. Brückner, *Synlett* **2000**, 1402-1404; b) D. Brückner, *Tetrahedron* **2006**, *62*, 3809-3814.

[84] D. Rodríguez, M. F. Martínez-Esperón, L. Castedo, C. Saá, *Synlett* **2007**, 1963-1965.

[85] a) S. Couty, M. Barbazanges, C. Meyer, J. Cossy, *Synlett* **2005**, 905-910; b) Y. Yang, X. Zhang, Y. Liang, *Tetrahedron Lett.* **2012**, *53*, 6557-6560; c) G. Evano, K. Jouvin, C. Theunissen, C. Guissart, A. Laouiti, C. Tresse, J. Heimburger, Y. Bouhoute, R. Veillard, M. Lecomte, A. Nitelet, S. Schweizer, N. Blanchard, C. Alayrac, A. C. Gaumont, *Chem. Commun.* **2014**; d) S. J. Mansfield, C. D. Campbell, M. W. Jones, E. A. Anderson, *Chem. Commun.* **2015**, *51*, 3316-3319.

[86] M. Muller, D. Bur, T. Tschamber, J. Streith, *Helv. Chim. Acta* **1991**, *74*, 767-773.

[87] a) Y. Dündar, S. Ünlü, E. Banoğlu, A. Entrena, G. Costantino, M.-T. Nunez, F. Ledo, M. F. Şahin, N. Noyanalpan, *Eur. J. Med. Chem.* **2009**, *44*, 1830-1837; b) W. A. Gregory, D. R. Brittelli, C. L. J. Wang, M. A. Wuonola, R. J. McRipley, D. C. Eustice, V. S. Eberly, A. M. Slee, M. Forbes, P. T. Bartholomew, *J. Med. Chem.* **1989**, *32*, 1673-1681; c) J. R. C. Moellering, *Ann. Intern. Med.* **2003**, *138*, 135-142; d) C. Puig, M. I. Crespo, N. Godessart, J. Feixas, J. Ibarzo, J.-M. Jiménez, L. Soca, I. Cardelús, A. Heredia, M. Miralpeix, J. Puig, J. Beleta, J. M. Huerta, M. López, V. Segarra, H. Ryder, J. M. Palacios, *J. Med. Chem.* **2000**, *43*, 214-223.

[88] a) S. V. D'Andrea, J. P. Freeman, J. Szmuszkovicz, *J. Org. Chem.* **1990**, *55*, 4356-4358; b) G. Butora, T. Hudlicky, S. P. Fearnley, A. G. Gum, M. R. Stabile, K. Abboud, *Tetrahedron Lett.* **1996**, *37*, 8155-8158; c) I. Nomura, C. Mukai, *J. Org. Chem.* **2004**, *69*, 1803-1812.

[89] a) U. Lerch, M. G. Burdon, J. G. Moffatt, *J. Org. Chem.* **1971**, *36*, 1507-1513; b) K. Pomeisl, A. Holý, R. Pohl, K. Horská, *Tetrahedron* **2009**, *65*, 8486-8492; c) R.-W. Wang, B. Gold, *Org. Lett.* **2009**, *11*, 2465-2468; d) U. Gellrich, J. Huang, W. Seiche, M. Keller, M. Meuwly, B. Breit, *J. Am. Chem. Soc.* **2010**, *133*, 964-975.

[90] A. D. Gillie, R. J. Reddy, P. W. Davies, *Adv. Synth. Catal.* in press: DOI 10.1002/adsc.201500905

[91] M. A. Cinellu, L. Maiore, G. Minghetti, F. Cocco, S. Stoccoro, A. Zucca, M. Manassero, C. Manassero, *Organometallics* **2009**, *28*, 7015-7024.

[92] A. Molina, M. A. de las Heras, Y. Martinez, J. J. Vaquero, J. García Navio, J. Alvarez-Builla, P. Gomez-Sal, R. Torres, *Tetrahedron* **1997**, *53*, 6411-6420.

[93] a) B. W. Michel, A. M. Camelio, C. N. Cornell, M. S. Sigman, *J. Am. Chem. Soc.* **2009**, *131*, 6076-6077; b) B. W. Michel, J. R. McCombs, A. Winkler, M. S. Sigman, *Angew. Chem. Int. Ed.* **2010**, *49*, 7312-7315; c) B. W. Michel, L. D. Steffens, M. S. Sigman, *J. Am. Chem. Soc.* **2011**, *133*, 8317-8325.

[94] A. H. Sato, K. Ohashi, K. Ito, T. Iwasawa, *Tetrahedron Lett.* **2013**, *54*, 2878-2881.

[95] a) A. S. K. Hashmi, R. Salathé, W. Frey, *Synlett* **2007**, 1763-1766; b) F. M. Istrate, A. K. Buzas, I. D. Jurberg, Y. Odabachian, F. Gagosz, *Org. Lett.* **2008**, *10*, 925-928.

[96] a) A. S. K. Hashmi, A. M. Schuster, F. Rominger, *Angew. Chem. Int. Ed.* **2009**, *48*, 8247-8249; b) A. S. Hashmi, *Gold Bull* **2009**, *42*, 275-279.

[97] S. Xu, J. Liu, D. Hu, X. Bi, *Green Chem.* **2015**, *17*, 184-187.

[98] W. Wang, B. Xu, G. B. Hammond, *J. Org. Chem.* **2009**, *74*, 1640-1643.

[99] a) W. Shi, F. Xiao, J. Wang, *J. Org. Chem.* **2005**, *70*, 4318-4322; b) F. Xiao, J. Wang, *J. Org. Chem.* **2006**, *71*, 5789-5791.

[100] a) M. Y. Karpeiskii, V. L. Florent'ev, *Russ. Chem. Rev.* **1969**, *38*, 540; b) I. J. Turchi, M. J. S. Dewar, *Chem. Rev.* **1975**, *75*, 389-437; c) D. L. Boger, *Chem. Rev.* **1986**, *86*, 781-793.

[101] S. Shimada, T. Tojo, *Chem. Pharm. Bull.* **1983**, *31*, 4247-4258.

[102] a) X. Sun, P. Janvier, G. Zhao, H. Bienaymé, J. Zhu, *Org. Lett.* **2001**, *3*, 877-880; b) P. Janvier, X. Sun, H. Bienaymé, J. Zhu, *J. Am. Chem. Soc.* **2002**, *124*, 2560-2567; c) R. Gámez-Montaño, E. González-Zamora, P. Potier, J. Zhu, *Tetrahedron* **2002**, *58*, 6351-6358; d) A. Fayol, J. Zhu, *Tetrahedron* **2005**, *61*, 11511-11519; e) C. Lalli, M. J. Bouma, D. Bonne , G. Masson, J. Zhu, *Chem. Eur. J.* **2011**, *17*, 880-889; f) Y. Su, M. J. Bouma, L. Alcaraz, M. Stocks, M. Furber, G. Masson, J. Zhu, *Chem. Eur. J.* **2012**, *18*, 12624-12627.

[103] a) J. I. Levin, S. M. Weinreb, *J. Am. Chem. Soc.* **1983**, *105*, 1397-1398; b) J. I. Levin, S. M. Weinreb, *J. Org. Chem.* **1984**, *49*, 4325-4332.

[104] a) C. Subramanyam, M. Noguchi, S. M. Weinreb, *J. Org. Chem.* **1989**, *54*, 5580-5585; b) M. Ohba, H. Kubo, H. Ishibashi, *Tetrahedron* **2000**, *56*, 7751-7761; c) M. Ohba, I. Natsutani, T. Sakuma, *Tetrahedron Lett.* **2004**, *45*, 6471-6474; d) M. Ohba, R. Izuta, E. Shimizu, *Chem. Pharm. Bull.* **2006**, *54*, 63-67; e) S. N. Goodman, D. M. Mans, J. Sisko, H. Yin, *Org. Lett.* **2012**, *14*, 1604-1607; f) M. Uosis-Martin, G. D. Pantoş, M. F. Mahon, S. E. Lewis, *J. Org. Chem.* **2013**, *78*, 6253-6263.

[105] a) R. Grigg, R. Hayes, J. L. Jackson, *J. Chem. Soc. D* **1969**, 1167-1168; b) H. Gotthardt, R. Huisgen, H. O. Bayer, *J. Am. Chem. Soc.* **1970**, *92*, 4340-4344.

[106] S. E. Whitney, B. Rickborn, *J. Org. Chem.* **1988**, *53*, 5595-5596.

[107] a) P. A. Jacobi, D. G. Walker, I. M. A. Odeh, *J. Org. Chem.* **1981**, *46*, 2065-2069; b) P. A. Jacobi, D. G. Walker, *J. Am. Chem. Soc.* **1981**, *103*, 4611-4613; c) P. A. Jacobi, T. A. Craig, D. G. Walker, B. A. Arrick, R. F. Frechette, *J. Am. Chem. Soc.* **1984**, *106*, 5585-5594; d) P. A. Jacobi, H. G. Selnick, *J. Am. Chem. Soc.* **1984**, *106*, 3041-3043.

[108] a) P. A. Jacobi, C. S. R. Kaczmarek, U. E. Udodong, *Tetrahedron Lett.* **1984**, *25*, 4859-4862; b) A. Padwa, M. A. Brodney, B. Liu, K. Satake, T. Wu, *J. Org. Chem.* **1999**, *64*, 3595-3607; c) L. A. Paquette, I. Efremov, *J. Am. Chem. Soc.* **2001**, *123*, 4492-4501.

[109] A. Fayol, J. Zhu, *Org. Lett.* **2004**, *6*, 115-118.

[110] a) K. A. Parker, M. R. Adamchuk, *Tetrahedron Lett.* **1978**, *19*, 1689-1692; b) R. Pedrosa, C. Andrés, J. Nieto, *J. Org. Chem.* **2000**, *65*, 831-839; c) F. I. Zubkov, V. P. Zaytsev, E. V. Nikitina, V. N. Khrustalev, S. V. Gozun, E. V. Boltukhina, A. V. Varlamov, *Tetrahedron* **2011**, *67*, 9148-9163.

[111] a) N. V. Vasil'ev, V. M. Koshelev, D. V. Romanov, K. A. Lyssenko, M. Y. Antipin, G. V. Zatonskii, *Russ. Chem. Bull.* **2005**, *54*, 1680-1685; b) G. V. Suárez-Moreno, E. González-Zamora, F. Méndez, *Org. Lett.* **2011**, *13*, 6358-6361.

[112] S. Kotha, K. Singh, *Eur. J. Org. Chem.* **2007**, 5909-5916.

[113] T. Fukuyama, C.-K. Jow, M. Cheung, *Tetrahedron Lett.* **1995**, *36*, 6373-6374.

[114] E. J. Kantorowski, M. J. Kurth, *Tetrahedron* **2000**, *56*, 4317-4353.

[115] C. L. Perrin, G. M. L. Arrhenius, *J. Am. Chem. Soc.* **1982**, *104*, 2839-2842.

[116] S. R. Chirapu, J. N. Bauman, H. Eng, T. C. Goosen, T. J. Strelevitz, S. C. Sinha, R. L. Dow, M. G. Finn, *Bioorg. Med. Chem. Lett.* **2014**, *24*, 1144-1147.

[117] V. G. Nenajdenko, E. P. Zakurdaev, E. V. Prusov, E. S. Balenkova, *Tetrahedron* **2004**, *60*, 11719-11724.

[118] a) E. J. Goldstein, D. M. Citron, M. Hudspeth, S. Hunt Gerardo, C. V. Merriam, *Antimicrob. Agents Chemother.* **1997**, *41*, 1552-1557; b) A. B. Brueggemann, K. C. Kugler, G. V. Doern, *Antimicrob. Agents Chemother.* **1997**, *41*, 1594-1597; c) M. Baumann, I. R. Baxendale, *Beilstein J. Org. Chem.* **2013**, *9*, 2265-2319; d) G. Li, L. Wu, Q. Fu, Z. Tang, X. Zhang, *Sci. China Chem.* **2013**, *56*, 307-311.

[119] a) D. Enders, O. Niemeier, A. Henseler, *Chem. Rev.* **2007**, *107*, 5606-5655; b) X. Bugaut, F. Glorius, *Chem. Soc. Rev.* **2012**, *41*, 3511-3522; c) M. Fevre, J. Pinaud, Y. Gnanou, J. Vignolle, D. Taton, *Chem. Soc. Rev.* **2013**, *42*, 2142-2172.

[120] a) S. Díez-González, N. Marion, S. P. Nolan, *Chem. Rev.* **2009**, *109*, 3612-3676; b) G. C. Fortman, S. P. Nolan, *Chem. Soc. Rev.* **2011**, *40*, 5151-5169; c) J. D. Egbert, C. S. J. Cazin, S. P. Nolan, *Catal. Sci. Technol.* **2013**, *3*, 912-926; d) S. P. Nolan, *Acc. Chem. Res.* **2011**, *44*, 91-100.

[121] A. J. Arduengo, L. I. Iconaru, *Dalton Trans.* **2009**, 6903-6914.

[122] a) F. E. Hahn, L. Wittenbecher, R. Boese, D. Bläser, *Chem. Eur. J.* **1999**, *5*, 1931-1935; b) C. J. O'Brien, E. A. B. Kantchev, G. A. Chass, N. Hadei, A. C. Hopkinson, M. G. Organ, D. H. Setiadi, T.-H. Tang, D.-C. Fang, *Tetrahedron* **2005**, *61*, 9723-9735; c) H. Buhl, C. Ganter, *Chem. Commun.* **2013**, *49*, 5417-5419.

[123] a) R. L. Knight, F. J. Leeper, *J. Chem. Soc., Perkin Trans. 1* **1998**, 1891-1894; b) D. Enders, U. Kallfass, *Angew. Chem. Int. Ed.* **2002**, *41*, 1743-1745; c) M. S. Kerr, J. Read de Alaniz, T. Rovis, *J. Am. Chem. Soc.* **2002**, *124*, 10298-10299; d) M. S. Kerr, J. Read de Alaniz, T. Rovis, *J. Org. Chem.* **2005**, *70*, 5725-5728.

[124] a) F. Glorius, G. Altenhoff, R. Goddard, C. Lehmann, *Chem. Commun.* **2002**, 2704-2705; b) S. Würtz, C. Lohre, R. Fröhlich, K. Bergander, F. Glorius, *J. Am. Chem. Soc.* **2009**, *131*, 8344-8345; c) J.-N. Levy, C. M. Latham, L. Roisin, N. Kandziora, P. D. Fruscia, A. J. P. White, S.

Woodward, M. J. Fuchter, *Org. Biomol. Chem.* **2012**, *10*, 512-515; d) J. K. Park, H. H. Lackey, M. D. Rexford, K. Kovnir, M. Shatruk, D. T. McQuade, *Org. Lett.* **2010**, *12*, 5008-5011.

[125] a) F. Wang, L.-j. Liu, W. Wang, S. Li, M. Shi, *Coord. Chem. Rev.* **2012**, *256*, 804-853; b) V. Cesar, S. Bellemin-Laponnaz, L. H. Gade, *Chem. Soc. Rev.* **2004**, *33*, 619-636.

[126] a) A. Fürstner, M. Alcarazo, H. Krause, C. W. Lehmann, *J. Am. Chem. Soc.* **2007**, *129*, 12676-12677; b) M. Alcarazo, T. Stork, A. Anoop, W. Thiel, A. Fürstner, *Angew. Chem. Int. Ed.* **2010**, *49*, 2542-2546.

[127] A. Miyashita, Y. Suzuki, M. Kobayashi, N. Kuriyama, T. Higashino, *Heterocycles* **1996**, *43*, 509-512.

[128] M. Alcarazo, S. J. Roseblade, A. R. Cowley, R. Fernández, J. M. Brown, J. M. Lassaletta, *J. Am. Chem. Soc.* **2005**, *127*, 3290-3291.

[129] M. Nonnenmacher, D. Kunz, F. Rominger, T. Oeser, *J. Organomet. Chem.* **2007**, *692*, 2554-2563.

[130] a) M. Tsimerman, D. Mallik, T. Matsuo, T. Otani, K. Tamao, M. G. Organ, *Chem. Commun.* **2012**, *48*, 10352-10354; b) J. Zhang, J. Fu, X. Su, X. Wang, S. Song, M. Shi, *Chem. Asain J.* **2013**, *8*, 552-555; c) G. Pelletier, A. B. Charette, *Org. Lett.* **2013**, *15*, 2290-2293.

[131] C. Burstein, C. W. Lehmann, F. Glorius, *Tetrahedron* **2005**, *61*, 6207-6217.

[132] M. A. Schmidt, M. Movassaghi, *Tetrahedron Lett.* **2007**, *48*, 101-104.

[133] C. Lohre, R. Fröhlich, F. Glorius, *Synthesis* **2008**, 2221-2228.

[134] a) L. Hintermann, *Beilstein J. Org. Chem.* **2007**, *3*, 22; b) L. Benhamou, E. Chardon, G. Lavigne, S. Bellemin-Laponnaz, V. César, *Chem. Rev.* **2011**, *111*, 2705-2733.

[135] a) C.-H. Chien, S. Fujita, S. Yamoto, T. Hara, T. Yamagata, M. Watanabe, K. Mashima, *Dalton Trans.* **2008**, 916-923; b) T. Samanta, B. Kumar Rana, G. Roymahapatra, S. Giri, P. Mitra, R. Pallepogu, P. Kumar Chattaraj, J. Dinda, *Inorg. Chim. Acta* **2011**, *375*, 271-279; c) M. Kriechbaum, M. List, R. J. F. Berger, M. Patzschke, U. Monkowius, *Chem. Eur. J.* **2012**, *18*,

5506-5509; d) J.-L. Zhang, L.-A. Chen, R.-B. Xu, C.-F. Wang, Y.-P. Ruan, A.-E. Wang, P.-Q. Huang, *Tetrahedron: Asymmetry* **2013**, *24*, 492-498.

[136] a) J. T. Hutt, Z. D. Aron, *Org. Lett.* **2011**, *13*, 5256-5259; b) J. T. Hutt, J. Jo, A. Olasz, C.-H. Chen, D. Lee, Z. D. Aron, *Org. Lett.* **2012**, *14*, 3162-3165.

[137] C. Grohmann, T. Hashimoto, R. Fröhlich, Y. Ohki, K. Tatsumi, F. Glorius, *Organometallics* **2012**, *31*, 8047-8050.

[138] A. J. Arduengo, R. L. Harlow, M. Kline, *J. Am. Chem. Soc.* **1991**, *113*, 361-363.

[139] M. Nonnenmacher, D. Kunz, F. Rominger, T. Oeser, *Chem. Commun.* **2006**, *0*, 1378-1380.

[140] M. Espina, I. Rivilla, A. Conde, M. M. Díaz-Requejo, P. J. Pérez, E. Álvarez, R. Fernández, J. M. Lassaletta, *Organometallics* **2015**, *34*, 1328-1338.

[141] X. Liu, S. Pan, J. Wu, Y. Wang, W. Chen, *Organometallics* **2012**, *32*, 209-217.

[142] J. M. O'Brien, K.-s. Lee, A. H. Hoveyda, *J. Am. Chem. Soc.* **2010**, *132*, 10630-10633.

[143] Z. Niu, J. Chen, Z. Chen, M. Ma, C. Song, Y. Ma, *J. Org. Chem.* **2015**, *80*, 602-608.

[144] a) A. Ros, D. Monge, M. Alcarazo, E. Álvarez, J. M. Lassaletta, R. Fernández, *Organometallics* **2006**, *25*, 6039-6046; b) S. J. Roseblade, A. Ros, D. Monge, M. Alcarazo, E. Álvarez, J. M. Lassaletta, R. Fernández, *Organometallics* **2007**, *26*, 2570-2578; c) A. Ros, M. Alcarazo, J. Iglesias-Sigüenza, E. Díez, E. Álvarez, R. Fernández, J. M. Lassaletta, *Organometallics* **2008**, *27*, 4555-4564; d) J. Iglesias-Sigüenza, A. Ros, E. Díez, A. Magriz, A. Vázquez, E. Álvarez, R. Fernández, J. M. Lassaletta, *Dalton Trans.* **2009**, 8485-8488.

[145] J. Sprinz, G. Helmchen, *Tetrahedron Lett.* **1993**, *34*, 1769-1772.

[146] J. Francos, F. Grande-Carmona, H. Faustino, J. Iglesias-Sigüenza, E. Díez, I. Alonso, R. Fernández, J. M. Lassaletta, F. López, J. L. Mascareñas, *J. Am. Chem. Soc.* **2012**, *134*, 14322-14325.

[147] a) K.-i. Yamada, Y. Matsumoto, K. B. Selim, Y. Yamamoto, K. Tomioka, *Tetrahedron* **2012**, *68*, 4159-4165; b) M. He, J. R. Struble, J. W. Bode, *J. Am. Chem. Soc.* **2006**, *128*, 8418-8420.

[148] Y. Ma, S. Wei, J. Lan, J. Wang, R. Xie, J. You, *J. Org. Chem.* **2008**, *73*, 8256-8264.

[149] R. W. Alder, M. E. Blake, S. Bufali, C. P. Butts, A. G. Orpen, J. Schutz, S. J. Williams, *J. Chem. Soc., Perkin Trans. 1* **2001**, 1586-1593.

[150] a) C. J. Cathey, E. C. Constable, M. J. Hannon, D. A. Tohcer, M. D. Ward, *J. Chem. Soc., Chem. Commun.* **1990**, 621-622; b) A. Bheemaraju, J. W. Beattie, Y. Danylyuk, J. Rochford, S. Groysman, *Eur. J. Inorg. Chem.* **2014**, *2014*, 5865-5873.

[151] I. C. Calder, T. M. Spotswood, W. H. P. Sasse, *Tetrahedron Lett.* **1963**, *4*, 95-100.

[152] a) V. Gierz, A. Seyboldt, C. Maichle-Mössmer, K. W. Törnroos, M. T. Speidel, B. Speiser, K. Eichele, D. Kunz, *Organometallics* **2012**, *31*, 7893-7901; b) C. Schulte to Brinke, T. Pape, F. E. Hahn, *Dalton Trans.* **2013**, *42*, 7330-7337.

[153] a) R. Visbal, A. Laguna, M. C. Gimeno, *Chem. Commun.* **2013**, *49*, 5642-5644; b) A. Collado, A. Gomez-Suarez, A. R. Martin, A. M. Z. Slawin, S. P. Nolan, *Chem. Commun.* **2013**, *49*, 5541-5543; c) O. Santoro, A. Collado, A. M. Z. Slawin, S. P. Nolan, C. S. J. Cazin, *Chem. Commun.* **2013**, *49*, 10483-10485.

[154] a) A. Poater, B. Cosenza, A. Correa, S. Giudice, F. Ragone, V. Scarano, L. Cavallo, *Eur. J. Inorg. Chem.* **2009**, *2009*, 1759-1766; b) H. Clavier, S. P. Nolan, *Chem. Commun.* **2010**, *46*, 841-861.

[155] www.molnac.unisa.it/OMtools/sambvca.php.

[156] M. Brill, A. Collado, D. B. Cordes, A. M. Z. Slawin, M. Vogt, H. Grützmacher, S. P. Nolan, *Organometallics* **2015**, *34*, 263-274.

[157] M. R. Fructos, T. R. Belderrain, P. de Frémont, N. M. Scott, S. P. Nolan, M. M. Díaz-Requejo, P. J. Pérez, *Angew. Chem. Int. Ed.* **2005**, *44*, 5284-5288.

[158] P. Marshall, R. L. Jenkins, W. Clegg, R. W. Harrington, S. K. Callear, S. J. Coles, I. A. Fallis, A. Dervisi, *Dalton Trans.* **2012**, *41*, 12839-12846.

[159] T. Dröge, F. Glorius, *Angew. Chem. Int. Ed.* **2010**, *49*, 6940-6952.

[160] D. J. Nelson, S. P. Nolan, *Chem. Soc. Rev.* **2013**, *42*, 6723-6753.

[161] C. A. Tolman, *Chem. Rev.* **1977**, *77*, 313-348.

[162] R. A. Kelly Iii, H. Clavier, S. Giudice, N. M. Scott, E. D. Stevens, J. Bordner, I. Samardjiev, C. D. Hoff, L. Cavallo, S. P. Nolan, *Organometallics* **2007**, *27*, 202-210.

[163] S. Leuthäußer, D. Schwarz, H. Plenio, *Chem. Eur. J.* **2007**, *13*, 7195-7203.

[164] D. A. Valyaev, R. Brousses, N. Lugan, I. Fernández, M. A. Sierra, *Chem. Eur. J.* **2011**, *17*, 6602-6605.

[165] J. Iglesias-Sigüenza, A. Ros, E. Díez, M. Alcarazo, E. Álvarez, R. Fernández, J. M. Lassaletta, *Dalton Trans.* **2009**, 7113-7120.

[166] a) F. Hanasaka, Y. Tanabe, K.-i. Fujita, R. Yamaguchi, *Organometallics* **2006**, *25*, 826-831; b) R. Corberán, M. Sanaú, E. Peris, *Organometallics* **2006**, *25*, 4002-4008.

[167] a) N. Marion, R. S. Ramón, S. P. Nolan, *J. Am. Chem. Soc.* **2009**, *131*, 448-449; b) P. Nun, R. S. Ramón, S. Gaillard, S. P. Nolan, *J. Organomet. Chem.* **2011**, *696*, 7-11.

[168] Y. Xu, X. Hu, J. Shao, G. Yang, Y. Wu, Z. Zhang, *Green Chem.* **2015**, *17*, 532-537.

[169] J. A. Goodwin, A. Aponick, *Chem. Commun.* **2015**, *51*, 8730-8741.

[170] H. E. Gottlieb, V. Kotlyar, A. Nudelman, *J. Org. Chem.* **1997**, *62*, 7512-7515.

[171] S. C. G. Biagini, S. E. GibsoneThomas, S. P. Keen, *J. Chem. Soc., Perkin Trans. 1* **1998**, 2485-2500.

[172] S. Surprenant, W. D. Lubell, *J. Org. Chem.* **2006**, *71*, 848-851.

[173] C. Jahns, T. Hoffmann, S. Müller, K. Gerth, P. Washausen, G. Höfle, H. Reichenbach, M. Kalesse, R. Müller, *Angew. Chem. Int. Ed.* **2012**, *51*, 5239-5243.

[174] A. A. Arutyunyan, R. G. Melik-Ogadzhanyan, L. G. Alaverdova, S. A. Papoyan, Y. Z. Ter-Zakharyan, É. V. Kazaryan, G. M. Paronikyan, T. P. Sarkisyan, *Pharm. Chem. J.* **1989**, *23*, 837-840.

[175] C. Soede-Huijbregts, M. van Laren, F. B. Hulsbergen, J. Raap, J. Lugtenburg, *J. Labelled Compd. Radiopharm.* **2001**, *44*, 831-841.

[176] I. Ugarriza, U. Uria, L. Carrillo, J. L. Vicario, E. Reyes, *Chem. Eur. J.* **2014**, *20*, 11650-11654.

[177] A. G. Cameron, A. T. Hewson, *J. Chem. Soc., Perkin Trans. 1* **1983**, *0*, 2979-2982.

[178] N. Sakai, K. Tamura, K. Shimamura, R. Ikeda, T. Konakahara, *Org. Lett.* **2012**, *14*, 836-839.

[179] S. Dohi, K. Moriyama, H. Togo, *Eur. J. Org. Chem.* **2013**, 7815-7822.

[180] K. Okano, N. Mitsuhashi, H. Tokuyama, *Chem. Commun.* **2010**, *46*, 2641-2643.

[181] D. Pulido, F. Albericio, M. Royo, *Org. Lett.* **2014**, *16*, 1318-1321.

[182] M. Gemperli, W. Hofmann, M. Rottenberg, *Helv. Chim. Acta* **1965**, *48*, 939-945.

[183] N. B. Palakurthy, B. Mandal, *Tetrahedron Lett.* **2011**, *52*, 7132-7134.

[184] M. Ordóñez, R. De la Cruz-Cordero, M. Fernández-Zertuche, M. Angel Muñoz-Hernández, O. García-Barradas, *Tetrahedron: Asymmetry* **2004**, *15*, 3035-3043.

[185] K. L. Jensen, E. A. Standley, T. F. Jamison, *J. Am. Chem. Soc.* **2014**, *136*, 11145-11152.

[186] K.-T. Yip, J.-H. Li, O.-Y. Lee, D. Yang, *Org. Lett.* **2005**, *7*, 5717-5719.

[187] J. Xie, Z.-Z. Huang, *Angew. Chem. Int. Ed.* **2010**, *49*, 10181-10185.

[188] P. Gesche, F. Klinger, W. Müller, J. Streith, H. Strub, R. Sustmann, *Chem. Ber.* **1985**, *118*, 4682-4706.

[189] J. F. King, J. Y. L. Lam, S. Skonieczny, *J. Am. Chem. Soc.* **1992**, *114*, 1743-1749.

[190] S. O'Sullivan, E. Doni, T. Tuttle, J. A. Murphy, *Angew. Chem. Int. Ed.* **2014**, *53*, 474-478.

[191] D. C. Johnson, T. S. Widlanski, *J. Org. Chem.* **2003**, *68*, 5300-5309.

[192] A. Yoshimura, M. W. Luedtke, V. V. Zhdankin, *J. Org. Chem.* **2012**, *77*, 2087-2091.

[193] O. Kreye, S. Wald, M. A. R. Meier, *Adv. Synth. Catal.* **2013**, *355*, 81-86.

[194] B. Urones, A. M. Martinez, N. Rodriguez, R. G. Arrayas, J. C. Carretero, *Chem. Commun.* **2013**, *49*, 11044-11046.

[195] X. Tang, L. Huang, C. Qi, X. Wu, W. Wu, H. Jiang, *Chem. Commun.* **2013**, *49*, 6102-6104.

[196] D. C. Baker, A. Mayasundari, J. Mao, S. C. Johnson, S. Yan, (The University of Tennessee Research Foundation) US6562850 (B1) **2003**, p. 14.

[197] X. Fan, L.-A. Fu, N. Li, H. Lv, X.-M. Cui, Y. Qi, *Org. Biomol. Chem.* **2013**, *11*, 2147-2153.

[198] A. Kumar, G. Ye, Y. Ahmadibeni, K. Parang, *J. Org. Chem.* **2006**, *71*, 7915-7918.

[199] X. Zhang, B. Cao, S. Yu, X. Zhang, *Angew. Chem. Int. Ed.* **2010**, *49*, 4047-4050.

[200] D. Farran, A. M. Z. Slawin, P. Kirsch, D. O'Hagan, *J. Org. Chem.* **2009**, *74*, 7168-7171.

[201] H.-J. Li, R. Guillot, V. Gandon, *J. Org. Chem.* **2010**, *75*, 8435-8449.

[202] M. L. N. Rao, D. N. Jadhav, P. Dasgupta, *Org. Lett.* **2010**, *12*, 2048-2051.

[203] Y. Araki, K. Kobayashi, M. Yonemoto, Y. Kondo, *Org. Biomol. Chem.* **2011**, *9*, 78-80.

[204] M. F. Jacobsen, J. E. Moses, R. M. Adlington, J. E. Baldwin, *Org. Lett.* **2005**, *7*, 641-644.

[205] R. Liu, G. N. Winston-McPherson, Z.-Y. Yang, X. Zhou, W. Song, I. A. Guzei, X. Xu, W. Tang, *J. Am. Chem. Soc.* **2013**, *135*, 8201-8204.

[206] R. B. Dateer, B. S. Shaibu, R.-S. Liu, *Angew. Chem. Int. Ed.* **2012**, *51*, 113-117.

[207] A. Mukherjee, R. B. Dateer, R. Chaudhuri, S. Bhunia, S. N. Karad, R.-S. Liu, *J. Am. Chem. Soc.* **2011**, *133*, 15372-15375.

[208] W. D. Mackay, M. Fistikci, R. M. Carris, J. S. Johnson, *Org. Lett.* **2014**, *16*, 1626-1629.

[209] N. Riddell, K. Villeneuve, W. Tam, *Org. Lett.* **2005**, *7*, 3681-3684.

[210] D. A. Alonso, E. Alonso, C. Nájera, D. J. Ramón, M. Yus, *Tetrahedron* **1997**, *53*, 4835-4856.

[211] F. Medina, C. Michon, F. Agbossou-Niedercorn, *Eur. J. Org. Chem.* **2012**, 6218-6227.

[212] A. J. Walkinshaw, W. Xu, M. G. Suero, M. J. Gaunt, *J. Am. Chem. Soc.* **2013**, *135*, 12532-12535.

[213] C. Zhao, X. Jia, X. Wang, H. Gong, *J. Am. Chem. Soc.* **2014**, *136*, 17645-17651.

[214] J.-C. Hsieh, Y.-C. Chen, A.-Y. Cheng, H.-C. Tseng, *Org. Lett.* **2012**, *14*, 1282-1285.